Validation of Urban Freeway Models

DETAILS

0 pages | 8.5 x 11 | PAPERBACK
ISBN 978-0-309-43312-9 | DOI 10.17226/22282

AUTHORS

Hranac, Robert; Barkley, Tiffany; Sambana, Kavya; Derstine, Brian; Mirchandani, Pitu; Zhou, Zhuoyang; and Soyoung Ahn

The Second
STRATEGIC HIGHWAY RESEARCH PROGRAM

SHRP 2 REPORT S2-L33-RW-1

Validation of Urban Freeway Models

Robert Hranac, Tiffany Barkley, Kavya Sambana, and Brian Derstine
Iteris, Inc.
Berkeley, California

Pitu Mirchandani and Zhuoyang Zhou
Arizona State University
Phoenix, Arizona

Soyoung Ahn
University of Wisconsin–Madison

TRANSPORTATION RESEARCH BOARD

WASHINGTON, D.C.
2015
www.TRB.org

Subject Areas

Highways
Operations and Traffic Management
Planning and Forecasting

The Second Strategic Highway Research Program

America's highway system is critical to meeting the mobility and economic needs of local communities, regions, and the nation. Developments in research and technology—such as advanced materials, communications technology, new data collection technologies, and human factors science—offer a new opportunity to improve the safety and reliability of this important national resource. Breakthrough resolution of significant transportation problems, however, requires concentrated resources over a short time frame. Reflecting this need, the second Strategic Highway Research Program (SHRP 2) has an intense, large-scale focus, integrates multiple fields of research and technology, and is fundamentally different from the broad, mission-oriented, discipline-based research programs that have been the mainstay of the highway research industry for half a century.

The need for SHRP 2 was identified in *TRB Special Report 260: Strategic Highway Research: Saving Lives, Reducing Congestion, Improving Quality of Life,* published in 2001 and based on a study sponsored by Congress through the Transportation Equity Act for the 21st Century (TEA-21). SHRP 2, modeled after the first Strategic Highway Research Program, is a focused, time-constrained, management-driven program designed to complement existing highway research programs. SHRP 2 focuses on applied research in four areas: Safety, to prevent or reduce the severity of highway crashes by understanding driver behavior; Renewal, to address the aging infrastructure through rapid design and construction methods that cause minimal disruptions and produce lasting facilities; Reliability, to reduce congestion through incident reduction, management, response, and mitigation; and Capacity, to integrate mobility, economic, environmental, and community needs in the planning and designing of new transportation capacity.

SHRP 2 was authorized in August 2005 as part of the Safe, Accountable, Flexible, Efficient Transportation Equity Act: A Legacy for Users (SAFETEA-LU). The program is managed by the Transportation Research Board (TRB) on behalf of the National Research Council (NRC). SHRP 2 is conducted under a memorandum of understanding among the American Association of State Highway and Transportation Officials (AASHTO), the Federal Highway Administration (FHWA), and the National Academy of Sciences, parent organization of TRB and NRC. The program provides for competitive, merit-based selection of research contractors; independent research project oversight; and dissemination of research results.

SHRP 2 Report S2-L33-RW-1

ISBN: 978-0-309-27424-1

Copyright Information

Note: SHRP 2 report numbers convey the program, focus area, project number, and publication format. Report numbers ending in "w" are published as web documents only.

Notice

The project that is the subject of this report was a part of the second Strategic Highway Research Program, conducted by the Transportation Research Board with the approval of the Governing Board of the National Research Council.

The members of the technical committee selected to monitor this project and review this report were chosen for their special competencies and with regard for appropriate balance. The report was reviewed by the technical committee and accepted for publication according to procedures established and overseen by the Transportation Research Board and approved by the Governing Board of the National Research Council.

The opinions and conclusions expressed or implied in this report are those of the researchers who performed the research and are not necessarily those of the Transportation Research Board, the National Research Council, or the program sponsors.

The Transportation Research Board of the National Academies, the National Research Council, and the sponsors of the second Strategic Highway Research Program do not endorse products or manufacturers. Trade or manufacturers' names appear herein solely because they are considered essential to the object of the report.

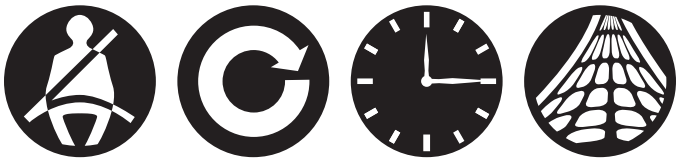

SHRP 2 Reports

Available by subscription and through the TRB online bookstore:

www.mytrb.org/store

Contact the TRB Business Office:
202-334-3213

More information about SHRP 2:

www.TRB.org/SHRP2

THE NATIONAL ACADEMIES

Advisers to the Nation on Science, Engineering, and Medicine

The **National Academy of Sciences** is a private, nonprofit, self-perpetuating society of distinguished scholars engaged in scientific and engineering research, dedicated to the furtherance of science and technology and to their use for the general welfare. On the authority of the charter granted to it by Congress in 1863, the Academy has a mandate that requires it to advise the federal government on scientific and technical matters. Dr. Ralph J. Cicerone is president of the National Academy of Sciences.

The **National Academy of Engineering** was established in 1964, under the charter of the National Academy of Sciences, as a parallel organization of outstanding engineers. It is autonomous in its administration and in the selection of its members, sharing with the National Academy of Sciences the responsibility for advising the federal government. The National Academy of Engineering also sponsors engineering programs aimed at meeting national needs, encourages education and research, and recognizes the superior achievements of engineers. Dr. C. D. (Dan) Mote, Jr., is president of the National Academy of Engineering.

The **Institute of Medicine** was established in 1970 by the National Academy of Sciences to secure the services of eminent members of appropriate professions in the examination of policy matters pertaining to the health of the public. The Institute acts under the responsibility given to the National Academy of Sciences by its congressional charter to be an adviser to the federal government and, on its own initiative, to identify issues of medical care, research, and education. Dr. Victor J. Dzau is president of the Institute of Medicine.

The **National Research Council** was organized by the National Academy of Sciences in 1916 to associate the broad community of science and technology with the Academy's purposes of furthering knowledge and advising the federal government. Functioning in accordance with general policies determined by the Academy, the Council has become the principal operating agency of both the National Academy of Sciences and the National Academy of Engineering in providing services to the government, the public, and the scientific and engineering communities. The Council is administered jointly by both Academies and the Institute of Medicine. Dr. Ralph J. Cicerone and Dr. C. D. (Dan) Mote, Jr., are chair and vice chair, respectively, of the National Research Council.

The **Transportation Research Board** is one of six major divisions of the National Research Council. The mission of the Transportation Research Board is to provide leadership in transportation innovation and progress through research and information exchange, conducted within a setting that is objective, interdisciplinary, and multimodal. The Board's varied activities annually engage about 7,000 engineers, scientists, and other transportation researchers and practitioners from the public and private sectors and academia, all of whom contribute their expertise in the public interest. The program is supported by state transportation departments, federal agencies including the component administrations of the U.S. Department of Transportation, and other organizations and individuals interested in the development of transportation. **www.TRB.org**

www.national-academies.org

SHRP 2 STAFF

Ann M. Brach, *Director*
Stephen J. Andrle, *Deputy Director*
Cynthia Allen, *Editor*
Kenneth Campbell, *Chief Program Officer, Safety*
Jared Cazel, *Editorial Assistant*
JoAnn Coleman, *Senior Program Assistant, Capacity and Reliability*
Eduardo Cusicanqui, *Financial Officer*
Richard Deering, *Special Consultant, Safety Data Phase 1 Planning*
Shantia Douglas, *Senior Financial Assistant*
Charles Fay, *Senior Program Officer, Safety*
Carol Ford, *Senior Program Assistant, Renewal and Safety*
James Hedlund, *Special Consultant, Safety Coordination*
Alyssa Hernandez, *Reports Coordinator*
Ralph Hessian, *Special Consultant, Capacity and Reliability*
Andy Horosko, *Special Consultant, Safety Field Data Collection*
William Hyman, *Senior Program Officer, Reliability*
Linda Mason, *Communications Officer*
David Plazak, *Senior Program Officer, Capacity and Reliability*
Rachel Taylor, *Senior Editorial Assistant*
Dean Trackman, *Managing Editor*
Connie Woldu, *Administrative Coordinator*

ACKNOWLEDGMENTS

This work was sponsored by the Federal Highway Administration in cooperation with the American Association of State Highway and Transportation Officials. It was conducted in the second Strategic Highway Research Program (SHRP 2), which is administered by the Transportation Research Board of the National Academies. The project was managed by William Hyman, Senior Program Officer for SHRP 2 Reliability.

The research reported was performed by Iteris, Inc., supported by Arizona State University and the University of Wisconsin. Robert Hranac of Iteris, Inc., was the principal investigator. The other authors of this report are Tiffany Barkley, Kavya Sambana, and Brian Derstine of Iteris, Inc.; Pitu Mirchandani and Zhuoyang Zhou of Arizona State University; and Soyoung Ahn of the University of Wisconsin–Madison.

Iteris, Inc., received technical assistance about the source data from the following agencies: Minnesota Department of Transportation (MnDOT), Utah Department of Transportation (UDOT), Washington State Department of Transportation, and the California Department of Transportation (CalTrans).

FOREWORD

William Hyman, *SHRP 2 Senior Program Officer, Reliability*

This report describes the methodology, data, conclusions, and enhanced models regarding the validation of two sets of models developed in SHRP 2 Reliability Project L03, Analytical Procedures for Determining the Impacts of Reliability Mitigation Strategies. The significance of the L03 models is they were among the first models that could be used to predict travel time reliability.

Loosely speaking, reliability is defined as how travel time changes over time. More rigorously, reliability is defined as "the level of consistency in travel conditions over time . . . measured by describing the distribution of travel times that occur over a substantial period of time."[1] Specific reliability measures can be derived from the travel time distribution, such as the standard deviation and the Travel Time Index (n), or TTI_n, which is the nth percentile of the travel time distribution divided by the free-flow travel time.

Two sets of models were developed in Project L03, the data-poor and the data-rich models. The data-poor models predict a measure of reliability as a function of just the mean Travel Time Index, except for the on-time measures. Because these data-poor models have but one independent variable, these simple models provide a great deal of versatility in estimating reliability. Data-poor models enable the use of straightforward equations for predicting reliability in sketch planning and in complex modeling systems such as a trip-based demand model married to a network model.

The data-rich models predict a measure of the variability of travel time as a function of a number of important variables that Project L03 found to be meaningful explanatory variables: the demand-to-capacity ratio, lane-hours lost (due to traffic incidents or work zones), and rainfall. The data-rich models can be used to predict or estimate reliability when any of these causal variables appear in an equation and data are available.

Both the data-poor and data-rich models were estimated from data collected over a year from a subset of urban freeway segments in seven cities. The data-poor models apply to all time slices throughout a day, whereas four sets of data-rich models concerning different moments of the TTI distribution (mean, 99th, 95th, 90th, 80th, 50th, and 10th percentiles) were estimated for the peak hour, the peak period, the midday, and weekdays.

The objectives of Project L33, Validation of Urban Freeway Models, were threefold: (1) attempt to validate the "data-poor" and "data-rich" models, (2) develop enhanced models if justified, and (3) promote acceptance and use of the L03 type of models for planning, programming, project development, design, systems operations, and further research.

[1] Cambridge Systematics, Texas Transportation Institute, University of Washington, and Dowling Associates. 2006. *NCHRP Web-Only Document 97: Guide to Effective Freeway Performance Measurement: Final Report and Guidebook*. Transportation Research Board of the National Academies, Washington, D.C.

In conducting the validation, the research team was prohibited from using data that were used to estimate the data-poor and data-rich models. Validation data came from California, Minnesota, Utah (Salt Lake City), and Washington (Spokane) and totaled 323 segment-years covering both midday and peak periods. L03 models used data from some of these same places, but the same data were not used in the validation, as required.

The project used two criteria for assessing the validity of the L03 models. The first was the difference between the predicted and measured values of the dependent variable. The second was whether the estimated models satisfied the assumptions of linear regression.

This report describes the degree to which the different models perform well in terms of prediction and satisfying regression assumptions. The data-poor models predicted acceptably well as documented here but had some shortcomings in terms of satisfying the regression assumptions. Three sets of enhanced models were developed. The research team could not find satisfactory enhancements to the data-rich models. The degree to which the data-rich models predict well and satisfy the assumptions of linear regression is also described in the report.

CONTENTS

Executive Summary

Overview

The goal of the SHRP 2 L33 Validation of Urban Freeways project is to assess and enhance the predictive travel time reliability models developed in the SHRP 2 L03 project, Analytical Procedures for Determining the Impacts of Reliability Mitigation Strategies. SHRP 2 L03, which concluded in 2010, developed two categories of reliability models to be used for the estimation or prediction of travel time reliability within planning, programming, and systems management contexts: data-rich and data-poor models.

The L33 project was tasked with (1) validating the data-rich and data-poor equations with new data sets; (2) assessing the validation outcomes to recommend potential enhancements; (3) exploring enhancements and developing a final set of predictive equations; (4) validating the enhanced models; and (5) developing a clear set of application guidelines for practitioners to use with the project outputs.

The work outputs of this project include a set of recalibrated data-poor models, a set of enhanced data-rich models, and revised application guidelines for using the models.

Models

Data-poor, the first category of L03 models, predicts a select set of travel time reliability measures for urban freeway sections based only on the mean travel time for the section. This category of models was intended for use in locations with low availability of traffic and related types of data. The second category—data-rich models—predicts a similar set of travel time reliability measures based on the following input measures related to the causes of congestion and unreliability: (1) the lane-hours lost caused by incidents; (2) the hours of precipitation exceeding 1/20th of an inch; (3) the average demand-to-capacity ratio; and/or (4) the 99th-percentile demand-to-capacity ratio. In cases where one or more of these pieces of data are not available, the L03 project provides heuristic approaches to estimate them from commonly available data. Both models predict reliability over the course of the year. The data-poor models can be fit to any defined time period. The data-rich models estimate or predict travel time reliability within four defined time periods: peak hour, peak period, midday, and weekday.

The L03 models were calibrated using data collected in metropolitan areas from around the country. They were validated using data collected in the Seattle, Washington, region.

Method

Both the validation and the enhancement tasks rely on the collection of traffic, incident, weather, and capacity data sets collected from a diverse set of metropolitan areas, with care taken to avoid using the same data collected in the L03 project. The L33 project collected the data sets needed

for the data-rich and data-poor models in the Los Angeles, California; Minneapolis–Saint Paul, Minnesota; Sacramento, California; Salt Lake City, Utah; San Diego and San Francisco, California; and Spokane, Washington, metropolitan regions.

The validation was performed by processing the collected data in accordance with L03-established methodologies and using it to compare the predicted reliability metrics with the measured ones. The validation assessed both the error of each predictive equation and whether the results met the generalized assumptions of regression modeling.

The enhancement was performed in two ways: (1) recalibration of all of the L03 models using data collected in the California regions and the Minneapolis region; and (2) testing new model forms with the L33 data sets. Performance of the recalibrated and new models was measured in the same way as the validation: assessing the error of each predictive equation and whether the results met the generalized assumptions of regression modeling.

The data-poor enhancement process tested the performance of three new model forms to predict the 95th-, 90th-, and 80th-percentile Travel Time Indices (TTIs): (1) a single parameter power form model; (2) a two-parameter power form model; and (3) a two-parameter polynomial model.

Validation Findings

The validation for the data-poor models yielded the following findings:

1. The errors for most of the models across the study regions were acceptable.
2. The models violated the assumptions of regression, particularly in that the residuals did not average to zero.

From these results, it was concluded that the best way to proceed with the data-poor work was to compare the results of recalibrating the existing equations using the new data sets with the results of the performance of new model forms.

The validation for the data-rich models revealed the following key insights:

1. The performance of the models varied regionally, with the highest errors measured in the California regions. Additionally, the models tended to systematically overpredict reliability in some regions and underpredict it in others.
2. The performance of the models varied by time period, with the highest errors measured during the peak period.
3. The error was highest for the equations that predict higher moments of the travel time distribution (such as the 95th- and 99th-percentile TTIs).
4. The models systematically violated a number of the assumptions of regression, leading the team to conclude that they may be missing one or more important variables for predicting reliability.

In addition to these validation findings, the team noted that a number of the study segments, particularly those in Salt Lake City and Spokane, did not meet the L03 requirements for having a peak hour and a peak period. This suggested the need for a revision of these definitions, to ensure that all segments can get estimation results for these important time periods.

From the data-rich validation results, the team concluded that the models would best be improved by enhancement, specifically through seeking additional variables to include in the equations and exploring modifications to the model functional form.

Enhancement Findings

Enhancement was explored for the data-rich models, but no suitable enhancements resulting in performance improvements were found.

The data-poor enhancement process yielded the following findings:

1. In general, the recalibrated L03 models yielded reasonable error values (measured by the mean square error), but still violated the assumptions of generalized regression.
2. The new models yielded similar or improved error values compared with the recalibrated L03 models and better satisfied the assumptions of regression.

Overall, the L33 research team recommends that the SHRP 2 program adopt the new data-poor models. They allow for a consistent model form between all of the predictive equations and better capture the intuitive increasing rate of change between the mean TTI and the percentile TTI as the mean TTI increases.

CHAPTER 1

Background

Context

One of key objectives of the SHRP 2 Reliability program research is to develop methods for researchers and practitioners to evaluate the causal factors of travel time unreliability. The Federal Highway Administration (FHWA) defined three types of sources that contribute to congestion and travel time variability: (1) traffic-influencing events, like incidents, work zones, and weather; (2) traffic demand, either through day-to-day variability or special events; and (3) physical highway features, like traffic control devices (such as ramp meters) and physical bottlenecks (*1*). Various projects within the SHRP 2 Reliability program have investigated various pieces of how to understand the relationship between these sources and travel time variability. These efforts include how the source data can be measured and processed (SHRP 2 L02), how simulation models can incorporate nonrecurrent congestion sources to generate travel time distributions (SHRP 2 L04), how nonrecurrent congestion impacts on travel time reliability can be incorporated into the *Highway Capacity Manual* (SHRP 2 L08), and how the reliability improvements of various interventions can be predicted (SHRP 2 L03).

The SHRP 2 L03 project collected traffic, incident, and weather data on urban freeway sections from around the United States and used it to develop cross-sectional statistical models to predict various moments of the travel time distribution based on the explanatory variables. To accommodate the needs of model users with varying quantities of data available to them, the L03 team developed two types of models:

- Data-poor models, in which travel time reliability is a function of the mean travel time; and
- Data-rich models, in which travel time reliability is a function of some combination of incident lane hours lost, hours of rainfall, and the demand-to-capacity ratio.

These L03 models were calibrated in sites around the country and validated using data collected in the Seattle metropolitan area. The models were also adapted and implemented in the SHRP 2 L07 project within a spreadsheet tool to evaluate the cost-effectiveness of highway design features.

The SHRP 2 L33 project, Validation of Urban Freeway Models, had three specific goals: (1) perform further validation of the data-rich and data-poor predictive urban freeway travel time reliability models developed in the SHRP 2 L03 project; (2) enhance the models to improve their prediction of the reliability impacts of various reliability improvement strategies; and (3) validate the enhanced models to promote their acceptance and use among researchers and practitioners.

In conducting research on travel time reliability, it should be noted that, while it is relatively straightforward to calculate reliability using measured data, it is a challenging task to predict reliability at the individual route level using a model. This is because people make route choice decisions dynamically in the real world, especially with the recent trends of traffic and incident information made available in real time to the traveling public.

L03 Review

This section summarizes the L03 predictive model work to provide a framing for the work done in L33. More information on L03 can be found in this report in Appendix A.

Modeling Approach

For the predictive models, the L03 project team collected traffic, incident, work zone, and weather data in eight metropolitan areas: Houston, Texas; Minneapolis, Minnesota; Los Angeles, San Francisco, and San Diego, California; Atlanta, Georgia; Jacksonville, Florida; and Seattle, Washington. Data were

collected on a total of 81 urban freeway study sections, which shared the following characteristics:

- Relatively homogeneous in terms of traffic and geometric conditions
- Represent portions of trips taken by travelers
- No midsection freeway-to-freeway interchanges

From this data set, the L03 team calculated a number of explanatory variables to test for inclusion in the models. Illustrative examples of these variables, as well as the reliability metrics computed as potential dependent variables, are shown in Table 1.1. It is important to note that the reliability metrics shown in this table and used in the modeling are calculated as the volume-weighted average of all of the 5-min-level Travel Time Indices in the given time period over a year. This is a critical piece of the analysis chain, as it means that the ultimate travel time distributions and results are weighted toward the time periods that are the most heavily traveled. This is in contrast to a facility-level perspective, which treats each measurement equally regardless of how many vehicles experienced it.

Following initial investigation of the relationships between the assembled variables and the calculated reliability metrics, the L03 team proposed two model forms:

1. "A detailed deterministic model that uses all of the data being collected to a maximum degree (data-rich model)"
2. "A simpler model based on the fact that many of the applications [*Highway Capacity Manual* (HCM) and travel demand forecasting models] work in an environment with limited data (data-poor model)"

Each of these models is described in further detail below.

Data-Rich Models

The data-rich models were calibrated to predict reliability measures within four different time periods:

- Peak hour: 60-min period during which the space mean speed is less than 45 mph

Table 1.1. L03 Modeling Analysis Data Set

Category	Sample Measures
Dependent Variables	
Reliability Metrics	• Mean, standard deviation, median, mode, minimum, and percentile travel times and TTIs • Buffer indices, planning time index, skew statistics, and misery index • On-time percentages
Independent Variables	
Area Operations Characteristics	• Number of service patrol trucks • Service patrol trucks per mile • Quick Clearance Law? • Number of ramp meters, dynamic message signs, and closed circuit television (CCTV) cameras
Service Patrols	• Number of service patrol trucks covering section • Percentage of time periods when trucks are active
Capacity and Volume Characteristics	• Start and end times of peak hour and peak period • Calculated and imputed vehicle miles traveled • Average of demand-to-capacity ratio on all section links • Highest demand-to-capacity ratio of all links on the section
Incident Characteristics	• Number of incidents • Incident rate per 100 million vehicle miles • Incident lane-hours lost • Incident shoulder hours lost • Mean, standard deviation, and 95th percentile of incident duration
Event Characteristics	• Number of work zones • Work zone lane-hours lost • Work zone shoulder hours lost • Mean, standard deviation, and 95th percentile of work zone duration
Weather Characteristics	• Number of hours with precipitation amounts exceeding various thresholds • Number of hours with measurable snow • Number of hours with frozen precipitation • Number of hours with fog

Table 1.2. L03 Data-Rich Explanatory Variables and RMSE by Model

Period		10th	Mean	50th	80th	95th	99th
Peak Hour	Variable	dc_{crit}, ILHL, RainHrs	dc_{crit}, ILHL	dc_{crit}, ILHL	dc_{crit}, ILHL	dc_{crit}, ILHL, RainHrs	dc_{crit}, ILHL
	RMSE	10–20%	20–30%	20–30%	30–40%	30–40%	>40%
Peak Period	Variable	dc_{crit}, ILHL, RainHrs	dc_{crit}, ILHL	dc_{crit}, ILHL	dc_{crit}, ILHL, RainHrs	dc_{crit}, ILHL, RainHrs	dc_{crit}, ILHL, RainHrs
	RMSE	<10%	10–20%	20–30%	20–30%	30–40%	30–40%
Midday	Variable	dc_{crit}	dc_{crit}	dc_{crit}	dc_{crit}	dc_{crit}	dc_{crit}
	RMSE	<10%	<10%	20–30%	<10%	20–30%	30–40%
Weekday	Variable	$dc_{average}$	$dc_{average}$, ILHL	$dc_{average}$	$dc_{average}$, ILHL	$dc_{average}$, ILHL	$dc_{average}$, ILHL
	RMSE	<10%	20–30%	<10%	10–20%	30–40%	>40%

- Peak period: period of at least 75 min during which is the space mean speed is less than 45 mph
- Midday: 11:00 a.m.–2:00 p.m., Monday–Friday
- Weekday: All day, Monday–Friday

The team selected a natural logarithmic form for the regression model, because it is able to predict a TTI of 1 when the independent variables are 0. Root mean square error (RMSE) was used as the goodness-of-fit measure to compare between models with different combinations of independent variables. Variables were allowed to stay in the model equation with an alpha level of 0.1.

After evaluating the potential independent variables, the L03 team ultimately selected the following to predict reliability within the defined time periods:

- Incident lane-hours lost (ILHL)
- Hours of precipitation exceeding 0.05 in. (RainHrs)
- Critical demand-to-capacity ratio (dc_{crit})
- Average demand-to-capacity ratio ($dc_{average}$)

Note that demand cannot be directly measured, and methods to calculate this and other independent variables are given in detail in Appendix C.

Table 1.2 shows the explanatory variables that were used to predict different moments of the travel time index distribution (column names) within the defined time periods (row names). Below the explanatory variables, it also displays the RMSE for each model measured during the calibration process.

Data-Poor Models

The data-poor model was first envisioned to take advantage of commonly available independent variables (such as annual collisions per million, vehicle miles traveled, speed limit, and yearly demand profiles). However, exploratory analysis showed promising relationships between the mean travel time and all selected reliability metrics. Because the mean travel time is a ready output from planning and operational tools such as travel demand and simulation models, this relationship became the focus of the data-poor model development.

Unlike the data-rich models, the data-poor models were not calibrated for specific time periods. The original set of data-poor equations developed in L03 and presented in the L03 final report use an exponential form to relate the mean TTI with measures of reliability. The data-poor models were developed to predict some reliability metrics not directly pulled from the travel time distribution. The definitions for these are

- PctTripsOnTimeX: The percentage of on-time trips made with respect to *X* times the median TTI
- PctTripsOnTimeXmph: The percentage of on-time trips made with respect to a speed threshold of *X* mph

The functional form and calibration RMSEs for these models are shown in Tables 1.3 and 1.4. These original data-poor models were revised with new model forms or updated with new coefficients following the finalization of the L03 final report and were included in an appendix to the final report. No calibration errors were presented for these revised equations. The new functional forms are shown in Tables 1.3 and 1.4. The revised models for the TTI moment predictions were validated and explored for enhancement in the L33 project.

Validation

The L03 final report shows validation results for a select set of the data-rich and original data-poor models using data

Table 1.3. Data-Poor Functional Form and RMSE by Model, Part 1

		10th	Median	80th	90th	95th
Original Models	Form	exponential	exponential	exponential	exponential	exponential
	RMSE	<10%	<10%	<10%	<10%	10–20%
Revised Models	Form	natural log	natural log	natural log	natural log	natural log
	RMSE	na	na	na	na	na

Note: No calibration errors were presented for the L03 revised data-poor models; na = not applicable.

Table 1.4. Data-Poor Functional Form and RMSE by Model, Part 2

		PctTrips OnTime10mph	PctTrips OnTime25mph	PctTrips OnTime50mph	PctTrips OnTime45mph	PctTrips OnTime30mph
Original Models	Form	exponential	exponential	exponential	exponential	exponential
	RMSE	<10%	<10%	10–20%	10–20%	<10%
Revised Models	Form	NA	NA	exponential	exponential	sigmoidal
	RMSE	na	na	na	na	na

Note: No calibration errors were presented for the L03 revised data-poor models; NA = not available; na = not applicable.

collected on 26 freeway segments in the Seattle metropolitan area. Table 1.5 shows the validation error (the percentage difference between the measured and the predicted values) for each roadway section for each validated model. Positive errors indicate that the model overpredicted the TTI (thus predicting that the segment is less reliable than it actually is) and negative errors indicate that the model underpredicted the TTI (thus predicting that the segment is more reliable than it actually is).

The L03 team noted that the models tend to underpredict the weekday TTIs in the Seattle region and speculated that it may be due to the lack of a rain variable in the weekday models, which raises errors in regions like Seattle that experience a lot of rainfall. The data-poor model exhibits the same underprediction trend, particularly with the 95th-percentile equation. The L03 project team recommended further validation of the models to address these high errors.

Research Questions

To evaluate and enhance the L03 predictive models described above, the L33 project was guided by the following research questions:

- What are the right explanatory variables to use to predict travel time reliability?
- Is it possible to have single models that can be applied in all regions?
- What are the most useful measures for the predictive models to output?
- What is the right functional form for the reliability models?

Final Report Structure

Following this background chapter, the remainder of this final report is structured as follows:

- *Chapter 2: Data* describes the data sets used in the L03 model validation and L33 model enhancement and validation stages of this project
- *Chapter 3: Existing Model Validation* presents the validation results for the L03 data-rich and data-poor models
- *Chapter 4: Enhanced Models and Application Guidelines* presents the recalibration and new model results for the data-rich and data-poor models and discusses recommendations for applying the models

This report also contains the following five appendices, each of which contains one of the work products of the L33 project.

- *Appendix A: Review of L03 and Related Models* is a technical memorandum discussing the work performed in the SHRP 2 L03 project and other SHRP 2 Reliability projects that developed predictive models.

Table 1.5. L03 Validation Errors

Roadway Section	Peak Period			Weekday			Data-Poor	
	Mean	80th	95th	Mean	80th	95th	80th	95th
I-405 Bellevue northbound	+30 to 40%	Over +40%	Over +40%	Under +10%	+10 to 20%	+10 to 20%	Under +10%	+20 to 30%
I-405 Eastgate northbound	+10 to 20%	+10 to 20%	+30 to 40%	NA	Under +10%	Under +10%	Under +10%	+30 to 40%
I-405 Eastgate southbound	–10 to 20%	–10 to 20%	Under –10%	–10 to 20%	–10 to 20%	–10 to 20%	Under +10%	–20 to 30%
I-405 Kennydale southbound	–10 to 20%	–10 to 20%	–10 to 20%	–10 to 20%	–30 to 40%	–30 to 40%	Under –10%	–20 to 30%
I-405 Kirkland northbound	Under +10%	Under +10%	+20 to 30%	Under +10%	Under +10%	+20 to 30%	+10 to 20%	+30 to 40%
I-405 Kirkland southbound	Under –10%	Under +10%	+10 to 20%	Under –10%	Under +10%	+20 to 30%	Under +10%	+30 to 40%
I-405 North northbound	Under +10%	Under +10%	+20 to 30%	Under +10%	Under +10%	+10 to 20%	Under +10%	+20 to 30%
I-405 North southbound	–30 to 40%	Over –40%	Over –40%	Under +10%	–10 to 20%	–20 to 30%	–10 to 20%	Over –40%
I-405 South northbound	–30 to 40%	–30 to 40%	–20 to 30%	–20 to 30%	Over –40%	Over –40%	–10 to 20%	–20 to 30%
I-405 South southbound	Under +10%	Under +10%	+10 to 20%	+10 to 20%	+20 to 30%	+10 to 20%	Under +10%	+10 to 20%
I-5 Everett northbound	Under +10%	Under –10%	–10 to 20%	Under +10%	Under +10%	–30 to 40%	+20 to 30%	Over –40%
I-5 Everett southbound	+20 to 30%	+20 to 30%	+30 to 40%	Under +10%	+10 to 20%	+20 to 30%	Under +10%	Under +10%
I-5 Lynnwood northbound	+10 to 20%	+20 to 30%	Under –10%	Under +10%	Under +10%	–10 to 20%	Under +10%	+20 to 30%
I-5 Lynnwood southbound	Under –10%	Under –10%	–10 to 20%	Under –10%	Under +10%	–20 to 30%	+10 to 20%	–30 to 40%
I-5 South northbound	+10 to 20%	+20 to 30%	+30 to 40%	Under +10%	+10 to 20%	Under +10%	+10 to 20%	+30 to 40%
I-5 South southbound	+10 to 20%	Under +10%	+20 to 30%	Under +10%	Under +10%	+20 to 30%	+10 to 20%	+30 to 40%
I-5 Tukwila northbound	+20 to 30%	+10 to 20%	+10 to 20%	Under +10%	Under +10%	Under +10%	Under +10%	+20 to 30%
I-5 Tukwila southbound	Over +40%	Over +40%	Over +40%	Under +10%	Under +10%	+20 to 30%	Under +10%	Under +10%
I-90 Bellevue westbound	+20 to 30%	+30 to 40%	+30 to 40%	Under +10%	Under +10%	+10 to 20%	+10 to 20%	+20 to 30%
I-90 Bridge eastbound	+10 to 20%	Under +10%	Under +10%	Under +10%	Under +10%	+20 to 30%	Under +10%	+30 to 40%
I-90 Bridge westbound	Under –10%	–10 to 20%	–10 to 20%	Under –10%	Under +10%	–10 to 20%	+10 to 20%	–10 to 20%
I-90 Issaquah westbound	+10 to 20%	+10 to 20%	+10 to 20%	Under +10%	Under +10%	+10 to 20%	Under +10%	+20 to 30%
SR 167 Auburn northbound	Under –10%	Under –10%	Under +10%	Under –10%	–10 to 20%	+20 to 30%	Under –10%	–20 to 30%
SR 167 Auburn southbound	–10 to 20%	–20 to 30%	–20 to 30%	Under –10%	–10 to 20%	–30 to 40%	Under +10%	–20 to 30%
SR 167 Renton northbound	Under +10%	+20 to 30%	–10 to 20%	Under +10%	+10 to 20%	–20 to 30%	Under +10%	+20 to 30%
SR 167 Renton southbound	Under +10%	Under +10%	–10 to 20%	Under +10%	Under +10%	–10 to 20%	Under +10%	+20 to 30%

Note: NA = not available.

- *Appendix B: Validation Plan* is a technical report outlining the data collection and analysis strategy for validating the L03 data-rich and data-poor models.
- *Appendix C: Data-Rich Validation* is a technical memorandum containing detailed validation results for the data-rich models.
- *Appendix D: Data-Poor Validation* is a technical memorandum containing detailed validation results for the data-poor models.
- *Appendix E: Model Enhancements* is a technical memorandum showing the results of the data-poor model recalibration and enhancement.

Reference

1. Federal Highway Administration, U.S. Department of Transportation. *Traffic Congestion and Reliability: Trends and Advanced Strategies for Congestion Mitigation.* http://www.ops.fhwa.dot.gov/congestion_report/chapter2.htm. Accessed on January 9, 2014.

CHAPTER 2

Data

Sites

The L33 team calibrated and validated its models using urban freeway data collected in the following metropolitan areas:

- San Diego;
- San Francisco;
- Sacramento, California;
- Los Angeles;
- Minneapolis–Saint Paul, Minnesota;
- Spokane, Washington; and
- Salt Lake City, Utah.

Details about the study segments and data sets are provided in the L33 validation plan included in Appendix B. The San Diego, San Francisco Bay Area, Sacramento, and Los Angeles metropolitan regions (grouped together into a California data set), Salt Lake City, and Spokane data were collected from the 3-year period between January 1, 2010, and December 31, 2012. The Minnesota data were collected from the 3-year period between June 1, 2009, and May 31, 2012.

The L33 team selected these sites in part because their agencies collect and archive continuous, high quality traffic data. These characteristics are also critical for L33 validation and enhancement activities. As such, this project used data collected in many of the same locations as L03. The L33 project team ensured that the model validation performed in L33 does not use the same data collected during the same time frame on the same freeways segments as was used to calibrate or validate the models in L03. Because this is a critical requirement, the L33 team conducted a thorough review of the data set.

The roadway sections that were studied within each of these regions were selected in accordance with the application guidelines of the L03 data-rich and data-poor models through the following criteria:

- Length of around 5 mi (range from 2 to 10 mi)
- Good data quality over a year
- Monitored by point detectors with no more than an average spacing of ¾ mi, or monitored by automated vehicle identification (AVI) technologies at the section origin and destination
- No midsection freeway-to-freeway interchanges or bottlenecks
- Relative homogeneity in terms of traffic and geometric conditions

Processing

This section briefly describes the data processing that was performed to generate the dependent and independent variables for the validation of the data-rich and data-poor models. Further detail on these steps is provided in the L33 validation plan included in Appendix B.

Traffic Data

For the validation, traffic data is needed to calculate (1) the dependent TTI reliability measures; (2) the mean TTI independent variable for the data-poor models; (3) the demand-to-capacity ratios used as independent variables for some of the data-rich models; and (4) the peak hour and peak period time slice definitions.

Raw traffic data were extracted from the Performance Measurement System (PeMS) deployment databases for each study location. The raw data consisted of 5-min traffic flow, occupancy, and speed for each detector station along a roadway section. The following steps were taken to turn the raw data points into section-level TTI reliability statistics over a year:

1. Calculate 5-min vehicle miles traveled (VMT) and vehicle hours traveled (VHT) at each detector station (link) using the link's volume, speed, and length (the distance halfway to the nearest neighboring stations in the upstream and downstream directions)

2. Aggregate the link-level data to section-level 5-min VMT, VHT, space mean speed, TTI, and travel time
3. Exclude 5-min data points collected when fewer than 50% of the section's detectors were not working
4. Group the 5-min section-level data into the peak hour, peak period, midday, and weekday time slices over an entire year, and calculate for each section-year-time slice combination the
   - Mean TTI
   - Percentile TTIs (10th, 50th, 80th, 95th, and 99th)
   - On-time statistics [percentage of trips (VMT) made within 1.1*x* the median travel time and within 1.25*x* the median travel time]
   - Failure statistics [percentage of trips (VMT)] with speeds less than 50 mph, 45 mph, and 30 mph

The peak hour and peak period time slices used in Step 4 were calculated from the outputs of Step 3 as follows:

- *Peak Hour*: Identify the 60-min period on non-holiday weekdays with the lowest average speed. Each consecutive section speed must be less than or equal to 45 mph.
- *Peak Period*: Identify non-holiday, weekday time periods of at least 75 min during which the average section speeds are less than or equal to 45 mph.

Demand-to-Capacity Ratios

The following two forms of the demand-to-capacity (D/C) ratio were used as independent variables in the data-rich models:

- *Critical demand-to-capacity ratio*: The critical demand of a section is calculated as the highest 99th-percentile demand measured on a link on the segment during the given time period (peak hour or peak period) over a year.
- *Average demand-to-capacity ratio*: The average demand is calculated as the average demand measured on all links on the segment during the given time period (peak hour or peak period) over a year.

The capacity used in both ratios is the hourly capacity according to National Cooperative Highway Research Program (NCHRP 387) methodologies. The demand is summed up over all 5-min periods in the time slice over a single day. Since only volume, not demand, can be directly measured by loop detectors, demand was computed using the methodology developed in L03 and summarized in Appendix B.

To give an example of this process, for a single day, the D/C ratio during the midday period is equal to the sum of all of the 5-min demands over the 3-hour midday period divided by the hourly capacity. The 99th-percentile D/C ratio over the year is the 99th-percentile D/C ratio over all midday periods in the year. The average D/C ratio over the year is the mean of all the midday D/C ratios over the year.

Incident Lane-Hours Lost

The number of incident lane-hours lost on a roadway section over the year is an independent variable in some of the data-rich models. Estimating this number for a roadway section requires two key pieces of information from each incident: (1) the number of lanes it blocked and (2) its duration. In datasets for which one or both of these variables were unavailable, they were estimated from the L03 final report equations based on the agency incident clearance policies and the presence of shoulders.

Hours of Precipitation Exceeding 0.05 in.

The number of hours of precipitation exceeding 0.05 in. on a roadway section over a year is an independent variable in some of the data-rich models. Hourly weather data from the National Weather Service (NWS) was used to compute the number of hours that had precipitation exceeding defined thresholds (ultimately, the number of hours where rainfall exceeded 0.05 in. was included in the data-rich model).

Characteristics

Data-Rich Independent Variables

This section describes and evaluates the independence of the data-rich independent variables that were input into each model in order to predict travel time reliability.

Peak Hour

The distributions of the critical demand-to-capacity ratio, incident lane-hours lost, and hours of rainfall exceeding 0.05 in., as well as some basic summary statistics for these variables, are shown in Figure 2.1. There is a fairly wide distribution of all of these variables, though no notable outliers.

Table 2.1 shows the correlation coefficients between the independent variables, and Figure 2.2 shows scatterplots illustrating these relationships. The critical demand-to-capacity ratio and the number of incident lane-hours lost exhibit the strongest, though still weak, linear relationship.

Peak Period

The distributions of the critical demand-to-capacity ratio, incident lane-hours lost, and hours of rainfall exceeding 0.05 in., as well as some basic summary statistics for these

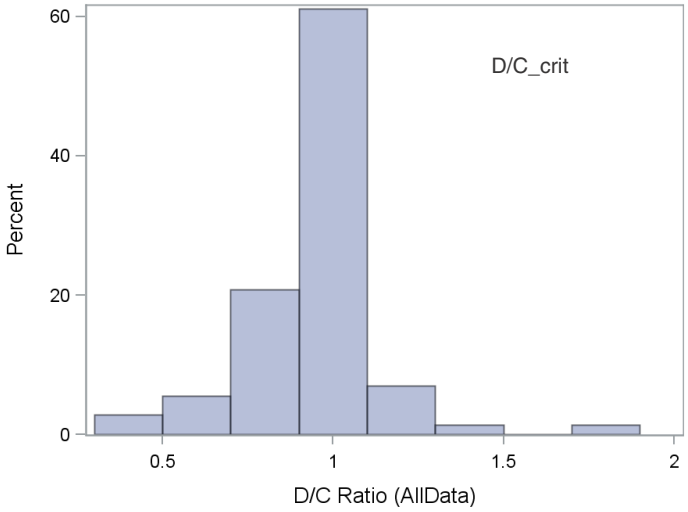

Variable	N	Mean	Std Dev	Minimum	Maximum
D/C	72	0.9564	0.1836	0.4093	1.8256
ILHL	72	11.3744	6.9121	0.0555	28.0741
Rain	72	5.4306	2.8720	0	14.000

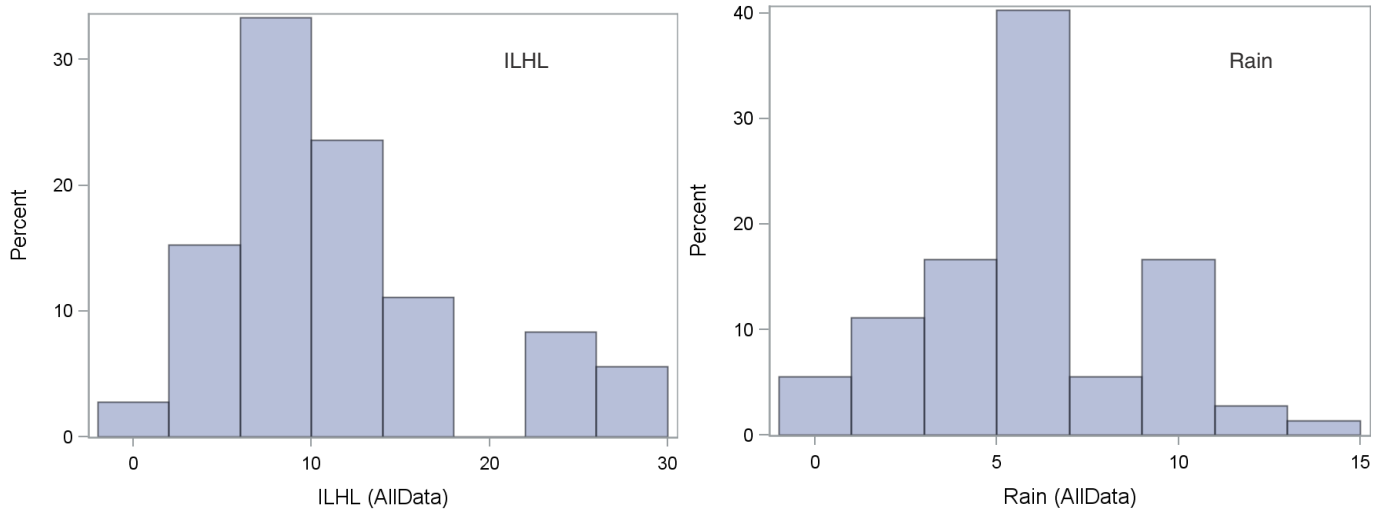

Figure 2.1. Independent variables summary, peak hour.

variables, are shown in Figure 2.3. As with the peak hour, each of the variables exhibits a wide distribution. This makes sense because the duration of the peak period varies from section to section, and as the peak period duration increases, the D/C ratio is certain to increase and the incident and rain terms are likely to increase.

Table 2.1. Correlation Coefficients between Independent Variables, Peak Hour

	D/C_{crit}	ILHL	Rain
D/C_{crit}	1	0.272	–0.14
ILHL	0.272	1	–0.21
Rain	–0.14	–0.21	1

Table 2.2 shows the correlation coefficients between the independent variables, and Figure 2.4 shows scatterplots illustrating these relationships. The relationships between variables in the peak period are much stronger than they are for the peak hour. The relationship between the critical-demand-to-capacity ratio and the incident lane-hours lost is particularly strong.

Midday

The distribution of the only independent variable in the midday models—the critical demand-to-capacity ratio—is shown in Figure 2.5. Most of the ratios are between 1 and 3.

Weekday

The distributions of the average demand-to-capacity ratio and the incident lane-hours lost, as well as some basic summary

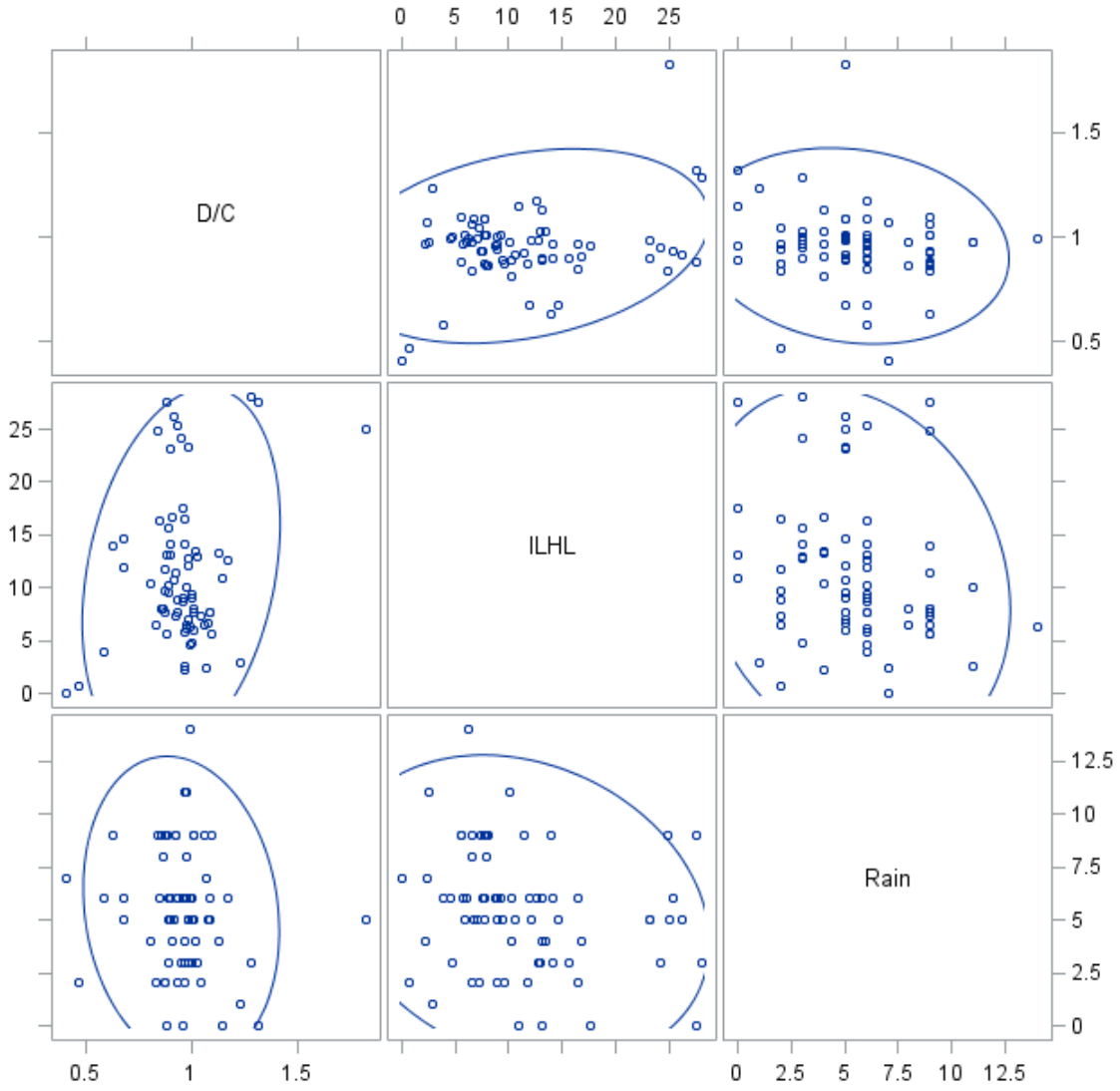

Figure 2.2. Relationships between independent variables, peak hour.

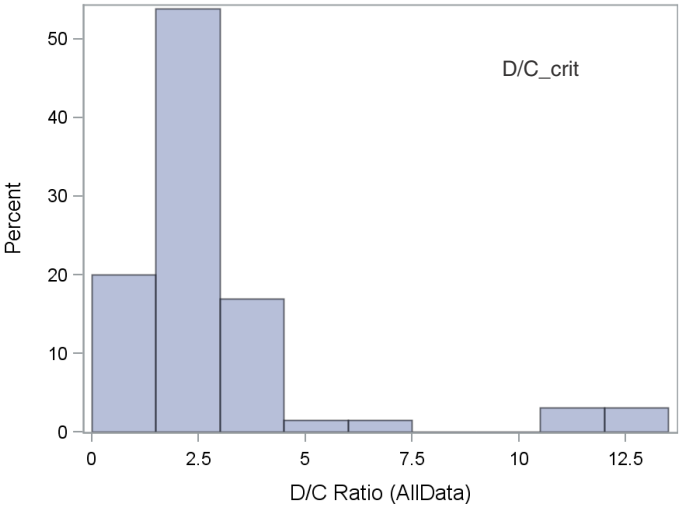

Variable	N	Mean	Std Dev	Minimum	Maximum
D/C	65	2.9666	2.5495	0.6878	12.3355
ILHL	65	36.7953	43.2505	-0.3721	194.3
Rain	65	11.4769	10.5994	0	60.0000

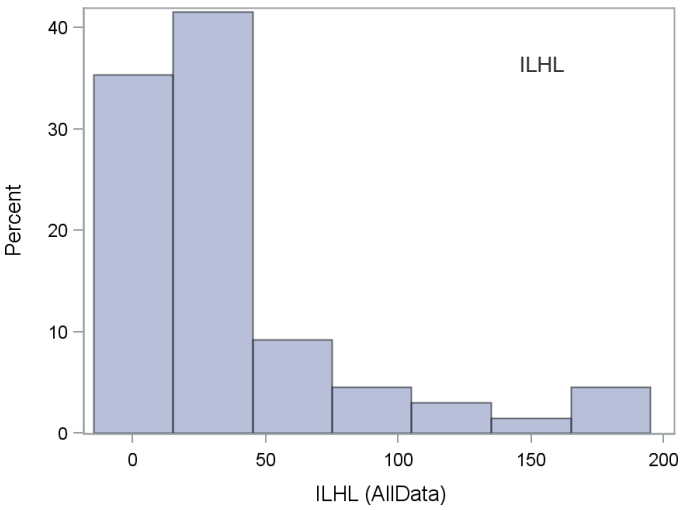

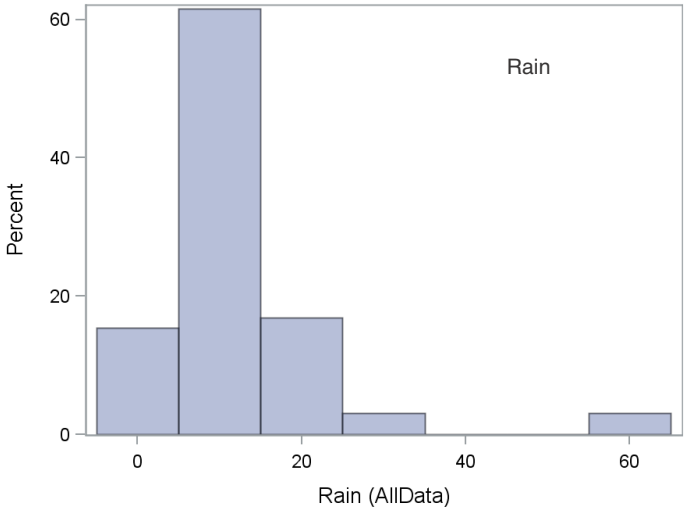

Figure 2.3. Independent variables summary, peak period.

Table 2.2. Correlation Coefficients between Independent Variables, Peak Period

	D/C_{crit}	ILHL	Rain
D/C_{crit}	1	0.917	0.637
ILHL	0.917	1	0.505
Rain	0.637	0.506	1

statistics for these variables, are shown in Figure 2.6. There are some potential outliers noticeable (in the incident lanes-hours lost distribution), which are around three times as high as the next-highest values. These were collected on a few of the Minneapolis roadway sections.

Figure 2.7 shows the scatterplot of the incident lane-hours lost against the average demand-to-capacity ratio. The linear relationship here is weak, with a correlation coefficient of 0.2.

Summary

Table 2.3 contains a summary of the correlation coefficients of the three independent variables for three time periods.

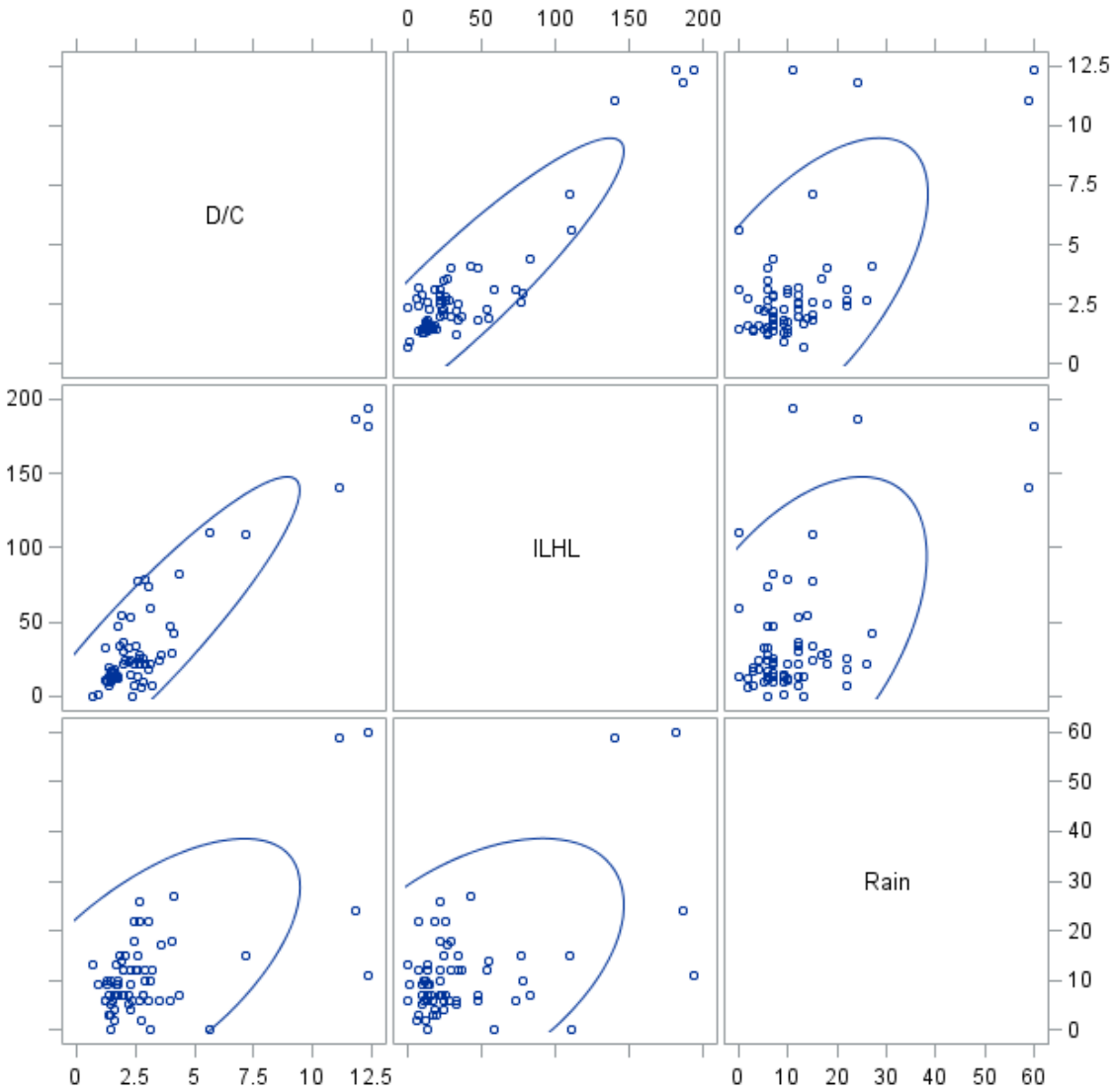

Figure 2.4. Relationships between independent variables, peak hour.

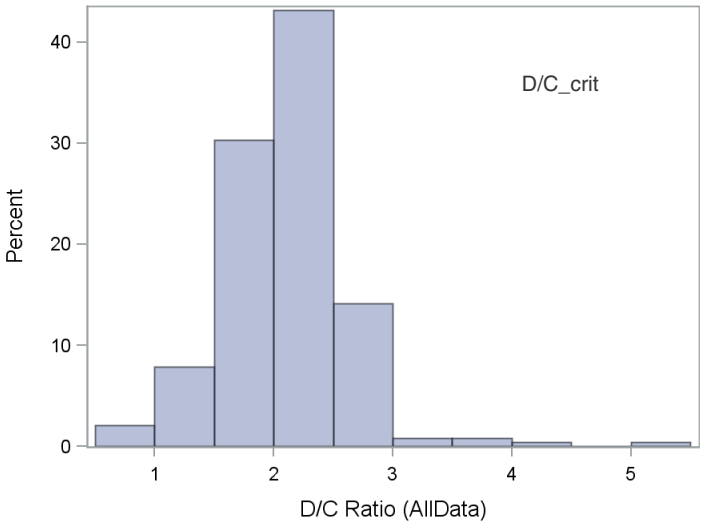

Variable	N	Mean	Std Dev	Minimum	Maximum
D/C	241	2.1211	0.5206	0.7477	5.1288
ILHL	241	12.3178	18.3531	0.3332	170.0
Rain	241	13.7178	7.84029	2.0000	28.0000

Figure 2.5. Independent variable summary, midday.

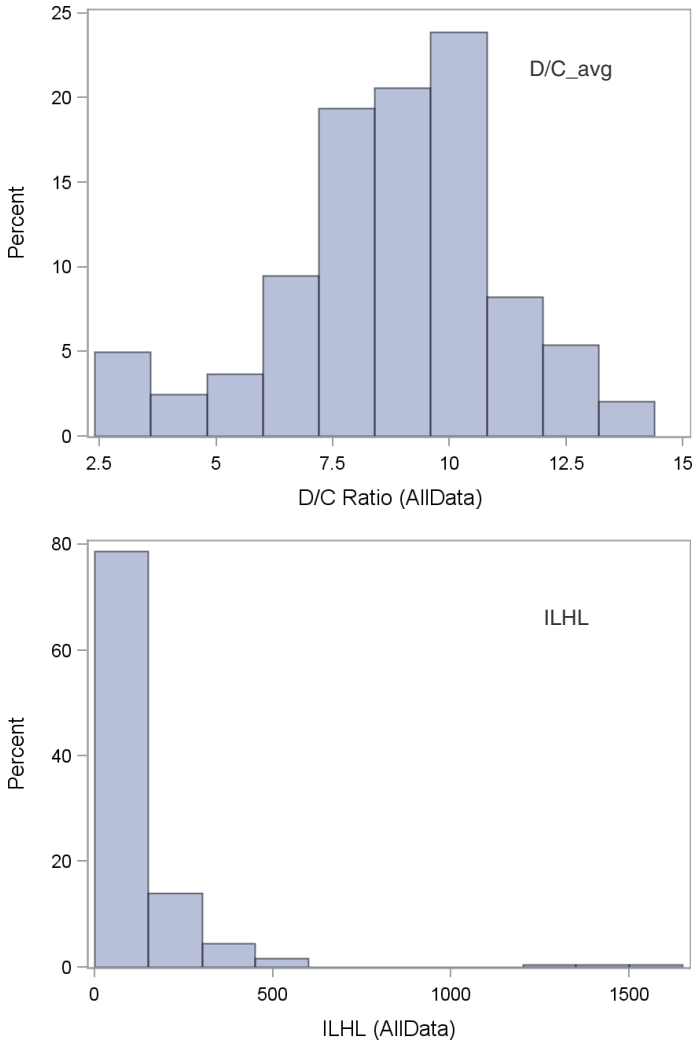

Variable	N	Mean	St Dev	Minimum	Maximum
D/C	243	8.7627	2.3575	2.5527	14.0683
ILHL	243	110.2	179.1	0.0164	1587.4
Rain	243	75.4444	30.7094	3.0000	119.0

Figure 2.6. Independent variables summary, weekday.

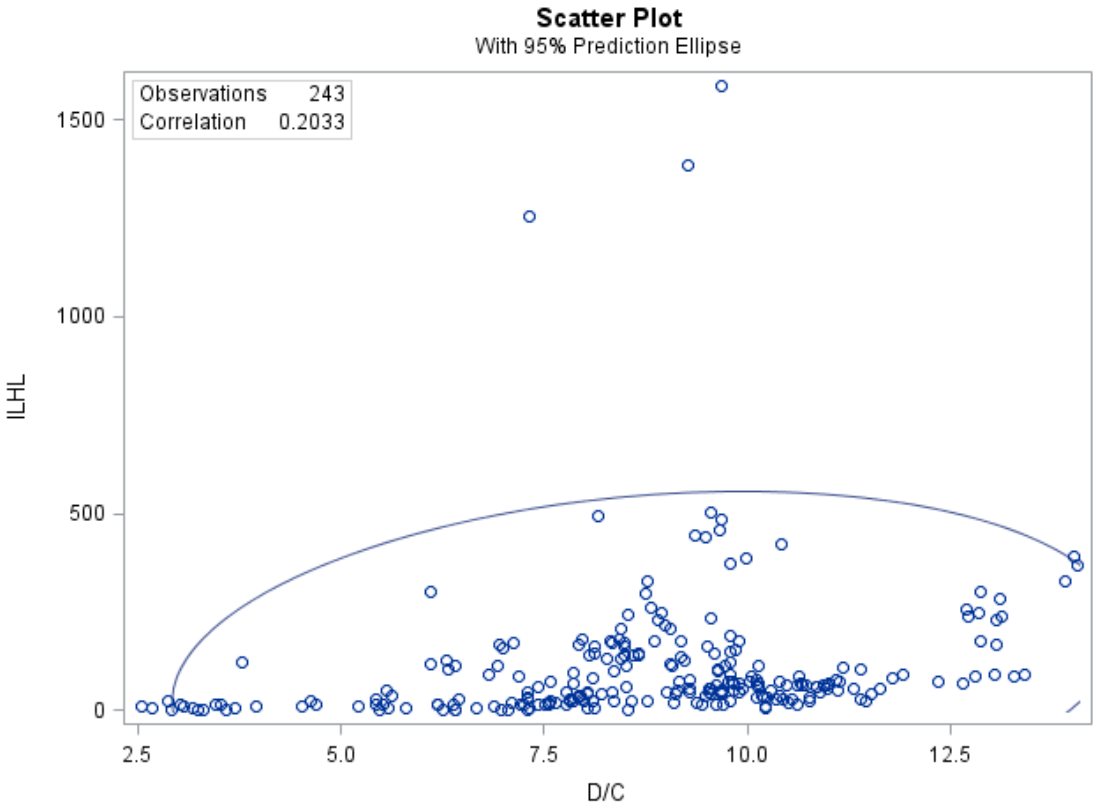

Figure 2.7. Relationship between independent variables, weekday.

Table 2.3. Correlation Coefficients of Independent Variables

		D/C			ILHL			Rain	
		Hour	**Period**	**Weekday**	**Hour**	**Period**	**Weekday**	**Hour**	**Period**
D/C	Hour	1			0.27			–0.14	
	Period		1			0.92			0.64
	Weekday			1			0.20		
ILHL	Hour	0.28			1			–0.21	
	Period		0.92			1			0.51
	Weekday			0.20			1		
Rain	Hour	–0.14			–0.21			1	
	Period		0.64			0.51			1

CHAPTER 3

Existing Model Validation

Overview

Following this overview section, which describes the metrics used to perform the validation, this chapter presents the validation results for the data-rich and the data-poor models. The complete results are included in Appendix C (Data-Rich Validation) and Appendix D (Data-Poor Validation).

The validation was performed by assessing the following two questions:

1. What is the model error?
2. Does the model meet the assumptions of generalized regression?

Model Error

The model error was quantified through the root mean square error (RMSE). The specific calculation of RMSE depends on the model form, so calculation details for the data-rich and data-poor models are contained in Appendix C and Appendix D.

Generalized Regression Model Assumptions

The following checks were performed to evaluate whether each model satisfied the assumptions of generalized regression:

Assessing whether each model adhered to a generalized regression model was performed quantitatively and qualitatively using (1) residual plots, to find any non-random patterns; (2) Student's *t*-test, to evaluate whether the means of the residuals are statistically different from zero; (3) histograms, to visually assess whether residuals are normally distributed; and (4) the Shapiro-Wilk test, to statistically assess whether residuals are normally distributed. Each of these tools is described below.

Residual Plots

To satisfy regression assumptions, the plot of residuals versus the predicted values must show that (1) the variance of the residuals is constant across all predicted values (homoscedastic) and (2) the mean of the residuals is constant across all predicted values (unbiased). This principal is illustrated in Figure 3.1 (*1*), which compares the ideal residual plot [unbiased and homoscedastic, in plot (a)] to other patterns. This comparison indicates that the assumptions of regression are not being met.

Student's t-Test

The one sample Student's *t*-test can be used to determine if the mean of the residuals is significantly different from zero in a statistical sense, which tests for systematic bias. With an unbiased model, the difference should be statistically insignificant. The *t*-value is calculated as

$$t = \frac{\bar{r} - \mu_0}{s/\sqrt{n}}$$

where $\bar{r}$ is the residual mean, s is the standard deviation of residuals, n is the sample size, and μ_0 is the specific mean value for comparison, set here to be zero. To draw a conclusion, if the calculated t value is larger than some threshold t_α (e.g., $\alpha = 5\%$) using a two-tailed t distribution table, the null hypothesis that the residuals have a mean of zero can be rejected with $(1 - \alpha)$ level of confidence. Or we say that the residual mean is significantly different from zero at α level of probability. If the corresponding p value is used to draw a conclusion, it means that if the null hypothesis were correct, then we would expect to obtain such a large t value on at most p percentage of occasions. The data-poor validation used a confidence level of 95%, and the data-rich validation used a confidence level of 90%.

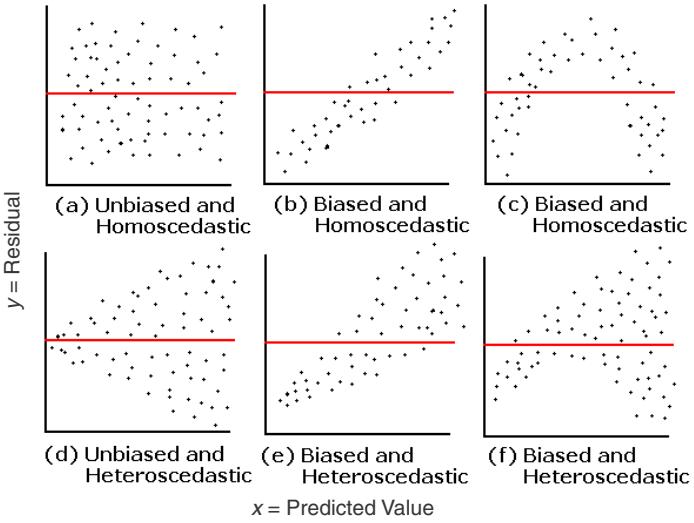

(a) Unbiased and homoscedastic. The residuals average to zero in each thin vertical strip and the standard deviation is the same all across the plot.

(b) Biased and homoscedastic. The residuals show a linear pattern, probably due to a lurking variable not included in the experiment.

(c) Biased and homoscedastic. The residuals show a quadratic pattern, possibly because of a nonlinear relationship. Sometimes a variable transform will eliminate the bias.

(d) Unbiased and heteroscedastic. The standard deviation is small to the left of the plot and large to the right: the residuals are heteroscedastic.

(e) Biased and heteroscedastic. The pattern is linear.

(f) Biased and heteroscedastic. The pattern is quadratic.

Figure 3.1. Residual plot examples.

Shapiro-Wilk Normality Test

The Shapiro-Wilk test was used in the data-rich validation to test whether the distribution of residuals is significantly different from the normal distribution in a statistical sense. The null hypothesis in this test states that the residuals are normally distributed. To draw a conclusion, if the *p*-value is less than a threshold, the null hypothesis that the residuals are normally distributed can be rejected with $(1 - \alpha)$ level of confidence. The threshold used here is $\alpha = 10\%$, which corresponds to a confidence level of 90%. The question of normality was also visually investigated using normality plots and residual histograms.

Data-Rich Validation

Process

There are six L03 data-rich models per analysis time slice (peak period, peak hour, weekday, and midday) to predict the mean TTI and the 99th-percentile, 95th-percentile, 80th-percentile, 50th-percentile, and 10th-percentile TTI, resulting in a total of 24 data models to be validated. The independent variables used in each model were described in Chapter 2, and the equations for each model are contained in Appendix C. Table 3.1 shows the total number of freeway section-years for which data was available within each region and time slice; the cells

Table 3.1. Data-Rich Validation Freeway Section Sample Sizes

Region	Peak Period	Peak Hour	Midday	Weekday
California	**43**	**43**	**140**	**142**
Minnesota	**19**	**25**	**60**	**60**
Salt Lake City	3	4	**32**	**30**
City of Spokane	0	0	9	11
All Data	**65**	**72**	**241**	**243**

Note: Bold numbers = regions and time periods used in the data-rich validation.

in bold indicate regions and time periods used in the data-rich validation. In the Salt Lake City and Spokane regions, very few of the roadway sections experienced traffic conditions that qualified under the peak period and peak hour definitions established in L03. Due to these small sample sizes, these region time periods were excluded from the validation results.

Results

Table 3.2 presents the data-rich root mean square errors (RMSEs) measured for each time period, model, and region. The main conclusion of the data-rich validation is that the average prediction errors measured by the RMSE for each model are not acceptable across many of the regions.

From a regional perspective, for all time slices except the weekday time period, the RMSEs are the highest when the models are applied to the California data set. During the weekday time period, the RMSEs are the highest when the models are applied to the Minnesota data set, and the lowest when applied to the Salt Lake City data set.

When the RMSEs are interpreted by the predicted measure, we see that, across all of the time periods, the highest RMSEs occur for the prediction of the 99th-percentile TTI. The RMSEs tend to decrease as the predicted TTI measure lowers (i.e., the RMSEs for the 50th-percentile models are lower than for the 80th-percentile models, which are lower than for the 95th-percentile models, and so on). This is to be expected, as there is naturally more variability among the validation data sections at the higher moments of the travel time distribution.

Table 3.2. Summary of Data-Rich RMSE Values by Model and Region

Model Details		RMSE Value by Region			
Analysis Time Slice	**Model**	**All Data**	**CA**	**MN**	**Salt Lake City**
Peak period	Mean TTI	96.94%	127.55%	21.59%	na
	99th Percentile	403.44%	607.76%	63.67%	na
	95th Percentile	251.95%	359.19%	45.85%	na
	80th Percentile	151.95%	206.54%	30.95%	na
	50th Percentile	89.55%	116.63%	23.15%	na
	10th Percentile	12.13%	14.43%	6.23%	na
Peak hour	Mean TTI	25.45%	26.97%	24.68%	na
	99th Percentile	50.74%	52.78%	47.46%	na
	95th Percentile	38.38%	40.19%	37.27%	na
	80th Percentile	35.13%	36.89%	34.06%	na
	50th Percentile	28.85%	32.41%	24.22%	na
	10th Percentile	18.50%	22.24%	12.14%	na
Midday	Mean TTI	6.24%	7.57%	4.07%	3.52%
	99th Percentile	32.32%	34.95%	25.86%	34.01%
	95th Percentile	15.62%	17.29%	14.01%	12.55%
	80th Percentile	8.99%	10.86%	6.61%	3.60%
	50th Percentile	5.43%	6.93%	2.09%	2.08%
	10th Percentile	1.81%	2.20%	0.80%	1.33%
Weekday	Mean TTI	19.74%	12.81%	35.99%	5.95%
	99th Percentile	72.91%	50.04%	141.72%	30.87%
	95th Percentile	83.82%	40.46%	197.82%	22.85%
	80th Percentile	29.28%	14.84%	59.43%	5.75%
	50th Percentile	4.68%	5.92%	1.71%	2.16%
	10th Percentile	0.81%	0.74%	0.48%	1.30%

Note: na = not applicable.

From a time period perspective, the highest RMSEs are seen during the peak period, which is defined specifically for each section to cover time periods of at least 75 min, during which the average speeds fall below 45 mph. The RMSEs are lower, though still high, for the peak hour models. Both the peak hour and peak period models are predicted by the critical D/C ratio, the incident lane-hours lost and, for some of the models, the precipitation factor. The RMSEs are the lowest during the midday period (11:00 a.m. to 2:00 p.m.), during which congestion tends to be minimal. The midday period TTIs are predicted only by the critical D/C ratio. RMSEs during the weekday period (predicted by the average D/C ratio and, for some of the models, the incident lane-hours lost), are slightly higher than they are for the midday period.

Results also indicate that the models violate many of the assumptions of generalized regression and thus have room for enhancement. Generally, a good regression model is expected to present randomly scattered residuals without obvious trends. However, increasing trends and other non-random patterns were observed in the residual plots of many of the models. This indicates that the models may not be able to sufficiently describe the relationship between the independent variables and the dependent variable. Table 3.3 summarizes the results of the *t*-test and normality test for each model, as applied to the AllData set. In the majority of cases, the null hypotheses for these tests were able to be rejected with 90% confidence, particularly in all but the peak hour time periods.

Data-Poor Validation

Process

The seven L03 data-poor models validated in this task were

1. 95th-percentile TTI = 1 + 3.6700 * ln(meanTTI)
2. 90th-percentile TTI = 1 + 2.7809 * ln(meanTTI)
3. 80th-percentile TTI = 1 + 2.1406 * ln(meanTTI)
4. Standard deviation of TTI = $0.71 * (\text{meanTTI} - 1)^{0.56}$
5. PctTripsOnTime50mph = $e^{(-0.20570*[\text{meanTTI}-1])}$
6. PctTripsOnTime45mph = $e^{(-1.5115*[\text{meanTTI}-1])}$
7. PctTripsOnTime30mph = $0.333 + [0.672/(1 + e^{(5.0366*[\text{meanTTI}-1.8256])})]$

Validation was performed using data collected on weekdays during the midday period (11:00 a.m. to 2:00 p.m.) and the peak period (a continuous time period of at least 75 min during which the space mean speed is less than 45 mph). This is consistent with the time periods that L03 used to calibrate the data-poor models.

Table 3.4 shows the number of freeway section-year data points available for validation within each region. As with the data-rich validation, the number of peak period data points available in Salt Lake City and Spokane were too few to be used in the analysis.

Table 3.3. Data-Rich Statistical Test Results by Model, All Regions

Model Details		Statistical Test Results	
Analysis Time Slice	**Model**	***t*-Test**	**Wilkes-Barr**
Peak period	Mean TTI	Reject	Reject
	99th Percentile	Reject	Reject
	95th Percentile	Reject	Reject
	80th Percentile	Reject	Reject
	50th Percentile	Reject	Reject
	10th Percentile	Reject	Reject
Peak hour	Mean TTI	Cannot Reject	Cannot Reject
	99th Percentile	Cannot Reject	Reject
	95th Percentile	Cannot Reject	Cannot Reject
	80th Percentile	Reject	Cannot Reject
	50th Percentile	Reject	Cannot Reject
	10th Percentile	Cannot Reject	Reject
Midday	Mean TTI	Reject	Reject
	99th Percentile	Reject	Reject
	95th Percentile	Reject	Reject
	80th Percentile	Reject	Reject
	50th Percentile	Cannot Reject	Reject
	10th Percentile	Reject	Reject
Weekday	Mean TTI	Reject	Reject
	99th Percentile	Reject	Reject
	95th Percentile	Reject	Reject
	80th Percentile	Reject	Reject
	50th Percentile	Cannot Reject	Reject
	10th Percentile	Reject	Reject

Table 3.4. Data-Poor Validation Freeway Section Sample Sizes

Time Period	CA	MN	Salt Lake City	Spokane	All Data
Midday	144	60	42	12	258
Peak Period	43	19	3	0	65
Total	187	79	45	12	323

Table 3.5. Summary of Data-Poor RMSE Values by Model and Region

Model	RMSE Value by Region				
	All Data	CA	MN	Salt Lake City	Spokane
95th Percentile	0.1820	0.2064	0.1716	0.0833	0.0688
90th Percentile	0.1189	0.1187	0.1502	0.0483	0.0604
80th Percentile	0.0684	0.0660	0.0896	0.0290	0.0447
Standard Deviation	0.0855	0.0839	0.1028	0.0586	0.0672
PctTripsOnTime50mph	0.0784	0.0891	0.0617	0.0552	0.0721
PctTripsOnTime45mph	0.0602	0.0681	0.0480	0.0433	0.0553
PctTripsOnTime30mph	0.0254	0.0247	0.0329	0.0134	0.0065

Results

Table 3.5 summarizes the root mean square error estimates for each model on all sections (All Data column) and by region. Overall, the RMSEs are generally acceptable for most of the models and regions. The model error is larger for the prediction of higher moments of the TTI distribution. This makes sense because the 95th-percentile TTIs are likely associated with very rare events (like a major incident or bad weather). We would expect these TTIs to vary greatly from section to section, making them harder to accurately model based solely on the mean TTI.

The main concern with the data-poor models following the validation effort is that they violate many of the assumptions of generalized regression. The *t*-test results of the AllData set for each model are shown in Table 3.6; for nearly all of the models, it was possible to reject the null hypothesis of zero residual mean with 95% confidence. The systematic bias of overpredicting or underpredicting the residuals varied regionally, with the models tending to show better-than-measured reliability measures in Minnesota and poorer-than-measured reliability measures in California. This lends support for building regional models rather than cross-sectional models.

Table 3.6. Data-Poor t-Test Results by Model, All Regions

Model	*t*-Test Results
95th Percentile	Reject
90th Percentile	Reject
80th Percentile	Reject
Standard Deviation	Reject
PctTripsOnTime50mph	Reject
PctTripsOnTime45mph	Reject
PctTripsOnTime30mph	Cannot Reject

Reference

1. DePaul University. Linear Regression. http://condor.depaul.edu/sjost/it223/documents/regress.htm. Accessed February 15, 2014.

CHAPTER 4

Enhanced Models and Application Guidelines

Overview

Enhancement was explored for the data-rich models, but no suitable enhancements resulting in performance improvements were found.

For the data-poor enhancement, the original L03 models were recalibrated using data collected in the Los Angeles, San Diego, Sacramento, San Francisco, and Minneapolis regions. Additionally, the research team explored the performance of three new model forms to predict the 95th-, 90th-, and 80th-percentile TTIs:

1. A one-parameter power model ($y = x^b$)
2. A two-parameter power model ($y = a \times x^b$)
3. A two-parameter polynomial model ($y = a \times x + b \times x^2$)

New models were explored for the 95th-, 90th-, and 80th-percentile models because they exhibited the worst performance in the validation assessment.

The results of the recalibration were compared with the performance of the three new model forms. Overall, the team found that the error values (measured in mean square error) for the recalibration and the new models were similar 95th- and 90th-percentile TTI predictions. For the 80th-percentile TTI equation, the mean square error (MSE) of the new models was approximately half that of the recalibrated model. All of the new models exhibited a better adherence to the assumptions of regression than the original model form.

In this chapter, the results section summarizes the results of the enhancement assessment and documents the equation outputs. The recommendations section discusses application guidelines for using the recommended models.

Results

Models

The models shown in Table 4.1 were developed from the All-Data set (containing data from the regions in California and the Minneapolis region). Further discussion of these equations, as well as the equations calibrated specifically to the California regions and the Minneapolis region, are included in Appendix E.

Performance

The performance of the recalibrated and new models was evaluated through consideration of the model statistics (mean square error and *F*-test results) and an assessment of how well the models meet the assumptions of regression. The details of the evaluation are presented in Appendix E in the form of model statistics, fit plots, observed versus predicted value plots, residuals versus predicted value plots, outlier and leverage plots, residual histograms, and normality plots.

Table 4.2 shows the mean square error results for the recalibrated and new models. In terms of MSE, the new models show the most significant improvement over the recalibrated model for the 80th-percentile TTI. The MSEs between the recalibrated and new models for the 95th- and 90th-percentile TTI predictions are comparable.

All of the recalibrated and new models satisfied the *F*-test, indicating overall validity. As seen in the residual versus predicted value plots, all of the new models exhibited improved residual patterns over the recalibrated L03 models. The new models still exhibited some issues with non-constant variance and residuals that are not perfectly normally distributed. As with the error, the best improvements in the residual patterns were seen for the 80th-percentile TTI model.

Table 4.1. Recalibrated and New Data-Poor Models

Model		Form
95th-Percentile TTI	Recalibration	95th-percentile $TTI_{AllData} = 1 + 3.4201\ln(\text{meanTTI})$
	1-param power	95th-percentile $TTI_{AllData} = \text{meanTTI}^{1.9566}$
	2-param power	95th-percentile $TTI_{AllData} = 1.0406 * \text{meanTTI}^{1.8821}$
	2-param polynomial	95th-percentile $TTI_{AllData} = 0.1494 * \text{meanTTI} + 0.8902 * \text{meanTTI}^2$
90th-Percentile TTI	Recalibration	90th-percentile $TTI_{AllData} = 1 + 2.8189 * \ln(\text{meanTTI})$
	1-param power	90th-percentile $TTI_{AllData} = \text{meanTTI}^{1.7324}$
	2-param power	90th-percentile $TTI_{AllData} = 1.0099 * \text{meanTTI}^{1.7137}$
	2-param polynomial	90th-percentile $TTI_{AllData} = 0.3528 * \text{meanTTI} + 0.6591 * \text{meanTTI}^2$
80th-Percentile TTI	Recalibration	80th-percentile $TTI_{AllData} = 1 + 2.1598 * \ln(\text{meanTTI})$
	1-param power	80th-percentile $TTI_{AllData} = \text{meanTTI}^{1.4448}$
	2-param power	80th-percentile $TTI_{AllData} = 0.9943 * \text{meanTTI}^{1.4559}$
	2-param polynomial	80th-percentile $TTI_{AllData} = 0.6166 * \text{meanTTI} + 0.3809 * \text{meanTTI}^2$
Standard Deviation TTI	Recalibration	$StdDevTTI_{AllData} = 0.7775 * (\text{meanTTI} - 1)^{0.6810}$
PctTripsOnTime50mph	Recalibration	$PctOnTimeTrip50mph_{AllData} = e^{-2.0293*[\text{meanTTI}-1]}$
PctTripsOnTime45mph	Recalibration	$PctOnTimeTrip45mph_{AllData} = e^{-1.4874*[\text{meanTTI}-1]}$
PctTripsOnTime30mph	Recalibration	$PctOnTimeTrip30mph_{AllData} = 0.3401 + \frac{0.6803}{1+\exp(4.5026 * [\text{meanTTI} - 1.7890])}$

Table 4.2. Data-Poor Enhancement Mean Square Error

Model		Form	MSE		
			All Data	CA	MN
95th Percentile	Recalibration	$y = 1 + a + \ln(x)$	0.0277	0.0255	0.0234
	1-param power	$y = x^b$	0.0300	0.0273	0.0408
	2-param power	$y = a \times x^b$	0.0286	0.0264	0.0345
	2-param polynomial	$y = a \times x + b \times x^2$	0.0289	0.0268	0.0352
90th Percentile	Recalibration	$y = 1 + \alpha + \ln(x)$	0.0137	0.0118	0.0110
	1-param power	$y = x^b$	0.0122	0.0118	0.0151
	2-param power	$y = a \times x^b$	0.0121	0.0118	0.0144
	2-param polynomial	$y = a \times x + b \times x^2$	0.0125	0.0121	0.0153
80th Percentile	Recalibration	$y = 1 + \alpha + \ln(x)$	0.00469	0.00410	0.00506
	1-param power	$y = x^b$	0.00239	0.00178	0.00384
	2-param power	$y = a \times x^b$	0.00237	0.00176	0.00389
	2-param polynomial	$y = a \times x + b \times x^2$	0.00245	0.00179	0.00436
Standard Deviation TTI	Recalibration[a]	$y = a \times (x - 1)^b$	0.00668	0.00630	0.00364
PctTripsOnTime50mph	Recalibration[a]	$y = e^{a(x-1)}$	0.00616	0.00765	0.00224
PctTripsOnTime45mph	Recalibration[a]	$y = e^{a(x-1)}$	0.00363	0.00451	0.00123
PctTripsOnTime30mph	Recalibration[a]	$y = a + (b - a)/\{1 + \exp[c * (x - d)]\}$	0.00053	0.00050	0.00031

[a]The recalibration for the 95th-percentile, 90th-percentile, and 80th-percentile models was performed following removal of two data points identified as outliers. The rest of the measures were recalibrated using all data points.

Application Guidelines

The research team recommends that the SHRP 2 program adopt the new L33 models. This recommendation is based on the following reasons:

1. The residual by predicted value plot shows improvement in the shape and in the balance of scatter around the origin, indicating that the new models better satisfy the assumptions of regression.
2. The new models allow for a consistent model form between different percentile TTI measures.
3. Since the variance of travel times tends to increase with the mean travel time, reliability model curves should show an increasing pattern at an increasing rate. The new models satisfy this characteristic in a way that the original L03 data-poor models do not.

APPENDIX A

Review of L03 and Related Models

Purpose

The purpose of this background technical memorandum, the deliverable for Task 1 of the second Strategic Highway Research Program (SHRP 2) L33 project, is to identify important findings and lessons learned that will help validate and extend the L03 predictive reliability models. To meet this objective, following this introduction the document is divided into four main sections. The first section conducts a review of SHRP 2 L03, including the modeling concept, data collection and processing procedures, and calibration and validation results. While the L33 research team had knowledge of the L03 project before conducting this literature survey, the team felt that it was critical to fully document the major components of the L03 process in order to identify opportunities for enhancement in data and modeling-related techniques. The second section conducts a survey of other predictive reliability models developed through the SHRP 2 Reliability program. The third section presents other reliability research conducted through SHRP 2 and other initiatives that can provide value to the L33 process. The final conclusions section summarizes the lessons learned from the background material for consideration in the L33 data collection, model validation, and model enhancement tasks.

Review of SHRP 2 L03

Overview

The purpose of the SHRP 2 L03 project was to develop analytical procedures to determine the impacts of reliability mitigation strategies. The project team explored this issue through the following analyses:

- *Congestion by Source.* This part of the project used data collected in Seattle to assess methodologies for assigning delay to the causes of congestion.
- *Before/After Studies.* The project team identified 17 improvements, categorized into the following, that could be analyzed with the project's continuously collected traffic data. These before/after reliability metrics were used to produce reliability adjustment factors that agencies can apply to various improvement scenarios to estimate the impact to travel time reliability.
  - Ramp metering;
  - Freeway service patrol implementation;
  - Bottleneck improvement;
  - General capacity increases;
  - Aggressive incident clearance program; and
  - High occupancy/toll (HOT) lane conversion.
- *Cross-Sectional Statistical Modeling.* Because only a limited number of before/after studies were observable in the project data sets, this portion of the project developed macroscale cross-sectional models that predict the overall travel time characteristics of a highway section. Two model forms were developed: data-rich and data-poor. These models are described and assessed in further sections of this appendix.

The remainder of this L03 project overview details the cross-sectional statistical modeling that ultimately produced the data-rich and data-poor models that will be validated and enhanced in the L33 project. It explains the modeling concept, the data collection and data processing methodologies used to generate travel time reliability statistics and explanatory factors, the estimation of independent variables, the final analysis data set, the model calibration and validation results, and the application guidelines. The summary concludes with a list of recommendations suggested by the L03 project team for further analysis.

Modeling Concept

The Phase 1 report of the L03 project proposed two model forms to focus on in the remainder of the project:

1. "A detailed deterministic model that uses all of the data being collected to a maximum degree (Data-Rich Model)"; and

2. "A simpler model based on the fact that many of the applications [*Highway Capacity Manual* (HCM) and travel demand forecasting models] work in an environment with limited data (Data-Poor Model)."

Figure A.1 shows the conceptual form of the data-rich model, which is composed of tiers of causal mechanisms that influence each other and, ultimately, travel time reliability. At a first level, the model conceives travel time reliability as a function of (1) the number of lanes; (2) the demand-to-capacity ratio; (3) primary incident capacity-hours lost; (4) secondary incident capacity-hours lost; (5) work zone capacity-hours lost; (6) weather factors; (7) traffic fluctuation; (8) active control; and (9) opposite direction incident-hours. All variables in the first tier, except for the number of lanes, are functions of further explanatory variables. For example, work zone capacity-hours lost is a function of lane-hours lost and shoulder-hours lost, which are functions of the work zone type and the work zone duration (which is a function of an agency's work zone policy). This model form allows high-level variables to be estimated from roadway characteristics and agency operational policies, which gives the model the power to estimate reliability improvements from capacity and demand-related interventions.

The data-poor model was first envisioned to take advantage of commonly available independent variables (such as annual collisions per million, vehicle miles traveled, speed limit, and yearly demand profiles). However, exploratory analysis showed promising relationships between the mean travel time and all selected reliability metrics. Because the mean travel time is a ready output from planning and operational tools such as travel demand and simulation models, this relationship became the focus of the data-poor model development.

Data Collection

The L03 project team developed a site selection design plan to collect data in metropolitan areas and along segments that meet a broad range of different criteria. These criteria are shown in Table A.1. Ultimately the project team elected to collect data in eight metropolitan areas that had mature data collection programs that could be leveraged in this project: (1) Atlanta, Georgia; (2) Houston, Texas; (3) Jacksonville, Florida; (4) Los Angeles, California; (5) Minneapolis, Minnesota; (6) San Diego, California; (7) San Francisco, California; and (8) Seattle, Washington. Details of these metropolitan areas and the types of data collected are shown in Table A.2.

The remainder of this section describes the data collection process for the key types of data collected in L03: (1) traffic, (2) incidents and work zones, (3) weather, and (4) capacity.

Traffic Data

Urban freeway traffic data were largely assembled from traffic management centers (TMCs) that have a history of maintaining quality traffic data. All of the study sections outside of Houston were monitored by fixed-point detectors that report volume as well as occupancy and/or speed. In Houston, the research team collected travel times from toll tag matches. In the San Francisco Bay area, data were collected from fixed-point sensors and toll tag matches.

A key piece of the traffic data collection was to select the segments to monitor and model. The L03 Phase 2 report states that "based on previous analyses conducted by the research team, such as those for the Federal Highway Administration's (FHWA's) Mobility Monitoring Program, the section length for urban freeways has generally been set at a length between two to five miles."

Figure A.2 shows the distribution of segment lengths studied in the L03 project. The segments had an average length of 5 miles, though some much longer segments were selected for the before-and-after analysis. Appendix G of the L03 final report states that sections should have the following characteristics:

1. Be relatively homogeneous in terms of traffic and geometric conditions;
2. Represent portions of trips taken by travelers; and
3. Have no mid-section freeway-to-freeway interchanges.

Incidents and Work Zones

For most sites, incident and work zone data were obtained from the private vendor Traffic.com. Traffic.com gathers incident data from a variety of sources and standardizes them into information on traffic incidents, special events, construction, severe weather, and other potentially traffic-influencing events. Each incident is either reported or confirmed and indicates the number of travel lanes blocked and the incident start and end time.

In some regions (Jacksonville, Atlanta, and Seattle), TMC-reported incidents were used as the primary incident data set.

Weather

Hourly weather data from weather stations in the study region were obtained from the National Climatic Data Center (NCDC) of the National Oceanic and Atmospheric Administration (NOAA). The hourly data contained information on the sky condition, visibility, obstructions to visibility, type and intensity of precipitation, precipitation accumulation, temperature, and wind characteristics.

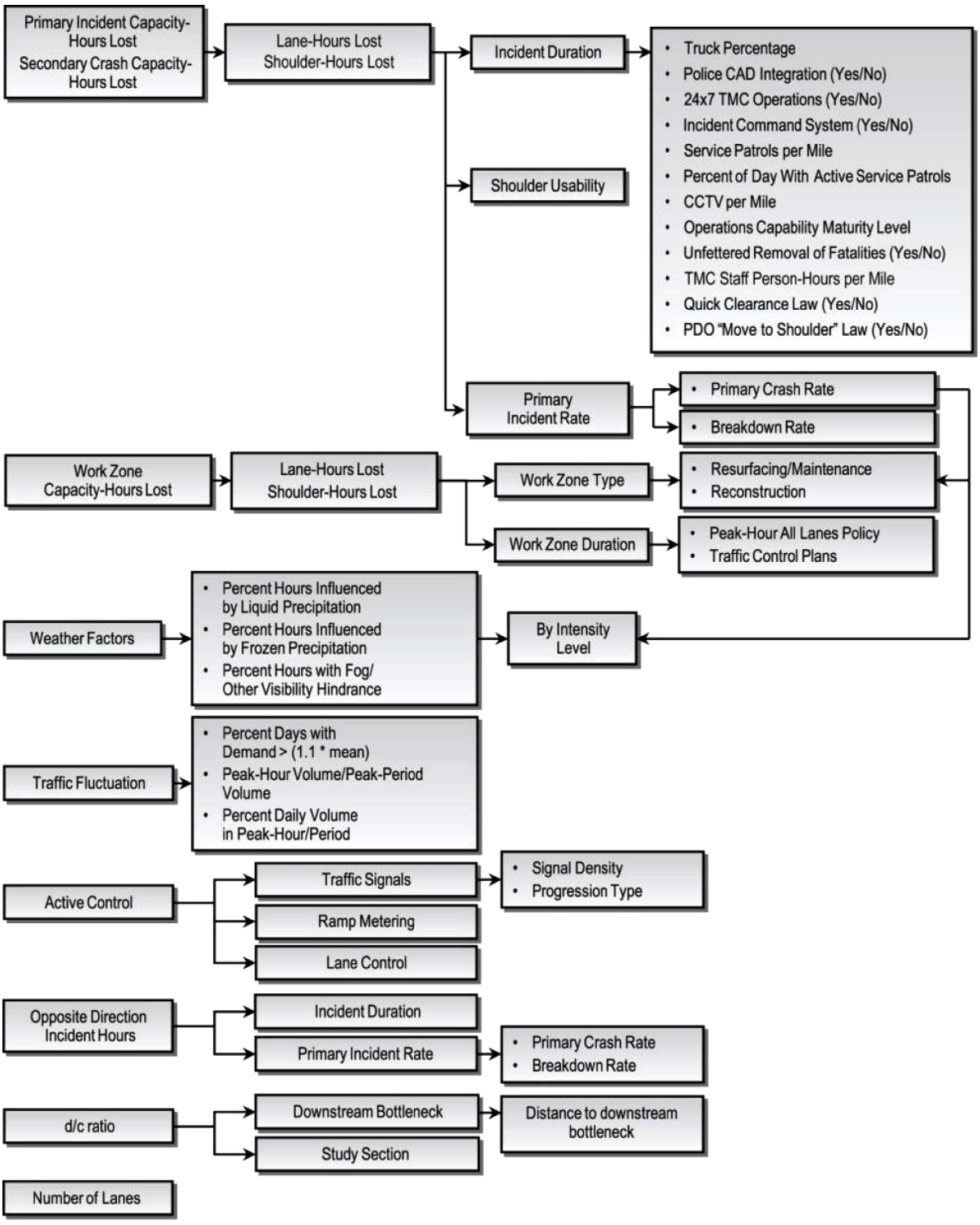

Notes: 1) " ⟶ " means "…is a function of..."
2) Primary Incident and Secondary Crash hours lost are modeled similarly.

Figure A.1. Data-rich modeling concept.

Table A.1. Site Selection Design Criteria

Factors	Levels	Highway Type		
		Urban		Rural
		Freeways	Signalized Arterials	Freeways
Area size	Small, medium	•	•	
	Large, very large	•	•	
Base congestion	Low (AADT/C^a < 7)			•
	Moderate (AADT/C ~ 9)	•	•	
	Severe (AADT/C ~ 12)	•	•	
Number of lanes	4	•	•	•
	6	•	•	
	8+	•	•	
Base crash rate[b]	Low	•	•	•
	High	•	•	•
Trucks (%)	<10%	•	•	•
	>10%	•	•	•
Traffic variability[c]	Low	•	•	•
	High	•	•	•
Traffic signal density	<2/mile		•	
	2–5/mile		•	
	>5/mile		•	
Proximity to major bottleneck	<1 mile downstream from segment	•		
	>5 miles downstream from segment	•		
Improvement type	Incident management	•	•	•
	Work zone management	•	•	•
	Weather management[d]	•		•
	Traffic device control[e]	•	•	
	Demand management	•	•	
	Special event management	•	•	
	Traveler information	•	•	•
	Physical expansion and/or changes	•	•	•

[a] AADT/C is annual average daily traffic-to-capacity ratio (specifically, two-way hourly capacity).
[b] Categories were based on comparison to each state's average crash rate by type of highway.
[c] For urban highways, traffic variability was determined based on the coefficient of variation (CV) of weekday peak period travel. For rural highways, the CV of the 24-hour volume was used.
[d] Weather management depended on what was being covered in other research activities, such as FHWA's Road Weather Research and Development Program.
[e] Ramp meter control on freeways; signal control on signalized arterials.

Table A.2. SHRP 2 L03 Study Sites

City	Number of Sections	Traffic Data	Incident/Work Zone Data	Weather Data
Houston	13	Toll Tag	Traffic.com	NCDC/NOAA
Minneapolis	16	Fixed Point	Traffic.com	NCDC/NOAA
Los Angeles	3	Fixed Point	Traffic.com	NCDC/NOAA
San Francisco Bay	4	Toll Tag/Fixed Point	Traffic.com	NCDC/NOAA
San Diego	6	Fixed Point	Traffic.com	NCDC/NOAA
Atlanta	10	Fixed Point, AirSage	GDOT (NaviGAtor)	NCDC/NOAA
Jacksonville	8	Fixed Point	TMC	NCDC/NOAA
Seattle	21	Fixed Point	TMC & CAD	NCDC/NOAA

Capacity

The project team also collected information to calculate the capacity of study segments. Geometric data were obtained from satellite photographs and 2007 Highway Performance Monitoring data. Relevant operating and improvement data were obtained from the state departments of transportation (DOTs).

Incident Management Activities

Incident management information was collected from the traffic incident management (TIM) self-assessment procedure, developed by the FHWA to capture the sophistication of incident management policies for modeling. The process results in a single numeric score.

The TIM self-assessment score ended up being available in only a few of the study locations, so it was ultimately not used in the statistical models.

Data Processing

Data were assembled for 81 urban freeway study segments. The ultimate statistical analysis data set summarizes reliability metrics for every study section over an entire year by peak hour, peak period, midday (weekdays 11:00 a.m. to 3:00 p.m.), weekday (all hours), and weekend and holiday. It consists of information in the categories listed in Table A.3 (intended to be illustrative, not exhaustive).

A number of computational steps were required to transform the raw data sets into the final cross-sectional analysis

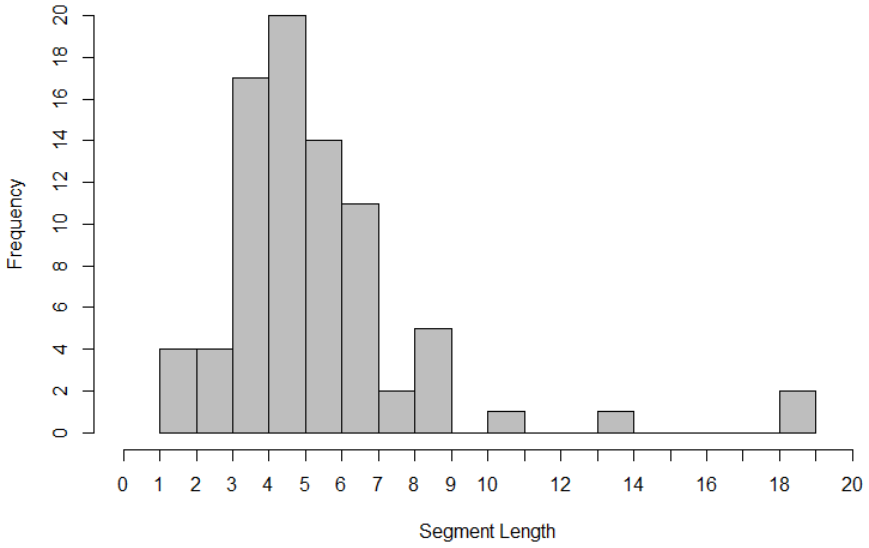

Figure A.2. Distribution of L03 segment lengths.

Table A.3. L03 Final Analysis Data Set

Category	Sample Measures
Reliability Metrics	• Mean, standard deviation, median, mode, minimum, and percentile travel times and travel time indices (TTIs) • Buffer indices, planning time index, skew statistics, and misery index • On-time percentages
Area Operations Characteristics	• Number of service patrol trucks • Service patrol trucks per mile • Quick clearance law? • Number of ramp meters, dynamic message signs, and closed-circuit televisions (CCTVs)
Service Patrols	• Number of service patrol trucks covering section • Percentage of time periods when trucks are active
Capacity and Volume Characteristics	• Start and end times of peak hour and peak period • Calculated and imputed vehicle miles traveled • Average of demand-to-capacity ratio on all section links • Highest demand-to-capacity ratio of all links on the section
Incident Characteristics	• Number of incidents • Incident rate per 100 million vehicle miles • Incident lane-hours lost • Incident shoulder-hours lost • Mean, standard deviation, and 95th percentile of incident duration
Event Characteristics	• Number of work zones • Work zone lane-hours lost • Work zone shoulder-hours lost • Mean, standard deviation, and 95th percentile of work zone duration
Weather Characteristics	• Number of hours with precipitation amounts exceeding various thresholds • Number of hours with measurable snow • Number of hours with frozen precipitation • Number of hours with fog

data set listed in Table A.3. The key steps described in this section are (1) quality control, (2) calculating speed, (3) calculating the travel time index, (4) defining the peak hour and peak period, (5) calculating demand in oversaturated conditions, and (6) associating incidents with segments.

Quality Control

The L03 final report states, "The processing began with quality control of the data as received from the TMCs. The data quality checks used were those developed for FHWA." The FHWA report cited is *Quality Control Procedures for Archived Operations Traffic Data: Synthesis of Practice and Recommendations: Final Report* (Texas Transportation Institute 2007).

Calculating Speed

The calculation of speed is a necessary processing step for data collected by single loop detectors. The L03 team did not have to do any of this processing because all of the collected data already supplied speeds that were either directly measured by the detector or were estimated in an upstream processing module. For example, in the case of the San Francisco, Los Angeles, and San Diego sites, traffic data were obtained from the Freeway Performance Measurement System (PeMS), which computes speeds based on 5-min measurements of volume and occupancy using a lane-, day of week-, and time-of-day specific *g*-factor (estimate of the average vehicle length).

Calculating Travel Time Index

All collected detector data were first aggregated to the 5-min level. At the 5-min level, volume and speed data were spatially aggregated across all lanes in a given direction then turned into vehicle miles traveled (VMT) and vehicle hours traveled (VHT), where

- VMT = volume $*$ detector zone length; and
- VHT = VMT/(Min(FreeFlowSpeed,Speed)).

The detector zone length spans the distance between the current detector and halfway to its nearest neighboring detectors in the upstream and downstream directions.

When aggregating to the section level, VMT and VHT were marked as missing if less than half of the detectors reported valid data for each of the 5-min periods. Otherwise, VMT and VHT were summed across all detectors on the segment, weighting by segment length. From these 5-min, segment VMT and VHT, TTI was computed through the following equations:

- SpaceMeanSpeed = VMT/VHT;
- TravelRate = 1/SpaceMeanSpeed; and
- TTI = MAX(1.0,[TravelRate/(1/FreeFlowSpeed)]).

In L03, the urban freeway free-flow speed was set to 60 mph. Under this computational framework, the TTI can never be lower than 1. The ultimate outputs of this processing are 5-min TTIs by segment.

Defining Peak Hour and Peak Period

Both the data-rich and data-poor models were structured to predict reliability within the peak hour, peak period, midday, and weekend time periods. Of these time periods, the peak hour and peak period are allowed to vary from segment to segment.

L03 defined the peak hour as the continuous 60-min period during which the space mean speed is less than 45 mph. For segments where this condition occurs for longer than 60 min, the peak hour is selected by comparing the following criteria among adjacent 60-min periods:

- Low space mean speed;
- High vehicle hours of travel; and
- High vehicle miles of travel.

Ultimately, the analyst selects the peak hour based on comparing observed data with local knowledge on conditions.

The peak period is defined as a continuous time period of at least 75 min during which the space mean speed is less than 45 mph. The distribution of the durations of the peak periods for the L03 segments is shown in Figure A.3.

Calculating Demand in Oversaturated Conditions

Demand is a critical explanatory variable in the L03 models. Since roadway detectors measure volume not demand, the L03 research team created a methodology for computing the demand during the oversaturated conditions that all selected study corridors experience during the peak hour and peak period.

The methodology takes inputs of 5-min link volumes and speeds. For any 5-min speed that falls below a defined threshold (35, 40, or 45 mph), the link is assumed to be in congestion, and the measured volume is not considered representative of the demand. Single 5-min periods when the speed increases above the defined threshold then decreases below the threshold in the subsequent 5-min period are also assumed to be congested.

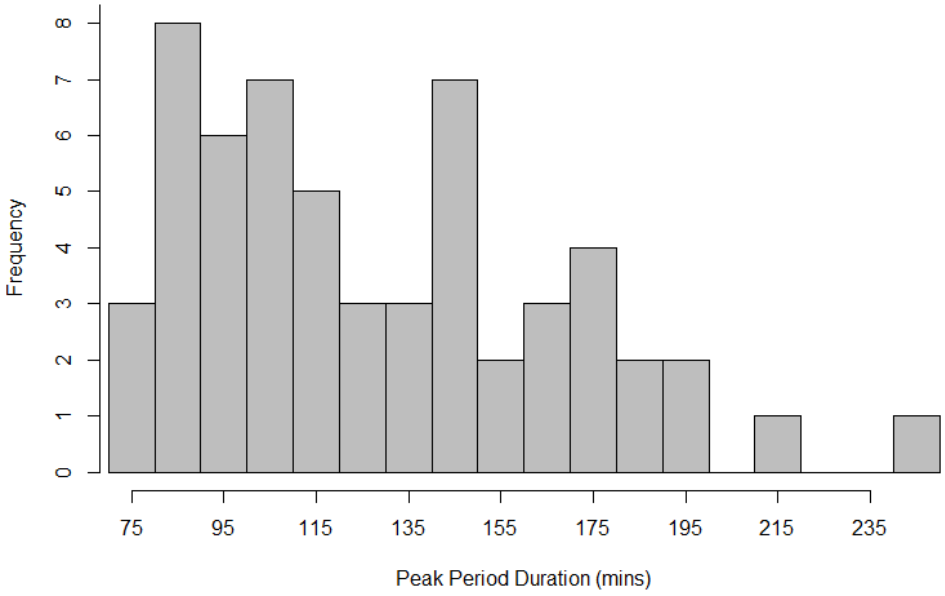

Figure A.3. L03 freeway segment peak period duration distributions.

Once the congested time period has been defined, it is split into two halves. The demand in the first half of congestion is assumed to be equal to the average volume measured in the two 5-min periods before the start of congestion. The demand in the second half of congestion is set such that the cumulative volume measured over the congested period is equal to the estimated cumulative demand. An illustration of the congestion definition methodology, applied to single loop detector in San Diego, is shown in Figure A.4.

The L03 final report states that the two 5-min periods after the termination of congestion need to be checked to ensure that the estimated demand curve fits smoothly to the observed cumulative volume curve. Additionally, the observed 5-min volume should not be significantly higher than the estimated demand for the second half of congestion. If necessary, the congested period can be extended to ensure a smooth transition. The importance of these steps is illustrated in Figure A.5, which shows the application of the demand-estimation process on a single day at six vehicle detector stations (VDSs) in Orange County, California. For VDSs 1201292 and 1202105, the estimation process appears to produce reasonable results. For VDSs 1201348 and 1201839, the estimated demands for the second half of the congested period are significantly lower than the measured volumes immediately following the congestion. For VDSs 1201419 and 1217710, the estimated second-half demands are higher that those estimated for the first half of congestion.

Associating Incidents with Segments

Spatially, incidents were assigned to segments if the incident's linear referencing information indicated that it occurred on the segment.

Temporally, for the peak hour, peak period, and midday models, an incident was assigned to a time slice if it began in or 15 min before the time slice, ended in the time slice, or spanned the time slice.

Estimation of Independent Variables

The final data-rich models contained a combination of up to three independent variables:

- The demand-to-capacity ratio (critical or average);
- Incident lane-hours lost (ILHL); and
- Hours of precipitation exceeding 0.05 in.

This section describes how each independent variable was calculated from the processed data sets.

Calculating the Demand-to-Capacity Ratio

The demand-to-capacity ratio is a critical input into all forms of the data-rich model. The previous section describes the process for calculating 5-min demand values from link-level measured volumes. Two forms of demand-to-capacity ratio were computed, stored, and used in the data-rich model:

- *Critical demand-to-capacity ratio.* The critical demand of a section is calculated as the highest 99th-percentile demand measured on a link on the segment during the given time period (peak hour or peak period) over a year.
- *Average demand-to-capacity ratio.* The average demand is calculated as the average demand measured on all links on the segment during the given time period (peak hour or peak period) over a year.

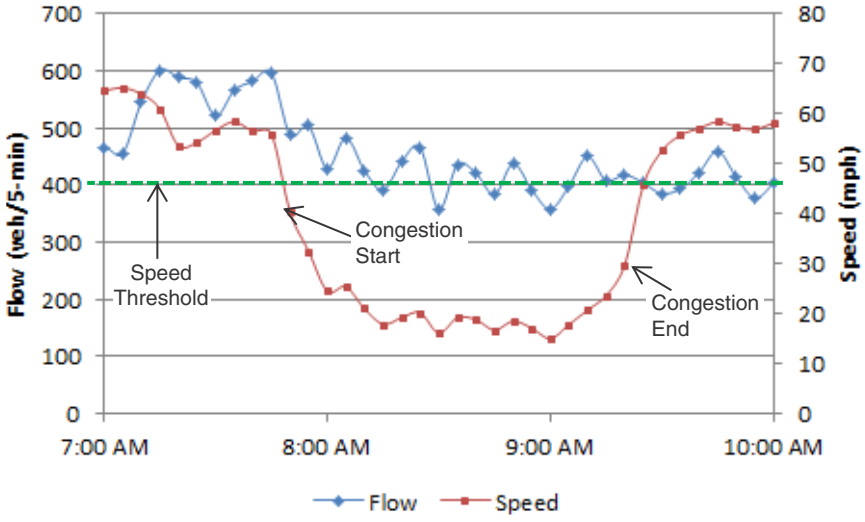

Figure A.4. L03 demand calculation concept.

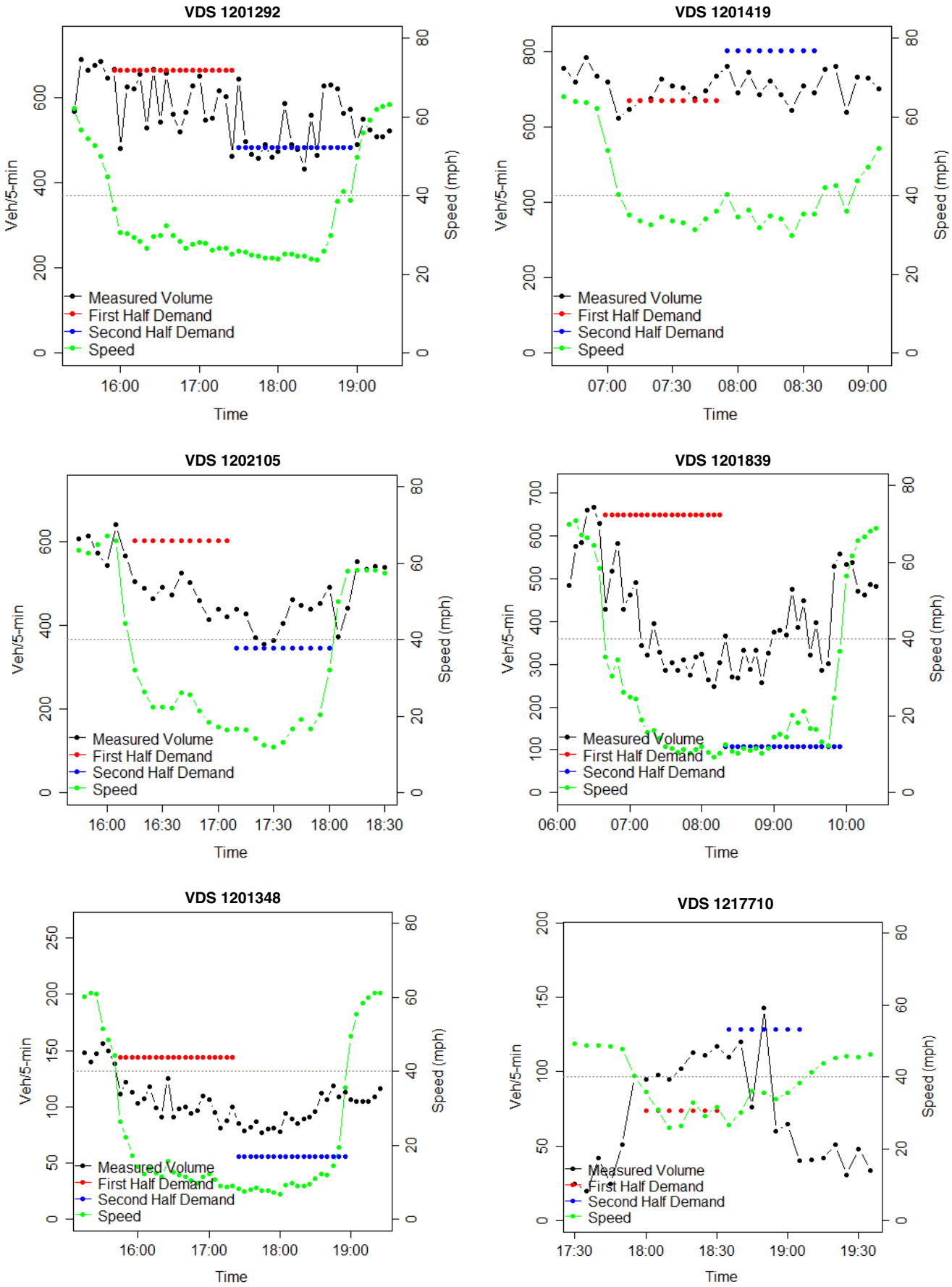

Figure A.5. Demand-estimation methodology applied to detector data in Orange County, California.

The capacity used in both ratios is the hourly capacity according to HCM methods.

Calculating Lane-Hours Lost

The lane-hours lost term in the model is meant to be the sum of lane-hours lost because of incidents and lane-hours lost because of work zones. The L03 project team only considered incidents in its developed models. Over a year, ILHL is calculated as follows:

$$\text{ILHL} = \text{number of incidents} * \text{lanes blocked} * \text{incident durations}$$

Through exploratory analysis, the L03 team developed the following guidelines for estimating the above parameters:

- If the incident rate is unavailable, it can be estimated by multiplying the crash rate by 4.545.
- If lanes blocked per incident is unavailable, it can be estimated as follows:
  - 0.476 if a usable shoulder is present and the agency moves lane-blocking incidents to the shoulder as quickly as possible;
  - 0.580 if lane-blocking incidents are not moved to the shoulder; and
  - 1.140 if usable shoulders are unavailable.

The L03 team concluded that while they had hoped to develop a statistical relationship between incident management policies and average incident duration, sufficient data were not available. The final report contains average incident durations in all of the study locations for use by practitioners.

Since the models are used to predict reliability measures within defined time periods (like the peak hour or peak period), the lane-hours lost because of a particular incident have to be assigned to these time periods. In L03, the total lane-hours lost caused by an incident were calculated and attributed to time periods based on the percentage of the active incident time spent in the time period. For example, if an incident that causes 10 lane-hours lost lasts from 8:00 a.m. to 9:00 a.m. on a section that has a peak period from 6:00 a.m. to 10:00 p.m. and a peak hour from 7:30 a.m. to 8:30 a.m., 10 lane-hours lost are contributed to the peak period and 5 lane-hours lost are contributed to the peak hour.

Calculating Precipitation

Hourly weather data from the National Weather Service (NWS) were used to compute the number of hours that had precipitation exceeding defined thresholds (ultimately, the number of hours where rainfall exceeded 0.05 in. was included in the data-rich model).

Final Analysis Data Set

The final analysis data set summarizes segment travel time reliability, demand, capacity, incidents, and weather conditions over an entire year. For TTI, the distribution and moments were computed as the volume-weighted average of all of the 5-min TTIs in the given time period over the year. This is a critical piece of the analysis chain, as it means that the ultimate travel time distributions and results are weighted toward the time periods that are the most heavily traveled. This is in contrast to a facility-level perspective, which treats each measurement equally regardless of how many vehicles experienced it.

Model Calibration

Data-Rich

The data-rich model contains three independent variables that predict travel time reliability over a year:

- The critical and average demand-to-capacity ratio;
- The ILHL; and
- The number of hours when precipitation exceeded 0.05 in.

Equations were fit for the peak hour, peak period, midday, and weekday time periods, and were developed to predict the mean and 10th, 50th, 80th, 95th, and 99th percentile for urban freeway sections. The equations are all listed in the attachment of this document.

Figure A.6 shows which of the independent variables (icons) were used in the models for the different TTI moments (columns) and time periods (row). The colors of the table show the root mean square error (RMSE) for each model during the calibration process. While the critical demand-to-capacity ratio and the ILHL were used in all of the peak hour and peak period equations, the hours of precipitation term was only used in six of the time period/moment equations. During the midday period, reliability is predicted only by the critical demand-to-capacity ratio. The RMSE generally increases with the higher TTI moments, likely because there is significantly more variability in the higher-percentile TTIs than in the mean, 10th-, and 50th-percentile TTIs across different segments.

Data-Poor

The data-poor model has only one independent variable: the mean TTI. Unlike the data-rich model, the data-poor predictive equations are not calibrated to specific time periods. Similar to the data-rich model, equations were developed to predict specific reliability metrics: the 80th-, 90th-, and 95th-percentile TTIs; the standard deviation TTI; the percentage of

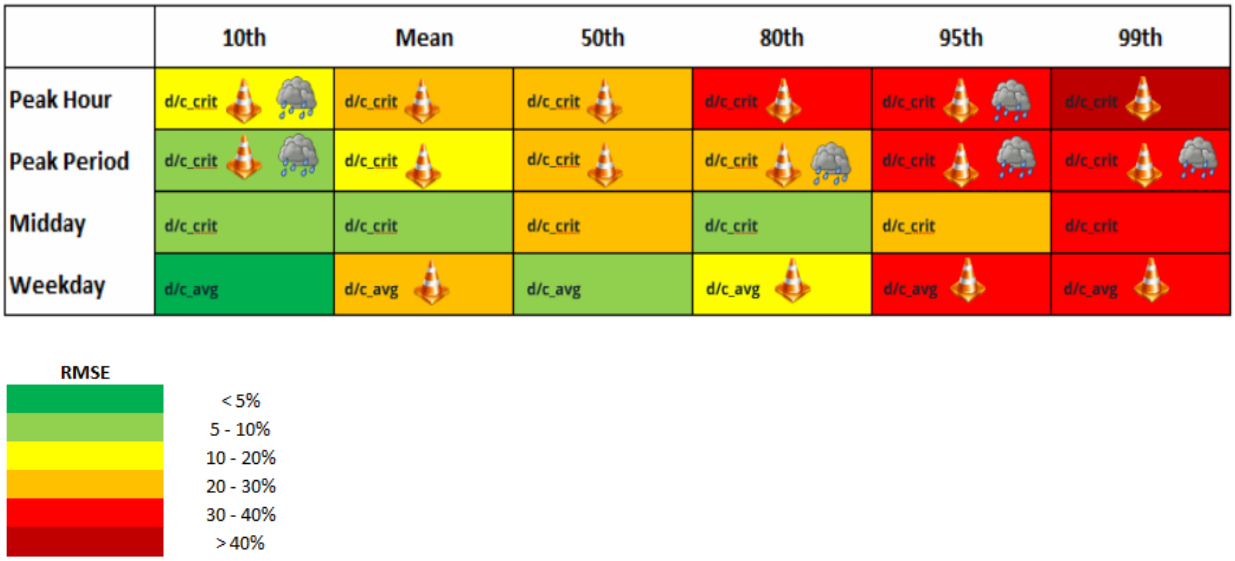

Figure A.6. RMSE of data-rich model calibration.

on-time trips made within 1.1 and 1.25 times the median TTI; and the percentage of on-time trips with 30-, 45-, and 50-mph speed thresholds.

Two sets of data-poor equations are presented in the L03 final report and have been included in the attachment of this document. The equations presented in the main body of the final report use an exponential form to relate the mean TTI with reliability. Appendix H, which supersedes the models in the body of the L03 report, presents a revised set of equations to account for the fact that the exponential form does not do well at estimating TTIs that exceed 2.0 (which are common in planning applications). The revised equations use the following forms:

- Natural log relationship for the percentile predictions;
- Exponential relationship with revised coefficients for the standard deviation prediction;
- Negative exponential form for the on-time measures for 45 and 50 mph; and
- Sigmoidal form for the on-time measure for 30 mph.

No revised equations were presented for the percentage of on-time trips made within 1.1 and 1.25 times the median TTI.

Figure A.7 shows the RMSE for each equation during the calibration process. No calibration results were presented for the revised equations in the final report.

Model Validation

The data-rich and data-poor models were both validated on 26 urban freeway sections in Seattle. The L03 final report presents validation errors (measured in percent difference between the actual and predicted values) for the following equations:

- Data-rich: mean, 80th-percentile, and 95th-percentile TTIs during the peak period and weekday (all 24-h) time periods, and
- Data-poor: 80th- and 95th-percentile TTIs.

The validation errors are shown in Figure A.8. The solid colors indicate sections on which the model overpredicted the TTI (thus predicting that the segment is less reliable than it actually is) and the striped colors indicate sections on which the model underpredicted the TTI (thus predicting that the segment is more reliable than it actually is).

As noted by the L03 project team, the models tend to underpredict the weekday TTIs in the Seattle region. The final report authors speculate that this may be because of

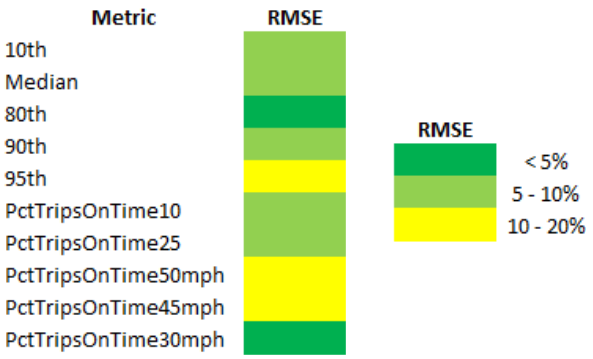

Figure A.7. Calibration root mean square error, data-poor equations.

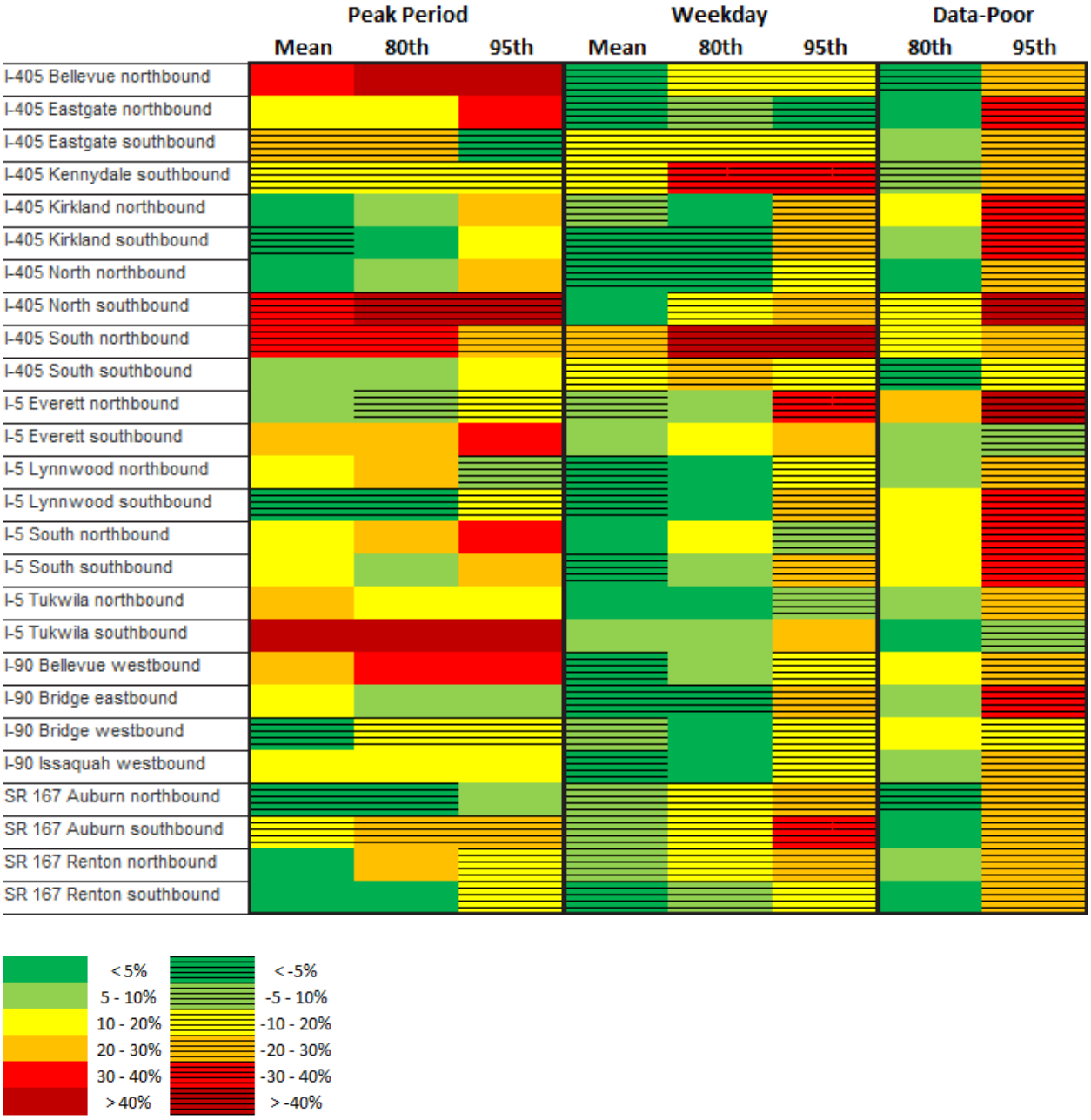

Figure A.8. Validation errors.

the lack of a rain variable in the weekday models; rain is an important factor in Seattle congestion. The data-poor model exhibits the same underprediction trend, particularly with the 95th-percentile equation. The L03 project team recommended further validation of the models to address these high errors.

Application Guidelines

Chapter 8 of the L03 final report contains application guidelines for using the project findings, including the data-rich and data-poor models to estimate the reliability impacts of various improvement scenarios. With respect to the model, it concludes that the data-poor models can be used to generate reliability statistics for many planning-level applications. Since the overall TTI from planning models includes only recurrent congestion, analysts must figure out how to incorporate nonrecurrent events into an overall mean TTI for use in the models. L03 provides an adjustment factor for doing this. For the data-rich models, the application guidelines include tables to link improvement actions with changes in the independent variables.

Recommendations

The L33 project team reviewed the L03 final report and final technical expert task group (TETG) presentation and communicated with the L03 principal investigator to assess the lessons learned and final conclusions from that project. The major findings and opportunities for L33 to further explore are as follows:

Geographic Scope

One issue with the L03 model validation and calibration steps is that winter weather was a factor in only one of the seven cities (Minneapolis). Additionally, all of the regions studied had well-developed incident management programs and other real-time operational activities. Further research should include more winter weather locations as well as more operationally diverse metropolitan areas.

Section Characteristics

All of the study sections shared two key characteristics: (1) all had three or more lanes per direction of travel, and (2) all regularly experienced severe congestion. Further work should consider sections with more diverse cross-sections and levels of congestion. These may be important factors because the impact of a lane blockage increases when there are fewer available lanes. Additionally, on severely congested segments, the relative impact of incidents, work zone, and inclement weather is less than on segments with less recurrent delay.

Additionally, L03 had some concerns about the performance of the data-poor models during extremely congested conditions. This is why revised models were included in the appendix of the final L03 report. It is recommended to validate and potentially recalibrate on sections that experience extremely congested conditions.

A further consideration is how capacity-restricting events like incidents and work zones are assigned to roadway sections. L03, as well as the SHRP 2 L08 project, Incorporation of Travel Time Reliability into the *Highway Capacity Manual,* assigned incidents to the section that they occur on. However, incidents that occur on one section often have impacts off of the section that are not captured in the L03 models. Similarly, incidents at the upstream end of a section may improve operations further downstream because of metering. These assumptions could be explored in further work.

Modification of Independent Variables

The L03 project team identified some opportunities for improving the estimation of independent variables in the models as well as potentially modifying them to produce better results. On the data-poor side, the team recommends a more rigorous approach for translating a recurring mean TTI into an overall mean TTI, ideally one that uses section-level incident and weather characteristics. On the data-rich side, results may be improved by altering the lane-hours-lost variable such that it is normalized by the total number of lanes at the location. Further exploration is also needed to figure out why this variable was not significant during the off-peak hours.

Additional Independent Variables

The two main identified opportunities for additional independent variables are (1) a representation of the number of lanes along a segment, and (2) a snowfall term.

Predictive Reliability Models

This section reviews the development and usage of other predictive travel time reliability models within the SHRP 2 Reliability program.

The SHRP 2 L05 project created a framework for how the various predictive reliability outputs of the SHRP 2 program can support different levels of analysis. Their findings, presented in Table A.4, identify three projects besides L03 that

Table A.4. Analysis Supported By SHRP 2 Reliability Predictive Models

Analysis Type/Scale	Supporting Tools
Sketch planning	L03 reliability prediction equations
Project planning	L07 hybrid method where data inputs are limited L08 multiscenario methods where additional data are available and more resolution in results are desired
Facility performance	L08 multiscenario methods most directly applicable L04 preprocessor (simulation manager) and postprocessor (trajectory processor) could be used, then the performance of an individual facility can be isolated
Travel demand forecasting	L03 reliability prediction equations and L07 method can be adapted as postprocessors L08 multiscenario methods could be used to develop custom functions for postprocessing
Traffic simulation	L04 preprocessor (simulation manager) and postprocessor (trajectory processor) most appropriate L08 scenario generator can be adapted

developed predictive travel time reliability models: L07, L04, and L08. Together the four projects support analyses at the sketch planning, project planning, facility performance, travel demand forecasting, and traffic simulation levels.

SHRP 2 L07: Evaluating Cost-Effectiveness of Highway Design Features

The purpose of the L07 project, which is still active, is to assess the role of various treatments in reducing nonrecurrent congestion. The output of the project is a spreadsheet-based tool that allows users to input specific roadway information and view the predicted reliability curve based on the L03 equations. The tool lets users compare an untreated TTI curve with treated TTI curves to view the effect of each treatment of reliability on a particular section of roadway.

The L07 project team made some revisions to the L03 models to adapt them to their spreadsheet application. The main motivation for the adaptations was to improve their applicability to sections on which congestion is dominated by nonrecurrent events. This largely applies to rural areas and small and medium urban areas (relevant to L33). The revised models have been submitted in a draft final report and are awaiting approval by the L07 TETG.

Revisions were made only to the data-rich models. The L07 team focused on the peak hour data-rich model from L03 but generalized it such that it could be applied to any hour of any day. The draft equations are presented in the attachment of this appendix.

The first major change is that L07 split the data-rich model into two separate equations: to be applied to sections and hours with a critical demand-to-capacity ratio of less than or more than 0.8. This change was made to allow for better results on lower demand sections given that the L03 peak hour equation focused on heavily congested segments. The equations use the same independent variables as the L03 peak hour model but also include a snowfall term that measures the number of hours during the time period when snowfall exceeded 0.01 in. Both equations also split the predicted TTI into two components, the nonprecipitation portion of the predicted TTI (which is exponential, with independent variables lane-hour lost and critical demand-to-capacity ratio) and the precipitation TTI. For the low-demand model, the coefficients are continuous, so the data-poor model can be used to calculate a continuous TTI density function. For the data-rich model, coefficients were developed to predict the 10th-, 50th-, 80th-, 95th-, and 99th-percentile TTIs.

The L07 revised equations were calibrated using data from Minnesota, processed by the L07 project team. According to the project team, calibration errors were not calculated; rather, the reasonableness of the values output by the spreadsheet were assessed and deemed to be acceptable for the spreadsheet application.

Both the L03 and L07 project team noted that the predictive equations are not optimal for predicting the travel time impacts of extremely rare events that affect the highest percentiles, because these events are so rare over the time frame of one year. As such, the L07 team is also developing a way to account for the reliability impacts of multihour incidents to directly manipulate the TTI curve after the predictive equations have been implemented.

SHRP 2 L04: Incorporating Reliability Performance Measures in Operations and Planning Modeling Tools

The purpose of the L04 project, which was completed in March 2013, was to develop software to apply simulation models in a way that more fully accounts for the factors that cause nonrecurrent congestion. The software consists of two modules: (1) a scenario generator that produces random inputs of incidents, work zones, weather, and other nonrecurrent congestion factors for the simulation; and (2) a trajectory processor that generates travel time distributions.

The L33 project team reviewed the SHRP 2 L04 Task 7 Report to understand the overlap between the two projects. Similar to the L03 team, the L04 team chose to focus their reliability analysis on the relationship between the mean travel times and measures of reliability (in the case of L07, the standard deviation travel time). In the exploratory analysis phase of the project, the L07 team tested three possible relationships between the mean travel time per mile and the standard deviation travel time per mile: (1) linear, (2) square root, and (3) quadratic. Since no real-world trajectory data were readily available, the relationships were tested using simulated trajectory data at the network, origin–destination, path, and link levels in Irvine, California; Baltimore, Maryland/Washington, D.C., and New York City. Travel time variability was considered in two ways: (1) the variation among vehicle travel times departing at the same time (origin–destination, path, and link levels); and (2) the variation by time of day (network-level). Ultimately, the quadratic model had the best goodness-of-fit (R-squared), but some of its coefficients had high p-values and violated accepted theory. The linear regression model was selected as the best model because it generally exhibited higher R-squared values than the quadratic model. In all models, the network-level had the highest slope (standard deviation increases faster with mean travel time) and the network-level the smallest slope. The linear relationship was validated using GPS probe data collected near Puget Sound. The validation yielded the following R-squared values:

- Origin–destination: 0.5770;
- Path: 0.3861; and
- Link: 0.6675.

These relationships were ultimately used to validate the results of the travel times output by the project's mesoscopic model. The L07 project team fit a linear regression model to the mean travel time per mile and standard deviation travel time per mile output by their mesoscopic model and compared the coefficients with those obtained from fitting the linear model to 4 hours of GPS trajectory data in New York City purchased from TomTom. The magnitudes of the coefficients were deemed comparable to those obtained for the simulated data, except at the network-level.

SHRP 2 L08: Incorporation of Travel Time Reliability into the *Highway Capacity Manual*

The SHRP 2 L08 project began in 2011 and is anticipated to end in the spring of 2013. The purpose of the L08 project is to develop analytic methods for potential incorporation of travel time reliability into the HCM. According to the draft final report, the project had two objectives: (1) to incorporate nonrecurring congestion impacts into the HCM and (2) to expand the HCM analysis horizon from a single study period to several weeks or months to assess variability. The project's methodology for freeways contains three components: (1) a data depository; (2) a scenario generator; and (3) a computational processor, each of which is described in turn.

The data depository contains required inputs to the scenario generator. At a segment-specific level, this includes segment geometries, free-flow speeds, lane patterns, segment types, and demand [which can be directly measured from field sensors over a sample of days or estimated from projections of annual average daily traffic (AADT)]. The depository also includes information about nonrecurrent congestion, such as the varying impacts it can have on traffic (for an incident, a shoulder closure versus a one-lane closure versus a two-lane closure); the probability of its occurrence during a particular time period; its duration; and the impact that it has on free-flow speed, demand, and capacity. These nonrecurrent congestion inputs have default values for cases where local data collection is not feasible. These inputs are fed into the scenario generator.

The freeway scenario generator (FSG) develops operational scenarios that a freeway facility may experience and the probability that they may occur during a particular time period. These scenarios are based on the nonrecurrent congestion inputs in the data depository. The methodology assumes that events are independent (thus, the probability that an incident and precipitation occur at the same time is equal to the product of their individual probabilities). The scenarios are ultimately expressed as demand and capacity parameters and fed into the core computation engine, which is an extension of the freeway evaluation tool (called FREEVAL-RL).

The FREEVAL-RL tool extended on past methodologies and was developed to generate a reliability report that characterizes the travel time distribution of a particular scenario.

Other Reliability Research

This section describes other recent research and implementation efforts into other aspects of understanding travel time reliability. It details predictive models in practice, best practices in data processing techniques, current research on the optimal reliability metrics, and recently developed methodologies for understanding the relationship between nonrecurrent congestion and reliability in the SHRP 2 program.

Predictive Models in Practice

The Florida Department of Transportation's (FDOT) Reliability Model was featured in the SHRP 2 L05 final report as a best practice example of using reliability performance measures in planning and programming. FDOT's preferred reliability statistic is the percentage of trips that arrive on time, defined as within 10 mph of the free-flow speed (the posted speed limit plus 5 mph) of the section. FDOT's predictive model calculates expected travel times for a set of predefined scenarios, along with the probability of each scenario occurring. Each scenario assumes some set of conditions including congestion level, weather, incidents, and work zones. For a particular section of road, the estimated travel times for each scenario are combined with the expected frequency of the scenario to create the travel time distribution for the section. This methodology is applied to the entire state freeway system, regardless of instrumentation. Each freeway is divided into sections, and the model applied to each of the 24 h in a day for each segment direction.

The model uses four major causes of congestion: recurring, incidents, weather, and work zones. Data inputs include hourly demand-to-capacity ratios derived from AADT and hourly and directional distributions of traffic. Travel times are determined for each segment for each scenario according to the following:

- *Recurring congestion component.* Determined through HCM planning applications and CORSIM (corridor simulation traffic software) travel time estimations.
- *Incident component.* Impact determined by capacity reduction. Probability determined from FDOT crash data during different work zone and precipitation conditions, and an assumed ratio of non-blocking to lane-blocking events.
- *Weather component.* Impact assumed to be 6% speed reduction for light rain and 12% for heavy rain. Probability of clear weather (<0.01 in./h), light rain (0.01 to 0.5 in./h), and

heavy rain (>0.5 in./h) determined from Weather Underground data.
- *Work Zone component.* Impact determined by capacity reduction. No data available, so constant probabilities assumed during particular times of day (3% overnight, 1% otherwise).

The data produced by this model are used for systemwide reporting and to set project priorities.

Data Processing

Applying best practices of traffic data processing techniques is an important component of the L33 project; how the data is quality controlled, aggregated, and turned into travel times as input into the model calibration ultimately affects the validity and applicability of the final results.

The SHRP 2 project that most fully addressed traffic data processing is L02, Establishing Monitoring Programs for Mobility and Travel Time Reliability. Chapters 3, 4, and 6 of the draft final report document methodologies for identifying and imputing bad traffic data from point detectors and filtering unrepresentative travel times from automated vehicle identification (AVI) and automated vehicle location (AVL) data sources. Figure A.9 illustrates these processing steps to show the computations that need to be performed on each type of data. Many of the findings in the L02 final documents directly relate to the required data processing needed to validate the L03 data-rich and data-poor models, including

1. Filtering detector data to remove samples with poor data quality;
2. Filtering AVI travel times to remove unrepresentative travel times;
3. Calculating segment and route travel times from time-mean-speeds; and
4. Estimating individual vehicle travel time probability density functions (PDFs) from facility-average travel times.

Reliability Metrics

Many of the SHRP 2 Reliability projects have performed user surveys and analysis to determine the optimal measures for summarizing reliability for different audiences. The L03 project explored measures commonly used in the United States and Europe to identify the set of measures to use in projects. Exploratory analysis showed that index measures (like the buffer index and planning time index) are not optimal for tracking reliability improvements because some improvements can make the mean (or median) travel time improve more than the 95th percentile travel time, thus showing a worsening in reliability. General consensus among the SHRP 2 Reliability projects and other research is that the best measures are those that provide information on the underlying travel time distributions. The L03 reliability models predict the mean, median, and 10th-, 80th-, 90th-, and 95th- percentile travel times. From these values, skew can be computed. The L07 extended-L03 models generate continuous probability density functions in the low-demand equation of their predictive model.

While the goal of reliability monitoring and prediction is to provide a full PDF of travel time conditions, the PDF can be developed in different ways. In an ideal monitoring environment, and one that will be possible in the future, travel times can be collected from every individual vehicle traversing a segment. In this case, a PDF of 5-min-level travel times can be assembled in one of two ways: (1) an individual traveler-level PDF, which is based on the full set of travel times measured across all vehicles that made the trip during

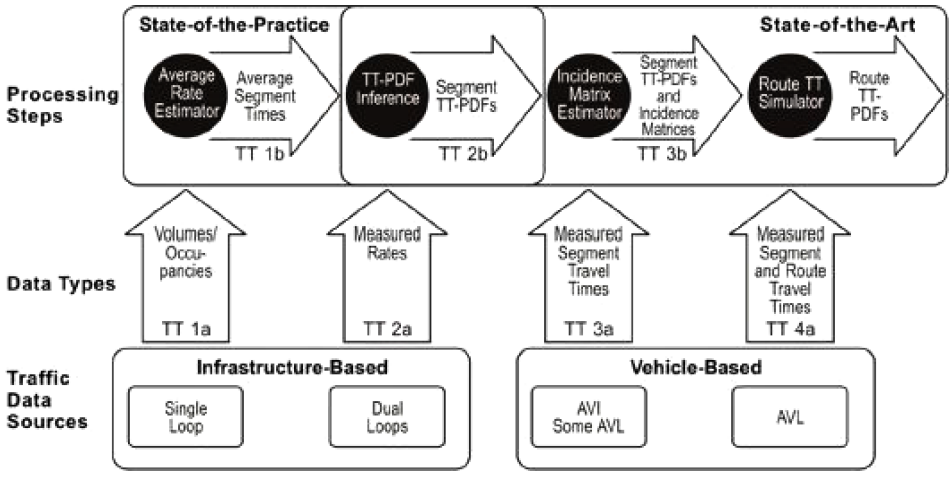

Figure A.9. L02 data processing by technology.

that 5-min period over a year, or (2) a facility-level PDF, in which the individual vehicle travel times are averaged within each 5-min period, and the PDF is composed of the 5-min average travel times across the year. The L02 project developed methodologies and guidance on developing both types of PDFs from different detection technologies. The L03 project produced a different PDF; the average 5-min travel times across a year were put into travel time bins, then each bin was weighted by the number of travel times in the bin as well as the average volume on the segment across all the time periods that experienced that travel time. This is similar to the individual traveler-level PDF in that it weights travel times by the number of vehicles that experienced them, but different in that it does not capture the variability of travel times within a single 5-min period.

Nonrecurrent Congestion Methodologies

A major piece of the SHRP 2 Reliability program is figuring out how the factors of nonrecurrent congestion affect travel time reliability. FHWA identified seven sources of nonrecurrent congestion: (1) incidents, (2) weather, (3) work zones, (4) fluctuation in demand, (5) special events, (6) traffic control devices, and (7) inadequate base capacity. This section addresses the outputs from the SHRP 2 program that seek to quantify the relationship between nonrecurrent congestion and reliability.

SHRP 2 L03

Outside of the predictive reliability model research, the L03 team performed a detailed congestion-by-source analysis using the collected Seattle data. The work was performed by associating disruptions with travel times and delay. The analysts used 5-min delay and travel time data and data on the sources of congestion to assign influence variables to time periods affected by disruptions, grouped into incidents, incidents involving lane closures, vehicle crashes, active construction events, bad weather, and rubbernecking (delay in the opposite direction of travel of the incident). Methodologies were also developed to relate off-segment congestion influences to the segment being studied. Performance during the disruptions was compared with the segment's baseline performance. The results of the analysis ultimately summarize the percentage of delay caused by the different types of disruptions.

SHRP 2 L02

The L02 project performed similar analyses but related the sources of congestion to the underlying travel time PDFs. The project's guidebook recommends six steps for assessing the reliability impacts of influencing factors:

1. Select the region or facilities of interest.
2. Select a timeframe of interest.
3. Assemble travel rate data for each facility.
4. Generate PDFs for each facility.
5. Understand variations in reliability as a result of congestion.
6. Develop cumulative distribution functions (CDFs) for each combination or recurring congestion level and nonrecurring event.

An example of the final step is shown in Figure A.10.

SHRP 2 L08

The L08 project has performed significant analysis into quantifying the reliability impact of nonrecurrent congestion events to feed into the HCM update. In the L08 project, variability in demand, weather, and incidents are the nonrecurrent congestion factors that affect travel time reliability. The

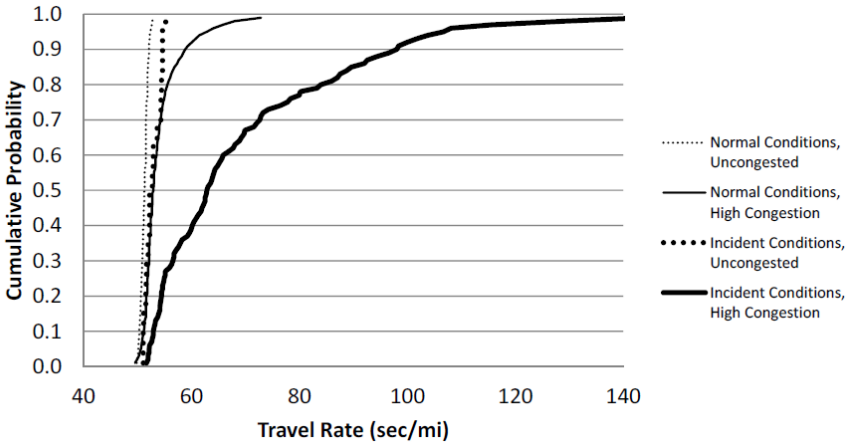

Figure A.10. Influencing factor CDF, L02.

L08 methodology incorporates these factors by discretizing a particular factor into a category and estimating the probability that each category of factor will occur during a particular time period. Demand is categorized into different demand patterns that are facility-specific and organized by day of week and month. The probability of each demand pattern occurring within a particular time period is then easily computed from the frequency of that demand pattern by day of week and month in the study period. Weather is categorized into the HCM categories shown to impact travel time: medium rain, heavy rain, light snow, light-medium snow, medium-heavy snow, heavy snow, very low visibility, minimal visibility, and normal weather. The frequency of these categories can easily be estimated from hourly weather data. Incidents are grouped into six categories based on their severity or capacity impacts: no incident, shoulder closure, one-lane closure, two-lane closure, three-lane closure, and four-lane closure. Probabilities can be computed from empirical data.

Conclusions

This final section summarizes lessons learned from the background review and details potential opportunities for further exploration in the L33 project.

Validating in Multiple Regions with Diverse Characteristics

The L03 data-rich and data-poor models were validated in only one location, Seattle, a metropolitan area that had vastly different weather patterns from any of the calibration locations. As such, it is critical that the L33 project performs the validation at multiple sites with a wide range in climate and operational policies.

Finding Sufficiently Detailed Data Sets

The L03 team experienced significant challenges in acquiring data sets that had a sufficient level of detail needed to calibrate the predictive models, particularly with regard to disruptions like incidents and lane closures. In one example, the L03 team thought that the Traffic.com data it had purchased in most of the study areas contained lane closure data but, on further investigation, determined that lane closure data was infrequently and inconsistently reported. In another example, the L03 team had planned to incorporate an agency's incident clearance policies into the data-rich predictive model by using agency-reported TIM scores, but subsequently learned that only a few of the study areas had reported TIM scores. These experiences highlight the importance of seeking out data sources, guaranteeing their availability, and making sure that together they can be used to estimate all of the desired model variables.

Implementing Best Practices of Data Processing

A major portion of L03 resources were spent on quality controlling and processing the collected traffic and incident data, a necessary effort for ensuring valid model results. In the time since the L03 analysis was conducted, the L02 project, which focused on monitoring travel time reliability, has been completed and published and is in the process of being implemented. The timing of the L33 project is such that it is well-positioned to take advantage of the best practices in traffic and nonrecurrent congestion source data processing established by the SHRP 2 program.

Accurately Capturing Demand

SHRP 2 research has found the complex interaction between demand and capacity to be a critical determinant of travel time reliability. The L03 project established an empirical approach for estimating demand for every 5-min period, but exploratory analysis performed by the L33 team has shown that this can produce inaccurate results in a number of cases. This estimation process appears to be an opportunity for improvement in the L33 project.

Capturing the Right Independent Variables

The L03 project found that the demand-to-capacity ratio, the ILHL, and the number of hours with precipitation exceeding 0.05 in. to be the key predictors of reliability in a data-rich environment. However, the L03 team recommended that further investigation consider modifying the ILHL variable to account for the total number of lanes at the location. In extending the L03 data-rich models, the L07 project team modified the precipitation variable to also include hours of snowfall exceeding 0.01 in. A major focus of the L33 project will be to assess whether the modification of existing independent variables or the addition of further independent variables reduce the calibration and validation errors.

Further Investigation of the Relationship Between the Mean Travel Time and Reliability

Both the L03 and L04 projects independently arrived at the conclusion that measures of travel time reliability can be predicted with reasonable accuracy from the mean travel time. However, when the L03 team validated the data-poor model in Seattle, they noted that it significantly underpredicted high percentile travel times, even though the model had strong goodness-of-fit in the calibration stage. The L33 team plans to investigate whether this relationship is the ideal form for a predictive data-poor model.

Measuring the Travel Time Probability Density Function

In measuring the travel time probability density functions of each study section for calibration and validation of the data-rich and data-poor models, the L03 project team weighted each measured travel time bin by the frequency it occurred as well as the average volume on the segment across the 5-min time periods that experienced that travel time. According to the L03 principal investigator, this was done to ensure that the models will still be applicable in the future when it is possible to directly measure travel times from every vehicle traversing a segment. However, the PDF approximated in L03 is still fundamentally different from that assembled from individual vehicle travel times, which accounts for the variability of travel times between different vehicles traversing the same segment at the same time. In L33, the project team wants to explore the PDF assumption made in L03 and assess the value of providing models to predict other PDF forms.

Predicting a Travel Time Probability Density Function

Recent reliability research concludes that the closer one can get to measuring or predicting the full travel time probability density function the better the understanding of reliability will be. A full PDF can support the computation of any travel time reliability measure. The L07 team has already extended the L03 models such that, for low-demand conditions, they can predict a continuous PDF. The L33 team plans to evaluate revised equations and methodologies that can provide a fuller picture of segment-level travel time reliability.

References

Barkley, T., R. Hranac, and K. Petty. Relating Travel Time Reliability and Nonrecurrent Congestion with Multistate Models. In *Transportation Research Record: Journal of the Transportation Research Board, No. 2278,* Transportation Research Board of the National Academies, Washington, D.C., 2012.

Cambridge Systematics, Inc. Final Report. *SHRP 2 Report S2-L05-RW-1: Incorporating Reliability Performance Measures into the Transportation Planning and Programming Processes.* Transportation Research Board of the National Academies, Washington, D.C., 2014.

Cambridge Systematics, Inc. Technical Reference. *SHRP 2 Report S2-L05-RW-1: Incorporating Reliability Performance Measures into the Transportation Planning and Programming Processes.* Transportation Research Board of the National Academies, Washington, D.C., 2014.

Cambridge Systematics, Inc.; Texas Transportation Institute; University of Washington; Dowling Associates; Street Smarts; H. Levinson, and H. Rakha. Final Report. *SHRP 2 Report S2-L03-RR-1: Analytical Procedures for Determining the Impacts of Reliability Mitigation Strategies.* Transportation Research Board of the National Academies, Washington, D.C., 2013.

Cambridge Systematics, Inc.; Texas Transportation Institute; University of Washington; Dowling Associates; Street Smarts; H. Levinson, and H. Rakha. Phase 1 Report. SHRP 2 L03 Project, Analytical Procedures for Determining the Impacts of Reliability Mitigation Strategies. Transportation Research Board of the National Academies, Washington, D.C., 2009.

Cambridge Systematics, Inc.; Texas Transportation Institute; University of Washington; Dowling Associates; Street Smarts; H. Levinson, and H. Rakha. Phase 2 Report. SHRP 2 L03 Project, Analytical Procedures for Determining the Impacts of Reliability Mitigation Strategies. Transportation Research Board of the National Academies, Washington, D.C., 2009.

Delcan, Northwestern University, and Parsons Brinckerhoff. Draft Task 7 Report. *SHRP 2 Report S2-L04-RW-2: Incorporating Reliability Performance Measures in Operations and Planning Modeling Tools.* Transportation Research Board of the National Academies, Washington, D.C., 2013.

ITRE, Iteris, Kittelson & Associates, National Institute of Statistical Sciences, University of Utah, Rensselaer Polytechnic University, and A. Khattak of Planitek. Final Report. *SHRP 2 Report S2-L02-RR-1: Establishing Monitoring Programs for Travel Time Reliability.* Transportation Research Board of the National Academies, Washington, D.C., 2012.

Kittelson & Associates, Inc.; Cambridge Systematics; ITRE; and Texas A&M Research Foundation. Draft Final Report. *SHRP 2 Report S2-L08-RW-1: Incorporation of Travel Time Reliability into the Highway Capacity Manual.* Transportation Research Board of the National Academies, Washington, D.C., 2013.

Kwon, J., T. Barkley, R. Hranac, K. Petty, and N. Compin. Decomposition of Travel Time Reliability into Various Sources: Incidents, Weather, Work Zones, Special Events, and Base Capacity. In *Transportation Research Record: Journal of the Transportation Research Board, No. 2229,* Transportation Research Board of the National Academies, Washington, D.C., 2011.

Kwon, J., M. Mauch, and P. Varaiya. Components of Congestion. In *Transportation Research Record: Journal of the Transportation Research Board, No. 1959,* Transportation Research Board of the National Academies, Washington, D.C., 2006.

Mahmassani, H., T. Hou, and H. Dong. Characterizing Travel Time Reliability in Vehicular Networks: Deriving a Robust Relation for Reliability Analysis. In *Transportation Research Record: Journal of the Transportation Research Board, No. 2315,* Transportation Research Board of the National Academies, Washington, D.C., 2012.

McLeod, D., L. Elefteriadou, and L. Jin. *Travel Time Reliability as a Performance Measure: Applying Florida's Predictive Model on the State's Freeway System.* Submitted for Presentation and Publication to the TRB 2012 Annual Meeting. October 2011.

MRI Global. Draft Final Report. *SHRP 2 Report S2-L07-RR-1: Identification and Evaluation of the Cost-Effectiveness of Highway Design Features to Reduce Nonrecurrent Congestion.* Transportation Research Board of the National Academies, Washington, D.C., 2013.

Pu, W. Analytic Relationships Between Travel Time Reliability Measures. In *Transportation Research Record: Journal of the Transportation Research Board, No. 2254,* Transportation Research Board of the National Academies, Washington, D.C., 2011.

Texas Transportation Institute. 2007. *Quality Control Procedures for Archived Operations Traffic Data: Synthesis of Practice and Recommendations: Final Report.* Federal Highway Administration, U.S. Department of Transportation, Washington, D.C.

Van Lint, J. W. C., and H. J. van Zuylen. Monitoring and Predictive Travel Time Reliability. In *Transportation Research Record: Journal of the Transportation Research Board, No. 1917,* Transportation Research Board of the National Academies, Washington, D.C. 2005.

Appendix A Attachment

This attachment lists the equations for the data-rich and data-poor models from L03 and L07 projects, which are noted in Appendix A.

L03 Data-Rich Equations, Chapter 7 of Final Report

Peak Period

mean TTI = $e^{(0.09677 * dc_{crit} + 0.00862 * ILHL + 0.00904 * Rain05Hrs)}$ (1)

RMSE = 18.8%; alpha level of coefficients: <0.0001, <0.0001, 0.0189 (in order of appearance in the equations)

99th-percentile TTI = $e^{(0.33477 * dc_{crit} + 0.012350 * ILHL + 0.025315 * Rain05Hrs)}$ (2)

RMSE = 39.8%; alpha level of coefficients: <0.0001, 0.0002, 0.0022

95th-percentile TTI = $e^{(0.23233 * dc_{crit} + 0.01222 * ILHL + 0.01777 * Rain05Hrs)}$ (3)

RMSE = 32.3%; alpha level of coefficients: <0.0001, <0.0001, 0.0078

80th-percentile TTI = $e^{(0.13992 * dc_{crit} + 0.01118 * ILHL + 0.01271 * Rain05Hrs)}$ (4)

RMSE = 25.8%; alpha level of coefficients: <0.0001, <0.0001, 0.0163

50th-percentile TTI = $e^{(0.09335 * dc_{crit} + 0.00932 * ILHL)}$ (5)

RMSE = 20.5%; alpha level of coefficients: <0.0001, <0.0001

10th-percentile TTI = $e^{(0.01180 * dc_{crit} + 0.00145 * ILHL)}$ (6)

RMSE = 6.7%; alpha level of coefficients: 0.0169, 0.0060

Peak Hour

mean TTI = $e^{(0.27886 * dc_{crit} + 0.01089 * ILHL + 0.02935 * Rain05Hrs)}$ (7)

RMSE = 26.4%; alpha level of coefficients: 0.0008, 0.0094, 0.0838

99th-percentile TTI = $e^{(1.13062 * dc_{crit} + 0.01242 * ILHL)}$ (8)

RMSE = 41.3%; alpha level of coefficients: <0.0001, 0.0477

95th-percentile TTI = $e^{(0.63071 * dc_{crit} + 0.01219 * ILHL + 0.04744 * Rain05Hrs)}$ (9)

RMSE = 38.3%; alpha level of coefficients: <0.0001, 0.0436, 0.0553

80th-percentile TTI = $e^{(0.52013 * dc_{crit} + 0.01544 * ILHL)}$ (10)

RMSE = 34.1%; alpha level of coefficients: <0.0001, 0.0031

50th-percentile TTI = $e^{(0.29097 * dc_{crit} + 0.01380 * ILHL)}$ (11)

RMSE = 28.3%; alpha level of coefficients: <0.0001, 0.0015

10th-percentile TTI = $e^{(0.07643 * dc_{crit} + 0.00405 * ILHL)}$ (12)

RMSE = 15.2%; alpha level of coefficients: 0.0081, 0.0748

Midday (11:00 a.m. to 2:00 p.m., Weekdays)

mean TTI = $e^{(0.02599 * dc_{crit})}$ (13)

RMSE = 7.5%; alpha level of coefficient: <0.0001

99th-percentile TTI = $e^{(0.19167 * dc_{crit})}$ (14)

RMSE = 33.4%; alpha level of coefficient: <0.0001

$$95\text{th-percentile TTI} = e^{(0.07812 * dc_{crit})} \quad (15)$$

RMSE = 21.8%; alpha level of coefficient: <0.0001

$$80\text{th-percentile TTI} = e^{(0.02612 * dc_{crit})} \quad (16)$$

RMSE = 9.2%; alpha level of coefficient: <0.0001

$$50\text{th-percentile TTI} = e^{(0.01134 * dc_{crit})} \quad (17)$$

RMSE = 21.8%; alpha level of coefficient: <0.0001

$$10\text{th-percentile TTI} = e^{(0.00389 * dc_{crit})} \quad (18)$$

RMSE = 5.1%; alpha level of coefficient: <0.0016

Weekday

$$\text{mean TTI} = e^{(0.00949 * dc_{average} + 0.00067 * ILHL)} \quad (19)$$

RMSE = 29.3%; alpha level of coefficients: <0.0001, 0.0051

$$99\text{th-percentile TTI} = e^{(0.07028 * dc_{average} + 0.00222 * ILHL)} \quad (20)$$

RMSE = 38.9%; alpha level of coefficients: <0.0001, 0.0261

$$95\text{th-percentile TTI} = e^{(0.03632 * dc_{average} + 0.00282 * ILHL)} \quad (21)$$

RMSE = 31.8%; alpha level of coefficients: <0.0001, 0.0007

$$80\text{th-percentile TTI} = e^{(0.00842 * dc_{average} + 0.00117 * ILHL)} \quad (22)$$

RMSE = 14.7%; alpha level of coefficients: 0.0004, 0.0023

$$50\text{th-percentile TTI} = e^{(0.0021 * dc_{average})} \quad (23)$$

RMSE = 4.7%; alpha level of coefficients: <0.0001

$$10\text{th-percentile TTI} = e^{(0.00047 * dc_{average})} \quad (24)$$

RMSE = 2.0%; alpha level of coefficients: 0.0121

L03 Data-Poor Equations, Appendix H of Final Report

$$\text{meanTTI} = 1.0274 * \text{RecurringmeanTTI}^{1.2204} \quad (25)$$

More work remains to be done to make this adjustment more sensitive to the effect of disruptions. Revised section-level equations are as follows:

$$95\text{th-percentile TTI} = 1 + 3.6700 * \ln(\text{meanTTI}) \quad (26)$$

$$90\text{th-percentile TTI} = 1 + 2.7809 * \ln(\text{meanTTI}) \quad (27)$$

$$80\text{th-percentile TTI} = 1 + 2.1406 * \ln(\text{meanTTI}) \quad (28)$$

$$\text{StdDevTTI} = 0.71 * (\text{meanTTI} - 1)^{0.56} \quad (29)$$

$$\text{PctTripsOnTime50mph} = e^{(-2.0570 * [\text{meanTTI} - 1])} \quad (30)$$

$$\text{PctTripsOnTime45mph} = e^{(-1.5115 * [\text{meanTTI} - 1])} \quad (31)$$

$$\text{PctTripsOnTime30mph} = 0.333 + \left[0.672/\left(1 + e^{(5.0366 * [\text{meanTTI} - 1.8256])}\right)\right] \quad (32)$$

L03 Data-Poor Equations, Chapter 7 of Final Report

$$95\text{th-percentile TTI} = \text{meanTTI}^{1.8834} \quad (33)$$

RMSE = 15.7%; alpha level of coefficient < 0.0001

$$90\text{th-percentile TTI} = \text{meanTTI}^{1.6424} \quad (34)$$

RMSE = 9.4%; alpha level of coefficient < 0.0001

$$80\text{th-percentile TTI} = \text{meanTTI}^{1.365} \quad (35)$$

RMSE = 4.5%; alpha level of coefficient < 0.0001

$$\text{median TTI} = \text{meanTTI}^{0.8601} \quad (36)$$

RMSE = 6.3%; alpha level of coefficient < 0.0001

$$10\text{th-percentile TTI} = \text{MeanTTI}^{0.1524} \quad (37)$$

RMSE = 5.4%; alpha level of coefficient < 0.0001

$$\text{PctTripsOnTime10} = 1 - \left(0.4396 * [\text{meanTTI} - 1]^{0.4361}\right) \quad (38)$$

RMSE = 8.4%

where PctTripsOnTime10 is the percentage of trips that occur below the threshold of 1.1 * median TTI.

$$\text{PctTripsOnTime25} = 1 - \left(0.2861 * [\text{meanTTI} - 1]^{0.5251}\right) \quad (39)$$

RMSE = 7.5%

where PctTripsOnTime25 is the percentage of trips that occur below the threshold of 1.25 * median TTI.

$$\text{PctTripsOnTime50mph} = 1 - \left(0.8985 * [\text{meanTTI} - 1]^{0.6387}\right)$$

RMSE = 18.0% (40)

where PctTripsOnTime50mph is the percentage of trips that occur at space mean speeds above the threshold of 50 mph.

$$\text{PctTripsOnTime45mph} = 1 - \left(0.8203 * [\text{meanTTI} - 1]^{0.7692}\right)$$

RMSE = 14.0% (41)

Table A.5. TTI Prediction Model Coefficients

N (percentile)	D/C ≤ 0.8[a]				D/C > 0.8					
	a_n	b_n	c_n	d_n	a_n	b_n	$c1_n$	$c2_n$	$d1_n$	$d2_n$
10	0.01400	0.00099	0.00015	0.00037	0.07643	0.00405	1.364	–28.34	0.178	15.55
50	0.07000	0.00495	0.00075	0.00184	0.29097	0.01380	0.966	–6.74	0.345	3.27
80	0.11214	0.00793	0.00120	0.00310	0.52013	0.01544	0.630	6.89	0.233	5.24
95	0.19763	0.01557	0.00197	0.01056	0.63071	0.01219	0.639	5.04	0.286	1.67
99	0.47282	0.04170	0.00300	0.02293	1.13062	0.01242	0.607	5.27	0.341	–0.55

[a] Coefficients for $D/C \le 0.8$ are continuous functions of n. See text below for more description.

where PctTripsOnTime45mph is the percentage of trips that occur at space mean speeds above the threshold of 45 mph.

$$\text{PctTripsOnTime30mph} = 1 - \left(0.4139 * [\text{meanTTI} - 1]^{1.5527}\right)$$

$$\text{RMSE} = 4.4\% \qquad (42)$$

where PctTripsOnTime30mph is the percentage of trips that occur at space mean speeds above the threshold of 30 mph.

$$\text{standard deviation} = 0.6182 * (\text{meanTTI} - 1)^{0.5404} \qquad (43)$$

$R^2 = 0.781$; alpha levels of coefficients < 0.0001

L07 Model Equations, Chapter 4 of Final Report

$$\text{TTI}_n = \begin{cases} \text{TTI}_{\text{NP},n} \times e^{(c_n R_{05"} + d_n S_{01"})} & \text{for } D/C \le 0.8 \\ \dfrac{\text{TTI}_{\text{NP},n}}{N_{\text{days}}} \times \left[N_{\text{NP}} + V_{\text{FF}} \left(\dfrac{R_{05"}}{c1_n V_{\text{FF}} + c2_n \text{TTI}_{\text{NP},n}} + \dfrac{S_{01"}}{d1_n V_{\text{FF}} + d2_n \text{TTI}_{\text{NP},n}} \right) \right] & \text{for } D/C > 0.8 \end{cases} \qquad (44)$$

where

TTI_n = the predicted nth-percentile travel time index
$\text{TTI}_{\text{NP},n}$ = the nonprecipitation portion of $\text{TTI}_n = e^{(a_n D/C + b_n \text{LHL})}$
LHL = lane-hours lost due to incidents and work zones (see L07 report Chapter 4)
D/C = demand-to-capacity ratio (see L07 final report Section 4.2.2)
$R_{05"}$ = number of hours in time slice with rain exceeding 0.05 in. (See L07 final report Chapter 4)
$S_{01"}$ = number of hours in time slice with snow exceeding 0.01 in. (See L07 final report Chapter 4)
N_{days} = number of hours in time slice (365)
N_{NP} = number of hours in time slice with no precipitation = $N_{\text{days}} - R_{05\text{ in.}} - S_{01\text{ in.}}$
V_{FF} = free-flow travel time on segment, mph
a_n, b_n = nth-percentile coefficients for nonprecipitation components (D/C and LHL). (See L07 final report Table 4.5)
c_n, d_n = nth-percentile coefficients for rain and snow components, respectively ($D/C < 0.8$). (See L07 final report Table 4.5)
$c1_n, c2_n$ = nth-percentile coefficients for rain component ($D/C > 0.8$). (See L07 final report Table 4.5)
$d1_n, d2_n$ = nth-percentile coefficients for snow component ($D/C > 0.8$). (See L07 final report Table 4.5)

For the $D/C \le 0.8$ models, the four coefficients (a_n, b_n, c_n, d_n) were developed as continuous functions of the TTI percentile (n), allowing prediction of any percentile value (the entire cumulative TTI curve), not just the five percentiles shown in Table A.5.

These coefficient functions are built with subcoefficients, as shown in the equation below (with values in Table A.6).

$$\text{coeff}_n = wn + xy^{z(n-1)} \qquad (45)$$

where

coeff_n = one of the four coefficients in the TTI_n formula (a_n, b_n, c_n, d_n)
n = percentile (scaled between 0 and 1.0)
w, x, y, z = subcoefficient (shown in Table A.6)

Table A.6. Subcoefficient Values for TTI Prediction Model (D/C < 0.8)

coeff_n	Subcoefficients			
	w	x	y	z
a_n	0.14	0.504	96	9
b_n	0.0099	0.0481	96	9
c_n	0.00149	0.0197	68	6
d_n	0.00367	0.0248	36	7

APPENDIX B

Validation Plan

Purpose

The purpose of this document is to detail the data collection and analysis plans for performing the validation of the L03 data-rich and data-poor models. As such, this document contains three sections. The data collection plan section describes the data used in the L03 project, lists the data requirements for model validation, and details the metropolitan areas and data sets available for validation and enhancement activities. The analysis plan lists the steps needed to transform the raw collected data into the final analysis data sets for model validations. Finally, the conclusions section synthesizes the validation design.

Data Collection Plan

Overview

The L03 team calibrated and validated its models using urban freeway data collected in the following metropolitan areas:

- Atlanta, Georgia (calibration);
- Houston, Texas (calibration);
- Jacksonville, Florida (calibration);
- Los Angeles, California (calibration);
- Minneapolis–St. Paul, Minnesota (calibration);
- San Diego, California (calibration);
- San Francisco, California (calibration); and
- Seattle, Washington (validation).

The L03 team selected these sites in part because their agencies collect and archive continuous, high-quality traffic data. These characteristics are also critical for L33 validation and enhancement activities. As such, this validation plan proposes to use data collected in many of the same locations. The L33 project team will ensure that the model validation performed in L33 does not use the same data collected during the same time frame on the same freeways segments as were used to calibrate or validate the models in L03. Because this is a critical requirement, this data collection plan reviews the regions and data sets used in L03.

Validation Data Characteristics

This section lists the metropolitan area and data sets requirements, as well as the optimal data set features, for performing the data-rich and data-poor model validation. These requirements and features have been developed by evaluating the L03 data processing methodologies and application guidelines.

Metropolitan Area Requirements

- Region must have continuous archived data for at least one urban freeway;
- Selected regions must offer a wide variety of seasonal weather conditions; and
- At least five regions must be selected for validation.

Data Set Requirements

- At least a year of traffic data must be available;
- At least a year of hourly precipitation data must be available (data-rich only);
- At least a year of incident data must be available (data-rich only); and
- Urban freeway sections must offer high-quality traffic data collected from detectors at a dense spacing.

Optimal Data Set Features

- At least a year of work zone data are available;
- At least a year of travel time data collected from technologies other than point detectors are available; and
- Incident data contain detailed and accurate information on the lane blockages and duration.

Proposed Regions

Overview

This section details the characteristics of the metropolitan areas and data sets that the L33 team has identified as suitable for use in the model validation and/or enhancement stages of this project.

The L33 team has identified 10 metropolitan areas from which to acquire data for validation and enhancement purposes. These metropolitan regions, which are listed with key characteristics in Table B.1 and further detailed in the rest of this section, were selected based on the criteria defined in the validation data characteristics. Five of the sites were also used in the L03 project. For L33, the project team has made efforts to acquire more recent data than were used for calibration and validation in L03. A chart comparing the data by region used in L03 with the traffic data available to the L33 team is shown in Figure B.1.

Atlanta

The L33 team possesses 6 months of archived traffic data and 3 months of archived incident and work zone data collected through the SHRP 2 L02 project.

L02 collected two types of traffic data in Atlanta:

(1) Data from camera and radar detectors collected in real time from the Georgia Department of Transportation's (GDOT) Navigator Advanced Transportation Management System (ATMS) and speed; and

(2) Travel time data acquired from data-reseller Navteq (now NOKIA).

The point detector data has been quality controlled using L02 methodologies and is aggregated to the 5-min level, which is consistent with the L03 model data needs. The Navteq data have also been aggregated to the 5-min level.

The L33 team also has 3 months of incident and work zone data, collected in L02 from Atlanta traffic management centers through the Navigator system. The incident and work zone data are highly detailed: they contain information on the type of incident, the number of lanes blocked, and the incident duration. This information is sufficient to directly calculate incident-lane-hours-lost by time period.

Archived hourly weather data are available from the National Climatic Data Center for multiple sensors in the metropolitan area.

The L03 data-rich and data-poor models were calibrated using Atlanta traffic and incident data collected from Navigator during the 2006 to 2008 timeframe. Maps of L02 data coverage and L03 study corridors are shown in Figure B.2. L03 does not have any Atlanta data from these years, so any L33 analysis will not temporally overlap with that of L03.

The L02 data set does not contain the full year of data required for L03 model validation. The incident data may be explored during validation to test the L03 relationships developed between the average number of lanes blocked per incident and the roadway geometry and incident clearance policies, as well as the ratio of collisions to incidents. This

Table B.1. Site Selection Matrix

Region	Traffic Data	L03 Site	Other Sources			Use in L33		
			Incidents	Work Zones	Weather	Data-Rich Validation	Data-Poor Validation	Enhancement
Atlanta	Detectors	X	X	X	X			X
	Navteq							X
Las Vegas	Detectors		X	X	X	X	X	X
Los Angeles	Detectors	X	X	X	X	X	X	X
Minneapolis	Detectors	X	X		X	X	X	X
Sacramento	Detectors		X	X	X	X	X	X
	Bluetooth							X
San Diego	Detectors	X	X	X	X	X	X	X
Salt Lake City	Detectors		X	X	X	X	X	X
San Francisco	Detectors	X	X	X	X	X	X	X
	Toll Tag	X				X	X	X
Spokane	Detectors		X	X	X	X	X	X
Washington, D.C.	Detectors		X		X	X	X	X

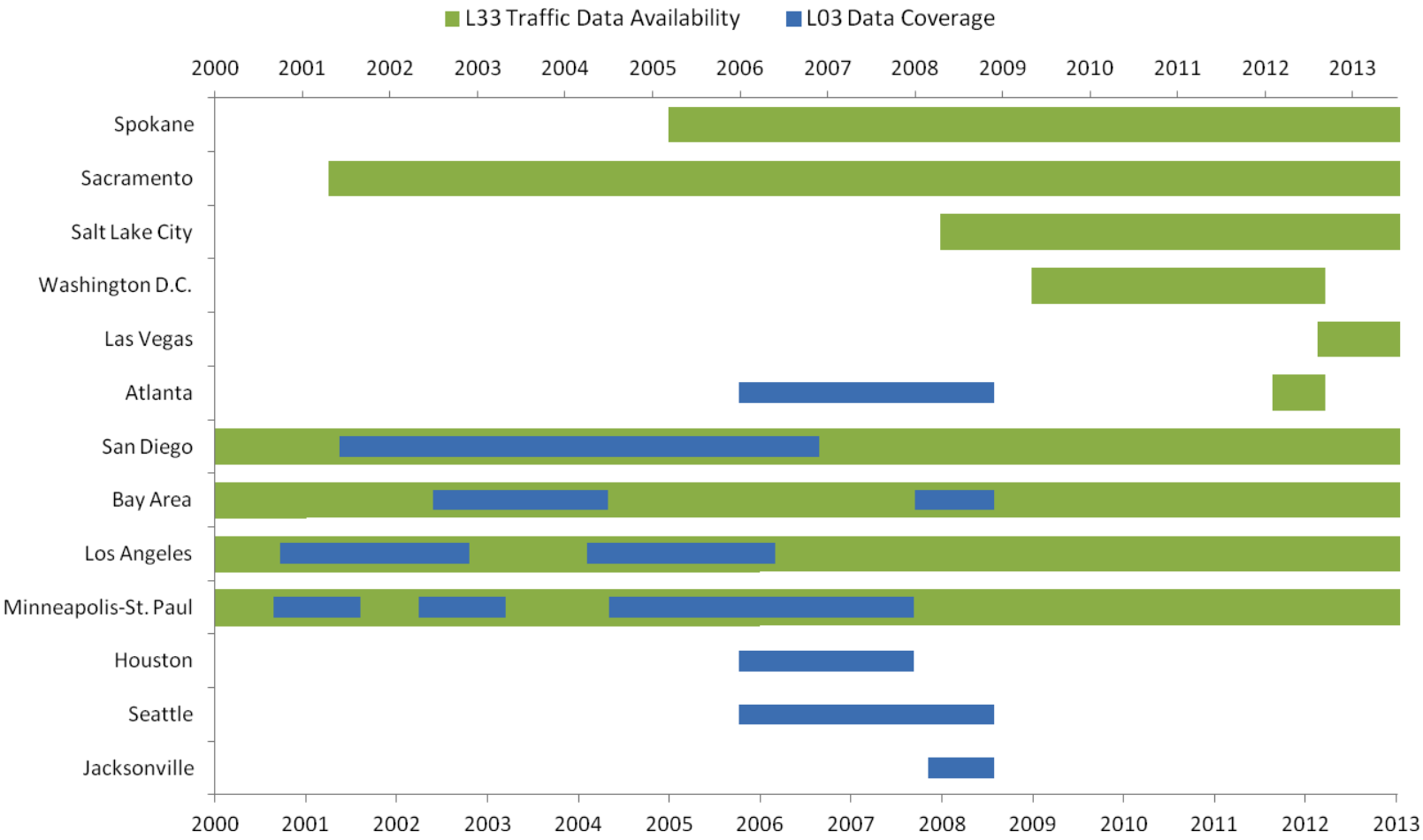

Figure B.1. L33 data availability and L03 data coverage. Note that validation will not be performed on the same freeway sections and years that were used to calibrate the L03 data-rich and data-poor models. In other words, no L03 data will be used in the L33 validation.

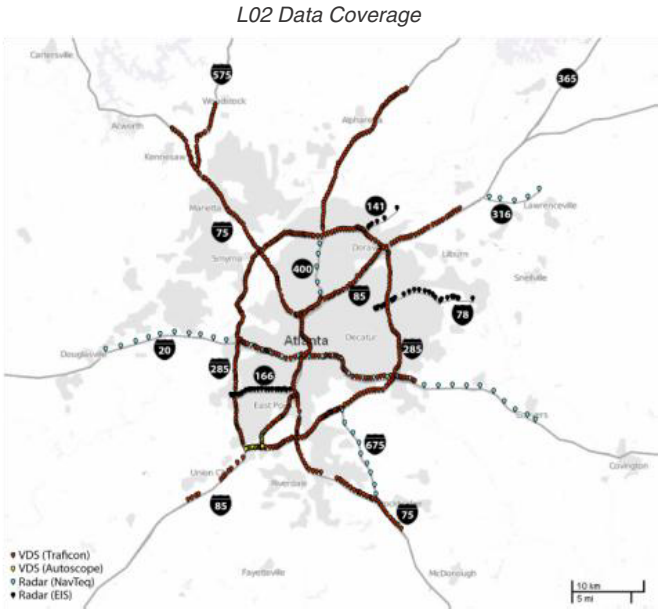

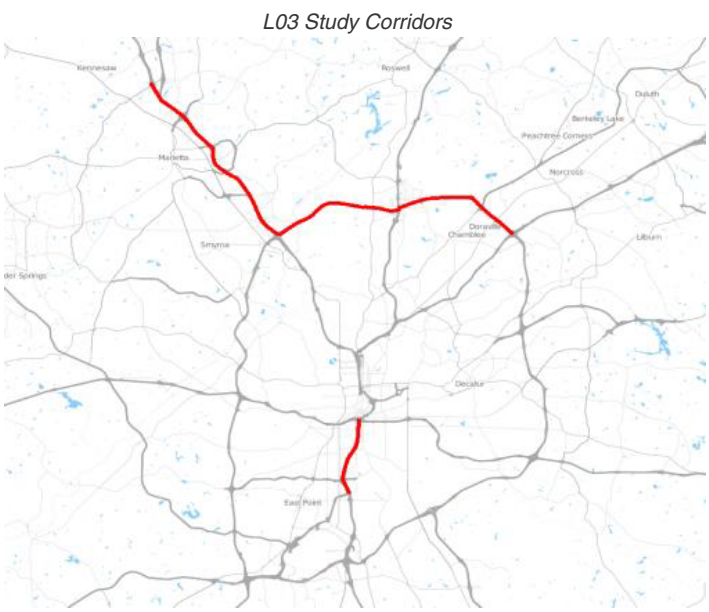

Figure B.2. Atlanta data availability and L03 usage.

investigation is further detailed in the analysis plan section of this document. This data set may also be further explored in the enhancement phase of this project as needed.

Las Vegas

The L33 team has a year (March 2012 to March 2013) of traffic, incident, and work zone data collected from the Regional Transportation Commission of Southern Nevada (RTC) Freeway and Arterial System of Transportation (FAST) via Iteris' Performance Measurement System (PeMS).

The traffic data were collected from point detectors; data coverage is shown in the speed map in Figure B.3. The traffic data have been quality controlled per L02 methodologies and are available at a 5-min granularity.

The incident and work zone data were collected from the FAST Traffic Management Center (TMC) and contain highly detailed information on the duration, lane blockage, and type of activity. This information is sufficient to directly calculate incident-lane-hours-lost by time period.

Archived hourly weather data are available from the National Climatic Data Center for multiple sensors in the metropolitan area.

No Las Vegas data were used in the L03 project, so this site adds regional diversity to the validation activities.

Los Angeles

Multiple years of traffic, incident, and work zone data are available in Los Angeles County and Orange County through the Caltrans PeMS.

The traffic data are collected from loop and radar detectors, are quality controlled per L02 methodologies, and are aggregated to the 5-min level. The spacing of detectors in Los Angeles County is very dense, but the percentage of working detectors has always hovered around 60%. The spacing in neighboring Orange County is of comparable density with much higher quality data (70% to 90% working detectors since 2009).

Figure B.3. Las Vegas data availability.

The L33 team has possession of two sources of incident data in the Los Angeles region, and throughout California, collected via PeMS:

(1) Incidents from the California Highway Patrol (CHP) collected in real time from the CHP media feed; and
(2) Traffic accidents from the Caltrans Traffic Accident Surveillance and Analysis System (TASAS), which contains severity and lane blockages, but no duration.

The CHP data contain the type of incident and duration but no standardized indication of the number of lanes blocked. The L33 team is currently exploring ways to parse the CHP log details, which often indicate lane blockages in free-text form, to estimate the number of lanes blocked. The TASAS accidents are compiled by Caltrans through accident reports. They report the accident severity and lane blockage but only include the incident start time (no duration information). As such, these data may not be usable in the data-rich model but may be explored in conjunction with the CHP data to obtain a ratio between the number of collisions and the number of overall incidents.

Work zone information is also available in this region, and throughout California, via PeMS. PeMS continuously collects and archives work zone information from the Caltrans Lane Closure System, which is used by Caltrans staff to plan, approve, and manage lane closures. PeMS data contain detailed information on the work zone start and end times, type of work, number of lanes closed, and estimated traffic impact. This information is sufficient to calculate the lane-hours-lost caused by work zones.

Archived hourly weather data are available from the National Climatic Data Center for multiple sensors in the metropolitan area.

In Los Angeles, the L03 team used traffic data collected from PeMS and incident data collected from traffic.com on two study segments in 2001, 2002, 2004, 2005, and 2006. The usage of Los Angeles data in L33 will not overlap in time and space with the usage in L03. Maps of Los Angeles data coverage and L03 study corridors are shown in Figure B.4.

Minneapolis

The L33 project team currently has 10 years of traffic data in the Minneapolis–St. Paul region archived in the Minnesota Department of Transportation's (MnDOT) PeMS. The data have been quality controlled per L02 methodologies and are available at a 5-min granularity.

The MnDOT PeMS also has slightly more than a year of traffic incident data archived from MnDOT's Intelligent Roadway Information System (IRIS) ATMS. To supplement this, the L03 project team has acquired an additional 4 years (2008 to 2012) of archived incident data from MnDOT. This incident data contain incident duration, type, and an indication of the traffic impact. This information is sufficient to calculate incident-lane-hours-lost by time period for input into the data-rich model.

No work zone data are available in Minneapolis.

In Minneapolis, the L03 team used traffic data collected from MnDOT and incident data from traffic.com in 2001 to 2007 to calibrate the data-rich and data-poor models. The usage of Minneapolis data in L33 will not overlap in time and space with

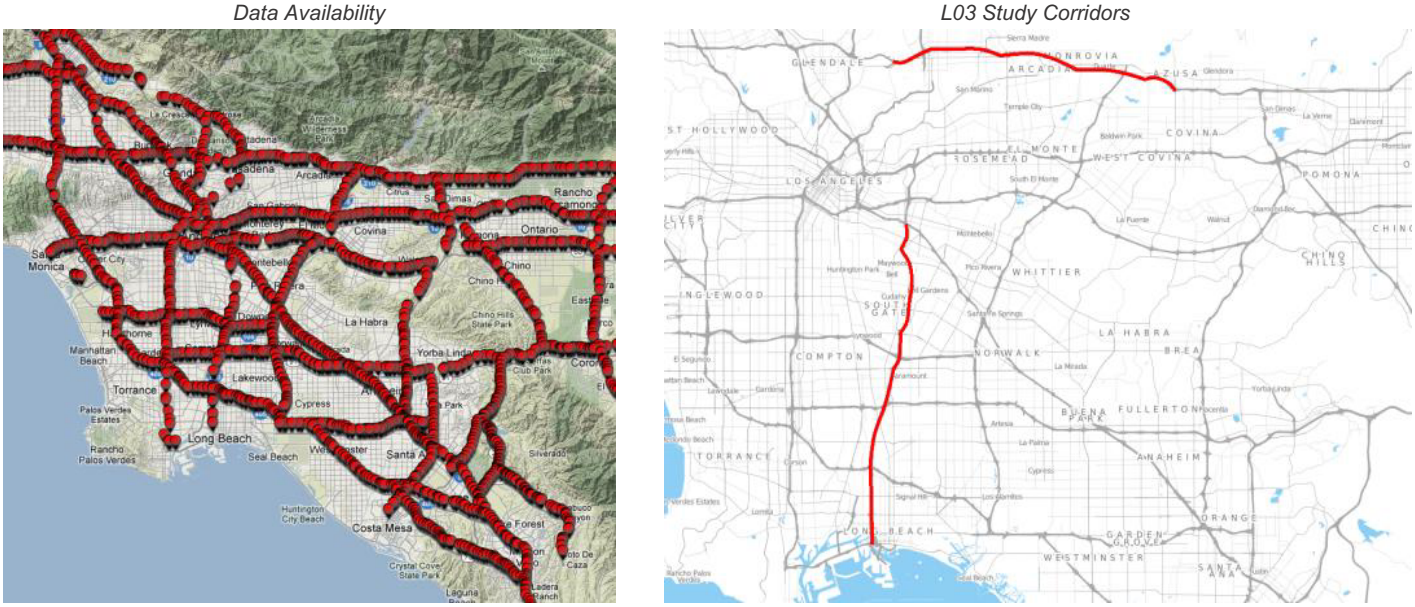

Figure B.4. Los Angeles data availability and L03 usage.

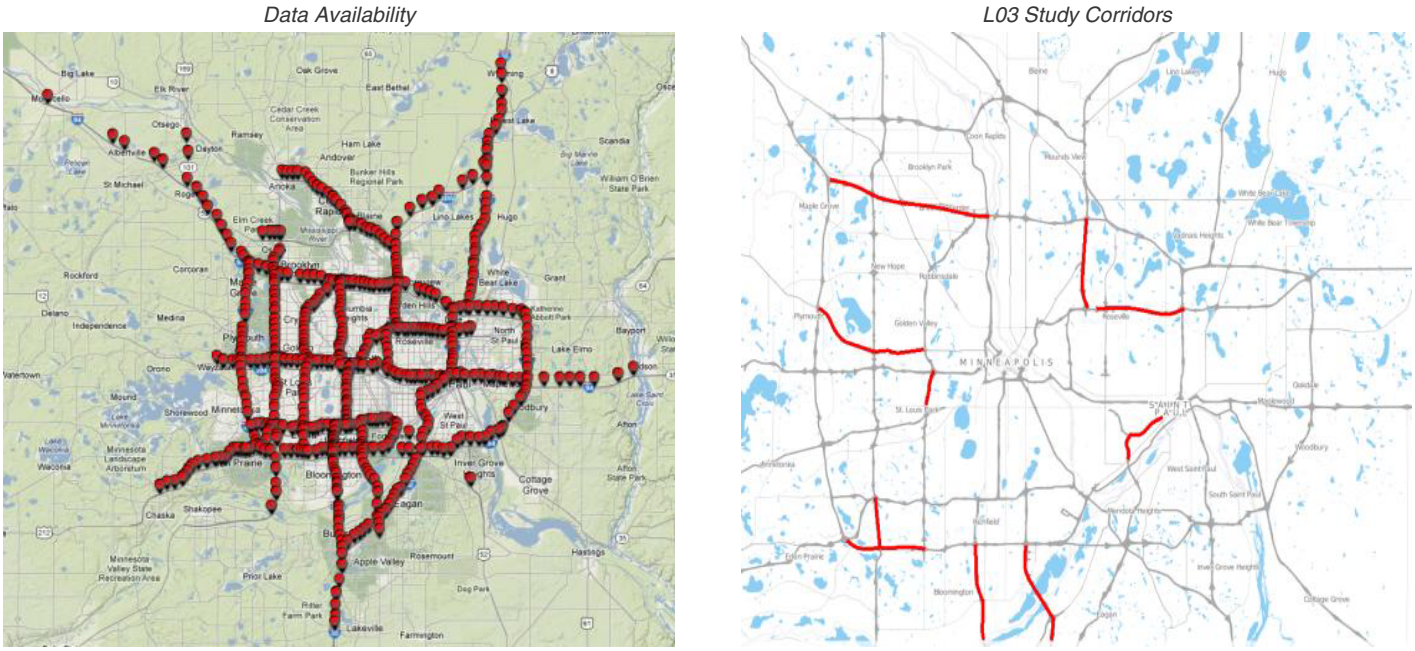

Figure B.5. Minneapolis–St. Paul data availability and L03 usage.

the usage in L03. Maps of Minneapolis data coverage and L03 study corridors are shown in Figure B.5. Even though Minneapolis was studied fairly extensively in L03, it is a critical validation region for L33 given its severe winter weather conditions.

Sacramento

Multiple years of traffic, incident, and work zone data are available in the Sacramento region through the Caltrans PeMS. The types of data available are the same as those described for Los Angeles. A map of the available traffic detection network is shown in Figure B.6.

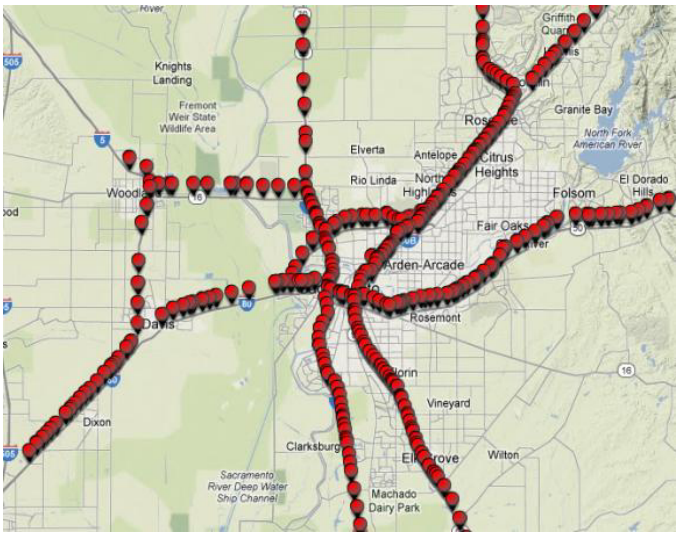

Figure B.6. Sacramento data availability.

In addition, the L02 project's case study efforts in Lake Tahoe included the collection of 4 months of Bluetooth data on a segment of Interstate 5 near downtown Sacramento. The remainder of the L02 data collected to support this case study was on rural freeways, so it is not useful for the L33 project. This quantity of Bluetooth data is not sufficient for validation purposes, but it will be critical for exploring Bayesian approaches in later phases of the project.

Archived hourly weather data are available from the National Climatic Data Center for multiple sensors in the metropolitan area.

No Sacramento data were used in the L03 project, so this site adds regional diversity to the validation activities. Additionally, the extreme fog conditions that this region can experience present an added vector into the weather analysis portion of the L33 project.

Salt Lake City

Multiple years of traffic data are available in the Salt Lake City region through the Utah Department of Transportation's (UDOT) PeMS. The data have been quality controlled and are available at a 5-min granularity. A map of the detection coverage is shown in Figure B.7.

UDOT's PeMS system does not contain any archived incident or work zone data. The L33 team is currently working with staff at the UDOT Traffic Operations Center to acquire archived incident and work zone data collected by the center's ATMS, with an anticipated delivery date of July 8, 2013. The

Figure B.7. Salt Lake City data availability.

team has been guaranteed the availability of these data, but has not yet acquired them. As such, the exact details and format of the data are currently unknown.

Archived hourly weather data are available from the National Climatic Data Center for multiple sensors in the metropolitan area.

No Salt Lake City data were used in the L03 project, so this area contributes regional diversity as well as another severe winter weather site to the validation activities.

San Diego

Multiple years of traffic, incident, and work zone data are available in the San Diego region through the Caltrans PeMS. The types of data available are the same as those described for Los Angeles. Archived hourly weather data are available from the National Climatic Data Center for multiple sensors in the metropolitan area.

San Diego was a multimodal case study site for the L02 project. The L02 project leveraged all of the data sources described above to develop a framework for linking travel time variability with the sources of nonrecurrent congestion.

In San Diego, the L03 team used traffic data collected from PeMS and incident data from traffic.com in 2001 to 2006. The usage of San Diego data in L33 will not overlap in time and space with the usage in L03. Maps of San Diego PeMS data coverage and L03 study corridors are shown in Figure B.8.

San Francisco

Multiple years of traffic, incident, and work zone data are available in the San Francisco Bay Area through the Caltrans PeMS. The types of data available are the same as those described for Los Angeles. In the past few years, the quality of detector data in the Bay Area has decreased, so L33 study corridors will have to be carefully selected and may have to rely on older data. In addition to the point detector data, PeMS also contains matched toll tag travel times. Archived hourly weather data are available from the National Climatic Data Center.

In the Bay Area, the L03 team used point detector and toll tag data collected from PeMS and incident data from

Data Availability

L03 Study Corridors

Figure B.8. San Diego data availability and L03 usage.

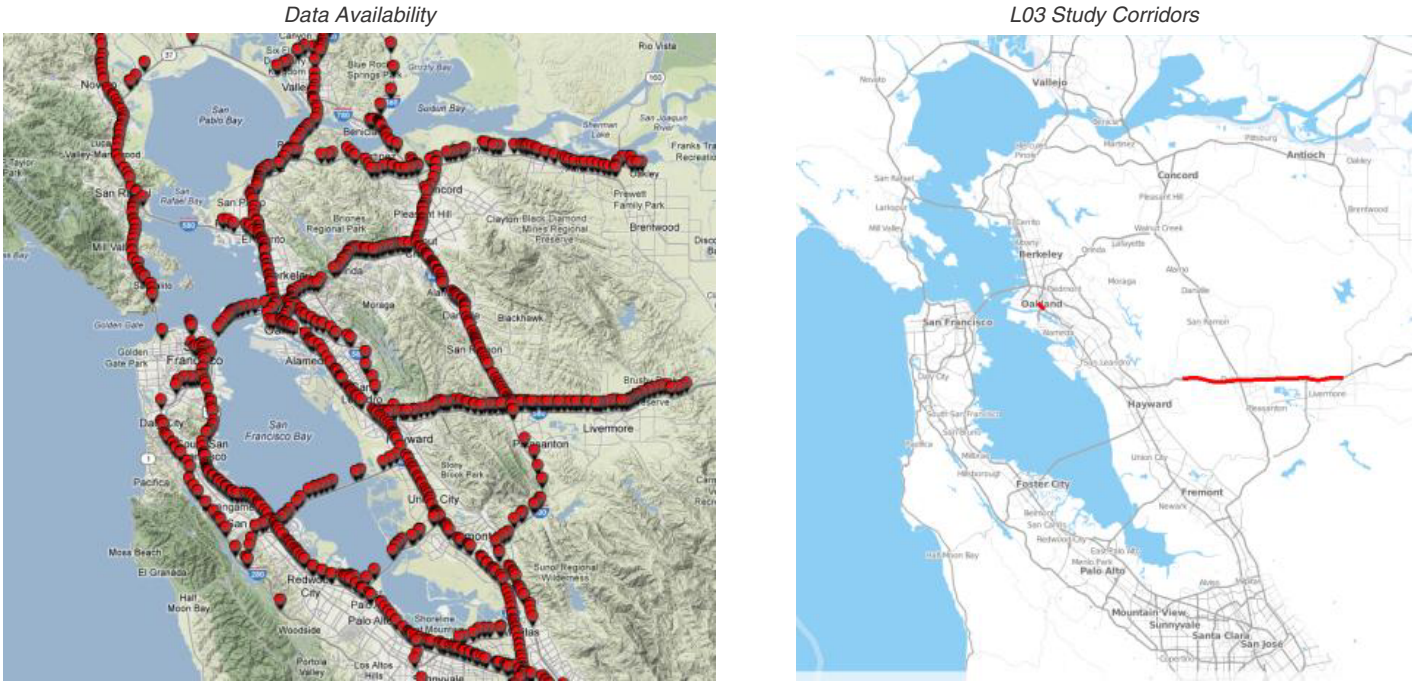

Figure B.9. San Francisco Bay Area data availability and L03 usage.

traffic.com in 2002. The usage of Bay Area data in L33 will not overlap in time and space with its usage in L03. Maps of Bay Area PeMS data coverage and L03 study corridors are shown in Figure B.9.

Spokane

Eight years of traffic data are available in the Spokane region via the Spokane Regional Transportation Management Center (SRTMC) PeMS. In Spokane, PeMS collects data from radar detectors that report data to the TMC. Figure B.10 shows the available detection network, which monitors the I-90 freeway through the city. The other available detection is on conventional highways. The traffic data have been quality controlled as recommended by the L02 reliability monitoring guidebook and are available at 5-min granularities as required by the L03 model validation.

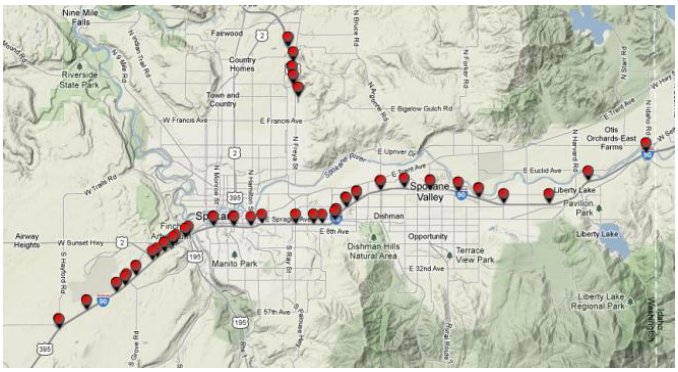

Figure B.10. Spokane data availability.

The project team also acquired incident and work zone data on I-90 in Spokane from the SRTMC. This data set has two pieces:

1. Incidents logged by TMC operators, and
2. Incident and work zone traveler alerts issued by the TMC.

The TMC log incidents contain the start time, free-text description of the incident, and free-text additional remarks. No incident end time is given. The traveler alerts contain start and end times and a description of the alert. Initial analysis of the data received from the SRTMC suggests that the traveler alert information is the better data set for calculating incident-lane-hours-lost for the data-rich model.

To supplement the TMC incidents, the L33 team acquired collision records from 2005 to 2012 for I-90 through Spokane from the Washington State Department of Transportation.

Archived hourly weather data are available from the National Climatic Data Center.

No data from Spokane were used in the L03 project, so this area contributes regional diversity as well as another severe winter weather site to the validation activities.

Washington, D.C.

The L33 team is in possession of 2 years of traffic data collected in Northern Virginia near Washington, D.C., during

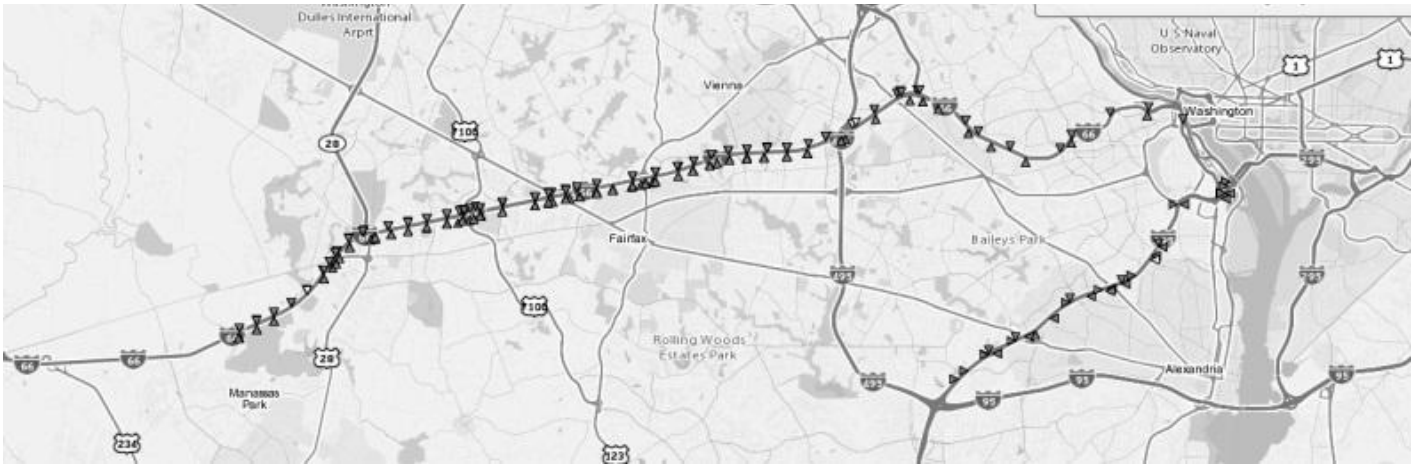

Figure B.11. Washington, D.C., data availability.

the L02 project. In L02, data from 2009 were obtained from the Regional Integrated Transportation Information System (RITIS), developed and maintained by the CATT Laboratory at the University of Maryland. Data from 2011 and 2012 were collected by the L02 monitoring system in real time from RITIS. The traffic data have been quality controlled as recommended by the L02 reliability monitoring guidebook and are available at 5-min granularities as required by the L03 model validation. A map of the traffic detection coverage is shown in Figure B.11. Data are available on US-66 and I-95 near Washington, D.C. The main issue with this data source is that the data were judged to be low quality in 2011, with an average of 70% of detectors not meeting the data-quality requirements. Data in 2009 are superior, so L33 analysis will likely focus on 2009.

The L33 project team has also acquired incident data for 2009 to 2011 from the University of Maryland. The incident data consist of detailed records on incident type, duration, and lane blockages over the duration of the incident. The availability and format of the work zone data in 2009 have not yet been confirmed.

Archived hourly weather data are available from the National Climatic Data Center.

No data from Washington, D.C., were used in L03, so this area contributes regional diversity as well as another severe winter weather site to the validation activities.

Summary

The L33 team proposes to perform validation and enhancement activities in 10 metropolitan areas around the United States. Together, these sites have the following characteristics:

- 9 sites have guaranteed access to traffic data over at least a year.
- 9 sites have guaranteed access to incident data over at least a year.
- 10 sites have guaranteed access to weather data of at least a year.
- 7 sites have guaranteed access to work zone data of at least a year.
- 7 sites have guaranteed access to at least 5 years of traffic, incident, and weather data.
- 3 sites have guaranteed access to traffic data collected by technologies other than point detectors.

The charts in Figure B.12 summarize the availability of the needed types of data in each of the 10 proposed metropolitan areas.

Analysis Plan

This analysis plan outlines the L33 team's proposal for turning the data sets described in the previous section into the final data sets required for validation of the data-rich and data-poor models. The plan consists of detailed instructions for nine tasks:

1. Select validation freeway sections,
2. Quality-control and aggregate traffic data,
3. Calculate the peak hour and peak period (data-rich only),
4. Calculate travel time reliability measures,
5. Calculate demand-to-capacity ratio variables (data-rich only),
6. Calculate incident-lane-hours-lost (data-rich only),
7. Calculate hours of precipitation exceeding 0.05 in. (data-rich only),
8. Validate data-rich and data-poor equations, and
9. Sensitivity testing on alternative data processing approaches.

In structuring this analysis plan, it was important to balance conducting validation in the same way as L03 with the desire to gauge model performance under different data

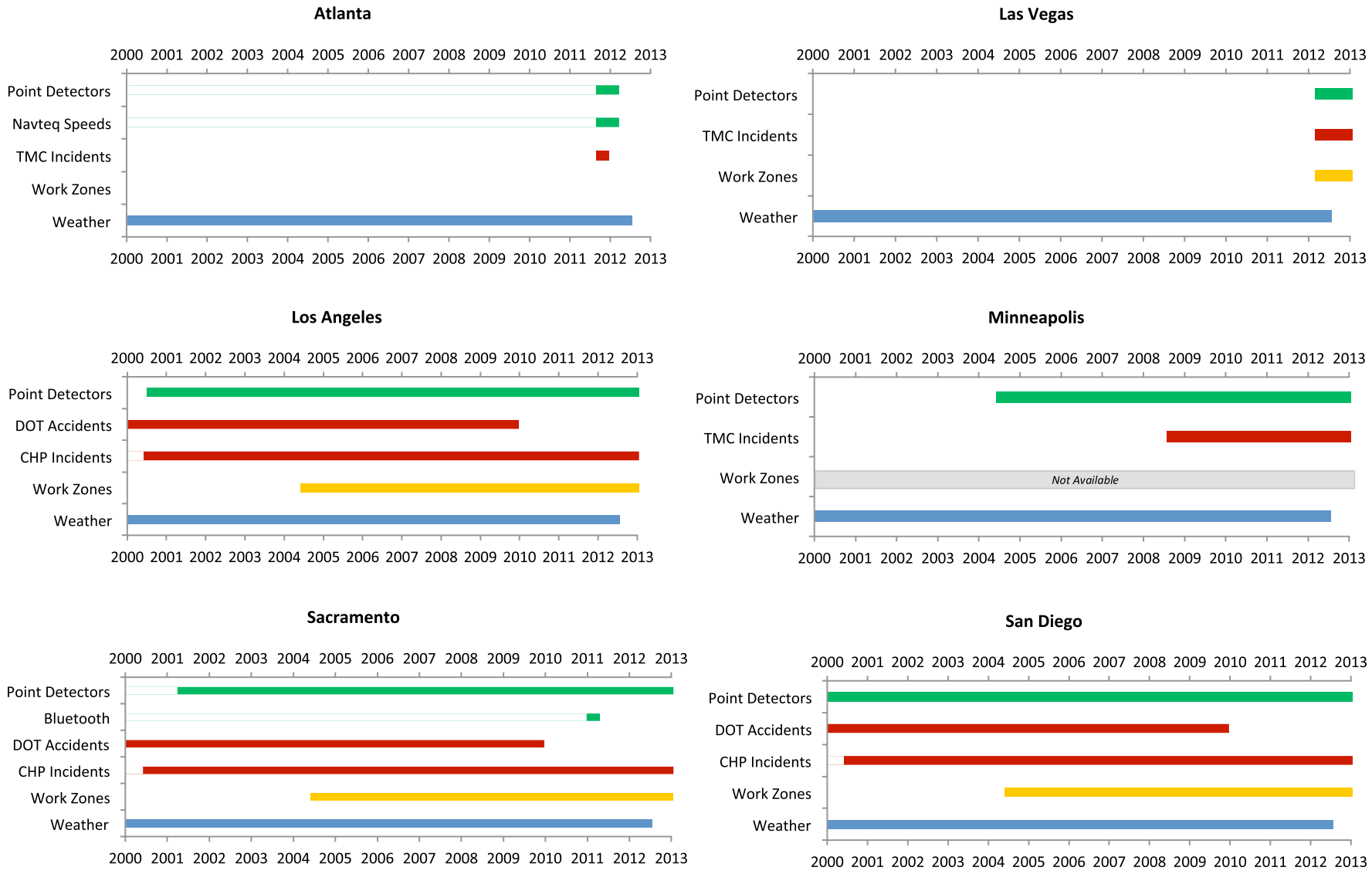

Figure B.12. Availability of the needed types of data in each of the 10 proposed metropolitan areas. (Continued on next page.)

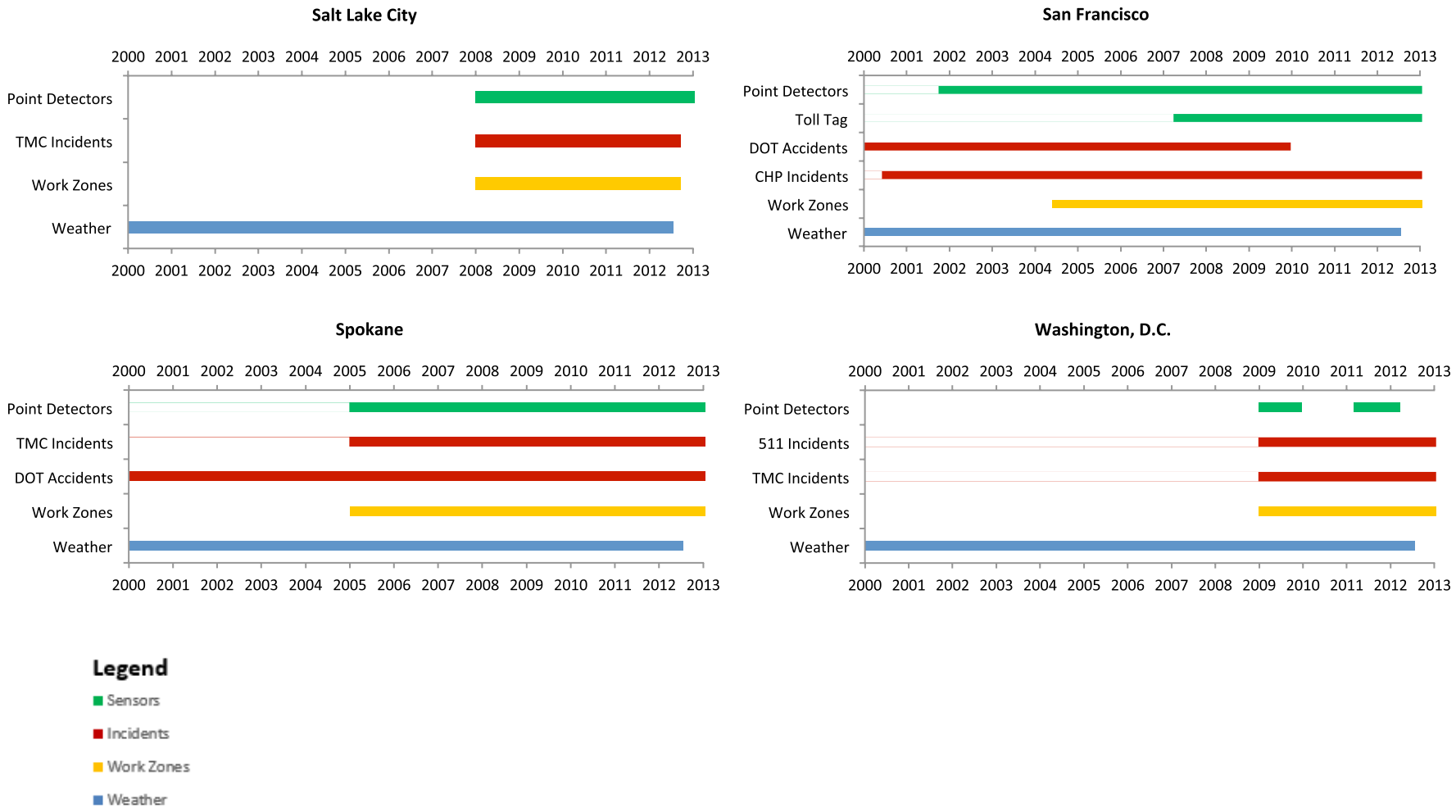

Figure B.12. Availability of the needed types of data in each of the 10 proposed metropolitan areas. (Continued from previous page.)

methodologies. The fact that the data-rich and data-poor model validation was only performed in one region is a major motivation for this validation task. Performing the validation using the same data processing and estimation methodologies as L03 tests the validity of the developed models for different regions and time periods. On the other hand, performing the validation using different processing methodologies and assumptions tests the model's sensitivity to the way the inputs are generated.

To address both forms of validation, this section is centered on a core validation analysis plan, which adheres as closely as possible to the L03 process, but also contains a set of supplemental experiments. Each of the 9 tasks contained in this section lists the inputs, outputs, and steps that will be used to perform the model validation as it was done in L03. Where relevant, supplemental experiments that generate separate data sets or perform other validation activities are listed. The goal of this structure is to assess the strengths and weaknesses of the L03 data-rich and data-poor models and the degree to which the validation errors are a function of the independent variable estimation process. These findings will guide the enhancement tasks of the L33 project.

Task 1: Select Validation Freeway Sections

The application guidelines of the L03 data-rich and data-poor models specify the freeway section characteristics required to achieve valid model results. The freeway sections used for validation in L33 will meet the following criteria:

- Length of around 5 mi (range from 2 to 10 mi);
- Good data quality over a year;
- Monitored by point detectors with no more than an average spacing of 3/4 mi, or monitored by automated vehicle identification (AVI) technologies at the section origin and destination;
- No mid-section freeway-to-freeway interchanges or bottlenecks; and
- Relative homogeneity in terms of traffic and geometric conditions.

Steps

1. Identify freeway segments with dense detector spacing.
2. Identify sections along the densely monitored segments that have a consistent number of lanes, have no mid-section freeway-to-freeway interchanges, and are approximately 5-mi long.
3. Identify yearlong periods with good data quality (average percent observed exceeding 75%).
4. Visually assess detector data to identify calibration issues.

Task 2: Quality-Control and Aggregate Traffic Data

In this step, the 5-min level traffic data available at the proposed study sites are aggregated to the section level and filtered to exclude data samples with poor quality. The required steps depend on the technology used to collect the traffic data; as such, separate steps are presented for point detector data and the toll tag travel times proposed for validation in the San Francisco Bay Area. The quality-control and aggregation plan for the point detector data is nearly identical to that used by L03, with the exception that, in L33, quality control has already been performed by upstream data collection systems according to L02 recommendations. For the toll tag data, the L03 final report does not suggest that any filtering was performed on the data. Because toll tag travel times are highly influenced by the presence of outlier data samples, the L33 team is currently performing exploratory analysis to identify an appropriate filtering and quality-control algorithm.

Point Detector Data

Inputs

- At least a year of 5-min detector station volumes (summed across all lanes) and speeds (volume-weighted average across all lanes) that have been quality controlled, cleaned, and imputed according to methodologies from the SHRP 2 L02 guide.

Outputs

- At least a year of 5-min section vehicle miles traveled (VMT), vehicle hours traveled (VHT), speed, travel time index (TTI), and travel times.

Steps

1. Calculate 5-min VMT and VHT at each detector station (link) using the link's length (the distance halfway to the nearest neighboring stations in the upstream and downstream directions):
   a. Link VMT = link length * 5-min volume, and
   b. Link VHT = link VMT/(Min(60 mph, 5-min speed)).
2. Aggregate the link-level data to section-level 5-min VMT, VHT, space mean speed (speed), TTI, and travel time:
   a. Section VMT = sum of link VMTs,
   b. Section VHT = sum of link VHTs,
   c. Section speed = Section VMT/Section VHT,
   d. Section TTI = Max(1.0, 60 mph * (1/Section speed)), and
   e. Section travel time (mins) = Section TTI * Section length.
3. Flag 5-min data points when less than 50% of the section's detectors data were not working. These data points will be excluded from all downstream analysis.

Supplemental Quality-Control Experiments

- Use a higher data-quality threshold in generating the section-level data by flagging 5-min data points when less than 90% of the section's detectors were not working. Assess the difference in the validation results in Task 9.
- Calculate the free-flow speed along each section and use that in the TTI equations, instead of 60 mph. Assess the difference in the validation results in Task 9.

Toll Tag Travel Times (San Francisco Bay Area Only)

Inputs

- At least a year of 5-min mean, median, minimum, 25th-percentile, 75th-percentile, and maximum travel times, and number of measured samples; and
- 5-min detector station volumes.

Outputs

- 5-min quality-controlled median travel times.

Steps

- To be determined following exploratory analysis currently underway by Iteris and Arizona State University.

Supplemental Data Collection Technology Experiments

- Collect toll tag travel times and point detector travel times on the same section. Assess the difference in the validation results in Task 9.

Task 3: Calculate the Peak Hour and Peak Period (Data-Rich Only)

This step is required to identify each section's peak hour and peak period in order to group data into the data-rich study time periods. The steps outlined below adhere to those used in L03.

Peak Hour

Inputs

- 5-min section speeds from Task 2.

Outputs

- Peak 60-min time period for each section, and
- Average 5-min weekday speeds over a year for each section.

Steps

1. Subset each section's data to include only non-holiday weekdays.
2. For each 5-min period, calculate the weekday average space-mean section speed.
3. For each section, identify the 12 consecutive 5-min periods that have the lowest average space mean speed.

Peak Period

Inputs

- 5-min average weekday speeds from peak hour calculation.

Outputs

- Peak time period (of at least 75 min) for each section.

Steps

- Identify time periods of at least 75 min where the average section speeds are less than or equal to 45 mph. If there are none, identify the 75 consecutive minutes that have the lowest average section speeds.

Supplemental Time Period Definition Experiments

- Test different definitions of the peak period.

Task 4: Calculate Travel Time Reliability Measures

The purpose of this task is to use the section-level traffic data from Task 2 and the peak hour/peak period definitions from Task 3 to generate yearly section travel time reliability measures for use in validation. The L03 models were developed to estimate volume-weighted travel time reliability measures. The L33 team plans to duplicate this methodology.

Inputs

- 5-min section data from Task 2, and
- Peak hour and peak period definitions from Task 3 (data-rich only).

Outputs (For Each Section and Time Period)

- Mean TTI;
- Percentile TTIs (10th, 50th, 80th, 95th, and 99th);
- On-time statistics [percentage of trips (VMT) made within 1.1*x* the median travel time and within 1.25*x* the median travel time]; and
- Failure statistics [percentage of trips (VMT) with speeds less than 50 mph, 45 mph, and 30 mph].

Steps

1. Group 5-min section data into the L03 model time periods (data-rich only):
   a. Peak hour: defined in Task 4;
   b. Peak period: defined in Task 4;

   c. Midday: Non-holiday weekdays from 11:00 a.m. to 2:00 p.m.; and
   d. Weekdays: Non-holiday weekdays, 24 h.
2. Calculate the outputs using VMT-weighting (consider the VMT in the frequency of each TTI weighting).

Task 5: Calculate Demand-to-Capacity Ratio Variables (Data-Rich Only)

This task consists of four subtasks: (1) calculate link capacity; (2) calculate link demand; (3) calculate section critical demand-to-capacity ratio; and (4) calculate section average demand-to-capacity ratio.

Task 5.1: Calculate Link Capacity

The L03 project team obtained the capacity of each link from the Highway Performance Monitoring System (HPMS) wherever it was provided. On sections where the capacity was not listed in HPMS, it was calculated using the capacity method for planning applications from Dowling et al.'s 1997 report, which considers the number of lanes, the percentage trucks, and the peak hour factor (which was fixed in L03). The L33 team plans to duplicate this approach during validation.

Inputs
- Number of lanes;
- Truck percentage; and
- Peak Hour Factor.

Outputs
- Link capacity by time period.

Steps
- Calculate capacity using NCHRP 387 methodologies.

Supplemental Capacity-Estimation Experiment
- Experiment with other capacity-estimation methodologies to be determined through exploratory analysis.

Task 5.2: Calculate Link Demand

The L03 project team assumed that when speeds fall below 45 mph on an urban freeway the measured volume is not an accurate estimate of the demand. The L33 team plans to implement the procedure that the L03 team developed to estimate the demand during congested conditions. The L33 team will evaluate the estimation results and explore alternative methods if the L03 method proves deficient.

Inputs
- 5-min link volumes and speeds.

Outputs
- 5-min link demand.

Steps
1. For each station, identify continuous 5-min periods when the measured speed falls below 45 mph. During these time periods, the link is assumed to be in congestion and the measured volume not representative of the demand. Single 5-min gaps during which speeds exceed 45 mph can still be included.
2. Split each congested time period into two halves.
3. The demand during the first half of congestion is assumed to be equal to the average volume measured in the two 5-min periods before the start of congestion.
4. The demand during the second half of congestion is set such that the cumulative volume measured over the congested period is equal to the estimated cumulative demand over the same time period.
5. Check that the two 5-min periods after the termination of congestion fit smoothly to observed cumulative volume curve. If they do not, extend the congested period to ensure a smooth transition.

Task 5.3: Calculate Section Critical Demand-to-Capacity Ratio

The data-rich models for the peak hour, peak period, and midday time periods all require the critical demand-to-capacity ratio. The L33 project team plans to compute this ratio using the L03 methodology, outlined here.

Inputs
- Link capacities from Task 5.1.
- 5-min link demands from Task 5.2.

Outputs
- For each section and time period (peak hour, peak period, and midday), the critical demand-to-capacity ratio.

Steps
1. For each link, calculate the demand during each weekday time period (peak hour, peak period, and midday).
2. Calculate the 99th-percentile demand-to-capacity ratio for each link over all time periods in the year.
3. For a section, choose the highest 99th-percentile demand-to-capacity ratio among all the links on the section as the independent variables.

Task 5.4: Calculate Section Average Demand-to-Capacity Ratio

The data-rich weekday models require the average demand-to-capacity ratio of each section. The L33 project team

plans to compute this ratio using the L03 methodology, outlined here.

INPUTS

- Link capacities from Task 5.1.
- 5-min link demands from Task 5.2.

OUTPUTS

- For each section and time period, the average demand-to-capacity ratio for a section.

STEPS

- For each link, calculate the demand-to-capacity ratio during each time period.
- For a section, calculate the average demand-to-capacity ratio across all of the links on the section during the time period.

Task 6: Calculate Incident-Lane-Hours-Lost Variable (Data-Rich Only)

All of the peak hour and peak period models, and some of the weekday models, require the yearly incident-lane-hours-lost. L03 calculated these values wherever possible from the raw incident data. The L33 project team plans to use this approach, outlined below.

Inputs

- Raw, time-stamped incident data collected within the metropolitan area.

Outputs

- For each section, incident-lane-hours-lost by time period over a year.

Steps

1. Using the incident location data, subset the raw incidents to those that occurred on the section.
2. For each time period, subset the incidents to those that started in or 15 min before, ended in, or spanned the entire time period.
3. For the portion of each incident that occurred during a time period, calculate the lane-hours-lost caused by the incident using information on the lane blockage and incident duration. If lane blockage and/or incident duration is not available in the incident data set, estimate them using L03 final report equations that estimate these values based on the agency incident clearance policies and the presence of shoulders.
4. For each section and time period, calculate the total incident-lane-hours-lost over the year as the independent variable.

Supplemental Analysis of Incident Data

- Use work zone data to calculate a work zone lane-hours-lost term. Assess how the addition of this term into the incident-lane-hours-lost variable affects the model performance in Task 9.
- Use detailed incident and collision data sets to validate the L03 equations for
  - Ratio of the incident rate to the crash rate (4.545); and
  - Average number of lanes blocked per incident: (a) with usable shoulder and policy to move lane-blocking incidents as quickly as possible (0.476); (b) with usable shoulder and no policy to move lane-blocking incidents (0.580); and (c) no usable shoulders (1.140).

Task 7: Calculate Hours of Precipitation Exceeding 0.05 in. (Data-Rich Only)

Some of the peak hour and peak period L03 data-rich models require inputs of the yearly number of hours of precipitation that exceeded 0.05 in. The L03 methodology leveraged hourly precipitation data from the National Climatic Data Center. This data source will also be used in L33, and processed as follows.

Inputs

- Hourly precipitation values at weather stations downloaded from the National Climatic Data Center.

Outputs

- For each section and time period, the number of hours of precipitation exceeding 0.05 in., for input as an independent variable into the data-rich model.

Steps

1. Pick the weather station that is closest to a section.
2. Download the hourly precipitation data.
3. For each time period, calculate the number of hours when the precipitation exceeded 0.05 in.

Task 8: Validate Data-Rich and Data-Poor Equations

In this step, the independent variables are input into the L03 data-rich and data-poor equations, and outputs are compared with the actual reliability measures calculated in Task 4.

Inputs

- Critical demand-to-capacity ratio for each section during the peak hour, peak period, and midday period (output of Task 5.3).
- Average demand-to-capacity ratio for each section on weekdays (output of Task 5.4).
- Number of hours when rainfall exceeds 0.05 in. for each section during the peak hour and peak period (output of Task 7).
- Incident-lane-hours-lost for each section during the peak hour, peak period, and weekday time periods (output of Task 6).
- The mean travel time, 10th-, 50th-, 80th-, 95th-, and 99th-percentile travel times, the percentage of on-time trips made within 1.1 and 1.25 times the median TTI, and the percentage of on-time trips with 30-, 45-, and 50-mph speed thresholds for each section and time period (outputs of Task 4).

Outputs

- For each section and model, the percentage error between the predicted and measured reliability metrics.
- For each model, the root mean square error across all sections.
- Where possible, test the statistical significance of the comparison between measured and predicted reliability metrics.

Validation Steps

To understand the performance of the data-rich and data-poor models across the regions proposed in the data collection plan, the L33 project team plans to focus validation efforts on the following travel time reliability statistics predicted by the L03 models:

- 80th-percentile TTI (data-poor and data-rich, all time periods);
- 95th-percentile TTI (data-poor and data-rich, all time periods); and
- Standard deviation (predicted by data-poor model only).

The team believes that focusing on these measures will provide ample insight into the performance of the L03 model forms, while allowing more resources to be spent collecting data and processing data from a wide range of sites. This will allow the L33 team to assess application guidelines for the L03 models while also gaining insight into potential model enhancements.

For the data-poor prediction, the L03 project team initially used power form models to relate the mean TTI with the reliability-related TTIs. However, these equations were revised in Appendix H of the L03 final report. The final L03 data-poor equations for the 80th-percentile TTI, 95th-percentile TTI, and the standard deviation are as follows:

$$80\text{th-percentile TTI} = 1 + 2.1406 * \ln(\text{meanTTI})$$

$$95\text{th-percentile TTI} = 1 + 3.6700 * \ln(\text{meanTTI})$$

$$\text{standard deviation of TTI} = 0.71(\text{meanTTI} - 1)^{0.56}$$

In these revisions, the L03 team changed the form of the percentile equations to assume that the 80th- and 95th-percentile TTIs are related to the log of the mean TTI. The standard deviation equation keeps the power form, but modifies the coefficient from the original equations. The L33 team plans to validate the three final L03 data-poor equations shown above.

For the data-rich prediction, there are four equations that predict each reliability measure, one for each of the following time periods: (1) peak hour, (2) peak period, (3) midday, and (4) weekday. The data-rich equations that will be validated are as follows:

Peak Hour

$$95\text{th-percentile TTI} = e^{0.63071 * dc_{crit} + 0.01219 * ILHL + 0.04744 * Rain05Hrs}$$

$$80\text{th-percentile TTI} = e^{0.52013 * dc_{crit} + 0.01544 * ILHL}$$

Peak Period

$$95\text{th-percentile TTI} = e^{0.23233 * dc_{crit} + 0.01222 * ILHL + 0.01777 * Rain05Hrs}$$

$$80\text{th-percentile TTI} = e^{0.13992 * dc_{crit} + 0.01118 * ILHL + Rain05Hrs}$$

Midday

$$95\text{th-percentile TTI} = e^{0.07812 * dc_{crit}}$$

$$80\text{th-percentile TTI} = e^{0.02612 * dc_{crit}}$$

Weekday

$$95\text{th-percentile TTI} = e^{0.03632 * dc_{average} * 0.00282 * ILHL}$$

$$80\text{th-percentile TTI} = e^{0.00842 * dc_{average} + 0.00117 * ILHL}$$

To validate the data-poor and data-rich equations listed above, the L33 team will calculate the following performance measures:

- Root mean square error (RMSE)

Denote the predicted response values as $\hat{y}$, real response values as y, then the residual r is defined as

$$r = \hat{y} - y$$

RMSE is defined as

$$RMSE = \sqrt{MSE(\hat{y})} = \sqrt{E\left[(\hat{y} - y)^2\right]} = \sqrt{\frac{\sum_{i=1}^{n} r^2}{n}}$$

RMSE can measure the magnitude of differences between the predicted and actual responses. However, there is no simple benchmark or threshold for an acceptable RMSE.

- Residual plots

Ideally, residual r is a random variable following a normal distribution with zero mean. Plotting out the distribution of residuals provides direct impression of the goodness of fit, presence of bias, and heteroscedasticity.

- Standard t-test of zero residual mean

The standard t-test can be used to determine if the mean of residuals is significantly different from zero (in a statistical sense). With an unbiased model, the difference should be statistically insignificant.

$$t = \frac{\bar{r} - \mu_0}{s/\sqrt{n}}$$

where $\bar{r}$ is the residual mean, s is the standard deviation of residuals, n is the sample size, and μ_0 is the specific mean value targeted, set as zero.

The end goals of the quantitative validation efforts are to determine: (1) How good are the L03 models? and (2) When and where can they be applied? To evaluate these questions, the L33 team will compare the log of residual variance as a measure of fit. When this measure is low then the model fits well; when high it fits poorly. This comparison will reveal how well the models perform during different time periods (peak versus non-peak), for different types of sections (e.g., number of lanes), and across different regions with varying weather conditions and driver populations. The results of this analysis will be used to develop application guidelines for the existing L03 models and recommendations for changes to be explored in model enhancement.

Task 9: Sensitivity Testing on Alternative Data Processing Approaches

This analysis plan contains a number of places in the analysis chain where the L33 team would like to explore alternate methods of performing the data processing or independent variable computations. Pursuing these methods will produce multiple validation data sets on some sections. After Task 8 is performed on each data set, the validation results can be compared to gauge the sensitivity of the models to the various data processing alternatives.

Conclusions

This validation plan proposes to perform validation of the L03 models using data collected at up to 250 different freeway section-year combinations located in nine metropolitan areas. In comparison, the model validation performed in L03 used data from 60 section-years in a single metropolitan area. The traffic data model inputs and measured reliability statistics will be gathered from agency detector data feeds as was done in L03, though no L03 data will be used in the L33 validation process. The incident-lane-hours-lost variable will be computed using dispatch and agency incident, crash, and work zone data sets. The L03 team used only incident data collected by the private sector in calibration and validation. Using agency incident data in L33 will allow for the assessment of model fit and development of application guidelines using data sets more likely to be used by agencies that are implementing the predictive models. The weather data used in L33 validation will be of the same form as that used in L03 hourly precipitation data from the National Climatic Data Center, though the L33 team is also exploring more spatially and temporally fine-grained weather data sets for enhancement tasks.

This experimental design presented in this validation plan will allow the L33 team to confidently assess how well the data-rich and data-poor models predict travel times in different metropolitan areas. The core validation and the supplemental validation experiments will yield information that will enable the L03 team to identify and prioritize potential enhancements to the L03 models, such as the estimation of new coefficients or the development of new model forms.

Reference

Dowling, R., W. Kittelson, J. Zegeer. 1997. *NCHRP Report 387: Planning Techniques to Estimate Speeds and Service Volumes for Planning Applications*. Transportation Research Board, National Research Council, Washington, D.C.

APPENDIX C

Data-Rich Validation

Overview

This appendix presents the validation analysis of the L03 data-rich models. Pages 143–145 of the L03 report contain six model equations that predict the following travel time index (TTI) reliability statistics (http: //www.trb.org/Main/Blurbs/166935 .aspx):

- mean TTI; and
- 99th-, 95th-, 80th-, 50th-, and 10th-percentile TTI.

In the L03 project, these models were termed "data-rich" because they predict a wide set of reliability measures based on different combinations of four data variables:

- dc_{crit}, the critical demand-to-capacity (D/C) ratio on the study section;
- $dc_{average}$, the average D/C ratio on the study section;
- ILHL (incident-lane-hours-lost), the annual lane hours lost because of incidents on the study section, during the analysis time slice; and
- Rain05Hrs, the annual hours of rainfall ≥0.05 in. on the study section, during the analysis time slice.

The L03 project calibrated these data-rich models using data collected in a number of metropolitan areas, but only validated the models on roadway sections in the Seattle metropolitan area. The goal of this stage of the L33 project is to quantify the effectiveness of these models using new data sets collected from around the country.

The rest of this appendix is organized as follows. Section 2 presents the validation procedure, including the data gathering and the techniques used to measure the effectiveness of the L03 data-rich models. Section 3 presents the validation results for each time slice, including results for the model overall and by region. Finally, Section 4 summarizes the conclusions. There is also an attachment that contains detailed regional validation results.

Validation Procedure

Models

There are six L03 data-rich models per analysis time slice (peak period, peak hour, weekday, and midday), resulting in a total of 24 data models to be validated. The models to be validated in this task are as follows:

Peak Period Models

1. $\text{meanTTI} = e^{(0.09677*dc_{crit}+0.00862*\text{ILHL}+0.00904*Rain05Hrs)}$
2. $\text{99th-percentile TTI} = e^{(0.33477*dc_{crit}+0.012350*\text{ILHL}+0.025315*\text{Rain05Hrs})}$
3. $\text{95th-percentile TTI} = e^{(0.23233*dc_{crit}+0.01222*\text{ILHL}+0.01777*\text{Rain05Hrs})}$
4. $\text{80th-percentile TTI} = e^{(0.13992*dc_{crit}+0.01118*\text{ILHL}+0.01271*\text{Rain05Hrs})}$
5. $\text{50th-percentile TTI} = e^{(0.09335*dc_{crit}+0.00932*\text{ILHL})}$
6. $\text{10th-percentile TTI} = e^{(0.01180*dc_{crit}+0.00145*\text{ILHL})}$

Peak Hour Models

1. $\text{mean TTI} = e^{(0.27886*dc_{crit}+0.01089*\text{ILHL}+0.02935*\text{Rain05Hrs})}$
2. $\text{99th-percentile TTI} = e^{(1.13062*dc_{crit}+0.01242*\text{ILHL})}$
3. $\text{95th-percentile TTI} = e^{(0.63071*dc_{crit}+0.01219*\text{ILHL}+0.04744*\text{Rain05Hrs})}$
4. $\text{80th-percentile TTI} = e^{(0.52013*dc_{crit}+0.01544*\text{ILHL})}$
5. $\text{50th-percentile TTI} = e^{(0.29097*dc_{crit}+0.0138*\text{ILHL})}$
6. $\text{10th-percentile TTI} = e^{(0.07643*dc_{crit}+0.00405*\text{ILHL})}$

Midday Models

1. mean TTI = $e^{(0.2599*dc_{crit})}$
2. 99th-percentile TTI = $e^{(0.19167*dc_{crit})}$
3. 95th-percentile TTI = $e^{(0.07812*dc_{crit})}$
4. 80th-percentile TTI = $e^{(0.02612*dc_{crit})}$
5. 50th-percentile TTI = $e^{(0.01134*dc_{crit})}$
6. 10th-percentile TTI = $e^{(0.00389*dc_{crit})}$

Weekday Models

1. mean TTI = $e^{(0.00949*dc_{average}+0.00067*ILHL)}$
2. 99th-percentile TTI = $e^{(0.07028*dc_{average}+0.00222*ILHL)}$
3. 95th-percentile TTI = $e^{(0.03632*dc_{average}+0.00282*ILHL)}$
4. 80th-percentile TTI = $e^{(0.00842*dc_{average}+0.00117*ILHL)}$
5. 50th-percentile TTI = $e^{(0.0021*dc_{average})}$
6. 10th-percentile TTI = $e^{(0.00047*dc_{average})}$

Root mean square error (RMSE) and the alpha level of the model coefficients are the only model fit statistics presented in the L03 report for each of these models. Without the full model fit outputs, much of the L33 validation had to focus on evaluating the extent to which these models adhere to the assumptions required for generalized regression.

Data

The data used in the validation were collected from the Los Angeles, San Francisco Bay Area, Sacramento, and San Diego metropolitan regions (grouped together into a "California" data set); Minneapolis–St. Paul, Minnesota; Salt Lake City, Utah; and Spokane, Washington. Details about the study segments, data sets, and data processing techniques are provided in the L33 Validation Plan report. The California, Salt Lake City, and Spokane data were collected from the 3-year period between January 1, 2010, and December 31, 2012. The Minnesota data were collected from the 3-year period between June 1, 2009, and May 31, 2012.

Validation was performed using data collected on weekdays during the following analysis time slices:

1. Peak period: a continuous time period of at least 75 min during which the space mean speed is less than 45 mph;
2. Peak hour: a continuous 60-min period during which the space mean speed is less than 45 mph;
3. Midday period: 11:00 a.m.–2:00 p.m.; and
4. Weekday period: 12:00 a.m.–11:55 p.m.

This is consistent with the time periods that L03 used to calibrate and validate the data-rich models.

Table C.1 summarizes the sample size of data by region and time period used in the validation. Each value represents the number of section-years for which the D/C ratios, ILHL, rain, and TTI reliability statistics were calculated from the collected data. Only the highlighted cells in Table C.1 were used in the data-rich validation analysis, as these were the locations and time periods that had a sufficient sample size for analysis. In the validation, the input variables were plugged into the model equations to calculate the TTI reliability statistics, which were then compared to the measured values.

Table C.1 shows that far fewer section-year data points were generated for the peak period and peak hour time slices than for the midday and weekday time slices. This is because many segments did not meet the L03 definition of having a peak period or peak hour. In Spokane, none of the sections met these criteria. In Salt Lake City, only seven section-years met these criteria. This reduces the regional variation among the validation data sets, and suggests that the peak period definition needs to be re-evaluated in the model enhancement stage. In addition to the lack of a notable peak period in the Spokane and Salt Lake City data sets, in general, the travel times in these data sets exhibited much less variation and unreliability than in the California (CA) and Minnesota (MN) sites. This should be kept in mind when evaluating the validation results.

Measures

For each model, the goals of the validation were to quantify the model error and determine whether the model follows the key assumptions of generalized regression. This section first describes the method of determining the prediction error and then presents the performance measures that were evaluated.

Table C.1. Final Data-Rich Validation Sample Sizes (Section-Years)

Site	Peak Period	Peak Hour	Midday	Weekday
CA	43	43	140	142
MN	19	25	60	60
Salt Lake City	3	4	32	30
City of Spokane	0	0	9	11
All Data	65	72	241	243

Performance Measures

Root Mean Square Error

Because the data-rich models are in the exponential form, the prediction error is defined differently here than it was for the data poor validation. The research team assumes that the data-rich models are produced by first taking the logarithm transformation of the response data and then fitting it with a linear regression model. This implicitly assumes that the error term in the exponential form model is multiplicative and not additive. This is a typical way to develop a regression model for log-normally distributed data.

Denote the predicted response values from the model as $\hat{y}$ and the measured response values as y. The linear regression model form is

$$\ln(\hat{y}) = \beta X$$

The prediction error (residual) r is thus defined as:

$$r = \ln(\hat{y}) - \ln(y) \quad \text{(C.1)}$$

A positive mean r implies that the model systemically overestimates values based on new data.

Because the data-rich models are in exponential form and built by using the logarithm transformation of reliability measurements and linear regression method, the error (residual) defined above is a multipliable term in the form of e^r. Taking the exponential function for both sides of Equation 1 leads to the following Equation 2:

$$y = \hat{y}e^{-r} \quad \text{(C.2)}$$

or equally,

$$e^r = \frac{\hat{y}}{y}$$

Then, subtracting 1 from both sides of the equation, the formula for the percent deviation of the predicted TTI reliability metric from its measured value is obtained. That is,

$$e^r - 1 = \frac{(\hat{y} - y)}{y}$$

This definition states that the data-rich model overestimates or underestimates the response variable by a percentage of $(e^r - 1) * 100\%$ compared to the measured data. Note that when r is close to zero, $e^r - 1 \approx r$.

In the rest of this appendix, the RMSE values presented are the modified RMSE values, calculated according to the following procedure:

- The ordinary RMSE values are calculated using the residual defined as $r = \ln(\hat{y}) - \ln(y)$;
- The redefined RMSE is calculated by $RMSE' = e^{RMSE} - 1$; and
- The presented values are $RMSE' * 100\%$, which is referred as RMSE in the rest of this data-rich model validation appendix.

Note that the statistical analysis tables and the residual plots are produced using r, because it is r that needs to satisfy the linear regression assumptions.

Student's t-Test

The one sample Student's t-test can be used to determine if the mean of the residuals is significantly different from zero in a statistical sense, which tests for systematic bias. With an unbiased model, the difference should be statistically insignificant. The t-value is calculated as

$$t = \frac{\bar{r} - \mu_0}{s/\sqrt{n}}$$

where $\bar{r}$ is the residual mean, s is the standard deviation of residuals, n is the sample size, and μ_0 is the specific mean value for comparison, set here to be zero. To draw a conclusion, if the calculated t value is larger than some threshold t_α (e.g., $\alpha = 5\%$) using a two-tailed t distribution table, the null hypothesis that the residuals have a mean of zero can be rejected with $(1 - \alpha)$ level of confidence. Or, say that the residual mean is significantly different from zero at α level of probability. If the corresponding p value is used to draw a conclusion, it means that if the null hypothesis were correct, then we would expect to obtain such a large t value on at most p percentage of occasions. For the validation, we use a 90% level of confidence.

Shapiro-Wilk Normality Test

The Shapiro-Wilk test can be used to determine whether the distribution of the residuals is significantly different from the normal distribution in a statistical sense. The null hypothesis in this test states that the residuals are normally distributed. To draw a conclusion, if the p-value is less than a threshold, the null hypothesis that the residuals are normally distributed can be rejected with $(1 - \alpha)$ level of confidence. The threshold used here is $\alpha = 10\%$.

Residual Plots

Ideally, residual r is a random variable that follows a normal distribution with zero mean. Plotting out the distribution of residuals allows for an assessment of the goodness of fit and the likelihood of the presence of bias and heteroscedasticity (unequal variance).

Data-Rich Model Validation

The data-rich models are categorized as peak period, peak hour, midday, and weekday models. For each category, there are six models for the different travel time reliability measures: mean TTI, 99th-percentile TTI, 95th-percentile TTI, 80th-percentile TTI, 50th-percentile TTI, and 10th-percentile TTI. The following subsections are named as "time period—reliability measure—region of the data set." Tables and figures for all data are shown in these subsections, while tables and figures for specific regions are shown in the attachment (Tables C.52 to C.111 and Figures C.73 to C.252).

Peak Period

Peak Period—Mean TTI

Peak Period—Mean TTI—All Data

Table C.2 presents the summary of the RMSE for this category. The largest RMSE appears in the CA data in the peak period mean TTI model validation. The RMSE for MN data is relatively small. Since the CA data account for the largest portion of the AllData set, the RMSE for AllData is also relatively large. These RMSE values only present a general impression of the model performance; further investigation on the residual analysis results provides more details on the model performance.

Table C.3 presents the statistical analysis of residuals resulting from predicting the validation data with the data-rich peak period mean TTI model. Ideally, the residuals should follow a normal distribution with a mean of zero. As shown in Table C.3.c, the Student's *t*-test for zero residual mean yields a *p*-value of 0.0119, meaning that we can reject the null hypothesis of zero residual mean with a confidence level of 90%. The Shapiro-Wilk normality test (Table C.3.d) rejects the hypothesis that the residuals follow a normal distribution as the *p*-value is less than 0.0001. The same conclusion can be drawn by observing the normality plot.

From the plot of residuals versus the predicted mean TTI (Figures C.1 through C.3), we can see that the residuals have an increasing trend where the maximum residual is reached at the largest predicted response value, and when the predicted value is smaller than approximately 0.5 the model tends to underestimate the response variable. This nonrandom pattern indicates that the data-rich model cannot perfectly predict the validation data and may be improved.

Table C.2. RMSE of Peak Period—Mean TTI

RMSE	All Data	CA	MN
Mean TTI	96.94%	127.55%	21.59%

Table C.3. Residual Analysis of Peak Period—Mean TTI—AllData

Table C.3.a. Basic Statistical Measures

Location		Variability	
Mean	0.2086	Std deviation	0.6499
Median	–0.007	Variance	0.4223
Minimum	–0.348	Range	3.0176
Maximum	2.6696	Interquartile range	0.3150

Table C.3.b. Basic Confidence Limits Assuming Normality

Parameter	Estimate	95% Confidence Limits	
Mean	0.2086	0.0476	0.3697
Std deviation	0.6499	0.5542	0.7858
Variance	0.4223	0.3071	0.6174

Table C.3.c. Tests for Location: Mu=0

Test	Statistic		*p*-Value	
Student's *t*	*t*	2.5884	Pr > |*t*|	0.0119

Table C.3.d. Tests for Normality

Test	Statistic		*p*-Value	
Shapiro-Wilk	*W*	0.5972	Pr < *W*	<0.0001

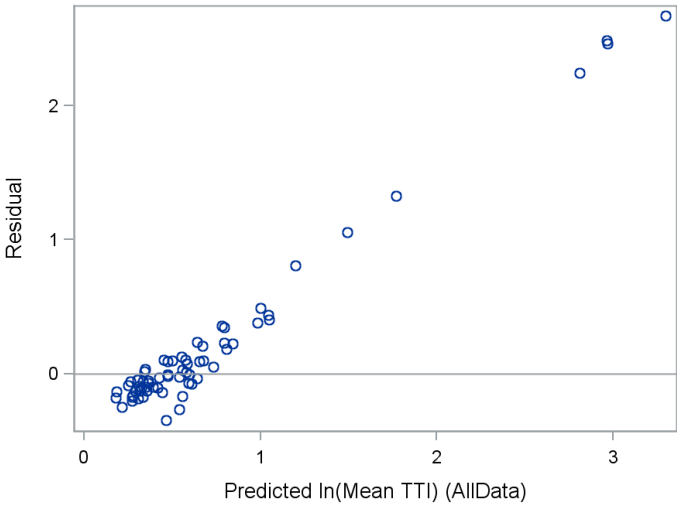

Figure C.1. Residual plot of peak period—mean TTI—AllData.

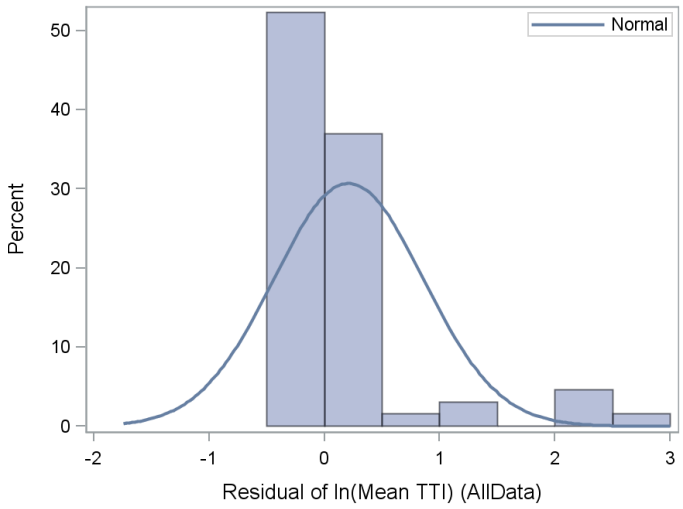

Figure C.2. Residual histogram of peak period—mean TTI—AllData.

Peak Period—Mean TTI—California

The residual plots in the peak period—mean TTI—CA looks similar to those in the AllData validation, since the CA validation data set accounts for most of the samples in the AllData set. The normality test result rejects the null hypothesis that the residuals follow a normal distribution. The Student's *t*-test for zero residual mean shows that we can reject the null hypothesis with a confidence level of 90%. The plot of residuals versus the predicted values shows an almost linear increasing relationship and tends to overestimate the mean TTI when the predicted value is larger than approximately 0.5. On the other hand, when the predicted value is smaller than 0.5, the models tend to underestimate the response variable as most residuals are under the zero reference line. These nonrandom patterns show that the model fits the validation data unsatisfactorily. All the associated plots and results for CA region are included in the attachment.

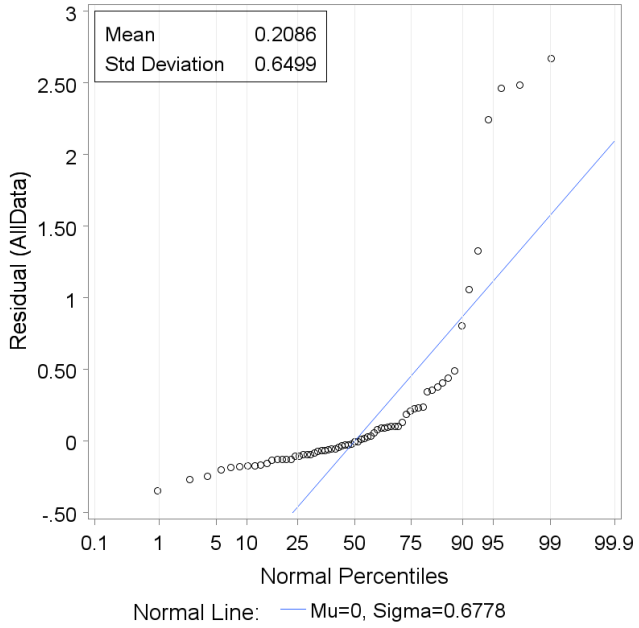

Figure C.3. Residual normality plot of peak period—mean TTI—AllData.

Peak Period—Mean TTI—Minnesota

In MN, the residuals increase with the predicted values. This nonrandom pattern shows that the model has the potential to be improved. The statistical tests show that we cannot reject the zero residual mean hypothesis but can reject the null hypothesis of normal distribution with a high confidence level. The histogram and the normality plot illustrate these conclusions. All the associated plots and results for MN region are included in the attachment.

Peak Period—99th-Percentile TTI

Peak Period—99th-Percentile TTI—All Data

The summary results for this category provided in Table C.4 indicate that the estimation error for the CA data set is as large as 607.76%. As the CA data set constitutes the most part of the AllData set, the RMSE for the AllData set is also relatively large (403.44%). The RMSE for the MN validation data set is 63.67%. This is relatively small compared to the AllData and the CA data sets but still indicates nonsatisfactory estimation performance, since it means an estimation error as large as 63.67% of the measured value.

The residual plot (Figure C.4) in validation analysis of the 99th-percentile TTI model using the AllData set shows a similar pattern to the validation of the mean TTI model using the same data set: residuals increase with the predicted value. Again, such nonrandom pattern shows that the model may have the potential for improvement. The normality plot shows that the residuals do not closely follow a normal distribution, which is also indicated in the normality test as a *p*-value less than 0.0001. The Student's *t*-test shows that the research team can reject the null hypothesis of zero residual mean with a confidence level of 90%. Table C.5 and Figures C.4 to C.6 present these results.

Peak Period—99th-Percentile TTI—California

The validation results for the peak period 99th-percentile TTI model using CA data set shows very similar pattern to that in the validation of percentile TTI model using AllData set. The

Table C.4. RMSE of Peak Period—99th-Percentile TTI

RMSE	All Data	CA	MN
Mean TTI	403.44%	607.76%	63.67%

Table C.5. Residual Analysis of Peak Period—99th-Percentile TTI—AllData

Table C.5.a. Basic Statistical Measures

Location		Variability	
Mean	0.5030	Std deviation	1.5480
Median	0.0020	Variance	2.3963
Minimum	–0.861	Range	7.4177
Maximum	6.5571	Interquartile range	0.9133

Table C.5.b. Basic Confidence Limits Assuming Normality

Parameter	Estimate	95% Confidence Limits	
Mean	0.5030	0.1194	0.8866
Std deviation	1.5480	1.3201	1.8717
Variance	2.3963	1.7427	3.5033

Table C.5.c. Tests for Location: Mu=0

Test	Statistic		*p*-Value	
Student's *t*	*t*	2.6197	Pr > |*t*|	0.0110

Table C.5.d. Tests for Normality

Test	Statistic		*p*-Value	
Shapiro-Wilk	*W*	0.6312	Pr < *W*	<0.0001

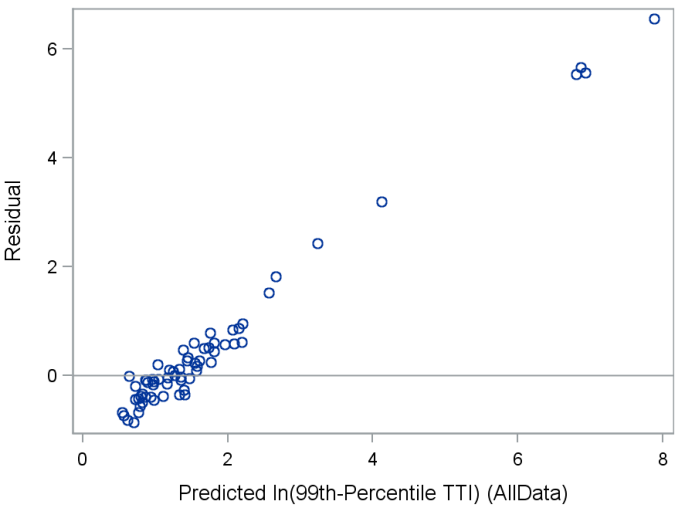

Figure C.4. Residual plot of peak period—99th-percentile TTI—AllData.

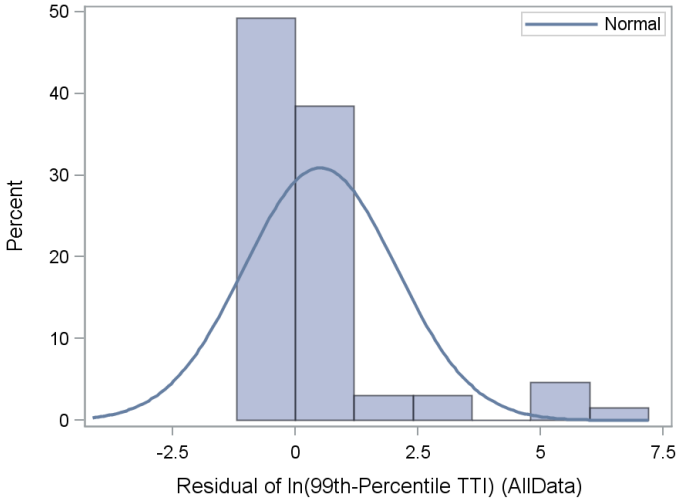

Figure C.5. Residual histogram of peak period—99th-percentile TTI—AllData.

zero residual mean hypothesis is rejected in the Student's *t*-test, and the null hypothesis of normal distribution is rejected in the normality test. The histogram and normality plots also show that the residuals do not closely follow a normal distribution. The plot of residuals versus predicted response values shows an almost linear increasing pattern as the predicted value increases. All the associated results for CA region are included in the attachment.

Peak Period—99th-Percentile TTI—Minnesota

In validating the 99th-percentile TTI model using the MN data set, the plot of residuals versus the predicted response

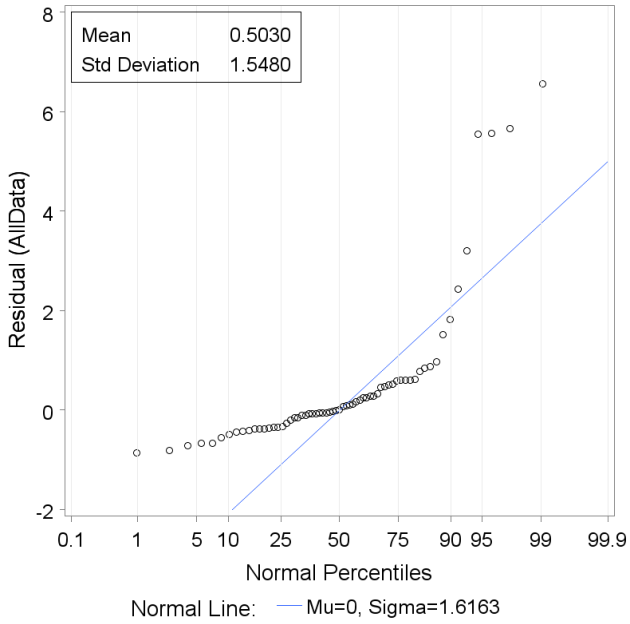

Figure C.6. Residual normality plot of peak period—99th-percentile TTI—AllData.

values does not indicate a good fit, evident from the increasing trend of the scattered points. The Student's *t*-test shows that the null hypothesis of zero residual mean can be rejected with a confidence level of 90%, while the Shapiro-Wilk normality test shows that null hypothesis of normal distribution cannot be rejected with 90% confidence level but can be rejected at a confidence level of 85%. All the associated results for MN region are included in the attachment.

Peak Period—95th-Percentile TTI

Peak Period—95th-Percentile TTI—All Data

The RMSE values for the peak period 95th-percentile TTI model are smaller than the corresponding values in the validation of the 99th-percentile TTI model. The largest value still comes from the CA data set, which is 359.19%, while the smallest is from the MN data, which is 45.85% as summarize in Table C.6.

The residual analysis for the 95th-percentile TTI model using AllData set shows that the Student's *t*-test rejects the null hypothesis of zero residual mean, as the *p*-value is only 0.0211. The Shapiro-Wilk rejects the null hypothesis of normal distribution with a high level of confidence (Table C.7). The residual plot (Figure C.7) shows a similar pattern as that in the previous models: the residual keeps increasing when the predicted value increases. The histogram and the normality plot (Figures C.8 and C.9) manifest the Shapiro-Wilk test result.

Peak Period—95th-Percentile TTI—California

The residual analysis results produced in the CA data validation shows that the null hypothesis of zero residual mean in the Student's *t*-test can be rejected with a confidence level of 90%, and the null hypothesis of a normal distribution can also be rejected with a high confidence in the normality test, as demonstrated in the histogram and the normality plot. The residual keeps increasing as the predicted value increases. All the associated results and plots for the CA region are included in the attachment.

Peak Period—95th-Percentile TTI—Minnesota

The residuals in the validation of the 95th-percentile model with the MN data set also present an increasing pattern in the residual plot. The Student's test rejects the zero residual mean with an over 90% level of confidence, and the Shapiro-Wilk

Table C.6. RMSE of Peak Period—95th-Percentile TTI

RMSE	All Data	CA	MN
Mean TTI	251.95%	359.19%	45.85%

Table C.7. Residual Analysis of Peak Period—95th-Percentile TTI—AllData

Table C.7.a. Basic Statistical Measures

Location		Variability	
Mean	0.3567	Std deviation	1.2161
Median	–0.025	Variance	1.4789
Minimum	–0.684	Range	5.7559
Maximum	5.0720	Interquartile range	0.5554

Table C.7.b. Basic Confidence Limits Assuming Normality

Parameter	Estimate	95% Confidence Limits	
Mean	0.3567	0.0553	0.6580
Std deviation	1.2161	1.0371	1.4704
Variance	1.4789	1.0755	2.1622

Table C.7.c. Tests for Location: Mu=0

Test	Statistic		*p*-Value	
Student's *t*	*t*	2.3646	Pr > |*t*|	0.0211

Table C.7.d. Tests for Normality

Test	Statistic		*p*-Value	
Shapiro-Wilk	*W*	0.6160	Pr < *W*	<0.0001

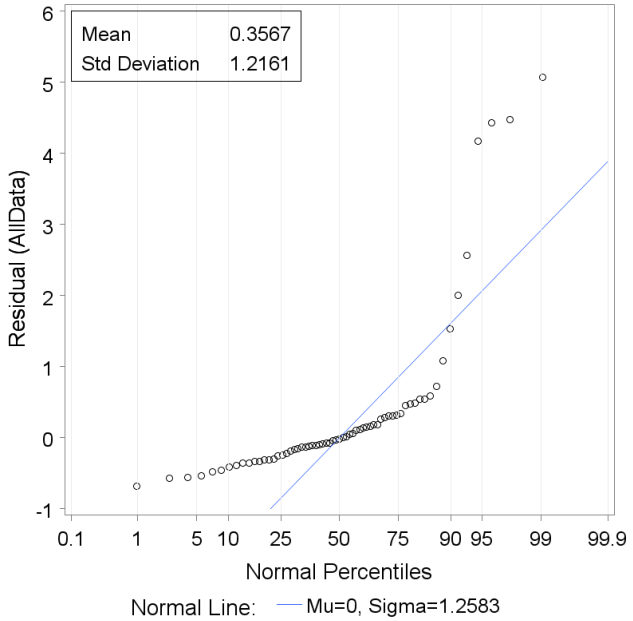

Figure C.7. Residual plot of peak period—95th-percentile TTI—AllData.

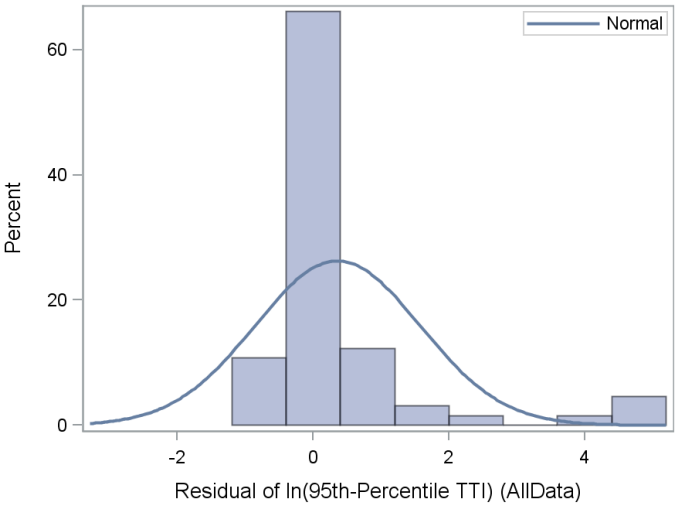

Figure C.8. Residual histogram of peak period—95th-percentile TTI—AllData.

normality test rejects the normal distribution hypothesis also with a high confidence level. All the associated results and plots for MN region are included in the attachment.

Peak Period—80th-Percentile TTI

Peak Period—80th-Percentile TTI—All Data

For the 80th-percentile TTI (Table C.8), the largest RMSE is seen in the CA data set (206.54%) and the RMSE from the MN data set is much smaller, at 30.95%. From the 99th-percentile TTI validation to the 80th-percentile TTI validation, the RMSE for the AllData set has decreased. This is attributed to the fact that smaller percentiles result in smaller response variable range. However, one should note that the reduced RMSEs do not necessarily mean better model performance as it is not instructive to compare the models in this way.

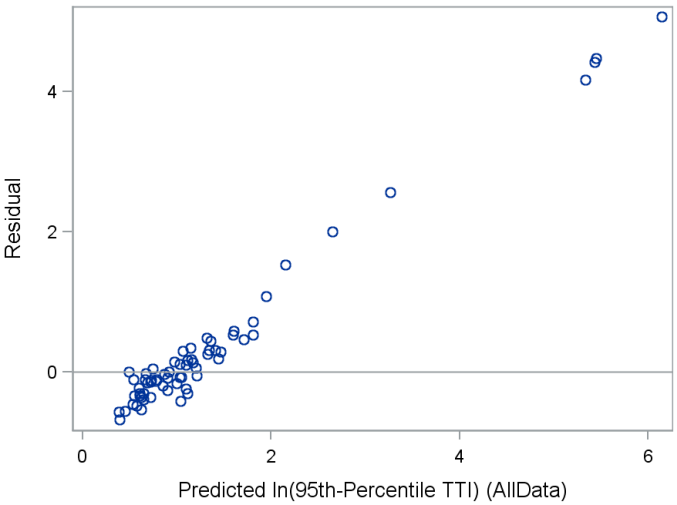

Figure C.9. Residual normality plot of peak period—95th-percentile TTI—AllData.

Table C.8. RMSE of Peak Period—80th-Percentile TTI

RMSE	All Data	CA	MN
Mean TTI	151.95%	206.54%	30.95%

The residual analysis results (Table C.9) show that the zero residual mean hypothesis can be rejected in the Student's *t*-test with a confidence level of 90%. The Shapiro-Wilk normality test rejects the null hypothesis of normal distribution at a confidence level of 90%, as also demonstrated in the normality plot. The residual plot (Figure C.10) shows an increasing trend in the residual value when the predicted response value increases. The residual histogram and normality plots are shown in Figures C.11 and C.12.

Peak Period—80th-Percentile TTI—California

For the 80th-percentile TTI validation using CA data, the Student's *t*-test rejects the null hypothesis of zero residual mean with a confidence level of 90%. The Shapiro-Wilk normality

Table C.9. Residual Analysis of Peak Period—80th-Percentile TTI—AllData

Table C.9.a. Basic Statistical Measures

Location		Variability	
Mean	0.2537	Std deviation	0.8954
Median	–0.058	Variance	0.8018
Minimum	–0.404	Range	4.0847
Maximum	3.6805	Interquartile range	0.4376

Table C.9.b. Basic Confidence Limits Assuming Normality

Parameter	Estimate	95% Confidence Limits	
Mean	0.2537	0.0319	0.4756
Std deviation	0.8954	0.7636	1.0827
Variance	0.8018	0.5831	1.1722

Table C.9.c. Tests for Location: Mu=0

Test	Statistic		*p*-Value	
Student's *t*	*t*	2.2845	Pr > |*t*|	0.0257

Table C.9.d. Tests for Normality

Test	Statistic		*p*-Value	
Shapiro-Wilk	*W*	0.5929	Pr < *W*	<0.0001

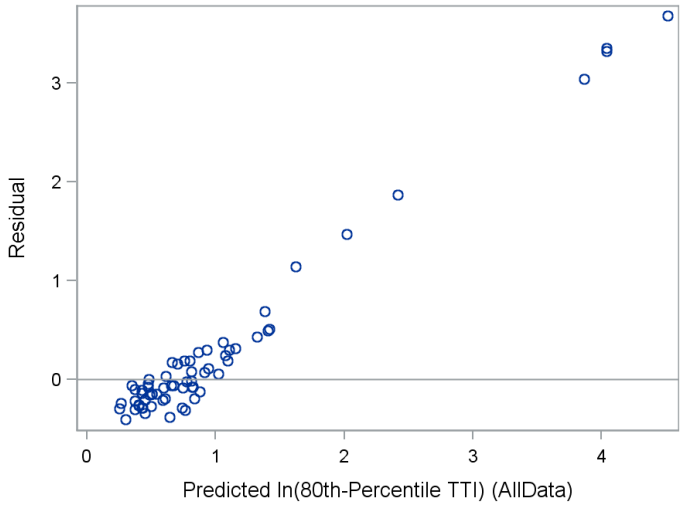

Figure C.10. Residual plot peak period—80th-percentile TTI—AllData.

test rejects the null hypothesis that the residuals follow a normal distribution at a confidence level of 90%. The residual plot shows a similar pattern to that in the AllData validation, with the residual increasing with the predicted value. This nonrandom pattern indicates that it may be possible to improve the data-rich model performance. All the associated results and plots for the CA region are included in the attachment.

Peak Period—80th-Percentile TTI—Minnesota

In MN, the residuals also show an increasing trend as the predicted response value increases. The Student's *t*-test shows that the null hypothesis of zero residual mean cannot be rejected with a confidence level of 90% but can be rejected with a confidence level of 80%. The Shapiro-Wilk normality test shows that the null hypothesis that the residuals follow a normal distribution can be rejected with the preset threshold

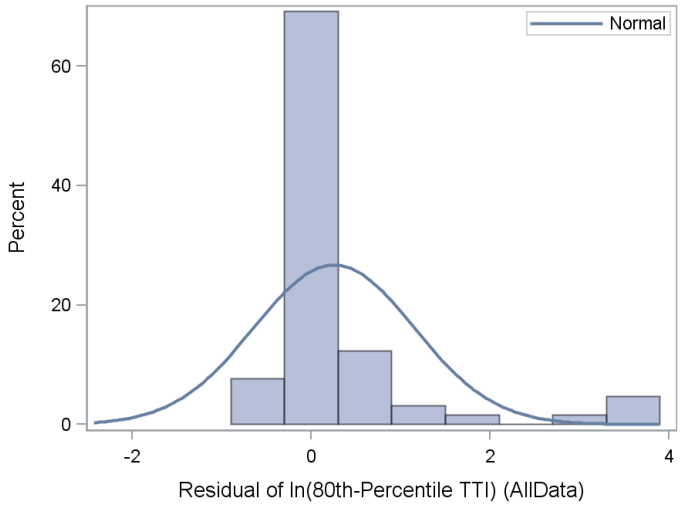

Figure C.11. Residual histogram of peak period—80th-percentile TTI—AllData.

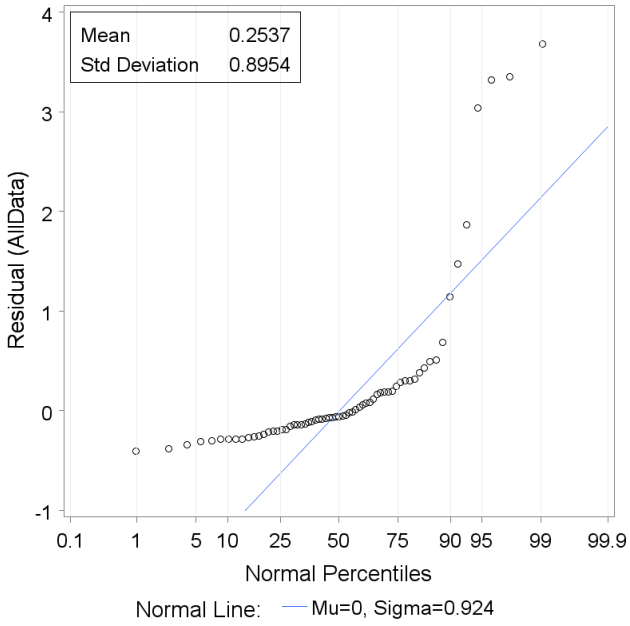

Figure C.12. Residual normality plot of peak period—80th-percentile TTI—AllData.

confidence level of 90%. All the associated results and plots for MN region are included in the attachment.

Peak Period—50th-Percentile TTI

Peak Period—50th-Percentile TTI—All Data

For the 50th-percentile TTI validation, the RMSE values show a similar pattern to that in the previous models: the largest value comes from the CA data (Table C.10).

The Student's *t*-test shows that the null hypothesis of zero residual mean can be rejected with a confidence level of 90% (Table C.11). The Shapiro-Wilk normality test result rejects the null hypothesis of normal distribution at a confidence level of 90%, which is also illustrated in the histogram (Figure C.14) and the normality plot (Figure C.15). The residual plot (Figure C.13) still shows an increasing trend similar to that in the previous models.

Peak Period—50th-Percentile TTI—California

The Student's *t*-test results show that the zero residual mean hypothesis can be rejected at a confidence level of 90%. The Shapiro-Wilk normality test result rejects the null hypothesis of normal distribution at the same threshold confidence level, which is also illustrated in the histogram and the normality

Table C.10. RMSE of Peak Period—50th-Percentile TTI

RMSE	All Data	CA	MN
Mean TTI	89.55%	116.63%	23.15%

Table C.11. Residual Analysis of Peak Period—50th-Percentile TTI—AllData

Table C.11.a. Basic Statistical Measures

Location		Variability	
Mean	0.2044	Std deviation	0.6106
Median	–0.017	Variance	0.3729
Minimum	–0.368	Range	2.8998
Maximum	2.5315	Interquartile range	0.2944

Table C.11.b. Basic Confidence Limits Assuming Normality

Parameter	Estimate	95% Confidence Limits	
Mean	0.2044	0.0531	0.3557
Std deviation	0.6106	0.5207	0.7383
Variance	0.3729	0.2712	0.5451

Table C.11.c. Tests for Location: Mu=0

Test	Statistic		*p*-Value	
Student's *t*	*t*	2.6990	Pr > |*t*|	0.0089

Table C.11.d. Tests for Normality

Test	Statistic		*p*-Value	
Shapiro-Wilk	*W*	0.6172	Pr < *W*	<0.0001

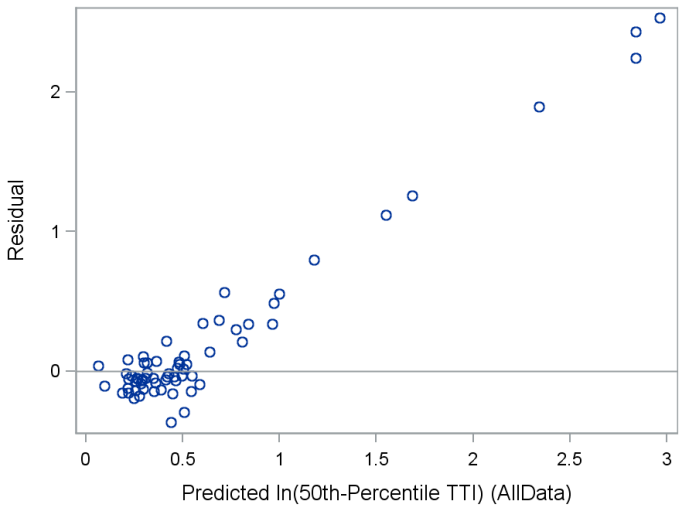

Figure C.13. Residual plot of peak period—50th-percentile TTI—AllData.

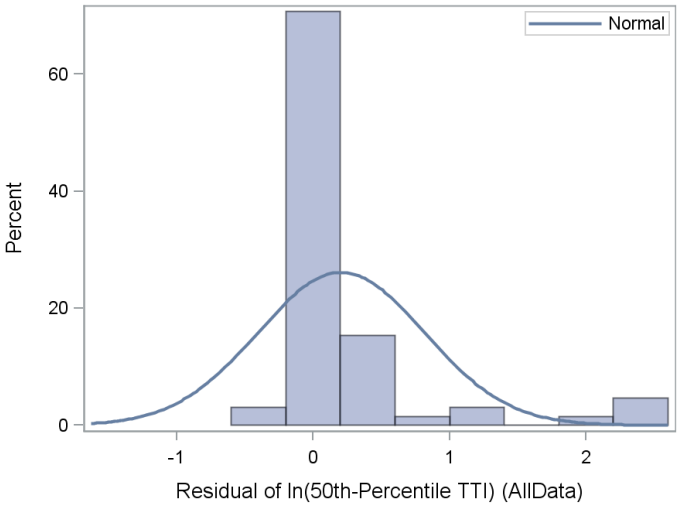

Figure C.14. Residual histogram of peak period—50th-percentile TTI—AllData.

plot. The plot of residuals versus the predicted values shows an increasing trend similar to that in the previous model validations. All the associated results and plots for the CA data are included in the attachment.

Peak Period—50th-Percentile TTI—Minnesota

In MN, the Student's *t*-test result shows that the null hypothesis of zero residual mean cannot be rejected with a confidence level of 90%, while the Shapiro-Wilk normality test result rejects the null hypothesis that the residuals follow a normal distribution. The increasing trend in the plot of residuals

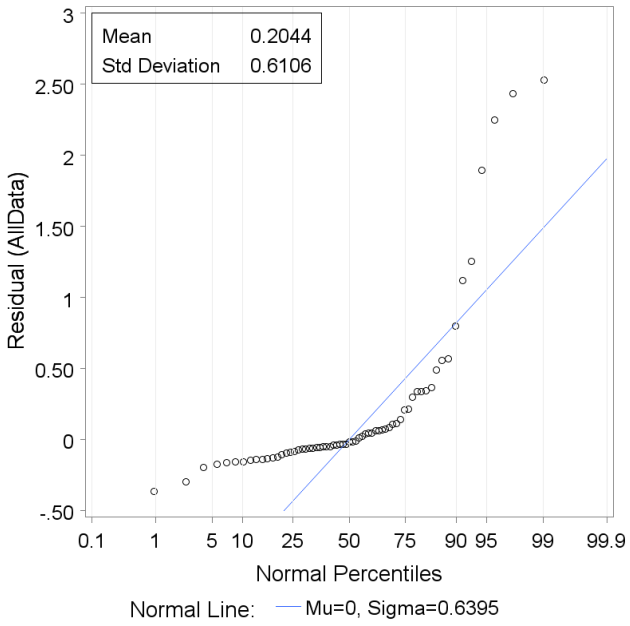

Figure C.15. Residual normality plot of peak period—50th-percentile TTI—AllData.

versus the predicted values still exists, and the histogram and the normality plot demonstrates the normality test results that the residuals are not closely following a normal distribution. All the associated results and plots for the MN data are included in the attachment.

Peak Period—10th-Percentile TTI

Peak Period—10th-Percentile TTI—All Data

The RMSE values for the validation of peak period 10th-percentile TTI data-rich model are all within 15% (Table C.12). However, as the 10th-percentile TTI data are within a small range themselves, the smaller RMSE values do not necessarily mean good model performance. Further investigation on the validation results for each data set is required.

The statistical validation using the AllData set shows that the zero residual mean hypothesis can be rejected with a confidence level of 90% in the Student's *t*-test, and the null hypothesis of normal distribution can be rejected with a confidence level of 90% in the Shapiro-Wilk normality test (Table C.13). The plot of residual versus the predicted value (Figure C.16) shows the problem of an increasing trend of residuals as the predicted value increases, as well as the nonconstant residual variance problem. These nonrandom patterns show that the model can potentially be improved further. The residual histogram and normality plots are shown in Figures C.17 and C.18.

Peak Period—10th-Percentile TTI—California

Validation of the CA data set generally produces similar results to the validation using the AllData set. The residual plot shows the increasing trend and the nonconstant residual variance problems. The Student's *t*-test cannot reject the zero residual mean hypothesis at the threshold confidence level of 90% as the *p*-value is as large as 0.1820. The hypothesis that the residuals follow a normal distribution is rejected in the Shapiro-Wilk normality test with a confidence level of 90%, which is illustrated in the histogram and the normality plot. All the associated results and plots for the CA data are included in the attachment.

Peak Period—10th-Percentile TTI—Minnesota

The MN data set validation results show that the assumption of zero residual mean is likely to be violated as the Student's *t*-test yields a *p*-value less than 0.0001, while the null hypothesis

Table C.12. RMSE of Peak Period—10th-Percentile TTI

RMSE	All Data	CA	MN
Mean TTI	12.13%	14.43%	6.23%

Table C.13. Residual Analysis of Peak Period—10th-Percentile TTI—AllData

Table C.13.a. Basic Statistical Measures

Location		Variability	
Mean	0.0333	Std deviation	0.1104
Median	0.0303	Variance	0.0122
Minimum	–0.344	Range	0.7344
Maximum	0.3906	Interquartile range	0.0600

Table C.13.b. Basic Confidence Limits Assuming Normality

Parameter	Estimate	95% Confidence Limits	
Mean	0.0333	0.0059	0.0606
Std deviation	0.1104	0.0941	0.1334
Variance	0.0122	0.0089	0.0178

Table C.13.c. Tests for Location: Mu=0

Test	Statistic		*p*-Value	
Student's *t*	*t*	2.4305	Pr > |*t*|	0.0179

Table C.13.d. Tests for Normality

Test	Statistic		*p*-Value	
Shapiro-Wilk	*W*	0.8479	Pr < *W*	<0.0001

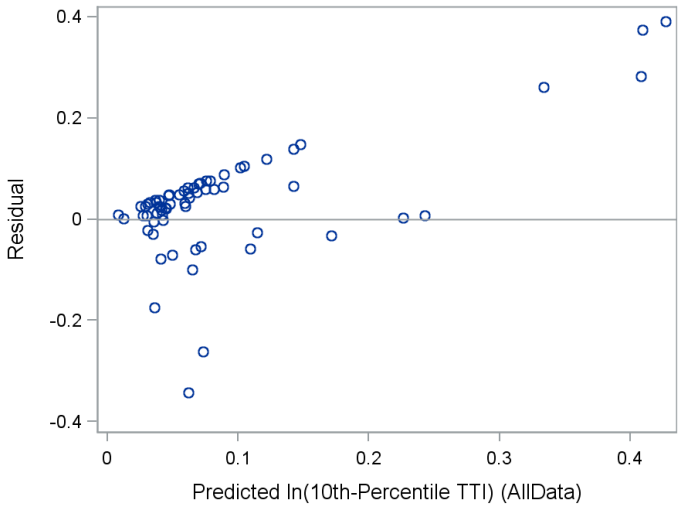

Figure C.16. Residual plot of peak period—10th-percentile TTI—AllData.

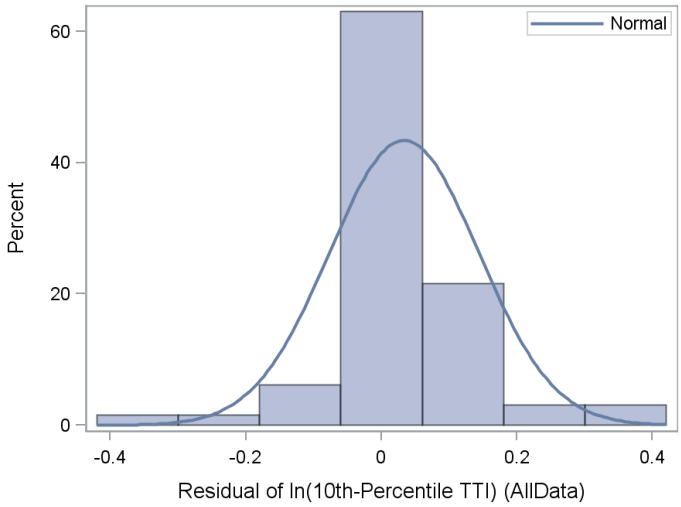

Figure C.17. Residual histogram of peak period—10th-percentile TTI—AllData.

that the residuals follow a normal distribution cannot be rejected in the Shapiro-Wilk normality test as the *p*-value is 0.6593. The residual plot shows that the residuals are all positive except for one. Meanwhile, a nonrandom increasing trend is obvious in the residual plot. All the associated results and plots for the MN data are included in the attachment.

Conclusions of the Data-Rich Peak Period Model Validation

The peak period data-rich model validation analyzed six models built in L03 using three data sets: the CA data set, the MN data set, and the AllData set, which included all the available peak period data.

The validation analysis indicates that the most significant problem is the increasing residual trend shown in the residual plots. A good regression model should present randomly scattered residuals without obvious trends. Additionally, the validation results rarely satisfy the zero residual mean or the normally distributed residual assumptions. Overall, the model form is not adequate and there is room to improve the models for better performance.

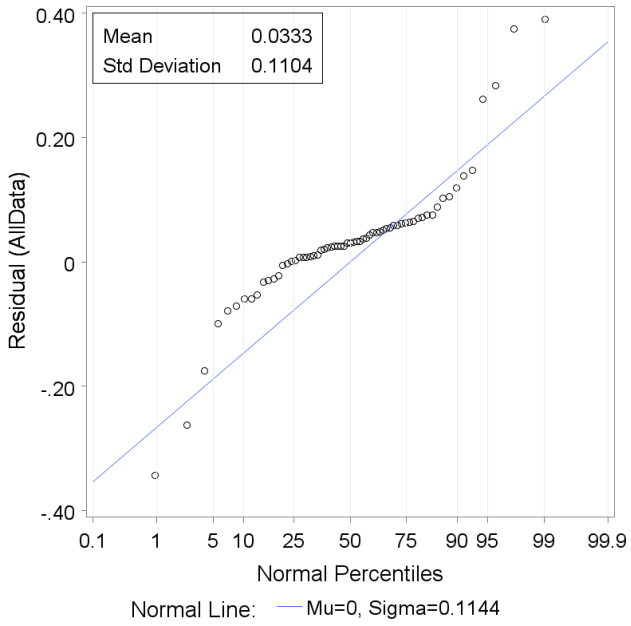

Figure C.18. Residual normality plot of peak period—10th-percentile TTI—AllData.

Peak Hour

Peak Hour—Mean TTI

Peak Hour—Mean TTI—All Data

The RMSE values of the three data sets used to validate the peak hour mean TTI model are all close to 25%, implying that on average the predicted mean TTI has an error in the magnitude of approximately one-fourth of the mean TTI itself (Table C.14). The corresponding RMSE in L03, at 26.4%, is of the same magnitude. Note that when comparing the L03 RMSE value with the validation RMSE values, the research team needs to keep in mind that the definition of RMSE in L33 may not be the same at that used in the L03, because of the limited knowledge of how the regression models were developed in L03.

The residual analysis presents relatively satisfying results (Table C.15). The Student's *t*-test for the zero residual mean and the Shapiro-Wilk normality test both yield *p*-values larger than 0.1, indicating that the research team does not have strong evidence to reject the null hypotheses that the residuals satisfy the zero residual mean and the normal distribution assumptions. The residual versus the predicted value plot (Figure C.19) generally presents a random pattern, although it may have a slight tendency of overestimation when the predicted value is large. The histogram (Figure C.20) and the normality plot (Figure C.21) both show that the residuals approximately display a normal distribution pattern. Overall, this data-rich model generally performs well given the above analysis.

Peak Hour—Mean TTI—California

The validation using the CA data set yields similar results to that using the AllData set. The Shapiro-Wilk normality test

Table C.14. RMSE of Peak Hour—Mean TTI

RMSE	All Data	CA	MN
Mean TTI	25.45%	26.97%	24.68%

Table C.15. Residual Analysis of Peak Hour—Mean TTI—AllData

Table C.15.a. Basic Statistical Measures

Location		Variability	
Mean	–0.030	Std deviation	0.2262
Median	–0.025	Variance	0.0512
Minimum	–0.547	Range	0.9459
Maximum	0.3987	Interquartile range	0.3138

Table C.15.b. Basic Confidence Limits Assuming Normality

Parameter	Estimate	95% Confidence Limits	
Mean	–0.030	–0.084	0.0227
Std deviation	0.2262	0.1944	0.2707
Variance	0.0512	0.0378	0.0733

Table C.15.c. Tests for Location: Mu=0

Test	Statistic		*p*-Value	
Student's *t*	*t*	–1.144	Pr > |*t*|	0.2565

Table C.15.d. Tests for Normality

Test	Statistic		*p*-Value	
Shapiro-Wilk	*W*	0.9763	Pr < *W*	0.1916

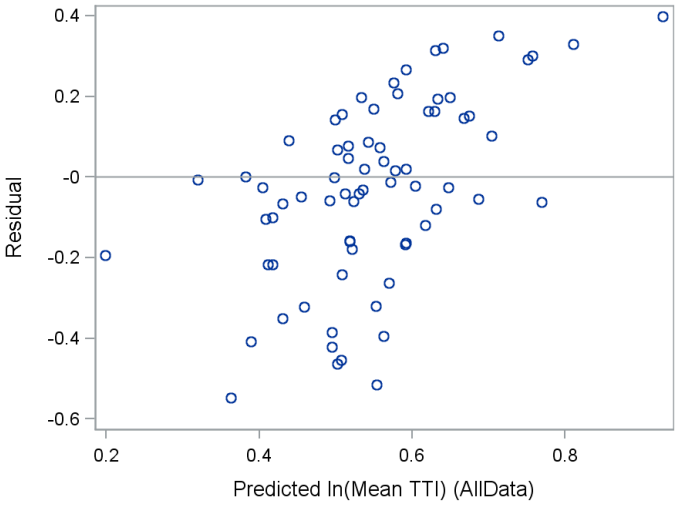

Figure C.19. Residual plot of peak hour—mean TTI—AllData.

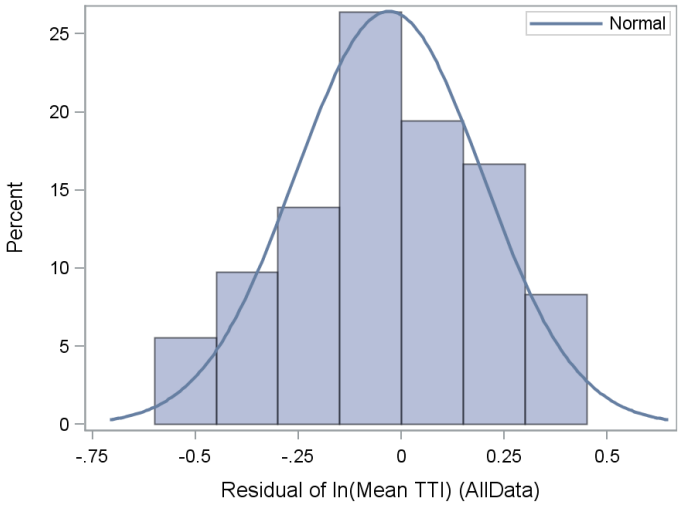

Figure C.20. Residual histogram of peak hour—mean TTI—AllData.

shows that the null hypothesis of normal distribution cannot be rejected with the threshold confidence level of 90%. The Student's *t*-test rejects the null hypothesis of zero residual mean with a high confidence level, which corresponds to the fact that the 95% confidence limits for the mean of residual both fall on the negative side. The residual versus the predicted value plot presents no strong unusual pattern except for a potential slight tendency of overestimation trend as the predicted value ln(mean TTI) increases, and that there are more negative residuals than positive ones. Overall, this validation result is also relatively satisfying. The associated results and plots for this category are included in the attachment.

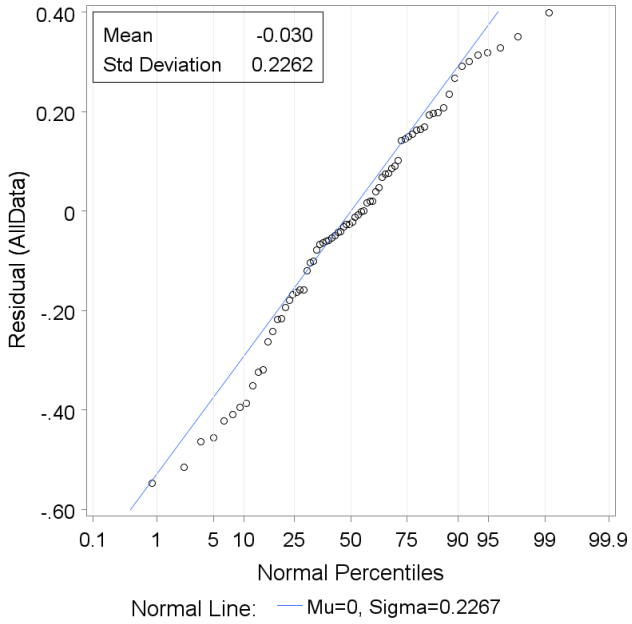

Figure C.21. Residual normality plot of peak hour—mean TTI—AllData.

Peak Hour—Mean TTI—Minnesota

The validation of the peak hour mean TTI model using the MN data set shows that the null hypothesis of the zero residual mean cannot be rejected with a confidence level of 90%. The normality test also shows that the null hypothesis cannot be rejected with the preset threshold confidence level but can be rejected with a confidence level of 85%. The residual plot displays a random pattern except for the potential increasing trend toward the upper right corner. Generally, this model performs satisfactorily. The associated results and plots for this category are included in the attachment.

Peak Hour—99th-Percentile TTI

Peak Hour—99th-Percentile TTI—All Data

The RMSE values are all close to 50% in the peak hour 99th-percentile TTI model validation (Table C.16). Because the 99th-percentile TTI usually represents some extreme or usual value in the TTI distribution, it is expected to have a relatively large prediction error. The RMSE value in the L03 report is 41.3%, smaller than all the RMSE values produced in this validation. This may indicate that the validation set presents different characteristics than the training data set.

The residual analysis using the AllData set is summarized by Table C.17 and Figures C.22 to C.24. The Student's *t*-test shows no strong confidence to reject the zero residual mean hypothesis, while the normality test rejects the null hypothesis of normal distribution with a confidence level of 90%. The residual plot presents a problematic pattern; the model tends to underestimate the response variable when the predicted value is small, and it tends to overestimate the response variable when the predicted value is large. Such a pattern may indicate that the samples located in the bottom left and the upper right corners are potential outliers. A closer look into the details of the validation data set reveals that the coefficient of the D/C predictor is 1.13062, dominating the prediction results. Those potential outlier samples are likely to have a different relationship between the D/C ratio and the response variable when compared to that in the training data samples used in L03. The model performs better when the predicted ln(99th-percentile TTI) is within (1, 1.5) where the residuals are within (–0.5, 0.5), or that the predicted 99th-percentile TTI is within (2.72, 4.48).

Table C.16. RMSE of Peak Hour—99th-Percentile TTI

RMSE	All Data	CA	MN
Mean TTI	50.74%	52.78%	47.46%

Table C.17. Residual Analysis of Peak Hour—99th-Percentile TTI—AllData

Table C.17.a. Basic Statistical Measures

Location		Variability	
Mean	–0.057	Std deviation	0.4092
Median	–0.080	Variance	0.1675
Minimum	–0.911	Range	2.3174
Maximum	1.4057	Interquartile range	0.3618

Table C.17.b. Basic Confidence Limits Assuming Normality

Parameter	Estimate	95% Confidence Limits	
Mean	–0.057	–0.153	0.0391
Std deviation	0.4092	0.3516	0.4897
Variance	0.1675	0.1236	0.2398

Table C.17.c. Tests for Location: Mu=0

Test	Statistic		*p*-Value	
Student's *t*	*t*	–1.183	Pr > |*t*|	0.2407

Table C.17.d. Tests for Normality

Test	Statistic		*p*-Value	
Shapiro-Wilk	*W*	0.9464	Pr < *W*	0.0040

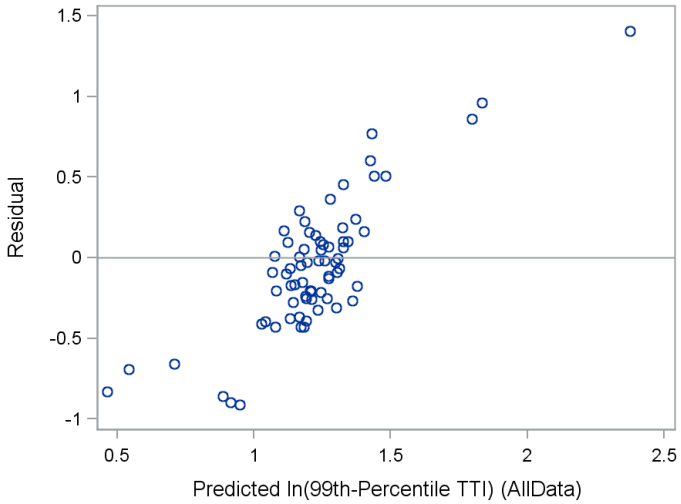

Figure C.22. Residual plot of peak hour—99th-percentile TTI—AllData.

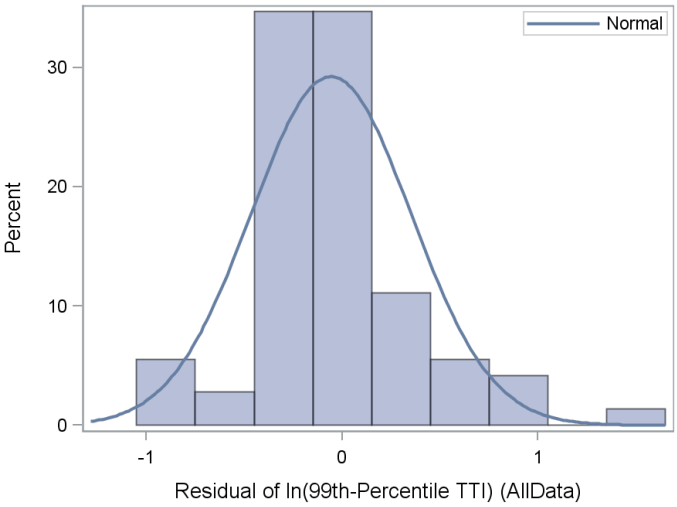

Figure C.23. Residual histogram of peak hour—99th-percentile TTI—AllData.`

Peak Hour—99th-Percentile TTI—California

Validation using the CA data presents similar results to that using the AllData set. Again, the model performs best when the predicted ln(99th-percentile TTI) is within (1, 1.5). The Student's *t*-test shows that the zero residual mean hypothesis cannot be rejected, while the Shapiro-Wilk normality test rejects the null hypothesis of normal distribution with a confidence level of 90%. The histogram and the normality plot manifest these tests results. All associated results and plots are included in the attachment.

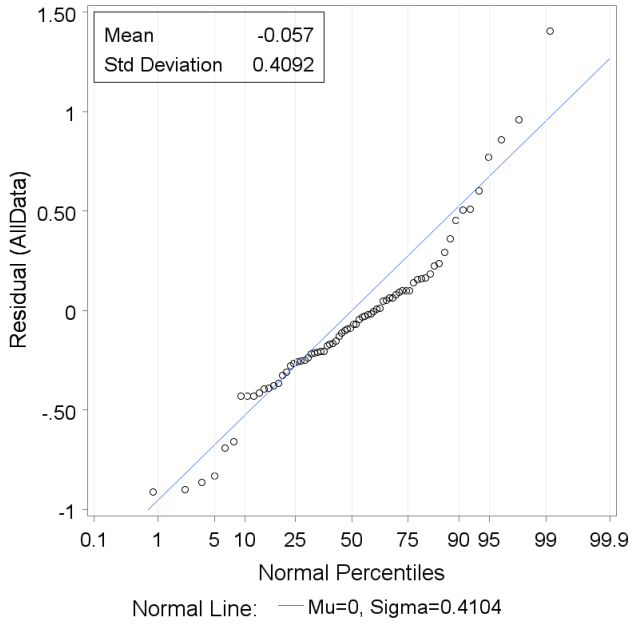

Figure C.24. Residual normality plot of peak hour—99th-percentile TTI—AllData.

Peak Hour—99th-Percentile TTI—Minnesota

The residual plot using the MN data set do not presents any strong unusual pattern except for the three underestimated samples located in the bottom left corner of the plot, which may be potential outliers. The Student's *t*-test rejects the zero residual mean with a confidence level of 90%, while the Shapiro-Wilk test cannot reject the null hypothesis of normal distribution with the preset confidence level. All associated results and plots are included in the attachment.

Peak Hour—95th-Percentile TTI

Peak Hour—95th-Percentile TTI—All Data

The RMSE values from the validation of the 95th-percentile TTI are summarized in Table C.18. The largest value still comes from the CA data set, which is 40.19%. The RMSE for the AllData set is 38.38%, which is almost equal to the RMSE of 38.3% for the peak hour 95th-percentile TTI model in the L03 report.

From this validation it is apparent that neither the zero residual mean hypothesis nor the normal distribution hypothesis can be rejected with the preset threshold confidence level, indicating satisfaction to these two model assumptions (Table C.19). The histogram and the normality plot also present good shape (Figures C.26 and C.27). However, the plot of residual versus the predicted reveals a problematic pattern: the increasing trend of residual as the predicted value increases (Figure C.25). It shows that the model tends to underestimate ln(95th-percentile TTI) when this predicted value is small while overestimate it when this predicted value is large. This pattern shows that although the model satisfies the zero residual mean and the normal distribution of residual assumptions, the model form may still be inadequate and might be improved.

Peak Hour—95th-Percentile TTI—California

The validation using the CA data set yields a similar pattern to that using the AllData set. The research team cannot reject the zero residual mean hypothesis or the normal distribution hypothesis with the preset threshold confidence, indicating these two model assumptions are satisfied. However, the residual plot shows a nonrandom increasing pattern, which indicates that the model form may not be adequate to predict the validation data set. All associated results and plots are included in the attachment.

Table C.18. RMSE of Peak Hour—95th-Percentile TTI

RMSE	All Data	CA	MN
Mean TTI	38.38%	40.19%	37.27%

Table C.19. Residual Analysis of Peak Hour—95th-Percentile TTI—AllData

Table C.19.a. Basic Statistical Measures

Location		Variability	
Mean	–0.037	Std deviation	0.3250
Median	0.0129	Variance	0.1056
Minimum	–0.757	Range	1.7162
Maximum	0.9590	Interquartile range	0.4056

Table C.19.b. Basic Confidence Limits Assuming Normality

Parameter	Estimate	95% Confidence Limits	
Mean	–0.037	–0.113	0.0397
Std deviation	0.3250	0.2792	0.3889
Variance	0.1056	0.0780	0.1512

Table C.19.c. Tests for Location: Mu=0

Test	Statistic		*p*-Value	
Student's *t*	*t*	–0.957	Pr > |*t*|	0.3419

Table C.19.d. Tests for Normality

Test	Statistic		*p*-Value	
Shapiro-Wilk	*W*	0.9850	Pr < *W*	0.5515

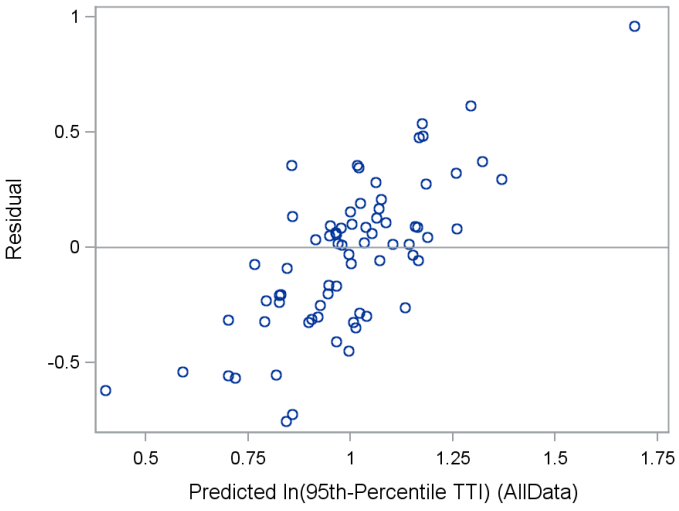

Figure C.25. Residual plot of peak hour—95th-percentile TTI—AllData.

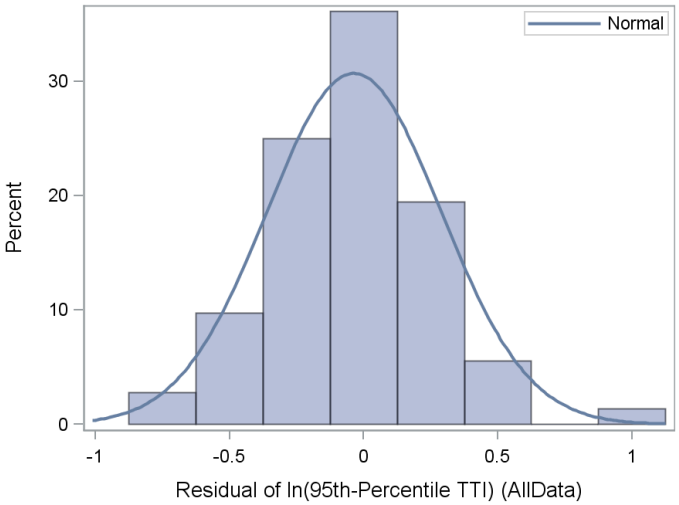

Figure C.26. Residual histogram of peak hour—95th-percentile TTI—AllData.

Peak Hour—95th-Percentile TTI—Minnesota

The validation results using the MN data set show that the research team cannot reject the zero residual mean assumption or the normal distribution of residual assumption with a confidence level of 90%, as the *p*-values in the Student's *t*-test and the Shapiro-Wilk test are both larger than 0.1. The histogram and the normality plot manifest these hypothesis-testing results. However, the plot of residual versus the predicted value displays a possible increasing trend, implying that the model may be biased. All associated results and plots are included in the attachment.

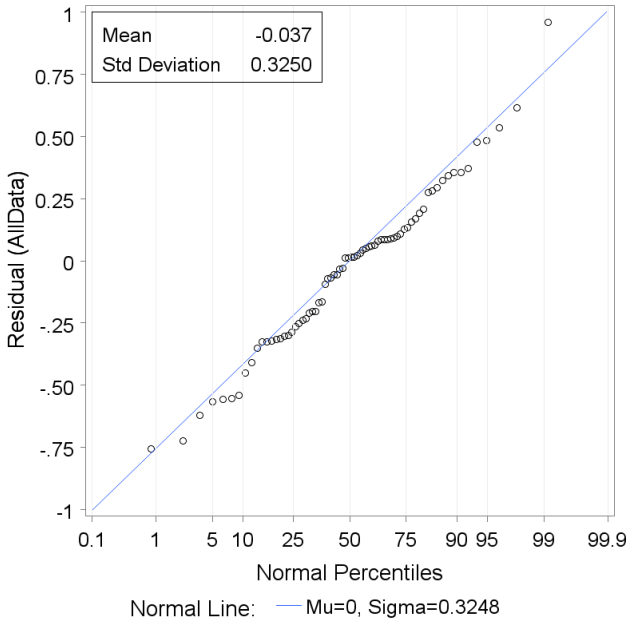

Figure C.27. Residual normality plot of peak hour—95th-percentile TTI—AllData.

Table C.20. RMSE of Peak Hour—80th-Percentile TTI

RMSE	All Data	CA	MN
Mean TTI	35.13%	36.89%	34.06%

Peak Hour—80th-Percentile TTI

Peak Hour—80th-Percentile TTI—All Data

The RMSE values for the validation of the 80th-percentile TTI model using the AllData, CA, and MN data sets are close to one another, at around 35% (Table C.20). The RMSE for the corresponding model in the L03 report is 34.1%, which is close to the validation RMSE values.

Table C.21 and Figures C.28 to C.30 summarize the validation results for the 80th-percentile TTI model using the AllData set. The Student's *t*-test rejects the null hypothesis of zero residual mean with a confidence level of 90%, while the Shapiro-Wilk normality test yields a *p*-value of 0.2959, indicating that the null hypothesis of normal distribution cannot be rejected with the preset threshold confidence level. The plot of residual versus the predicted ln(80th-percentile TTI) implies that bias might exist shown as the tendency of underestimating the response variable when the predicted value is small and overestimating it when the predicted value is large.

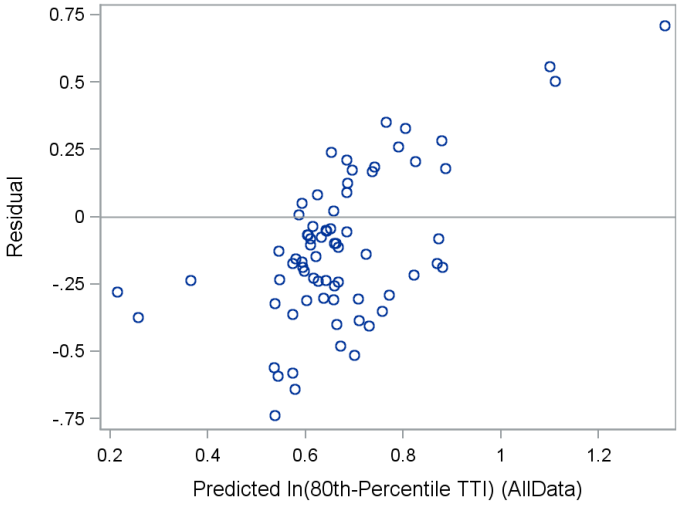

Figure C.28. Residual plot of peak hour—80th-percentile TTI—AllData.

Table C.21. Residual Analysis of Peak Hour—80th-Percentile TTI—AllData

Table C.21.a. Basic Statistical Measures

Location		Variability	
Mean	–0.116	Std deviation	0.2798
Median	–0.143	Variance	0.0783
Minimum	–0.738	Range	1.4482
Maximum	0.7099	Interquartile range	0.3335

Table C.21.b. Basic Confidence Limits Assuming Normality

Parameter	Estimate	95% Confidence Limits	
Mean	–0.116	–0.182	–0.050
Std deviation	0.2798	0.2403	0.3347
Variance	0.0783	0.0578	0.1120

Table C.21.c. Tests for Location: Mu=0

Test	Statistic		*p*-Value	
Student's *t*	*t*	–3.517	Pr > |*t*|	0.0008

Table C.21.d. Tests for Normality

Test	Statistic		*p*-Value	
Shapiro-Wilk	*W*	0.9797	Pr < *W*	0.2959

Peak Hour—80th-Percentile TTI—California

The validation of the 80th-percentile TTI model using the CA data set shows that the model does not perform well enough. The Student's *t*-test and the Shapiro-Wilk normality test reject their null hypotheses with a confidence level of 90%, implying violation of the zero residual mean assumption and

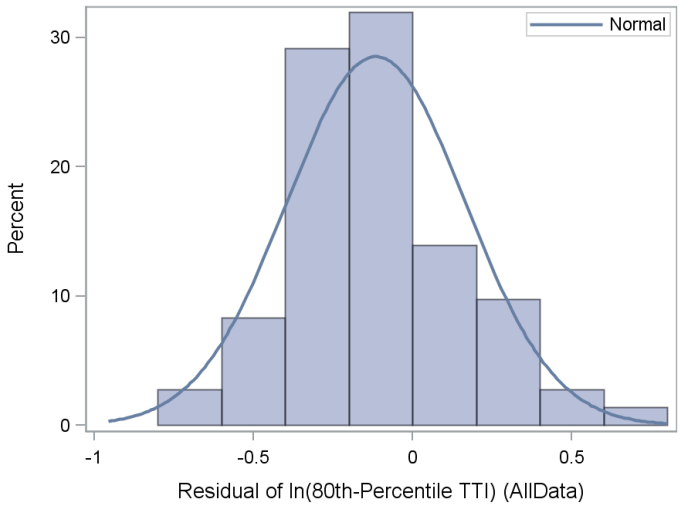

Figure C.29. Residual histogram of peak hour—80th-percentile TTI—AllData.

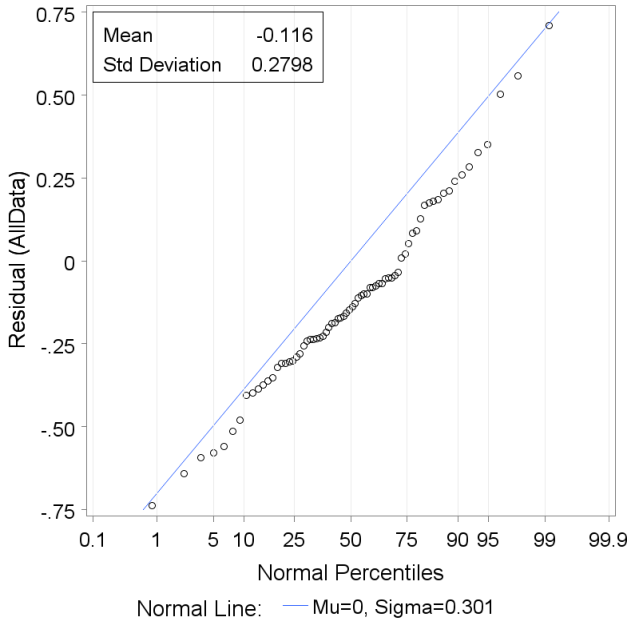

Figure C.30. Residual normality plot of peak hour—80th-percentile TTI—AllData.

the normal distribution of residual assumption. The residual versus predicted value plot shows that the model tends to overestimate when the predicted value is large, and that there are more negative residuals than positive ones. All these observations suggest that the model can be improved. All associated results and plots are included in the attachment.

Peak Hour—80th-Percentile TTI—Minnesota

The statistical analysis results summarized in the attachment show that the Student's *t*-test rejects the null hypothesis of zero residual mean with a confidence level of 90%, and the Shapiro-Wilk normality test rejects the null hypothesis of normal distribution with the same confidence level. However, the plot of residual versus the predicted value presents no strong nonrandom pattern, except for the three potential outliers located at the bottom left corner. Because the basic model assumptions are violated, the model performance may be improved. Note that the failure to pass the statistical tests may result from the existence of those potential outliers.

Peak Hour—50th-Percentile TTI

Peak Hour—50th-Percentile TTI—All Data

The RMSE values for the peak hour 50th-percentile TTI model validation are summarized in Table C.22. The largest RMSE value comes from the CA data set. This is the same as all previous validation exercises presented in this appendix. The RMSE for the corresponding model in L03 is 28.3%, which is close to the RMSE for AllData set.

Table C.22. RMSE of Peak Hour—50th-Percentile TTI

RMSE	All Data	CA	MN
Mean TTI	28.85%	32.41%	24.22%

The validation results of the peak hour 50th-percentile TTI model using the AllData set are summarized in Table C.23 and Figures C.31 to C.33. The Student's *t*-test yields a *p*-value of 0.0115, showing strong evidence to reject the null hypothesis of zero residual mean. The Shapiro-Wilk test yields a *p*-value of 0.6028, indicating that the null hypothesis of normal distribution of residuals cannot be rejected. The plot of residuals versus predicted values shows that the residual variance is much larger when the ln(50th-percentile TTI) is around 0.4 than it is otherwise. The histogram also shows that the mean of the residual distribution is shifted to the left

Table C.23. Residual Analysis of Peak Hour—50th-Percentile TTI—AllData

Table C.23.a. Basic Statistical Measures

Location		Variability	
Mean	–0.075	Std deviation	0.2440
Median	–0.066	Variance	0.0595
Minimum	–0.624	Range	1.0277
Maximum	0.4035	Interquartile range	0.3580

Table C.23.b. Basic Confidence Limits Assuming Normality

Parameter	Estimate	95% Confidence Limits	
Mean	–0.075	–0.132	–0.017
Std deviation	0.2440	0.2096	0.2919
Variance	0.0595	0.0439	0.0852

Table C.23.c. Tests for Location: Mu=0

Test	Statistic		*p*-Value	
Student's *t*	*t*	–2.596	Pr > |*t*|	0.0115

Table C.23.d. Tests for Normality

Test	Statistic		*p*-Value	
Shapiro-Wilk	*W*	0.9859	Pr < *W*	0.6028

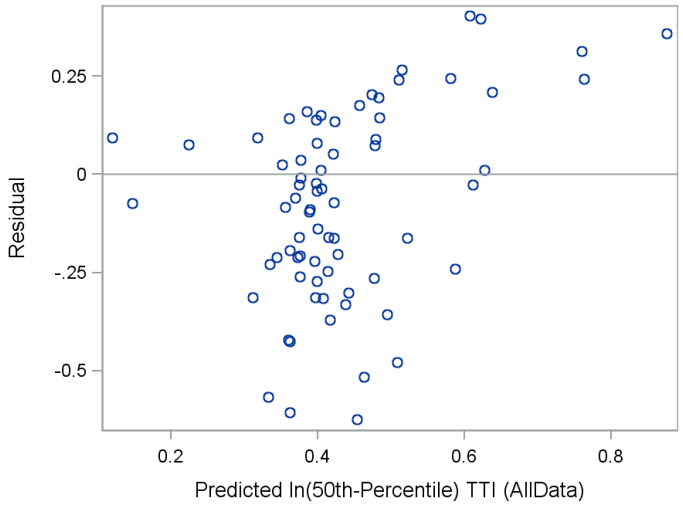

Figure C.31. Residual plot of peak hour—50th-percentile TTI—AllData.

side of the zero reference line, which corresponds to the 95% limits for residual mean shown in Table C.23.

Peak Hour—50th-Percentile TTI—California

The validation using the CA data set yields similar results to that using the AllData set: the Student's *t*-test rejects the null hypothesis of zero residual mean while the Shapiro-Wilk normality test cannot reject the null hypothesis of normal distribution. The histogram and the normality plot demonstrate these conclusions. The residual plot shows that there are many more negative residual samples than positive residual samples, and the prediction variance is much larger when the predicted ln(50th-percentile TTI) is around 0.4 than otherwise. The 95% confidence limits of residual mean are both negative, manifesting

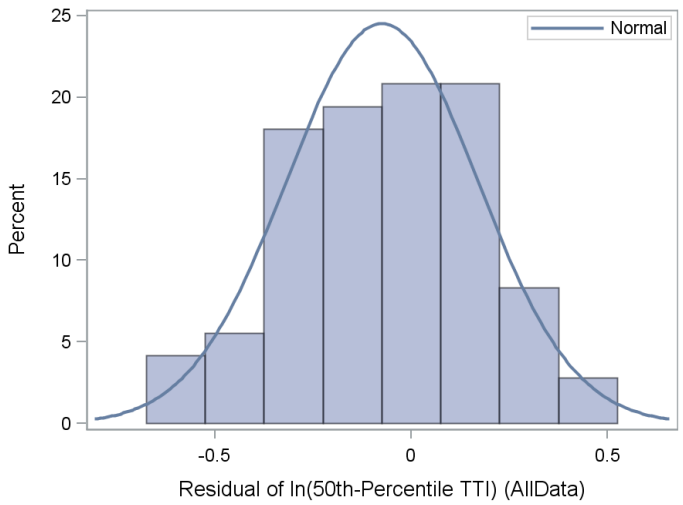

Figure C.32. Residual histogram of peak hour—50th-percentile TTI—AllData.

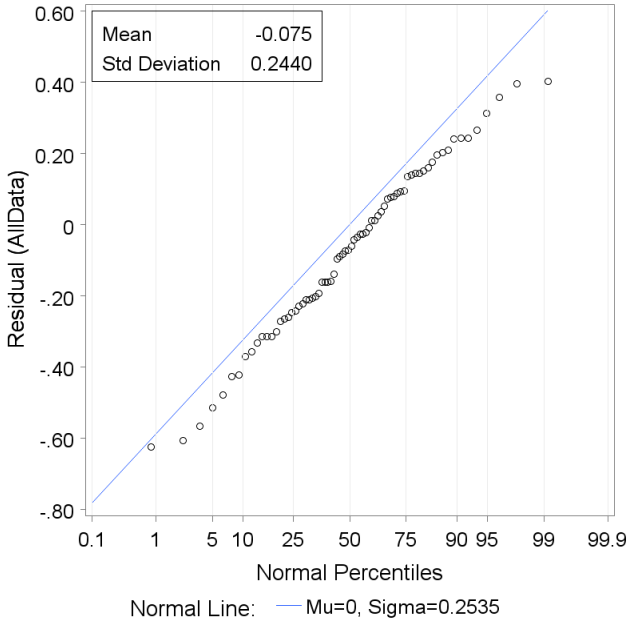

Figure C.33. Residual normality plot of peak hour—50th-percentile TTI—AllData.

the same fact that there are more negative residuals than positive ones. All associated results and plots are included in the attachment.

Peak Hour—50th-Percentile TTI—Minnesota

The validation analysis using the MN data set presents satisfying results. The Student's *t*-test and the Shapiro-Wilk test show evidence that we cannot reject the zero residual mean hypothesis and the normal distribution hypothesis. The histogram and normality plot demonstrate these conclusions. The plot of residuals versus predicted values does not display any strong unusual pattern, except for two potential outliers located in the upper right corner. Given the RMSE of 24.22%, which is smaller than the corresponding RMSE value in L03, the research team concludes that this model performs satisfactorily for the MN validation data set. All associated results and plots are included in the attachment.

Peak Hour—10th-Percentile TTI

Peak Hour—10th-Percentile TTI—All Data

The RMSE values in the validation of the 10th-percentile TTI model are summarized in Table C.24. The largest one comes

Table C.24. RMSE of Peak Hour—10th-Percentile TTI

RMSE	All Data	CA	MN
Mean TTI	18.50%	22.24%	12.14%

from the CA data set. The RMSE for this model in the L03 report is 15.2%, which is larger than the MN RMSE but smaller than the other two. Judging by the single criteria of RMSE this model performs the best for the MN data set and performs the poorest for the CA data set.

The validation of the 10th-percentile TTI model using the AllData set shows that the zero residual mean hypothesis in the Student's *t*-test cannot be rejected with a confidence level of 90%, while the normal distribution of residual hypothesis can be rejected at the preset threshold confidence level (Table C.25). The plot of residuals versus predicted values (Figure C.34) shows that the prediction variance is much larger when the predicted ln(10th-percentile TTI) falls within (0.1, 0.15) than otherwise. Those seven samples located below the –0.2 reference line may be outliers that this model cannot predict well, and they may represent different relationships between the three independent variables and the dependent variable other than those represented in the data-rich model. The histogram

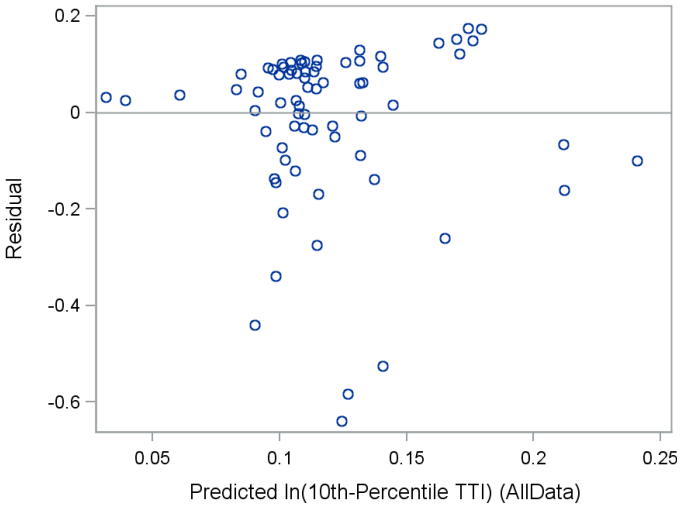

Figure C.34. Residual plot of peak hour—10th-percentile TTI—AllData.

(Figure C.35) shows that the distribution of residuals has a long left tail and that there are more positive than negative samples. The residual normality plot is shown in Figure C.36.

PEAK HOUR—10TH-PERCENTILE TTI—CALIFORNIA

The validation using the CA data set shows that the zero residual mean hypothesis and the normal distribution hypothesis can be rejected with a confidence level of 90% in their respective statistical tests. The histogram and the normality plot demonstrate these conclusions. The plot of residuals versus the predicted ln(10th-percentile TTI) has the same nonconstant variance and potential outlier problems as seen in the validation using the AllData set. All associated results and plots are included in the attachment.

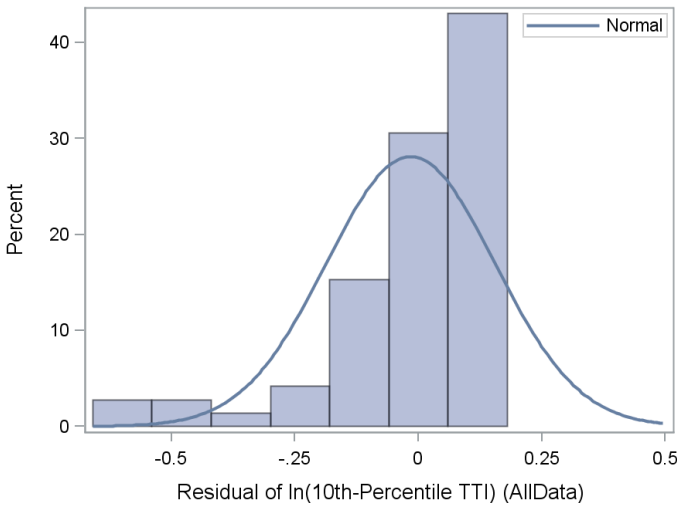

Figure C.35. Residual histogram of peak hour—10th-percentile TTI—AllData.

Table C.25. Residual Analysis of Peak Hour—10th-Percentile TTI—AllData

Table C.25.a. Basic Statistical Measures

Location		Variability	
Mean	–0.016	Std deviation	0.1702
Median	0.0392	Variance	0.0290
Minimum	–0.640	Range	0.8136
Maximum	0.1739	Interquartile range	0.1643

Table C.25.b. Basic Confidence Limits Assuming Normality

Parameter	Estimate	95% Confidence Limits	
Mean	–0.016	–0.056	0.0241
Std deviation	0.1702	0.1462	0.2037
Variance	0.0290	0.0214	0.0415

Table C.25.c. Tests for Location: Mu=0

Test	Statistic		*p*-Value	
Student's *t*	*t*	–0.794	Pr > |*t*|	0.4297

Table C.25.d. Tests for Normality

Test	Statistic		*p*-Value	
Shapiro-Wilk	*W*	0.7949	Pr < *W*	<0.0001

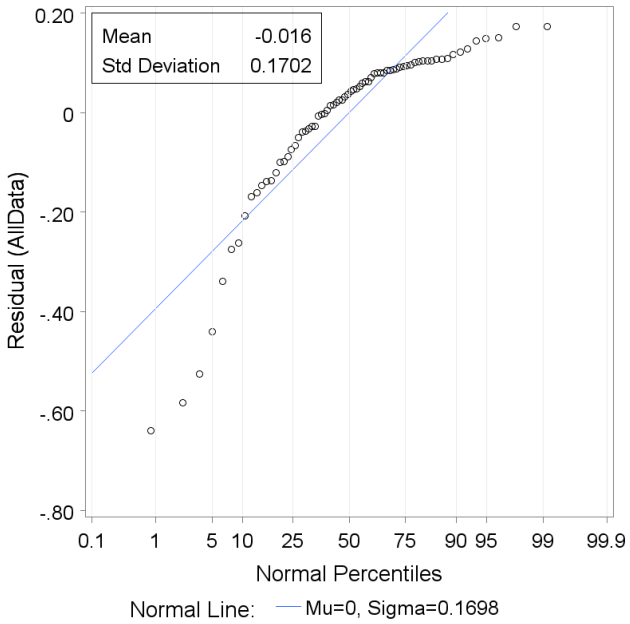

Figure C.36. Residual normality plot of peak hour—10th-percentile TTI—AllData.

Peak Hour—10th-Percentile TTI—Minnesota

The validation using the MN data set shows that the zero residual mean and the normal distribution of residuals assumptions are likely violated as the Student's *t*-test and the Shapiro-Wilk normality test both reject their null hypotheses. The plot of residuals versus predicted values shows that most of the residuals are positive, and there is one potential outlier located at the bottom right of the figure. The violation of assumptions and the unusual patterns shown in the residual plots indicate that the peak hour 10th-percentile TTI does not perform satisfactorily using the MN data set. All associated results and plots are included in the attachment.

Conclusions of the Data-Rich Peak Hour Model Validation

Based on the RMSE values, the data-rich peak hour models generally perform the best with the MN data set and the poorest with the CA data set. The most satisfying validation results were seen in the validation of the 50th-percentile TTI model using the MN data set, where both the zero residual mean assumption and the normal distribution assumption passed their respective statistical tests, and the residual plot did not show any unusual patterns.

It is apparent that violations of basic regression assumptions were common in these validation results. The models may not be able to sufficiently describe the relationship between the independent variables and the dependent variables as there are some nonrandom patterns in the residual plots. All of these findings indicate that the models can potentially be improved for better performance.

Midday Models

The midday models depend only on the critical D/C ratio, in the form of

$$y = e^{\beta x}$$

Thus, the prediction accuracy relies on the correction of the exponential relationship between the D/C ratio and the mean TTI.

Midday—Mean TTI

Midday—Mean TTI—All Data

The RMSE for the training data set is 7.5% in the L03 report (Table C.26). In the validation, the largest RMSE comes from the CA data set, which is almost the same as the L03 report. The smallest is 3.52%, which is almost half of the L03 report. Based on the single criteria of RMSE, this data-rich model performs satisfactorily for the validation data sets, and even better than its performance for the training data set. However, the small RMSE value may result from the characteristics of the data sets; it does not necessarily indicate satisfying performance.

The validation of the midday mean TTI model using the AllData set shows that the Student's *t*-test rejects the zero residual mean hypothesis with a confidence level of 90%, and the Shapiro-Wilk normality test also rejects the null hypothesis of normal distribution (Table C.27). Thus, it is likely that the zero residual mean assumption and the assumption that the residuals follow a normal distribution are violated. The distorted shape in the normality plot (Figure C.37) and the histogram (Figure C.38) demonstrate these hypothesis-testing conclusions. The plot of residuals versus predicted values (Figure C.39) presents some problematic patterns: there are more positive residuals than negative ones, and there are some potential outliers with large absolute residual values. These observations indicate that the model may not perform satisfactorily.

Midday—Mean TTI—California

The validation of the midday mean TTI model using the CA data set presents similar results to that using the AllData set. The null hypothesis of zero residual mean can be rejected in

Table C.26. RMSE of Midday—Mean TTI

RMSE	All Data	CA	MN	Salt Lake City
Mean TTI	6.24%	7.57%	4.07%	3.52%

Table C.27. Residual Analysis of Midday—Mean TTI—AllData

Table C.27.a. Basic Statistical Measures

Location		Variability	
Mean	0.0199	Std deviation	0.0573
Median	0.0349	Variance	0.0033
Minimum	–0.443	Range	0.5167
Maximum	0.0741	Interquartile range	0.0329

Table C.27.b. Basic Confidence Limits Assuming Normality

Parameter	Estimate	95% Confidence Limits	
Mean	0.0199	0.0126	0.0272
Std deviation	0.0573	0.0526	0.0630
Variance	0.0033	0.0028	0.0040

Table C.27.c. Tests for Location: Mu=0

Test	Statistic		*p*-Value	
Student's *t*	*t*	5.3837	Pr > |*t*|	<0.0001

Table C.27.d. Tests for Normality

Test	Statistic		*p*-Value	
Shapiro-Wilk	*W*	0.5446	Pr < *W*	<0.0001

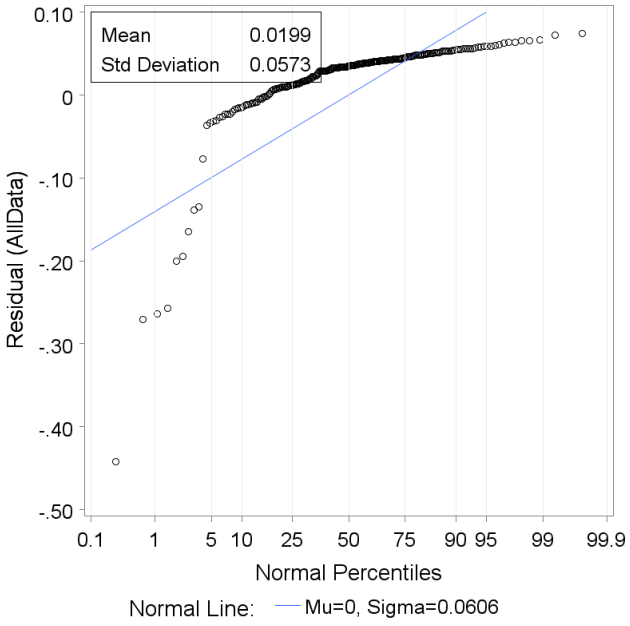

Figure C.37. Residual normality plot of midday—mean TTI—AllData.

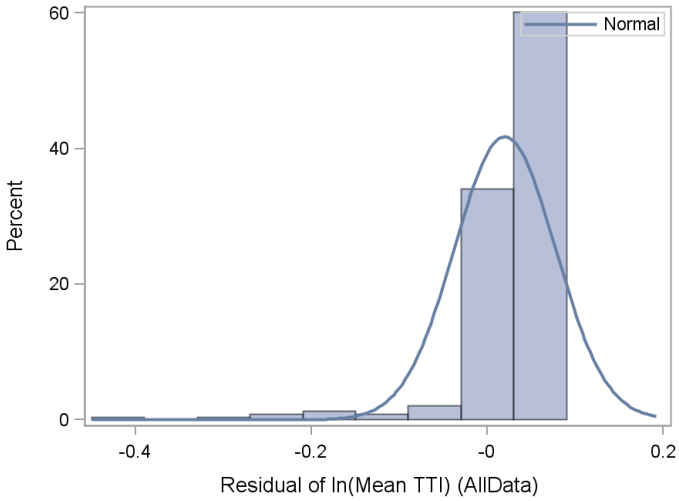

Figure C.38. Residual histogram of midday—mean TTI—AllData.

the Student's *t*-test with a confidence level of 90%. The null hypothesis of normal distribution can also be rejected with the threshold confidence level in the normality test. The plot of residuals versus predicted values shows that most samples have positive residuals, while there are also potential outliers with large negative residuals. All associated results and plots are included in the attachment.

Midday—Mean TTI—Minnesota

The validation of the midday mean TTI model using the MN data set also shows similar pattern to that using the AllData set. The zero residual mean and the normal distribution of residual hypotheses can be rejected in the statistical tests with

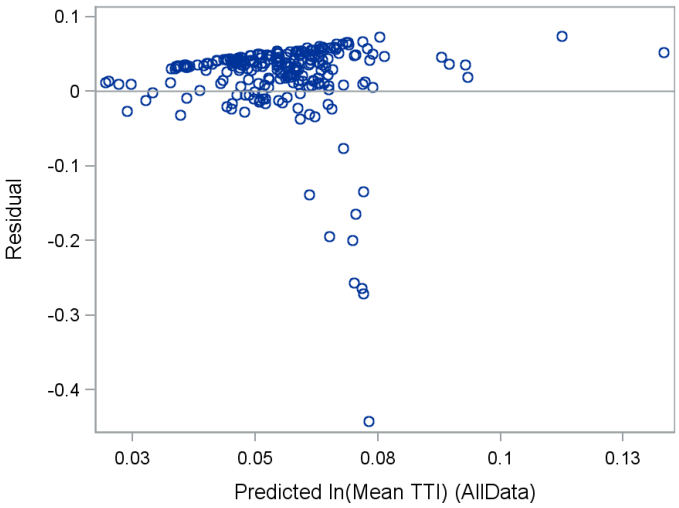

Figure C.39. Residual plot of midday—mean TTI—AllData.

a confidence level of 90%. The histogram and the normality plot show the deviation of the residual distribution from a normal distribution. The residual versus the predicted value plot displays that there are more positive residuals than negative ones and that there is a potential outlier located at the bottom right of the figure. This indicates that the model may be problematic in predicting the mean TTI for MN data. All associated results and plots are included in the attachment.

Midday—Mean TTI—Salt Lake City

The validation results for the midday mean TTI model using the Salt Lake City data are summarized in the attachment. It is apparent that the zero residual mean hypothesis can be rejected with a confidence level of 90%, and the normal distribution of residual hypothesis can also be rejected with the same threshold confidence level. The histogram and the normality plot demonstrate that the residual distribution deviates from the normal distribution. The zero reference line in the plot of residual versus the predicted value acts like a separating line. It separates the residuals into two sets, indicating that the model may not perform satisfactorily.

Midday—99th-Percentile TTI

Midday—99th-Percentile TTI—All Data

The RMSE values for each validation data set are summarized in Table C.28. The corresponding RMSE value in the data-rich appendix is 33.4%, which is close to the RMSE values for the AllData set, the CA data set, and the Salt Lake City data set. The RMSE for MN data set is smaller. A closer look at the validation details provides further details on the model performance for each validation data set.

The validation of the midday 99th-percentile TTI model using the AllData set shows that the zero residual mean assumption, the assumption that the residuals follow a normal distribution and the constant residual variance assumptions may be violated (Table C.29). The Student's *t*-test rejects the null hypothesis of zero residual mean with a confidence level of 90%, and the Shapiro-Wilk normality test rejects the null hypothesis of normal distribution with the same threshold confidence level. The plot of residual versus the predicted value (Figure C.40) shows that the variance of residual tends

Table C.28. RMSE of Midday—99th-Percentile TTI

RMSE	All Data	CA	MN	Salt Lake City
Mean TTI	32.32%	34.95%	25.86%	34.01%

Table C.29. Residual Analysis of Midday—99th-Percentile TTI—AllData

Table C.29.a. Basic Statistical Measures

Location		Variability	
Mean	0.1946	Std deviation	0.2019
Median	0.2451	Variance	0.0407
Minimum	–0.535	Range	1.2456
Maximum	0.7110	Interquartile range	0.1892

Table C.29.b. Basic Confidence Limits Assuming Normality

Parameter	Estimate	95% Confidence Limits	
Mean	0.1946	0.1689	0.2202
Std deviation	0.2019	0.1853	0.2217
Variance	0.0407	0.0343	0.0491

Table C.29.c. Tests for Location: Mu=0

Test	Statistic		*p*-Value	
Student's *t*	*t*	14.962	Pr > |*t*|	<0.0001

Table C.29.d. Tests for Normality

Test	Statistic		*p*-Value	
Shapiro-Wilk	*W*	0.8792	Pr < *W*	<0.0001

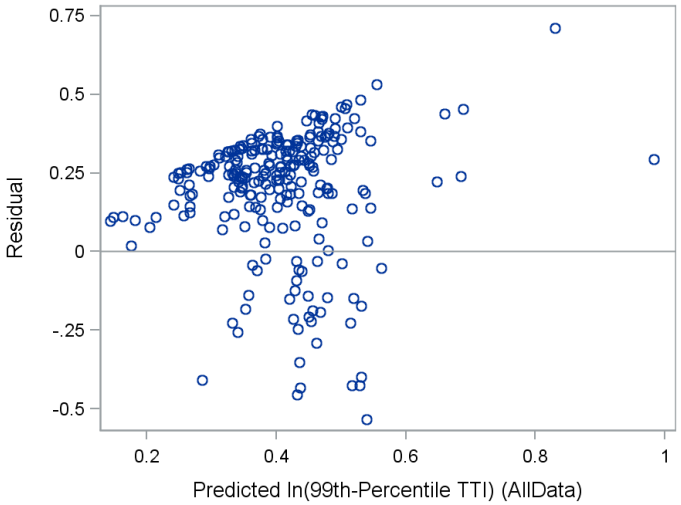

Figure C.40. Residual plot of midday—99th-percentile TTI—AllData.

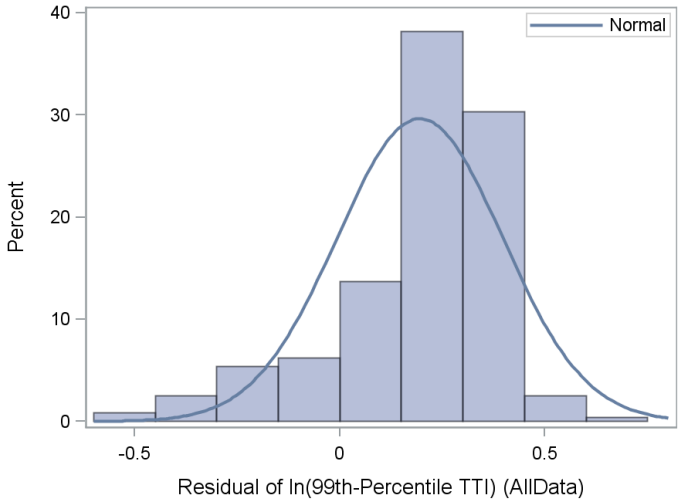

Figure C.41. Residual histogram of midday—99th-percentile TTI—AllData.

to increase with the increase in predicted values. All these observations imply that the predictive capability of the model may be insufficient. The residual histogram and normality plot are shown in Figure C.41 and Figure C.42.

Midday—99th-Percentile TTI—California

Since the CA data set constitutes the largest portion of the AllData set, the validation of the midday 99th-percentile TTI model using the CA data set shows similar results to that using the AllData set. The zero residual mean hypothesis test and the normality hypothesis test both reject the null hypotheses,

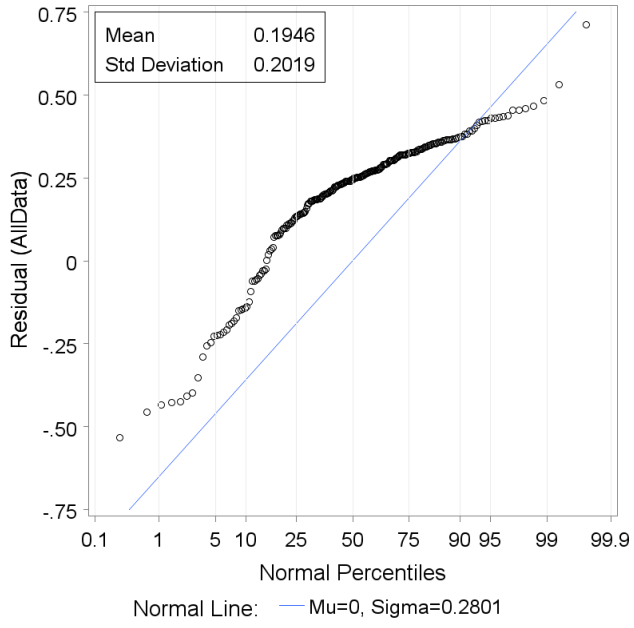

Figure C.42. Residual normality plot of midday—99th-percentile TTI—AllData.

respectively, with a confidence level of 90%. The residual versus the predicted value plot shows that a nonconstant residual variance problem may exist. All associated results and plots are included in the attachment.

Midday—99th-Percentile TTI—Minnesota

In this validation the zero residual mean hypothesis and the normal distribution of residual hypothesis again fail to pass the statistical tests, respectively. The histogram and the normality plot demonstrate these conclusions. The plot of residuals versus the predicted values shows two unusual patterns: more positive residuals and the potential outliers when the predicted value is around 0.45. Thus, the model may not perform satisfactorily. All associated results and plots are included in the attachment.

Midday—99th-Percentile TTI—Salt Lake City

The Salt Lake City data validation of the midday 99th-percentile TTI model shows that the zero residual mean hypothesis and the normal distribution of residual hypothesis can be rejected again with a confidence level of 90% in the respective statistical tests. The plot of residuals versus the predicted values show that the model constantly overestimates ln(99th-percentile TTI), excluding one sample with a large negative residual located at the bottom of the figure.

Midday—95th-Percentile TTI

Midday—95th-Percentile TTI—All Data

The RMSE for this midday 95th-percentile TTI model for the training data set in the L03 report is 21.8%. The research team can see that the RMSE values for all the validation data sets are smaller than 21.8% (Table C.30). This could be a result of the varying characteristics of the data sets instead of improved performance. The research team needs to investigate the validation details to see if the model satisfies the basic regression model assumptions.

The validation results for the midday 95th-percentile TTI model using the AllData set shows that the zero residual mean hypothesis can be rejected with a confidence level of 90% in the Student's *t*-test, and that the normal distribution hypothesis can be rejected with the same threshold confidence level in the normality test (Table C.31). The histogram (Figure C.44) and the normality plot (Figure C.45) demonstrate the deviation of the residual distribution from a

Table C.30. RMSE of Midday—95th-Percentile TTI

RMSE	All Data	CA	MN	Salt Lake City
Mean TTI	15.62%	17.29%	14.01%	12.55%

Table C.31. Residual Analysis of Midday—95th-Percentile TTI—AllData

Table C.31.a. Basic Statistical Measures

Location		Variability	
Mean	0.0752	Std deviation	0.1244
Median	0.1084	Variance	0.0155
Minimum	–0.662	Range	0.9157
Maximum	0.2537	Interquartile range	0.0821

Table C.31.b. Basic Confidence Limits Assuming Normality

Parameter	Estimate	95% Confidence Limits	
Mean	0.0752	0.0594	0.0910
Std deviation	0.1244	0.1142	0.1366
Variance	0.0155	0.0130	0.0187

Table C.31.c. Tests for Location: Mu=0

Test	Statistic		*p*-Value	
Student's *t*	*t*	9.3841	Pr > |*t*|	<0.0001

Table C.31.d. Tests for Normality

Test	Statistic		*p*-Value	
Shapiro-Wilk	*W*	0.6845	Pr < *W*	<0.0001

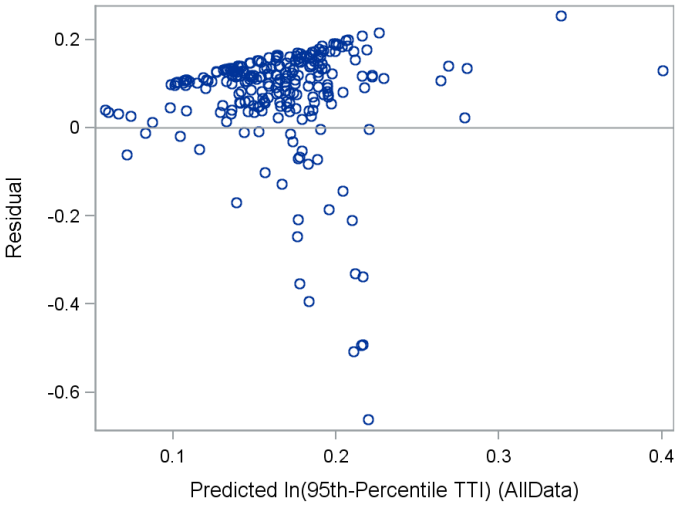

Figure C.43. Residual plot of midday—95th-percentile TTI—AllData.

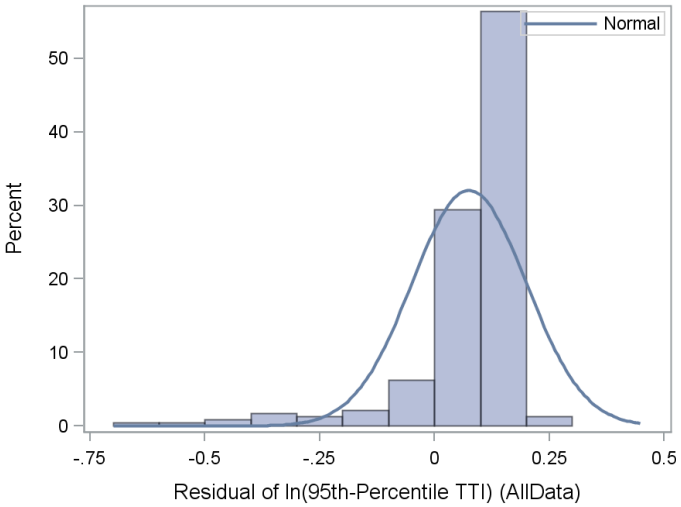

Figure C.44. Residual histogram of midday—95th-percentile TTI—AllData.

normal distribution. The plot of residual versus the predicted value (Figure C.44) presents an overestimation problem and the nonconstant residual variance problem. Generally this model does not perform satisfactorily. The plot of residual versus the predicted value is shown in Figure C.43.

Midday—95th-Percentile TTI—California

Validation of the CA data set presents similar results as that of the validation using the AllData set. The zero residual mean assumption and the normal distribution assumption are likely to be violated since they fail to pass the Student's

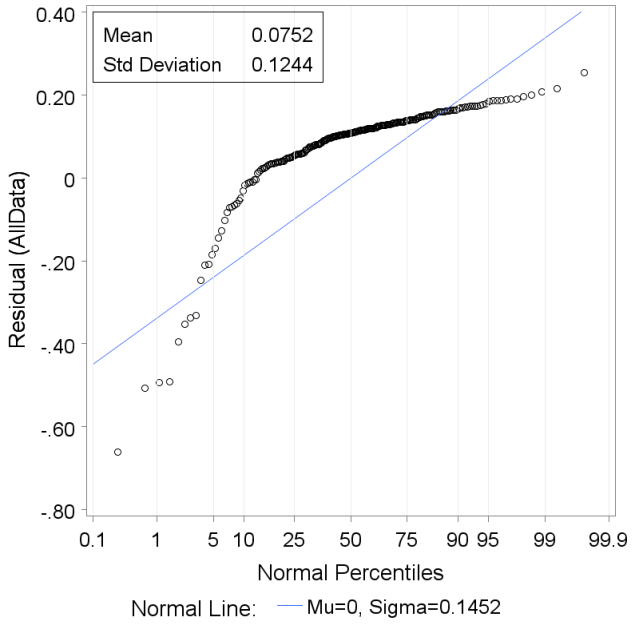

Figure C.45. Residual normality plot of midday—95th-percentile TTI—AllData.

t-test and the normality test. The residual plot shows that the model tends to overestimate the response variable. There are also some potential outliers located on the bottom side to the zero reference line when the ln(95th percentile TTI) is around 0.2. All associated results and plots are included in the attachment.

Midday—95th-Percentile TTI—Minnesota

The validation of the MN data set presents similar problems as that of the validation using the CA data set. The zero residual mean assumption and the normal distribution assumption are likely to be violated as the Student's *t*-test and the Shapiro-Wilk normality test reject the null hypotheses with a confidence level of 90%. The plot of residuals versus the predicted values shows that the model tends to overestimate the response variable while some potential outliers with large negative residuals exist when the ln(95th-percentile TTI) is around 0.18. All associated results and plots are included in the attachment.

Midday—95th-Percentile TTI—Salt Lake City

The validation of the midday 95th-percentile TTI model using the Salt Lake City data set shows that the zero residual mean assumption and the normal distribution assumption are unlikely to be satisfied. The plot of residuals versus the predicted values shows that the model consistently overestimates the ln(95th-percentile TTI) except for one potential outlier with large negative residual located at the bottom of the figure, where ln(95th-percentile TTI) is around 0.14. All associated results and plots are included in the attachment.

Midday—80th-Percentile TTI

Midday—80th-Percentile TTI—All Data

The largest RMSE in the validation of the midday 80th-percentile TTI model comes from the CA data set at 10.86% (Table C.32). The smallest comes from the Salt Lake City data set, which is 3.6%. The RMSE for this model in the L03 report is 9.2%, which is smaller than the RMSE of the CA data set but larger than the RMSE values for the other three data sets. Based on the single criteria of RMSE, the research team may reach the conclusion that the model performs satisfactorily for the validation data sets. However, as discussed previously, the RMSE might easily lead to misleading conclusions and further investigation of the validation details is required to evaluate whether the model assumptions are satisfied.

Table C.32. RMSE of Midday—80th-Percentile TTI

RMSE	All Data	CA	MN	Salt Lake City
Mean TTI	8.99%	10.86%	6.61%	3.60%

Table C.33. Residual Analysis of Midday—80th-Percentile TTI—AllData

Table C.33.a. Basic Statistical Measures

Location		Variability	
Mean	0.0116	Std deviation	0.0854
Median	0.0360	Variance	0.0073
Minimum	–0.627	Range	0.7005
Maximum	0.0737	Interquartile range	0.0462

Table C.33.b. Basic Confidence Limits Assuming Normality

Parameter	Estimate	95% Confidence Limits	
Mean	0.0116	0.0008	0.0224
Std deviation	0.0854	0.0784	0.0938
Variance	0.0073	0.0062	0.0088

Table C.33.c. Tests for Location: Mu=0

Test	Statistic		*p*-Value	
Student's *t*	*t*	2.1077	Pr > |*t*|	0.0361

Table C.33.d. Tests for Normality

Test	Statistic		*p*-Value	
Shapiro-Wilk	*W*	0.5139	Pr < *W*	<0.0001

The validation results show that the Student's *t*-test rejects the null hypothesis of zero residual mean with a confidence level of 90%, and the Shapiro-Wilk normality test rejects the null hypothesis with the same threshold confidence level (Table C.33). The plot of residuals versus the predicted values (Figure C.46) manifests a problematic pattern in that the model tends to overestimate the response variable, resulting in more positive residuals. Additionally, potential outliers characterized by large negative residuals can be noted from the plot. The residual histogram and normality plots are shown in Figures C.47 and C.48.

Midday—80th-Percentile TTI—California

In this validation the Student's *t*-test cannot reject the null hypothesis of zero residual mean with a confidence level of 90%, while the Shapiro-Wilk normality test rejects the null hypothesis of normal distribution with the threshold confidence level of 90%. The residual plot for the CA data set

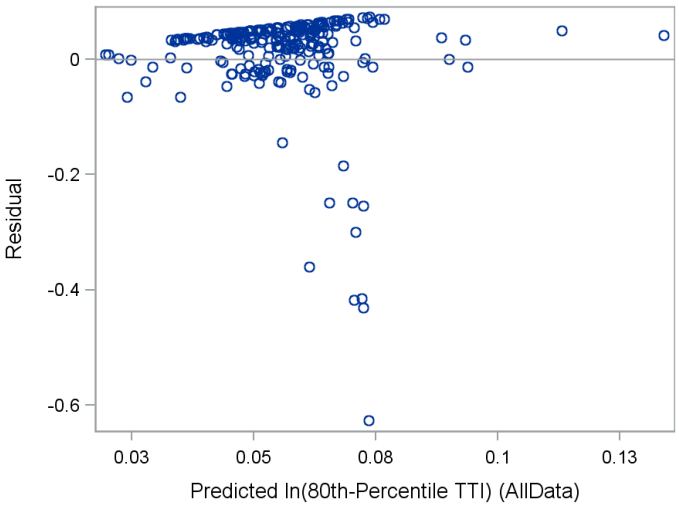

Figure C.46. Residual plot of midday—80th-percentile TTI—AllData.

shows similar problems noted in the validation results of the AllData set (i.e., more positive residuals and potential outliers). All associated results and plots are included in the attachment.

Midday—80th-Percentile TTI—Minnesota

The validation of the midday 80th-percentile TTI model using the MN data set shows that the zero residual mean assumption and the normal distribution assumption are likely to be violated, as they fail to pass the respective statistical tests. The residuals versus the predicted values plot shows that the model tends to overestimate the response variable as there are more positive residuals than negative ones. There are also two potential outliers with large negative residuals. All associated results and plots are included in the attachment.

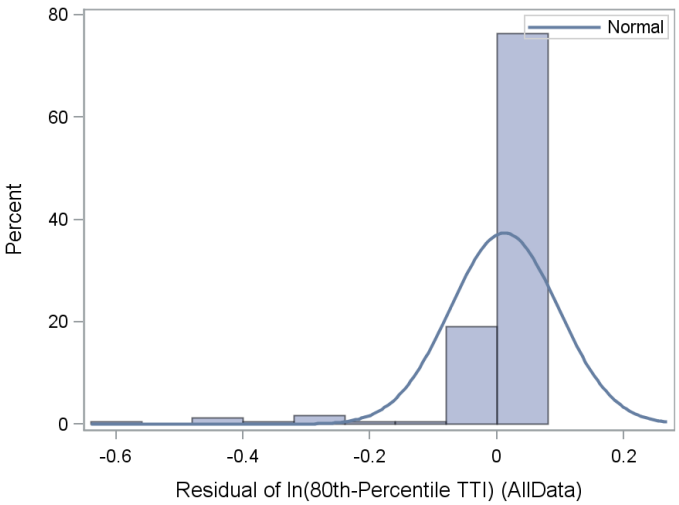

Figure C.47. Residual histogram of midday—80th-percentile TTI—AllData.

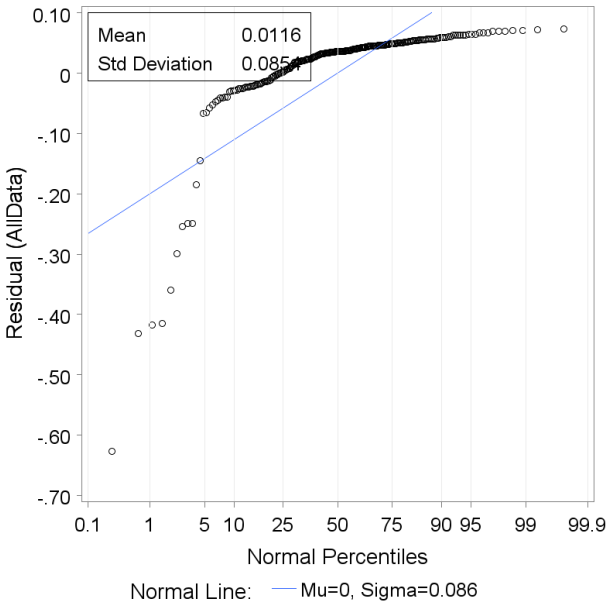

Figure C.48. Residual normality plot of midday—80th-percentile TTI—AllData.

Midday—80th-Percentile TTI—Salt Lake City

In this validation the null hypothesis of zero residual mean is rejected by the Student's *t*-test, and the null hypothesis of normal distribution of residual is also rejected in the normality test with a confidence level of 90%. The plot of residuals versus the predicted values has an unusual pattern where the upper bound of residuals has a linearly increasing pattern. Such nonrandomness indicates that the model may not be able to adequately describe the relationship between the independent variables and the dependent variable. All associated results and plots are included in the attachment.

Midday—50th-Percentile TTI

Midday—50th-Percentile TTI—All Data

The RMSE for the midday 50th-percentile TTI model is 21.8% in the L03 report. This number is suspicious since it is larger than the RMSE for the midday 80th-percentile TTI model (9.2%) and equals to the RMSE for the midday 95th-percentile TTI model (21.8%). Since the *p*th-percentile TTI value generally decreases as the percentage *p* decreases, the large RMSE value for midday 50th-percentile TTI is unexpected. The RMSE values for the same model using the validation data sets are all smaller than 7% (Table C.34). If the

Table C.34. RMSE of Midday—50th-Percentile TTI

RMSE	All Data	CA	MN	Salt Lake City
Mean TTI	5.43%	6.93%	2.09%	2.08%

training data set used in L03 is similar to the validation data sets, then the RMSE value in the L03 report should not have been this large, which indicates that it could be erroneous. For the validation data sets the research team can see that the largest value still comes from the CA data set while the smallest ones come from the MN and the Salt Lake City sets. It should be noted again that such small RMSE values might not necessarily indicate good model performance.

In this validation the zero residual mean hypothesis cannot be rejected with a confidence level of 90%, while the normal distribution hypothesis can be rejected with the same threshold confidence level (Table C.35). The histogram (Figure C.50) and the normality plot (Figure C.51) demonstrate the fact that the residual distribution does not closely follow a normal distribution. Note that the zero residual mean hypothesis passing the Student's *t*-test successfully could be because of the existence of potential outliers with large negative residuals, which can be identified in the plot of residuals versus the predicted values (Figure C.49) and the histogram.

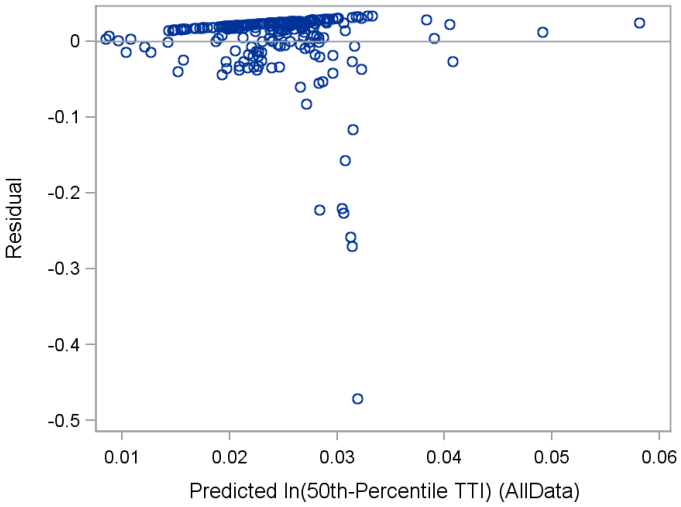

Figure C.49. Residual plot of midday—50th-percentile TTI—AllData.

From the plot of residuals versus the predicted values it is also evident that the upper bound of residuals increases linearly, which should not be the case if the regression model was behaving as expected.

Midday—50th-Percentile TTI—California

The validation of the midday 50th-percentile TTI model using the CA data set presents similar results to that using the AllData set. The null hypothesis of normal distribution fails to pass the Shapiro-Wilk test with a 90% confidence level, while the null hypothesis of zero residual mean cannot be rejected as the Student's *t*-test yields a *p*-value larger than 0.1. The residual plots again present the previously identified problems: nonrandom residual pattern and potential outliers. The above discussion indicates that the model may not

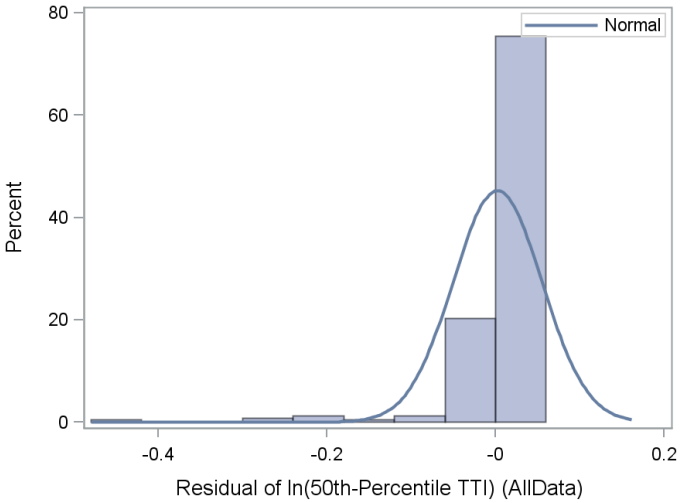

Figure C.50. Residual histogram of midday—50th-percentile TTI—AllData.

Table C.35. Residual Analysis of Midday—50th-Percentile TTI—AllData

Table C.35.a. Basic Statistical Measures

Location		Variability	
Mean	0.0023	Std deviation	0.0529
Median	0.0184	Variance	0.0028
Minimum	–0.471	Range	0.5043
Maximum	0.0333	Interquartile range	0.0226

Table C.35.b. Basic Confidence Limits Assuming Normality

Parameter	Estimate	95% Confidence Limits	
Mean	0.0023	–0.004	0.0090
Std deviation	0.0529	0.0486	0.0581
Variance	0.0028	0.0024	0.0034

Table C.35.c. Tests for Location: Mu=0

Test	Statistic		*p*-Value	
Student's *t*	*t*	0.6760	Pr > |*t*|	0.4997

Table C.35.d. Tests for Normality

Test	Statistic		*p*-Value	
Shapiro-Wilk	*W*	0.4486	Pr < *W*	<0.0001

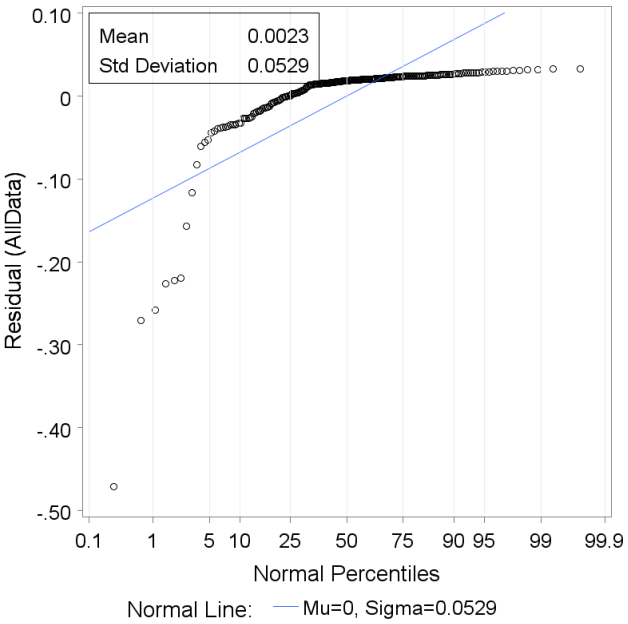

Figure C.51. Residual normality plot of midday—50th-percentile TTI—AllData.

perform satisfactorily. All associated results and plots are included in the attachment.

Midday—50th-Percentile TTI—Minnesota

In this validation the Student's *t*-test and the Shapiro-Wilk test both reject their null hypothesis with a confidence level of 90%, indicating that the zero residual mean assumption and the normal distribution of residuals assumption are likely to be violated. The plot of residuals versus the predicted values presents a nonrandom pattern of residuals, with the residuals increasing almost linearly on the upper bound. A well-behaving regression model should produce residuals randomly distributed along the zero reference line without any patterns. All associated results and plots are included in the attachment.

Midday—50th-Percentile TTI—Salt Lake City

The Salt Lake City validation results show that the zero residual mean hypothesis and the normal distribution hypothesis can be rejected with a confidence level of 90%. The residuals versus the predicted values plot indicates some nonrandom patterns on the upper bound of residuals. Hence, although the RMSE value for this data set is only 2.08%, the model does not perform satisfactorily. All associated results and plots are included in the attachment.

Midday—10th-Percentile TTI

Midday—10th-Percentile TTI—All Data

The RMSE value of the midday 10th-percentile TTI is 5.1% for the training data set in the L03 report. This is larger than all RMSE values for the validation data sets. The largest validation RMSE still comes from the CA data set, while the smallest comes from the MN data set (Table C.36).

Table C.36. RMSE of Midday—10th-Percentile TTI

RMSE	All Data	CA	MN	Salt Lake City
Mean TTI	1.81%	2.20%	0.80%	1.33%

In this validation the Student's *t*-test rejects the null hypothesis of zero residual mean with a confidence level of 90%, and the normality test also rejects the null hypothesis of normal distribution (Table C.37). The residual plots (Figure C.52) also reveal some problematic patterns. The histogram (Figure C.53) and the normality plot (Figure C.54) demonstrate the hypothesis-testing results, while the plot of residuals versus the predicted values shows an increasing upper bound of residuals as well as large negative residuals, indicating inadequacy of the model.

Table C.37. Residual Analysis of Midday—10th-Percentile TTI—AllData

Table C.37.a. Basic Statistical Measures

Location		Variability	
Mean	0.0021	Std deviation	0.0178
Median	0.0071	Variance	0.0003
Minimum	–0.138	Range	0.1547
Maximum	0.0168	Interquartile range	0.0038

Table C.37.b. Basic Confidence Limits Assuming Normality

Parameter	Estimate	95% Confidence Limits	
Mean	0.0021	–17E-5	0.0044
Std deviation	0.0178	0.0164	0.0196
Variance	0.0003	0.0003	0.0004

Table C.37.c. Tests for Location: Mu=0

Test	Statistic		*p*-Value	
Student's *t*	*t*	1.8177	Pr > |*t*|	0.0704

Table C.37.d. Tests for Normality

Test	Statistic		*p*-Value	
Shapiro-Wilk	*W*	0.4378	Pr < *W*	<0.0001

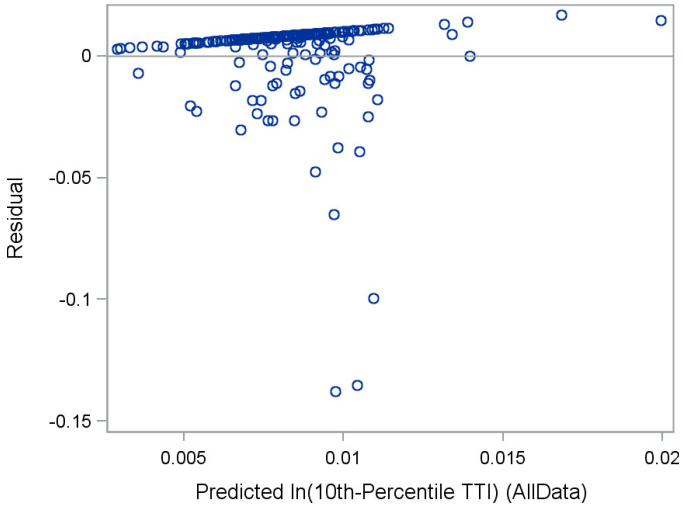

Figure C.52. Residual plot of midday—10th-percentile TTI—AllData.

Midday—10th-Percentile TTI—California

The validation of the midday 10th-percentile TTI model using the CA data set presents similar results to that using the AllData set, except that zero residual mean hypothesis has passed the Student's *t*-test. However, this success of passing the hypothesis test could be attributed to the existence of large negative residuals, which can be seen from the residuals versus the predicted values plot. The normality test again rejects its null hypothesis. The upper bound of residuals in the plot of residuals versus the predicted values also presents a linearly increasing trend. These observations suggest that the model does not perform the prediction satisfactorily. All associated results and plots are included in the attachment.

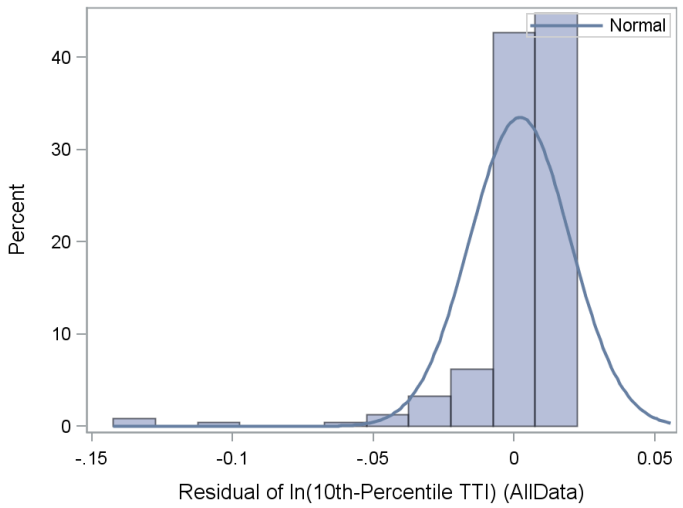

Figure C.53. Residual histogram of midday—10th-percentile TTI—AllData.

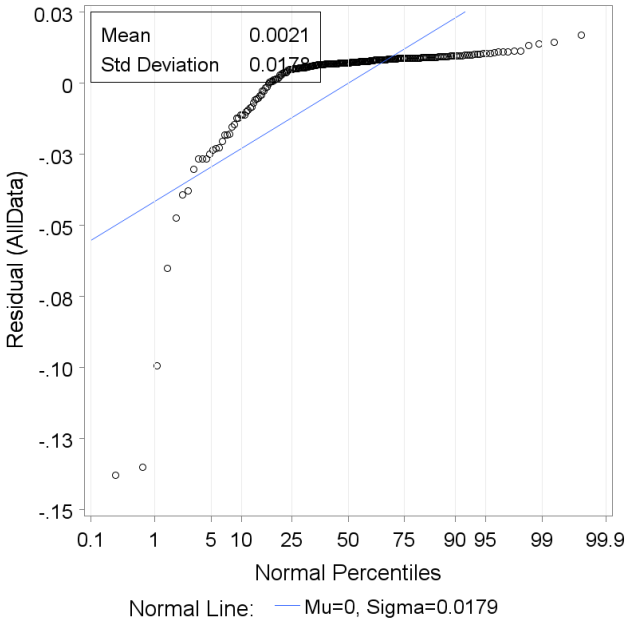

Figure C.54. Residual normality plot of midday—10th-percentile TTI—AllData.

Midday—10th-Percentile TTI—Minnesota

In this validation neither the null hypothesis of zero residual mean nor the null hypothesis of normal distribution pass their respective statistical tests, indicating the violation of basic regression model assumptions. The plot of residual versus the predicted value shows an unusual pattern. Most of the residuals form an increasing linear shape above the zero reference line. However, the vertical axis value tells that these residuals are all approximately equal to 0.01, which is also revealed from the almost zero residual variance in the table included in the attachment. A well-performing model should have randomly distributed residuals rather than what is seen here.

Midday—10th-Percentile TTI—Salt Lake City

In this validation the Student's *t*-test yields a *p*-value of 0.5199, indicating that the null hypothesis of zero residual mean with a confidence level of 90% cannot be rejected. The Shapiro-Wilk normality test rejects the null hypothesis of normal distribution. The plot of residual versus the predicted value presents a nonrandom pattern above the zero reference line, and there are some points below the zero reference line with relatively large negative residuals that may be potential outliers. All associated results and plots are included in the attachment.

Conclusions of the Data-Rich Midday Model Validation

The validation of the midday models does not present satisfying results. Violations of the basic regression model assumptions are consistently seen in the validation results. However, the most

problematic issue is the nonrandom patterns shown in the residual plots, which indicate that the model is not adequate.

It may be mentioned again that the comparison of the L03 RMSE values and the current RMSE values is based on the assumption that they are defined in the same way. However, because of the limited knowledge on how the L03 models were built, the comparison of the current validation results with the L03 results cannot be ascertained completely. In addition, the RMSE of 21.8% for the midday 50th-percentile TTI provided in the L03 report seems to be erroneous.

Weekday Models

The weekly models either have two independent variables (the average D/C ratio and the ILHL), or only one (the average D/C ratio), so the weather condition does not influence the prediction of the weekday travel time reliability metrics in the data-rich weekday models. The data-rich weekday 50th-percentile TTI model and the data-rich weekday 10th-percentile TTI model determine the response value using the average D/C ratio alone.

Weekday—Mean TTI

Weekday—Mean TTI—All Data

The RMSE value for the data-rich weekday mean TTI model is 29.3% in the L03 report, which is only smaller than RMSE for the MN validation data set, as illustrated in Table C.38. The RMSE for the AllData set is 19.74, which is about 10% less. The smallest is from the Salt Lake City data set, which is only 5.95%. Since the RMSE alone cannot lead to confident conclusions, further investigation on the validation details is required.

The validation of the weekday mean TTI model using the AllData set shows that the zero residual mean hypothesis can be rejected with a 90% confidence level in the Student's *t*-test (Table C.39). The null hypothesis of normal distribution can be rejected with the same threshold confidence level in the Shapiro-Wilk normality test. The histogram (Figure C.56) and the normality plot (Figure C.57) also illustrate that the residual distribution is distorted and deviates from a normal distribution. The plot of residuals versus the predicted values (Figure C.55) shows a strong pattern, with the residual value increasing with the predicted value. Also, the model tends to overestimate the response.

Table C.38. RMSE of Weekday—Mean TTI

RMSE	All Data	CA	MN	Salt Lake City
Mean TTI	19.74%	12.81%	35.99%	5.95%

Table C.39. Residual Analysis of Weekday—Mean TTI—AllData

Table C.39.a. Basic Statistical Measures

Location		Variability	
Mean	0.1212	Std deviation	0.1336
Median	0.1072	Variance	0.0178
Minimum	–0.234	Range	1.3799
Maximum	1.1458	Interquartile range	0.0887

Table C.39.b. Basic Confidence Limits Assuming Normality

Parameter	Estimate	95% Confidence Limits	
Mean	0.1212	0.1043	0.1381
Std deviation	0.1336	0.1226	0.1466
Variance	0.0178	0.0150	0.0215

Table C.39.c. Tests for Location: Mu=0

Test	Statistic		*p*-Value	
Student's *t*	*t*	14.150	Pr > |*t*|	<0.0001

Table C.39.d. Tests for Normality

Test	Statistic		*p*-Value	
Shapiro-Wilk	*W*	0.6754	Pr < *W*	<0.0001

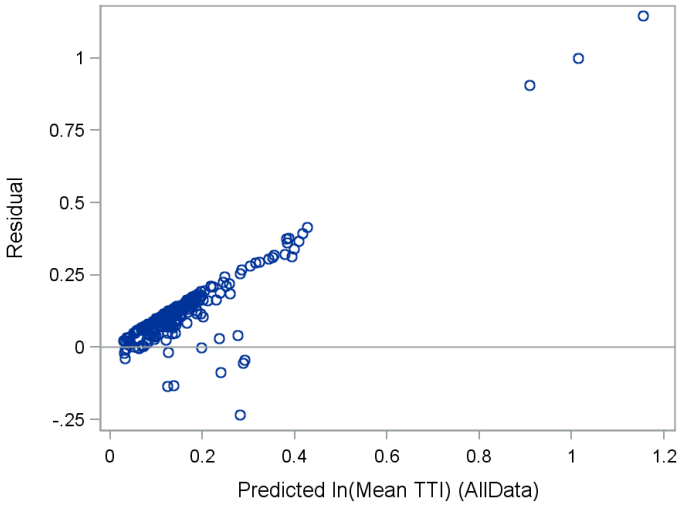

Figure C.55. Residual plot of weekday—mean TTI—AllData.

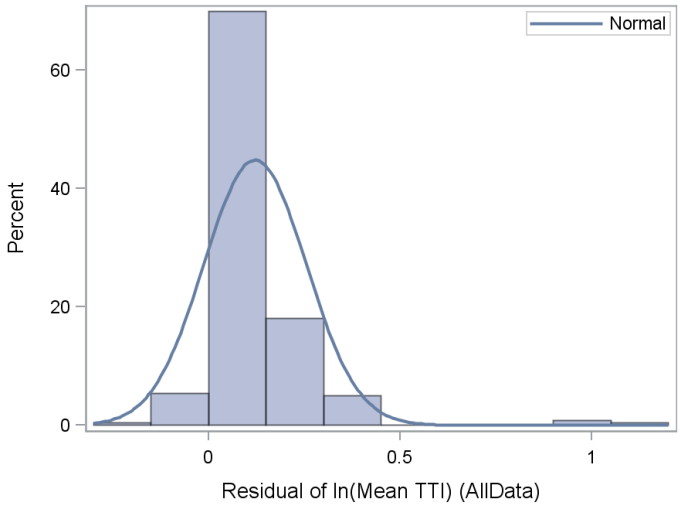

Figure C.56. Residual histogram of weekday—mean TTI—AllData.

Weekday—Mean TTI—California

In the validation of the weekday mean TTI model using the CA data set, the null hypothesis of zero residual mean can be rejected with a confidence level of 90%, and the null hypothesis of normal distribution can be rejected with the same threshold confidence level. The plot of residuals versus the predicted values shows problematic patterns, with the residuals increasing as the predicted values increase and that the model tending to overestimate the response variable. All associated results and plots are included in the attachment.

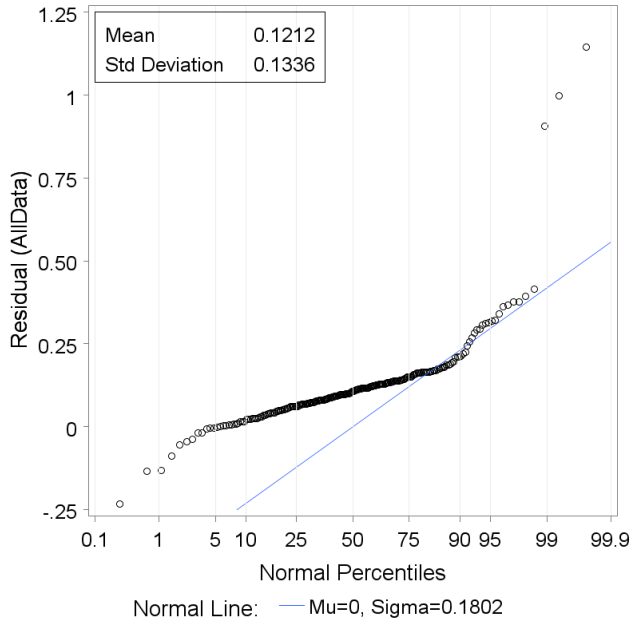

Figure C.57. Residual normality plot of weekday—mean TTI—AllData.

Weekday—Mean TTI—Minnesota

In this validation both the Student's *t*-test and the Shapiro-Wilk normality test reject the null hypotheses. The most significant problem is the nonrandom pattern shown in the residual versus the predicted value plot. The model is evidently biased toward the positive side, as all except one of the residual samples are above the zero reference line. The residuals also increase with the predicted value, which should not happen if the model is well behaving. All associated results and plots are included in the attachment.

Weekday—Mean TTI—Salt Lake City

This validation shows that the model does not perform satisfactorily. The zero mean hypothesis and the normality hypothesis are rejected in the statistical tests, but the most important unusual pattern is the nonrandomness shown in the plot of residuals versus the predicted values. The increasing trend and the overestimation tendency can be observed, which indicates that the model form may not be adequate. All associated results and plots are included in the attachment.

Weekday—99th-Percentile TTI

Weekday—99th-Percentile TTI—All Data

The RMSE value is 38.9% in the L03 report for the data-rich weekday 99th-percentile model. The RMSE for the AllData set is nearly twice as high, at 72.91%. The RMSE for the MN data set is the largest at 141.72%, which is highly influenced by the extreme values in the prediction. More details can be found in the validation analysis of the MN data set (Table C.40).

Validating the weekday 99th-percentile TTI model using the AllData set shows that the model has the follow problematic issues (Table C.41). The zero residual mean Student's *t*-test yields a *p*-value less than 0.001, showing strong evidence that the null hypothesis can be rejected. The 95% confidence interval for the residual mean is [0.2732, 0.3842], implying that the model is biased toward the positive side. The normality test also rejects the null hypothesis. The plot of residuals versus the predicted values (Figure C.58) shows an overestimation tendency caused by more positive residual samples and an increasing trend. The residual histogram and normality plots are shown in Figures C.59 and C.60.

Table C.40. RMSE of Weekday—99th-Percentile TTI

RMSE	All Data	CA	MN	Salt Lake City
Mean TTI	72.91%	50.04%	141.72%	30.87%

Table C.41. Residual Analysis of Weekday—99th-Percentile TTI—AllData

Table C.41.a. Basic Statistical Measures

Location		Variability	
Mean	0.3287	Std deviation	0.4389
Median	0.2902	Variance	0.1926
Minimum	–0.480	Range	4.0280
Maximum	3.5480	Interquartile range	0.3872

Table C.41.b. Basic Confidence Limits Assuming Normality

Parameter	Estimate	95% Confidence Limits	
Mean	0.3287	0.2732	0.3842
Std deviation	0.4389	0.4030	0.4818
Variance	0.1926	0.1624	0.2322

Table C.41.c. Tests for Location: Mu=0

Test	Statistic		*p*-Value	
Student's *t*	*t*	11.674	Pr > |*t*|	<0.0001

Table C.41.d. Tests for Normality

Test	Statistic		*p*-Value	
Shapiro-Wilk	*W*	0.7270	Pr < *W*	<0.0001

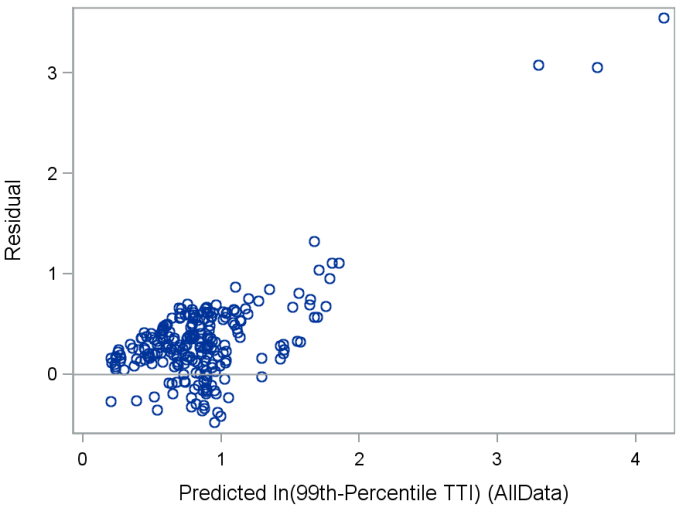

Figure C.58. Residual plot of midday—99th-percentile TTI—AllData.

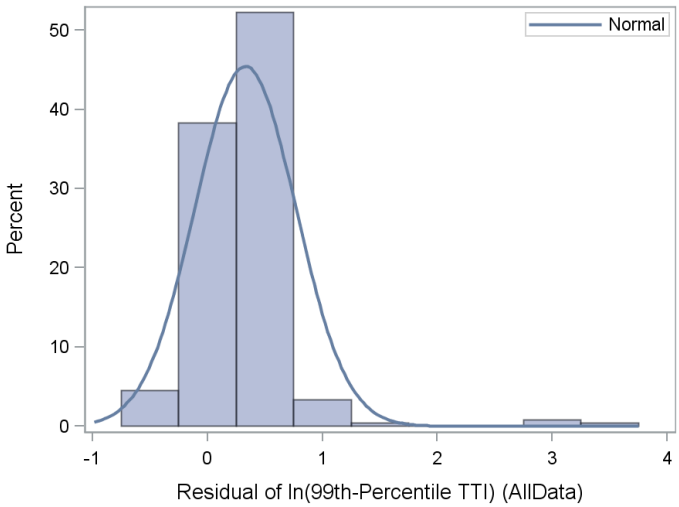

Figure C.59. Residual histogram of midday—99th-percentile TTI—AllData.

WEEKDAY—99TH-PERCENTILE TTI—CALIFORNIA

In this validation both the 95% confidence limits for the zero residual mean are positive, which accords with the Student's *t*-test results. The normality test also rejects the null hypothesis with a confidence level of 90%. The residual versus the predicted value plot manifests the overestimation tendency and the potential outliers. It should also be noted that the variance of residuals is relatively large, compared to the scale of the predicted value. These problems may render the model not reliable to predict unseen samples. All associated results and plots are included in the attachment.

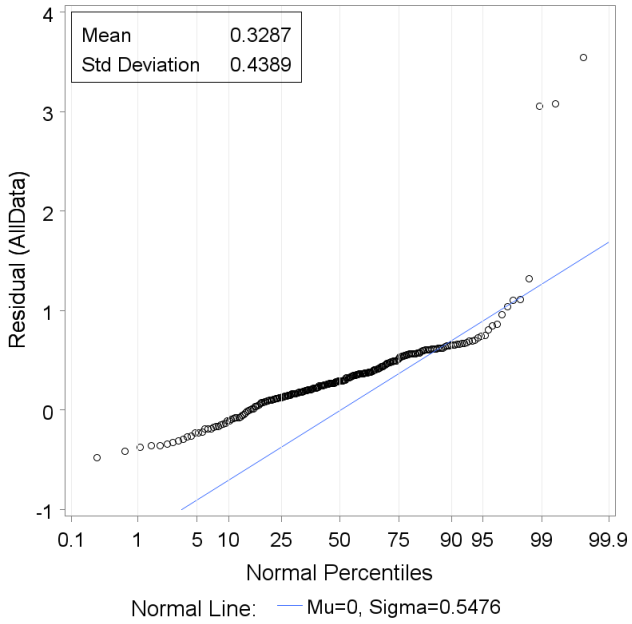

Figure C.60. Residual normality plot of midday—99th-percentile TTI—AllData.

Weekday—99th-Percentile TTI—Minnesota

In this validation the zero residual mean assumption and the normal distribution assumption seem to be violated as the Student's *t*-test and the Shapiro-Wilk normality test reject their null hypotheses. The residual versus the predicted value plot renders unusual patterns, with the residuals increasing with the predicted values. There are also more positive residuals than negative ones. All associated results and plots are included in the attachment.

Weekday—99th-Percentile TTI—Salt Lake City

In this validation the Student's *t*-test and the normality test show strong evidence to reject the null hypotheses. The plot of residuals versus the predicted values generally shows a random pattern, except for there being more samples located in the upper left corner than anywhere else. In addition, the model still tends to yield more positive residuals than negative ones. All associated results and plots are included in the attachment.

Weekday—95th-Percentile TTI

Weekday—95th-Percentile TTI—All Data

The RMSE for the data-rich weekday 95th-percentile TTI is 31.8% for the L03 report, which is only larger than the RMSE value for the Salt Lake City data set. The MN RMSE is again influenced by the extreme values in the data set. The AllData RMSE is 83.32%, which is also influenced by the extreme values (Table C.42).

The validation results show that null hypothesis of zero residual mean can be rejected with a confidence level of 90%, as the *p*-value is less than 0.0001, and the null hypothesis of normal distribution can also be rejected with the same threshold confidence level (Table C.43). The plot of residuals versus the predicted values (Figure C.61) shows similar problems to those seen in the validation of the 99th-percentile TTI model. The increasing trend and the unbalanced pattern indicate that the model may be biased and that there may be an influential variable that is not included in the model. Note that the variance of residuals is relatively large given the scale of the predicted value. The residual histogram and normality plots are shown in Figures C.62 and C.63.

Weekday—95th-Percentile TTI—California

In this validation the null hypotheses in the Student's *t*-test and the Shapiro-Wilk normality test are rejected. The plot of

Table C.42. RMSE of Weekday—95th-Percentile TTI

RMSE	All Data	CA	MN	Salt Lake City
Mean TTI	83.82%	40.46%	197.82%	22.85%

Table C.43. Residual Analysis of Weekday—95th-Percentile TTI—AllData

Table C.43.a. Basic Statistical Measures

Location		Variability	
Mean	0.3416	Std deviation	0.5050
Median	0.2780	Variance	0.2550
Minimum	–0.406	Range	4.7819
Maximum	4.3758	Interquartile range	0.2729

Table C.43.b. Basic Confidence Limits Assuming Normality

Parameter	Estimate	95% Confidence Limits	
Mean	0.3416	0.2778	0.4054
Std deviation	0.5050	0.4637	0.5544
Variance	0.2550	0.2150	0.3073

Table C.43.c. Tests for Location: Mu=0

Test	Statistic		*p*-Value	
Student's *t*	*t*	10.545	Pr > |*t*|	<0.0001

Table C.43.d. Tests for Normality

Test	Statistic		*p*-Value	
Shapiro-Wilk	*W*	0.6022	Pr < *W*	<0.0001

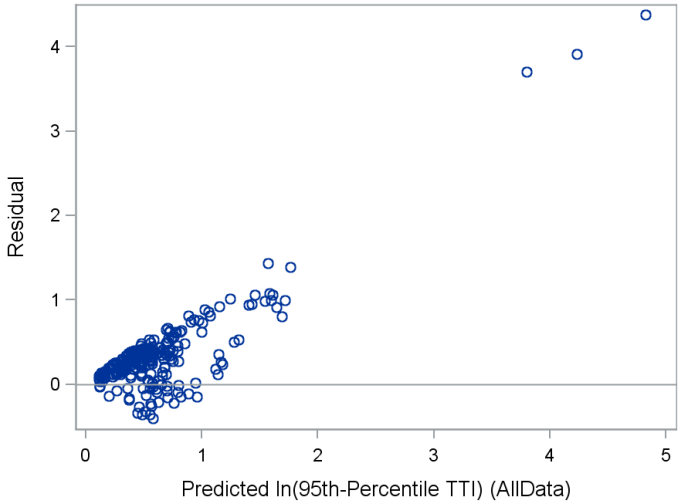

Figure C.61. Residual plot of midday—95th-percentile TTI—AllData.

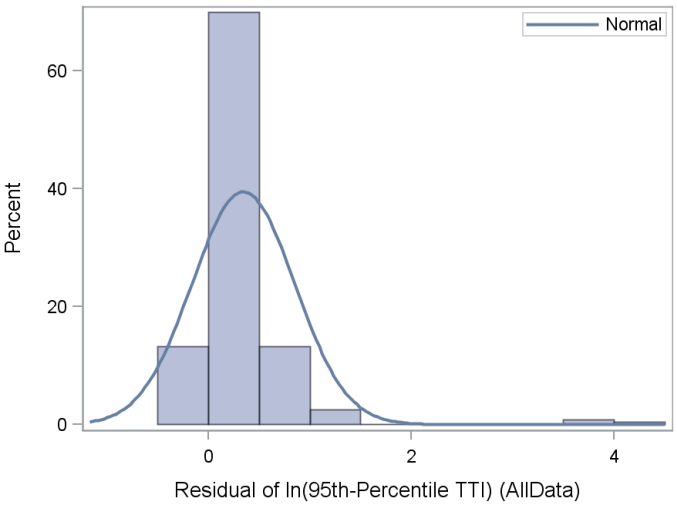

Figure C.62. Residual histogram of midday—95th-percentile TTI—AllData.

residuals versus the predicted values shows that the variation of residuals is relatively large given the scale of the predicted value. The increasing tendency and the fact that there are more positive residuals than negative ones indicate that the model may be biased and unreliable. All associated results and plots are included in the attachment.

Weekday—95th-Percentile TTI—Minnesota

The validation analysis of this data set is highly influenced by the potential outliers. The associated extremely large residuals make the RMSE value unusually large. The mean of residuals is also biased toward these extreme values. The statistical tests yield nearly zero *p*-values indicating strong evidence that the null hypotheses can be rejected with a confidence level of 90%. The plot of residuals versus the predicted values indicates potential outliers as well as other unusual patterns. There are more positive residuals than negative ones, and the residuals do not render a random pattern but rather an increasing trend. These unusual patterns demonstrate that the model may not be reliable for predicting unseen samples. All associated results and plots are included in the attachment.

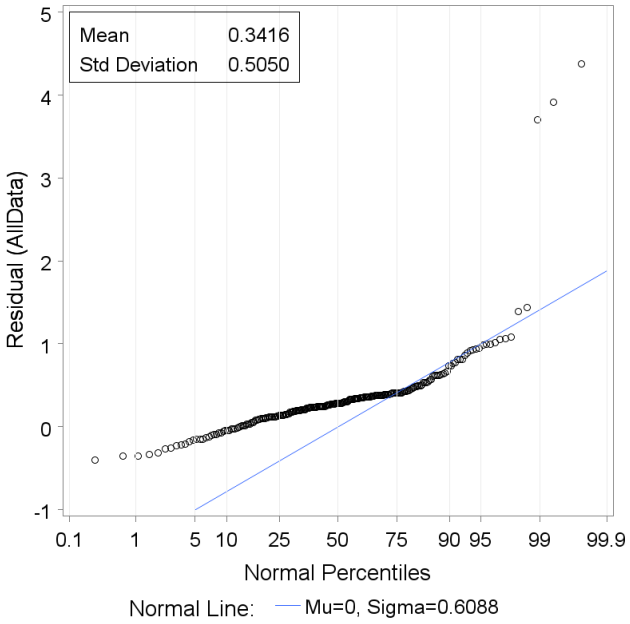

Figure C.63. Residual normality plot of midday—95th-percentile TTI—AllData.

Weekday—95th-Percentile TTI—Salt Lake City

In this validation the Student's *t*-test rejects the zero residual mean hypothesis with a confidence level of 90%, and the normality test rejects the normal distribution hypothesis with the same threshold confidence level. The residual versus the predicted value plot display a generally random pattern except that there is a cluster of residuals located in the upper left of the plot that plays an influential role in the overall positive residual mean. All associated results and plots are included in the attachment.

Weekday—80th-Percentile TTI

Weekday—80th-Percentile TTI—All Data

The RMSE value for the data-rich weekday 80th-percentile TTI model is 14.7% in the L03 report, which is almost the same as the RMSE for the CA validation data set. The RMSE for the Salt Lake City data set is much smaller, which may due to the small scale and variance of the validation data. The RMSE for the MN data set is the largest because of the extreme values (Table C.44).

In the validation of the 80th-percentile TTI using the AllData set, the Student' *t*-test yields a *p*-value less than 0.0001, indicating that the null hypothesis of zero residual mean can be rejected (Table C.45). The normality test also indicates strong evidence to reject the null hypothesis of normal distribution. The plot of residuals versus the predicted values (Figure C.64) is still problematic as most of the residual samples are above the zero reference line, and the increasing trend is obvious. Given these observations, the model does not perform satisfactorily for predicting the AllData set. The residual histogram and normality plots are shown in Figures C.65 and C.66.

Table C.44. RMSE of Weekday—80th-Percentile TTI

RMSE	All Data	CA	MN	Salt Lake City
Mean TTI	29.28%	14.84%	59.43%	5.75%

Table C.45. Residual Analysis of Weekday—80th-Percentile TTI—AllData

Table C.45.a. Basic Statistical Measures

Location		Variability	
Mean	0.1186	Std deviation	0.2282
Median	0.0958	Variance	0.0521
Minimum	–0.387	Range	2.2166
Maximum	1.8296	Interquartile range	0.1441

Table C.45.b. Basic Confidence Limits Assuming Normality

Parameter	Estimate	95% Confidence Limits	
Mean	0.1186	0.0897	0.1474
Std deviation	0.2282	0.2096	0.2506
Variance	0.0521	0.0439	0.0628

Table C.45.c. Tests for Location: Mu=0

Test	Statistic		*p*-Value	
Student's *t*	*t*	8.0997	Pr > |*t*|	<0.0001

Table C.45.d. Tests for Normality

Test	Statistic		*p*-Value	
Shapiro-Wilk	*W*	0.6720	Pr < *W*	<0.0001

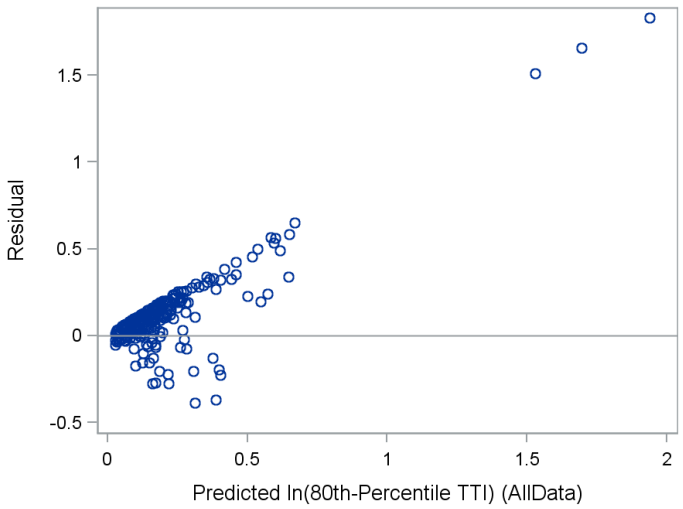

Figure C.64. Residual plot of midday—80th-percentile TTI—AllData.

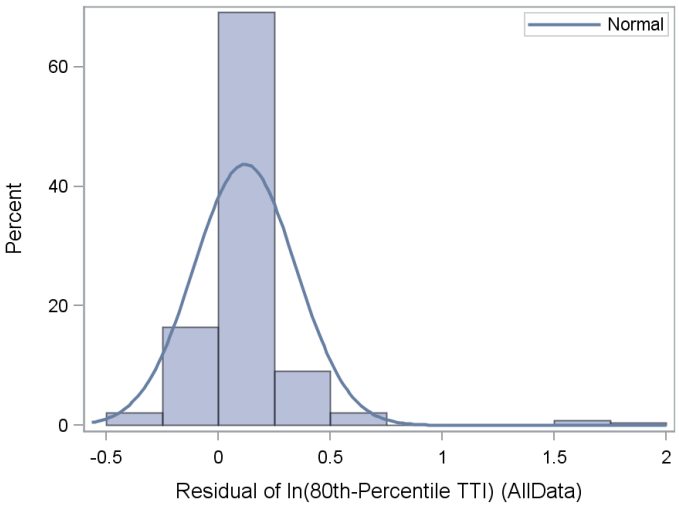

Figure C.65. Residual histogram of midday—80th-percentile TTI—AllData.

Weekday—80th-Percentile TTI—California

In this validation the Student's *t*-test and the normality test reject their null hypotheses, indicating violation of the zero residual mean assumption and the normal distribution assumption. The plot of residuals versus predicted values reveals a non-constant residual variance problem; additionally, the residuals are unbalanced with more positive residuals than negative. All associated results and plots are included in the attachment.

Weekday—80th-Percentile TTI—Minnesota

The MN validation problems are similar to those of the validation of the AllData set. The zero residual mean hypothesis

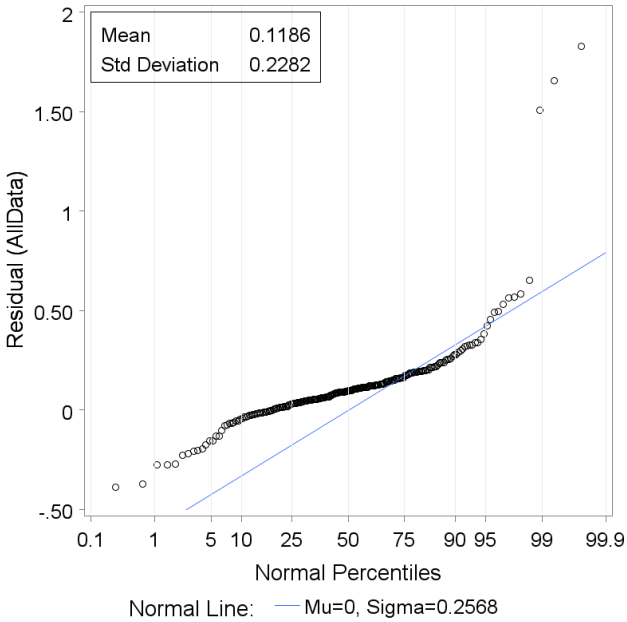

Figure C.66. Residual normality plot of midday—80th-percentile TTI—AllData.

and the normal distribution null hypotheses are rejected. The plot of residuals versus the predicted values shows an obvious increasing trend with mostly positive residuals. The range of the residuals is relatively large compared with the range of the predicted values. These observations indicate that the model does not perform satisfactorily. All associated results and plots are included in the attachment.

Weekday—80th-Percentile TTI—Salt Lake City

In this validation the predicted value is within a small range, from around 0.04 to around 0.16, which should be kept in mind when evaluating the small RMSE and the small residual values. The Student's *t*-test rejects the null hypothesis of zero residual mean with a confidence level of 90%, and the normality test rejects the null hypothesis of normal distribution with the same threshold level of confidence. The residual plot shows an increasing trend of residuals. Generally the model does not perform satisfactorily enough. All associated results and plots are included in the attachment.

Weekday—50th-Percentile TTI

Weekday—50th-Percentile TTI—All Data

The data-rich weekday 50th-percentile TTI model does not include the ILHL as an independent variable, thus the extreme values in the ILHL data in MN does not influence the prediction of the weekday 50th-percentile TTI. The MN RMSE value is the smallest, at only 1.71%. The largest RMSE value comes from the CA data set, which is 5.92% (Table C.46). The RMSE in the L03 report for the same model is 4.7%.

The residual plot indicates the presence of potential outliers with relatively large residuals below the zero reference line, showing a potential problem with increasing residual variance (Table C.47). Also, the residuals above the zero reference line exhibit a slightly increasing linear trend. Given a maximum predicted value of 0.03, the variance of the residuals below the zero reference line seems unusual. There is strong evidence shown in the Student's *t*-test that the zero residual mean hypothesis cannot be rejected as the *p*-value is 0.8746. The research team noted that the residual mean is negatively close to zero, but the histogram (Figure C.68) and the plot of residuals versus the predicted values (Figure C.67) indicate that there are more positive residual samples than negative ones, which implies that the large negative residuals may have influenced the Student's *t*-test results. The normality

Table C.46. RMSE of Weekday—50th-Percentile TTI

RMSE	All Data	CA	MN	Salt Lake City
Mean TTI	4.68%	5.92%	1.71%	2.16%

Table C.47. Residual Analysis of Weekday—50th-Percentile TTI—AllData

Table C.47.a. Basic Statistical Measures

Location		Variability	
Mean	–46E-5	Std deviation	0.0458
Median	0.0146	Variance	0.0021
Minimum	–0.399	Range	0.4271
Maximum	0.0282	Interquartile range	0.0197

Table C.47.b. Basic Confidence Limits Assuming Normality

Parameter	Estimate	95% Confidence Limits	
Mean	–46E-5	–0.006	0.0053
Std deviation	0.0458	0.0421	0.0503
Variance	0.0021	0.0018	0.0025

Table C.47.c. Tests for Location: Mu=0

Test	Statistic		*p*-Value	
Student's *t*	*t*	–0.158	Pr > |*t*|	0.8746

Table C.47.d. Tests for Normality

Test	Statistic		*p*-Value	
Shapiro-Wilk	*W*	0.4735	Pr < *W*	<0.0001

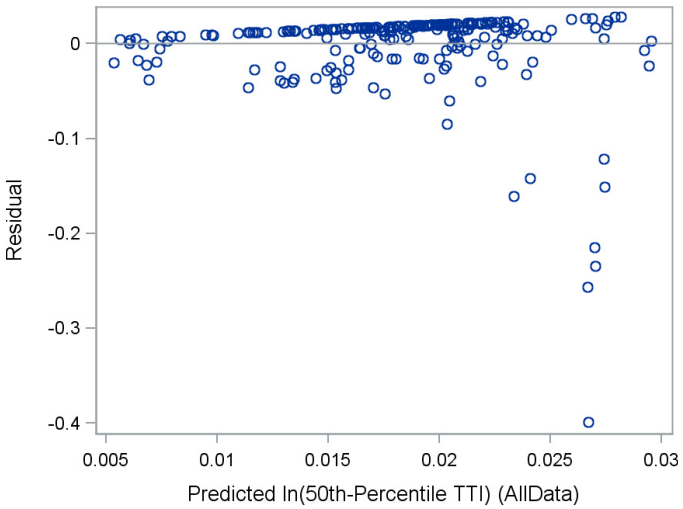

Figure C.67. Residual plot of midday—50th-percentile TTI—AllData.

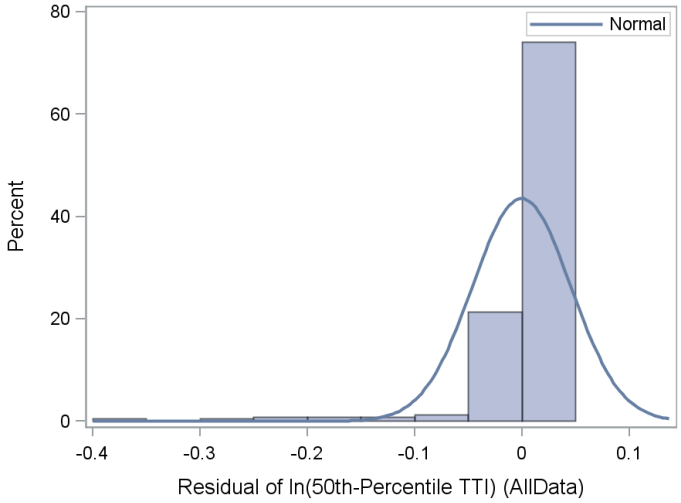

Figure C.68. Residual histogram of midday—50th-percentile TTI—AllData.

test rejects the normal distribution assumption. The residual normality plot is shown in Figure C.69.

WEEKDAY—50TH-PERCENTILE TTI—CALIFORNIA

This validation presents similar results to the validation of the same model using the AllData set. The Student's *t*-test yields a *p*-value large enough that the null hypothesis cannot be rejected with a confidence level of 90%. The normality test indicates that the null hypothesis of normal distribution can be rejected with the threshold confidence level. The plot of residuals versus the predicted values has some potential outliers below the zero reference line. All associated results and plots are included in the attachment.

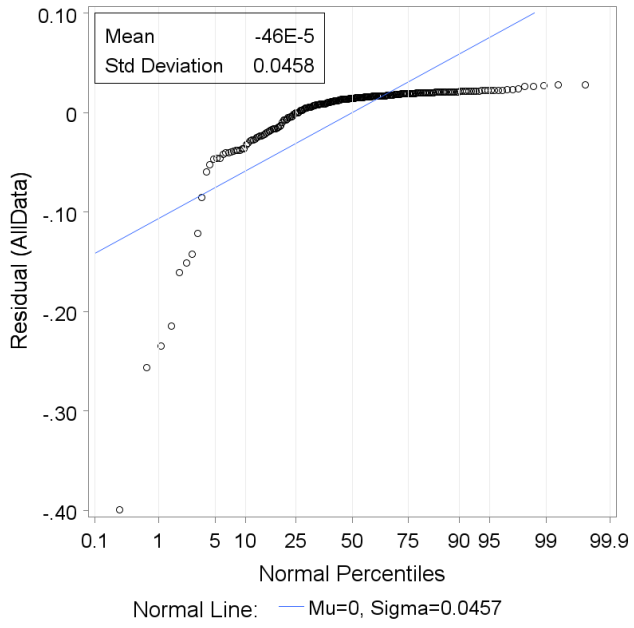

Figure C.69. Residual normality plot of midday—50th-percentile TTI—AllData.

WEEKDAY—50TH-PERCENTILE TTI—MINNESOTA

In this validation the null hypothesis of zero residual mean and the null hypothesis of normal distribution are rejected by the statistical tests. The plot of residuals versus the predicted values shows that there are more positive residuals than negative ones and that the upper bound of residuals shows a linearly increasing trend. The residual scale is much smaller than that for the CA data set. All associated results and plots are included in the attachment.

WEEKDAY—50TH-PERCENTILE TTI—SALT LAKE CITY

In this validation the standard deviation of the residual is 0.0215. Although seeming small, it is as large as the scale of the predicted values. The Student's *t*-test cannot reject the null hypothesis of zero residual mean, as the *p*-value is larger than 10%. The normality test rejects the null hypothesis of normal distribution, as the *p*-value is less than 0.001. The plot of residuals versus the predicted values does not show satisfying results as the upper bound of residuals follows a linear trend. The residual range is large compared with the range of the predicted value, affirming that the corresponding standard deviation is relatively large. All associated results and plots are included in the attachment.

Weekday—10th-Percentile TTI

WEEKDAY—10TH-PERCENTILE TTI—ALL DATA

The RMSE value for the data-rich weekday 10th-percentile TTI model is 2.0% in the L03 report. The largest RMSE comes from the Salt Lake City data set. However, all the RMSE values in the validation investigation are smaller than the RMSE in the L03 report (Table C.48).

In this validation the residual plots reveal several concerns (Table C.49). The histogram and the normality test results indicate violation of the normal distribution assumption. The plot of residuals versus the predicted values shows that most of the residuals are slightly larger than zero, and the upper bound shows a linear trend with slightly increasing values (Figure C.70). There are also many samples with large negative residuals located below the zero reference line, compared with the small scale of predicted values. The Student's *t*-test rejects the null hypothesis of zero residual mean. The

Table C.48. RMSE of Weekday—10th-Percentile TTI

RMSE	All Data	CA	MN	Salt Lake City
Mean TTI	0.81%	0.74%	0.48%	1.30%

Table C.49. Residual Analysis of Weekday—10th-Percentile TTI—AllData

Table C.49.a. Basic Statistical Measures

Location		Variability	
Mean	0.0014	Std deviation	0.0080
Median	0.0040	Variance	0.0001
Minimum	–0.062	Range	0.0685
Maximum	0.0066	Interquartile range	0.0017

Table C.49.b. Basic Confidence Limits Assuming Normality

Parameter	Estimate	95% Confidence Limits	
Mean	0.0014	0.0004	0.0024
Std deviation	0.0080	0.0073	0.0088
Variance	0.0001	54E-6	0.0001

Table C.49.c. Tests for Location: Mu=0

Test	Statistic		*p*-Value	
Student's *t*	*t*	2.6645	Pr > |*t*|	0.0082

Table C.49.d. Tests for Normality

Test	Statistic		*p*-Value	
Shapiro-Wilk	*W*	0.5123	Pr < *W*	<0.0001

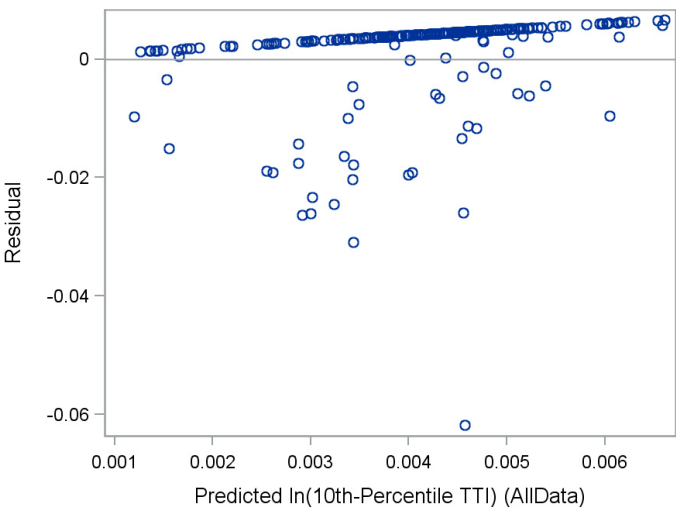

Figure C.70. Residual plot of midday—10th-percentile TTI—AllData.

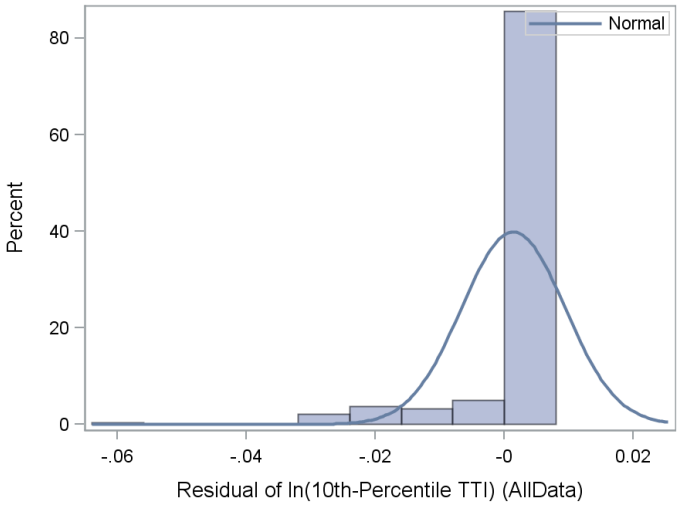

Figure C.71. Residual histogram of midday—10th-percentile TTI—AllData.

residual histogram and normality plots are shown in Figures C.71 and C.72.

Weekday—10th-Percentile TTI—California

In this validation the Student's *t*-test rejects the null hypothesis of zero residual mean with a confidence level of 90%, and the normality test rejects the null hypothesis of normal distribution with the same threshold confidence level. The plot of residuals versus the predicted values illustrates similar patterns as observed from the validation of the AllData set. All associated results and plots are included in the attachment.

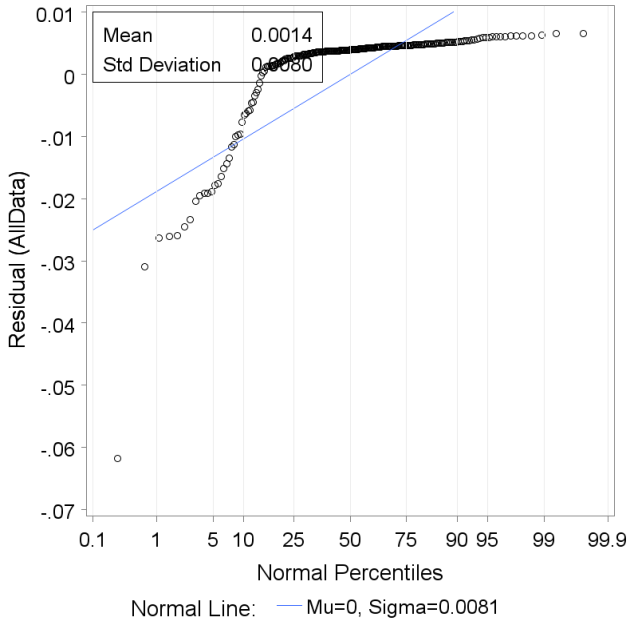

Figure C.72. Residual normality plot of midday—10th-percentile TTI—AllData.

Weekday—10th-Percentile TTI—Minnesota

In this validation the null hypothesis of zero residual mean and the null hypothesis of normal distribution are rejected with a confidence level of 90%. The plot of residuals versus the predicted values shows an almost linearly increasing trend with the exception of three samples located in the lower right corner of the plot. It does not exhibit the random pattern expected from a good regression model. This indicates that the model may have missed some important independent variables. All associated results and plots are included in the attachment.

Weekday—10th-Percentile TTI—Salt Lake City

In this validation the Student's *t*-test shows that the zero residual mean hypothesis can be rejected with a confidence level of 90%, and the normality test also shows that the null hypothesis of normal distribution can be rejected with the threshold confidence level. The plot of residual versus the predicted value presents a nonrandom pattern with large negative residuals below the zero reference line, as the predicted response is within a smaller range. All associated results and plots are included in the attachment.

Conclusions of the Data-Rich Weekday Model Validation

Most of the validations show an increasing trend of residuals in the residual versus predicted value plot. These nonrandom patterns indicate that the assumption of the relationship between the dependent and independent variables is questionable, regardless of the size of the RMSE values. It is important to note that the RMSE criterion has inherited drawbacks and that the assumption of the relationship between variables described by the adopted model is critical.

The MN data set has several potential outliers caused primarily by extremely large ILHL values that yield large residuals. These unusual residuals influence the statistical test results and the RMSE values.

Overall, the data-rich weekday models do not perform satisfactorily.

Conclusions

The validation of the L03 data-rich models was performed on three regional data sets: California, Minnesota, and Salt Lake City, along with the combined overall data set (AllData). The main conclusion is that the average prediction errors (measured by the RMSE) for each model are not acceptable across many of the regions. The RMSEs for each model and data set are presented in Table C.50.

From a regional perspective, for all time slices except the weekday time period, the RMSEs are the highest when the models are applied to the California data set. During the weekday time period, the RMSEs are the highest when the models are applied to the Minnesota data set, and the lowest when applied to the Salt Lake City data set. The high RMSEs for the weekday time period in the Minnesota data set are caused by several potential outliers influenced by very high ILHL values. When the RMSEs are interpreted by the predicted measure, it is evident that, across all of the time periods, the highest RMSEs occur for the prediction of the 99th-percentile TTI. The RMSEs tend to decrease as the predicted TTI measure lowers (i.e., the RMSEs for the 50th-percentile models are lower than for the 80th-percentile models, which are lower than for the 95th-percentile models, etc.). This is to be expected, as there is naturally more variability among the validation data sections at the higher moments of the travel time distribution. In particular, the RMSEs for the 10th-percentile travel time prediction are very low, especially during the midday and weekday time periods, when it is expected that the 10th-percentile travel time to be very close to the free-flow travel time.

From a time period perspective, the highest RMSEs are seen during the peak period, which is defined specifically for each section to cover time periods of at least 75 min during which the average speeds fall below 45 mph. The RMSEs are lower, though still high, for the peak hour models. The peak hour and peak period models are predicted by the critical D/C ratio, the ILHL and, for some of the models, the precipitation factor. The RMSEs are the lowest during the midday period (11:00 a.m.–2:00 p.m.), during which congestion tends to be minimal. The midday period TTIs are predicted only by the critical D/C ratio. RMSEs during the weekday period (predicted by the average D/C ratio and, for some of the models, the ILHL), are slightly higher than they are for the midday period.

Results also indicate that the models violate many of the assumptions of generalized regression and thus have room for enhancement. Generally, a good regression model is expected to present randomly scattered residuals without obvious trends. However, increasing trends and other nonrandom patterns were observed in the residual plots of many of the models. This indicates that the models may not be able to sufficiently describe the relationship between the independent variables and the dependent variable. Table C.51 summarizes the results of the *t*-test and normality test for each model as applied to the AllData set.

These results indicate that the models tend to either systematically overpredict the reliability measure (i.e., indicate that a section is less reliable than it actually is) or underpredict the reliability measure (i.e., indicate that a section is more reliable than it actually is). In all time periods except for the peak hour,

Table C.50. Summary of RMSE Values for Each Model by Region

Model Details		RMSE Value by Region			
Analysis Time Slice	Model	All Data	CA	MN	Salt Lake City
Peak period	Mean TTI	96.94%	127.55%	21.59%	–
	99th Percentile	403.44%	607.76%	63.67%	–
	95th Percentile	251.95%	359.19%	45.85%	–
	80th Percentile	151.95%	206.54%	30.95%	–
	50th Percentile	89.55%	116.63%	23.15%	–
	10th Percentile	12.13%	14.43%	6.23%	–
Peak hour	Mean TTI	25.45%	26.97%	24.68%	–
	99th Percentile	50.74%	52.78%	47.46%	–
	95th Percentile	38.38%	40.19%	37.27%	–
	80th Percentile	35.13%	36.89%	34.06%	–
	50th Percentile	28.85%	32.41%	24.22%	–
	10th Percentile	18.50%	22.24%	12.14%	–
Midday	Mean TTI	6.24%	7.57%	4.07%	3.52%
	99th Percentile	32.32%	34.95%	25.86%	34.01%
	95th Percentile	15.62%	17.29%	14.01%	12.55%
	80th Percentile	8.99%	10.86%	6.61%	3.60%
	50th Percentile	5.43%	6.93%	2.09%	2.08%
	10th Percentile	1.81%	2.20%	0.80%	1.33%
Weekday	Mean TTI	19.74%	12.81%	35.99%	5.95%
	99th Percentile	72.91%	50.04%	141.72%	30.87%
	95th Percentile	83.82%	40.46%	197.82%	22.85%
	80th Percentile	29.28%	14.84%	59.43%	5.75%
	50th Percentile	4.68%	5.92%	1.71%	2.16%
	10th Percentile	0.81%	0.74%	0.48%	1.30%

the null hypothesis of the normality test was rejected for all models, indicating that the residuals are nonnormally distributed. During the peak period, midday, and weekday time periods, the null hypothesis of the *t*-test was rejected for nearly all of the models, indicating that the mean of the residuals is nonzero. The null hypotheses of these tests were most frequently not rejected during the peak hour time period, but only the mean TTI model of this time period performed satisfactorily well when considering the pattern of residuals.

Further investigation of the residual patterns by time period shows that during the peak period each of the models tends to underpredict the measured TTI at low TTI values and overpredict it at higher TTIs. The residuals also tend to get larger as the TTI increases. The peak hour models also exhibit a tendency to underpredict the measured TTI at low TTI values and overpredict it at higher TTIs. During the midday period the main problem with the residuals is that they exhibit nonconstant variance, as seen through the cone-shaped residual plots of the models, and have a tendency to overpredict the TTI. During the weekday period, the residuals of the models are mostly positive, indicating a tendency to consistently overpredict the TTI.

Table C.51. Summary of Student's t-Test and Shapiro-Wilk Normality Test Results for AllData Set

Model Details		Null Hypothesis Result	
Analysis Time Slice	**Model**	***t*-Test[a]**	**Normality Test[b]**
Peak period	Mean TTI	Reject	Reject
	99th Percentile	Reject	Reject
	95th Percentile	Reject	Reject
	80th Percentile	Reject	Reject
	50th Percentile	Reject	Reject
	10th Percentile	Reject	Reject
Peak hour	Mean TTI	Cannot Reject	Cannot Reject
	99th Percentile	Cannot Reject	Reject
	95th Percentile	Cannot Reject	Cannot Reject
	80th Percentile	Reject	Cannot Reject
	50th Percentile	Reject	Cannot Reject
	10th Percentile	Cannot Reject	Reject
Midday	Mean TTI	Reject	Reject
	99th Percentile	Reject	Reject
	95th Percentile	Reject	Reject
	80th Percentile	Reject	Reject
	50th Percentile	Cannot Reject	Reject
	10th Percentile	Reject	Reject
Weekday	Mean TTI	Reject	Reject
	99th Percentile	Reject	Reject
	95th Percentile	Reject	Reject
	80th Percentile	Reject	Reject
	50th Percentile	Cannot Reject	Reject
	10th Percentile	Reject	Reject

[a] *t*-test results indicate whether the null hypothesis assumption that the residuals satisfy zero residual mean can be rejected or not with a certain confidence level.
[b] Normality test results indicate whether the null hypothesis assumption that the residuals satisfy the normal distribution can be rejected or not with a certain confidence level.

Appendix C Attachment

Peak Period

Mean TTI Model

Peak Period—Mean TTI Model—California

Table C.52. Residual Analysis of Peak Period—Mean TTI—California

Table C.52.a. Basic Statistical Measures

Location		Variability	
Mean	0.3287	Std deviation	0.7626
Median	0.0533	Variance	0.5815
Minimum	–0.3479	Range	3.0176
Maximum	2.6696	Interquartile range	0.2987

Table C.52.b. Basic Confidence Limits Assuming Normality

Parameter	Estimate	95% Confidence Limits	
Mean	0.3287	0.0940	0.5634
Std deviation	0.7626	0.6288	0.9692
Variance	0.5815	0.3954	0.9394

Table C.52.c. Tests for Location: Mu=0

Test	Statistic		*p*-Value	
Student's *t*	*t*	2.8263	Pr > |*t*|	0.0072

Table C.52.d. Tests for Normality

Test	Statistic		*p*-Value	
Shapiro-Wilk	*W*	0.6453	Pr < *W*	<0.0001

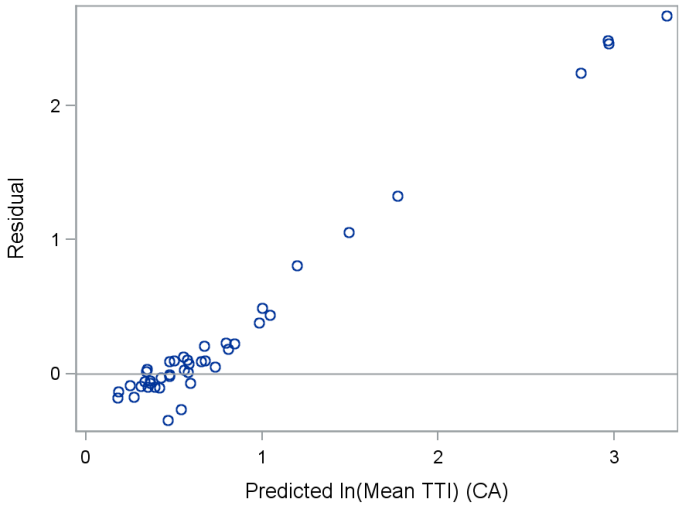

Figure C.73. Residual plot of peak period—mean TTI—California.

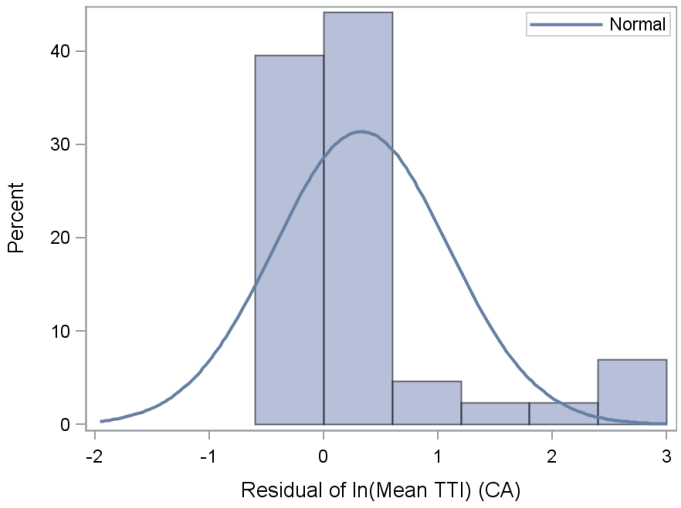

Figure C.74. Residual histogram of peak period—mean TTI—California.

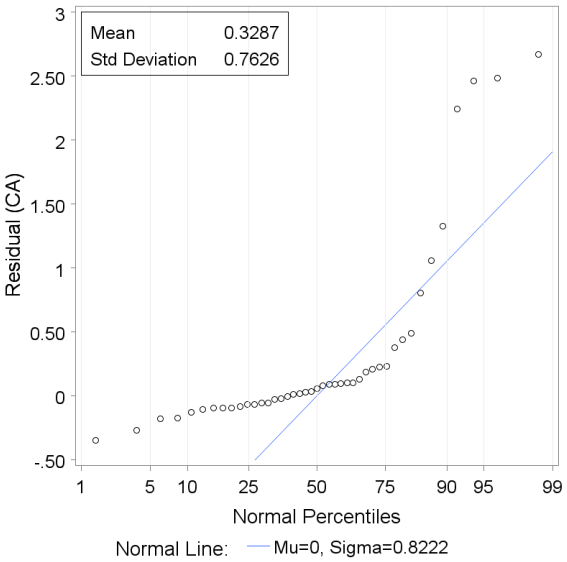

Figure C.75. Residual normality plot of peak period—mean TTI—California.

MINNESOTA

Table C.53. Residual Analysis of Peak Period—Mean TTI—Minnesota

Table C.53.a. Basic Statistical Measures

Location		Variability	
Mean	–0.009	Std deviation	0.2006
Median	–0.073	Variance	0.0402
Minimum	–0.247	Range	0.6507
Maximum	0.4042	Interquartile range	0.2395

Table C.53.b. Basic Confidence Limits Assuming Normality

Parameter	Estimate	95% Confidence Limits	
Mean	–0.009	–0.106	0.0873
Std deviation	0.2006	0.1516	0.2966
Variance	0.0402	0.0230	0.0880

Table C.53.c. Tests for Location: Mu=0

Test	Statistic		*p*-Value	
Student's *t*	*t*	–0.205	Pr > |*t*|	0.8401

Table C.53.d. Tests for Normality

Test	Statistic		*p*-Value	
Shapiro-Wilk	*W*	0.8416	Pr < *W*	0.0049

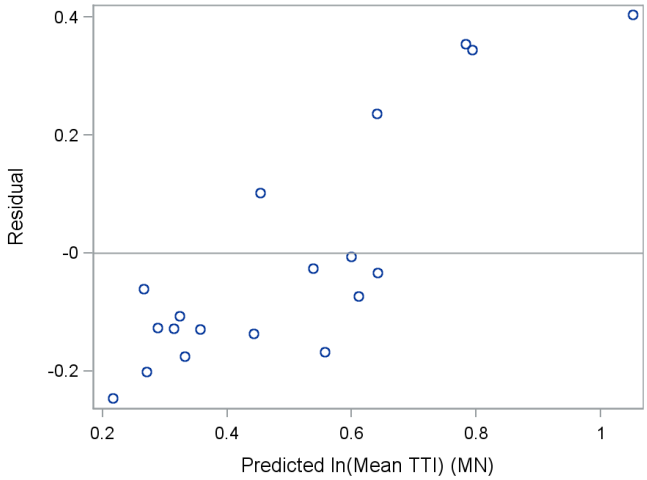

Figure C.76. Residual plot of peak period—mean TTI—Minnesota.

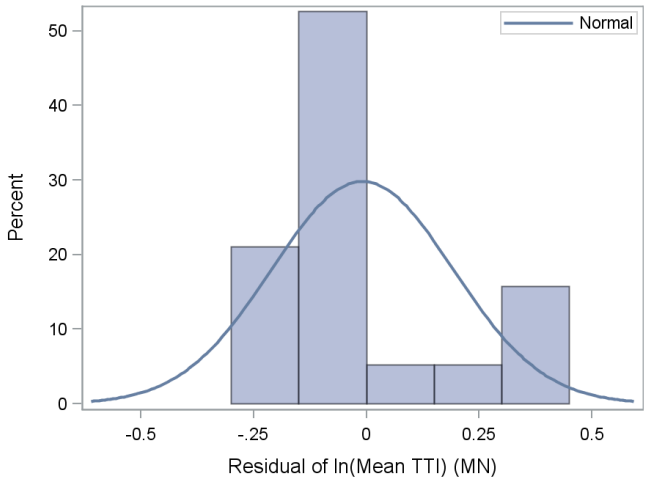

Figure C.77. Residual histogram of peak period—mean TTI—Minnesota.

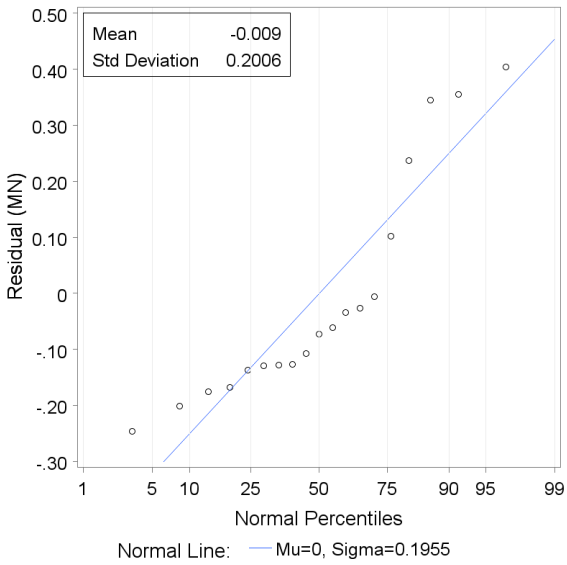

Figure C.78. Residual normality plot of peak period—mean TTI—Minnesota.

99th-Percentile TTI Model

California

Table C.54. Residual Analysis of Peak Period—99th-Percentile TTI—California

Table C.54.a. Basic Statistical Measures

Location		Variability	
Mean	0.8780	Std deviation	1.7696
Median	0.2508	Variance	3.1316
Minimum	–0.725	Range	7.2825
Maximum	6.5571	Interquartile range	0.8412

Table C.54.b. Basic Confidence Limits Assuming Normality

Parameter	Estimate	95% Confidence Limits	
Mean	0.8780	0.3334	1.4226
Std deviation	1.7696	1.4591	2.2492
Variance	3.1316	2.1291	5.0590

Table C.54.c. Tests for Location: Mu=0

Test	Statistic		*p*-Value	
Student's *t*	*t*	3.2534	Pr > |*t*|	0.0023

Table C.54.d. Tests for Normality

Test	Statistic		*p*-Value	
Shapiro-Wilk	*W*	0.6600	Pr < *W*	<0.0001

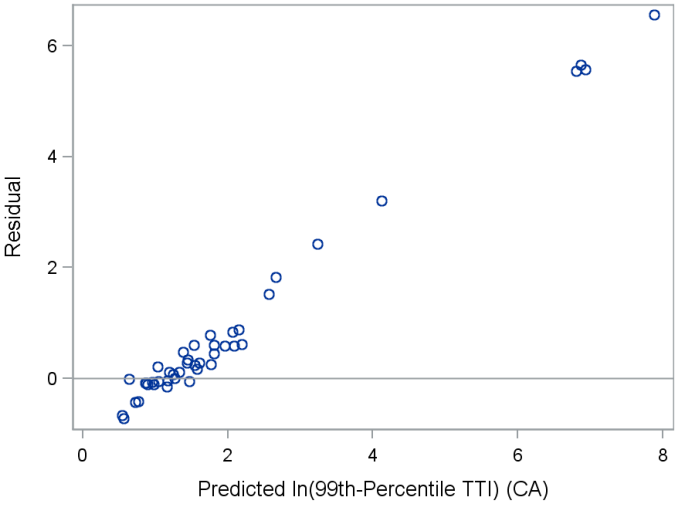

Figure C.79. Residual plot of peak period—99th-percentile TTI—California.

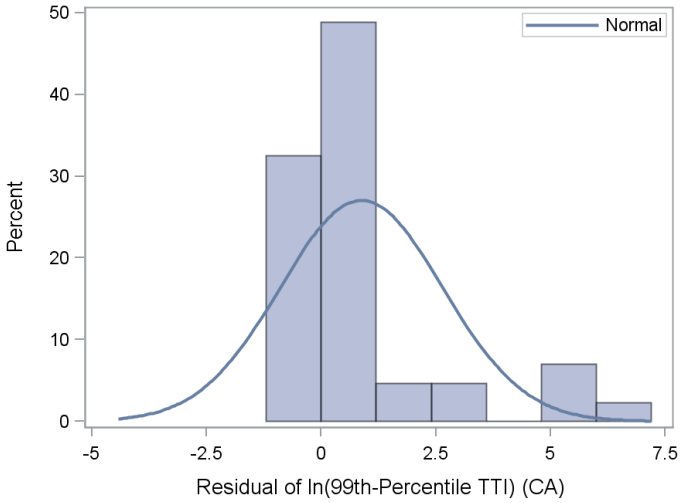

Figure C.80. Residual histogram of peak period—99th-percentile TTI—California.

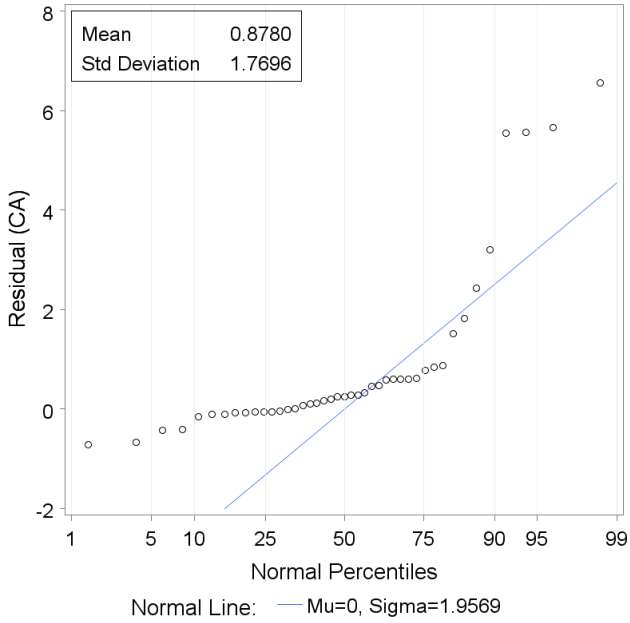

Figure C.81. Residual normality plot of peak period—99th-percentile TTI—California.

Minnesota

Table C.55. Residual Analysis of Peak Period—99th-Percentile TTI—Minnesota

Table C.55.a. Basic Statistical Measures

Location		Variability	
Mean	–0.201	Std deviation	0.4622
Median	–0.332	Variance	0.2137
Minimum	–0.861	Range	1.8231
Maximum	0.9624	Interquartile range	0.4244

Table C.55.b. Basic Confidence Limits Assuming Normality

Parameter	Estimate	95% Confidence Limits	
Mean	–0.201	–0.424	0.0221
Std deviation	0.4622	0.3493	0.6836
Variance	0.2137	0.1220	0.4673

Table C.55.c. Tests for Location: Mu=0

Test	Statistic		*p*-Value	
Student's *t*	*t*	–1.893	Pr > |*t*|	0.0746

Table C.55.d. Tests for Normality

Test	Statistic		*p*-Value	
Shapiro-Wilk	*W*	0.9208	Pr < *W*	0.1171

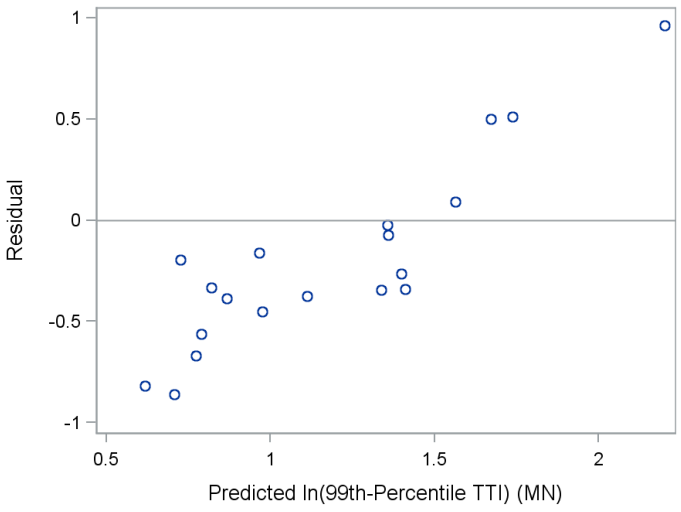

Figure C.82. Residual plot of peak period—99th-percentile TTI—Minnesota.

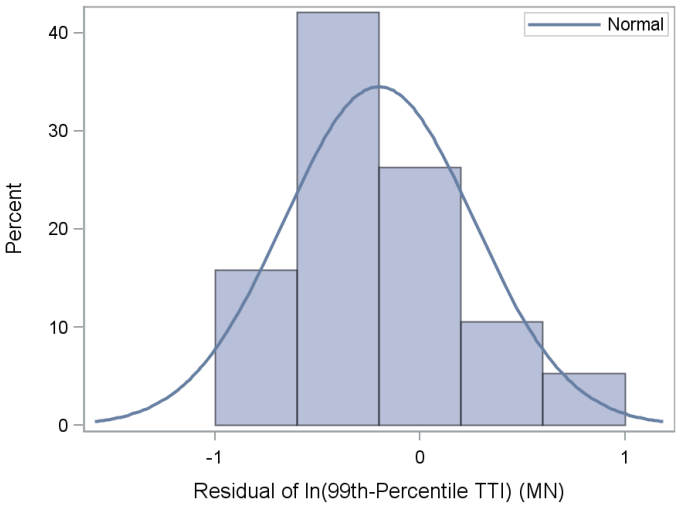

Figure C.83. Residual histogram of peak period—99th-percentile TTI—Minnesota.

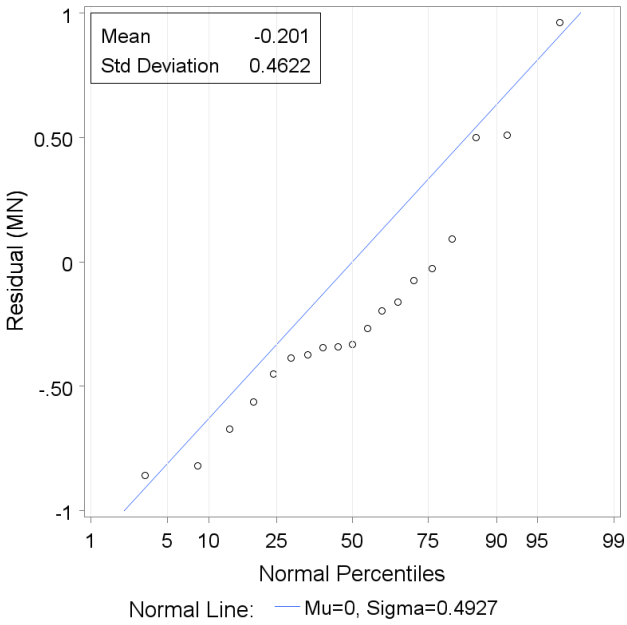

Figure C.84. Residual normality plot of peak period—99th-percentile TTI—Minnesota.

95th-Percentile TTI Model

California

Table C.56. Residual Analysis of Peak Period—95th-Percentile TTI—California

Table C.56.a. Basic Statistical Measures

Location		Variability	
Mean	0.6326	Std deviation	1.4032
Median	0.1346	Variance	1.9691
Minimum	–0.684	Range	5.7559
Maximum	5.0720	Interquartile range	0.6441

Table C.56.b. Basic Confidence Limits Assuming Normality

Parameter	Estimate	95% Confidence Limits	
Mean	0.6326	0.2007	1.0645
Std deviation	1.4032	1.1570	1.7835
Variance	1.9691	1.3387	3.1810

Table C.56.c. Tests for Location: Mu=0

Test	Statistic		*p*-Value	
Student's *t*	*t*	2.9562	Pr > |*t*|	0.0051

Table C.56.d. Tests for Normality

Test	Statistic		*p*-Value	
Shapiro-Wilk	*W*	0.6563	Pr < *W*	<0.0001

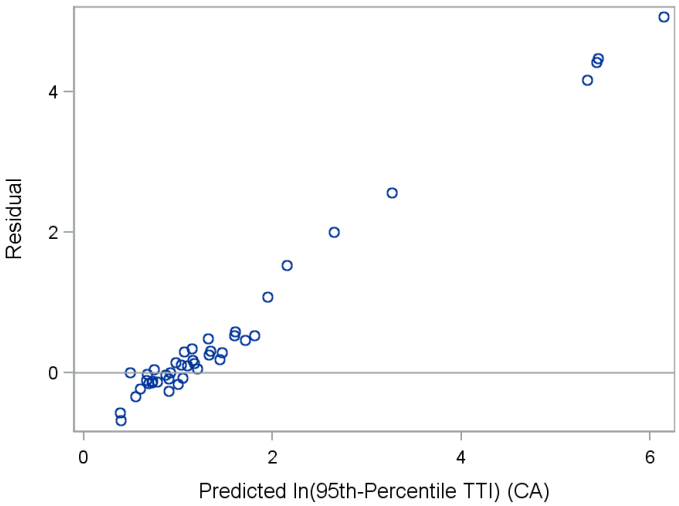

Figure C.85. Residual plot of peak period—95th-percentile TTI—California.

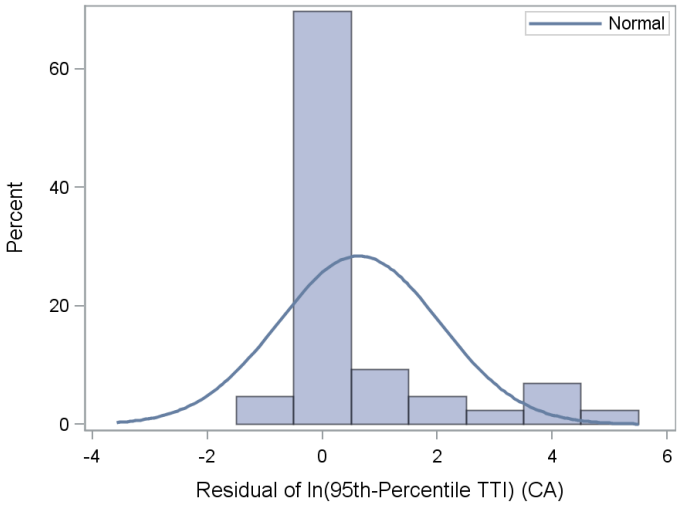

Figure C.86. Residual histogram of peak period—95th-percentile TTI—California.

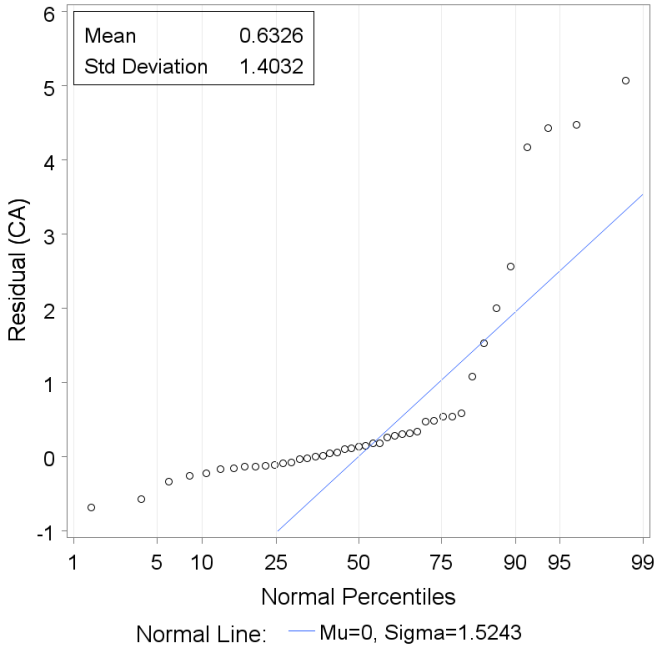

Figure C.87. Residual normality plot of peak period—95th-percentile TTI—California.

Minnesota

Table C.57. Residual Analysis of Peak Period—95th-Percentile TTI—Minnesota

Table C.57.a. Basic Statistical Measures

Location		Variability	
Mean	–0.161	Std deviation	0.3506
Median	–0.245	Variance	0.1229
Minimum	–0.566	Range	1.2796
Maximum	0.7138	Interquartile range	0.3646

Table C.57.b. Basic Confidence Limits Assuming Normality

Parameter	Estimate	95% Confidence Limits	
Mean	–0.161	–0.330	0.0077
Std deviation	0.3506	0.2649	0.5184
Variance	0.1229	0.0702	0.2688

Table C.57.c. Tests for Location: Mu=0

Test	Statistic		*p*-Value	
Student's *t*	*t*	–2.005	Pr > |*t*|	0.0602

Table C.57.d. Tests for Normality

Test	Statistic		*p*-Value	
Shapiro-Wilk	*W*	0.8942	Pr < *W*	0.0383

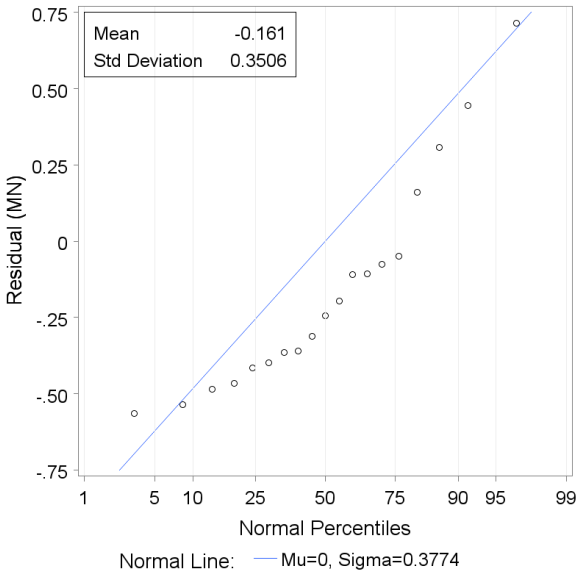

Figure C.88. Residual plot of peak period—95th-percentile TTI—Minnesota.

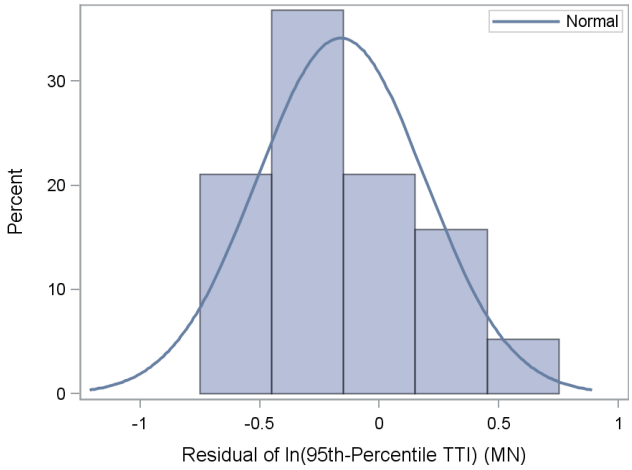

Figure C.89. Residual histogram of peak period—95th-percentile TTI—Minnesota.

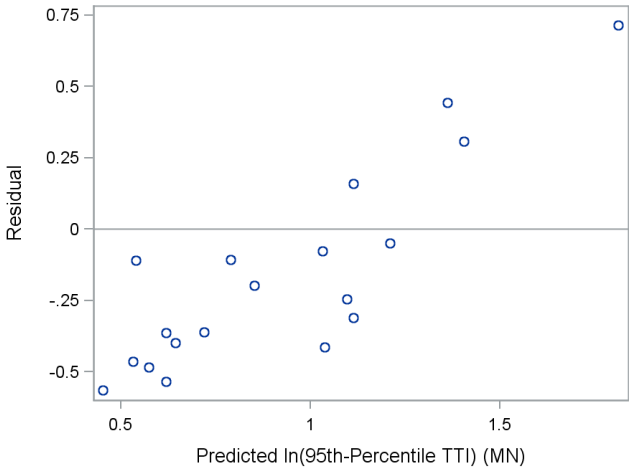

Figure C.90. Residual normality plot of peak period—95th-percentile TTI—Minnesota.

80th-Percentile TTI Model

California

Table C.58. Residual Analysis of Peak Period—80th-Percentile TTI—California

Table C.58.a. Basic Statistical Measures

Location		Variability	
Mean	0.4384	Std deviation	1.0430
Median	0.0584	Variance	1.0879
Minimum	–0.381	Range	4.0617
Maximum	3.6805	Interquartile range	0.4264

Table C.58.b. Basic Confidence Limits Assuming Normality

Parameter	Estimate	95% Confidence Limits	
Mean	0.4384	0.1174	0.7594
Std deviation	1.0430	0.8600	1.3257
Variance	1.0879	0.7396	1.7574

Table C.58.c. Tests for Location: Mu=0

Test	Statistic		*p*-Value	
Student's *t*	*t*	2.7565	Pr > |*t*|	0.0086

Table C.58.d. Tests for Normality

Test	Statistic		*p*-Value	
Shapiro-Wilk	*W*	0.6391	Pr < *W*	<0.0001

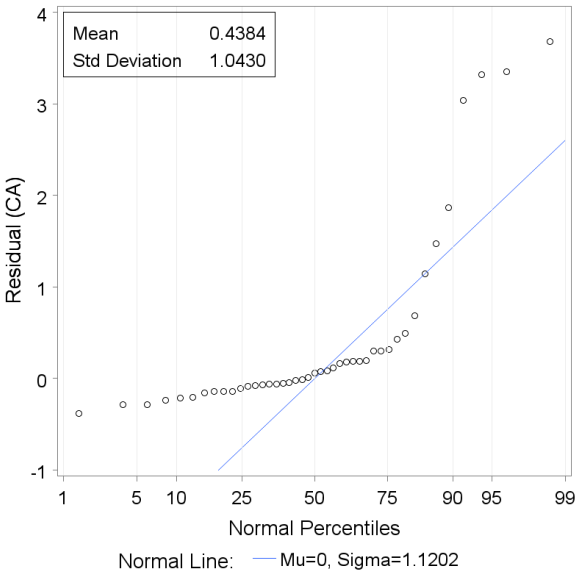

Figure C.91. Residual plot of peak period—80th-percentile TTI—California.

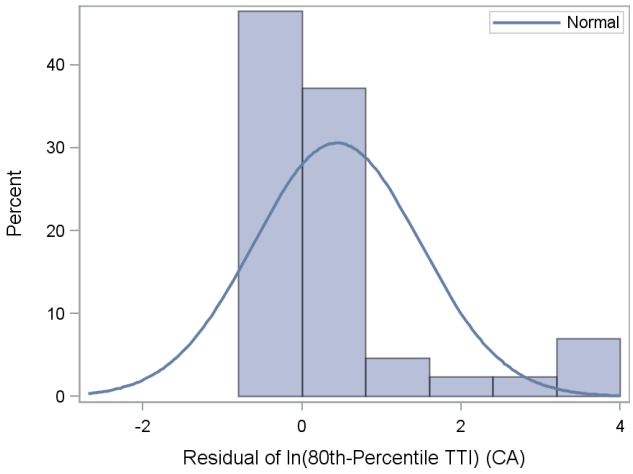

Figure C.92. Residual histogram of peak period—80th-percentile TTI—California.

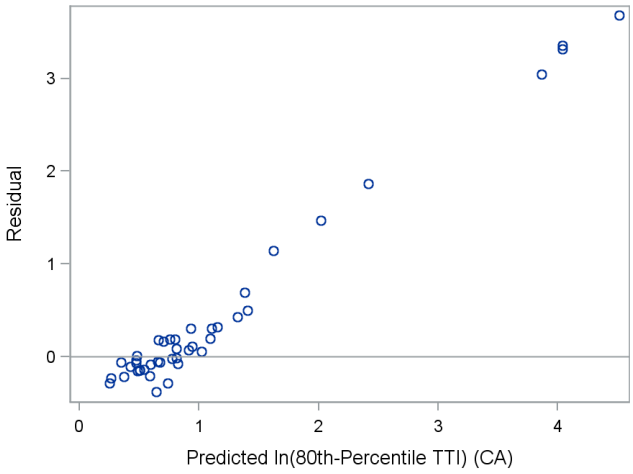

Figure C.93. Residual normality plot of peak period—80th-percentile TTI—California.

Minnesota

Table C.59. Residual Analysis of Peak Period—80th-Percentile TTI—Minnesota

Table C.59.a. Basic Statistical Measures

Location		Variability	
Mean	–0.089	Std deviation	0.2616
Median	–0.188	Variance	0.0684
Minimum	–0.404	Range	0.9128
Maximum	0.5086	Interquartile range	0.3141

Table C.59.b. Basic Confidence Limits Assuming Normality

Parameter	Estimate	95% Confidence Limits	
Mean	–0.089	–0.215	0.0372
Std deviation	0.2616	0.1976	0.3868
Variance	0.0684	0.0391	0.1496

Table C.59.c. Tests for Location: Mu=0

Test	Statistic		*p*-Value	
Student's *t*	*t*	–1.481	Pr > |*t*|	0.1560

Table C.59.d. Tests for Normality

Test	Statistic		*p*-Value	
Shapiro-Wilk	*W*	0.8741	Pr < *W*	0.0169

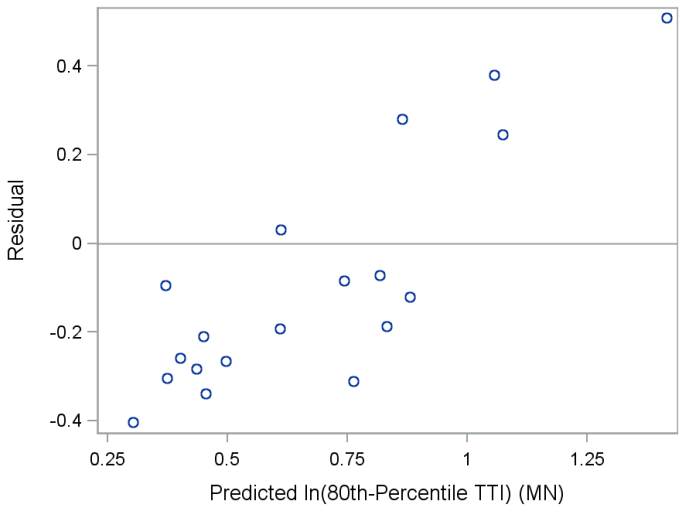

Figure C.94. Residual plot of peak period—80th-percentile TTI—Minnesota.

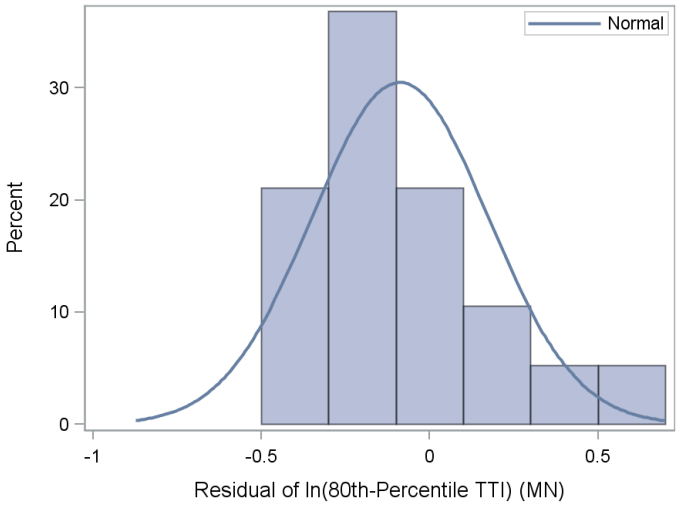

Figure C.95. Residual histogram of peak period—80th-percentile TTI—Minnesota.

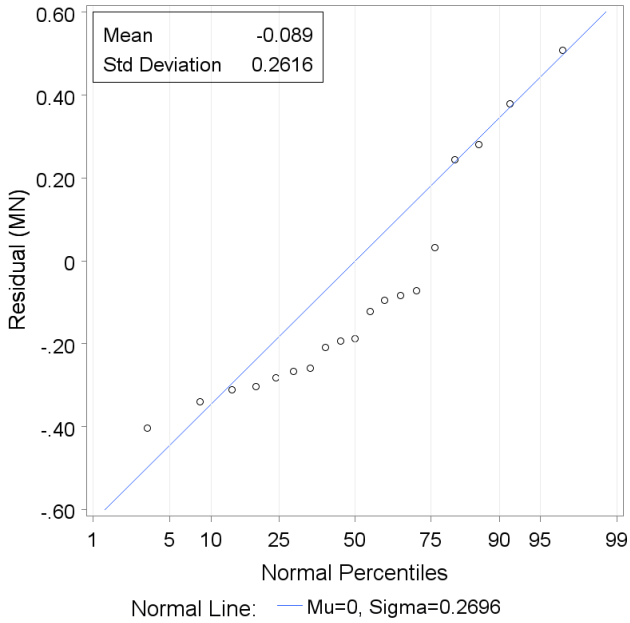

Figure C.96. Residual normality plot of peak period—80th-percentile TTI—Minnesota.

50th-Percentile TTI Model

California

Table C.60. Residual Analysis of Peak Period—50th-Percentile TTI—California

Table C.60.a. Basic Statistical Measures

Location		Variability	
Mean	0.2892	Std deviation	0.7254
Median	0.0125	Variance	0.5261
Minimum	–0.368	Range	2.8998
Maximum	2.5315	Interquartile range	0.3859

Table C.60.b. Basic Confidence Limits Assuming Normality

Parameter	Estimate	95% Confidence Limits	
Mean	0.2892	0.0660	0.5125
Std deviation	0.7254	0.5981	0.9219
Variance	0.5261	0.3577	0.8500

Table C.60.c. Tests for Location: Mu=0

Test	Statistic		*p*-Value	
Student's *t*	*t*	2.6147	Pr > |*t*|	0.0124

Table C.60.d. Tests for Normality

Test	Statistic		*p*-Value	
Shapiro-Wilk	*W*	0.6624	Pr < *W*	<0.0001

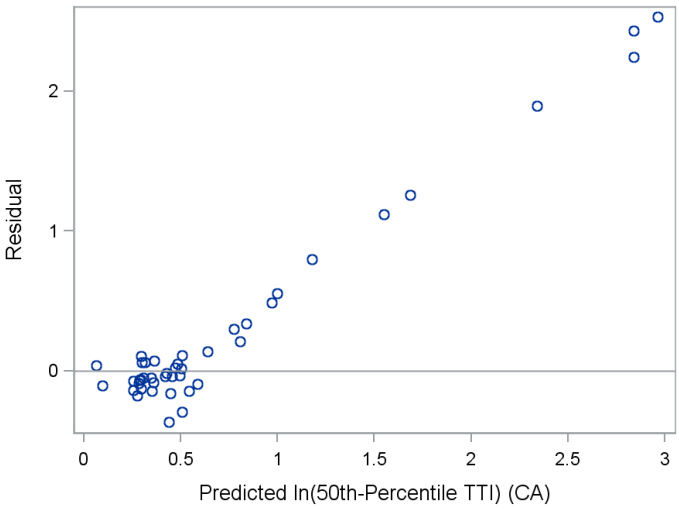

Figure C.97. Residual plot of peak period—50th-percentile TTI—California.

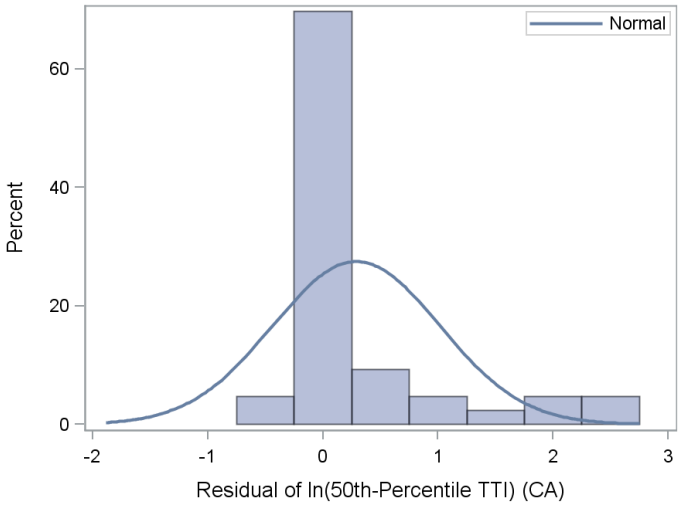

Figure C.98. Residual histogram of peak period—50th-percentile TTI—California.

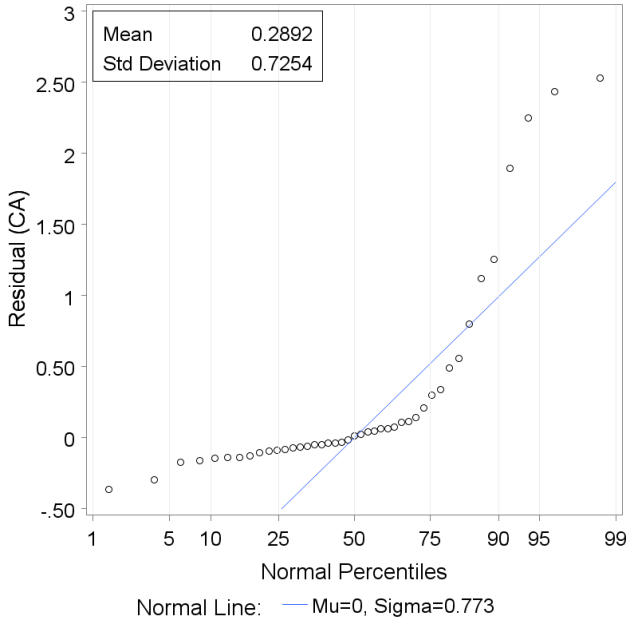

Figure C.99. Residual normality plot of peak period—50th-percentile TTI—California.

Minnesota

Table C.61. Residual Analysis of Peak Period—50th-Percentile TTI—Minnesota

Table C.61.a. Basic Statistical Measures

Location		Variability	
Mean	0.0574	Std deviation	0.2056
Median	–0.033	Variance	0.0423
Minimum	–0.158	Range	0.7232
Maximum	0.5649	Interquartile range	0.2754

Table C.61.b. Basic Confidence Limits Assuming Normality

Parameter	Estimate	95% Confidence Limits	
Mean	0.0574	–0.042	0.1565
Std deviation	0.2056	0.1554	0.3041
Variance	0.0423	0.0241	0.0925

Table C.61.c. Tests for Location: Mu=0

Test	Statistic		*p*-Value	
Student's *t*	*t*	1.2169	Pr > |*t*|	0.2394

Table C.61.d. Tests for Normality

Test	Statistic		*p*-Value	
Shapiro-Wilk	*W*	0.8309	Pr < *W*	0.0033

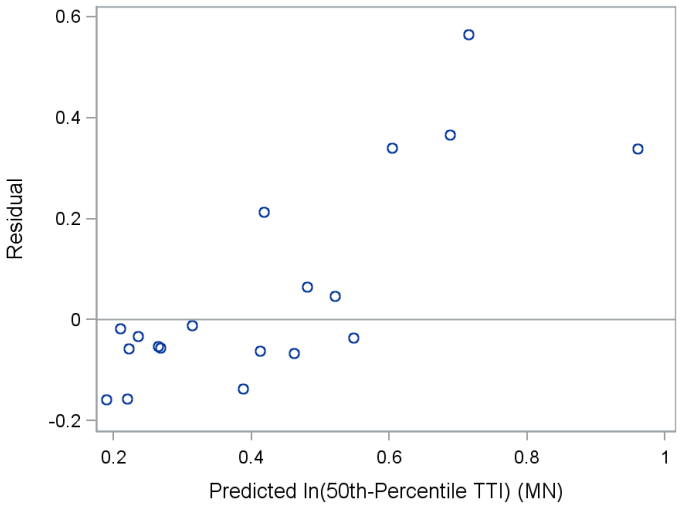

Figure C.100. Residual plot of peak period—50th-percentile TTI—Minnesota.

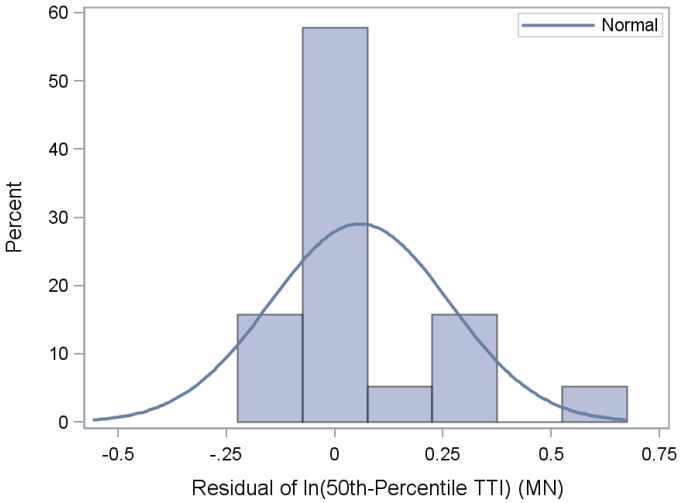

Figure C.101. Residual histogram of peak period—50th-percentile TTI—Minnesota.

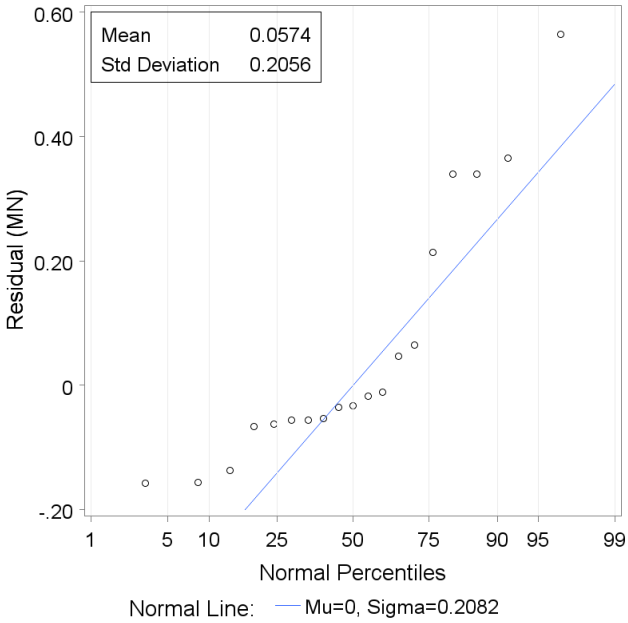

Figure C.102. Residual normality plot of peak period—50th-percentile TTI—Minnesota.

10th-Percentile TTI Model

California

Table C.62. Residual Analysis of Peak Period—10th-Percentile TTI—California

Table C.62.a. Basic Statistical Measures

Location		Variability	
Mean	0.0276	Std deviation	0.1335
Median	0.0234	Variance	0.0178
Minimum	–0.344	Range	0.7344
Maximum	0.3906	Interquartile range	0.0854

Table C.62.b. Basic Confidence Limits Assuming Normality

Parameter	Estimate	95% Confidence Limits	
Mean	0.0276	–0.013	0.0687
Std deviation	0.1335	0.1100	0.1696
Variance	0.0178	0.0121	0.0288

Table C.62.c. Tests for Location: Mu=0

Test	Statistic		*p*-Value	
Student's *t*	*t*	1.3572	Pr > |*t*|	0.1820

Table C.62.d. Tests for Normality

Test	Statistic		*p*-Value	
Shapiro-Wilk	*W*	0.8876	Pr < *W*	0.0005

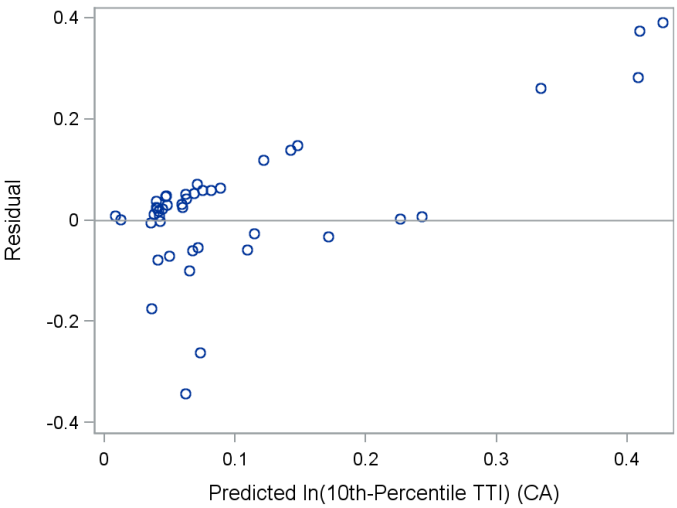

Figure C.103. Residual plot of peak period—10th-percentile TTI—California.

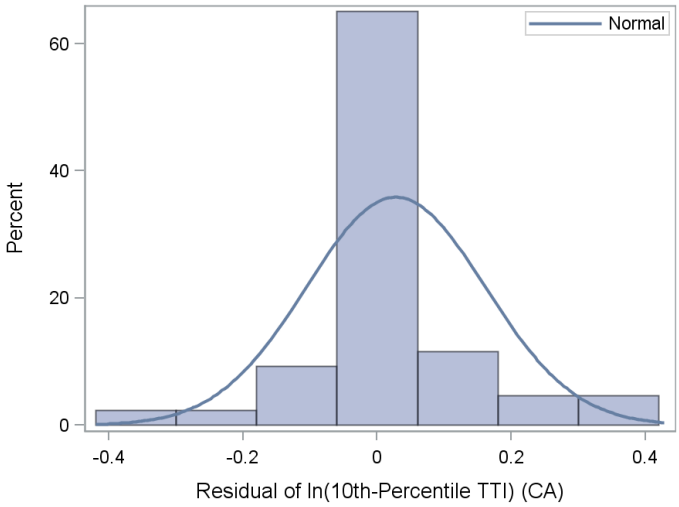

Figure C.104. Residual histogram of peak period—10th-percentile TTI—California.

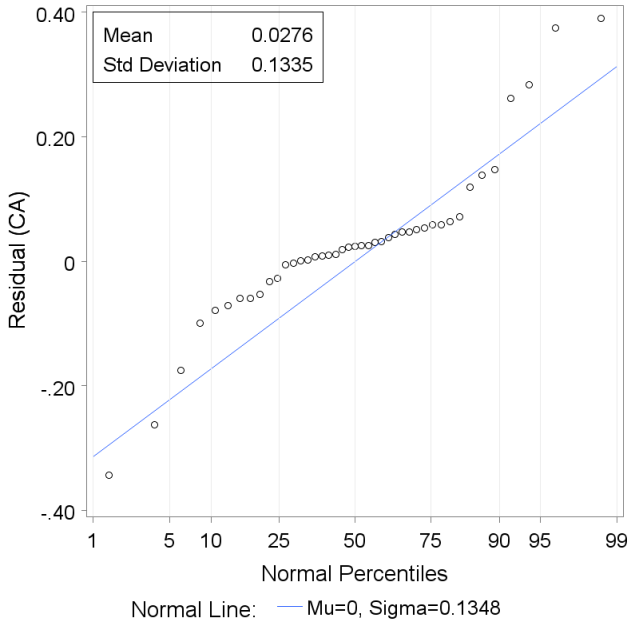

Figure C.105. Residual normality plot of peak period—10th-percentile TTI—California.

Minnesota

Table C.63. Residual Analysis of Peak Period—10th-Percentile TTI—Minnesota

Table C.63.a. Basic Statistical Measures

Location		Variability	
Mean	0.0521	Std deviation	0.0314
Median	0.0553	Variance	0.0010
Minimum	–0.023	Range	0.1273
Maximum	0.1046	Interquartile range	0.0457

Table C.63.b. Basic Confidence Limits Assuming Normality

Parameter	Estimate	95% Confidence Limits	
Mean	0.0521	0.0370	0.0673
Std deviation	0.0314	0.0238	0.0465
Variance	0.0010	0.0006	0.0022

Table C.63.c. Tests for Location: Mu=0

Test	Statistic		*p*-Value	
Student's *t*	*t*	7.2260	Pr > |*t*|	<0.0001

Table C.63.d. Tests for Normality

Test	Statistic		*p*-Value	
Shapiro-Wilk	*W*	0.9643	Pr < *W*	0.6593

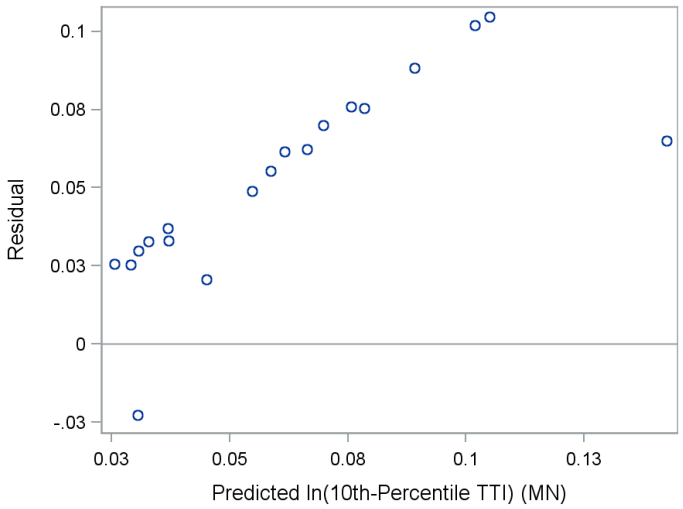

Figure C.106. Residual plot of peak period—10th-percentile TTI—Minnesota.

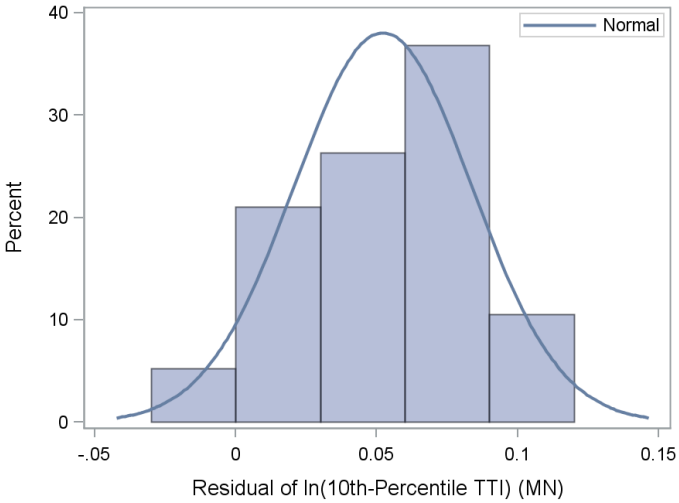

Figure C.107. Residual histogram of peak period—10th-percentile TTI—Minnesota.

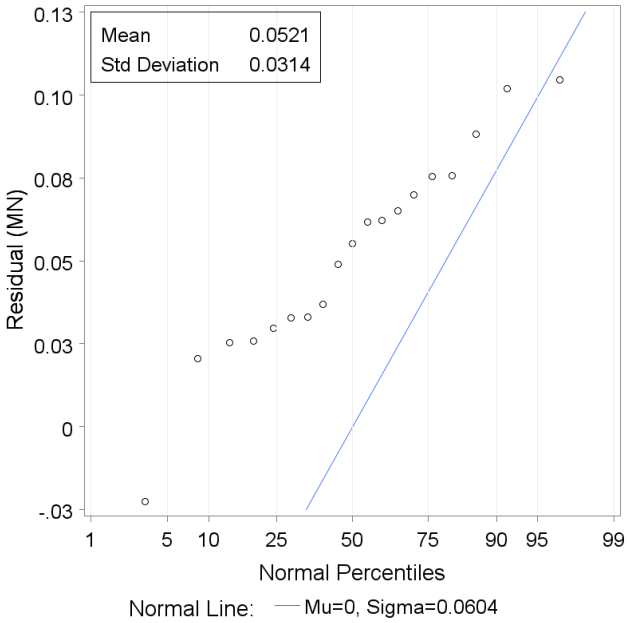

Figure C.108. Residual normality plot of peak period—10th-percentile TTI—Minnesota.

Peak Hour

Mean TTI Model

California

Table C.64. Residual Analysis of Peak Hour—Mean TTI—California

Table C.64.a. Basic Statistical Measures

Location		Variability	
Mean	–0.085	Std deviation	0.2258
Median	–0.055	Variance	0.0510
Minimum	–0.547	Range	0.9459
Maximum	0.3987	Interquartile range	0.2853

Table C.64.b. Basic Confidence Limits Assuming Normality

Parameter	Estimate	95% Confidence Limits	
Mean	–0.085	–0.155	–0.016
Std deviation	0.2258	0.1862	0.2870
Variance	0.0510	0.0347	0.0824

Table C.64.c. Tests for Location: Mu=0

Test	Statistic		*p*-Value	
Student's *t*	*t*	–2.470	Pr > |*t*|	0.0177

Table C.64.d. Tests for Normality

Test	Statistic		*p*-Value	
Shapiro-Wilk	*W*	0.9801	Pr < *W*	0.6519

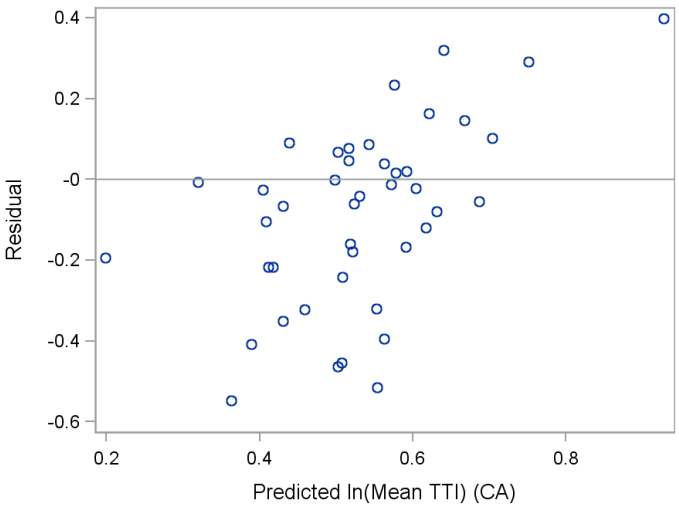

Figure C.109. Residual plot of peak hour—mean TTI—California.

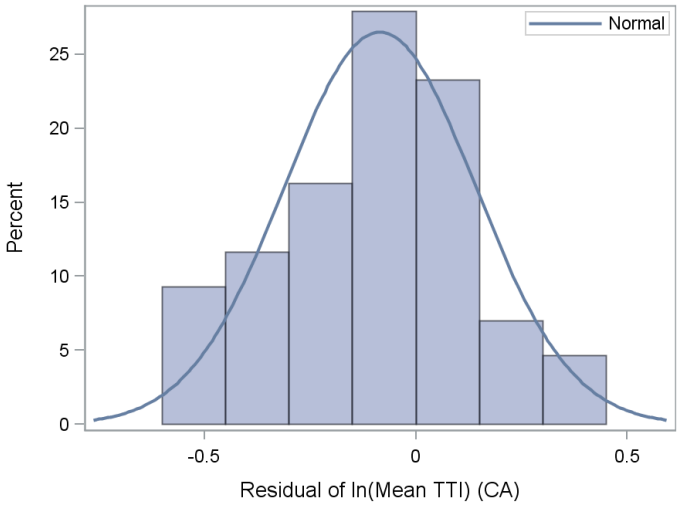

Figure C.110. Residual histogram of peak hour—mean TTI—California.

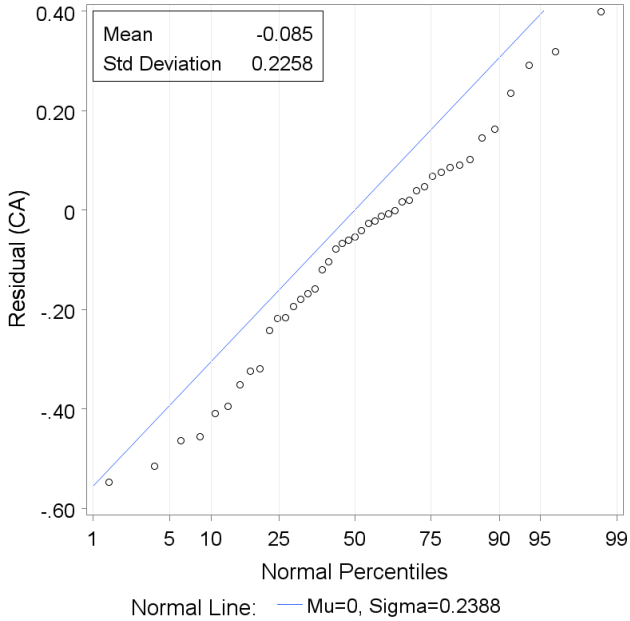

Figure C.111. Residual normality plot of peak hour—mean TTI—California.

Minnesota

Table C.65. Residual Analysis of Peak Hour—Mean TTI—Minnesota

Table C.65.a. Basic Statistical Measures

Location		Variability	
Mean	0.0549	Std deviation	0.2181
Median	0.1414	Variance	0.0476
Minimum	–0.422	Range	0.7718
Maximum	0.3501	Interquartile range	0.2612

Table C.65.b. Basic Confidence Limits Assuming Normality

Parameter	Estimate	95% Confidence Limits	
Mean	0.0549	–0.035	0.1449
Std deviation	0.2181	0.1703	0.3034
Variance	0.0476	0.0290	0.0920

Table C.65.c. Tests for Location: Mu=0

Test	Statistic		*p*-Value	
Student's *t*	*t*	1.2588	Pr > |*t*|	0.2202

Table C.65.d. Tests for Normality

Test	Statistic		*p*-Value	
Shapiro-Wilk	*W*	0.9361	Pr < *W*	0.1203

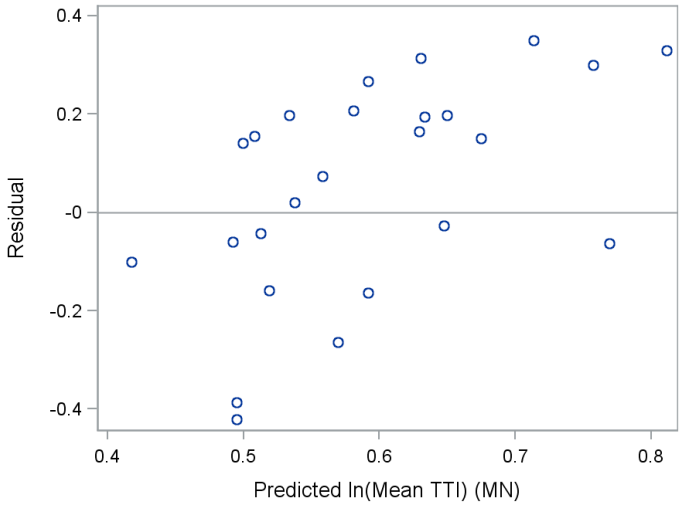

Figure C.112. Residual plot of peak hour—mean TTI—Minnesota.

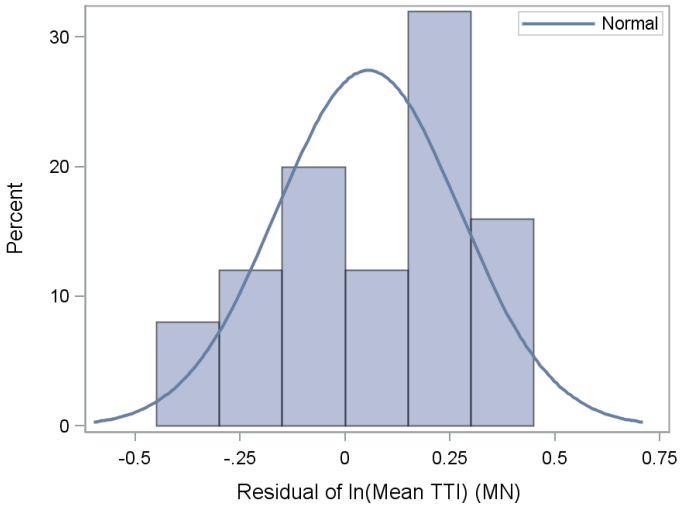

Figure C.113. Residual histogram of peak hour—mean TTI—Minnesota.

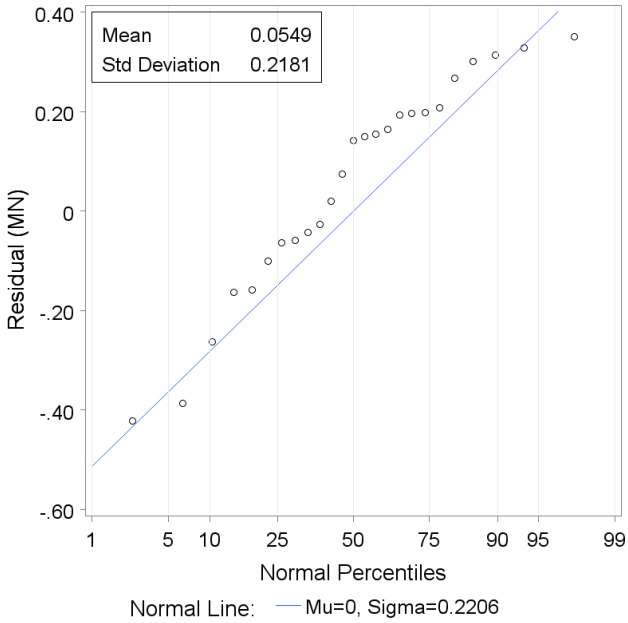

Figure C.114. Residual normality plot of peak hour—mean TTI—Minnesota.

99th-Percentile TTI Model

California

Table C.66. Residual Analysis of Peak Hour—99th-Percentile TTI—California

Table C.66.a. Basic Statistical Measures

Location		Variability	
Mean	0.0170	Std deviation	0.4285
Median	–0.046	Variance	0.1836
Minimum	–0.832	Range	2.2377
Maximum	1.4057	Interquartile range	0.3914

Table C.66.b. Basic Confidence Limits Assuming Normality

Parameter	Estimate	95% Confidence Limits	
Mean	0.0170	–0.115	0.1488
Std deviation	0.4285	0.3533	0.5446
Variance	0.1836	0.1248	0.2966

Table C.66.c. Tests for Location: Mu=0

Test	Statistic		*p*-Value	
Student's *t*	*t*	0.2594	Pr > |*t*|	0.7966

Table C.66.d. Tests for Normality

Test	Statistic		*p*-Value	
Shapiro-Wilk	*W*	0.9148	Pr < *W*	0.0036

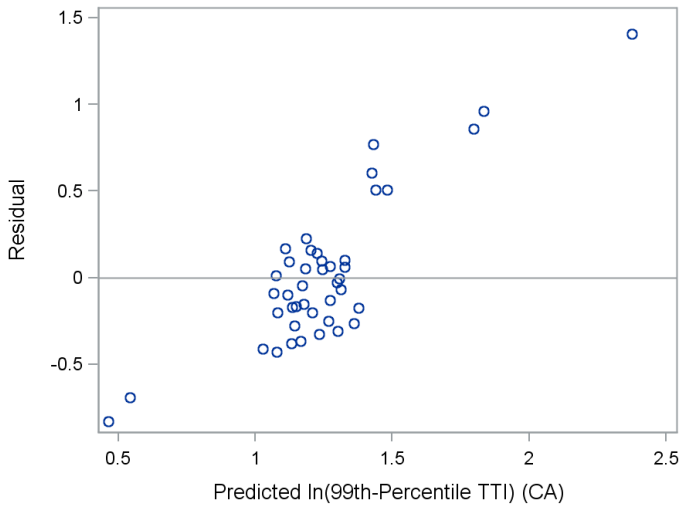

Figure C.115. Residual plot of peak hour—99th-percentile TTI—California.

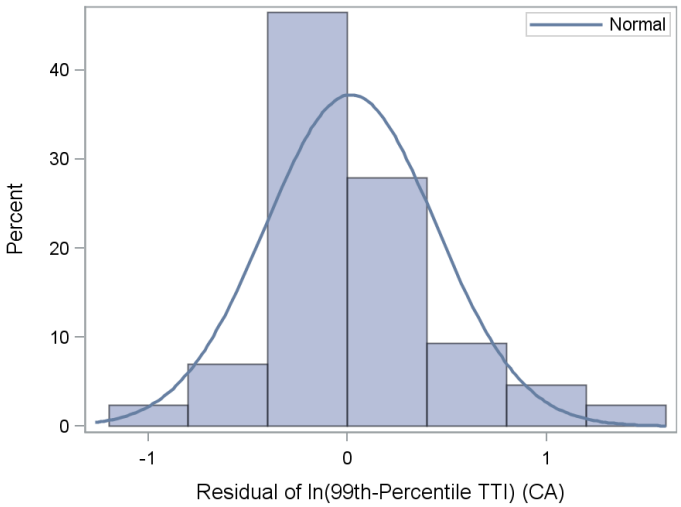

Figure C.116. Residual histogram of peak hour—99th-percentile TTI—California.

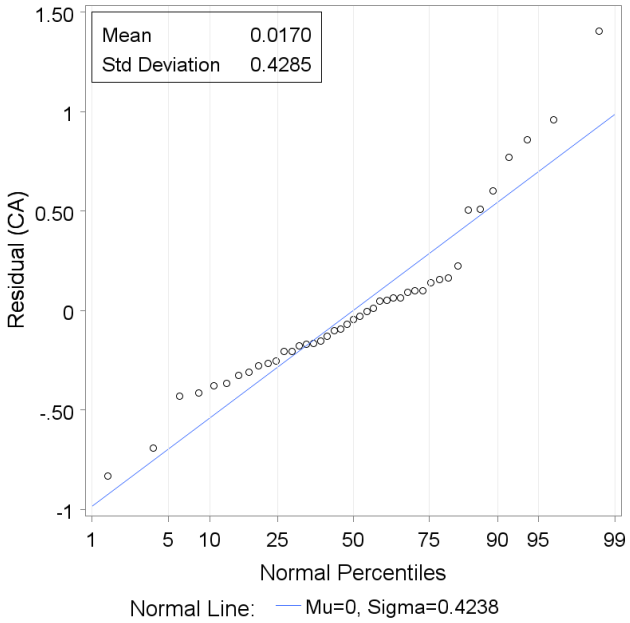

Figure C.117. Residual normality plot of peak hour—99th-percentile TTI—California.

Minnesota

Table C.67. Residual Analysis of Peak Hour—99th-Percentile TTI—Minnesota

Table C.67.a. Basic Statistical Measures

Location		Variability	
Mean	–0.156	Std deviation	0.3630
Median	–0.114	Variance	0.1318
Minimum	–0.912	Range	1.3634
Maximum	0.4517	Interquartile range	0.3377

Table C.67.b. Basic Confidence Limits Assuming Normality

Parameter	Estimate	95% Confidence Limits	
Mean	–0.156	–0.306	–0.006
Std deviation	0.3630	0.2835	0.5051
Variance	0.1318	0.0804	0.2551

Table C.67.c. Tests for Location: Mu=0

Test	Statistic		*p*-Value	
Student's *t*	*t*	–2.147	Pr > |*t*|	0.0421

Table C.67.d. Tests for Normality

Test	Statistic		*p*-Value	
Shapiro-Wilk	*W*	0.9409	Pr < *W*	0.1552

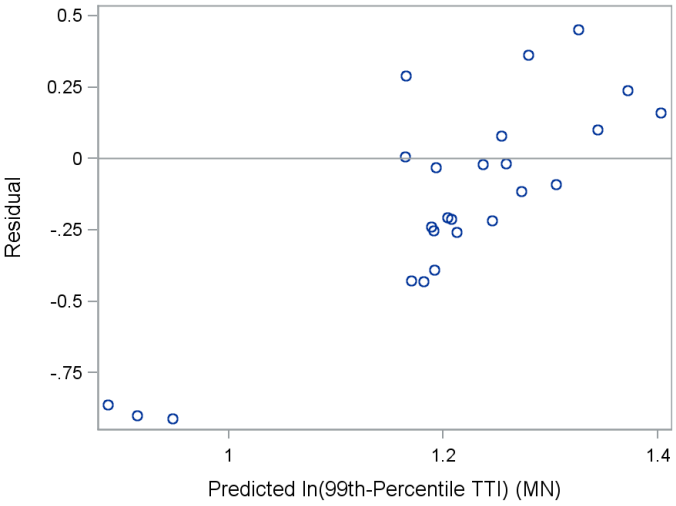

Figure C.118. Residual plot of peak hour—99th-percentile TTI—Minnesota.

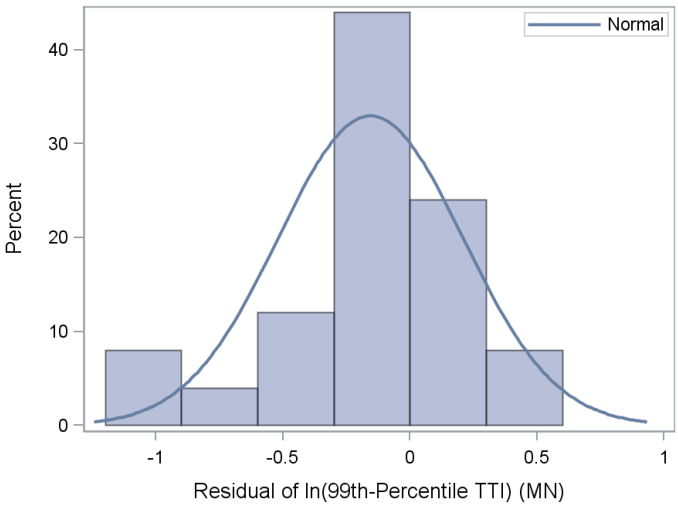

Figure C.119. Residual histogram of peak hour—99th-percentile TTI—Minnesota.

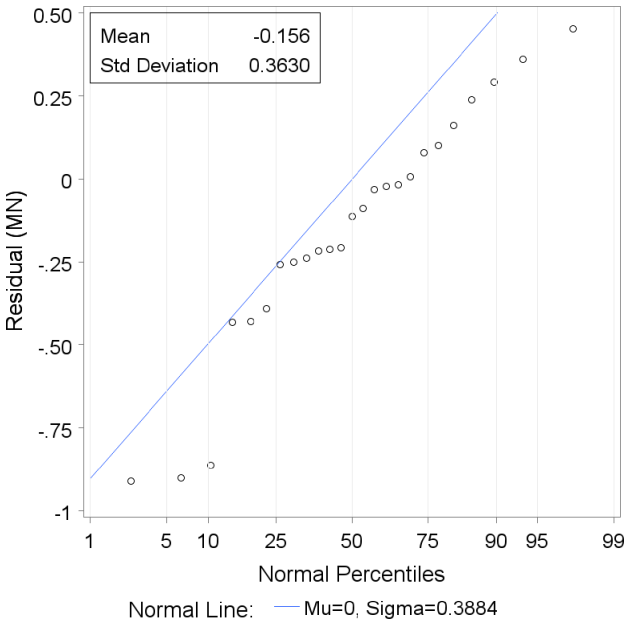

Figure C.120. Residual normality plot of peak hour—99th-percentile TTI—Minnesota.

95th-Percentile TTI Model

California

Table C.68. Residual Analysis of Peak Hour—95th-Percentile TTI—California

Table C.68.a. Basic Statistical Measures

Location		Variability	
Mean	–0.045	Std deviation	0.3387
Median	–0.057	Variance	0.1147
Minimum	–0.623	Range	1.5815
Maximum	0.9590	Interquartile range	0.4299

Table C.68.b. Basic Confidence Limits Assuming Normality

Parameter	Estimate	95% Confidence Limits	
Mean	–0.045	–0.150	0.0589
Std deviation	0.3387	0.2793	0.4305
Variance	0.1147	0.0780	0.1853

Table C.68.c. Tests for Location: Mu=0

Test	Statistic		*p*-Value	
Student's *t*	*t*	–0.877	Pr > |*t*|	0.3854

Table C.68.d. Tests for Normality

Test	Statistic		*p*-Value	
Shapiro-Wilk	*W*	0.9664	Pr < *W*	0.2357

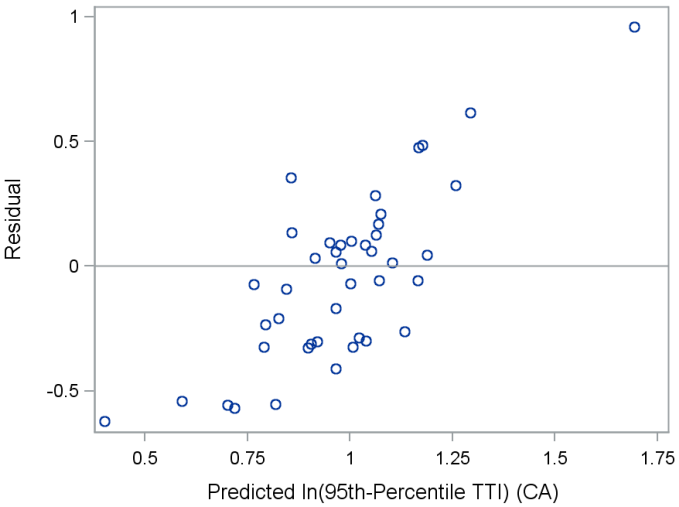

Figure C.121. Residual plot of peak hour—95th-percentile TTI—California.

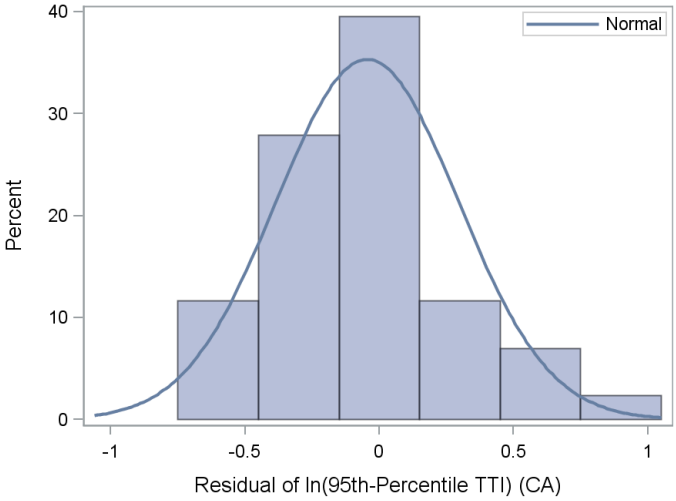

Figure C.122. Residual histogram of peak hour—95th-percentile TTI—California.

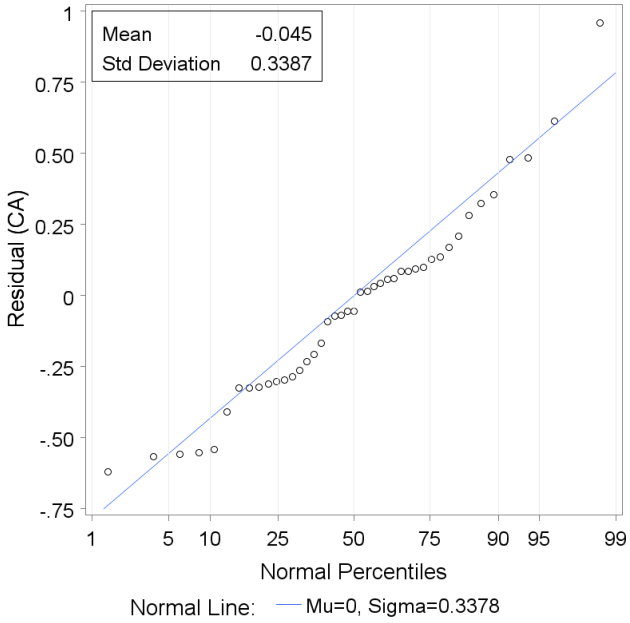

Figure C.123. Residual normality plot of peak hour—95th-percentile TTI—California.

Minnesota

Table C.69. Residual Analysis of Peak Hour—95th-Percentile TTI—Minnesota

Table C.69.a. Basic Statistical Measures

Location		Variability	
Mean	–0.012	Std deviation	0.3231
Median	0.0493	Variance	0.1044
Minimum	–0.757	Range	1.2923
Maximum	0.5351	Interquartile range	0.3942

Table C.69.b. Basic Confidence Limits Assuming Normality

Parameter	Estimate	95% Confidence Limits	
Mean	–0.012	–0.146	0.1212
Std deviation	0.3231	0.2523	0.4494
Variance	0.1044	0.0636	0.2020

Table C.69.c. Tests for Location: Mu=0

Test	Statistic		*p*-Value	
Student's *t*	*t*	–0.188	Pr > |*t*|	0.8522

Table C.69.d. Tests for Normality

Test	Statistic		*p*-Value	
Shapiro-Wilk	*W*	0.9464	Pr < *W*	0.2083

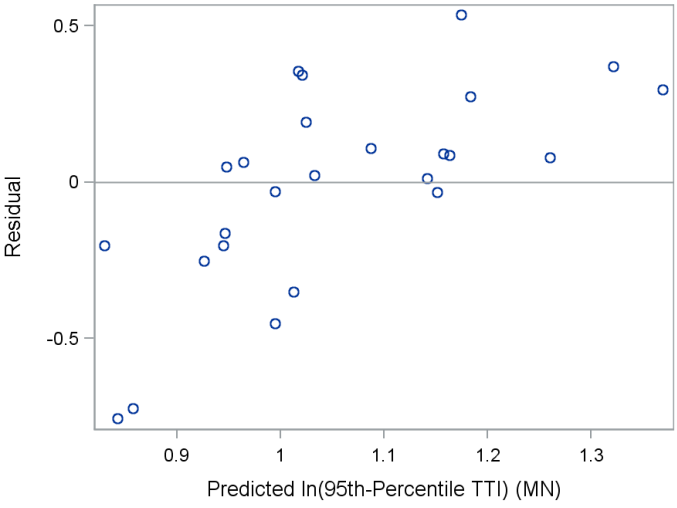

Figure C.124. Residual plot of peak hour—95th-percentile TTI—Minnesota.

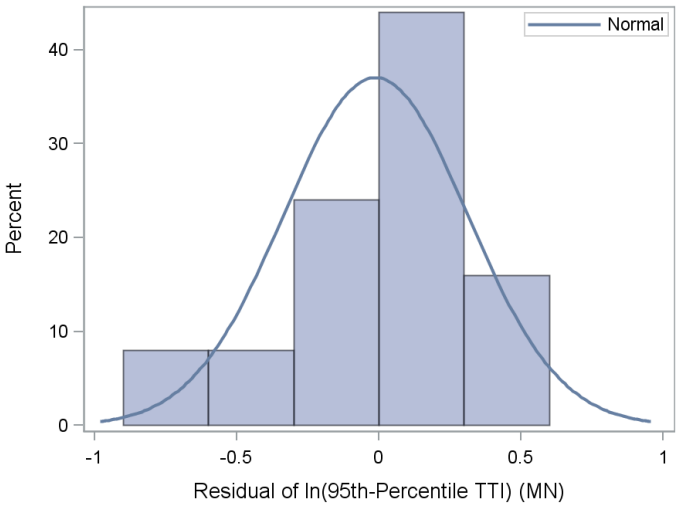

Figure C.125. Residual histogram of peak hour—95th-percentile TTI—Minnesota.

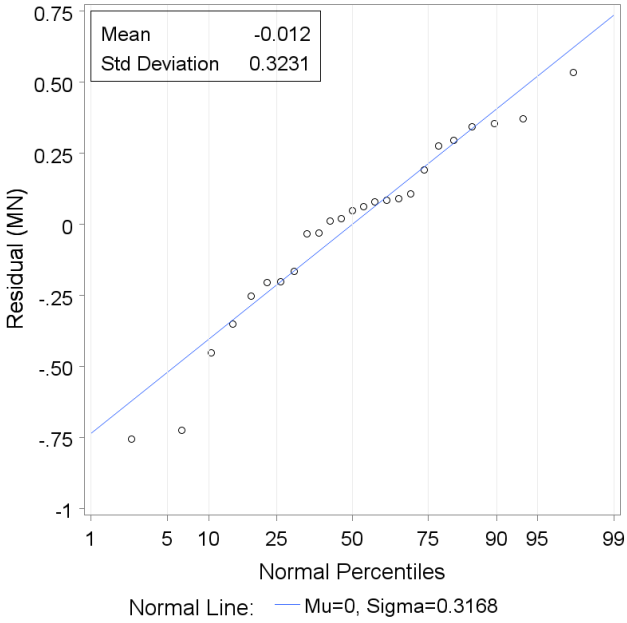

Figure C.126. Residual normality plot of peak hour—95th-percentile TTI—Minnesota.

80th-Percentile TTI Model

California

Table C.70. Residual Analysis of Peak Hour—80th-Percentile TTI—California

Table C.70.a. Basic Statistical Measures

Location		Variability	
Mean	–0.127	Std deviation	0.2908
Median	–0.187	Variance	0.0846
Minimum	–0.579	Range	1.2892
Maximum	0.7099	Interquartile range	0.2590

Table C.70.b. Basic Confidence Limits Assuming Normality

Parameter	Estimate	95% Confidence Limits	
Mean	–0.127	–0.216	–0.037
Std deviation	0.2908	0.2398	0.3696
Variance	0.0846	0.0575	0.1366

Table C.70.c. Tests for Location: Mu=0

Test	Statistic		*p*-Value	
Student's *t*	*t*	–2.855	Pr > |*t*|	0.0067

Table C.70.d. Tests for Normality

Test	Statistic		*p*-Value	
Shapiro-Wilk	*W*	0.9143	Pr < *W*	0.0035

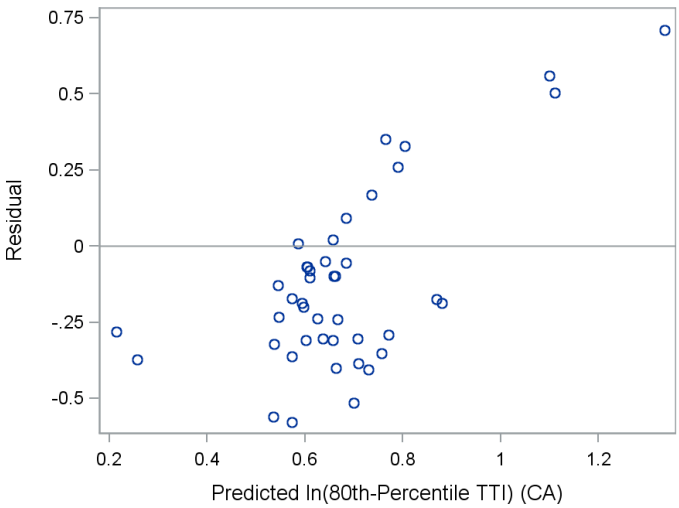

Figure C.127. Residual plot of peak hour—80th-percentile TTI—California.

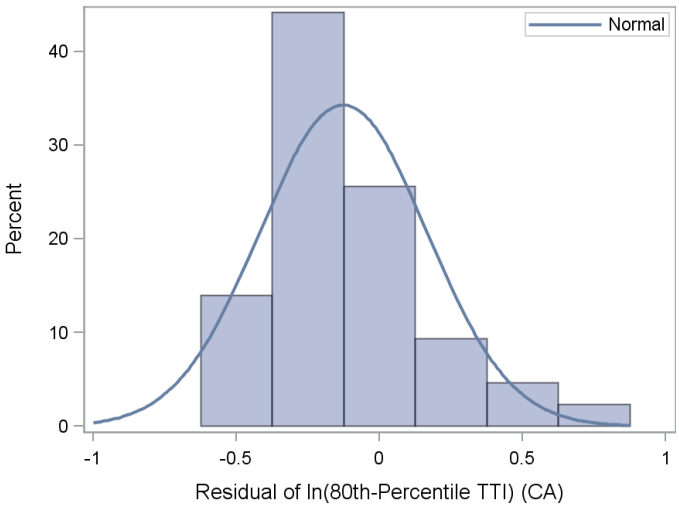

Figure C.128. Residual histogram of peak hour—80th-percentile TTI—California.

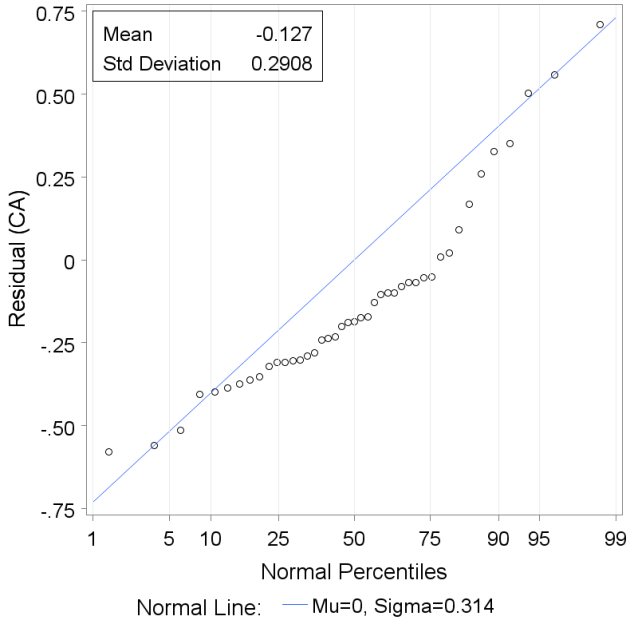

Figure C.129. Residual normality plot of peak hour—80th-percentile TTI—California.

Minnesota

Table C.71. Residual Analysis of Peak Hour—80th-Percentile TTI—Minnesota

Table C.71.a. Basic Statistical Measures

Location		Variability	
Mean	–0.102	Std deviation	0.2805
Median	–0.076	Variance	0.0787
Minimum	–0.738	Range	1.0207
Maximum	0.2824	Interquartile range	0.3547

Table C.71.b. Basic Confidence Limits Assuming Normality

Parameter	Estimate	95% Confidence Limits	
Mean	–0.102	–0.218	0.0139
Std deviation	0.2805	0.2190	0.3902
Variance	0.0787	0.0480	0.1523

Table C.71.c. Tests for Location: Mu=0

Test	Statistic		*p*-Value	
Student's *t*	*t*	–1.816	Pr > |*t*|	0.0818

Table C.71.d. Tests for Normality

Test	Statistic		*p*-Value	
Shapiro-Wilk	*W*	0.9279	Pr < *W*	0.0779

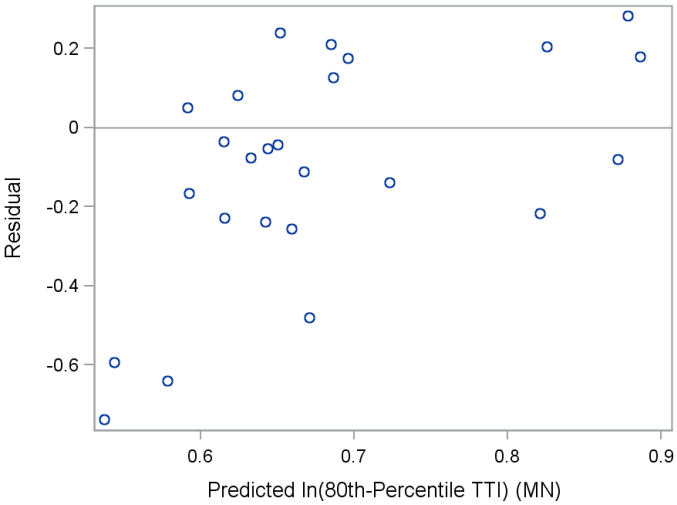

Figure C.130. Residual plot of peak hour—80th-percentile TTI—Minnesota.

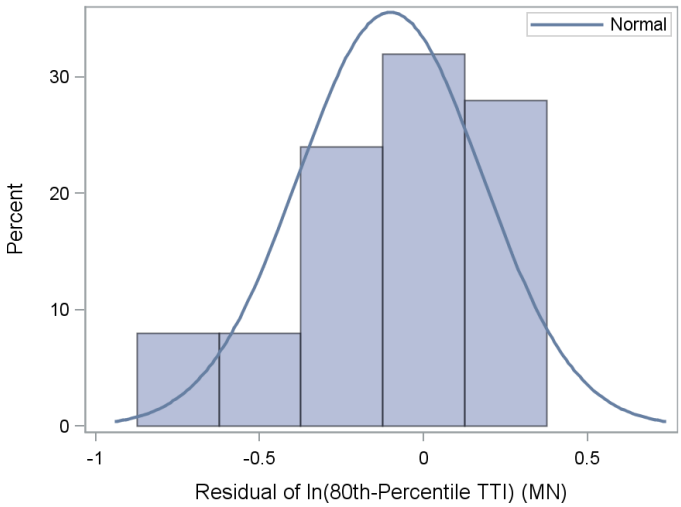

Figure C.131. Residual histogram of peak hour—80th-percentile TTI—Minnesota.

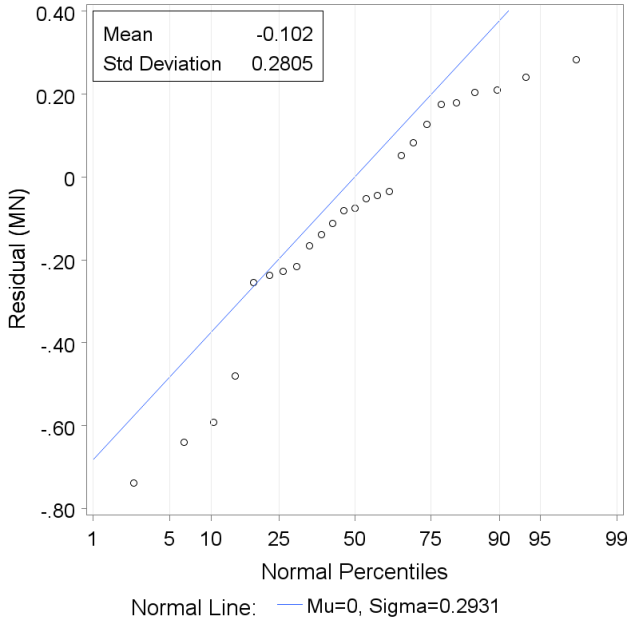

Figure C.132. Residual normality plot of peak hour—80th-percentile TTI—Minnesota.

50th-Percentile TTI Model

California

Table C.72. Residual Analysis of Peak Hour—50th-Percentile TTI—California

Table C.72.a. Basic Statistical Measures

Location		Variability	
Mean	–0.141	Std deviation	0.2458
Median	–0.161	Variance	0.0604
Minimum	–0.624	Range	0.9830
Maximum	0.3588	Interquartile range	0.3255

Table C.72.b. Basic Confidence Limits Assuming Normality

Parameter	Estimate	95% Confidence Limits	
Mean	–0.141	–0.216	–0.065
Std deviation	0.2458	0.2027	0.3125
Variance	0.0604	0.0411	0.0976

Table C.72.c. Tests for Location: Mu=0

Test	Statistic		*p*-Value	
Student's *t*	*t*	–3.750	Pr > |*t*|	0.0005

Table C.72.d. Tests for Normality

Test	Statistic		*p*-Value	
Shapiro-Wilk	*W*	0.9844	Pr < *W*	0.8187

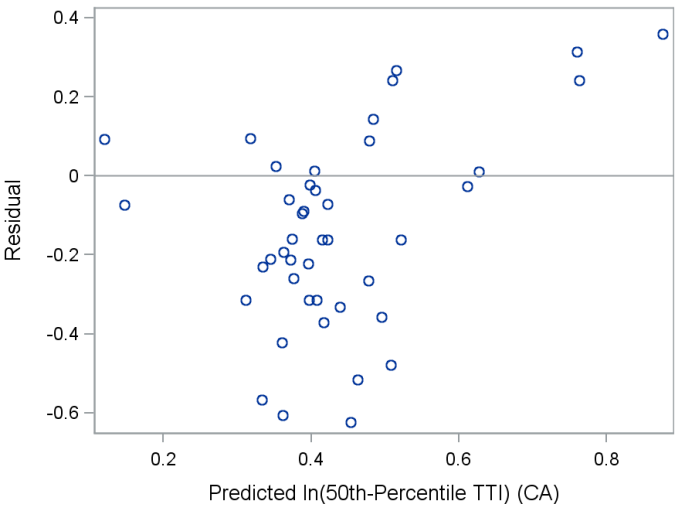

Figure C.133. Residual plot of peak hour—50th-percentile TTI—California.

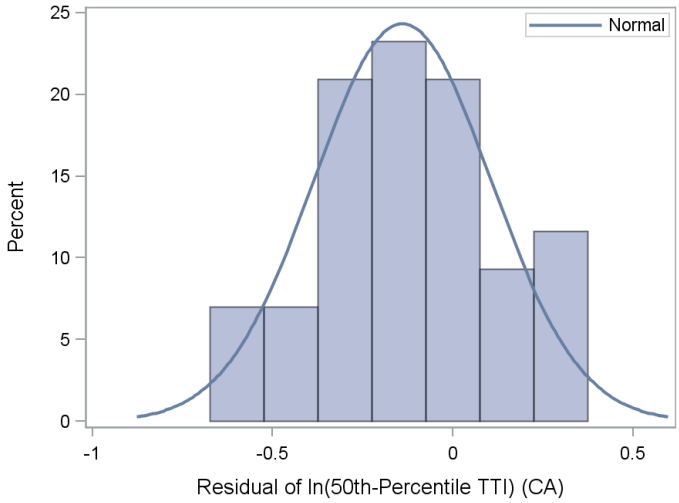

Figure C.134. Residual histogram of peak hour—50th-percentile TTI—California.

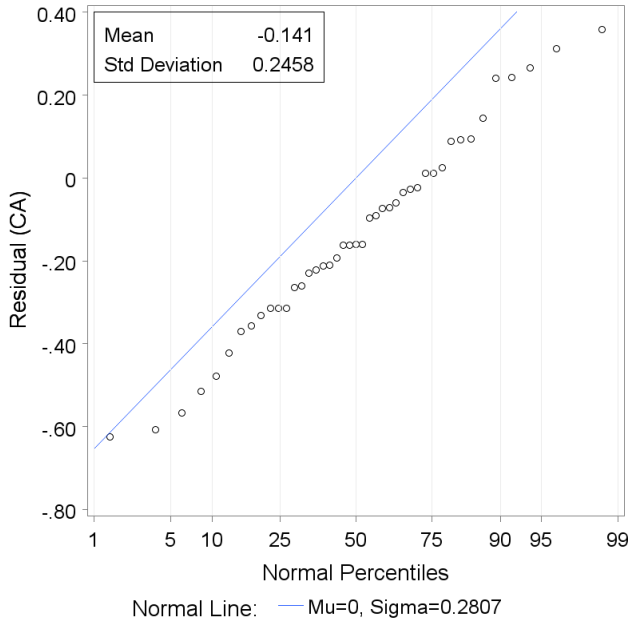

Figure C.135. Residual normality plot of peak hour—50th-percentile TTI—California.

Minnesota

Table C.73. Residual Analysis of Peak Hour—50th-Percentile TTI—Minnesota

Table C.73.a. Basic Statistical Measures

Location		Variability	
Mean	0.0219	Std deviation	0.2202
Median	0.0730	Variance	0.0485
Minimum	–0.426	Range	0.8297
Maximum	0.4035	Interquartile range	0.3632

Table C.73.b. Basic Confidence Limits Assuming Normality

Parameter	Estimate	95% Confidence Limits	
Mean	0.0219	–0.069	0.1128
Std deviation	0.2202	0.1719	0.3063
Variance	0.0485	0.0296	0.0938

Table C.73.c. Tests for Location: Mu=0

Test	Statistic		*p*-Value	
Student's *t*	*t*	0.4982	Pr > |*t*|	0.6228

Table C.73.d. Tests for Normality

Test	Statistic		*p*-Value	
Shapiro-Wilk	*W*	0.9545	Pr < *W*	0.3161

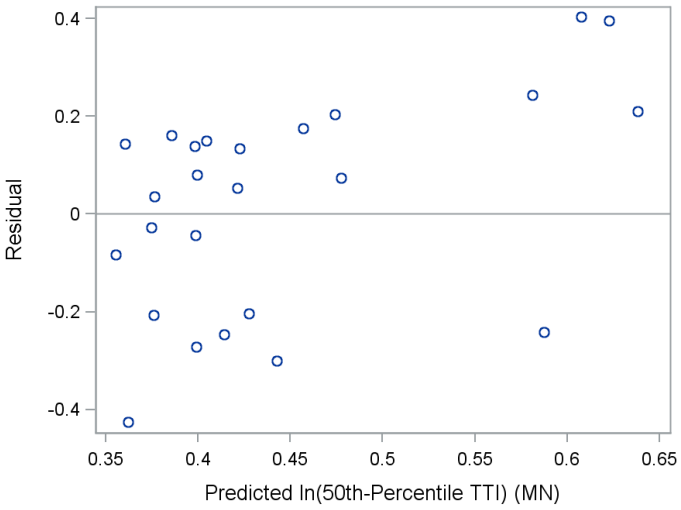

Figure C.136. Residual plot of peak hour—50th-percentile TTI—Minnesota.

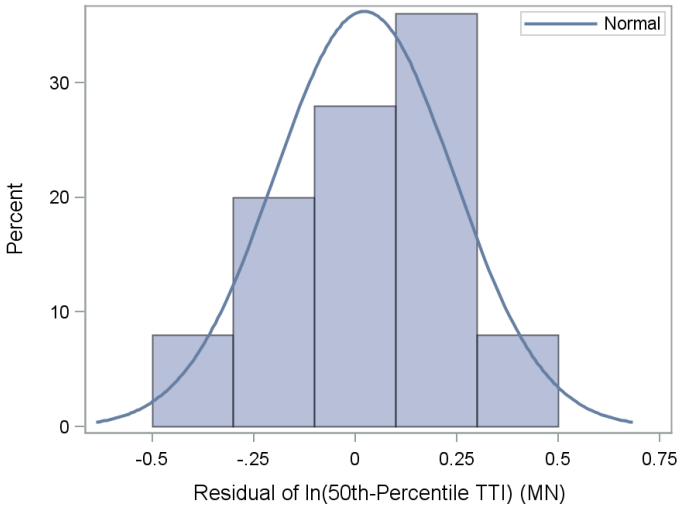

Figure C.137. Residual histogram of peak hour—50th-percentile TTI—Minnesota.

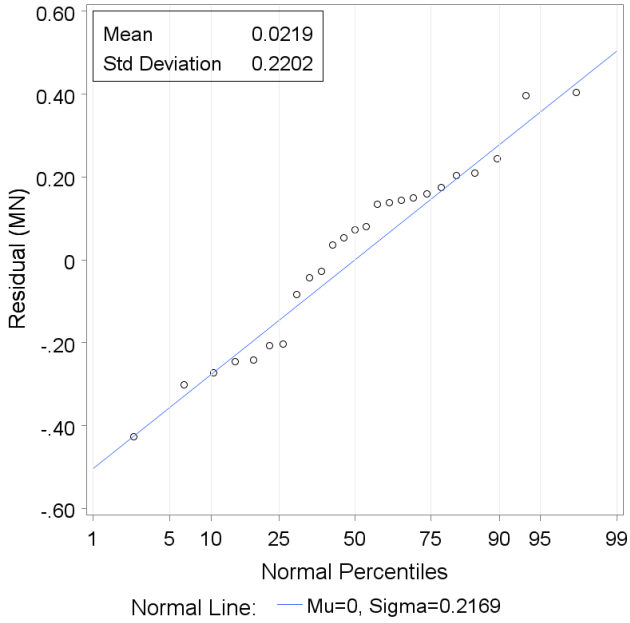

Figure C.138. Residual normality plot of peak hour—50th-percentile TTI—Minnesota.

10th-Percentile TTI Model

California

Table C.74. Residual Analysis of Peak Hour—10th-Percentile TTI—California

Table C.74.a. Basic Statistical Measures

Location		Variability	
Mean	–0.075	Std deviation	0.1886
Median	–0.027	Variance	0.0356
Minimum	–0.640	Range	0.7884
Maximum	0.1486	Interquartile range	0.1986

Table C.74.b. Basic Confidence Limits Assuming Normality

Parameter	Estimate	95% Confidence Limits	
Mean	–0.075	–0.133	–0.017
Std deviation	0.1886	0.1555	0.2397
Variance	0.0356	0.0242	0.0574

Table C.74.c. Tests for Location: Mu=0

Test	Statistic		*p*-Value	
Student's *t*	*t*	–2.603	Pr > |*t*|	0.0127

Table C.74.d. Tests for Normality

Test	Statistic		*p*-Value	
Shapiro-Wilk	*W*	0.8385	Pr < *W*	<0.0001

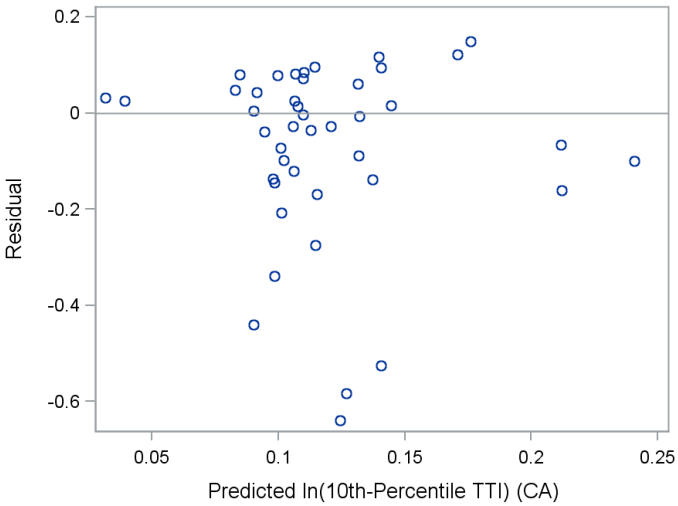

Figure C.139. Residual plot of peak hour—10th-percentile TTI—California.

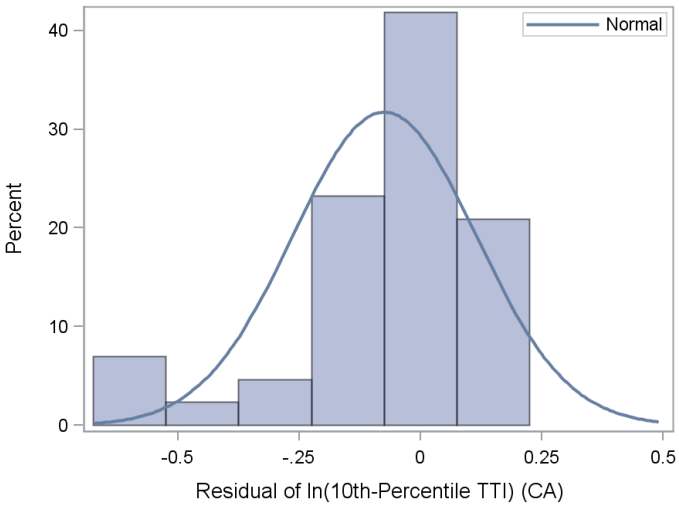

Figure C.140. Residual histogram of peak hour—10th-percentile TTI—California.

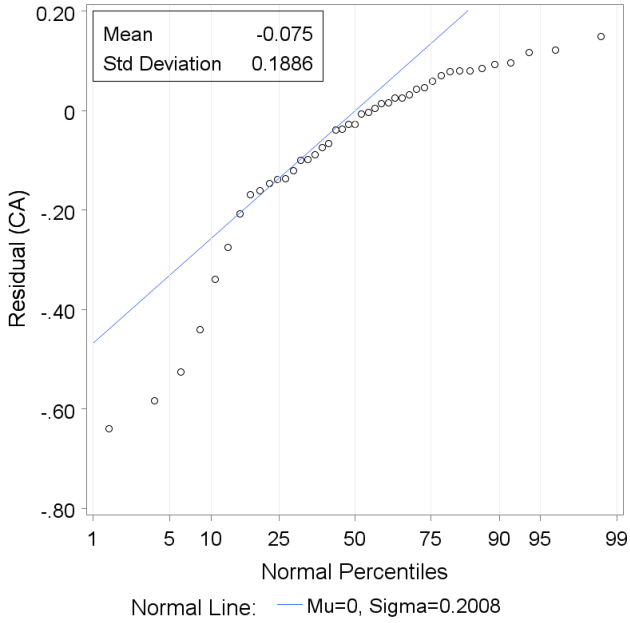

Figure C.141. Residual normality plot of peak hour—10th-percentile TTI—California.

Minnesota

Table C.75. Residual Analysis of Peak Hour—10th-Percentile TTI—Minnesota

Table C.75.a. Basic Statistical Measures

Location		Variability	
Mean	0.0770	Std deviation	0.0866
Median	0.1010	Variance	0.0075
Minimum	–0.261	Range	0.4352
Maximum	0.1739	Interquartile range	0.0461

Table C.75.b. Basic Confidence Limits Assuming Normality

Parameter	Estimate	95% Confidence Limits	
Mean	0.0770	0.0412	0.1128
Std deviation	0.0866	0.0677	0.1205
Variance	0.0075	0.0046	0.0145

Table C.75.c. Tests for Location: Mu=0

Test	Statistic		*p*-Value	
Student's *t*	*t*	4.4440	Pr > |*t*|	0.0002

Table C.75.d. Tests for Normality

Test	Statistic		*p*-Value	
Shapiro-Wilk	*W*	0.7271	Pr < *W*	<0.0001

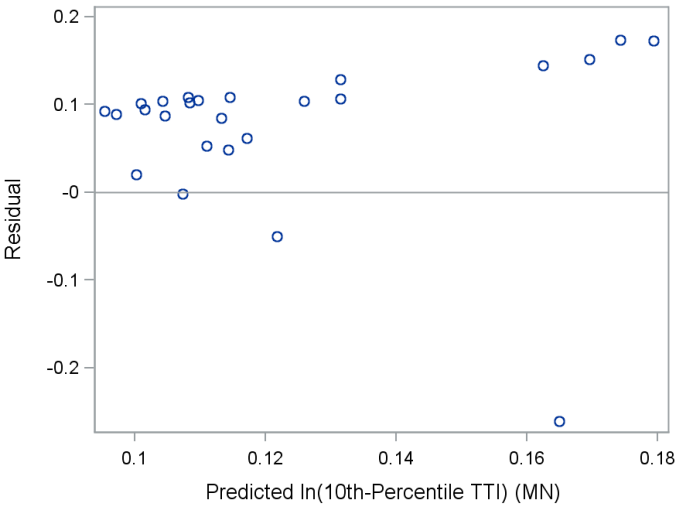

Figure C.142. Residual plot of peak hour—10th-percentile TTI—Minnesota.

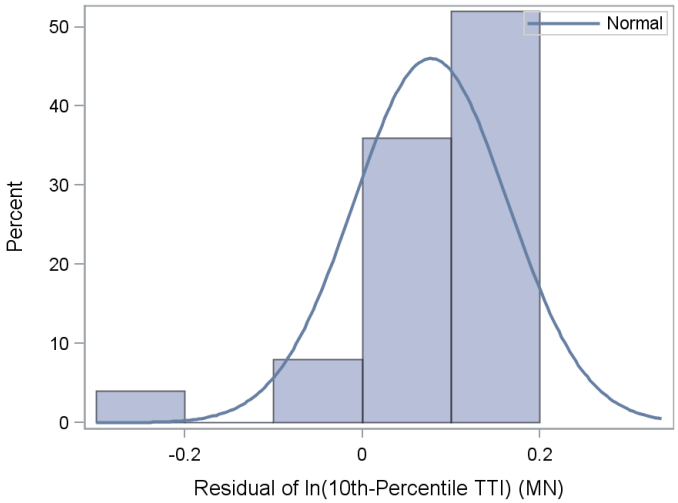

Figure C.143. Residual histogram of peak hour—10th-percentile TTI—Minnesota.

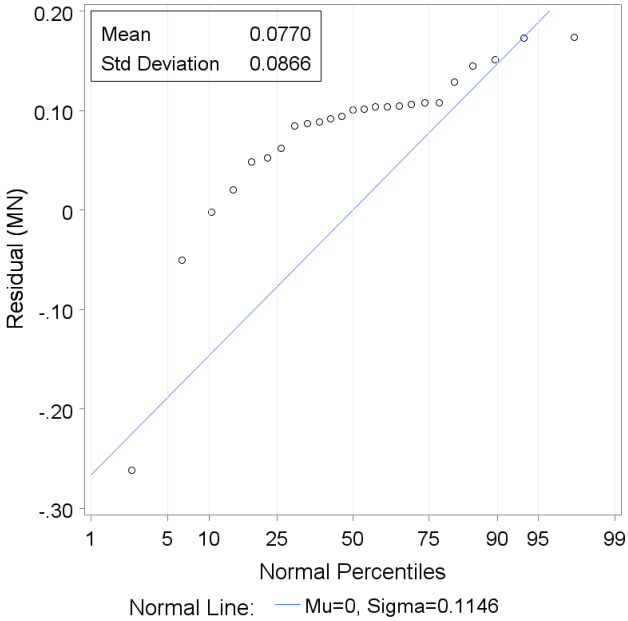

Figure C.144. Residual normality plot of peak hour—10th-percentile TTI—Minnesota.

Midday

Mean TTI Model

California

Table C.76. Residual Analysis of Midday—Mean TTI—California

Table C.76.a. Basic Statistical Measures

Location		Variability	
Mean	0.0164	Std deviation	0.0714
Median	0.0377	Variance	0.0051
Minimum	–0.443	Range	0.5167
Maximum	0.0741	Interquartile range	0.0370

Table C.76.b. Basic Confidence Limits Assuming Normality

Parameter	Estimate	95% Confidence Limits	
Mean	0.0164	0.0045	0.0283
Std deviation	0.0714	0.0639	0.0809
Variance	0.0051	0.0041	0.0065

Table C.76.c. Tests for Location: Mu=0

Test	Statistic		*p*-Value	
Student's *t*	*t*	2.7157	Pr > |*t*|	0.0075

Table C.76.d. Tests for Normality

Test	Statistic		*p*-Value	
Shapiro-Wilk	*W*	0.5476	Pr < *W*	<0.0001

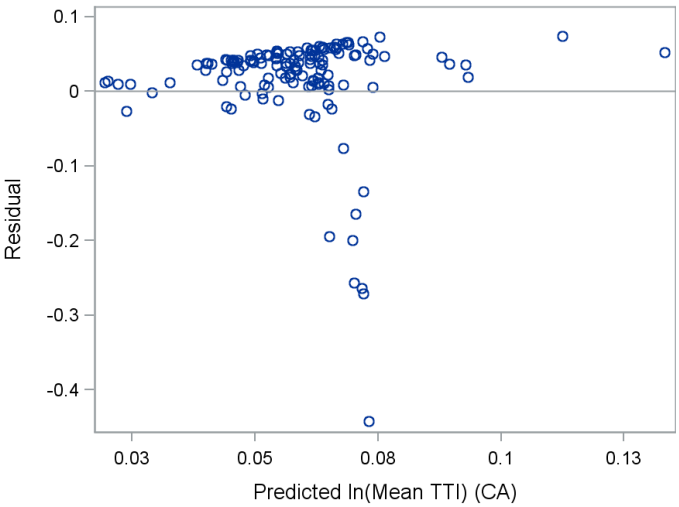

Figure C.145. Residual plot of midday—mean TTI—California.

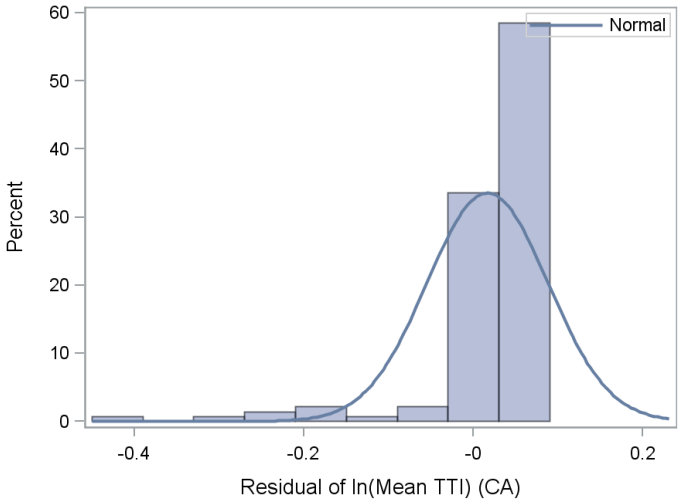

Figure C.146. Residual histogram of midday—mean TTI—California.

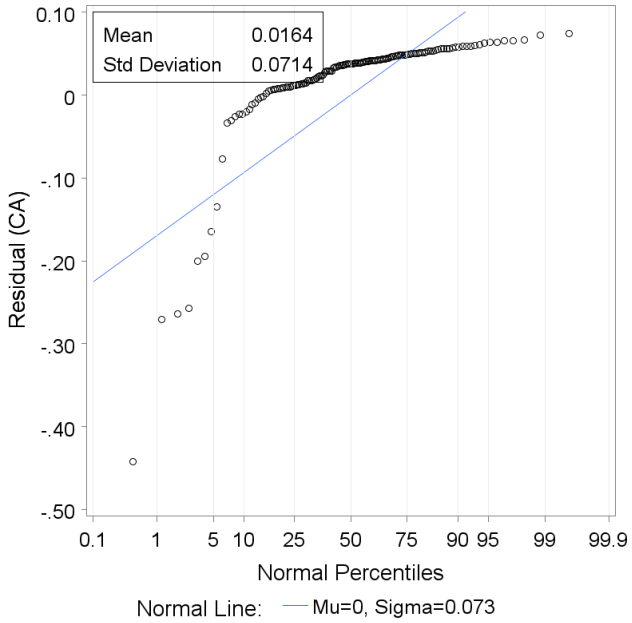

Figure C.147. Residual normality plot of midday—mean TTI—California.

Minnesota

Table C.77. Residual Analysis of Midday—Mean TTI—Minnesota

Table C.77.a. Basic Statistical Measures

Location		Variability	
Mean	0.0273	Std deviation	0.0294
Median	0.0339	Variance	0.0009
Minimum	–0.138	Range	0.1943
Maximum	0.0560	Interquartile range	0.0259

Table C.77.b. Basic Confidence Limits Assuming Normality

Parameter	Estimate	95% Confidence Limits	
Mean	0.0273	0.0197	0.0349
Std deviation	0.0294	0.0249	0.0358
Variance	0.0009	0.0006	0.0013

Table C.77.c. Tests for Location: Mu=0

Test	Statistic		*p*-Value	
Student's *t*	*t*	7.2065	Pr > |*t*|	<0.0001

Table C.77.d. Tests for Normality

Test	Statistic		*p*-Value	
Shapiro-Wilk	*W*	0.6904	Pr < *W*	<0.0001

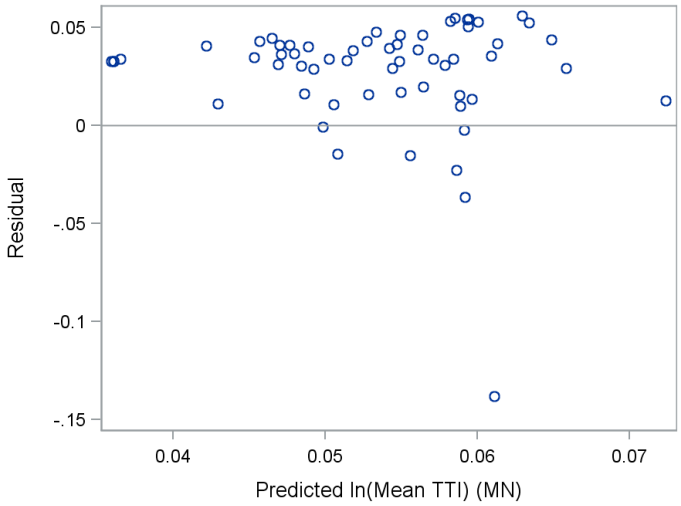

Figure C.148. Residual plot of midday—mean TTI—Minnesota.

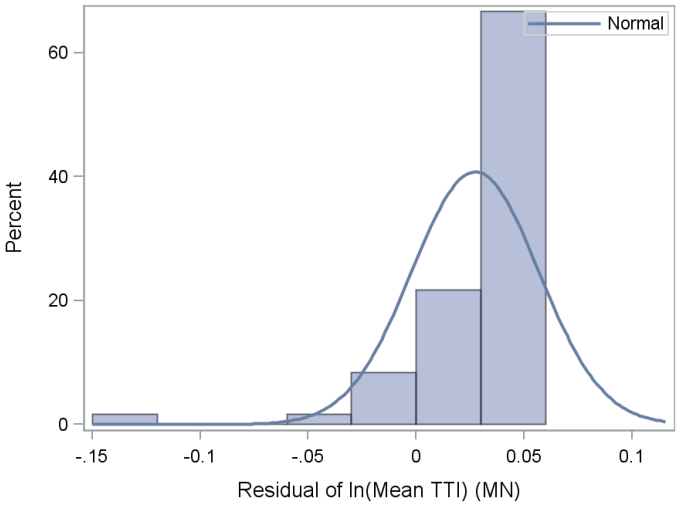

Figure C.149. Residual histogram of midday—mean TTI—Minnesota.

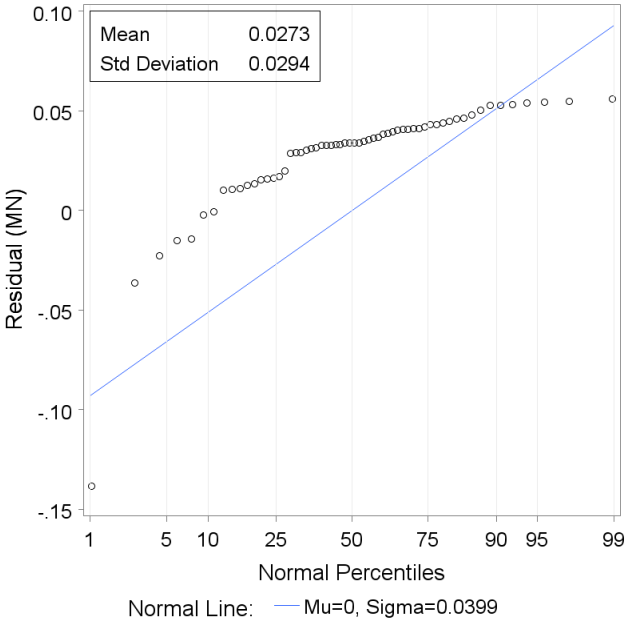

Figure C.150. Residual normality plot of midday—mean TTI—Minnesota.

Salt Lake City

Table C.78. Residual Analysis of Midday—Mean TTI—Salt Lake City

Table C.78.a. Basic Statistical Measures

Location		Variability	
Mean	0.0281	Std deviation	0.0206
Median	0.0342	Variance	0.0004
Minimum	–0.016	Range	0.0670
Maximum	0.0507	Interquartile range	0.0207

Table C.78.b. Basic Confidence Limits Assuming Normality

Parameter	Estimate	95% Confidence Limits	
Mean	0.0281	0.0207	0.0355
Std deviation	0.0206	0.0165	0.0274
Variance	0.0004	0.0003	0.0007

Table C.78.c. Tests for Location: Mu=0

Test	Statistic		*p*-Value	
Student's *t*	*t*	7.7165	Pr > |*t*|	<0.0001

Table C.78.d. Tests for Normality

Test	Statistic		*p*-Value	
Shapiro-Wilk	*W*	0.8171	Pr < *W*	<0.0001

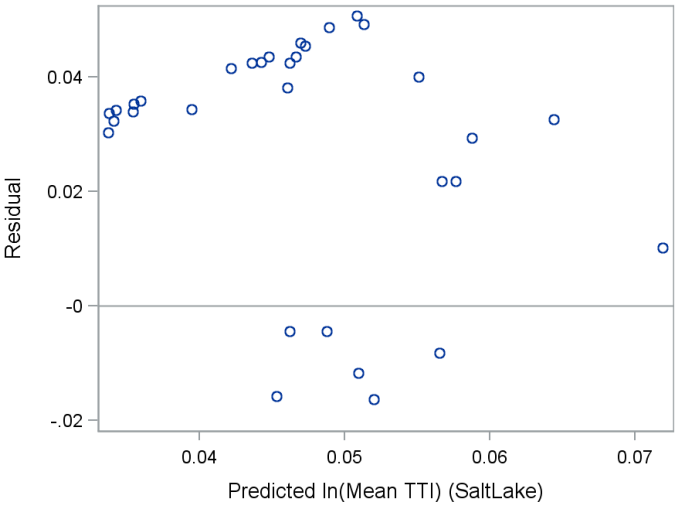

Figure C.151. Residual plot of midday—mean TTI—Salt Lake City.

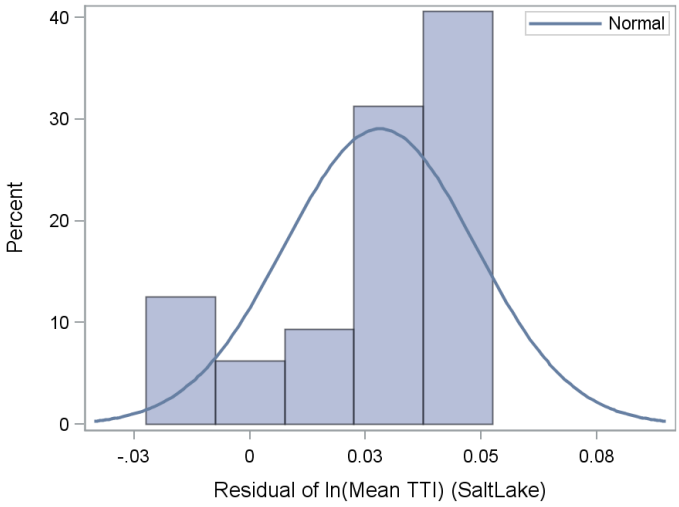

Figure C.152. Residual histogram of midday—mean TTI—Salt Lake City.

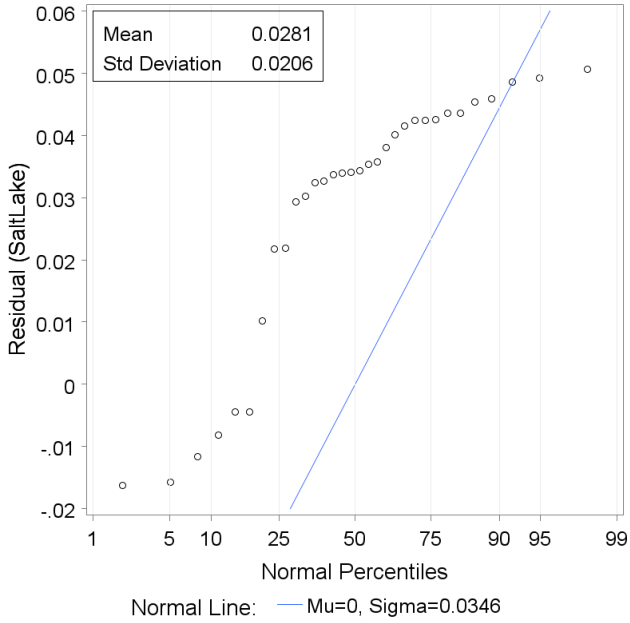

Figure C.153. Residual normality plot of midday—mean TTI—Salt Lake City.

99th-Percentile TTI Model

California

Table C.79. Residual Analysis of Midday—99th-Percentile TTI—California

Table C.79.a. Basic Statistical Measures

Location		Variability	
Mean	0.2094	Std deviation	0.2152
Median	0.2689	Variance	0.0463
Minimum	–0.535	Range	1.2456
Maximum	0.7110	Interquartile range	0.2254

Table C.79.b. Basic Confidence Limits Assuming Normality

Parameter	Estimate	95% Confidence Limits	
Mean	0.2094	0.1735	0.2454
Std deviation	0.2152	0.1926	0.2438
Variance	0.0463	0.0371	0.0595

Table C.79.c. Tests for Location: Mu=0

Test	Statistic		*p*-Value	
Student's *t*	*t*	11.517	Pr > |*t*|	<0.0001

Table C.79.d. Tests for Normality

Test	Statistic		*p*-Value	
Shapiro-Wilk	*W*	0.8888	Pr < *W*	<0.0001

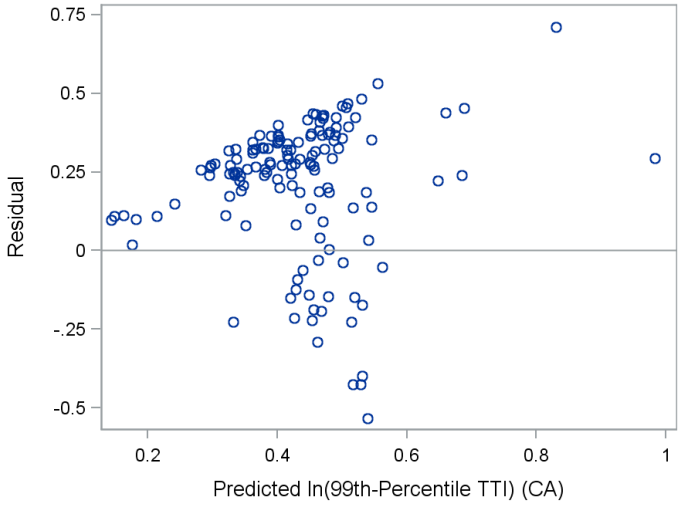

Figure C.154. Residual plot of midday—99th-percentile TTI—California.

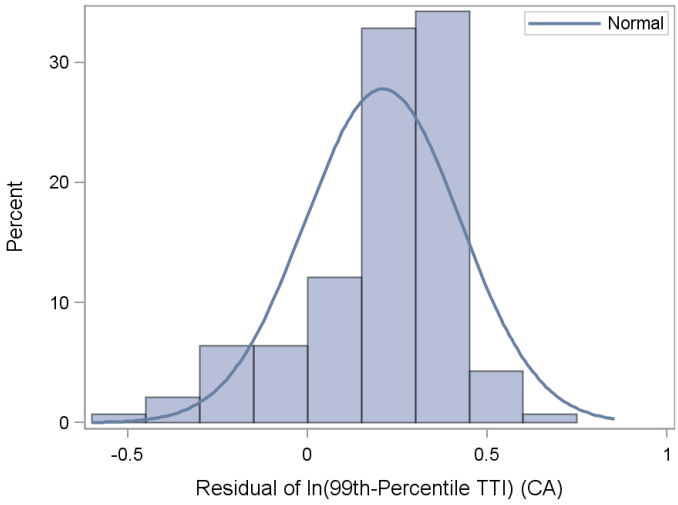

Figure C.155. Residual histogram of midday—99th-percentile TTI—California.

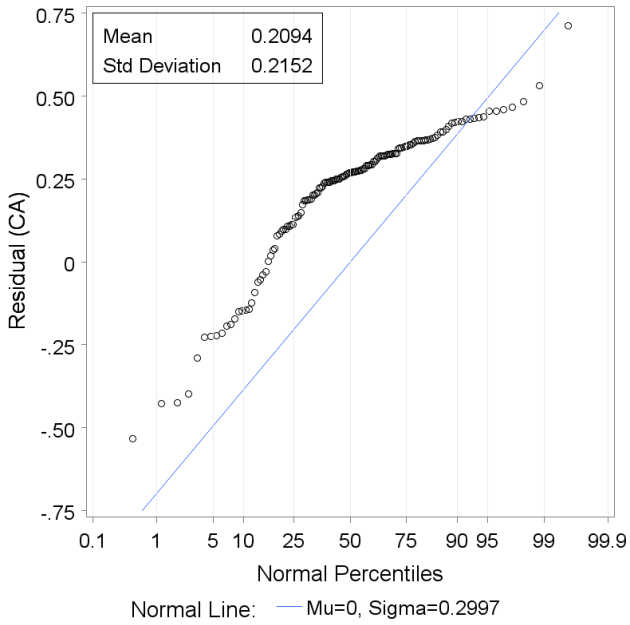

Figure C.156. Residual normality plot of midday—99th-percentile TTI—California.

Minnesota

Table C.80. Residual Analysis of Midday—99th-Percentile TTI—Minnesota

Table C.80.a. Basic Statistical Measures

Location		Variability	
Mean	0.1419	Std deviation	0.1825
Median	0.1902	Variance	0.0333
Minimum	–0.457	Range	0.8090
Maximum	0.3525	Interquartile range	0.1319

Table C.80.b. Basic Confidence Limits Assuming Normality

Parameter	Estimate	95% Confidence Limits	
Mean	0.1419	0.0948	0.1891
Std deviation	0.1825	0.1547	0.2225
Variance	0.0333	0.0239	0.0495

Table C.80.c. Tests for Location: Mu=0

Test	Statistic		*p*-Value	
Student's *t*	*t*	6.0250	Pr > |*t*|	<0.0001

Table C.80.d. Tests for Normality

Test	Statistic		*p*-Value	
Shapiro-Wilk	*W*	0.8145	Pr < *W*	<0.0001

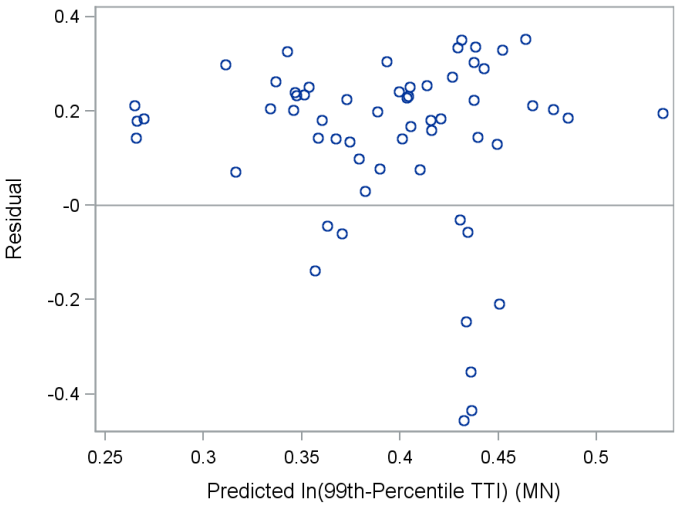

Figure C.157. Residual plot of midday—99th-percentile TTI—Minnesota.

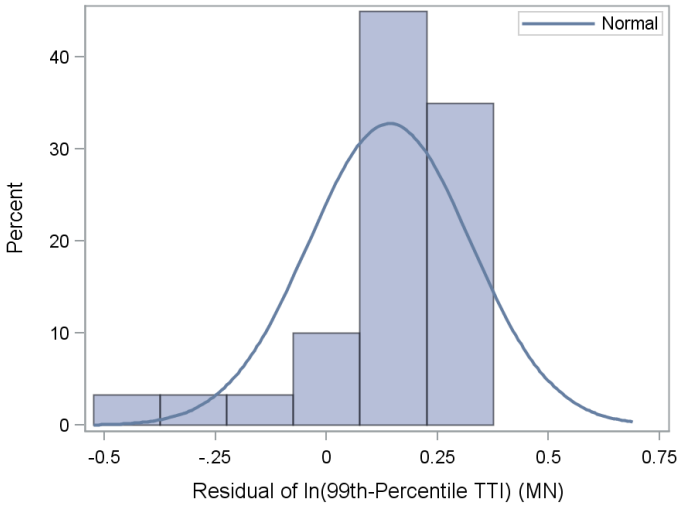

Figure C.158. Residual histogram of midday—99th-percentile TTI—Minnesota.

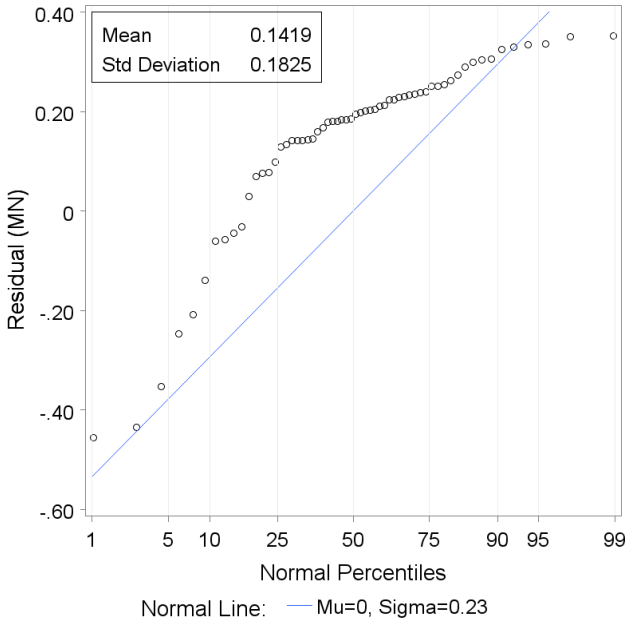

Figure C.159. Residual normality plot of midday—99th-percentile TTI—Minnesota.

Salt Lake City

Table C.81. Residual Analysis of Midday—99th-Percentile TTI—Salt Lake City

Table C.81.a. Basic Statistical Measures

Location		Variability	
Mean	0.2697	Std deviation	0.1158
Median	0.3032	Variance	0.0134
Minimum	–0.257	Range	0.6388
Maximum	0.3821	Interquartile range	0.0960

Table C.81.b. Basic Confidence Limits Assuming Normality

Parameter	Estimate	95% Confidence Limits	
Mean	0.2697	0.2279	0.3114
Std deviation	0.1158	0.0928	0.1539
Variance	0.0134	0.0086	0.0237

Table C.81.c. Tests for Location: Mu=0

Test	Statistic		*p*-Value	
Student's *t*	*t*	13.175	Pr > |*t*|	<0.0001

Table C.81.d. Tests for Normality

Test	Statistic		*p*-Value	
Shapiro-Wilk	*W*	0.6933	Pr < *W*	<0.0001

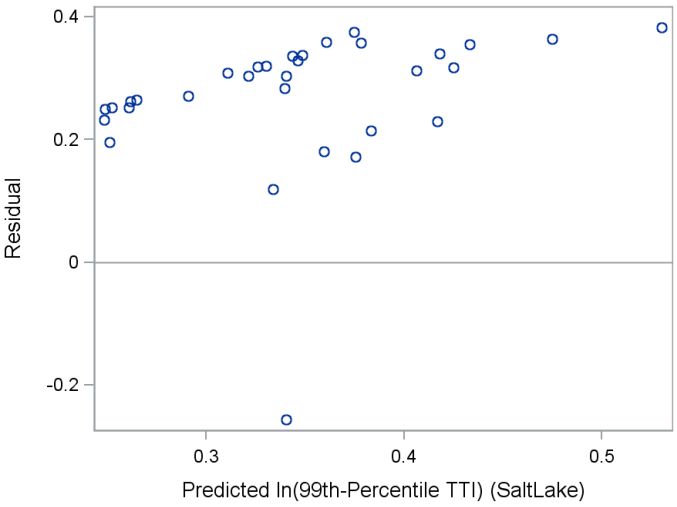

Figure C.160. Residual plot of midday—99th-percentile TTI—Salt Lake City.

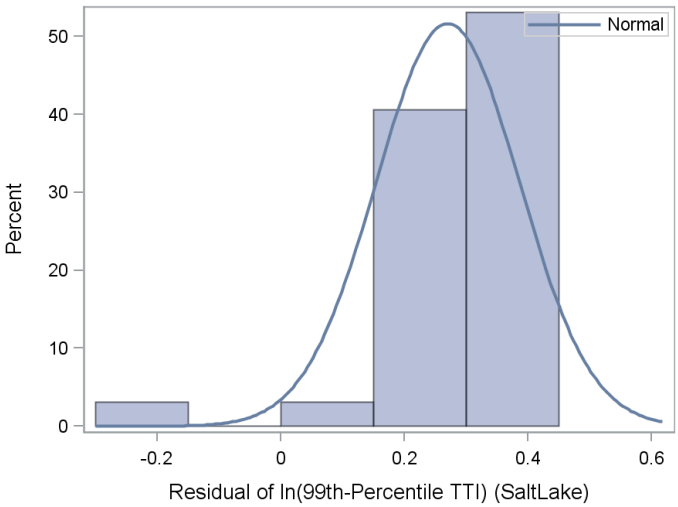

Figure C.161. Residual histogram of midday—99th-percentile TTI—Salt Lake City.

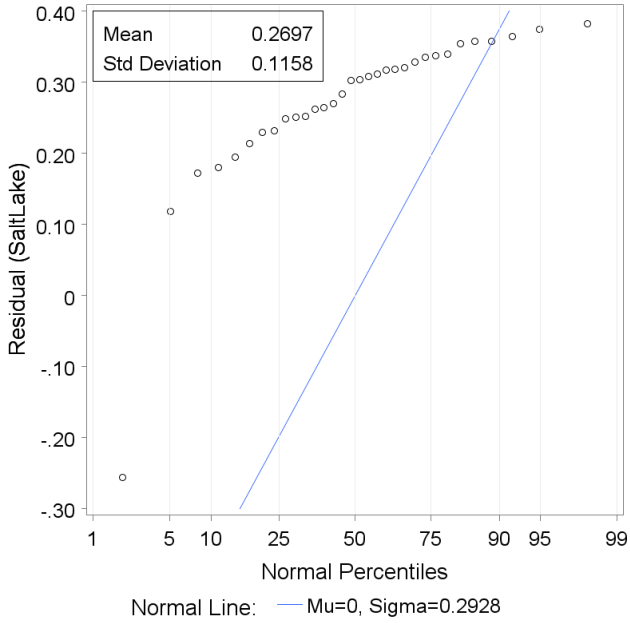

Figure C.162. Residual normality plot of midday—99th-percentile TTI—Salt Lake City.

95th-Percentile TTI Model

California

Table C.82. Residual Analysis of Midday—95th-Percentile TTI—California

Table C.82.a. Basic Statistical Measures

Location		Variability	
Mean	0.0787	Std deviation	0.1392
Median	0.1156	Variance	0.0194
Minimum	–0.662	Range	0.9157
Maximum	0.2537	Interquartile range	0.0949

Table C.82.b. Basic Confidence Limits Assuming Normality

Parameter	Estimate	95% Confidence Limits	
Mean	0.0787	0.0555	0.1020
Std deviation	0.1392	0.1246	0.1577
Variance	0.0194	0.0155	0.0249

Table C.82c. Tests for Location: Mu=0

Test	Statistic		*p*-Value	
Student's *t*	*t*	6.6931	Pr > |*t*|	<0.0001

Table C.82.d. Tests for Normality

Test	Statistic		*p*-Value	
Shapiro-Wilk	*W*	0.6580	Pr < *W*	<0.0001

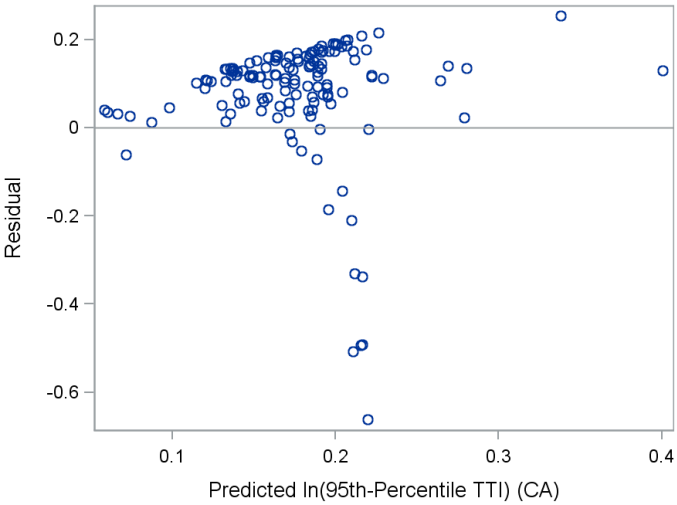

Figure C.163. Residual plot of midday—95th-percentile TTI—California.

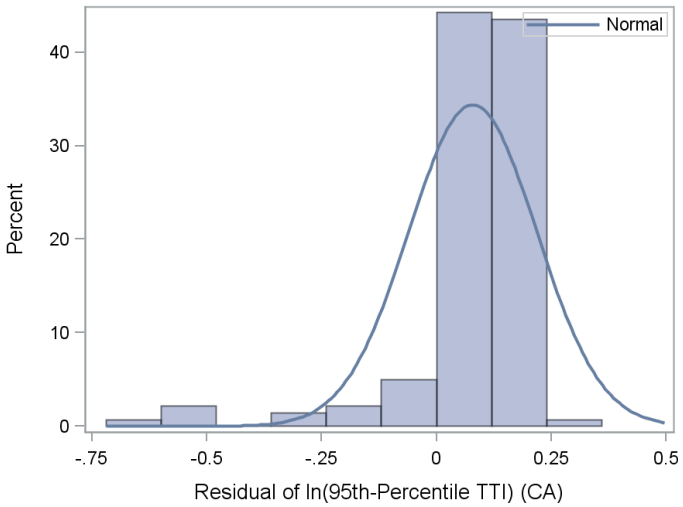

Figure C.164. Residual histogram of midday—95th-percentile TTI—California.

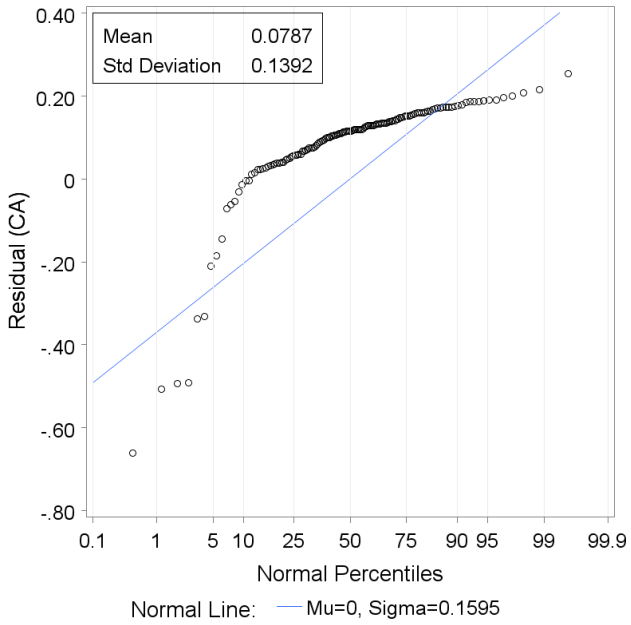

Figure C.165. Residual normality plot of midday—95th-percentile TTI—California.

Minnesota

Table C.83. Residual Analysis of Midday—95th-Percentile TTI—Minnesota

Table C.83.a. Basic Statistical Measures

Location		Variability	
Mean	0.0615	Std deviation	0.1168
Median	0.0957	Variance	0.0136
Minimum	–0.395	Range	0.5632
Maximum	0.1684	Interquartile range	0.0782

Table C.83.b. Basic Confidence Limits Assuming Normality

Parameter	Estimate	95% Confidence Limits	
Mean	0.0615	0.0313	0.0916
Std deviation	0.1168	0.0990	0.1424
Variance	0.0136	0.0098	0.0203

Table C.83.c. Tests for Location: Mu=0

Test	Statistic		*p*-Value	
Student's *t*	*t*	4.0784	Pr > |*t*|	0.0001

Table C.83.d. Tests for Normality

Test	Statistic		*p*-Value	
Shapiro-Wilk	*W*	0.7090	Pr < *W*	<0.0001

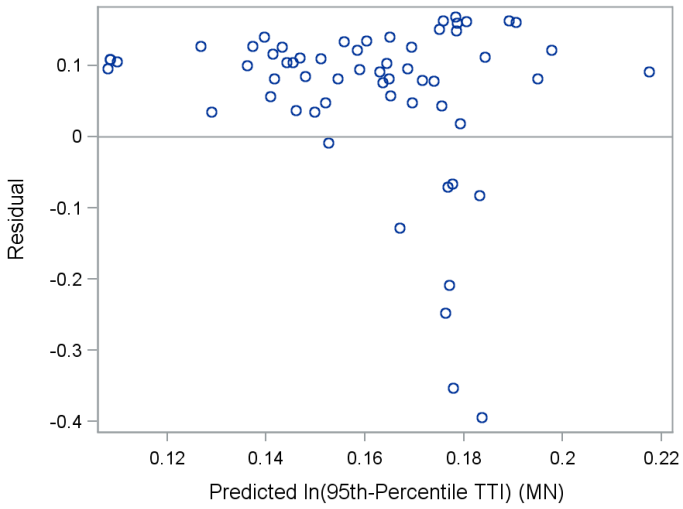

Figure C.166. Residual plot of midday—95th-percentile TTI—Minnesota.

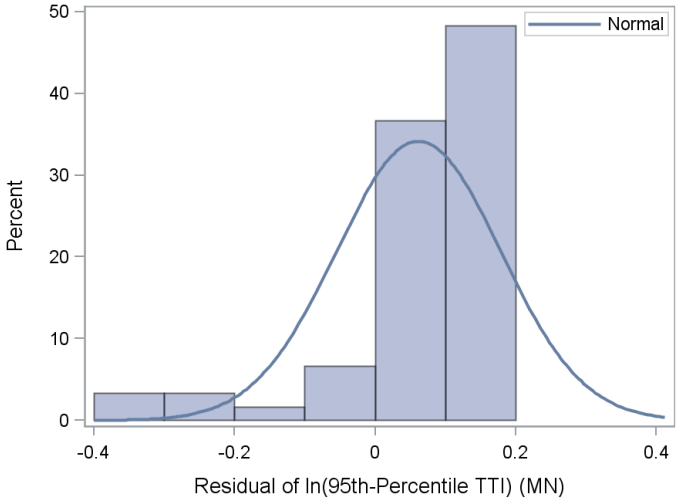

Figure C.167. Residual histogram of midday—95th-percentile TTI—Minnesota.

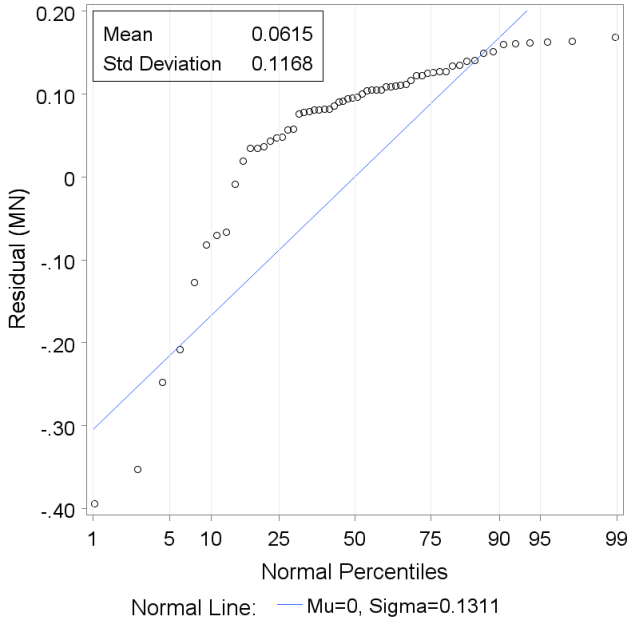

Figure C.168. Residual normality plot of midday—95th-percentile TTI—Minnesota.

Salt Lake City

Table C.84. Residual Analysis of Midday—95th-Percentile TTI—Salt Lake City

Table C.84.a. Basic Statistical Measures

Location		Variability	
Mean	0.1034	Std deviation	0.0583
Median	0.1182	Variance	0.0034
Minimum	–0.170	Range	0.3232
Maximum	0.1527	Interquartile range	0.0325

Table C.84.b. Basic Confidence Limits Assuming Normality

Parameter	Estimate	95% Confidence Limits	
Mean	0.1034	0.0824	0.1244
Std deviation	0.0583	0.0467	0.0775
Variance	0.0034	0.0022	0.0060

Table C.84.c. Tests for Location: Mu=0

Test	Statistic		*p*-Value	
Student's *t*	*t*	10.036	Pr > |*t*|	<0.0001

Table C.84.d. Tests for Normality

Test	Statistic		*p*-Value	
Shapiro-Wilk	*W*	0.6238	Pr < *W*	<0.0001

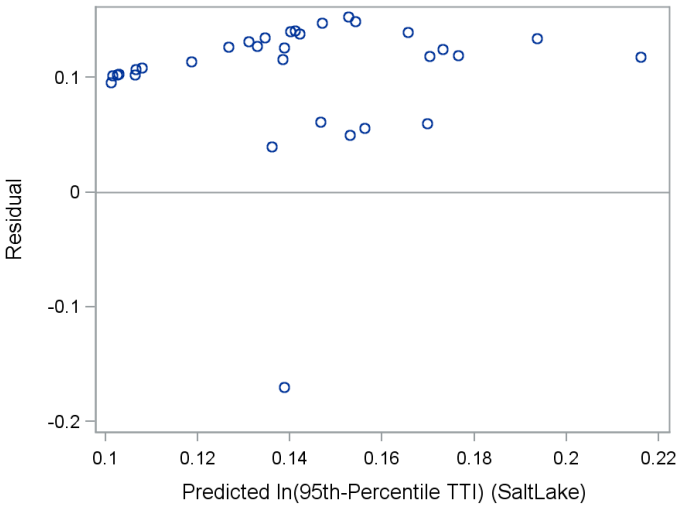

Figure C.169. Residual plot of midday—95th-percentile TTI—Salt Lake City.

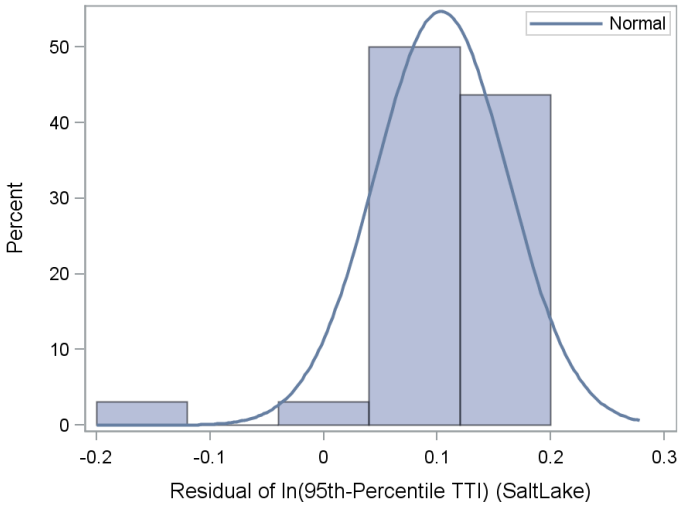

Figure C.170. Residual histogram of midday—95th-percentile TTI—Salt Lake City.

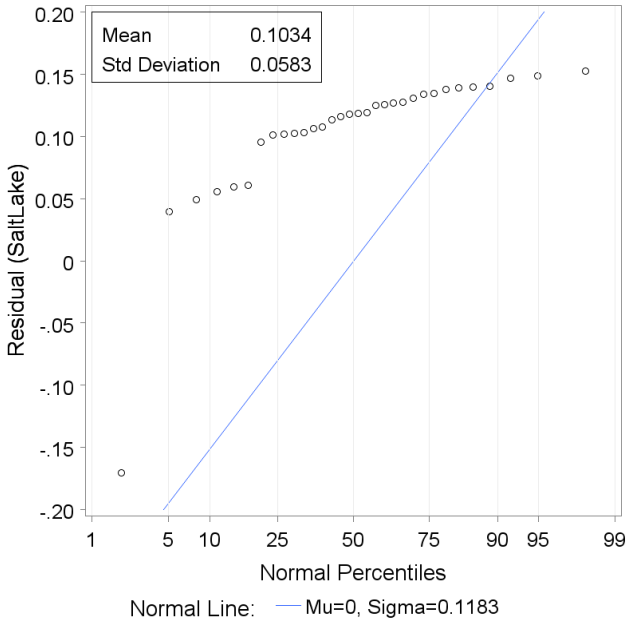

Figure C.171. Residual normality plot of midday—95th-percentile TTI—Salt Lake City.

80th-Percentile TTI Model

California

Table C.85. Residual Analysis of Midday—80th-Percentile TTI—California

Table C.85.a. Basic Statistical Measures

Location		Variability	
Mean	0.0047	Std deviation	0.1033
Median	0.0368	Variance	0.0107
Minimum	–0.627	Range	0.7005
Maximum	0.0737	Interquartile range	0.0517

Table C.85.b. Basic Confidence Limits Assuming Normality

Parameter	Estimate	95% Confidence Limits	
Mean	0.0047	–0.013	0.0220
Std deviation	0.1033	0.0925	0.1171
Variance	0.0107	0.0086	0.0137

Table C.85.c. Tests for Location: Mu=0

Test	Statistic		*p*-Value	
Student's *t*	*t*	0.5383	Pr > |*t*|	0.5912

Table C.85.d. Tests for Normality

Test	Statistic		*p*-Value	
Shapiro-Wilk	*W*	0.5368	Pr < *W*	<0.0001

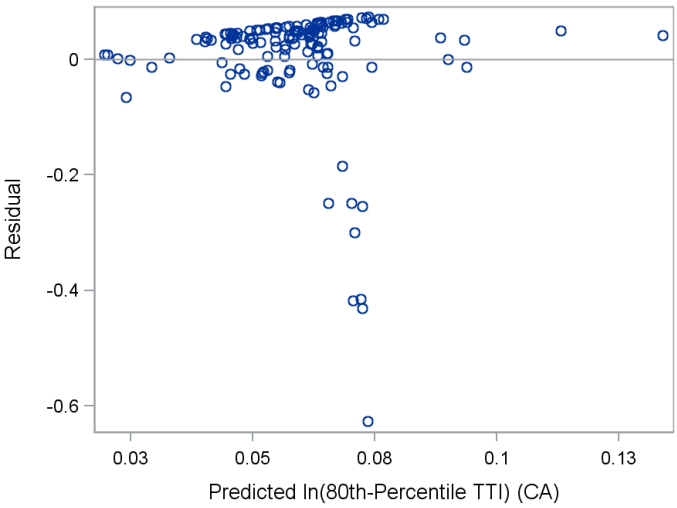

Figure C.172. Residual plot of midday—80th-percentile TTI—California.

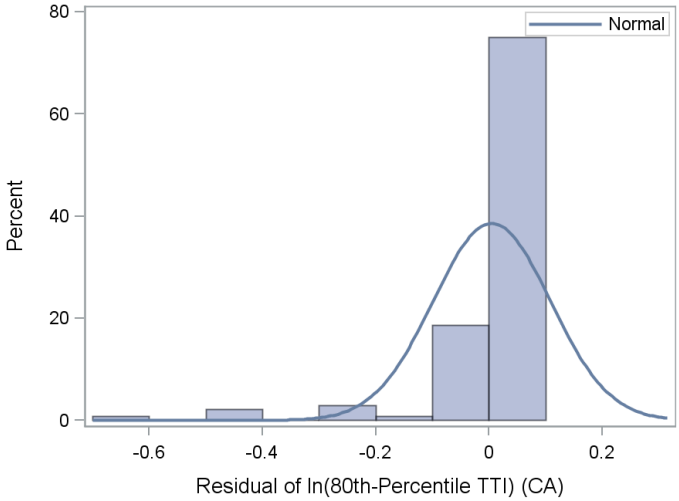

Figure C.173. Residual histogram of midday—80th-percentile TTI—California.

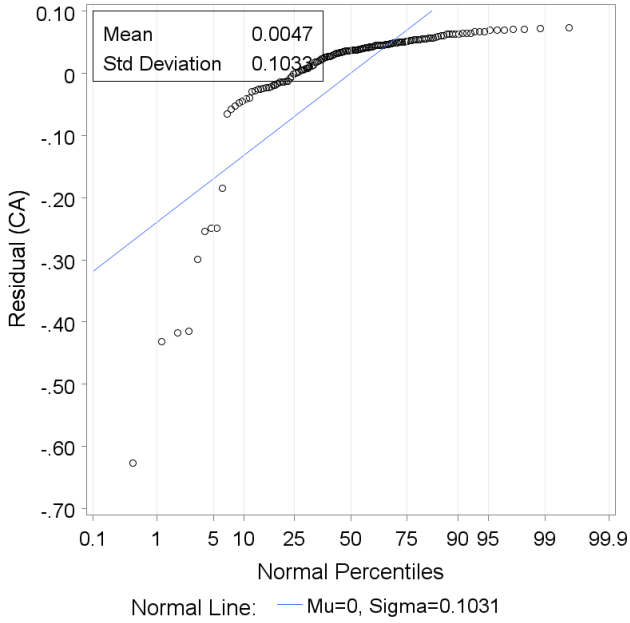

Figure C.174. Residual normality plot of midday—80th-percentile TTI—California.

Minnesota

Table C.86. Residual Analysis of Midday—80th-Percentile TTI—Minnesota

Table C.86.a. Basic Statistical Measures

Location		Variability	
Mean	0.0231	Std deviation	0.0602
Median	0.0365	Variance	0.0036
Minimum	–0.360	Range	0.4228
Maximum	0.0631	Interquartile range	0.0276

Table C.86.b. Basic Confidence Limits Assuming Normality

Parameter	Estimate	95% Confidence Limits	
Mean	0.0231	0.0075	0.0386
Std deviation	0.0602	0.0510	0.0734
Variance	0.0036	0.0026	0.0054

Table C.86.c. Tests for Location: Mu=0

Test	Statistic		*p*-Value	
Student's *t*	*t*	2.9669	Pr > |*t*|	0.0043

Table C.86.d. Tests for Normality

Test	Statistic		*p*-Value	
Shapiro-Wilk	*W*	0.4994	Pr < *W*	<0.0001

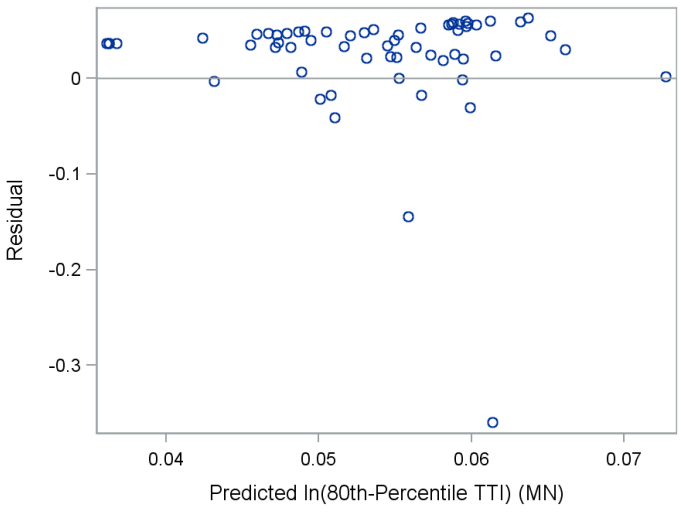

Figure C.175. Residual plot of midday—80th-percentile TTI—Minnesota.

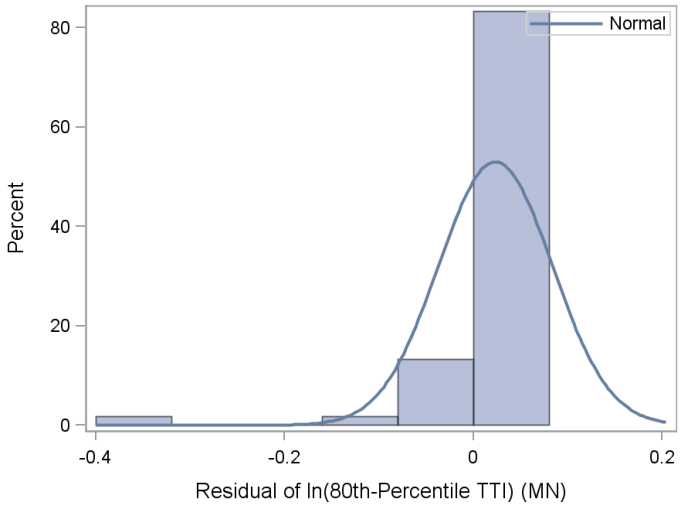

Figure C.176. Residual histogram of midday—80th-percentile TTI—Minnesota.

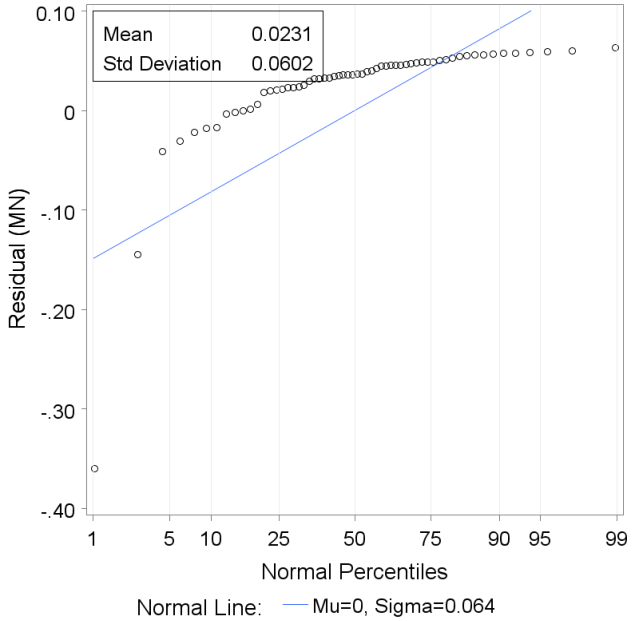

Figure C.177. Residual normality plot of midday—80th-percentile TTI—Minnesota.

Salt Lake City

Table C.87. Residual Analysis of Midday—80th-Percentile TTI—Salt Lake City

Table C.87.a. Basic Statistical Measures

Location		Variability	
Mean	0.0265	Std deviation	0.0238
Median	0.0350	Variance	0.0006
Minimum	–0.025	Range	0.0761
Maximum	0.0511	Interquartile range	0.0249

Table C.87.b. Basic Confidence Limits Assuming Normality

Parameter	Estimate	95% Confidence Limits	
Mean	0.0265	0.0179	0.0350
Std deviation	0.0238	0.0191	0.0316
Variance	0.0006	0.0004	0.0010

Table C.87.c. Tests for Location: Mu=0

Test	Statistic		*p*-Value	
Student's *t*	*t*	6.3027	Pr > |*t*|	<0.0001

Table C.87.d. Tests for Normality

Test	Statistic		*p*-Value	
Shapiro-Wilk	*W*	0.8161	Pr < *W*	<0.0001

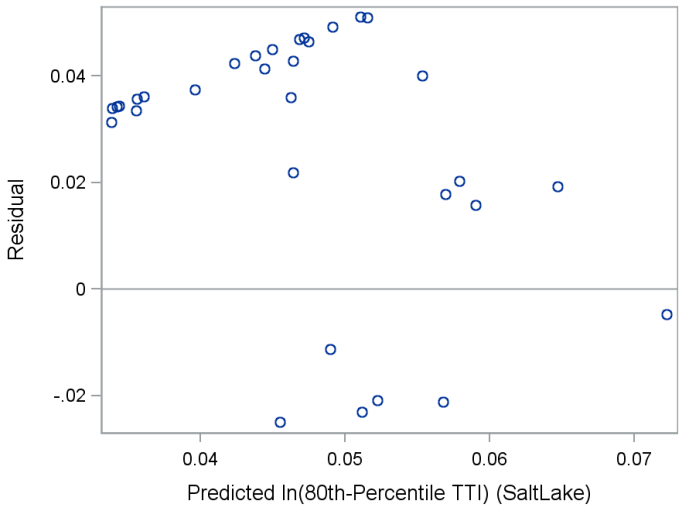

Figure C.178. Residual plot of midday—80th-percentile TTI—Salt Lake City.

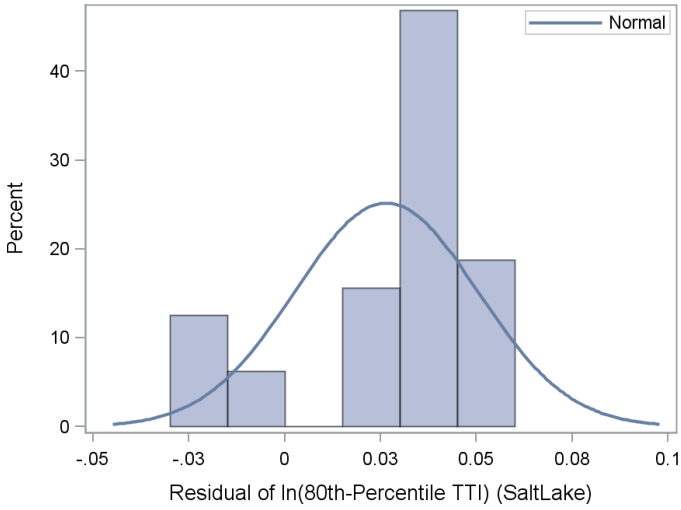

Figure C.179. Residual histogram of midday—80th-percentile TTI—Salt Lake City.

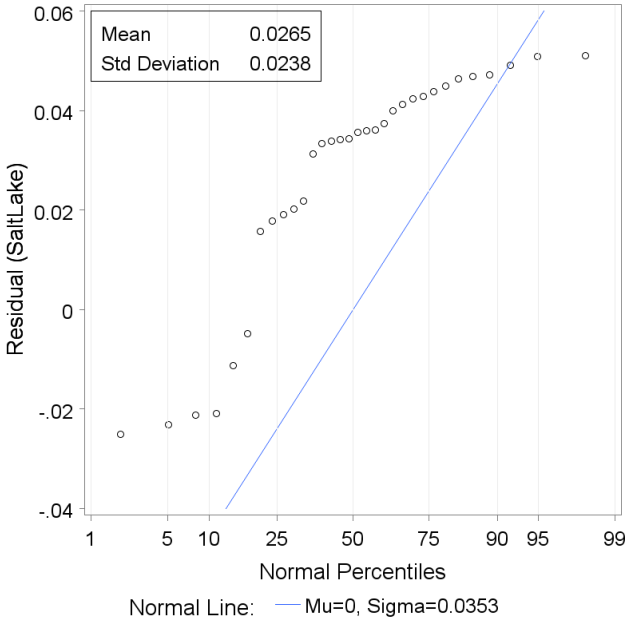

Figure C.180. Residual normality plot of midday—80th-percentile TTI—Salt Lake City.

50th-Percentile TTI Model

California

Table C.88. Residual Analysis of Midday—50th-Percentile TTI—California

Table C.88.a. Basic Statistical Measures

Location		Variability	
Mean	–0.004	Std deviation	0.0671
Median	0.0181	Variance	0.0045
Minimum	–0.471	Range	0.5043
Maximum	0.0333	Interquartile range	0.0258

Table C.88.b. Basic Confidence Limits Assuming Normality

Parameter	Estimate	95% Confidence Limits	
Mean	–0.004	–0.015	0.0070
Std deviation	0.0671	0.0601	0.0761
Variance	0.0045	0.0036	0.0058

Table C.88.c. Tests for Location: Mu=0

Test	Statistic		*p*-Value	
Student's *t*	*t*	–0.740	Pr > |*t*|	0.4607

Table C.88.d. Tests for Normality

Test	Statistic		*p*-Value	
Shapiro-Wilk	*W*	0.4886	Pr < *W*	<0.0001

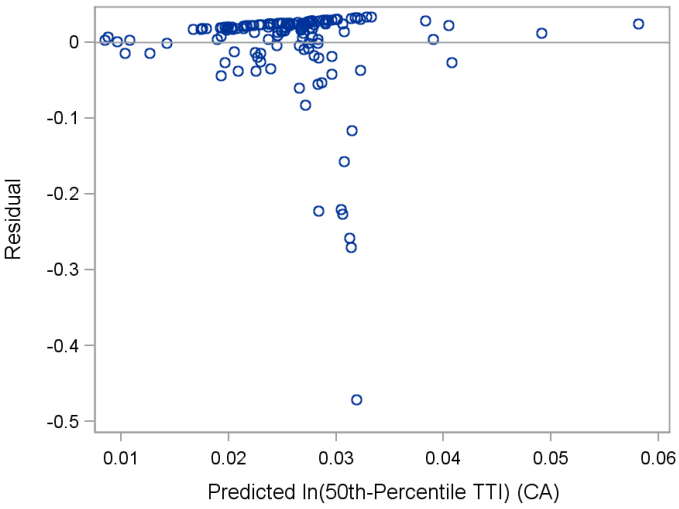

Figure C.181. Residual plot of midday—50th-percentile TTI—California.

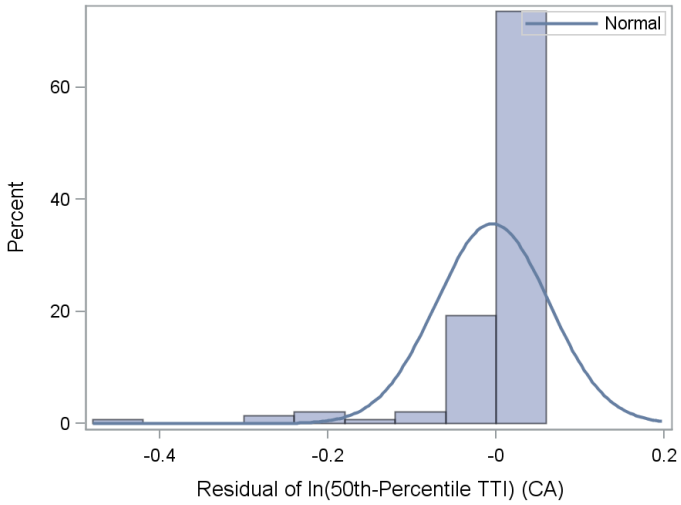

Figure C.182. Residual histogram of midday—50th-percentile TTI—California.

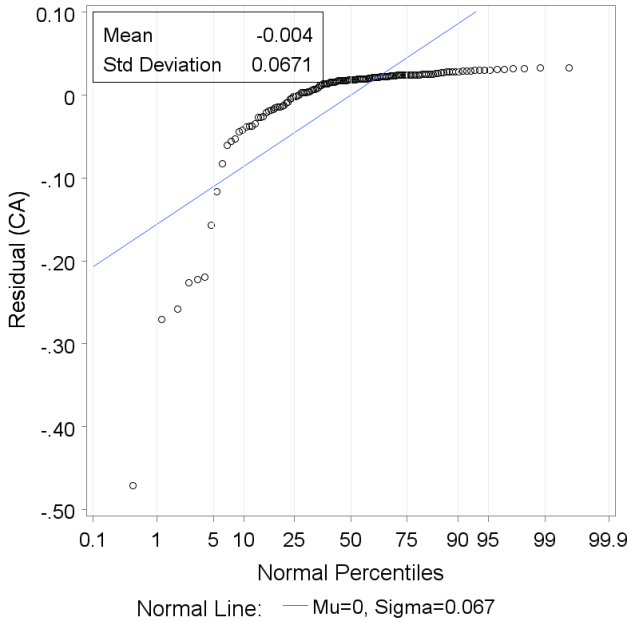

Figure C.183. Residual normality plot of midday—50th-percentile TTI—California.

Minnesota

Table C.89. Residual Analysis of Midday—50th-Percentile TTI—Minnesota

Table C.89.a. Basic Statistical Measures

Location		Variability	
Mean	0.0177	Std deviation	0.0108
Median	0.0208	Variance	0.0001
Minimum	–0.020	Range	0.0485
Maximum	0.0283	Interquartile range	0.0081

Table C.89.b. Basic Confidence Limits Assuming Normality

Parameter	Estimate	95% Confidence Limits	
Mean	0.0177	0.0150	0.0205
Std deviation	0.0108	0.0091	0.0131
Variance	0.0001	0.0001	0.0002

Table C.89.c. Tests for Location: Mu=0

Test	Statistic		*p*-Value	
Student's *t*	*t*	12.764	Pr > |*t*|	<0.0001

Table C.89.d. Tests for Normality

Test	Statistic		*p*-Value	
Shapiro-Wilk	*W*	0.7497	Pr < *W*	<0.0001

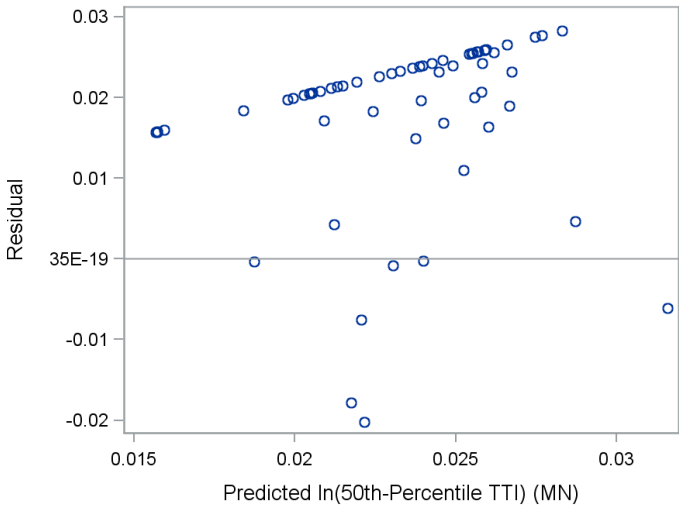

Figure C.184. Residual plot of midday—50th-percentile TTI—Minnesota.

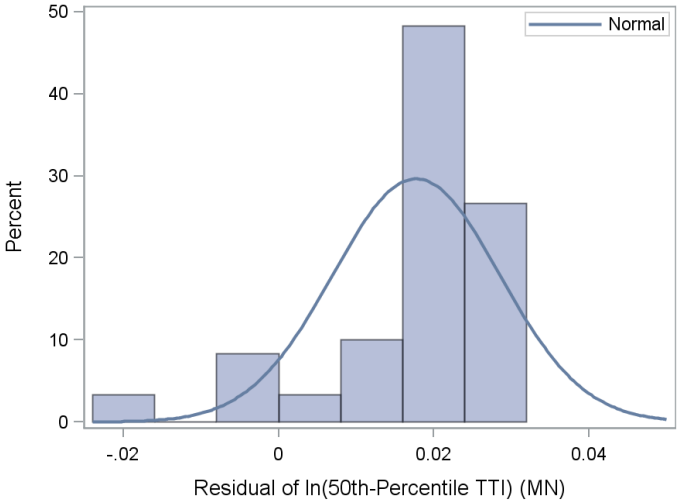

Figure C.185. Residual histogram of midday—50th-percentile TTI—Minnesota.

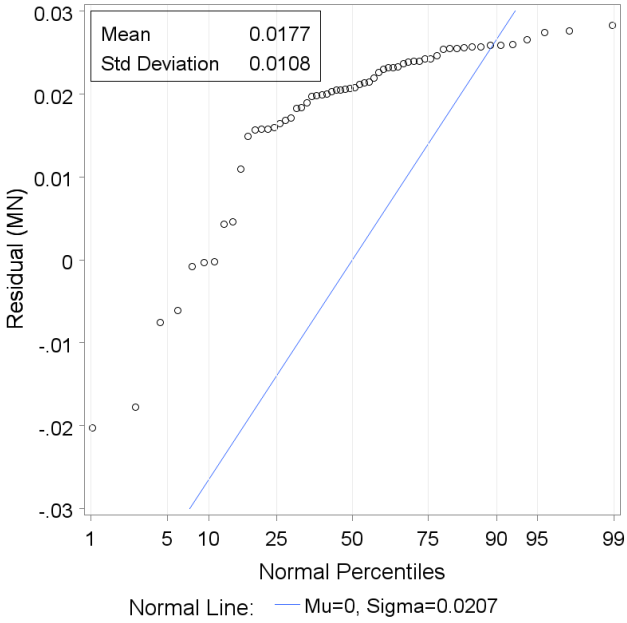

Figure C.186. Residual normality plot of midday—50th-percentile TTI—Minnesota.

Salt Lake City

Table C.90. Residual Analysis of Midday—50th-Percentile TTI—Salt Lake City

Table C.90.a. Basic Statistical Measures

Location		Variability	
Mean	0.0062	Std deviation	0.0199
Median	0.0152	Variance	0.0004
Minimum	–0.036	Range	0.0586
Maximum	0.0224	Interquartile range	0.0230

Table C.90.b. Basic Confidence Limits Assuming Normality

Parameter	Estimate	95% Confidence Limits	
Mean	0.0062	–93E-5	0.0134
Std deviation	0.0199	0.0159	0.0264
Variance	0.0004	0.0003	0.0007

Table C.90.c. Tests for Location: Mu=0

Test	Statistic		*p*-Value	
Student's *t*	*t*	1.7763	Pr > |*t*|	0.0855

Table C.90.d. Tests for Normality

Test	Statistic		*p*-Value	
Shapiro-Wilk	*W*	0.7216	Pr < *W*	<0.0001

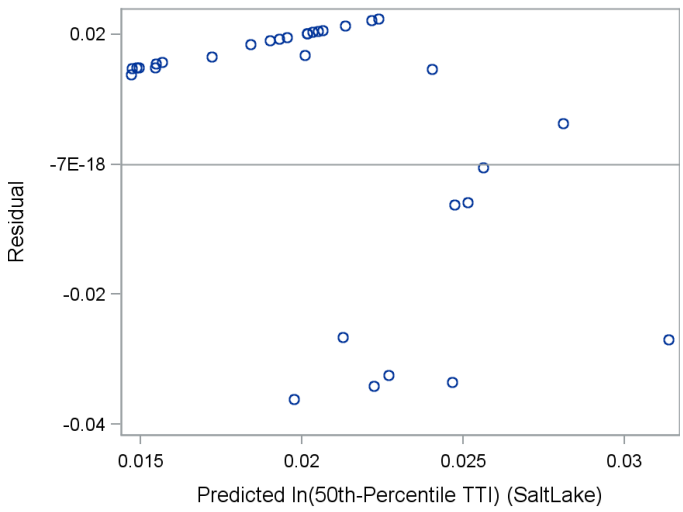

Figure C.187. Residual plot of midday—50th-percentile TTI—Salt Lake City.

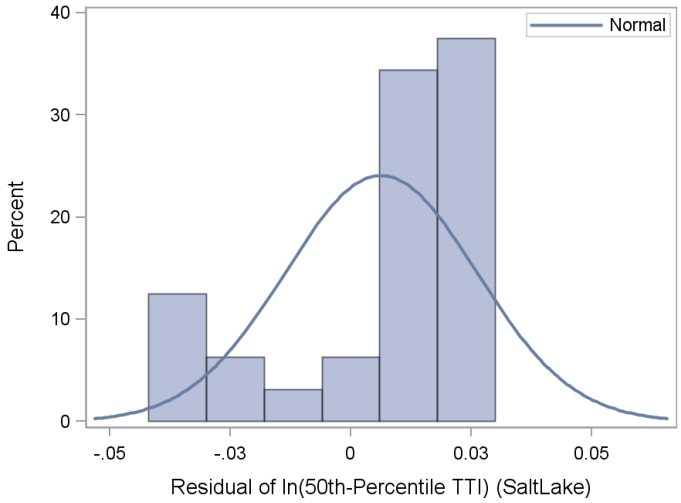

Figure C.188. Residual histogram of midday—50th-percentile TTI—Salt Lake City.

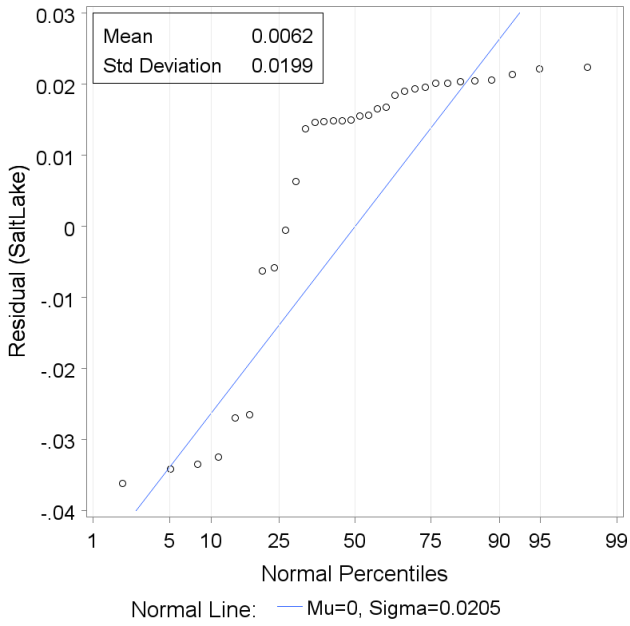

Figure C.189. Residual normality plot of midday—50th-percentile TTI—Salt Lake City.

10th-Percentile TTI Model

California

Table C.91. Residual Analysis of Midday—10th-Percentile TTI—California

Table C.91.a. Basic Statistical Measures

Location		Variability	
Mean	0.0016	Std deviation	0.0218
Median	0.0075	Variance	0.0005
Minimum	–0.138	Range	0.1547
Maximum	0.0168	Interquartile range	0.0050

Table C.91.b. Basic Confidence Limits Assuming Normality

Parameter	Estimate	95% Confidence Limits	
Mean	0.0016	–0.002	0.0052
Std deviation	0.0218	0.0195	0.0247
Variance	0.0005	0.0004	0.0006

Table C.91.c. Tests for Location: Mu=0

Test	Statistic		*p*-Value	
Student's *t*	*t*	0.8584	Pr > |*t*|	0.3922

Table C.91.d. Tests for Normality

Test	Statistic		*p*-Value	
Shapiro-Wilk	*W*	0.4094	Pr < *W*	<0.0001

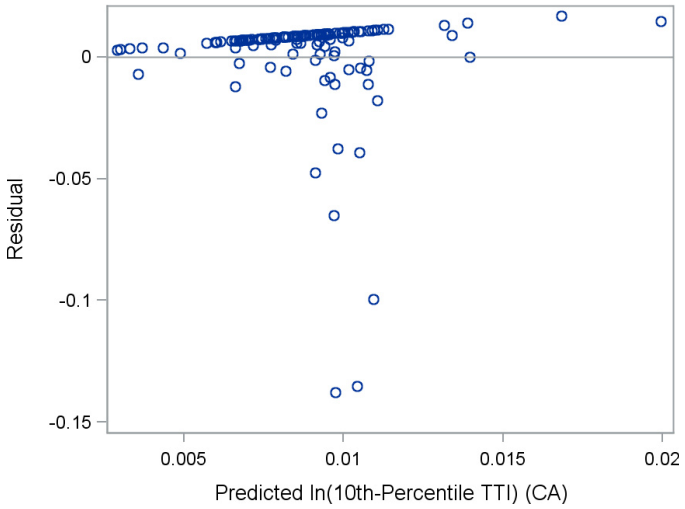

Figure C.190. Residual plot of midday—10th-percentile TTI—California.

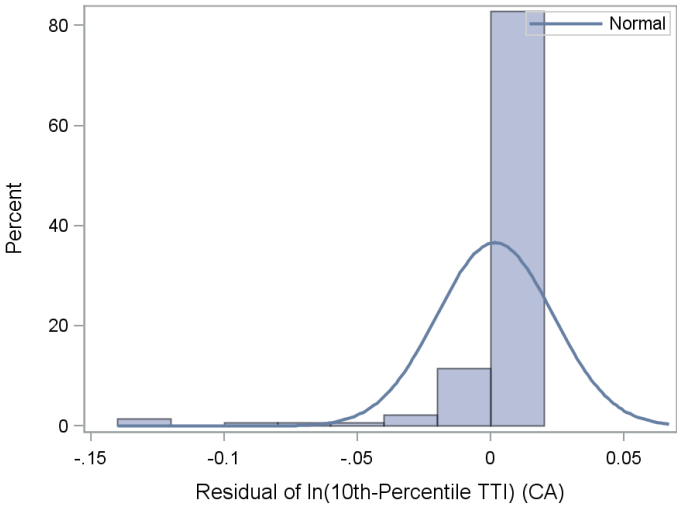

Figure C.191. Residual histogram of midday—10th-percentile TTI—California.

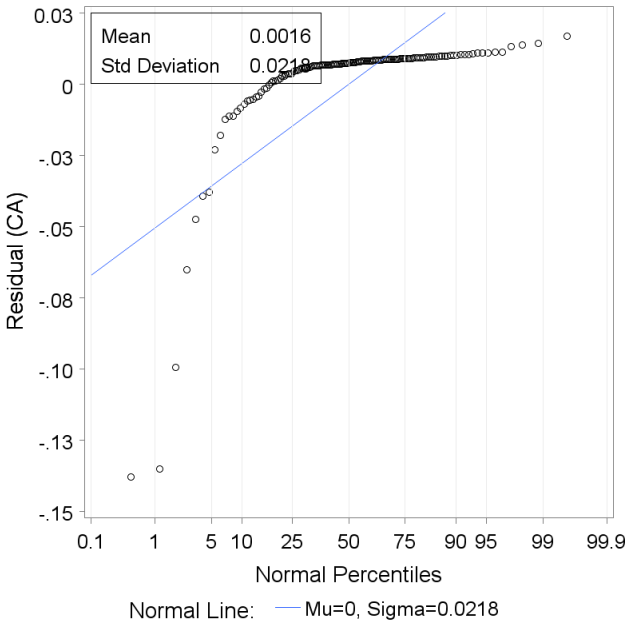

Figure C.192. Residual normality plot of midday—10th-percentile TTI—California.

Minnesota

Table C.92. Residual Analysis of Midday—10th-Percentile TTI—Minnesota

Table C.92.a. Basic Statistical Measures

Location		Variability	
Mean	0.0069	Std deviation	0.0041
Median	0.0079	Variance	171E-7
Minimum	–0.011	Range	0.0208
Maximum	0.0097	Interquartile range	0.0018

Table C.92.b. Basic Confidence Limits Assuming Normality

Parameter	Estimate	95% Confidence Limits	
Mean	0.0069	0.0058	0.0079
Std deviation	0.0041	0.0035	0.0050
Variance	171E-7	123E-7	254E-7

Table C.92.c. Tests for Location: Mu=0

Test	Statistic		*p*-Value	
Student's *t*	*t*	12.851	Pr > |*t*|	<0.0001

Table C.92.d. Tests for Normality

Test	Statistic		*p*-Value	
Shapiro-Wilk	*W*	0.5066	Pr < *W*	<0.0001

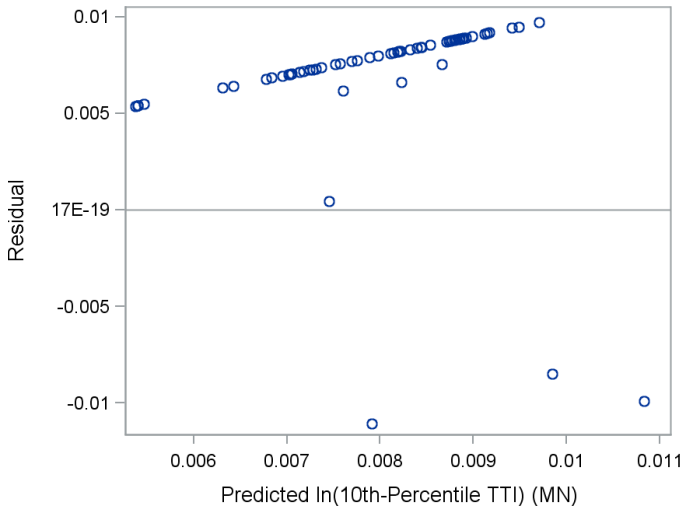

Figure C.193. Residual plot of midday—10th-percentile TTI—Minnesota.

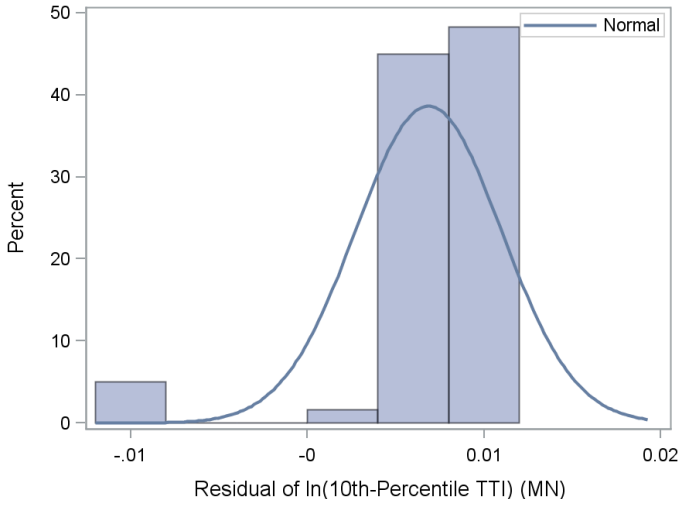

Figure C.194. Residual histogram of midday—10th-percentile TTI—Minnesota.

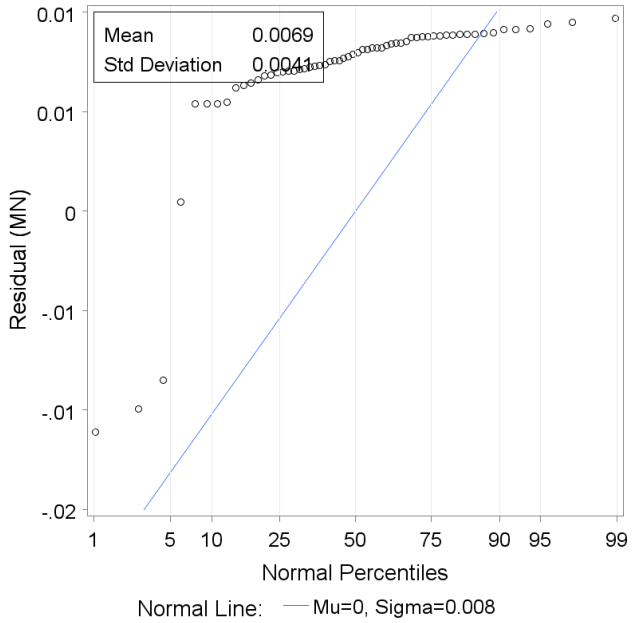

Figure C.195. Residual normality plot of midday—10th-percentile TTI—Minnesota.

Salt Lake City

Table C.93. Residual Analysis of Midday—10th-Percentile TTI—Salt Lake City

Table C.93.a. Basic Statistical Measures

Location		Variability	
Mean	–0.002	Std deviation	0.0133
Median	0.0053	Variance	0.0002
Minimum	–0.030	Range	0.0381
Maximum	0.0077	Interquartile range	0.0138

Table C.93.b. Basic Confidence Limits Assuming Normality

Parameter	Estimate	95% Confidence Limits	
Mean	–0.002	–0.006	0.0033
Std deviation	0.0133	0.0107	0.0177
Variance	0.0002	0.0001	0.0003

Table C.93.c. Tests for Location: Mu=0

Test	Statistic		*p*-Value	
Student's *t*	*t*	–0.651	Pr > |*t*|	0.5199

Table C.93.d. Tests for Normality

Test	Statistic		*p*-Value	
Shapiro-Wilk	*W*	0.6587	Pr < *W*	<0.0001

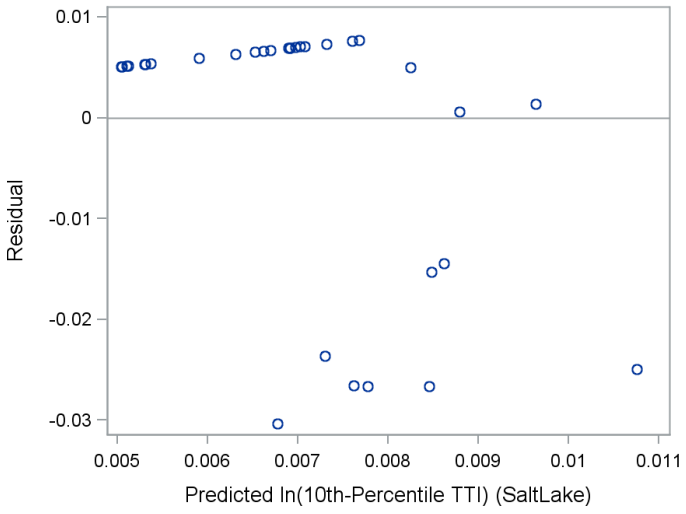

Figure C.196. Residual plot of midday—10th-percentile TTI—Salt Lake City.

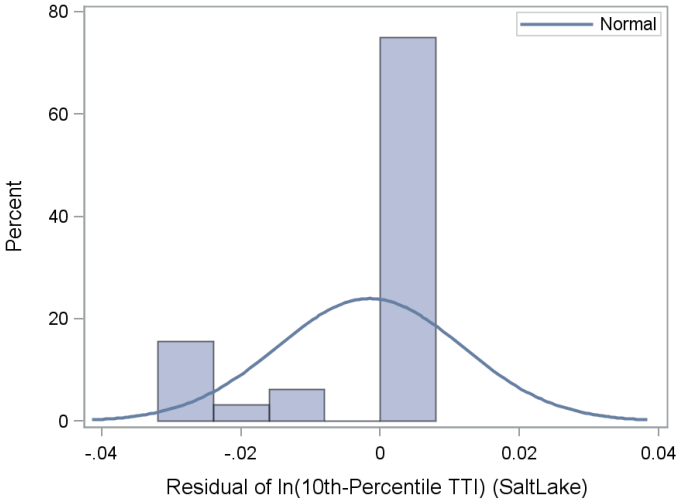

Figure C.197. Residual histogram of midday—10th-percentile TTI—Salt Lake City.

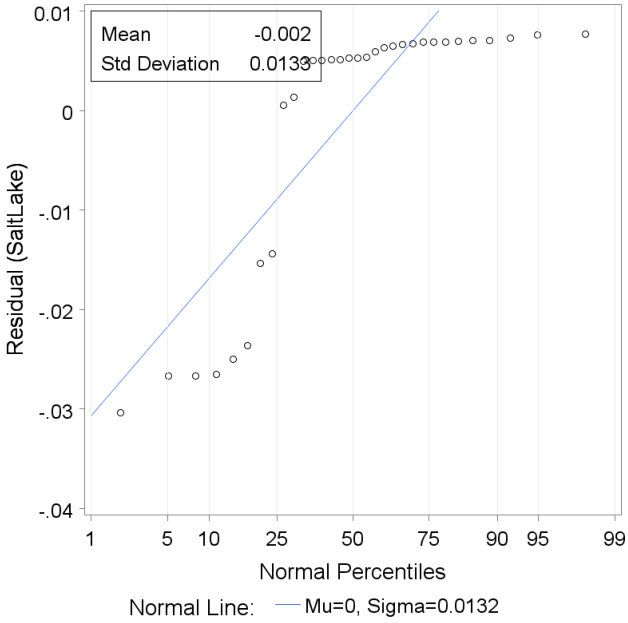

Figure C.198. Residual normality plot of midday—10th-percentile TTI—Salt Lake City.

Weekday

Mean TTI Model

California

Table C.94. Residual Analysis of Weekday—Mean TTI—California

Table C.94.a. Basic Statistical Measures

Location		Variability	
Mean	0.0936	Std deviation	0.0761
Median	0.0970	Variance	0.0058
Minimum	–0.234	Range	0.5556
Maximum	0.3215	Interquartile range	0.0605

Table C.94.b. Basic Confidence Limits Assuming Normality

Parameter	Estimate	95% Confidence Limits	
Mean	0.0936	0.0810	0.1063
Std deviation	0.0761	0.0682	0.0862
Variance	0.0058	0.0046	0.0074

Table C.94.c. Tests for Location: Mu=0

Test	Statistic		*p*-Value	
Student's *t*	*t*	14.660	Pr > |*t*|	<0.0001

Table C.94.d. Tests for Normality

Test	Statistic		*p*-Value	
Shapiro-Wilk	*W*	0.9011	Pr < *W*	<0.0001

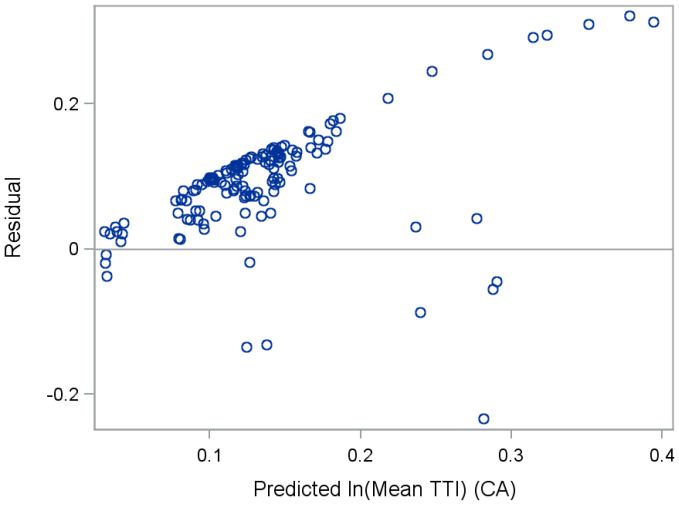

Figure C.199. Residual plot of weekday—mean TTI—California.

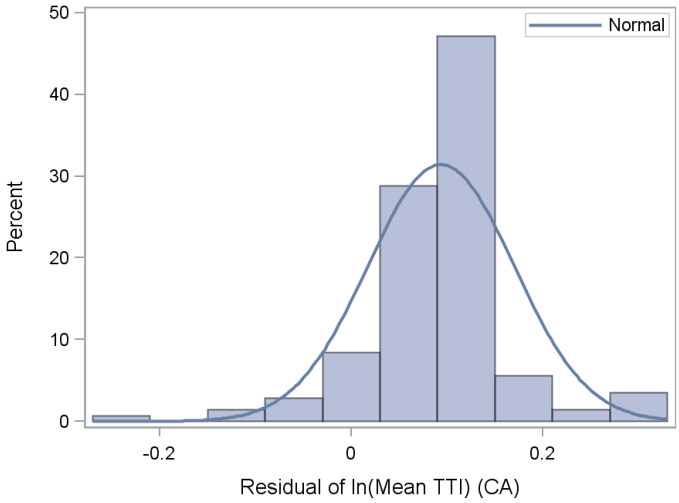

Figure C.200. Residual histogram of weekday—mean TTI—California.

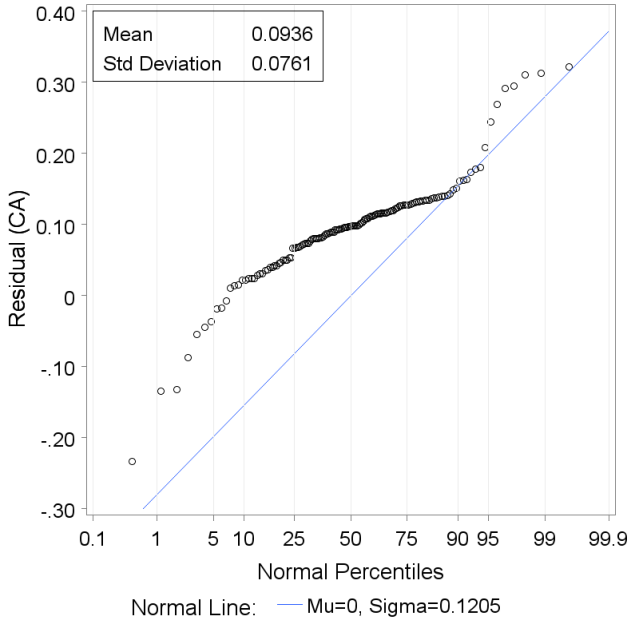

Figure C.201. Residual normality plot of weekday—mean TTI—California.

Minnesota

Table C.95. Residual Analysis of Weekday—Mean TTI—Minnesota

Table C.95.a. Basic Statistical Measures

Location		Variability	
Mean	0.2352	Std deviation	0.1997
Median	0.1658	Variance	0.0399
Minimum	–0.002	Range	1.1476
Maximum	1.1458	Interquartile range	0.0740

Table C.95.b. Basic Confidence Limits Assuming Normality

Parameter	Estimate	95% Confidence Limits	
Mean	0.2352	0.1836	0.2867
Std deviation	0.1997	0.1692	0.2435
Variance	0.0399	0.0286	0.0593

Table C.95.c. Tests for Location: Mu=0

Test	Statistic		*p*-Value	
Student's *t*	*t*	9.1235	Pr > |*t*|	<0.0001

Table C.95.d. Tests for Normality

Test	Statistic		*p*-Value	
Shapiro-Wilk	*W*	0.5745	Pr < *W*	<0.0001

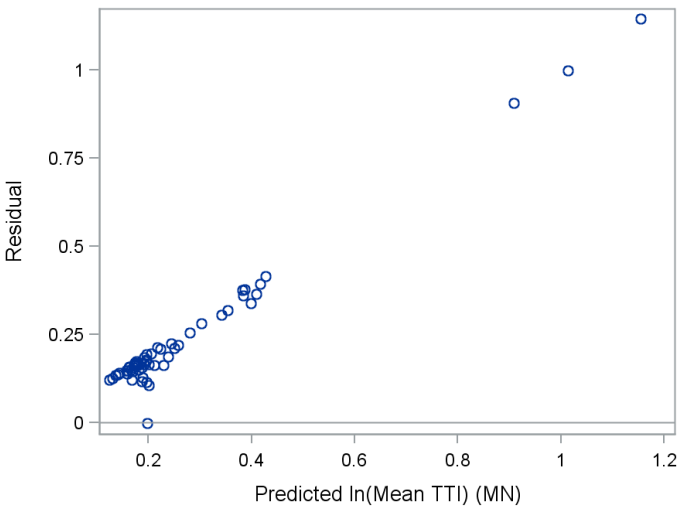

Figure C.202. Residual plot of weekday—mean TTI—Minnesota.

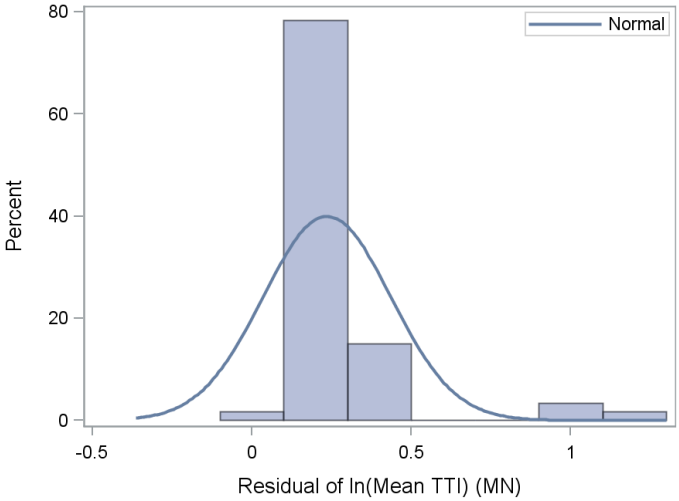

Figure C.203. Residual histogram of weekday—mean TTI—Minnesota.

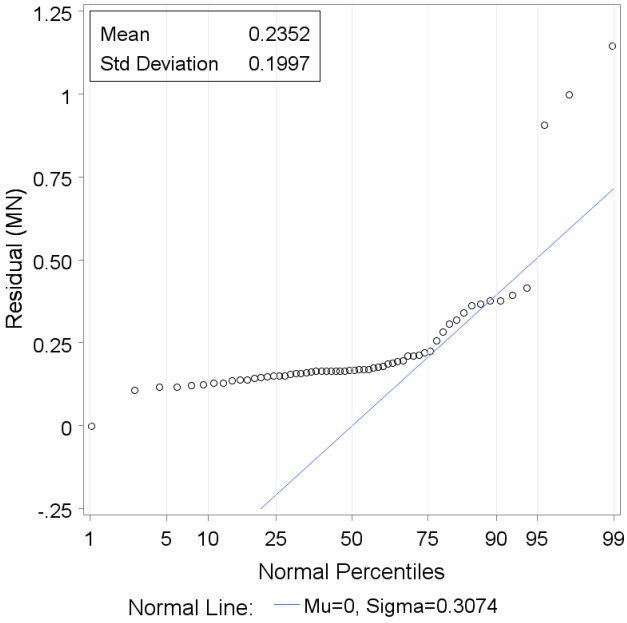

Figure C.204. Residual normality plot of weekday—mean TTI—Minnesota.

Salt Lake City

Table C.96. Residual Analysis of Weekday—Mean TTI—Salt Lake City

Table C.96.a. Basic Statistical Measures

Location		Variability	
Mean	0.0503	Std deviation	0.0290
Median	0.0597	Variance	0.0008
Minimum	–0.000	Range	0.1074
Maximum	0.1072	Interquartile range	0.0423

Table C.96.b. Basic Confidence Limits Assuming Normality

Parameter	Estimate	95% Confidence Limits	
Mean	0.0503	0.0394	0.0611
Std deviation	0.0290	0.0231	0.0390
Variance	0.0008	0.0005	0.0015

Table C.96.c. Tests for Location: Mu=0

Test	Statistic		*p*-Value	
Student's *t*	*t*	9.4868	Pr > |*t*|	<0.0001

Table C.96.d. Tests for Normality

Test	Statistic		*p*-Value	
Shapiro-Wilk	*W*	0.8662	Pr < *W*	0.0014

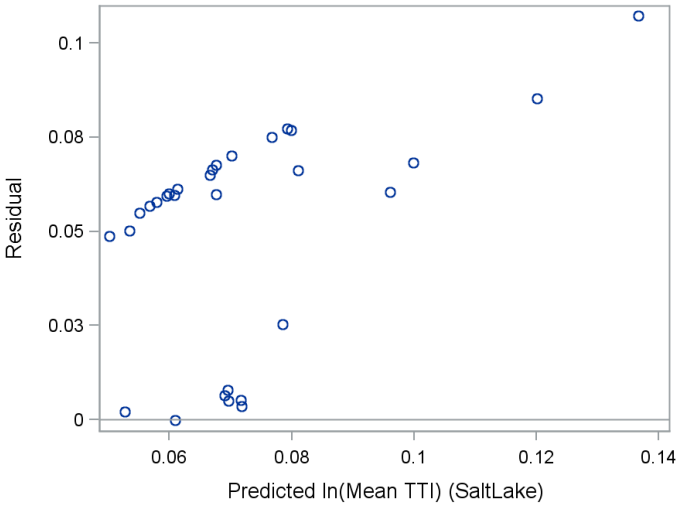

Figure C.205. Residual plot of weekday—mean TTI—Salt Lake City.

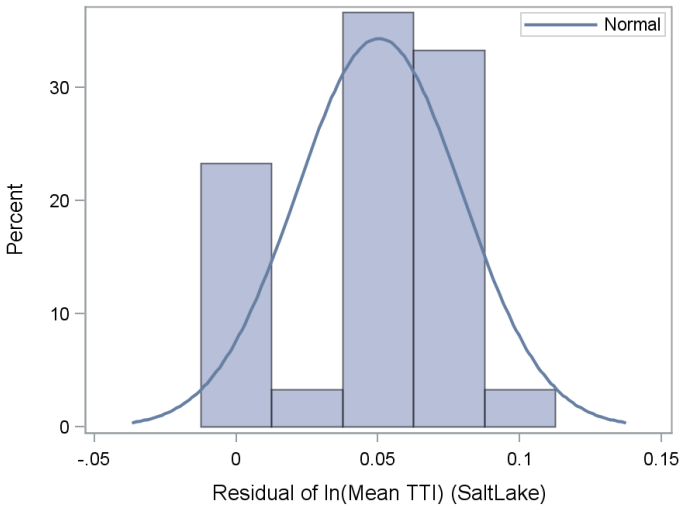

Figure C.206. Residual histogram of weekday—mean TTI—Salt Lake City.

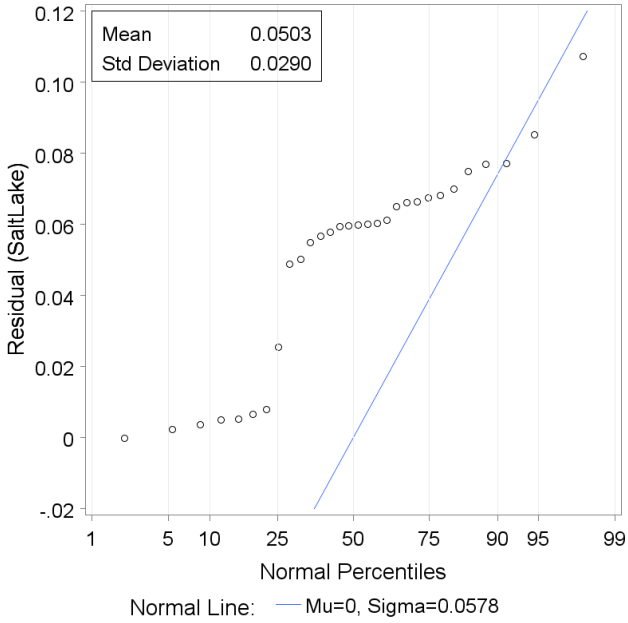

Figure C.207. Residual normality plot of weekday—mean TTI—Salt Lake City.

99th-Percentile TTI Model

California

Table C.97. Residual Analysis of Weekday—99th-Percentile TTI—California

Table C.97.a. Basic Statistical Measures

Location		Variability	
Mean	0.2965	Std deviation	0.2779
Median	0.2891	Variance	0.0772
Minimum	−0.362	Range	1.4728
Maximum	1.1110	Interquartile range	0.3403

Table C.97.b. Basic Confidence Limits Assuming Normality

Parameter	Estimate	95% Confidence Limits	
Mean	0.2965	0.2504	0.3426
Std deviation	0.2779	0.2489	0.3146
Variance	0.0772	0.0620	0.0990

Table C.97.c. Tests for Location: Mu=0

Test	Statistic		*p*-Value	
Student's *t*	*t*	12.714	Pr > |*t*|	<0.0001

Table C.97.d. Tests for Normality

Test	Statistic		*p*-Value	
Shapiro-Wilk	*W*	0.9824	Pr < *W*	0.0650

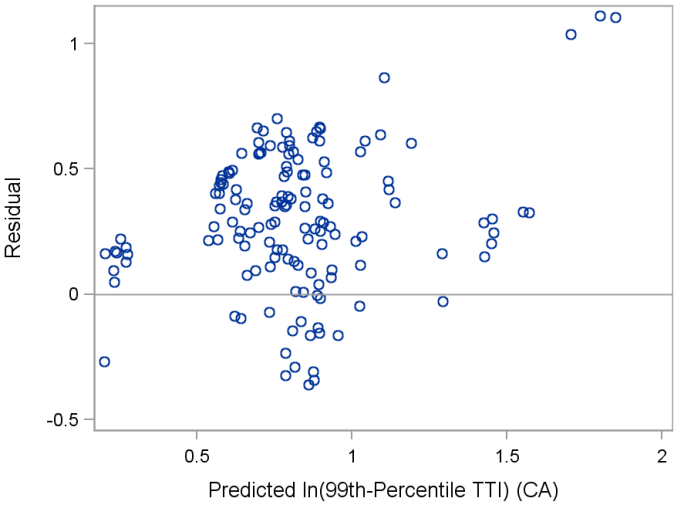

Figure C.208. Residual plot of weekday—99th-percentile TTI—California.

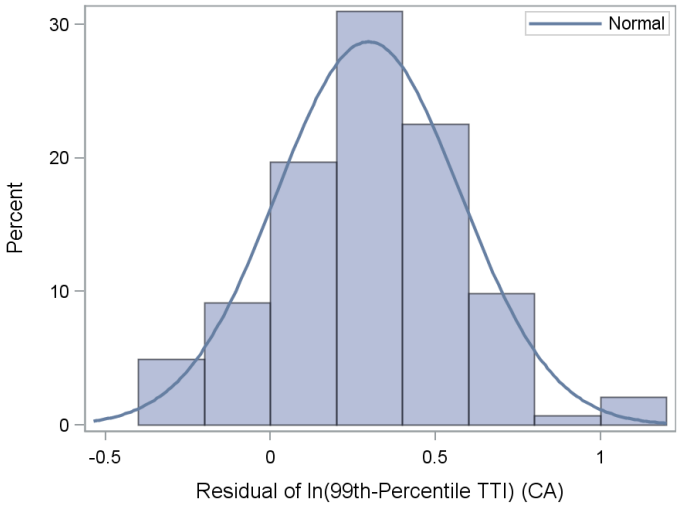

Figure C.209. Residual histogram of weekday—99th-percentile TTI—California.

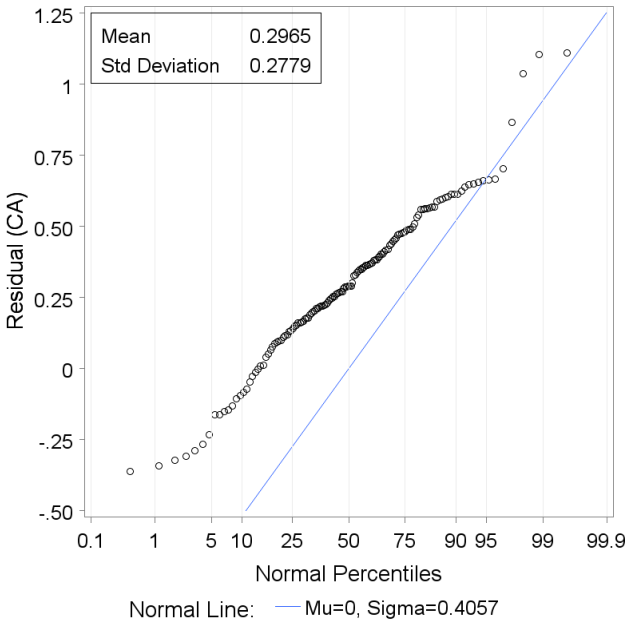

Figure C.210. Residual normality plot of weekday—99th-percentile TTI—California.

Minnesota

Table C.98. Residual Analysis of Weekday—99th-Percentile TTI—Minnesota

Table C.98.a. Basic Statistical Measures

Location		Variability	
Mean	0.5043	Std deviation	0.7305
Median	0.5237	Variance	0.5336
Minimum	–0.480	Range	4.0280
Maximum	3.5480	Interquartile range	0.5125

Table C.98.b. Basic Confidence Limits Assuming Normality

Parameter	Estimate	95% Confidence Limits	
Mean	0.5043	0.3156	0.6930
Std deviation	0.7305	0.6192	0.8909
Variance	0.5336	0.3834	0.7938

Table C.98.c. Tests for Location: Mu=0

Test	Statistic		*p*-Value	
Student's *t*	*t*	5.3476	Pr > |*t*|	<0.0001

Table C.98.d. Tests for Normality

Test	Statistic		*p*-Value	
Shapiro-Wilk	*W*	0.7169	Pr < *W*	<0.0001

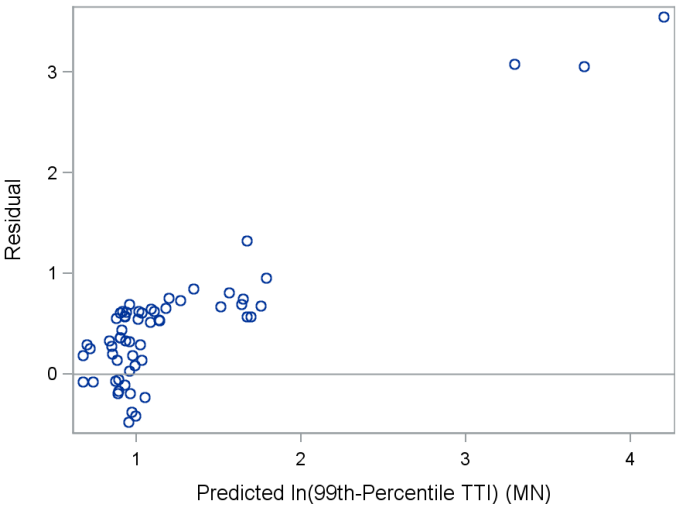

Figure C.211. Residual plot of weekday—99th-percentile TTI—Minnesota.

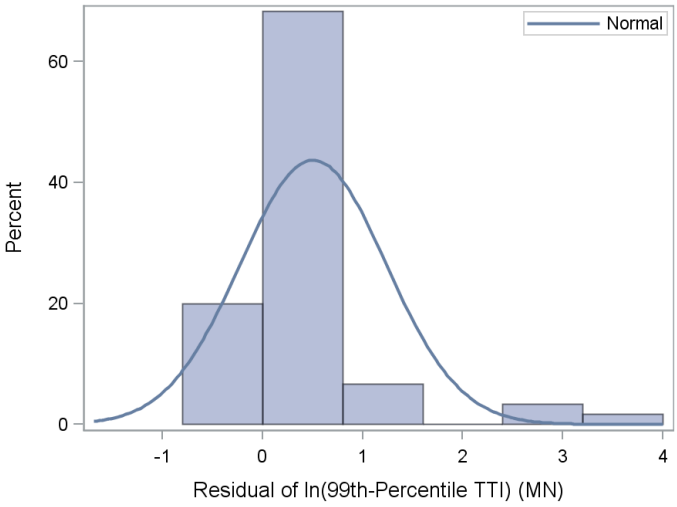

Figure C.212. Residual histogram of weekday—99th-percentile TTI—Minnesota.

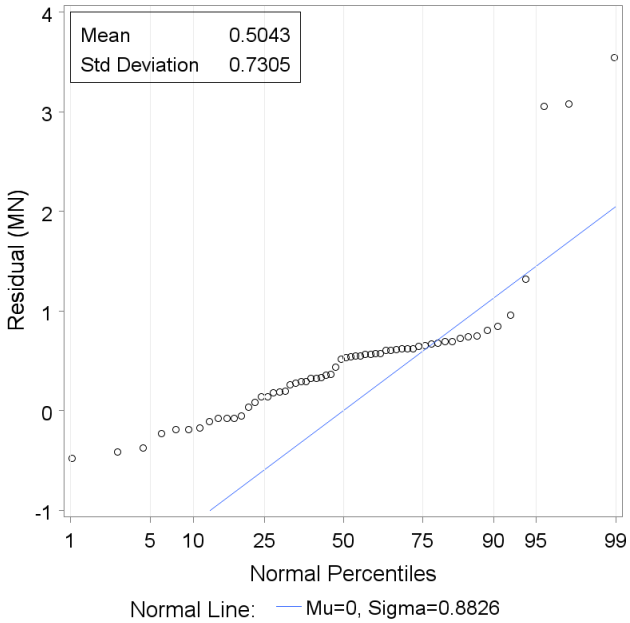

Figure C.213. Residual normality plot of weekday—99th-percentile TTI—Minnesota.

Salt Lake City

Table C.99. Residual Analysis of Weekday—99th-Percentile TTI—Salt Lake City

Table C.99.a. Basic Statistical Measures

Location		Variability	
Mean	0.2044	Std deviation	0.1778
Median	0.2447	Variance	0.0316
Minimum	–0.261	Range	0.6747
Maximum	0.4139	Interquartile range	0.1944

Table C.99.b. Basic Confidence Limits Assuming Normality

Parameter	Estimate	95% Confidence Limits	
Mean	0.2044	0.1380	0.2708
Std deviation	0.1778	0.1416	0.2390
Variance	0.0316	0.0201	0.0571

Table C.99.c. Tests for Location: Mu=0

Test	Statistic		*p*-Value	
Student's *t*	*t*	6.2975	Pr > |*t*|	<0.0001

Table C.99.d. Tests for Normality

Test	Statistic		*p*-Value	
Shapiro-Wilk	*W*	0.8601	Pr < *W*	0.0010

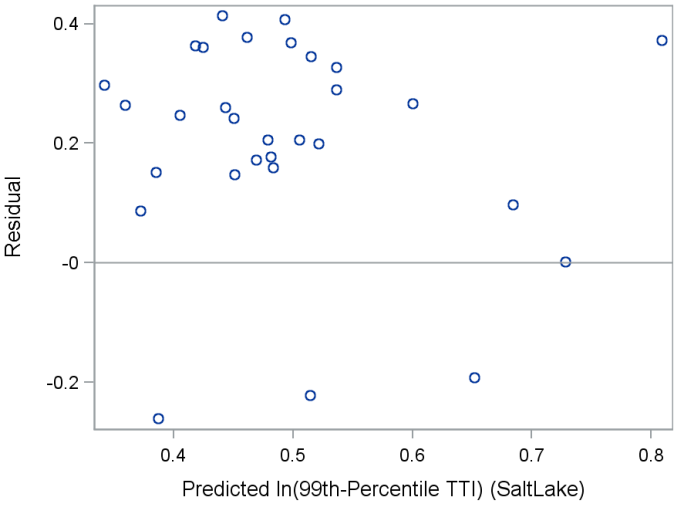

Figure C.214. Residual plot of weekday—99th-percentile TTI—Salt Lake City.

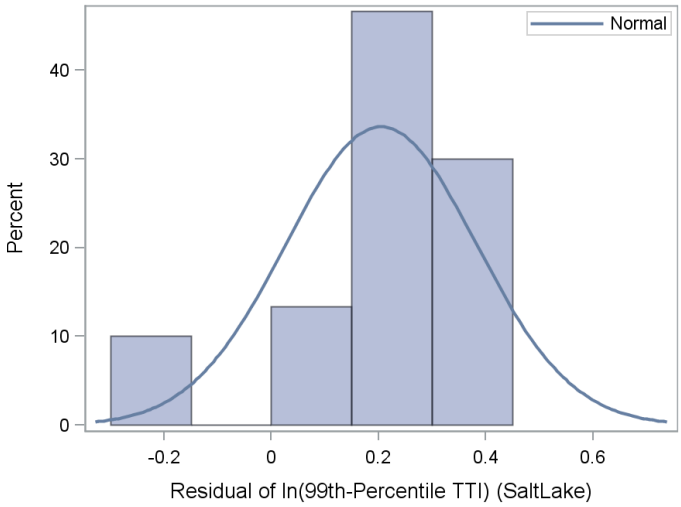

Figure C.215. Residual histogram of weekday—99th-percentile TTI—Salt Lake City.

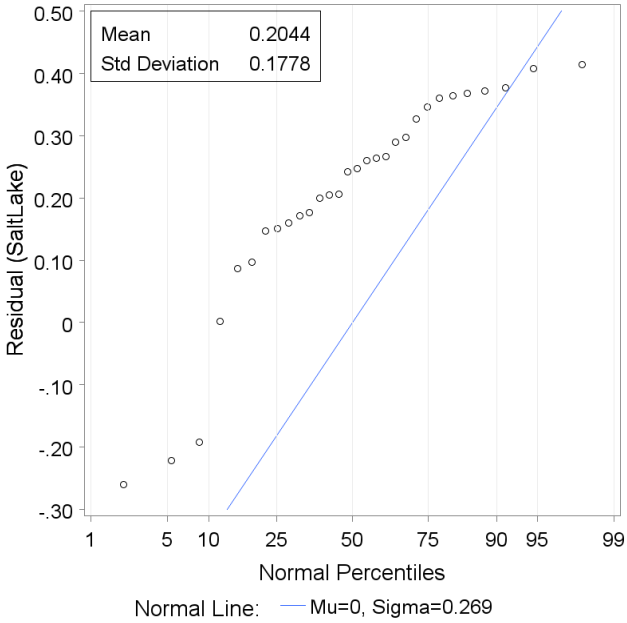

Figure C.216. Residual normality plot of weekday—99th-percentile TTI—Salt Lake City.

95th-Percentile TTI Model

California

Table C.100. Residual Analysis of Weekday—95th-Percentile TTI—California

Table C.100.a. Basic Statistical Measures

Location		Variability	
Mean	0.2369	Std deviation	0.2444
Median	0.2792	Variance	0.0597
Minimum	–0.406	Range	1.4594
Maximum	1.0533	Interquartile range	0.2651

Table C.100.b. Basic Confidence Limits Assuming Normality

Parameter	Estimate	95% Confidence Limits	
Mean	0.2369	0.1963	0.2774
Std deviation	0.2444	0.2189	0.2767
Variance	0.0597	0.0479	0.0766

Table C.100.c. Tests for Location: Mu=0

Test	Statistic		*p*-Value	
Student's *t*	*t*	11.549	Pr > |*t*|	<0.0001

Table C.100.d. Tests for Normality

Test	Statistic		*p*-Value	
Shapiro-Wilk	*W*	0.9378	Pr < *W*	<0.0001

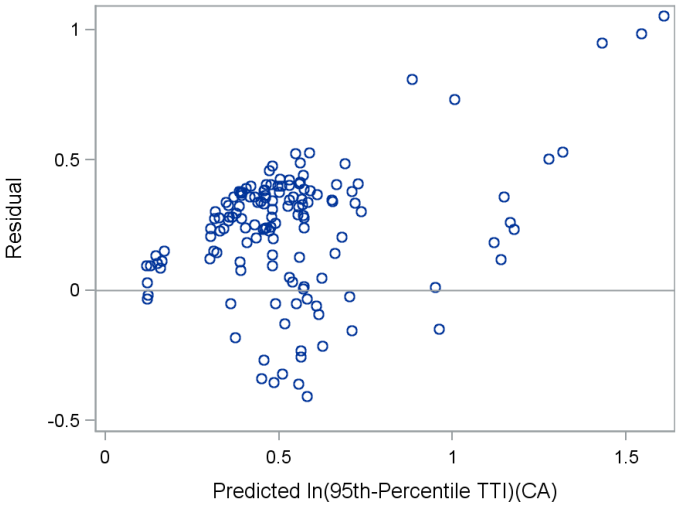

Figure C.217. Residual plot of weekday—95th-percentile TTI—California.

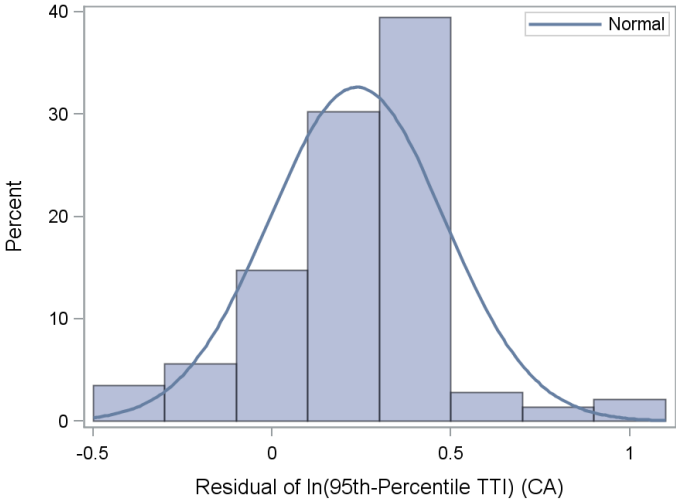

Figure C.218. Residual histogram of weekday—95th-percentile TTI—California.

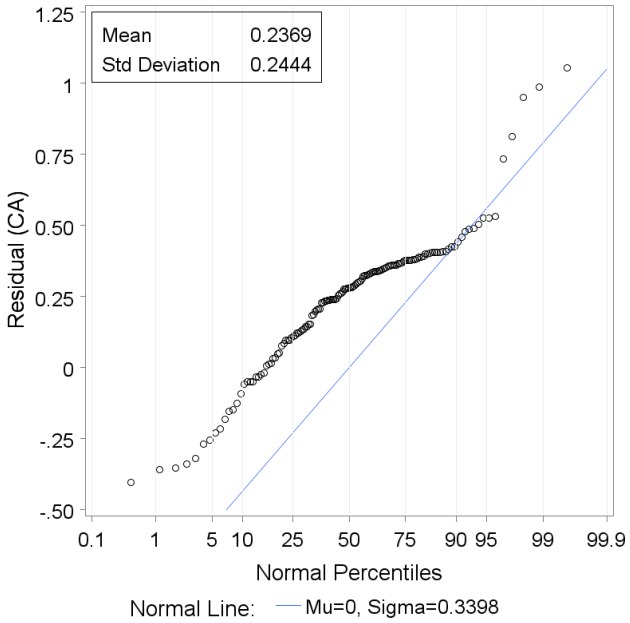

Figure C.219. Residual normality plot of weekday—95th-percentile TTI—California.

Minnesota

Table C.101. Residual Analysis of Weekday—95th-Percentile TTI—Minnesota

Table C.101.a. Basic Statistical Measures

Location		Variability	
Mean	0.6993	Std deviation	0.8449
Median	0.5499	Variance	0.7138
Minimum	–0.221	Range	4.5969
Maximum	4.3758	Interquartile range	0.4778

Table C.101.b. Basic Confidence Limits Assuming Normality

Parameter	Estimate	95% Confidence Limits	
Mean	0.6993	0.4811	0.9176
Std deviation	0.8449	0.7161	1.0304
Variance	0.7138	0.5128	1.0618

Table C.101.c. Tests for Location: Mu=0

Test	Statistic		*p*-Value	
Student's *t*	*t*	6.4118	Pr > |*t*|	<0.0001

Table C.101.d. Tests for Normality

Test	Statistic		*p*-Value	
Shapiro-Wilk	*W*	0.6407	Pr < *W*	<0.0001

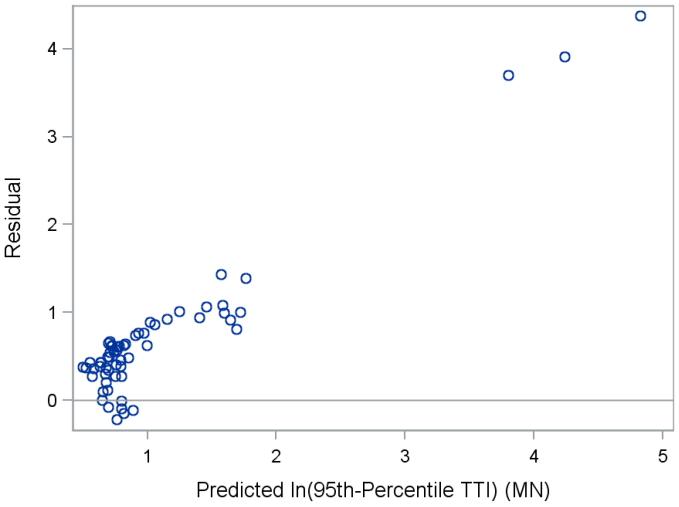

Figure C.220. Residual plot of weekday—95th-percentile TTI—Minnesota.

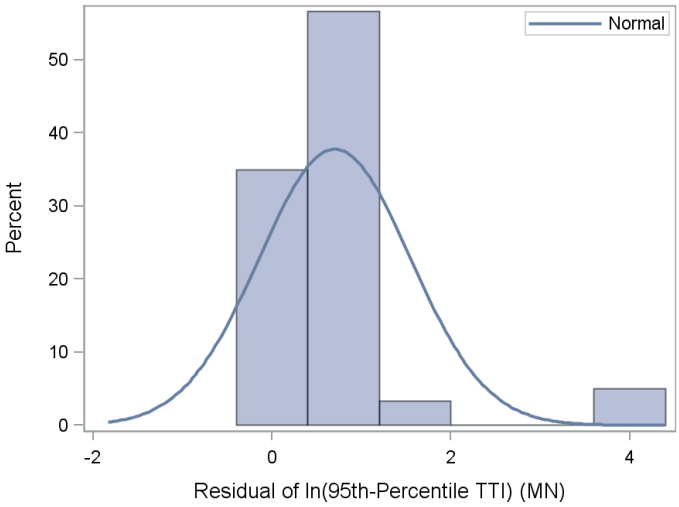

Figure C.221. Residual histogram of weekday—95th-percentile TTI—Minnesota.

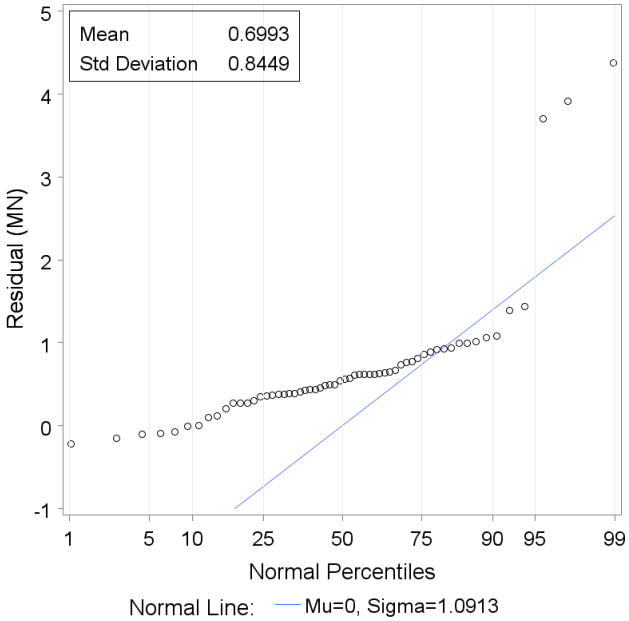

Figure C.222. Residual normality plot of weekday—95th-percentile TTI—Minnesota.

Salt Lake City

Table C.102. Residual Analysis of Weekday—95th-Percentile TTI—Salt Lake City

Table C.102.a. Basic Statistical Measures

Location		Variability	
Mean	0.1696	Std deviation	0.1185
Median	0.1951	Variance	0.0140
Minimum	–0.167	Range	0.5681
Maximum	0.4012	Interquartile range	0.1022

Table C.102.b. Basic Confidence Limits Assuming Normality

Parameter	Estimate	95% Confidence Limits	
Mean	0.1696	0.1254	0.2139
Std deviation	0.1185	0.0944	0.1593
Variance	0.0140	0.0089	0.0254

Table C.102.c. Tests for Location: Mu=0

Test	Statistic		*p*-Value	
Student's *t*	*t*	7.8406	Pr > |*t*|	<0.0001

Table C.102.d. Tests for Normality

Test	Statistic		*p*-Value	
Shapiro-Wilk	*W*	0.8312	Pr < *W*	0.0003

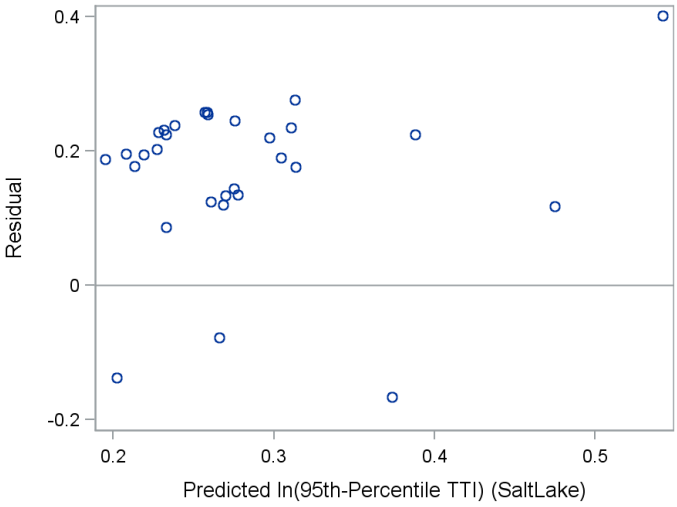

Figure C.223. Residual plot of weekday—95th-percentile TTI—Salt Lake City.

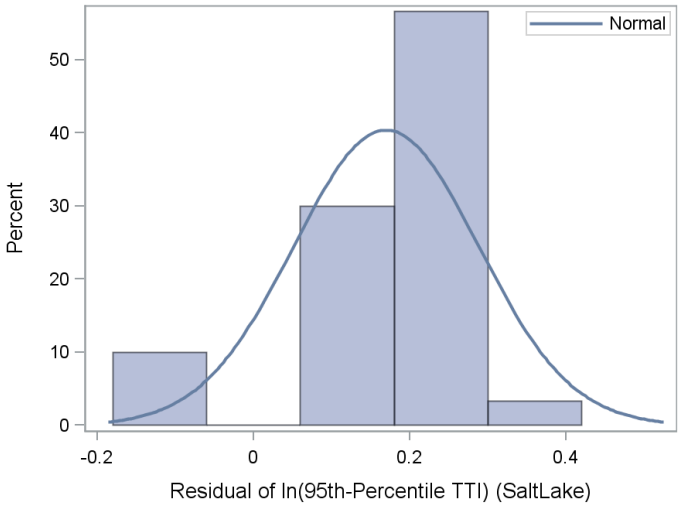

Figure C.224. Residual histogram of weekday—95th-percentile TTI—Salt Lake City.

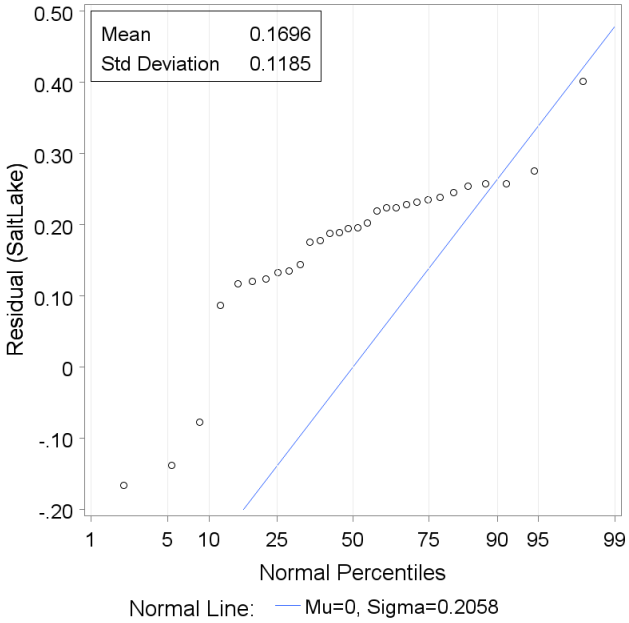

Figure C.225. Residual normality plot of weekday—95th-percentile TTI—Salt Lake City.

80th-Percentile TTI Model

California

Table C.103. Residual Analysis of Weekday—80th-Percentile TTI—California

Table C.103.a. Basic Statistical Measures

Location		Variability	
Mean	0.0564	Std deviation	0.1267
Median	0.0883	Variance	0.0161
Minimum	–0.387	Range	0.7396
Maximum	0.3527	Interquartile range	0.1138

Table C.103.b. Basic Confidence Limits Assuming Normality

Parameter	Estimate	95% Confidence Limits	
Mean	0.0564	0.0354	0.0774
Std deviation	0.1267	0.1135	0.1435
Variance	0.0161	0.0129	0.0206

Table C.103.c. Tests for Location: Mu=0

Test	Statistic		*p*-Value	
Student's *t*	*t*	5.3045	Pr > |*t*|	<0.0001

Table C.103.d. Tests for Normality

Test	Statistic		*p*-Value	
Shapiro-Wilk	*W*	0.9180	Pr < *W*	<0.0001

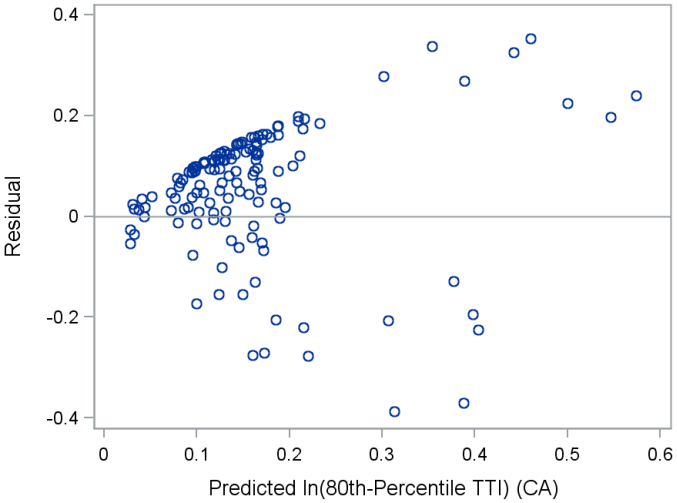

Figure C.226. Residual plot of weekday—80th-percentile TTI—California.

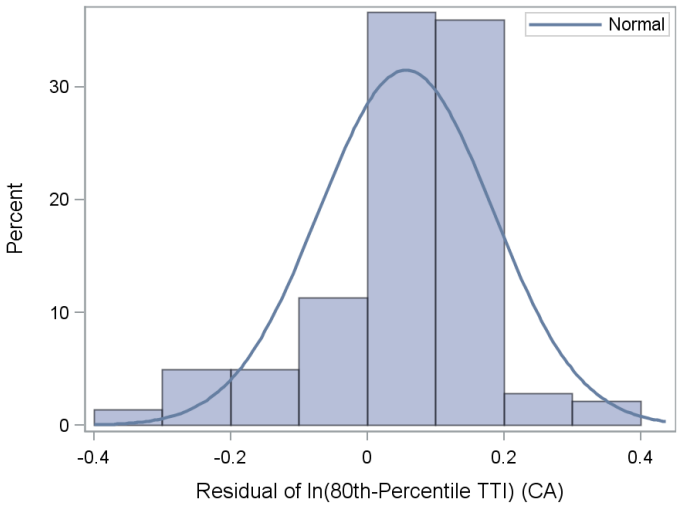

Figure C.227. Residual histogram of weekday—80th-percentile TTI—California.

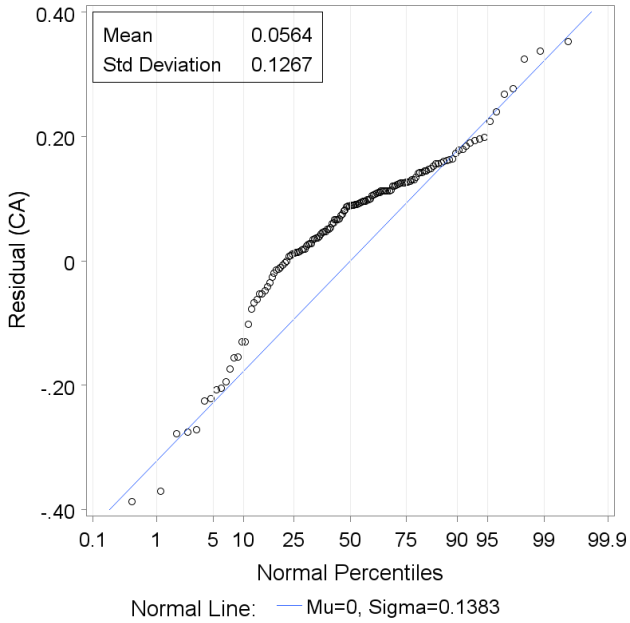

Figure C.228. Residual normality plot of weekday—80th-percentile TTI—California.

Minnesota

Table C.104. Residual Analysis of Weekday—80th-Percentile TTI—Minnesota

Table C.104.a. Basic Statistical Measures

Location		Variability	
Mean	0.3134	Std deviation	0.3484
Median	0.2155	Variance	0.1214
Minimum	–0.078	Range	1.9074
Maximum	1.8296	Interquartile range	0.1652

Table C.104.b. Basic Confidence Limits Assuming Normality

Parameter	Estimate	95% Confidence Limits	
Mean	0.3134	0.2234	0.4034
Std deviation	0.3484	0.2953	0.4249
Variance	0.1214	0.0872	0.1805

Table C.104.c. Tests for Location: Mu=0

Test	Statistic		*p*-Value	
Student's *t*	*t*	6.9691	Pr > |*t*|	<0.0001

Table C.104.d. Tests for Normality

Test	Statistic		*p*-Value	
Shapiro-Wilk	*W*	0.6274	Pr < *W*	<0.0001

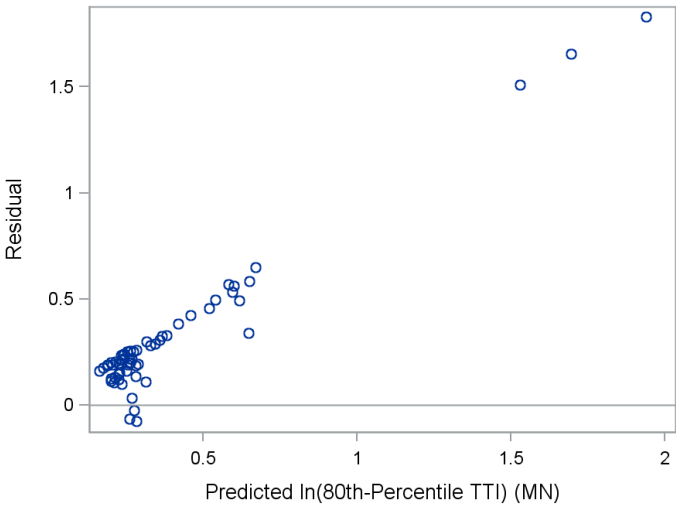

Figure C.229. Residual plot of weekday—80th-percentile TTI—Minnesota.

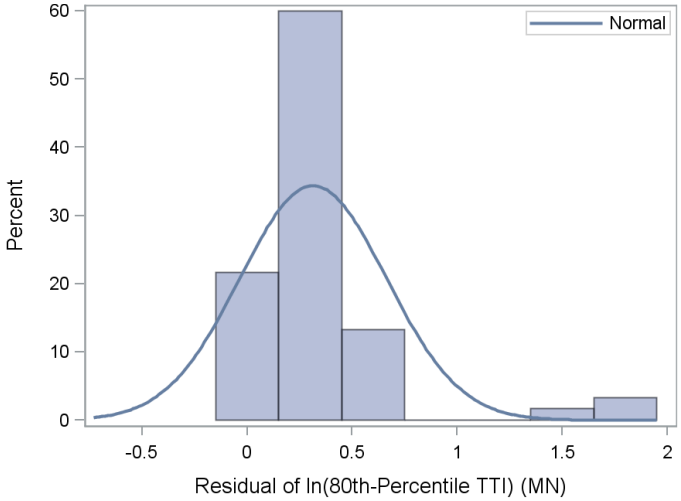

Figure C.230. Residual histogram of weekday—80th-percentile TTI—Minnesota.

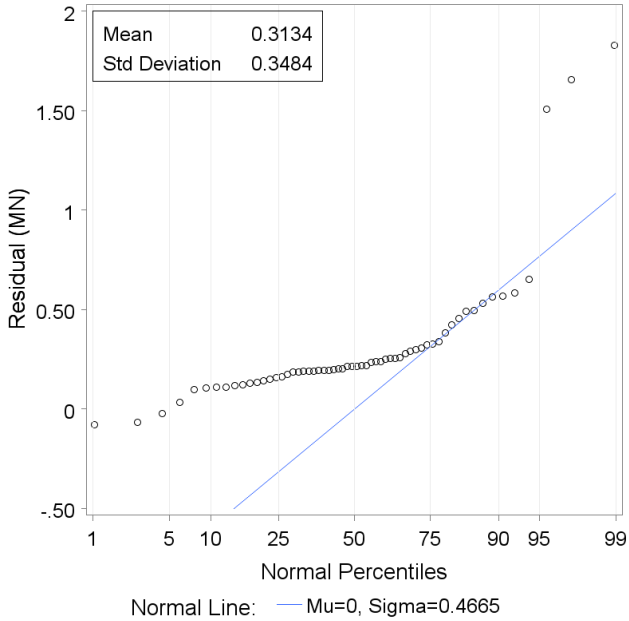

Figure C.231. Residual normality plot of weekday—80th-percentile TTI—Minnesota.

Salt Lake City

Table C.105. Residual Analysis of Weekday—80th-Percentile TTI—Salt Lake City

Table C.105.a. Basic Statistical Measures

Location		Variability	
Mean	0.0432	Std deviation	0.0360
Median	0.0533	Variance	0.0013
Minimum	–0.027	Range	0.1305
Maximum	0.1036	Interquartile range	0.0466

Table C.105.b. Basic Confidence Limits Assuming Normality

Parameter	Estimate	95% Confidence Limits	
Mean	0.0432	0.0298	0.0567
Std deviation	0.0360	0.0287	0.0485
Variance	0.0013	0.0008	0.0023

Table C.105.c. Tests for Location: Mu=0

Test	Statistic		*p*-Value	
Student's *t*	*t*	6.5668	Pr > |*t*|	<0.0001

Table C.105.d. Tests for Normality

Test	Statistic		*p*-Value	
Shapiro-Wilk	*W*	0.9118	Pr < *W*	0.0165

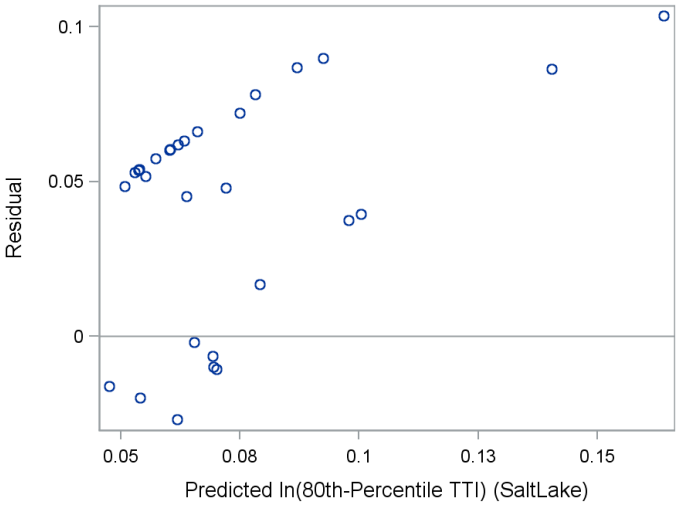

Figure C.232. Residual plot of weekday—80th-percentile TTI—Salt Lake City.

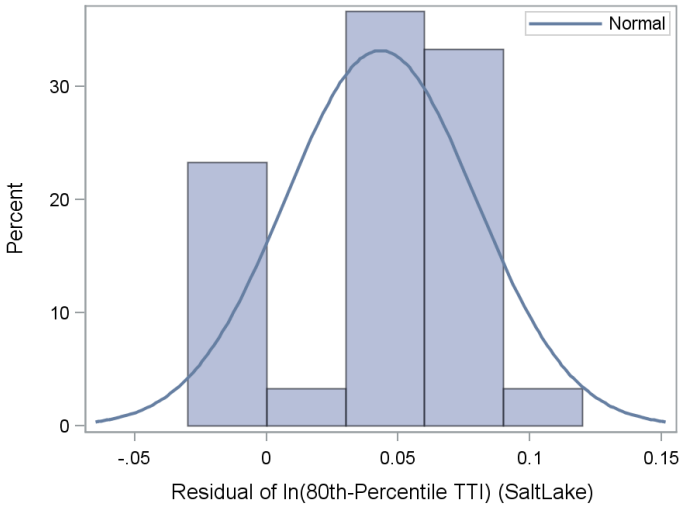

Figure C.233. Residual histogram of weekday—80th-percentile TTI—Salt Lake City.

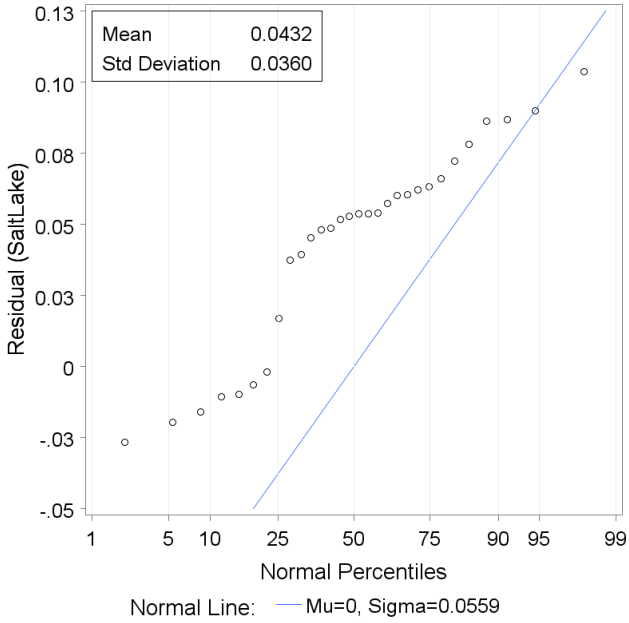

Figure C.234. Residual normality plot of weekday—80th-percentile TTI—Salt Lake City.

50th-Percentile TTI Model

California

Table C.106. Residual Analysis of Weekday—50th-Percentile TTI—California

Table C.106.a. Basic Statistical Measures

Location		Variability	
Mean	–0.005	Std deviation	0.0575
Median	0.0152	Variance	0.0033
Minimum	–0.399	Range	0.4271
Maximum	0.0282	Interquartile range	0.0247

Table C.106.b. Basic Confidence Limits Assuming Normality

Parameter	Estimate	95% Confidence Limits	
Mean	–0.005	–0.015	0.0042
Std deviation	0.0575	0.0515	0.0651
Variance	0.0033	0.0027	0.0042

Table C.106.c. Tests for Location: Mu=0

Test	Statistic		*p*-Value	
Student's *t*	*t*	–1.099	Pr > |*t*|	0.2735

Table C.106.d. Tests for Normality

Test	Statistic		*p*-Value	
Shapiro-Wilk	*W*	0.4980	Pr < *W*	<0.0001

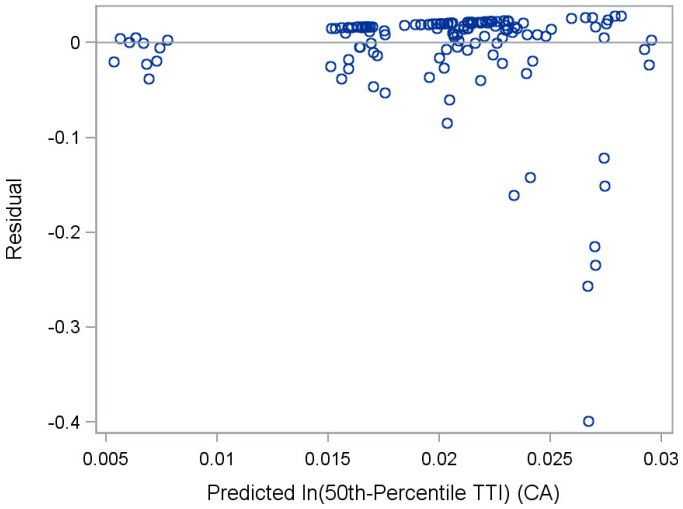

Figure C.235. Residual plot of weekday—50th-percentile TTI—California.

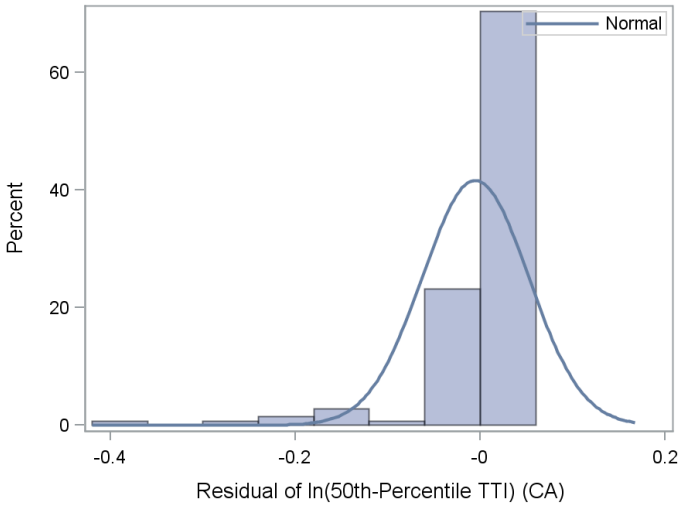

Figure C.236. Residual histogram of weekday—50th-percentile TTI—California.

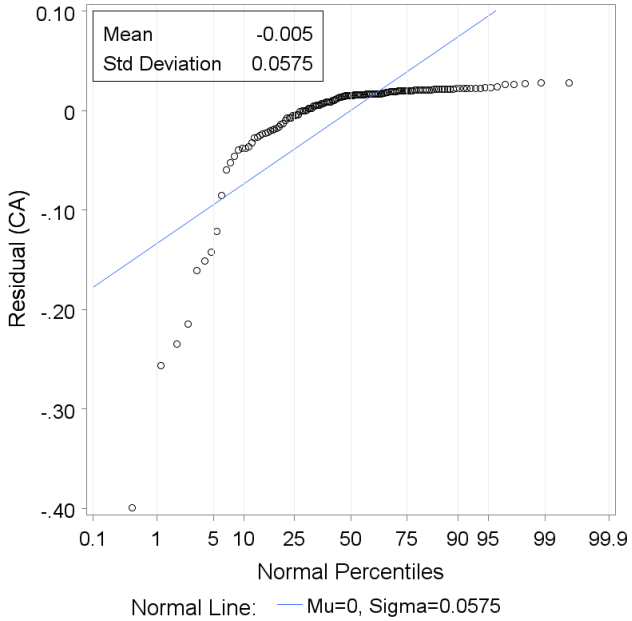

Figure C.237. Residual normality plot of weekday—50th-percentile TTI—California.

Minnesota

Table C.107. Residual Analysis of Weekday—50th-Percentile TTI—Minnesota

Table C.107.a. Basic Statistical Measures

Location		Variability	
Mean	0.0153	Std deviation	0.0074
Median	0.0178	Variance	543E-7
Minimum	–0.024	Range	0.0449
Maximum	0.0213	Interquartile range	0.0050

Table C.107.b. Basic Confidence Limits Assuming Normality

Parameter	Estimate	95% Confidence Limits	
Mean	0.0153	0.0134	0.0172
Std deviation	0.0074	0.0062	0.0090
Variance	543E-7	39E-6	0.0001

Table C.107.c. Tests for Location: Mu=0

Test	Statistic		*p*-Value	
Student's *t*	*t*	16.049	Pr > |*t*|	<0.0001

Table C.107.d. Tests for Normality

Test	Statistic		*p*-Value	
Shapiro-Wilk	*W*	0.6674	Pr < *W*	<0.0001

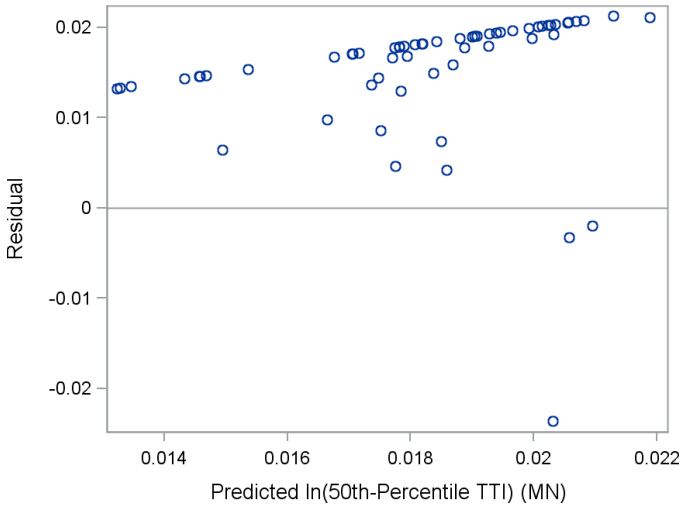

Figure C.238. Residual plot of weekday—50th-percentile TTI—Minnesota.

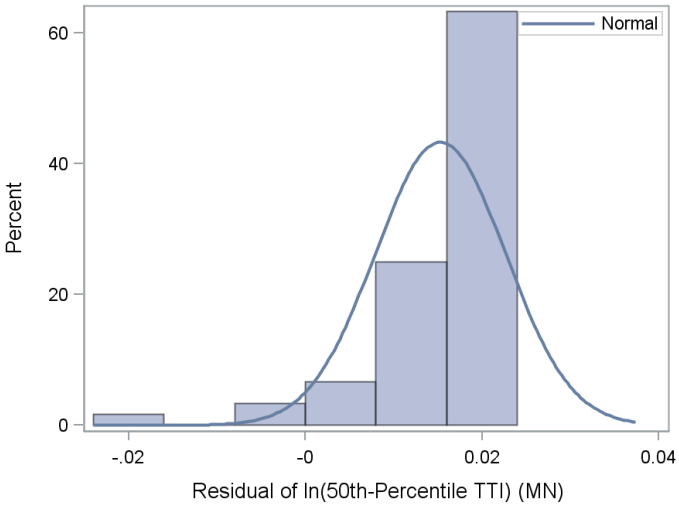

Figure C.239. Residual histogram of weekday—50th-percentile TTI—Minnesota.

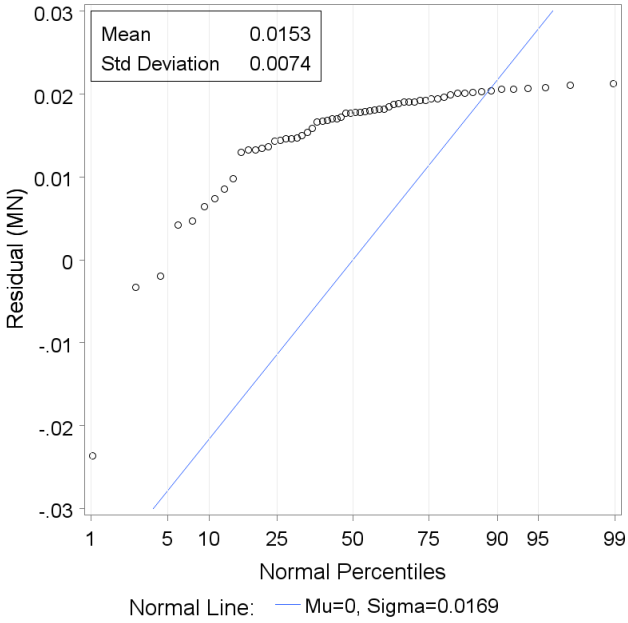

Figure C.240. Residual normality plot of weekday—50th-percentile TTI—Minnesota.

Salt Lake City

Table C.108. Residual Analysis of Weekday—50th-Percentile TTI—Salt Lake City

Table C.108.a. Basic Statistical Measures

Location		Variability	
Mean	–0.003	Std deviation	0.0215
Median	0.0102	Variance	0.0005
Minimum	–0.047	Range	0.0620
Maximum	0.0152	Interquartile range	0.0282

Table C.108.b. Basic Confidence Limits Assuming Normality

Parameter	Estimate	95% Confidence Limits	
Mean	–0.003	–0.011	0.0046
Std deviation	0.0215	0.0171	0.0289
Variance	0.0005	0.0003	0.0008

Table C.108.c. Tests for Location: Mu=0

Test	Statistic		*p*-Value	
Student's *t*	*t*	–0.865	Pr > |*t*|	0.3942

Table C.108.d. Tests for Normality

Test	Statistic		*p*-Value	
Shapiro-Wilk	*W*	0.7669	Pr < *W*	<0.0001

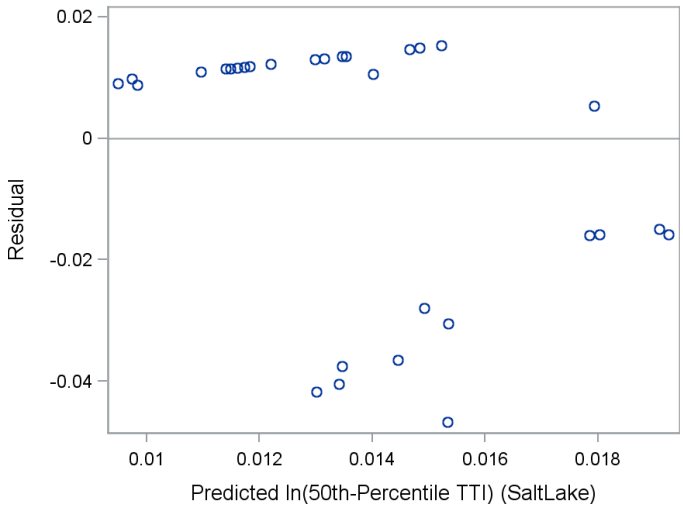

Figure C.241. Residual plot of weekday—50th-percentile TTI—Salt Lake City.

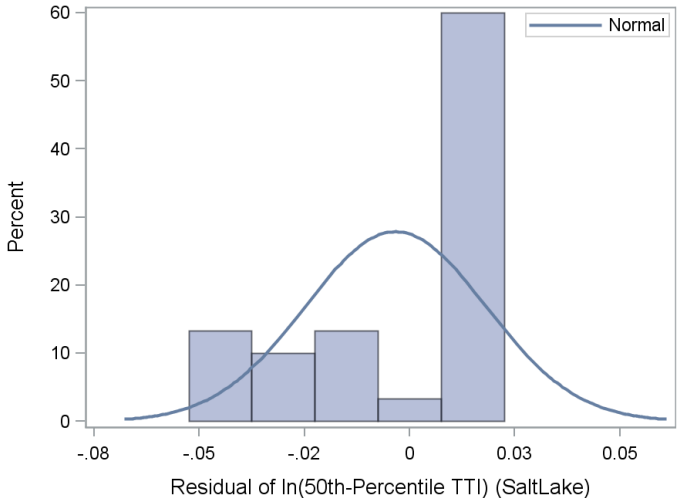

Figure C.242. Residual histogram of weekday—50th-percentile TTI—Salt Lake City.

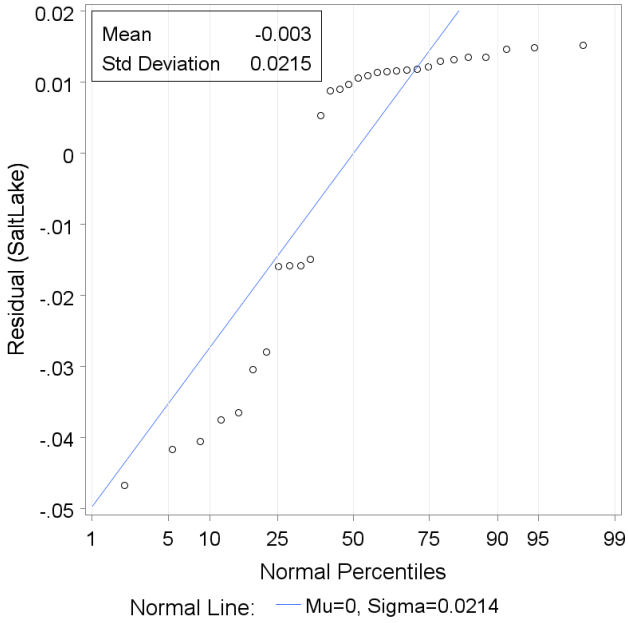

Figure C.243. Residual normality plot of weekday—50th-percentile TTI—Salt Lake City.

10th-Percentile TTI Model

California

Table C.109. Residual Analysis of Weekday—10th-Percentile TTI—California

Table C.109.a. Basic Statistical Measures

Location		Variability	
Mean	0.0028	Std deviation	0.0069
Median	0.0045	Variance	478E-7
Minimum	–0.062	Range	0.0685
Maximum	0.0066	Interquartile range	0.0013

Table C.109.b. Basic Confidence Limits Assuming Normality

Parameter	Estimate	95% Confidence Limits	
Mean	0.0028	0.0016	0.0039
Std deviation	0.0069	0.0062	0.0078
Variance	478E-7	383E-7	0.0001

Table C.109.c. Tests for Location: Mu=0

Test	Statistic		*p*-Value	
Student's *t*	*t*	4.7561	Pr > |*t*|	<0.0001

Table C.109.d. Tests for Normality

Test	Statistic		*p*-Value	
Shapiro-Wilk	*W*	0.3795	Pr < *W*	<0.0001

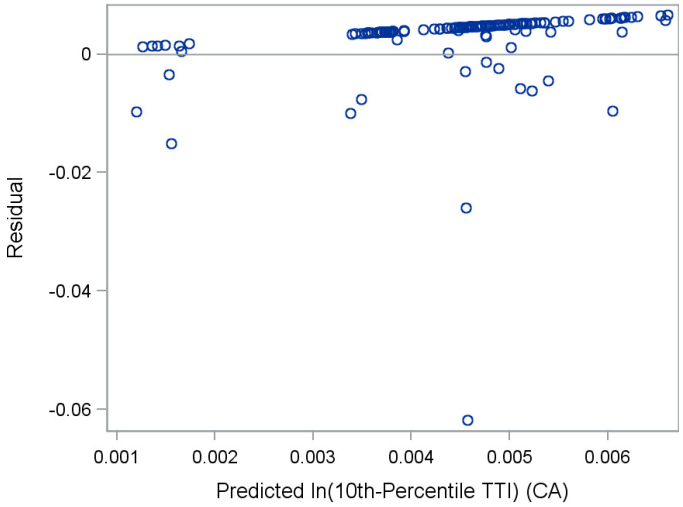

Figure C.244. Residual plot of weekday—10th-percentile TTI—California.

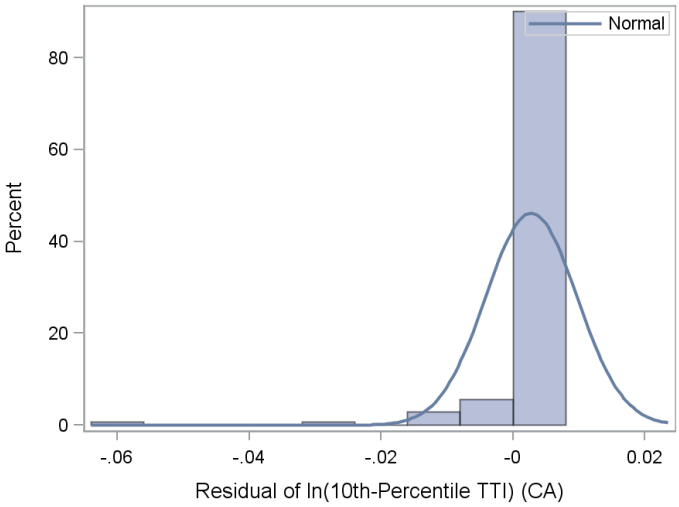

Figure C.245. Residual histogram of weekday—10th-percentile TTI—California.

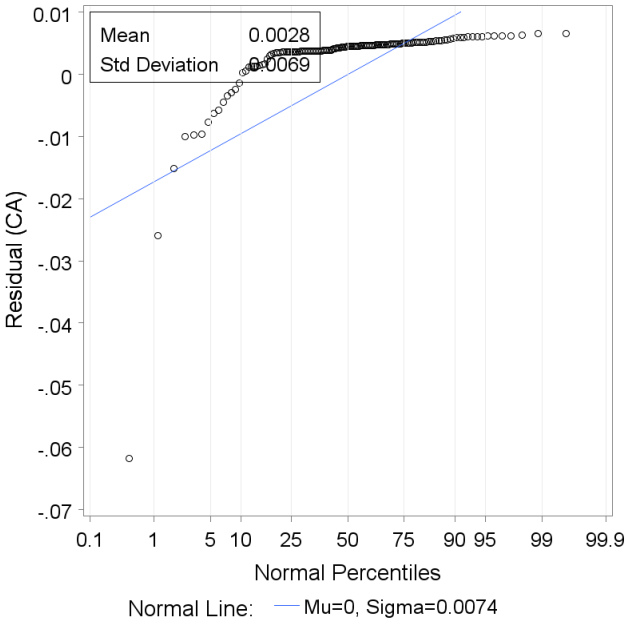

Figure C.246. Residual normality plot of weekday—10th-percentile TTI—California.

Minnesota

Table C.110. Residual Analysis of Weekday—10th-Percentile TTI—Minnesota

Table C.110.a. Basic Statistical Measures

Location		Variability	
Mean	0.0032	Std deviation	0.0036
Median	0.0041	Variance	13E-6
Minimum	–0.014	Range	0.0184
Maximum	0.0049	Interquartile range	0.0006

Table C.110.b. Basic Confidence Limits Assuming Normality

Parameter	Estimate	95% Confidence Limits	
Mean	0.0032	0.0023	0.0042
Std deviation	0.0036	0.0031	0.0044
Variance	13E-6	932E-8	193E-7

Table C.110.c. Tests for Location: Mu=0

Test	Statistic		*p*-Value	
Student's *t*	*t*	6.9862	Pr > |*t*|	<0.0001

Table C.110.d. Tests for Normality

Test	Statistic		*p*-Value	
Shapiro-Wilk	*W*	0.3382	Pr < *W*	<0.0001

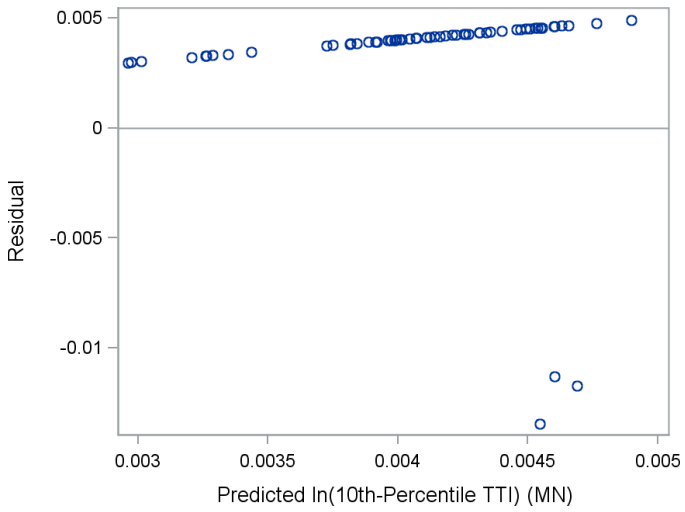

Figure C.247. Residual plot of weekday—10th-percentile TTI—Minnesota.

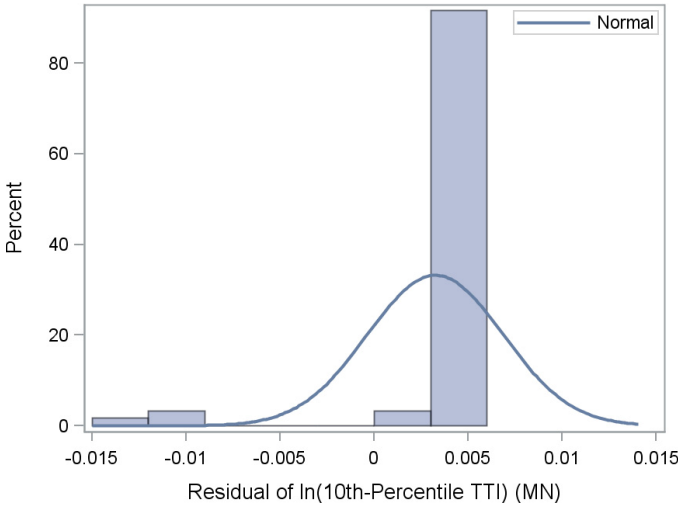

Figure C.248. Residual histogram of weekday—10th-percentile TTI—Minnesota.

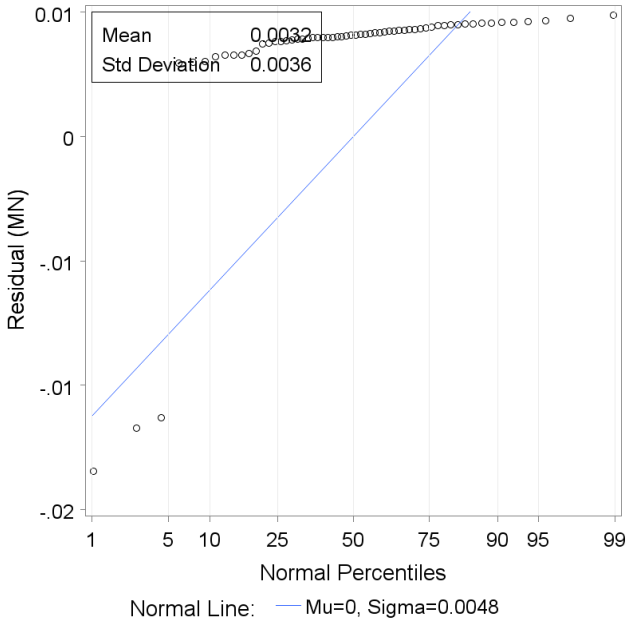

Figure C.249. Residual normality plot of weekday—10th-percentile TTI—Minnesota.

Salt Lake City

Table C.111. Residual Analysis of Weekday—10th-Percentile TTI—Salt Lake City

Table C.111.a. Basic Statistical Measures

Location		Variability	
Mean	–0.006	Std deviation	0.0119
Median	0.0023	Variance	0.0001
Minimum	–0.031	Range	0.0343
Maximum	0.0034	Interquartile range	0.0208

Table C.111.b. Basic Confidence Limits Assuming Normality

Parameter	Estimate	95% Confidence Limits	
Mean	–0.006	–0.010	–0.001
Std deviation	0.0119	0.0095	0.0160
Variance	0.0001	0.0001	0.0003

Table C.111.c. Tests for Location: Mu=0

Test	Statistic		*p*-Value	
Student's *t*	*t*	–2.567	Pr > |*t*|	0.0157

Table C.111.d. Tests for Normality

Test	Statistic		*p*-Value	
Shapiro-Wilk	*W*	0.7251	Pr < *W*	<0.0001

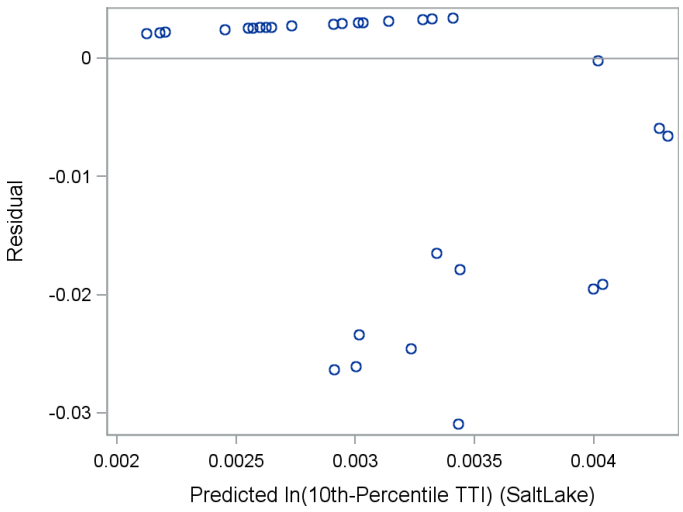

Figure C.250. Residual plot of weekday—10th-percentile TTI—Salt Lake City.

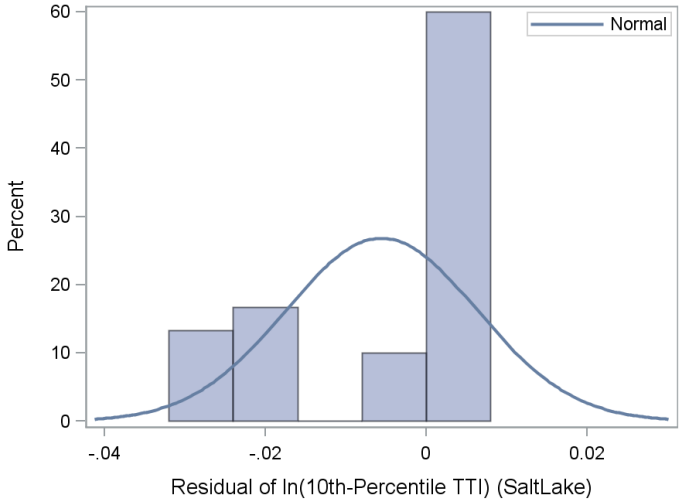

Figure C.251. Residual histogram of weekday—10th-percentile TTI—Salt Lake City.

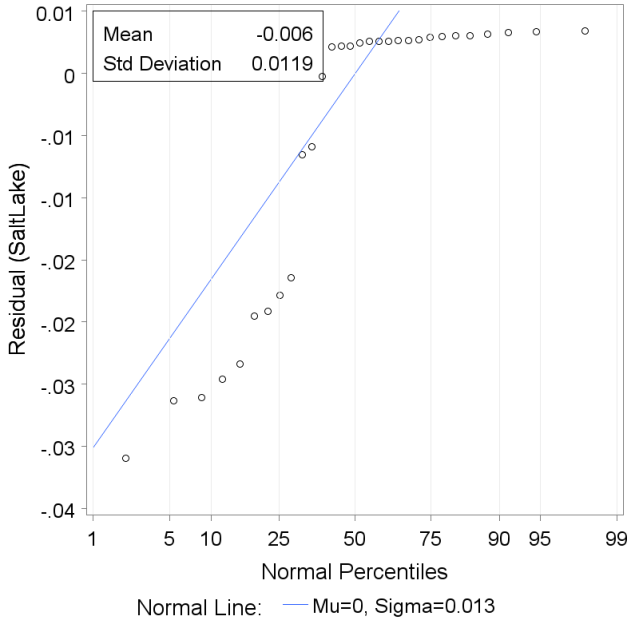

Figure C.252. Residual normality plot of weekday—10th-percentile TTI—Salt Lake City.

APPENDIX D

Data-Poor Validation

Overview

This appendix presents the validation analysis of the L03 data-poor models. Appendix H of the L03 Report contains a set of models that predict the following travel time index (TTI) reliability statistics:

- 95th-, 90th-, and 80th-percentiles
- Standard deviation
- Percentage of on-time trips relative to space mean speeds of 50 mph, 45 mph, and 30 mph

In the L03 project, these models were termed "data poor" because they enable the prediction of a wide set of reliability measures based only on estimates of the mean travel time index. The L03 project calibrated these data-poor models using data collected in a number of metropolitan areas but it did not perform any validation of the final predictive equations. The goal of this stage of the L33 project is to quantify the effectiveness of these models using new data sets collected from around the country.

The rest of this appendix is organized as follows. The next section presents the validation procedure, including the data gathering and the techniques used to measure the effectiveness of the L03 data-poor models. The following section presents the validation results for each model overall and by region. The final section summarizes the conclusions. There is also an attachment that contains detailed validation outputs (shown in Tables D.23 to D.50 and Figures D.57 to D.140).

Validation Procedure

Models

The seven L03 data-poor models validated in this task are

1. 95th-percentile TTI = 1 + 3.6700 * ln(meanTTI)
2. 90th-percentile TTI = 1 + 2.7809 * ln(meanTTI)
3. 80th-percentile TTI = 1 + 2.1406 * ln(meanTTI)
4. Standard deviation of TTI = 0.71 * $(\text{meanTTI} - 1)^{0.56}$
5. PctTripsOnTime50mph = $e^{(-0.20570*[\text{meanTTI}-1])}$
6. PctTripsOnTime45mph = $e^{(-1.5115*[\text{meanTTI}-1])}$
7. PctTripsOnTime30mph = $0.333 + [0.672/(1 + e^{(5.0366*[\text{meanTTI}-1.8256])})]$

Appendix H of the L03 Report, which contains these models, does not include any outputs from the statistical analyses used to form these equations. Without these outputs, much of the L33 validation had to focus on evaluating the extent to which these models adhere to the assumptions required for generalized regression.

Data

The data used in the validation were collected from the Los Angeles, San Francisco Bay Area, Sacramento, and San Diego metropolitan regions (grouped together into a "California" data set); Minneapolis–St. Paul, Minnesota; Salt Lake City, Utah; and Spokane, Washington. Details about the study segments, data sets, and data processing techniques are discussed in the L33 validation plan. The California, Salt Lake City, and Spokane data were collected from the three-year period between January 1, 2010, and December 31, 2012. The Minnesota data were collected from the three-year period between June 1, 2009, and May 31, 2012.

Validation was performed using data collected on weekdays during the midday period (11:00 a.m.–2:00 p.m.) and the peak period (a continuous time period of at least 75 min during which the space mean speed is less than 45 mph). This is consistent with the time periods that L03 used to calibrate the data-poor models.

Table D.1 summarizes the sample size of data by region and time period used in the validation. Each value represents the number of section-years for which the mean TTI and TTI reliability statistics were calculated from the collected data. In

Table D.1. L33 Validation Data Sample Size (Section-Years)

Period	CA	MN	Salt Lake City	Spokane	All Data
Midday	144	60	42	12	**258**
Peak period	43	19	3	0	**65**
Total	187	79	45	12	**323**

the validation, the mean TTI was plugged into the model equations to calculate the reliability statistics, which were then compared to the measured values.

Table D.1 shows that far fewer section-year data points were generated for the peak period than for the midday period. This is because many segments did not meet the L03 definition of having a peak period, defined as a time period of at least 75 min during which the mean speed is less than 45 mph. In Spokane, none of the sections met these criteria. In Salt Lake City, only three section-years (representing one section over 3 years) met these criteria. This reduces the regional variation among the validation data sets and suggests that the peak period definition needs to be reevaluated in the model enhancement stage. In addition to the lack of a notable peak period in the Spokane and Salt Lake City data sets, in general, the travel times in these data sets exhibited much less variation and unreliability than in the California (CA) and Minnesota (MN) sites. This should be kept in mind when evaluating the validation results.

D.2.3 Measures

For each model, the goals of the validation were to quantify the model error and determine whether the model follows the key assumptions of generalized regression. This section first describes the assumptions that were tested and then presents the performance measures that were evaluated.

D.2.3.1 Generalized Regression Model Assumptions

As part of model validation, we examine if the key assumptions of generalized regression models are violated. Generalized regression models have the following basic assumptions:

1. Generalized nonlinear functional form: the following formula states that the conditional mean of y_i given x_i is a continuous differential function f, that is,
   (a) $E[y_i|x_i] = f(x_i, \beta), i = 1, \ldots, n$
   (b) If this assumption is satisfied, the residuals should not show any nonrandom pattern (e.g., concave shape) in the residual plot. Otherwise, the model form may not be adequate.
2. Zero residual mean: the distribution of residuals has a mean of zero.
3. Homoscedasticity: the distribution of residuals has a constant variance.
4. Normal distribution of residual: it is assumed that residuals follow the normal distribution.

Performance Measures

For a systematic evaluation of the model assumptions, we used the performance measures proposed in the L33 validation plan: (1) root mean square error (RMSE); (2) residual plots; and (3) Student's *t*-test of zero residual mean. Each of these is described below.

Root Mean Square Error

Denote the predicted response values from the model as $\hat{y}$ and the measured response values as y. The prediction error (residual) r is thus defined as

$$r = \hat{y} - y$$

A positive mean r implies that the model systemically overestimates values based on new data. RMSE is defined as

$$\text{RMSE} = \sqrt{\text{MSE}(\hat{y})} = \sqrt{E\left[(\hat{y} - y)^2\right]} = \sqrt{\frac{\sum_{i=1}^{n} r^2}{n}}$$

RMSE measures the magnitude of differences between the predicted and measured responses. However, there is no simple benchmark or threshold for an acceptable RMSE.

Residual Plots

Ideally, residual r is a random variable that follows a normal distribution with zero mean. Plotting out the distribution of residuals allows for an assessment of the goodness of fit and the likelihood of the presence of bias and heteroscedasticity (unequal variance).

Student's t-Test of Zero Residual Mean

The one sample Student's *t*-test can be used to determine if the mean of the residuals is significantly different from zero in a statistical sense, which tests for systematic bias. With an unbiased model, the difference should be statistically insignificant. The *t*-value is calculated as

$$t = \frac{\bar{r} - \mu_0}{s/\sqrt{n}}$$

where $\bar{r}$ is the residual mean, s is the standard deviation of residuals, n is the sample size, and μ_0 is the specific mean

value for comparison, set here to be zero. To draw a conclusion, if the calculated *t*-value is larger than some threshold t_α (e.g., $\alpha = 5\%$) using a two-tailed *t* distribution table, the null hypothesis that the residuals have a mean of zero can be rejected with $(1t_\alpha)$ level of confidence. Or we say that the residual mean is significantly different from zero at α level of probability. If the corresponding *p*-value is used to draw a conclusion, it means that if the null hypothesis were correct, then we would expect to obtain such a large *t*-value on at most *p* percentage of occasions. For the validation, we use a 95% level of confidence.

Data-Poor Model Validation Results

This section contains the data-poor validation results, with subsections for each of the seven data-poor models. Each subsection is further divided into the following sections: (1) All Sites, which presents results aggregated across all regions; (2) Region Specific, which details model performance in each individual region; and (3) Summary, which includes conclusions on the model validation.

Each All Sites model section includes the following:

- A table listing the RMSE values at each study site;
- A scatter plot comparing the predicted TTI curve with the measured values;
- A scatter plot of the residuals by predicted TTI;
- A histogram showing the distribution of the residuals;
- A quantile-quantile plot (normality plot) of the residuals; and
- A series of tables showing various statistics about the residuals and the results of the *t*-test to check if the mean of the residuals is statistically different from zero.

Each region-specific section contains a scatter plot comparing the predicted TTI curve with the measured values, as well as a general discussion on the validation results. The outputs listed above are also included for each region in the attachment.

Each summary section contains a table listing whether the basic regression assumptions are satisfied based on statistical results and subjective observations of plots. The judgment is concluded in a qualitative way determining the satisfaction level of the assumptions, categorized as S (satisfactory) or NS (not satisfactory). Four criteria are summarized:

1. **Systematic nonlinear trend.** It is evaluated as "satisfactory" if the model can describe the validation data trend adequately, without some systematic biased pattern shown in the residual plot, in which case the residuals should be symmetrically distributed on both sides of the zero reference line in the residual plot.
2. **Residual: zero mean.** It is evaluated as "satisfactory" if the Student's *t*-test shows strong confidence (95% level) that the null hypothesis of zero residual mean cannot be rejected.
3. **Residual: constant variance.** It is evaluated as "satisfactory" if the distribution of residuals along the zero reference line does not show a cone shape or double bow shape.
4. **Residual: normal distribution.** It is evaluated as "satisfactory" if the residual distribution closely follows a normal distribution.

95th-Percentile TTI Model

All Sites

Table D.2 shows the RMSE for the 95th-percentile prediction by site. In terms of RMSE, the data-poor 95th-percentile TTI model fits the Spokane data the best, with an RMSE of only 0.0688. The error is highest with the California data set, which has an RMSE over 0.2. However, the RMSE criterion alone does not tell the whole story. As discussed in the Overview section of this appendix, the Spokane data set has very little variance compared to that of California. One needs to keep this issue in mind when examining the statistical results.

The scatter plot in Figure D.1 shows that the data-poor model can generally predict the trend of the 95th-percentile TTI data. Nonetheless, the residual plot in Figure D.2 exhibits a clear cone shape increasing in range, indicating a nonconstant variance

Table D.2. RMSE Summary, 95th-Percentile TTI

CA	MN	Salt Lake City	Spokane	All Data Sets
0.2064	0.1716	0.0883	0.0688	0.1820

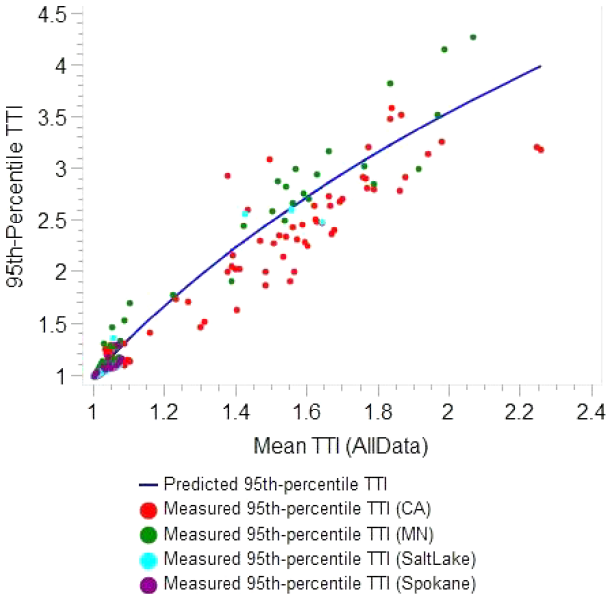

Figure D.1. Mean TTI versus 95th-percentile TTI.

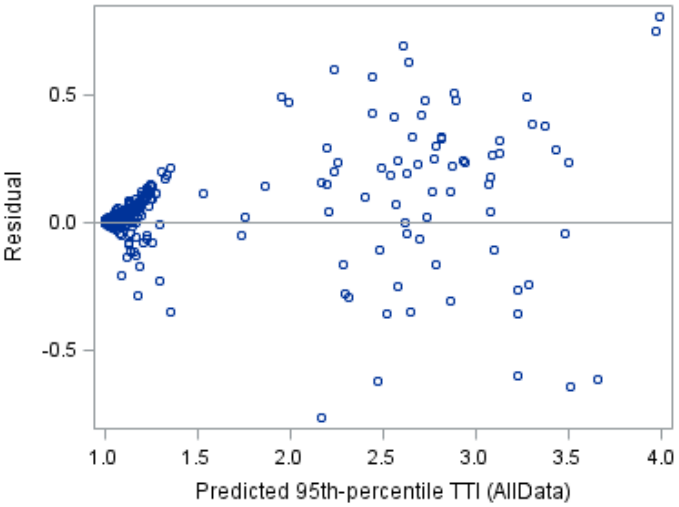

Figure D.2. Residual plot of the 95th-percentile TTI—AllData.

and suggesting that some data transformation may be needed to get a better fit to the data. The histogram in Figure D.3 and the normality plot in Figure D.4 show that the distribution of residuals close to the mean varies less than that for a normal distribution. The *t*-test results in Table D.3 show that the residual mean is larger than zero, meaning that the model tends to predict a higher 95th-percentile TTI than the data show.

Region Specific

California

The scatter plot of the California data set in Figure D.5 shows that the predicted 95th-percentile TTI curve follows a similar pattern to that of the measured data points. However, most of the residuals are positive, with an increasing error variance as the mean TTI increases. This indicates that the model tends to overpredict the 95th-percentile travel times in the California

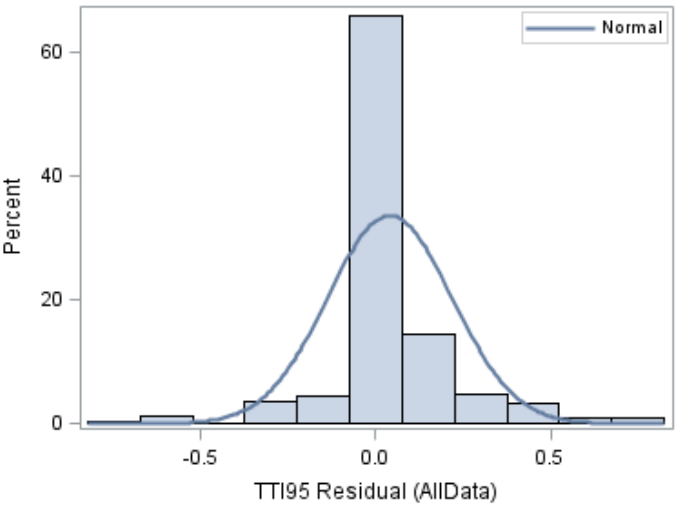

Figure D.3. Histogram of residuals—95th-percentile TTI—AllData.

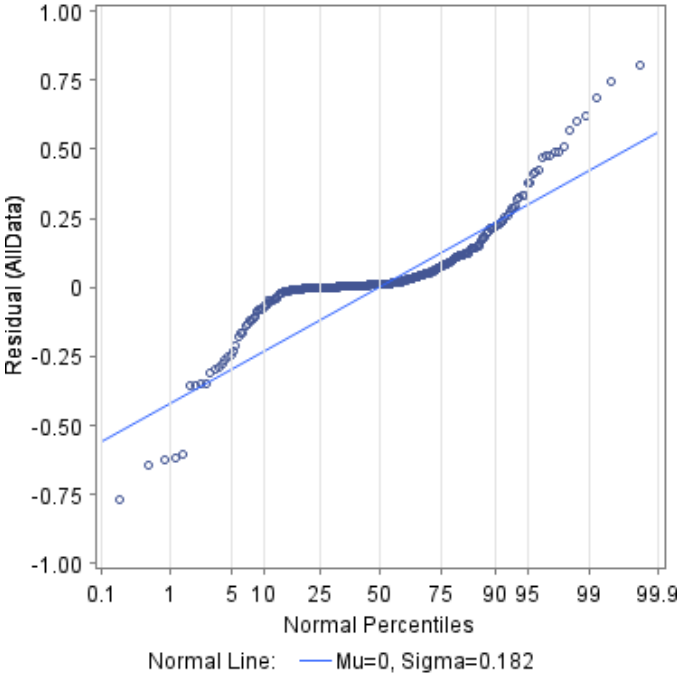

Figure D.4. Normality plot of residuals—95th-percentile TTI—AllData.

Table D.3. Residual Analysis Results—95th-percentile TTI—AllData

Table D.3.a. Basic Summary

Location		Variability	
Mean	0.0399	Std deviation	0.1779
Median	0.0108	Variance	0.0316
Min	–0.7684	Range	1.5732
Max	0.8048	Interquartile range	0.0767

Table D.3.b. Estimated Confidence Limits Assuming Normality

Parameter	Estimate	95% Confidence Limits	
Mean	0.0399	0.0204	0.0593
Std deviation	0.1779	0.1651	0.1927
Variance	0.0316	0.0273	0.0371

Table D.3.c. Student's t-Test of Zero Residual Mean

Test	Statistic	*p*-Value
Student's *t*-test	4.0291	<0.0001

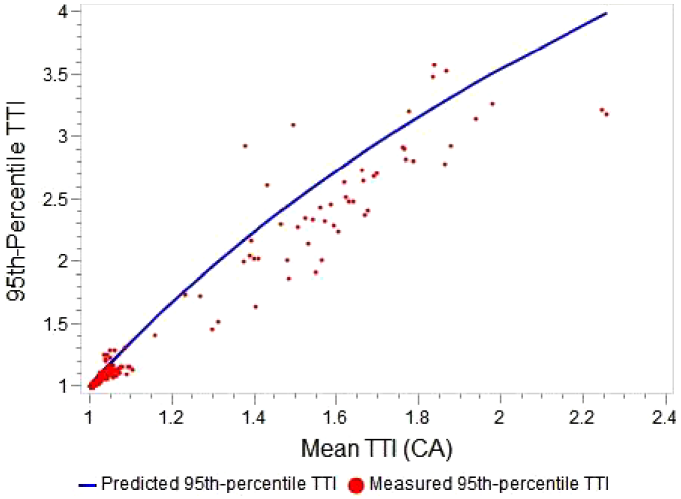

Figure D.5. Mean TTI versus 95th-percentile TTI, California.

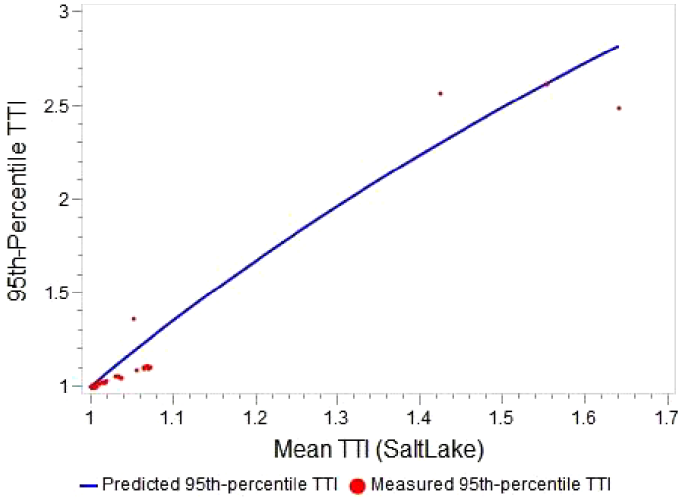

Figure D.7. Mean TTI versus 95th-percentile TTI, Salt Lake City.

regions. The *t*-test results reject the null hypothesis that the average of the residuals is zero.

Minnesota

The Minnesota data points are more evenly scattered on both sides of the data-poor model curve than were the California data points, as we can see from the scatter plot in Figure D.6. Analysis of the residuals shows a nonconstant error variance, implying that some type of variable transformation may be needed. The distribution of residuals is negatively skewed. The *t*-test results reject the null hypothesis that the average of the residuals is zero. In general, the model tends to underpredict the 95th-percentile travel times in the Minneapolis region.

Salt Lake City

The Salt Lake City data samples were mostly collected during a noncongested condition, as we can see from the scatter plot in Figure D.7. It has only three sparse points whose mean TTI is larger than 1.1. When the mean TTI is below 1.1, the real data pattern is much more flattened than the predicted curve, meaning that the model tends to overpredict the 95th-percentile travel time when mean conditions are relatively uncongested. As a result, there is some nonrandom pattern in the residuals when the predicted value is below 1.5. The normality analysis indicates less variability among the residuals than that of a normal distribution. The *t*-test results reject the null hypothesis that the average of the residuals is zero.

Spokane

The scatter plot of the Spokane results in Figure D.8 shows a cone shape, but this may be partly attributable to the scale of the plot. All section-years had a mean TTI of less than 1.08, which indicates a nearly free-flow condition. The residuals

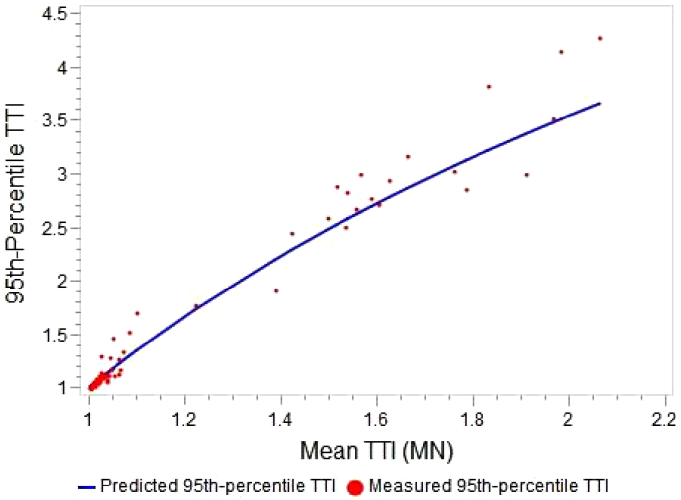

Figure D.6. Mean TTI versus 95th-percentile TTI, Minnesota.

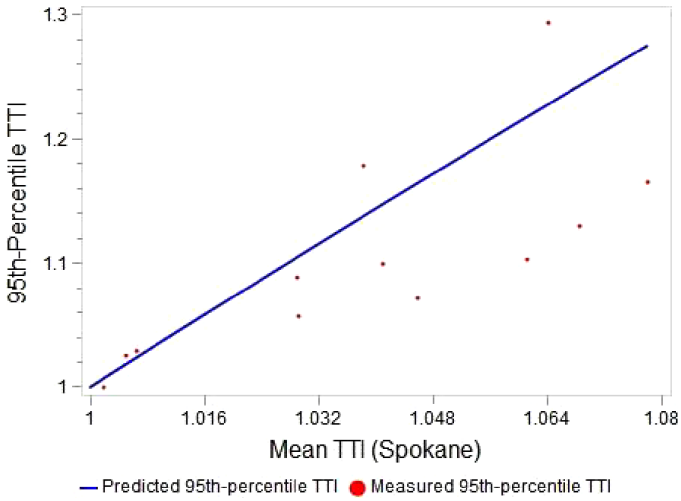

Figure D.8. Mean TTI versus 95th-percentile TTI, Spokane.

show a nonconstant variance, but none of the residuals are large. The residuals do not follow a normal distribution. The *t*-test of the zero residual mean gives a *p*-value of 0.0767, which means that we cannot reject the zero mean null hypothesis with a 95% level of confidence.

Summary

From the validation analysis for the 95th-percentile TTI, we can conclude that, in general, the existing model can explain the variation in the 95th-percentile TTI. However, the model does not fit each region's data set equally well. This may be due to the unique traffic flow characteristics of each region, which are difficult to generalize into a single model.

The residual analysis showed violations of the basic regression assumptions. Nonconstant variance of the residuals is the common problem in all of the regions. The zero residual mean assumption was rejected in all sites except for Spokane, with the model tending to overpredict the 95th-percentile TTI in California and Salt Lake City, and underpredict it in Minnesota. This implies that the nonlinear model form assumption may be violated. The Spokane data set exhibited the minimum RMSE among the four regional data sets. However, the sample size and variability of this data set are not large enough to draw confident statistical conclusions.

Table D.4 lists a summary of whether the generalized regression assumptions are satisfied (S) or not (NS). As mentioned in the beginning of this section, the conclusions are based on subjective observation of the plots as well as objective statistical analysis. The standards for the conclusions in the table are discussed in the previous section.

90th-Percentile TTI Model

All Sites

The RMSE table in Table D.5 shows that the 90th-percentile TTI model predicts consistently better than the 95th-percentile TTI for all four regional data sets. The largest RMSE shows up in the validation of the Minnesota data set, followed by that of the California data set. The largest RMSE is 0.15023. Overall, RMSE is 0.11890, close to that of the California data set, which may be because the dominant samples are coming from the California data set.

Table D.4. 95th-Percentile of TTI Model Validation Summary

Assumptions:	All	CA	MN	Salt Lake City	Spokane
Systematic nonlinear trend	NS	NS	S	NS	S
Residual: zero mean	NS	NS	NS	NS	S
Residual: constant variance	NS	NS	NS	NS	NS
Residual: normal distribution	NS	NS	NS	NS	NS

Note: NS = generalized regression assumptions are not satisfied; S = satisfied.

Table D.5. RMSE Summary, 90th-Percentile TTI

CA	MN	Salt Lake City	Spokane	All Data Sets
0.1187	0.1502	0.0483	0.0604	0.1189

The scatter plot in Figure D.9 and the residual plot in Figure D.10 clearly show that the data-poor model is unable to fully capture the data trend, resulting in a concave shape in the residual plot. The histogram in Figure D.11 and the

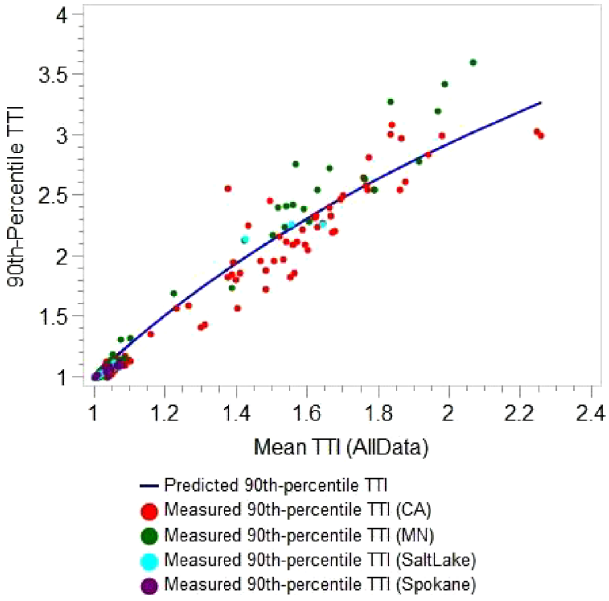

Figure D.9. Mean TTI versus 90th-percentile TTI.

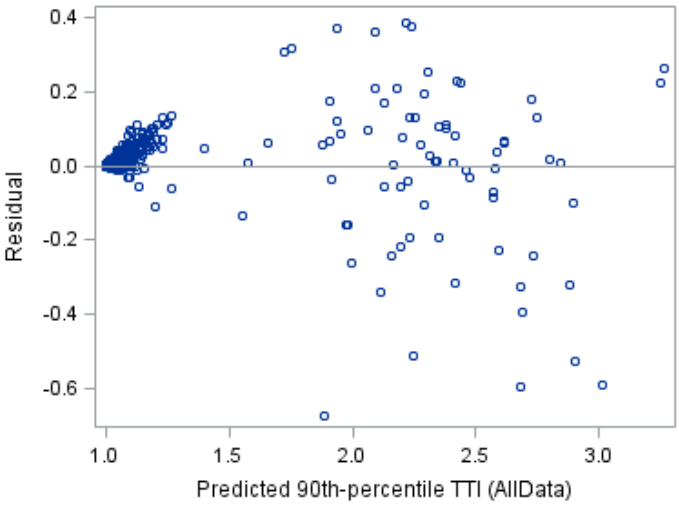

Figure D.10. Residual plot—90th-percentile TTI—AllData.

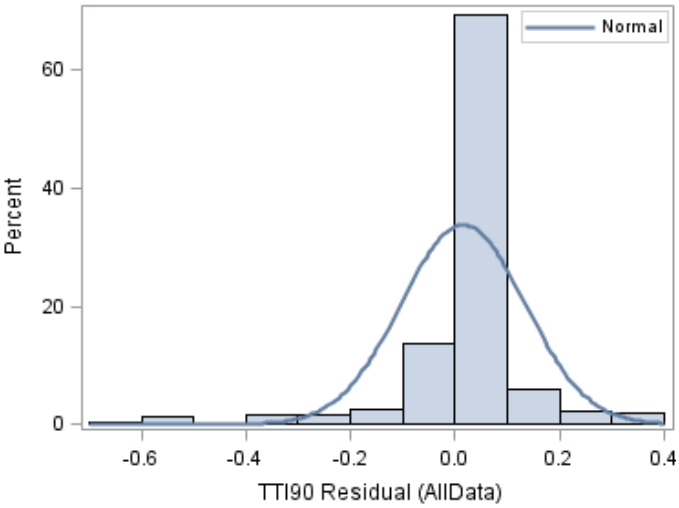

Figure D.11. Histogram of residuals.

normality plot in Figure D.12 indicate that the residual distribution has less variance compared with a normal distribution. The 95% confidence interval of estimated residual mean does not include zero, and the *t*-test yields a *p*-value of 0.0233 (Table D.6), indicating that the hypothesis of zero residual mean can be rejected.

Region Specific

CALIFORNIA

The California data samples fall around the predicted curve but tend to be smaller (Figure D.13). Residual analysis

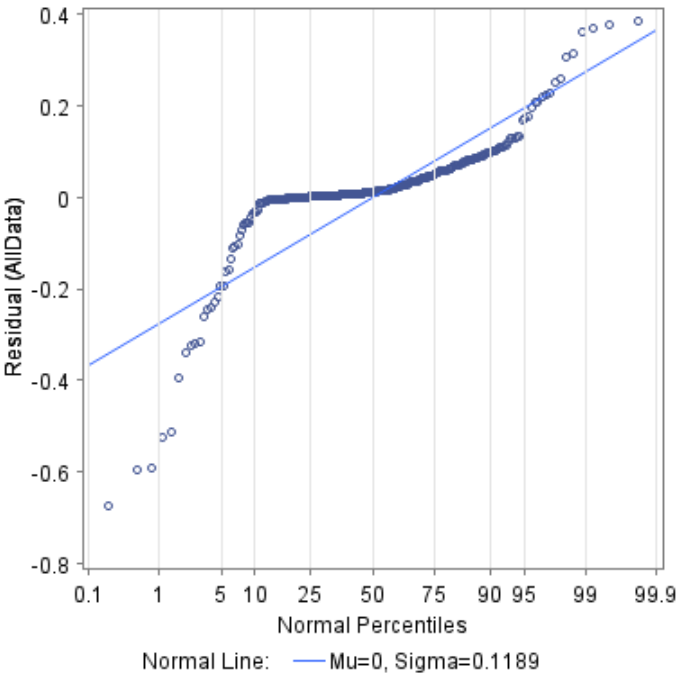

Figure D.12. Normality plot of residuals—90th-percentile TTI—AllData.

Table D.6. Statistical Residual Analysis Results—90th-percentile TTI—AllData

Table D.6.a. Basic Summary

Location		Variability	
Mean	0.0150	Std deviation	0.1181
Median	0.0118	Variance	0.0140
Min	–0.6737	Range	1.0585
Max	0.3848	Interquartile range	0.0503

Table D.6.b. Estimated Confidence Limits Assuming Normality

Parameter	Estimate	95% Confidence Limits	
Mean	0.0150	0.0020	0.0279
Std deviation	0.1181	0.1097	0.1280
Variance	0.0140	0.0120	0.0164

Table D.6.c. Student's t-Test of Zero Residual Mean

Test	Statistic	*p*-Value
Student's *t*-test	2.2790	0.0233

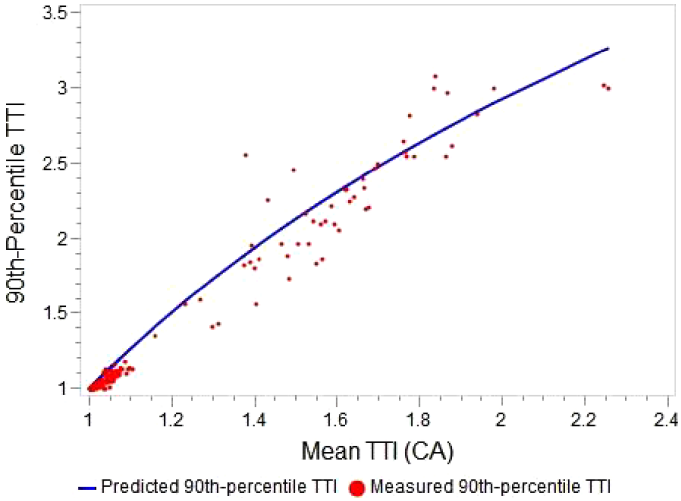

Figure D.13. Mean TTI versus 90th-percentile TTI, California.

confirms that most of the residuals are above the zero reference line, with a positive skew in the residual distribution. The estimated residual mean is 0.0358 with an estimated confidence interval of 0.0194 to 0.0522. The *t*-test rejects the zero residual mean hypothesis. Note that there is a potential outlier resulting in the maximal absolute residual value of 0.6737. However, since we do not have enough evidence to conclude that it should be removed from the data set, it is included in the validation analysis.

Minnesota

Unlike in California, in Minnesota the measured 90th-percentile TTI increases faster with the mean TTI than does the prediction. Like the 95th-percentile model, the 90th-percentile model in Minnesota tends to underpredict the measured 95th-percentile TTI (Figure D.14). The variance among the residuals is nonconstant, with the absolute value of the residual reaching its maximum as the predicted value reaches its maximum. The distribution of the residuals is negatively skewed compared with a normal distribution. The *t*-test results reject the zero residual mean hypothesis.

Salt Lake City

The Salt Lake City data set shows similar results to those in the 95th-percentile TTI model validation. In the area around the origin when the mean TTI is below 1.1, the measured data consistently fall below the predicted curve, as is shown in the scatter plot (Figure D.15) and the residual plot in the attachment (Figure D.75). The *t*-test results reject the zero residual mean null hypothesis.

Spokane

This 90th-percentile TTI data-poor model does not fit the Spokane data set very well, as shown in the scatter plot

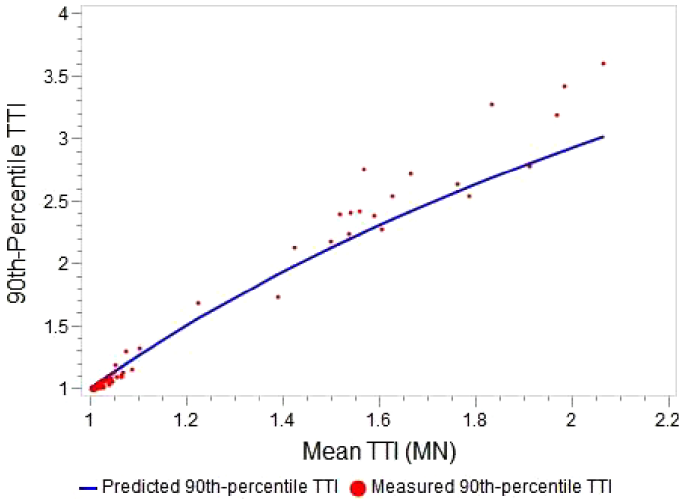

Figure D.14. Mean TTI versus 90th-percentile TTI, Minnesota.

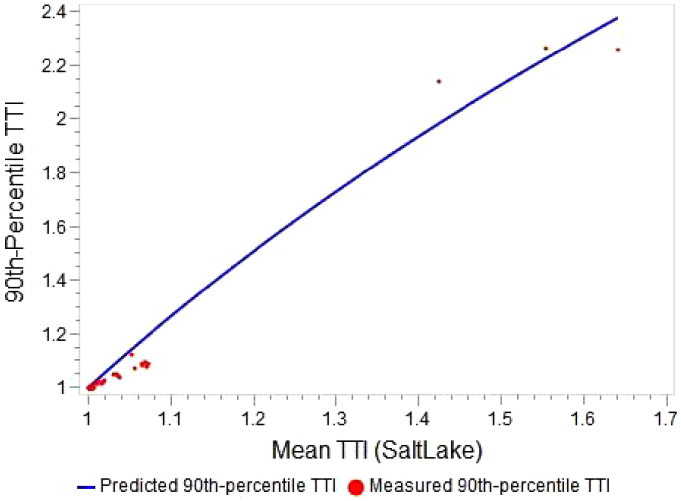

Figure D.15. Mean TTI versus 90th-percentile TTI, Salt Lake City.

(Figure D.16). However, since the data has relatively little variance, the absolute values of the residuals are small, with a maximum of 0.1118. The main problem with this model fit is that the residuals increase almost linearly with the predicted value. The distribution of the residuals is positively skewed and not normally distributed. The *t*-test results reject the zero residual mean null hypothesis.

Summary

The L03 90th-percentile TTI data-poor model generally fits the data better than the 95th-percentile model does, as shown by the lower RMSE values. This is probably due to the fact that the 90th-percentile TTI validation data has less overall variance than the 95th-percentile TTI data. The 90th-percentile TTI model tends to overpredict the 90th-percentile TTI in

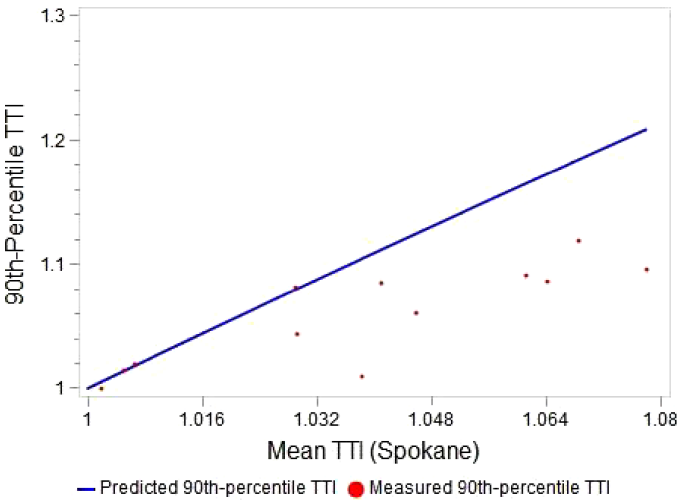

Figure D.16. Mean TTI versus 90th-percentile TTI, Spokane.

Table D.7. 90th-Percentile of TTI Model Validation Summary

Assumptions:	All	CA	MN	Salt Lake City	Spokane
Systematic nonlinear trend	NS	NS	NS	NS	NS
Residual: zero mean	NS	NS	NS	NS	NS
Residual: constant variance	NS	NS	NS	NS	NS
Residual: normal distribution	NS	NS	NS	NS	NS

Note: NS = generalized regression assumptions are not satisfied.

the California, Salt Lake City, and Spokane data sets and underestimate it in the Minnesota data. Residual analysis indicates violation of the basic normality, zero error mean, and constant error variance assumptions (summarized in Table D.7 with all "not satisfactory" assessments).

80th-Percentile TTI Model

All Sites

The RMSE values for the 80th-percentile TTI model, shown in Table D.8, are even smaller than those for the 90th-percentile TTI model. This is probably due to the fact that the 80th-percentile TTI validation data set has less variance. For each of the five data sets, RMSE is less than 0.1, which means that the mean 80th-percentile travel time prediction error is less than 10% of the corresponding free-flow travel time. In this sense, the model performs satisfactorily. However, we need more complicated validation analysis to see if the regression assumptions are satisfied.

The scatter plot (Figure D.17) and the residual plot (Figure D.18) clearly show that the data-poor model for the 80th-percentile TTI is unable to capture the trend of the response variable. In fact, the scattered data samples show a linear or convex shape, but the data-poor model shows a concave-like shape, resulting in concavely scattered residual points in the residual plot. The histogram (Figure D.19) and the normality plot (Figure D.20) both show that the residual distribution does not perfectly follow a normal distribution. The Student's *t*-test yields a *p*-value less than 0.0001, implying that we can reject the zero mean hypothesis (Table D.9).

Table D.8. RMSE Summary, 80th-Percentile TTI

CA	MN	Salt Lake City	Spokane	All Data Sets
0.0660	0.0896	0.0290	0.0447	0.0684

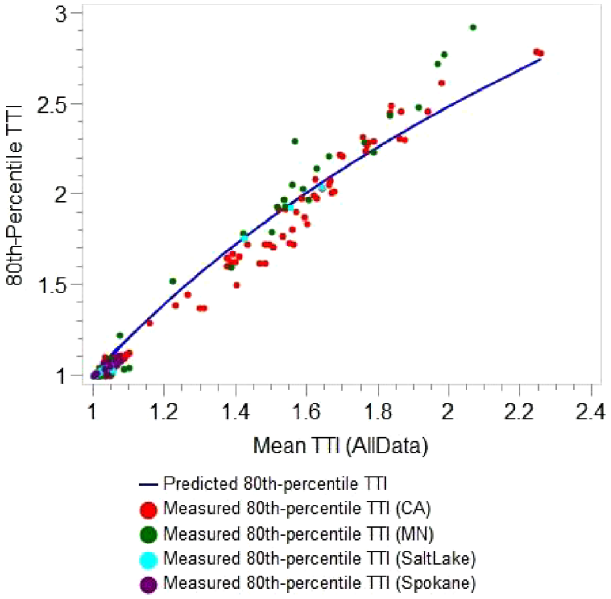

Figure D.17. Mean TTI versus 80th-percentile TTI.

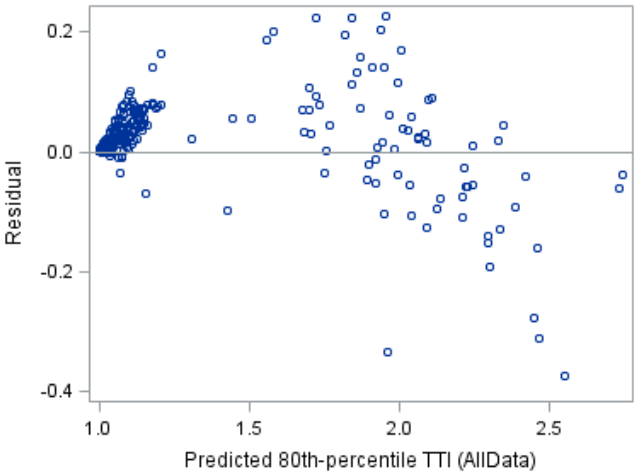

Figure D.18. Residual plot—80th-percentile TTI—AllData.

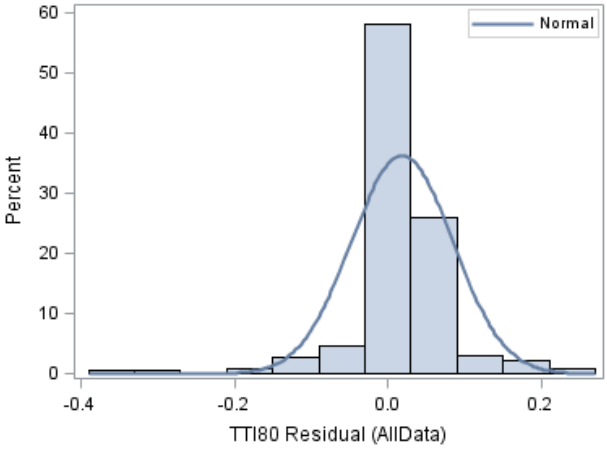

Figure D.19. Histogram of residuals—80th-percentile TTI—AllData.

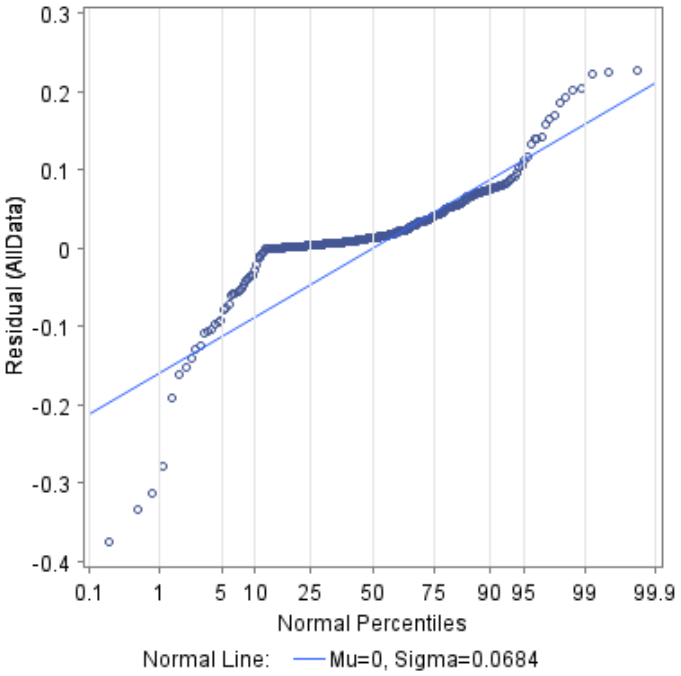

Figure D.20. Normality plot of residuals—80th-percentile TTI—AllData.

Table D.9. Statistical Residual Analysis Results—80th-percentile TTI—AllData

Table D.9.a. Basic Summary

Location		Variability	
Mean	0.0184	Std deviation	0.0660
Median	0.0135	Variance	0.0044
Min	–0.3750	Range	0.6014
Max	0.2263	Interquartile range	0.0379

Table D.9.b. Estimated Confidence Limits Assuming Normality

Parameter	Estimate	95% Confidence Limits	
Mean	0.0184	0.0111	0.0256
Std deviation	0.0660	0.0612	0.0715
Variance	0.0043	0.0037	0.0051

Table D.9.c. Student's t-Test of Zero Residual Mean

Test	Statistic	*p*-Value
Student's *t*-test	5.0051	<0.0001

Region Specific

California

The scatter plot of California data samples shows an initial tendency to fall below the predicted curve until the mean TTI exceeds 1.7, at which point the data samples tend to be above the predicted curve (Figure D.21). This obviously shows that the data-poor model fails to capture part of the variability in the response variable. The residual analysis shows nonconstant variance and a positively skewed distribution. The *t*-test results reject the zero residual mean hypothesis.

Minnesota

As in California, the 80th-percentile TTI data-poor model fails to sufficiently capture the measured data trend, especially when the mean TTI is beyond 1.5. In fact, the predicted curve shows a concave shape while the real data show a slight convex shape (Figure D.22). The nonconstant error variance problem also exists. The residuals are negatively skewed, just like for the 90th and 95th-percentile models in Minnesota. However, the *t*-test results show a *p*-value of 0.5049, meaning that we cannot reject the null hypothesis of zero mean.

Salt Lake City

The Salt Lake City data points all fall below the predicted line (Figure D.23), but the residuals are all very small (less than 0.1), meaning that the predicted values are very close to the true values. However, the residual distribution does not closely follow a normal distribution. The *t*-test results reject the zero residual mean null hypothesis.

Spokane

In the scatter plot for the Spokane results, sample points largely fall below the predicted line (Figure D.24), indicating that the model overestimates the 80th-percentile TTI. In addition, this

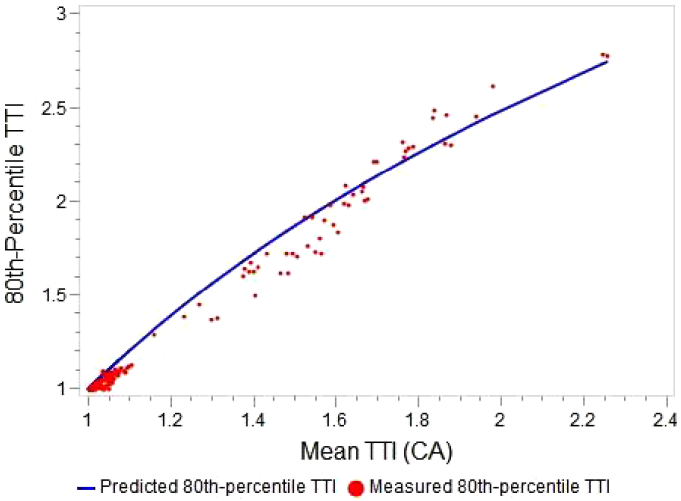

Figure D.21. Mean TTI versus 80th-percentile TTI, California.

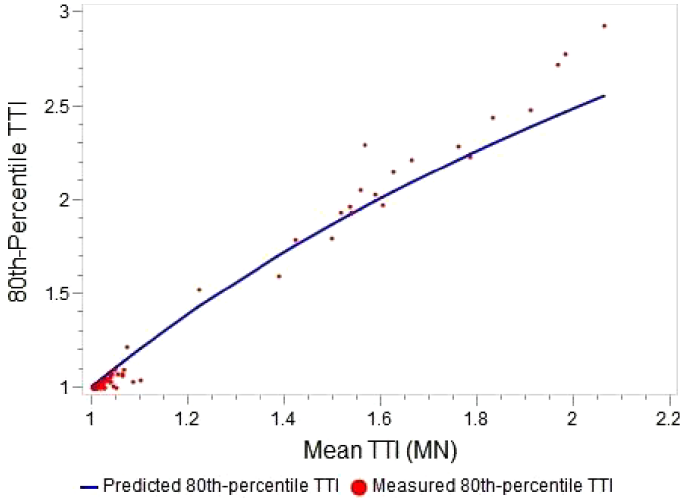

Figure D.22. 80th-percentile TTI versus mean TTI.

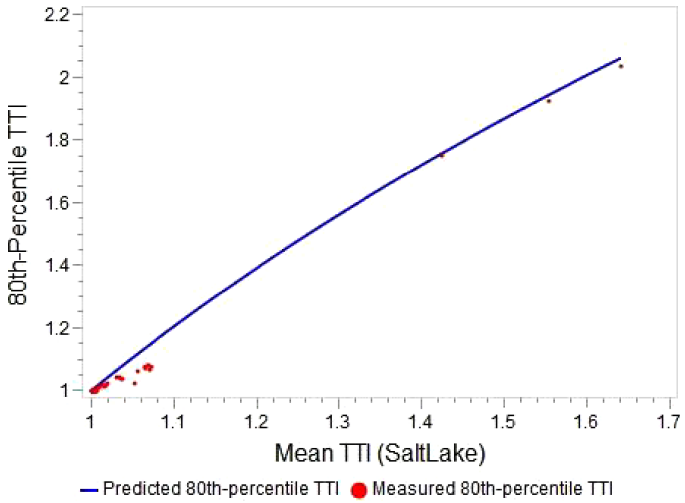

Figure D.23. 80th-percentile TTI versus mean TTI, Salt Lake City.

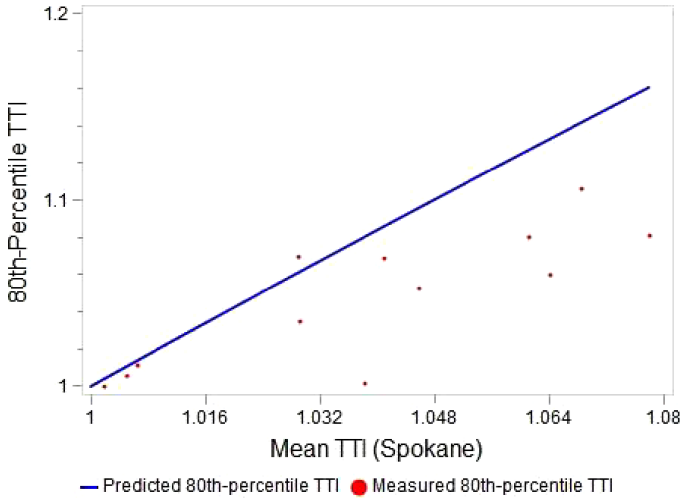

Figure D.24. 80th-percentile TTI versus mean TTI, Spokane.

Table D.10. 80th-Percentile of TTI Model Validation Summary

Assumptions:	All	CA	MN	Salt Lake City	Spokane
Systematic nonlinear trend	NS	NS	NS	NS	NS
Residual: zero mean	NS	NS	S	NS	NS
Residual: constant variance	NS	NS	NS	NS	NS
Residual: normal distribution	NS	NS	NS	NS	NS

Note: NS = generalized regression assumptions are not satisfied; S = satisfied.

overestimation tends to increase as the mean TTI increases, meaning that the residuals are positively correlated with the predicted values. The residuals are not normally distributed. The *t*-test results reject the zero residual mean null hypothesis.

Summary

Although the RMSE table shows that the average prediction error is within 10% of TTI, the validation analysis for the 80th-percentile TTI data-poor model shows that the lack of fit is obvious for all four data sets. Specifically, the model fails to capture the correct curvature of the California data and Minnesota data and tends to overestimate the 80th-percentile TTI for the Salt Lake City and Spokane data sets. Essentially they are the same problem, since the last two data sets have less variance and thus only represent the area with low mean TTIs. Nonnormally distributed residual, nonzero residual mean, and nonconstant error variance problems were all shown in the validation analysis (Table D.10), but the primary concern is the lack of fit for the curvature.

Standard Deviation of TTI Model

Overview

Table D.11 summarizes the RMSE for the data-poor standard deviation (std) of the TTI model. The magnitude of these values is not large since the standard deviation of TTI data itself has a small magnitude, mostly less than 1.1. The highest RMSE is in Minnesota while the lowest is in Salt Lake City.

The scatter plot (Figure D.25) and the residual plot (Figure D.26) together show that the model has lack of fit problems.

Table D.11. RMSE Summary, Standard Deviation of TTI

CA	MN	Salt Lake City	Spokane	All Data Sets
0.0839	0.1028	0.0586	0.0672	0.0855

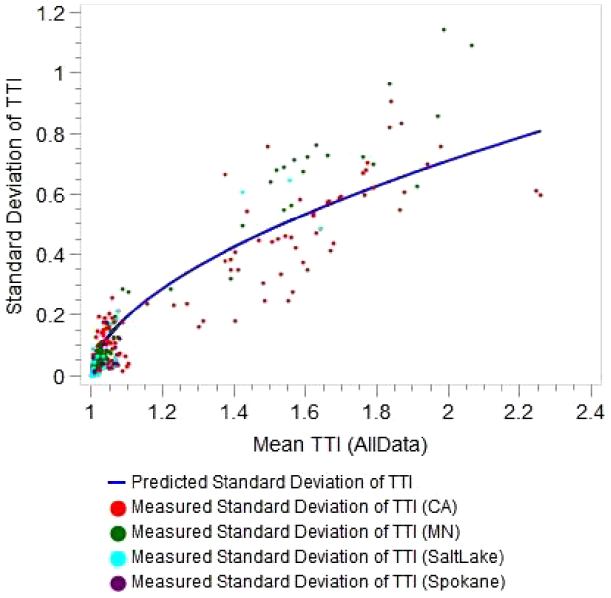

Figure D.25. Standard deviation TTI versus mean TTI.

The measured standard deviation increases faster than the predicted standard deviation. The histogram (Figure D.27) and the normality plot (Figure D.28) both indicate that the residual distribution approximately follows a normal curve, although a negative skew exists. In Table D.12, a *p*-value of 0.0430 in the Student's *t*-test demonstrates that the residual distribution does not have a zero mean.

Region Specific

California

The scatter plot of the California data set in Figure D.29 shows that most data points fall near the predicted curve. However, the shapes of the scattered points and the predicted line do not match very well; the predicted line initially tends to overestimate the standard deviation of TTI and then underestimates it at high mean TTIs. The residuals indicate nonconstant variance and a lack of fit problem. The residual distribution is close to normal, with a small positive skew. The *t*-test results reject the null hypothesis that the residual mean is zero.

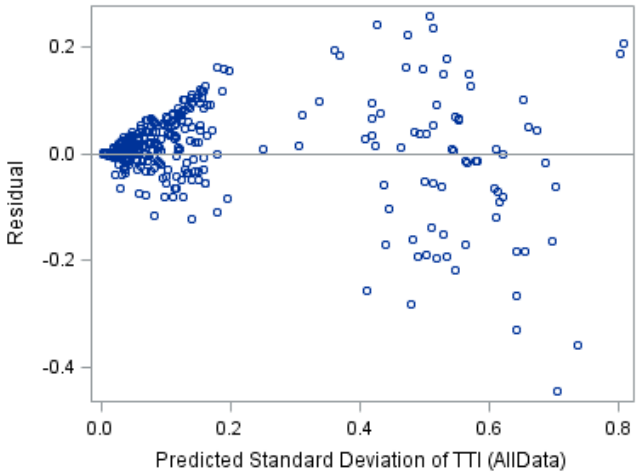

Figure D.26. Residual plot—standard deviation of TTI—AllData.

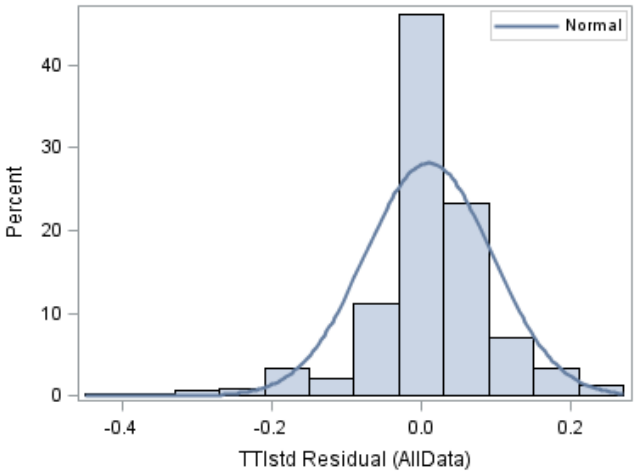

Figure D.27. Histogram of residuals—standard deviation of TTI—AllData.

Minnesota

The problem of lack of fit is obvious in the Minnesota data scatter plot. The model line fails to follow the upward trend in the measured data set, instead gradually flattening as the mean TTI increases (Figure D.30). The residual analysis confirms this problem and shows that the residual variance is nonconstant.

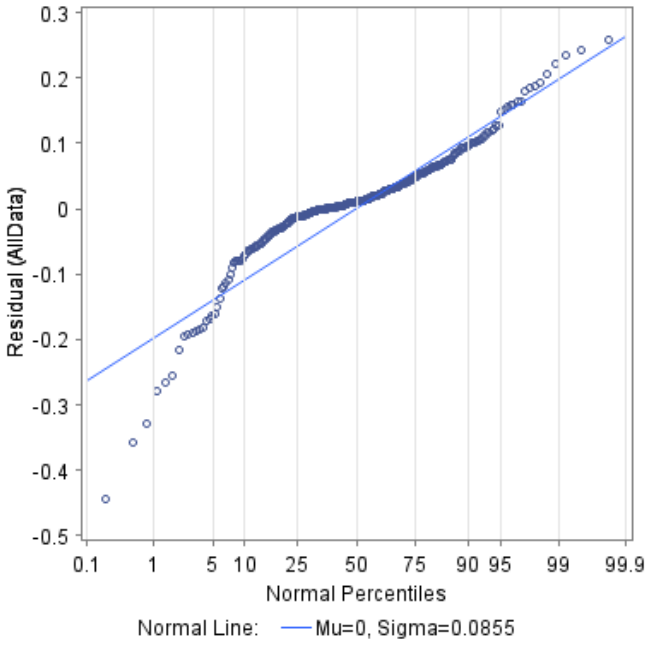

Figure D.28. Normality plot of residuals—standard deviation of TTI—AllData.

Table D.12. Statistical Residual Analysis Results—standard deviation of TTI

Table D.12.a. Basic Summary

Location		Variability	
Mean	0.0096	Std deviation	0.0850
Median	0.0110	Variance	0.0072
Min	−0.4453	Range	0.7044
Max	0.2590	Interquartile range	0.0626

Table D.12.b. Estimated Confidence Limits Assuming Normality

Parameter	Estimate	95% Confidence Limits	
Mean	0.0096	0.0003	0.0189
Std deviation	0.0851	0.0790	0.0922
Variance	0.0072	0.0062	0.0085

Table D.12.c. Student's t-Test of Zero Residual Mean

Test	Statistic	*p*-Value
Student's *t*-Test	2.0322	0.0430

The distribution of residuals is negatively skewed. The *t*-test results reject the null hypothesis of zero residual mean.

Salt Lake City

The standard deviation of a TTI data-poor model largely predicts the trend in the measured Salt Lake City data (Figure D.31). The residual analysis shows the nonconstant variance problem. The *t*-test has a *p*-value of 0.0907, meaning that we cannot reject the null hypothesis that the residual mean is zero.

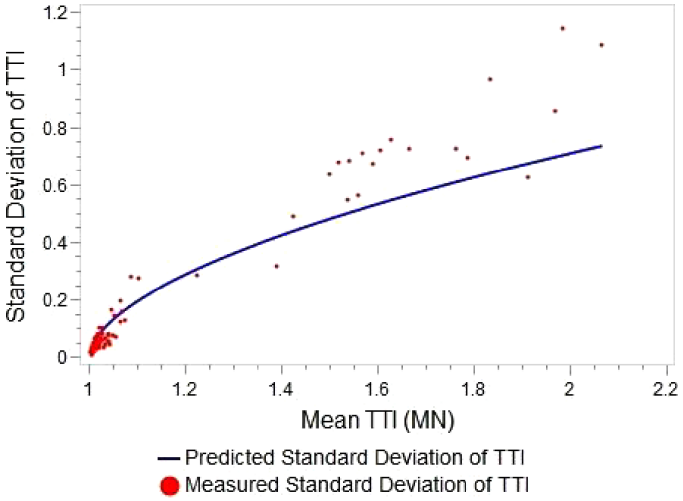

Figure D.30. Standard deviation TTI versus mean TTI, Minnesota.

Spokane

The mean TTI in the Spokane data spreads from 1.0 to 1.08. Thus the data has very little variance and is collected all in near free-flow conditions. Figure D.32 shows that only two data points fall to the left of the data-poor model curve while all other 10 points fall to the right of that curve. The residuals are scattered in an unbalanced way and have nonconstant variance. The distribution of residuals does not closely follow a normal distribution. The *t*-test results show that we can reject the null hypothesis that the residual mean is zero.

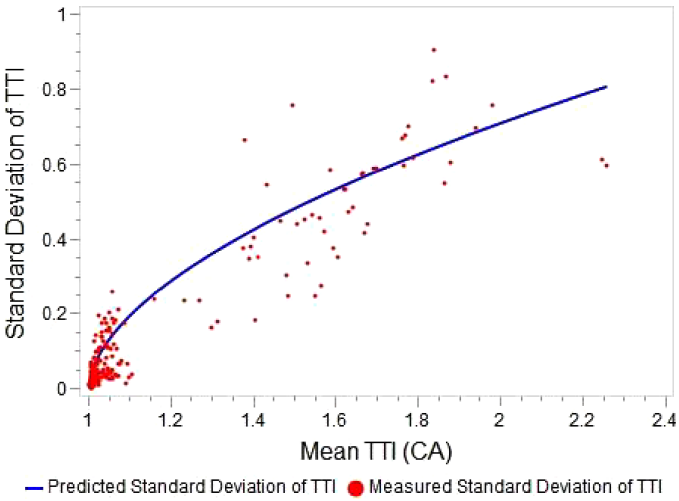

Figure D.29. Standard deviation TTI versus mean TTI, California.

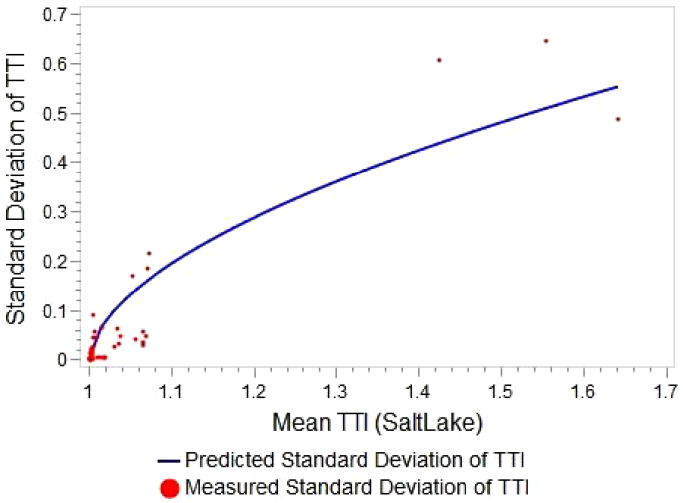

Figure D.31. Standard deviation TTI versus mean TTI, Salt Lake City.

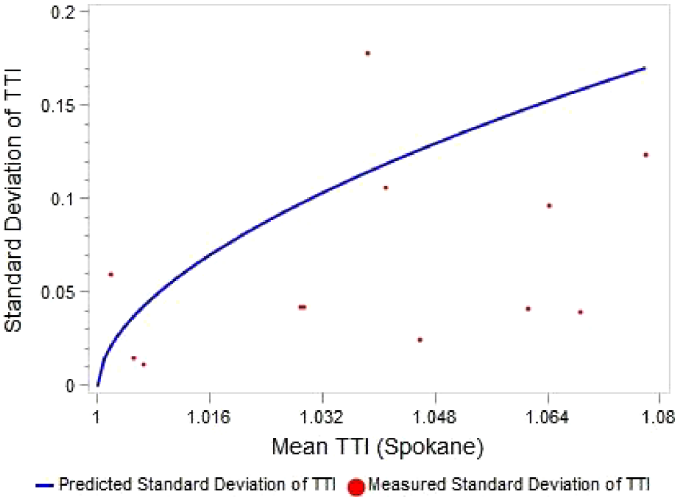

Figure D.32. Standard deviation TTI versus mean TTI, Spokane.

Summary

Overall, nonconstant variance is a problem for all data sets, and the nonzero residual mean is a problem for all data sets except for Salt Lake City. The California data set presents relatively good residual distributions that closely follow a normal distribution. Overall, though, we conclude that the standard deviation of TTI model does not adequately capture the measured data pattern. Table D.13 summarizes the validation results for this model based on subjective observation and objective statistical analysis.

Percentage of On-Time Trips with Over 50 mph Mean Speed

All Sites

Let "PctTripsOnTime50mph" denote a short name for "percentage of on-time trips with over 50 mph mean speed."

Table D.13. Standard Deviation of TTI Model Validation Summary

Assumptions:	All	CA	MN	Salt Lake City	Spokane
Systematic nonlinear trend	NS	NS	NS	S	NS
Residual: zero mean	NS	NS	NS	S	NS
Residual: constant variance	NS	NS	NS	NS	NS
Residual: normal distribution	S	S	NS	NS	NS

Note: NS = generalized regression assumptions are not satisfied; S = satisfied.

Table D.14. RMSE Summary, PctTripsOnTime50mph

CA	MN	Salt Lake City	Spokane	All Data Sets
0.0891	0.0617	0.0552	0.0721	0.0784

Similarly, in the next two sections, "PctTripsOnTime45mph" and "PctTripsOnTime30mph" are used for mean speed thresholds of 45 mph and 30 mph, respectively. The RMSE table for PctTripsOnTime50mph shows that the smallest RMSE comes from the Salt Lake City data, while the largest comes from the California data (Table D.14). However, all RMSE values are less than 0.1, or 10% of the number of all trips, which indicates good model performance.

The scatter plot (Figure D.33) shows that the data-poor model can generally predict the trend of PctTripsOnTime 50mph. However, the residual plot (Figure D.34) shows a clear nonrandom pattern when mean TTI is around 1.0, indicating that the model may be improved by some form of data transformation. The histogram (Figure D.35) and the normality plot (Figure D.36) both show that the residual distribution displays an almost perfect normal distribution shape when the residual is less than zero but differentiates from the normal distribution reference line when the residual is larger than zero. It is also shown that more samples have negative residuals than have positive residuals. The *t*-test results in Table D.15 demonstrate that the null hypothesis of the zero residual mean can be rejected with a 95% level

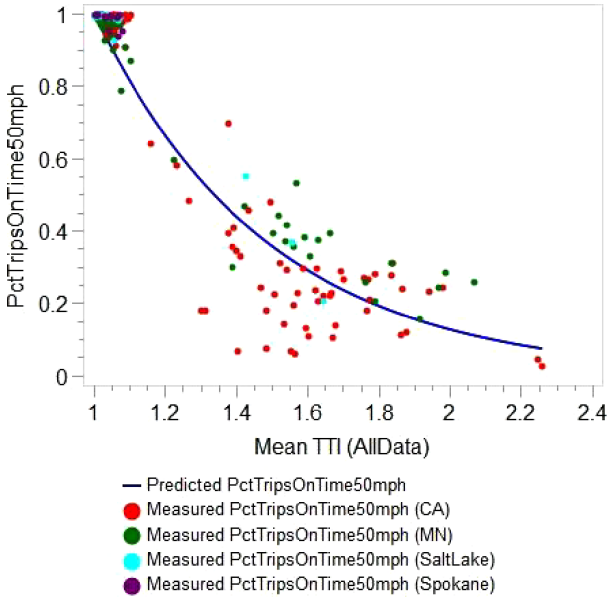

Figure D.33. PctTripsOnTime50mph versus mean TTI.

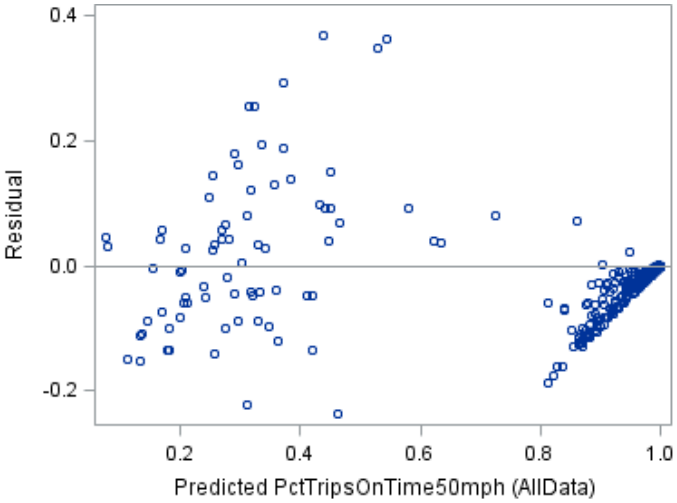

Figure D.34. Residual plot—PctTripsOnTime50mph—AllData.

of confidence since the *p*-value is less than 0.0001. Overall, the model performs satisfyingly to some extent but leaves room for improvement.

Region Specific

CALIFORNIA

The PctTripsOnTime50mph data-poor model tends to underestimate the response variable in California when the mean TTI is close to 1.0 (uncongested conditions). However, when the mean TTI becomes larger than 1.4, the data-poor model tends to overestimate the response variable

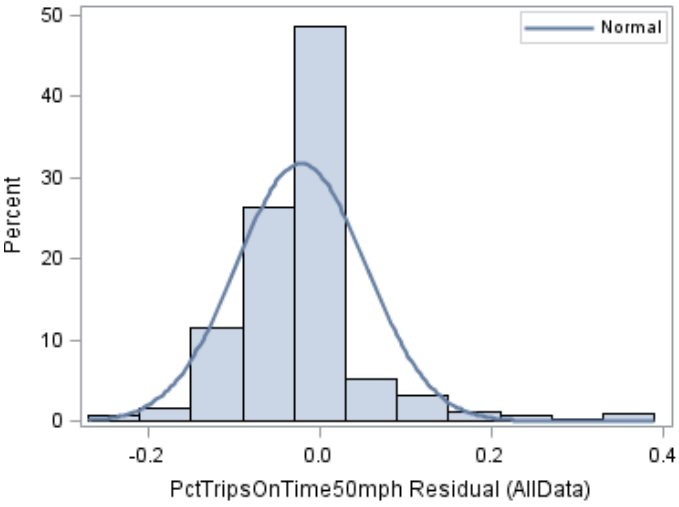

Figure D.35. Histogram of residuals—PctTripsOnTime50mph—AllData.

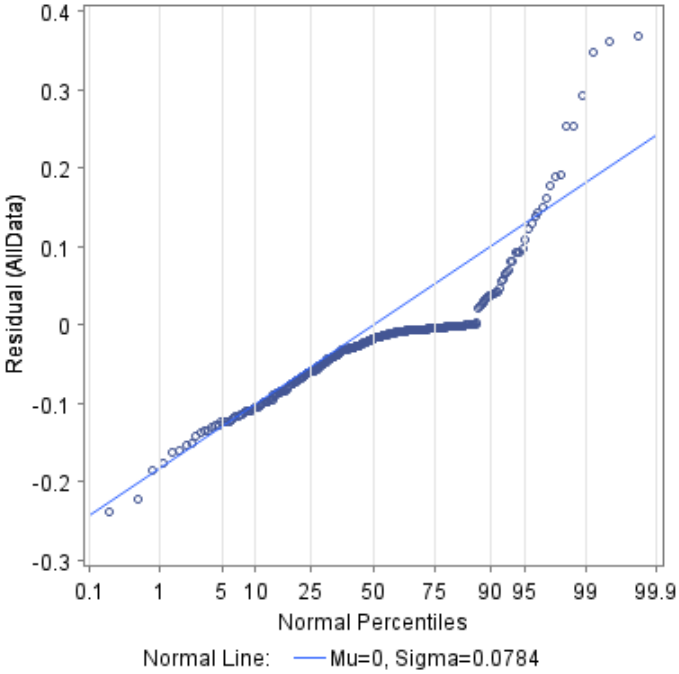

Figure D.36. Normality plot of residuals—PctTripsOnTime50mph—AllData.

Table D.15. Statistical Residual Analysis Results—PctTripsOnTime50mph—AllData

Table D.15.a. Basic Summary

Location		Variability	
Mean	–0.0221	Std deviation	0.0754
Median	–0.0172	Variance	0.0057
Min	–0.2374	Range	0.6062
Max	0.3687	Interquartile range	0.0565

Table D.15.b. Estimated Confidence Limits Assuming Normality

Parameter	Estimate	95% Confidence Limits	
Mean	–0.0221	–0.0303	–0.0138
Std deviation	0.0754	0.0700	0.0817
Variance	0.0057	0.0049	0.0067

Table D.15.c. Student's t-Test of Zero Residual Mean

Test	Statistic	*p*-Value
Student's *t*-Test	–5.2626	<0.0001

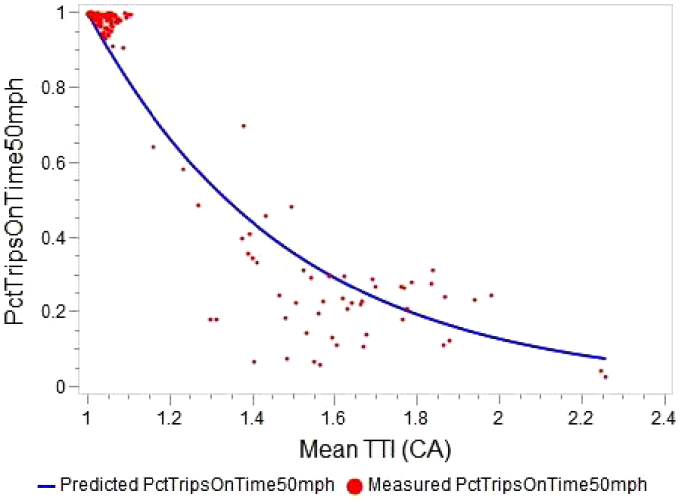

Figure D.37. PctTripsOnTime50mph versus mean TTI, California.

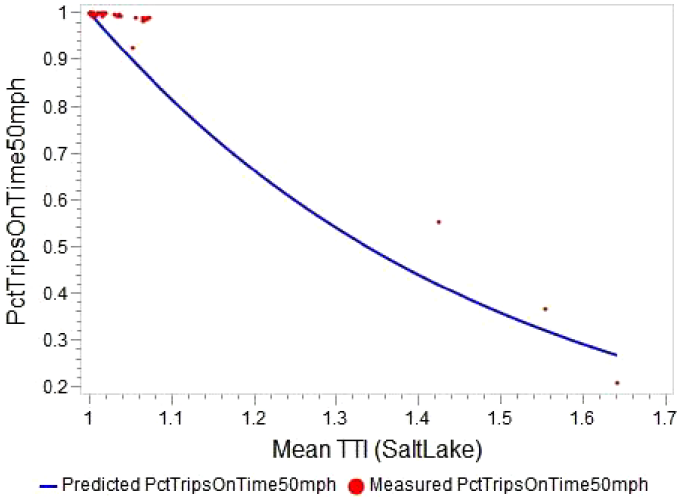

Figure D.39. PctTripsOnTime50mph versus mean TTI, Salt Lake City.

(Figure D.37). The residuals show nonconstant variance. The residual distribution approximately follows a normal distribution but with a positive skew. The *t*-test results show that evidence is not sufficient to reject the null hypothesis of zero residual mean.

Minnesota

In the Minnesota data validation, the data-poor model tends to consistently underestimate the response variable, as shown in Figure D.38. The nonconstant variance problem exists in this data set. The residuals do not closely follow a normal distribution and have a slight negative skew. The *t*-test results show strong evidence to reject the null hypothesis of zero residual mean.

Salt Lake City

The data-poor model fails to capture the Salt Lake City data pattern when the mean TTI is below 1.1, as shown in the scatter plot (Figure D.39). The nonconstant variance problem still exists, but the primary concern is the inability to predict the measured data trend. The distribution of residuals does not closely follow a normal distribution and is negatively skewed. The *t*-test results reject the zero residual mean hypothesis.

Spokane

The Spokane measured data all fall above the data-poor model line (Figure D.40). There is a positive correlation between the residuals and the predicted values. The residuals are not normally distributed but rather appear uniformly distributed.

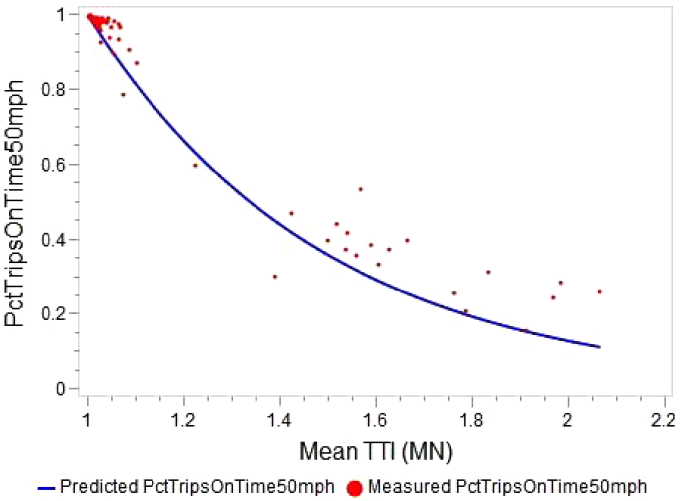

Figure D.38. PctTripsOnTime50mph versus mean TTI, Minnesota.

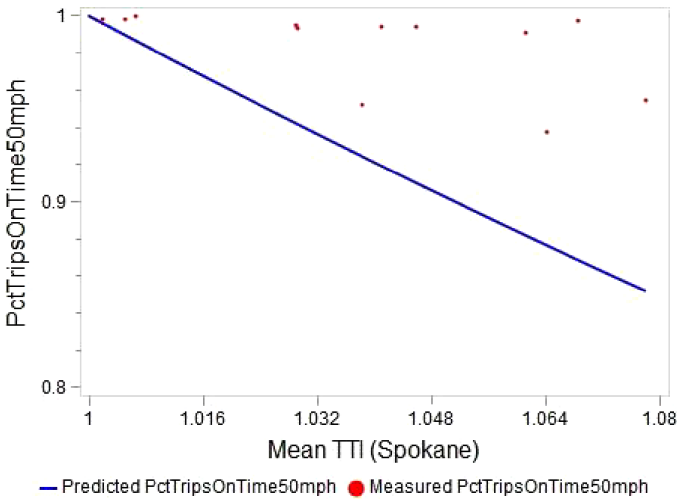

Figure D.40. PctTripsOnTime50mph versus mean TTI, Spokane.

Table D.16. PctTripsOnTime50mph Model Validation Summary

Assumptions:	All	CA	MN	Salt Lake	Spokane
Systematic nonlinear trend	NS	NS	NS	NS	NS
Residual: zero mean	NS	S	NS	NS	NS
Residual: constant variance	NS	NS	NS	NS	NS
Residual: normal distribution	NS	NS	NS	NS	NS

Note: NS = generalized regression assumptions are not satisfied; S = satisfied.

The *t*-test results show sufficient evidence to reject the zero residual mean hypothesis.

Summary

The PctTripsOnTime50mph data-poor model can largely predict the data trend of the measured validation data sets but tends to underestimate PctTripsOnTime50mph, especially when the mean TTI is small. The RMSE values are all below 0.1, indicating an average prediction error of less than 10% of the total number of trips. The California data has a weak indication of zero residual mean, but other data sets all show strong evidence of violating this assumption. The residual plots show that there is some uncaptured pattern in the data sets. The constant variance assumption cannot be satisfied in any data set; neither can the normal residual distribution assumption. Table D.16 summarizes these conclusions in a qualitative way.

Percentage of On-Time Trips with Over 45 mph Mean Speed

All Sites

The PctTripsOnTime45mph model validation results show that all the RMSE values are between 4% and 7%, which is an indication of relatively good performance (Table D.17). The scatter plot demonstrates that the data-poor model can largely predict the trend of the validation data, but it tends to underestimate the response when the mean TTI is below 1.1 (Figure D.41). A corresponding pattern along with an indication of nonconstant variance can be found in the residual plot (Figure D.42). The histogram (Figure D.43) and the normality plot (Figure D.44) both show that the residual

Table D.17. RMSE Summary, PctTripsOnTime45mph

CA	MN	Salt Lake City	Spokane	All Data Sets
0.0681	0.0480	0.0433	0.0553	0.0602

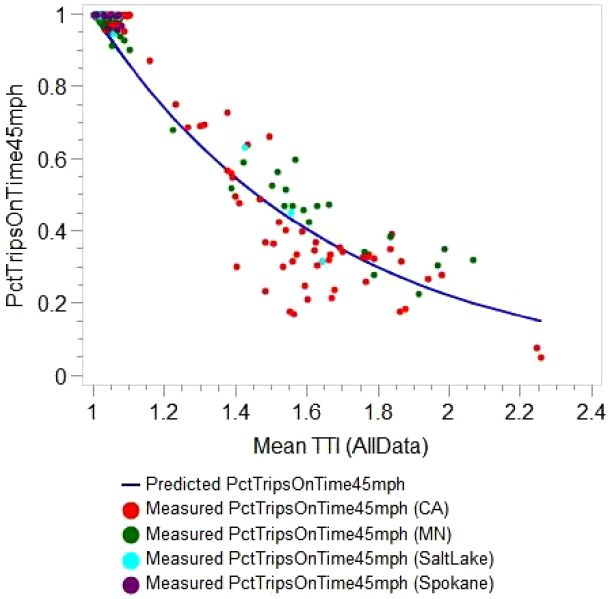

Figure D.41. PctTripsOnTime45mph versus mean TTI.

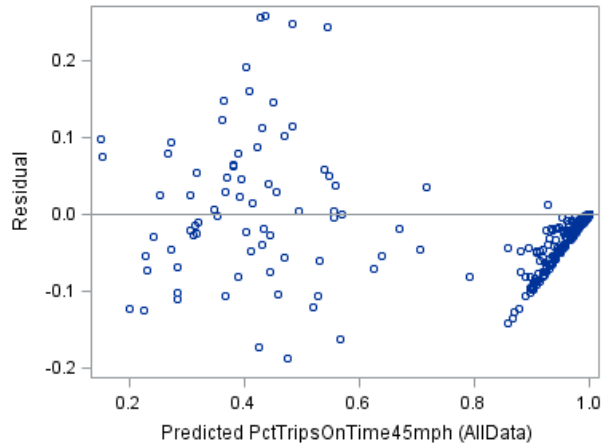

Figure D.42. Residual plot—PctTripsOnTime45mph—AllData.

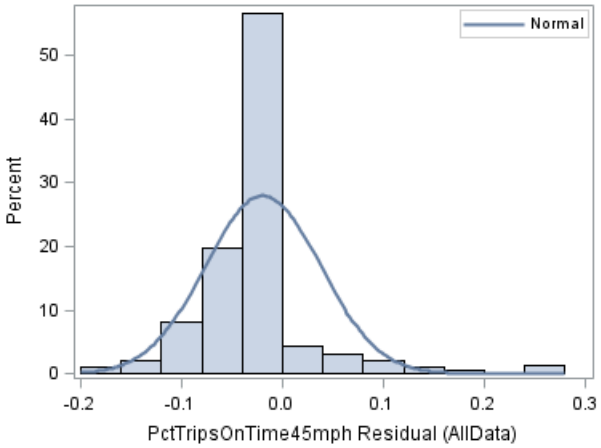

Figure D.43. Histogram of residuals—PctTripsOnTime45mph—AllData.

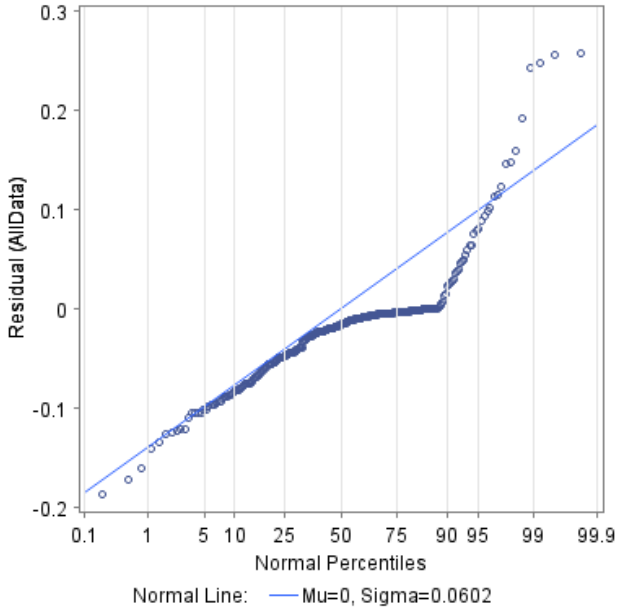

Figure D.44. Normality plot of residuals—PctTripsOnTime45mph—AllData.

distribution closely follows a normal distribution when the residual is less than zero but is skewed when the residual is larger than zero. The Student's *t*-test yields a *p*-value less than 0.0001, indicating that the null hypothesis can be rejected at a 95% level of confidence, as shown in Table D.18.

Region Specific

California

The data-poor model predicts a curve that generally approximates the measured trend. However, it tends to underestimate the response variable when the mean TTI is smaller than 1.1 while overestimating when the mean TTI is larger than 1.4 (Figure D.45). The residuals closely follow a normal distribution when the residuals are negative but are skewed when the residuals are positive. The *t*-test results imply that the zero mean residual assumption can be rejected.

Minnesota

The scatter plot (Figure D.46) and the residual analysis indicate that the data-poor model can predict the general pattern of the Minnesota data but tend to underestimate the response variable. The nonconstant variance problem also exists. The residuals do not appear to be normally distributed. The *t*-test shows strong evidence to reject the zero residual mean hypothesis.

Salt Lake City

The data-poor model tends to underestimate the response variable in the Salt Lake City validation data (Figure D.47). The nonconstant residual variance is evident, but the inadequate model trend problem is the primary concern. The residual distribution does not closely follow a normal distribution.

Table D.18. Statistical Residual Analysis Results—PctTripsOnTime45mph—AllData

Table D.18.a. Basic Summary

Location		Variability	
Mean	–0.0196	Std deviation	0.0570
Median	–0.0156	Variance	0.0033
Min	–0.1877	Range	0.4463
Max	0.2587	Interquartile range	0.0438

Table D.18.b. Estimated Confidence Limits Assuming Normality

Parameter	Estimate	95% Confidence Limits	
Mean	–0.0196	–0.0258	–0.0133
Std deviation	0.0570	0.0530	0.0618
Variance	0.0033	0.0028	0.0038

Table D.18.c. Student's t-Test of Zero Residual Mean

Test	Statistic	*p*-Value
Student's *t*-test	–6.1626	<0.0001

The *t*-test results indicate that we can reject the zero residual mean assumption.

Spokane

In the Spokane scatter plot (Figure D.48), sample points all fall above the data-poor model curve. As the mean TTI increases,

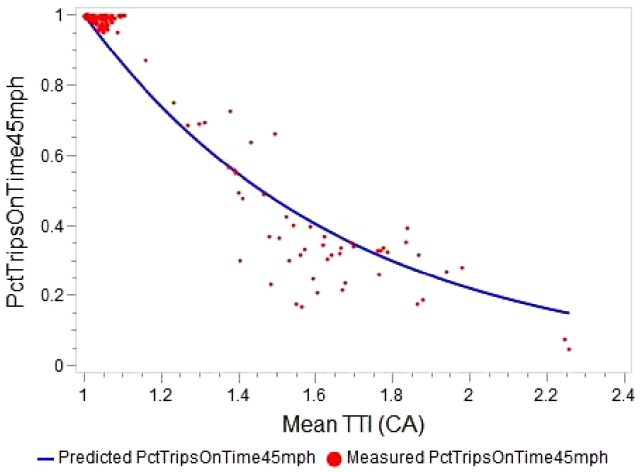

Figure D.45. PctTripsOnTime45mph versus mean TTI, California.

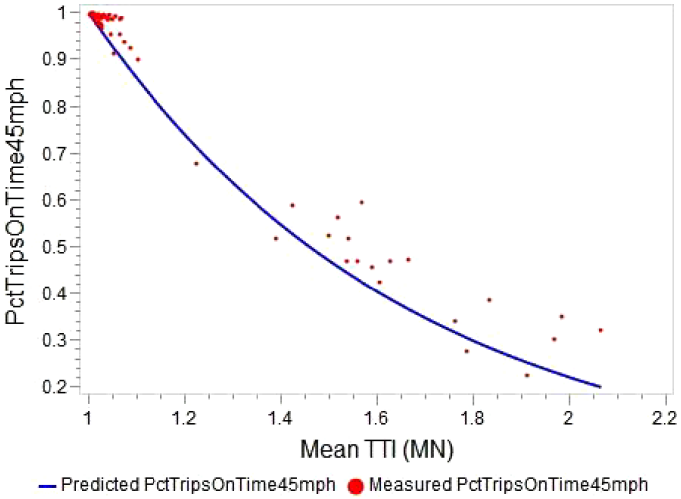

Figure D.46. PctTripsOnTime45mph versus mean TTI, Minnesota.

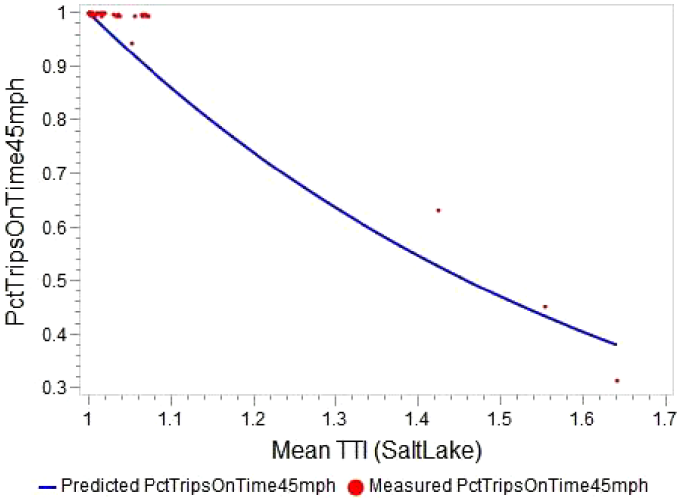

Figure D.47. PctTripsOnTime45mph versus mean TTI, Salt Lake City.

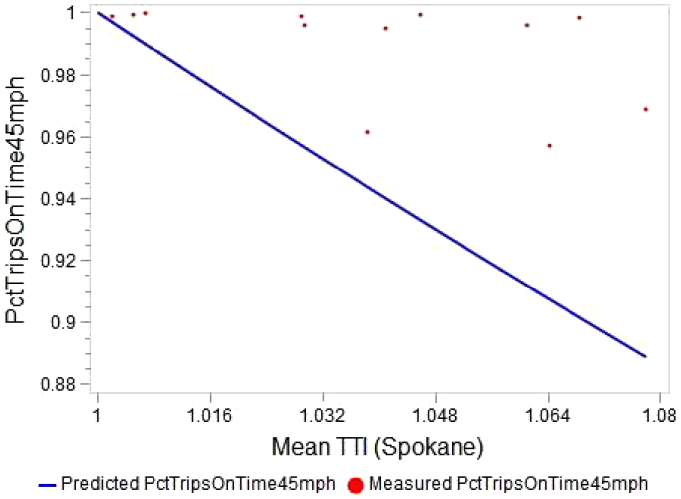

Figure D.48. PctTripsOnTime45mph versus mean TTI, Spokane.

Table D.19. PctTripsOnTime45mph Model Validation Summary

Assumptions:	All	CA	MN	Salt Lake	Spokane
Systematic nonlinear trend	NS	NS	NS	NS	NS
Residual: zero mean	NS	NS	NS	NS	NS
Residual: constant variance	NS	NS	NS	NS	NS
Residual: normal distribution	NS	NS	NS	NS	NS

Note: NS = generalized regression assumptions are not satisfied.

the measured PctTripsOnTime45mph decreases much more slowly than the predicted curve. The residuals are positively correlated with the predicted value, which implies lack of fit. Because the Spokane data have little variance, the prediction error is in fact not large. The residuals appear to be uniformly, rather than normally, distributed. The *t*-test results indicate that we can reject the zero residual mean assumption.

Summary

The PctTripsOnTime45mph data-poor model can predict the general trend of the validation data sets. However, evidence suggests that the models violate basic regression assumptions, meaning that the model has room for improvement. Specifically, the model tends to underestimate when mean TTI is small, which indicates lack of fit. Note that all residual means are negative. The constant residual variance assumption is found to be violated through examining the residual plot. Normal distribution of residuals and zero residual mean assumptions cannot be satisfied either.

Table D.19 summarizes the performance evaluation results qualitatively.

Percentage of On-Time Trips with Over 30 mph Mean Speed

All Sites

The PctTripsOnTime30mph data-poor model predicts the four validation data sets with a maximum RMSE of 0.0329, indicating good performance (Table D.20). The model largely captures the data trend (Figure D.49), and the residual plot (Figure D.50) shows a much better pattern than that in the previous two sections. However, a potential lack of fit is evidenced by the

Table D.20. RMSE Summary, PctTripsOnTime30mph

CA	MN	Salt Lake City	Spokane	All Data Sets
0.0247	0.0329	0.0134	0.00674	0.0254

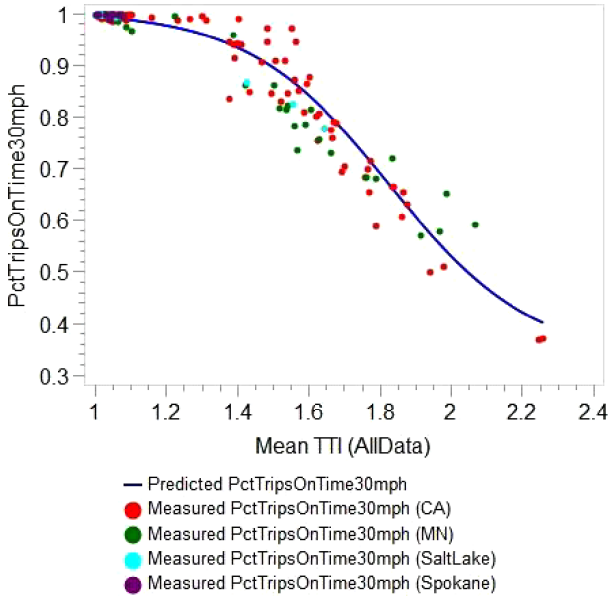

Figure D.49. PctTripsOnTime30mph versus mean TTI.

concave-like shape. A nonconstant variance problem is also indicated by the cone shape in the residual plot. The histogram and the normality plot (Figure D.51 and Figure D.52) show that the residual distribution has much less variance than that of a normal distribution but the residual mean is highly likely to be zero. The Student's *t*-test demonstrates this zero residual mean assumption with a *p*-value of 0.6689 (Table D.21).

Region Specific

California

The scatter plot of California data shows that the data-poor model closely predicts the measured data trend (Figure D.53). However, it is also clear that the model can still be improved

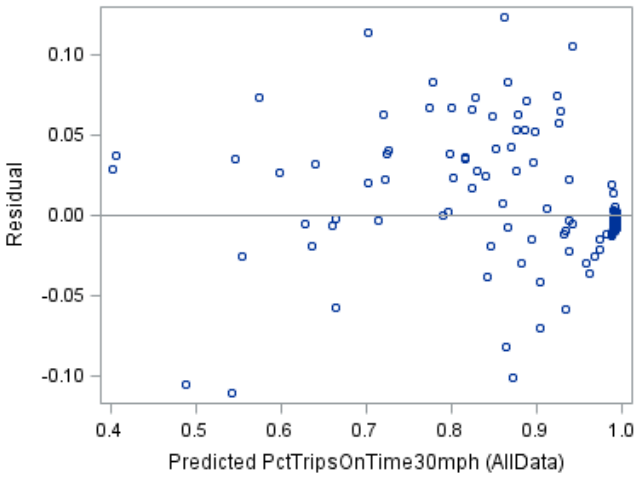

Figure D.50. Residual plot—PctTripsOnTime30mph—AllData.

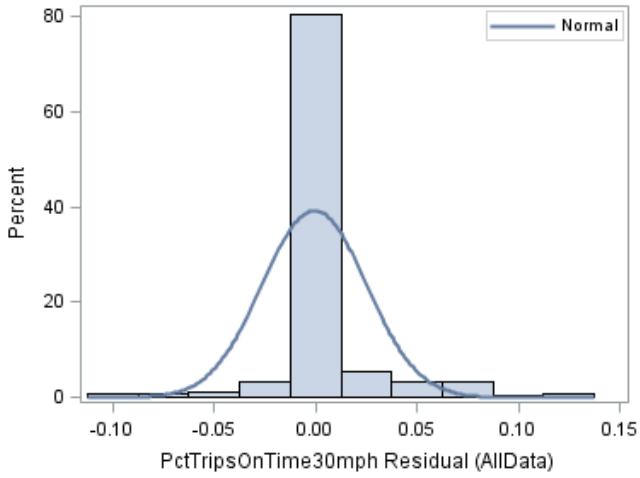

Figure D.51. Histogram of residuals—PctTripsOnTime30mph—AllData.

since the model tends to underestimate the response variable when the mean TTI is below 1.6 and to overestimate it when the mean TTI is above 1.6. The residual analysis indicates lack of fit and nonconstant variance. The residuals do not appear to be normally distributed. The *t*-test results show that the null hypothesis of zero residual mean cannot be rejected.

Minnesota

The scatter plot of Minnesota data also shows that this data-poor model generally follows the measured data trend but is obviously not adequate (Figure D.54). The residual plot included in the attachment shows a concave pattern, indicating some lack of fit. The nonconstant variance problem

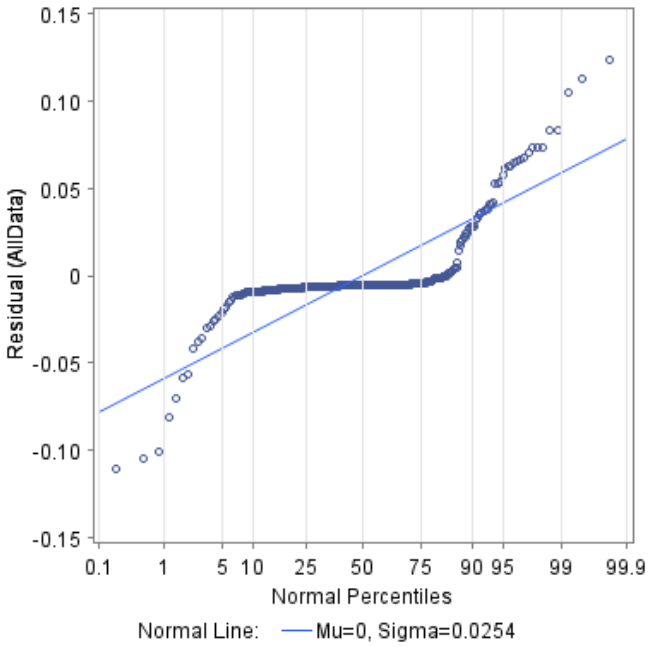

Figure D.52. Normality plot of residuals—PctTripsOnTime30mph—AllData.

Table D.21. Statistical Residual Analysis Results—PctTripsOnTime30mph—AllData

Table D.21.a. Basic Summary

Location		Variability	
Mean	–0.0006	Std deviation	0.0254
Median	–0.0055	Variance	0.0006
Min	–0.1103	Range	0.2336
Max	0.1233	Interquartile range	0.0021

Table D.21.b. Estimated Confidence Limits Assuming Normality

Parameter	Estimate	95% Confidence Limits	
Mean	–0.0006	–0.0034	0.0022
Std deviation	0.0254	0.0236	0.0275
Variance	0.0006	0.0006	0.0008

Table D.21.c. Student's t*-Test of Zero Residual Mean*

Test	Statistic	*p*-Value
Student's *t*-test	–0.4281	0.6689

may also exist. The *t*-test cannot reject the null hypothesis of zero residual mean.

Salt Lake City

The scatter plot of the Salt Lake City data set shows that the data-poor model follows the measured data but tends to

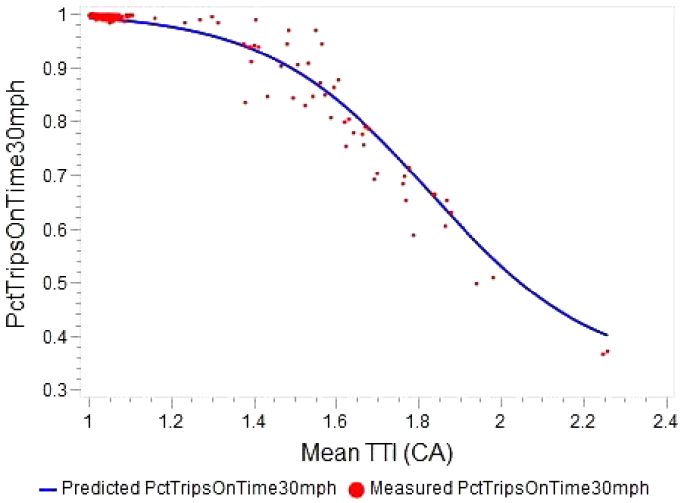

Figure D.53. PctTripsOnTime30mph versus mean TTI, California.

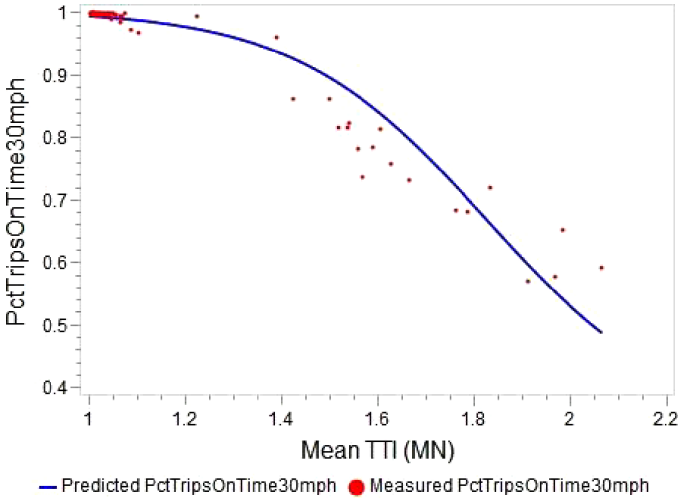

Figure D.54. PctTripsOnTime30mph versus mean TTI, Minnesota.

underestimate the response variable when the mean TTI is small, while overestimating it when the mean TTI is large (Figure D.55). The residuals do not appear to be normally distributed. The *t*-test results indicate that we cannot reject the zero residual mean null hypothesis.

Spokane

The scatter plot of the Spokane data shows that the data-poor model tends to underpredict the measured values (Figure D.56). The residuals do not appear to be normally distributed. The *t*-test results indicate that we can reject the zero residual mean hypothesis.

Summary

This PctTripsOnTime30mph data-poor model can largely predict the measured data trend but not with adequate fit. All but

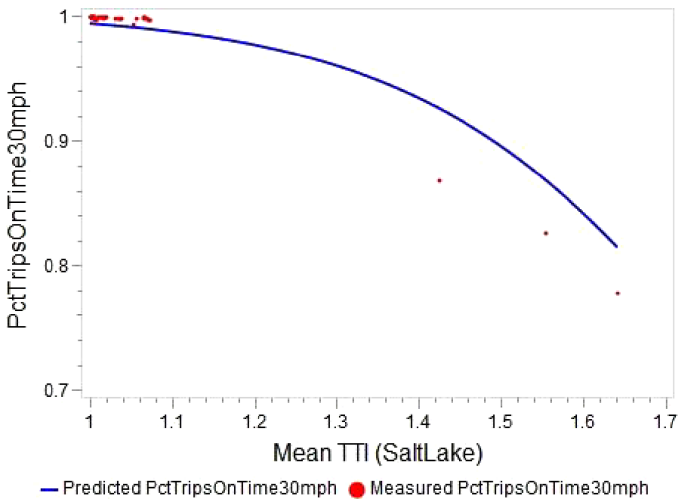

Figure D.55. PctTripsOnTime30mph versus mean TTI, Salt Lake City.

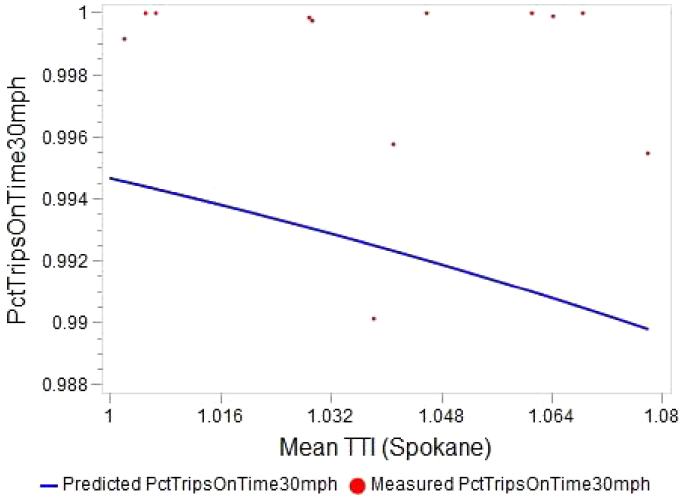

Figure D.56. PctTripsOnTime30mph versus mean TTI, Spokane.

the Spokane data satisfy the zero residual mean assumption. The normal-distributed residual assumption and the constant residual variance assumption are not satisfied in any regional data set. Potential improvements should address the slight concave pattern shown in the residual plot. Table D.22 summarizes the model validation results for the PctTripsOnTime30mph model.

Conclusions

The validation of the L03 data-poor models was performed on four regional data sets (California, Minnesota, Salt Lake City, and Spokane), as well as on the combined data sets overall. The main conclusion is that, while the average prediction error (measured by the RMSE) of each model is generally acceptable across the regions, the models violate many of the assumptions of generalized regression and thus have room for enhancement.

Table D.22. PctTripsOnTime30mph Model Validation Summary

Assumptions:	All	CA	MN	Salt Lake City	Spokane
Systematic nonlinear trend	NS	NS	NS	NS	NS
Residual: zero mean	S	S	S	S	NS
Residual: constant variance	NS	NS	NS	NS	NS
Residual: normal distribution	NS	NS	NS	NS	NS

Most of the models in nearly all of the regions violate the zero residual mean assumption, meaning that the models tend to either systematically overpredict the reliability measure (i.e., indicate that a section is less reliable than it actually is) or underpredict the reliability measure (i.e., indicate that a section is more reliable than it actually is). Interestingly, this systematic bias appears to vary regionally, with the models tending to underpredict the reliability measures in Minnesota and overpredict them in California. This lends support for building regional models rather than cross-sectional models, although insufficient data are an obstacle to regional modeling.

Additionally, most of the models in most of the regions violate the assumption of constant variance of the residuals. In just about all cases, the variance of the residuals increases with the mean TTI. This makes intuitive sense, as higher levels of baseline, recurrent congestion lead to more unreliable and unpredictable conditions. The models also tend to violate the assumptions that the residuals are normally distributed and that the model form can adequately predict the data trend. These problems all indicate that the data-poor model performance can be improved.

Another conclusion is that the model error is larger for the prediction of higher moments of the TTI distribution (i.e., the RMSEs are larger for the 95th-percentile model than for the 90th and 80th-percentile models). This makes sense because the 95th-percentile TTI is likely associated with very rare events (like a major incident or bad weather). We would thus expect these TTIs to vary greatly from section to section, making them harder to accurately model based solely on the mean TTI.

In interpreting these results and conclusions, it is important to understand how they are affected by the validation data set characteristics. Eighty percent of the section-year data included in this validation effort were collected during the weekday midday period, where mean TTIs were heavily clustered around 1. The RMSEs for this mean TTI area were very low, since section time periods that operate in free-flow conditions are relatively reliable. As illustrated by the consistent violation of the constant variance of residuals assumptions, the model error is much higher for larger mean TTIs, and these are the conditions under which systematic bias in the prediction is most evident. Unfortunately, due to the stringent definition of a peak period used in L03, very little of the Salt Lake City and Spokane data were able to contribute to this congested regime analysis, so we were only able to observe the model response to mean congested conditions at two sites (technically, the California data represent four regions). In the model enhancement phase, the research team hopes to loosen the peak period definition to be able to consider and evaluate more of the Salt Lake City and Spokane congestion.

Appendix D Attachment

95th-Percentile TTI Model

California

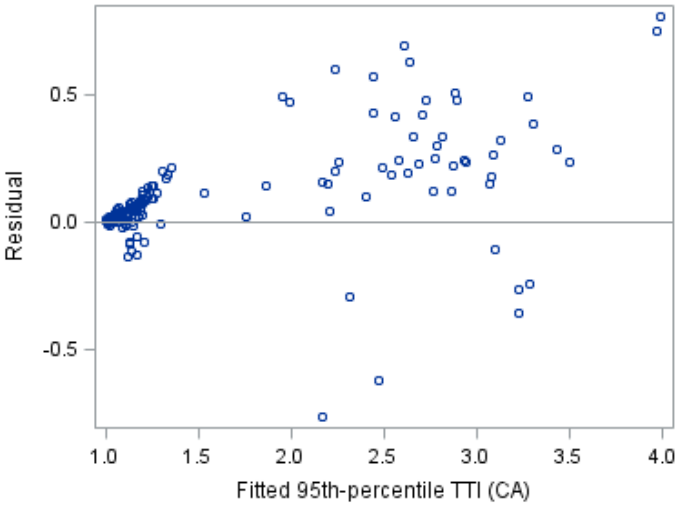

Figure D.57. Residual plot—95th-percentile TTI—California.

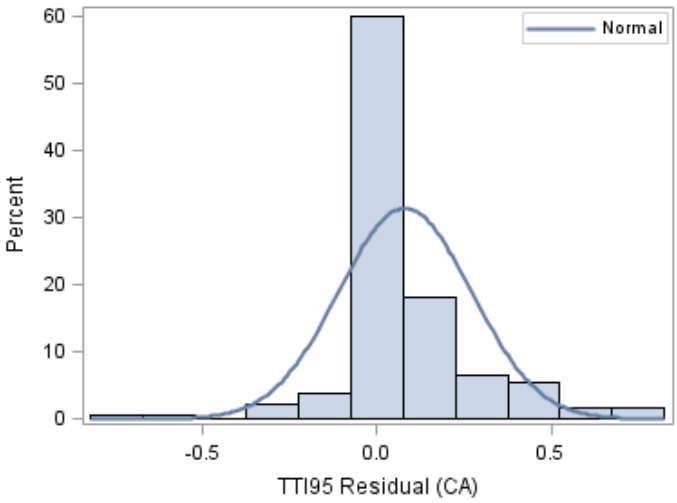

Figure D.58. Residual histogram—95th-percentile TTI—California.

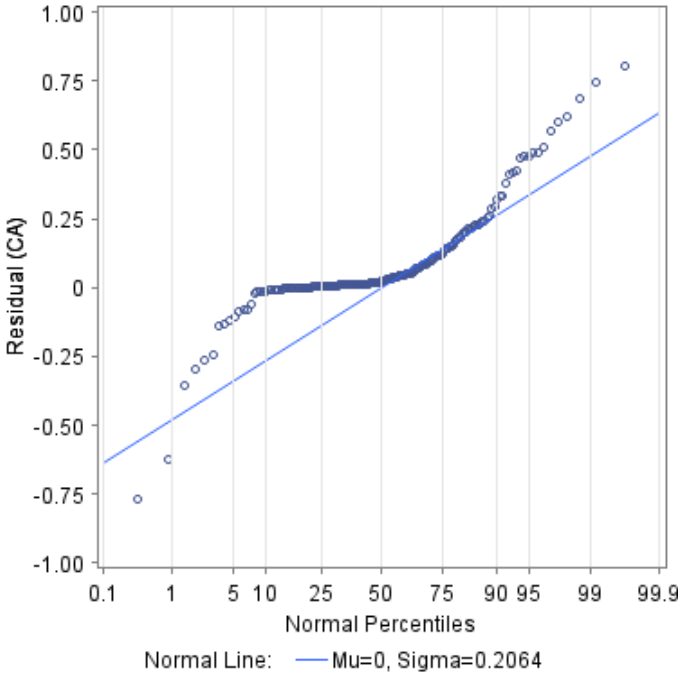

Figure D.59. Residual normality plot—95th-percentile TTI—California.

Table D.23. Residual Analysis—95th-Percentile TTI—California

Table D.23.a. Basic Summary

Location		Variability	
Mean	0.0799	Std deviation	0.1908
Median	0.0214	Variance	0.0364
Min	–0.7684	Range	1.5732
Max	0.8048	Interquartile range	0.1181

(continued on next page)

Table D.23. Residual Analysis—95th-Percentile TTI—California (continued)

Table D.23.b. Estimated Confidence Limits Assuming Normality

Parameter	Estimate	95% Confidence Limits	
Mean	0.0799	0.0524	0.1074
Std deviation	0.1908	0.1732	0.2124
Variance	0.0364	0.0300	0.0451

Table D.23.c. Student's t-Test of Zero Residual Mean

Test	Statistic	*p*-Value
Student's *t*-test	5.7275	<0.0001

Minnesota

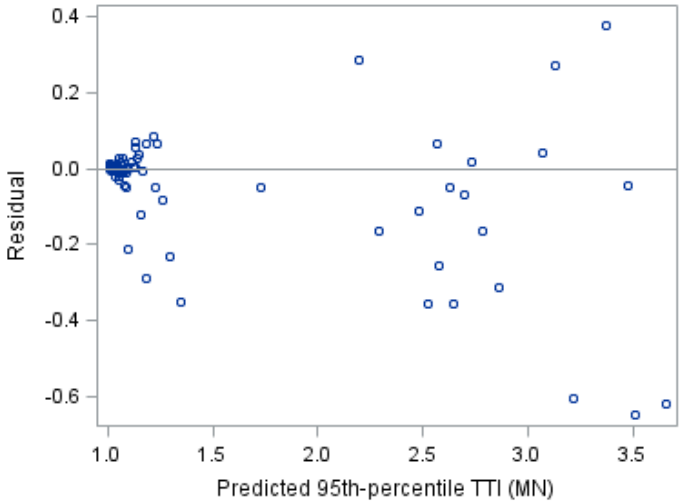

Figure D.60. Residual plot—95th-percentile TTI—Minnesota.

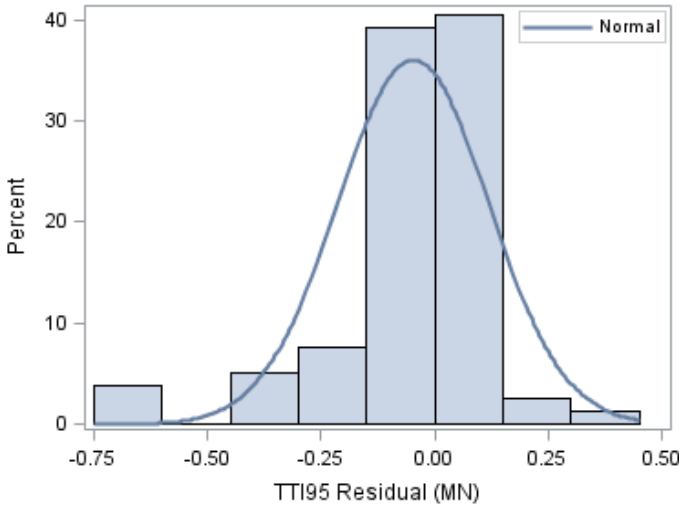

Figure D.61. Residual histogram—95th-percentile TTI—Minnesota.

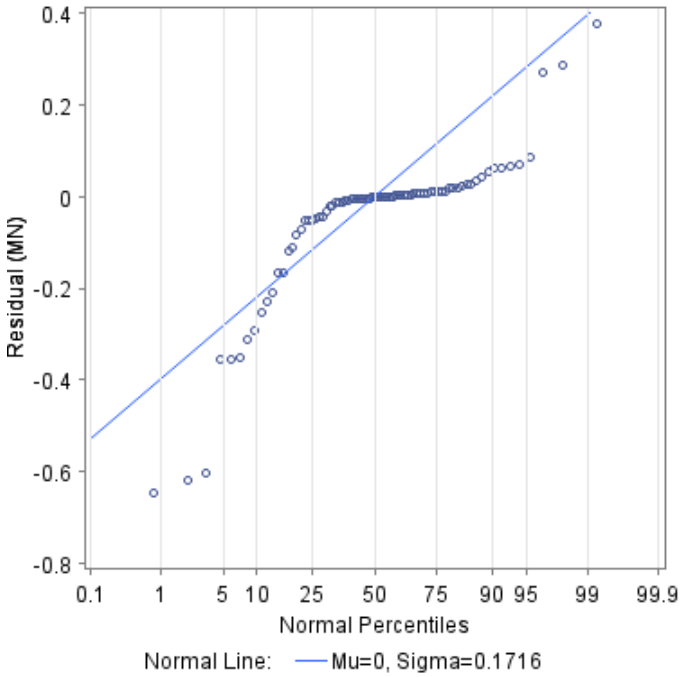

Figure D.62. Residual normality plot—95th-percentile TTI—Minnesota.

Table D.24. Residual Analysis—95th-percentile TTI—Minnesota

Table D.24.a. Basic Summary

Location		Variability	
Mean	–0.0474	Std deviation	0.1660
Median	–0.0016	Variance	0.0276
Min	–0.6480	Range	1.0239
Max	0.3760	Interquartile range	0.0618

Table D.24.b. Estimated Confidence Limits Assuming Normality

Parameter	Estimate	95% Confidence Limits	
Mean	–0.0473	–0.0845	–0.0102
Std deviation	0.1660	0.1435	0.1968
Variance	0.0276	0.0206	0.0387

Table D.24.c. Student's t-Test of Zero Residual Mean

Test	Statistic	*p*-Value
Student's *t*-test	–2.5351	0.0132

Salt Lake City

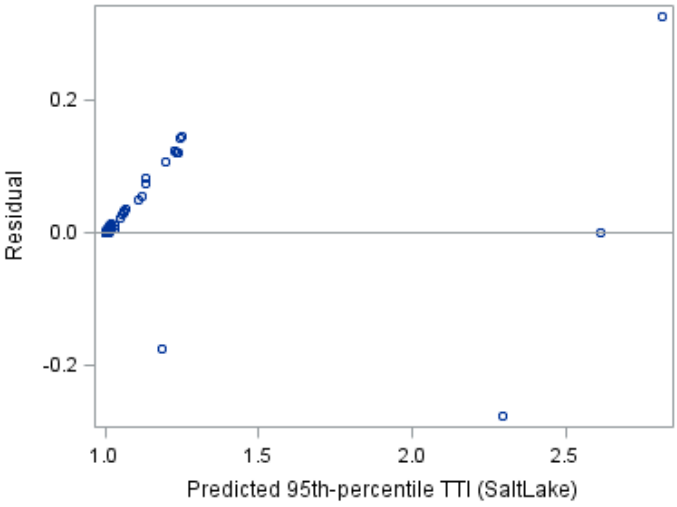

Figure D.63. Residual plot—95th-percentile TTI—Salt Lake City.

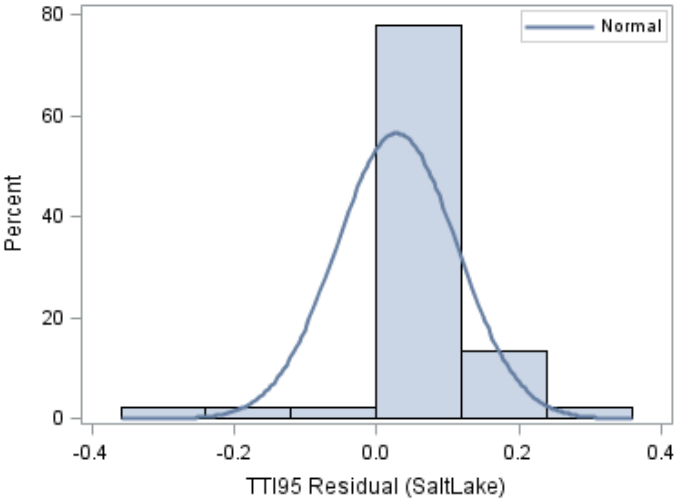

Figure D.64. Residual histogram—95th-percentile TTI—Salt Lake City.

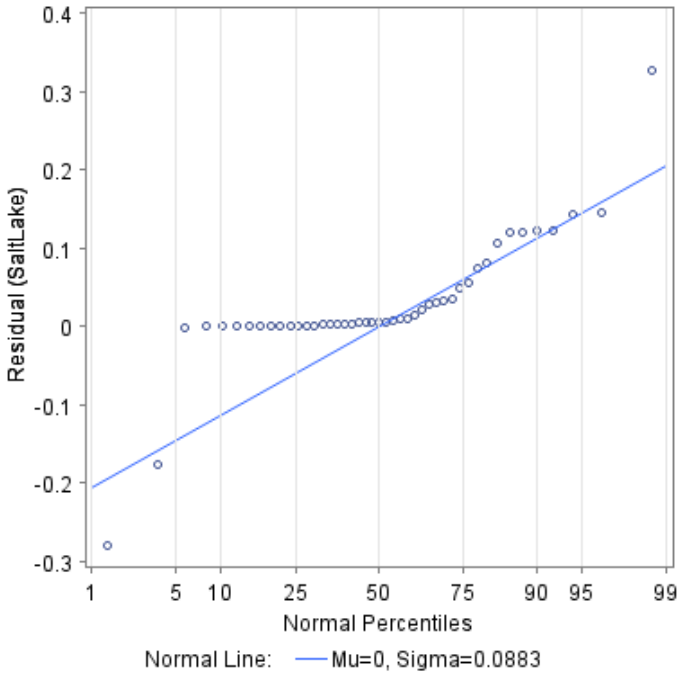

Figure D.65. Residual normality plot—95th-percentile TTI—Salt Lake City.

Table D.25. Residual Analysis—95th-Percentile TTI—Salt Lake City

Table D.25.a. Basic Summary

Location		Variability	
Mean	0.0279	Std deviation	0.0848
Median	0.0063	Variance	0.0072
Min	–0.2786	Range	0.6060
Max	0.3274	Interquartile range	0.0482

Table D.25.b. Estimated Confidence Limits Assuming Normality

Parameter	Estimate	95% Confidence Limits	
Mean	0.0279	0.0025	0.0534
Std deviation	0.0848	0.0702	0.1071
Variance	0.0072	0.0049	0.0115

Table D.25.c. Student's t-Test of Zero Residual Mean

Test	Statistic	*p*-Value
Student's *t*-test	2.2096	0.0324

Spokane

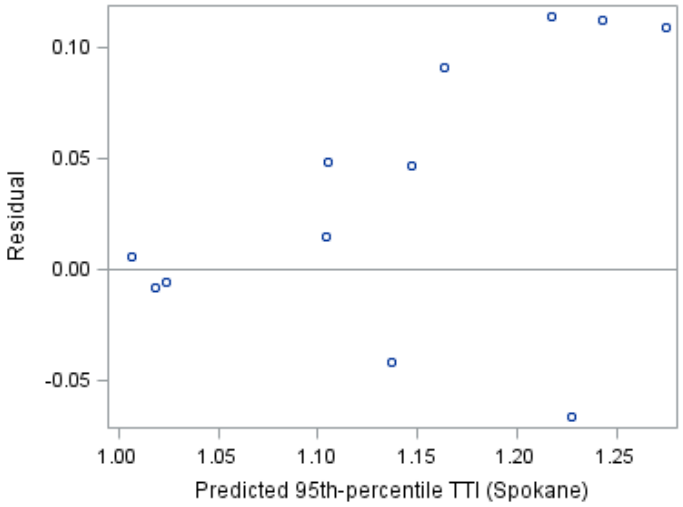

Figure D.66. Residual plot—95th-percentile TTI—Spokane.

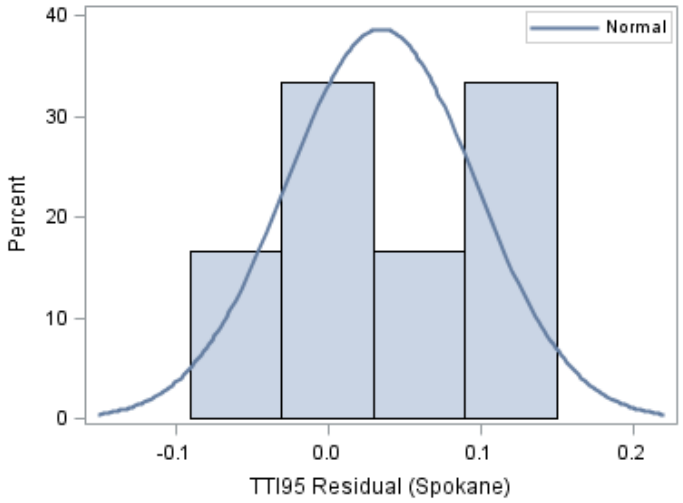

Figure D.67. Residual histogram—95th-percentile TTI—Spokane.

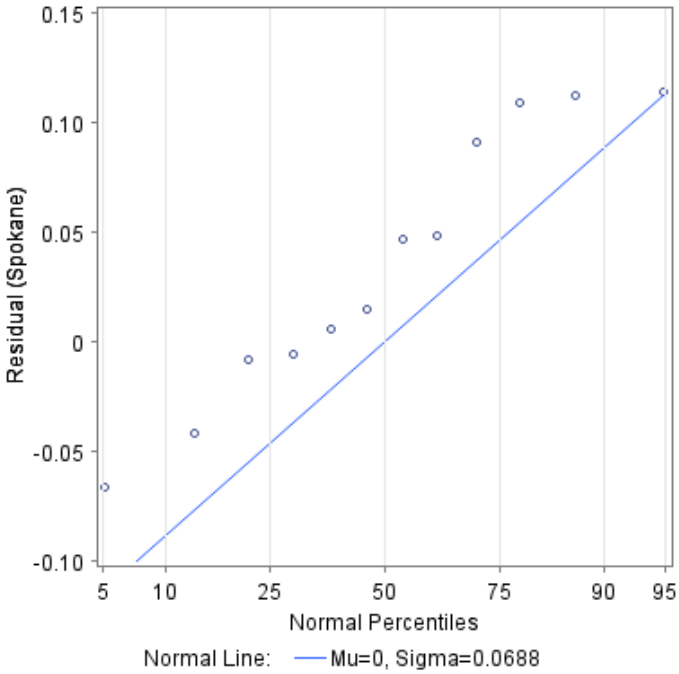

Figure D.68. Residual normality plot—95th-percentile TTI—Spokane.

Table D.26. Residual Analysis—95th-Percentile TTI—Spokane

Table D.26.a. Basic Summary

Location		Variability	
Mean	0.0349	Std deviation	0.0620
Median	0.0309	Variance	0.0038
Min	–0.0667	Range	0.1806
Max	0.1139	Interquartile range	0.1072

Table D.26.b. Estimated Confidence Limits Assuming Normality

Parameter	Estimate	95% Confidence Limits	
Mean	0.0349	–0.0044	0.0743
Std deviation	0.0620	0.0439	0.1052
Variance	0.0038	0.0019	0.0111

Table D.26.c. Student's t*-Test of Zero Residual Mean*

Test	Statistic	*p*-Value
Student's *t*-test	1.9534	0.0767

90th-Percentile TTI Model

California

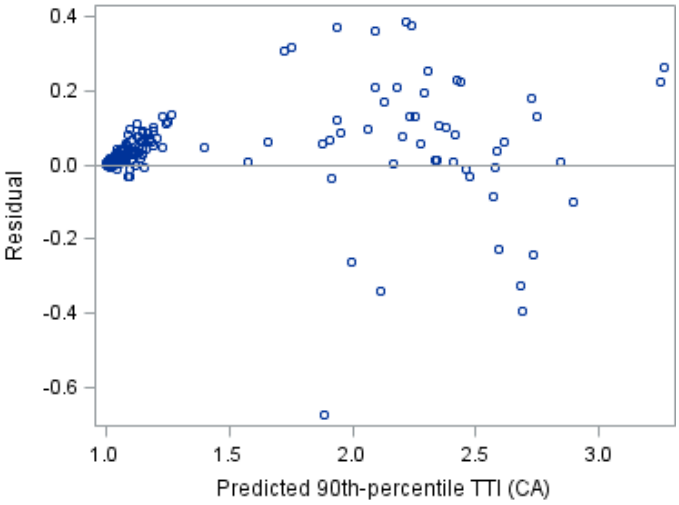

Figure D.69. Residual plot—90th-percentile TTI—California.

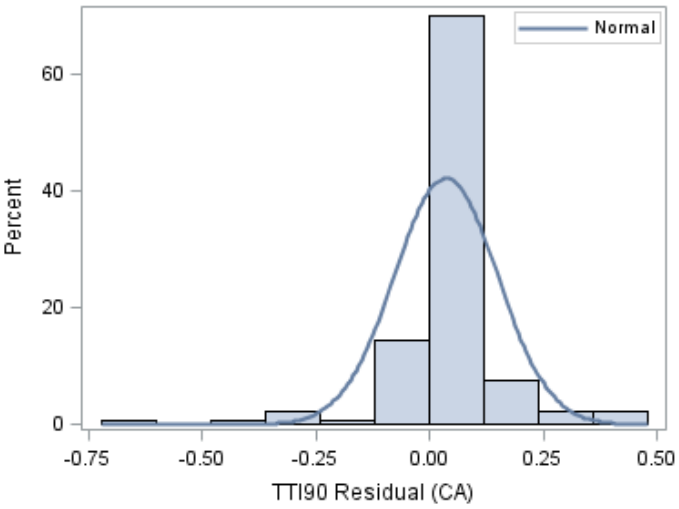

Figure D.70. Residual histogram—90th-percentile TTI—California.

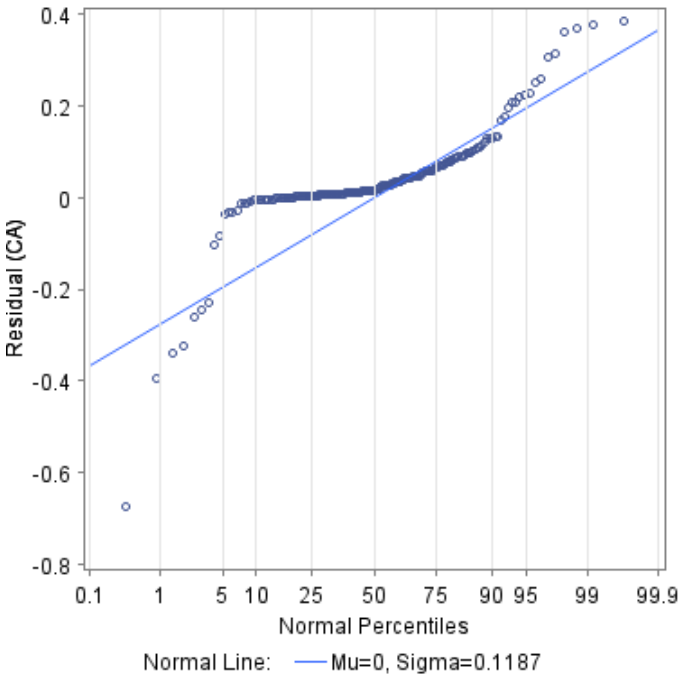

Figure D.71. Residual normality plot—90th-percentile TTI—California.

Table D.27. Residual Analysis—90th-Percentile TTI—California

Table D.27.a. Basic Summary

Location		Variability	
Mean	0.0358	Std deviation	0.1135
Median	0.0169	Variance	0.0129
Min	–0.6737	Range	1.0585
Max	0.3848	Interquartile range	0.0611

Table D.27.b. Estimated Confidence Limits Assuming Normality

Parameter	Estimate	95% Confidence Limits	
Mean	0.0358	0.0194	0.0522
Std deviation	0.1135	0.1030	0.1263
Variance	0.0129	0.0106	0.0160

Table D.27.c. Student's t-Test of Zero Residual Mean

Test	Statistic	*p*-Value
Student's *t*-test	4.3133	<0.0001

Minnesota

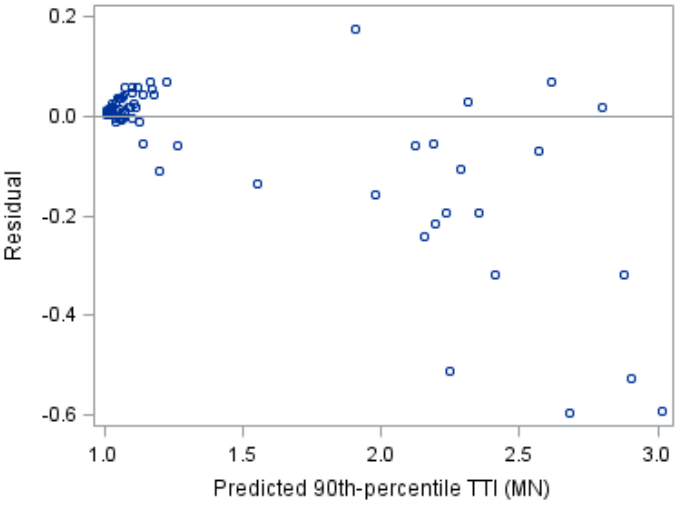

Figure D.72. Residual plot—90th-percentile TTI—Minnesota.

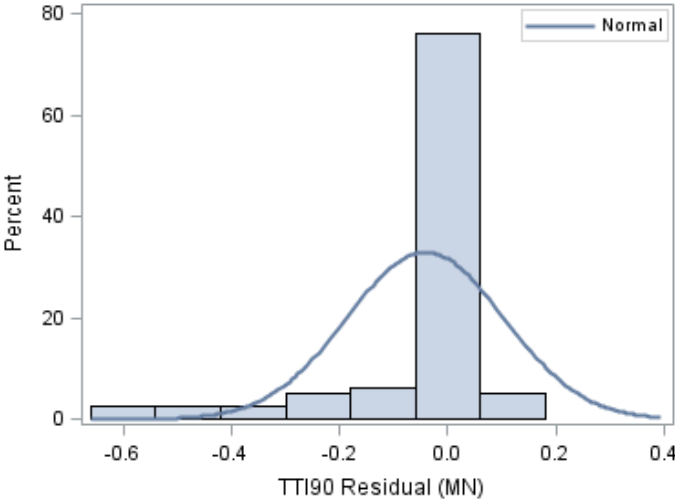

Figure D.73. Residual histogram—90th-percentile TTI—Minnesota.

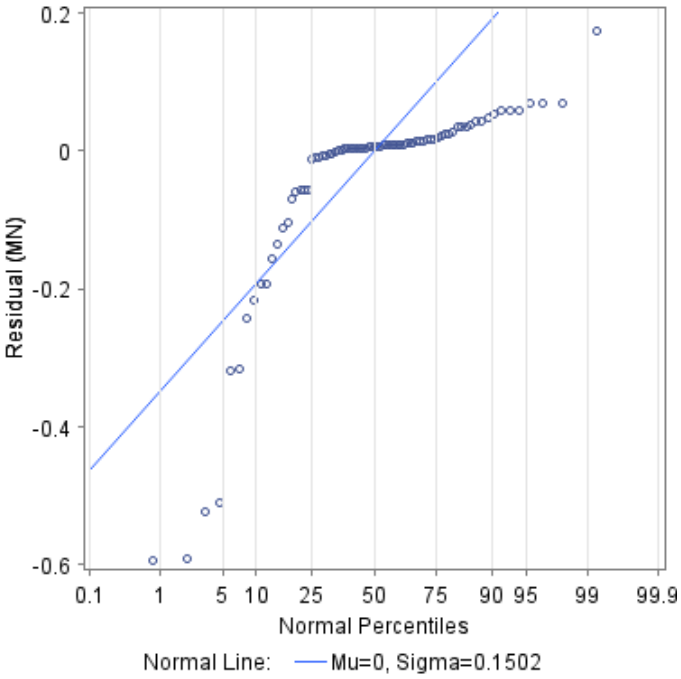

Figure D.74. Residual normality plot—90th-percentile TTI—Minnesota.

Table D.28. Residual Analysis—90th-Percentile TTI—Minnesota

Table D.28.a. Basic Summary

Location		Variability	
Mean	–0.0416	Std deviation	0.1453
Median	0.0064	Variance	0.0211
Min	–0.5958	Range	0.7700
Max	0.1742	Interquartile range	0.0297

Table D.28.b. Estimated Confidence Limits Assuming Normality

Parameter	Estimate	95% Confidence Limits	
Mean	–0.0416	–0.0741	–0.0090
Std deviation	0.1453	0.1256	0.1723
Variance	0.0211	0.0158	0.0297

Table D.28.c. Student's t-Test of Zero Residual Mean

Test	Statistic	*p*-Value
Student's *t*-test	–2.5415	0.0130

Salt Lake City

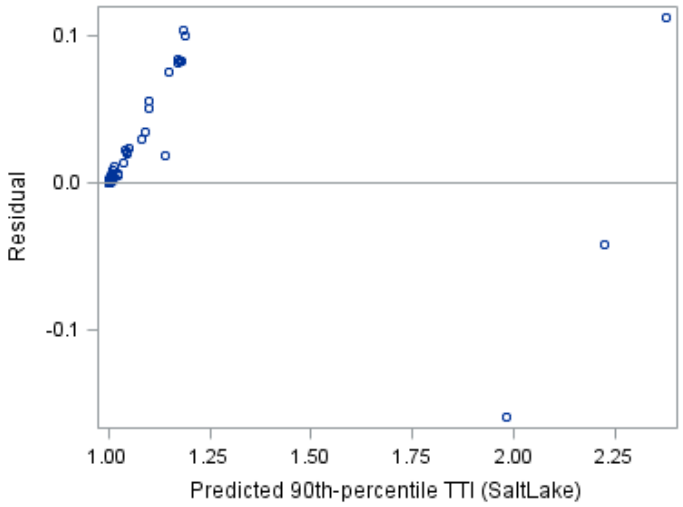

Figure D.75. Residual plot—90th-percentile TTI—Salt Lake City.

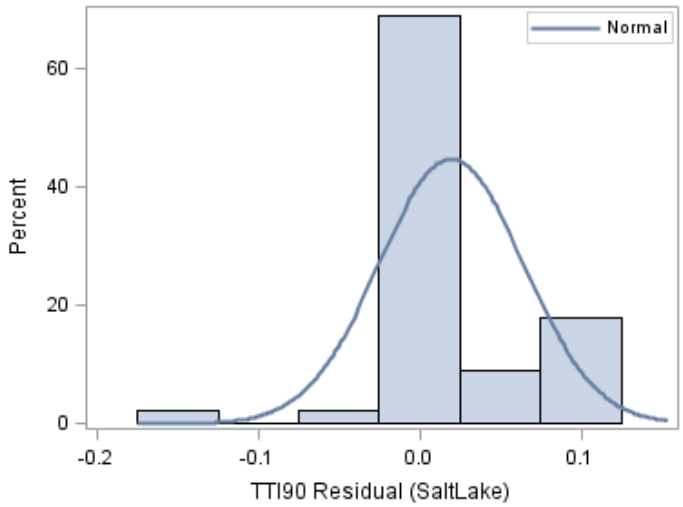

Figure D.76. Residual histogram—90th-percentile TTI—Salt Lake City.

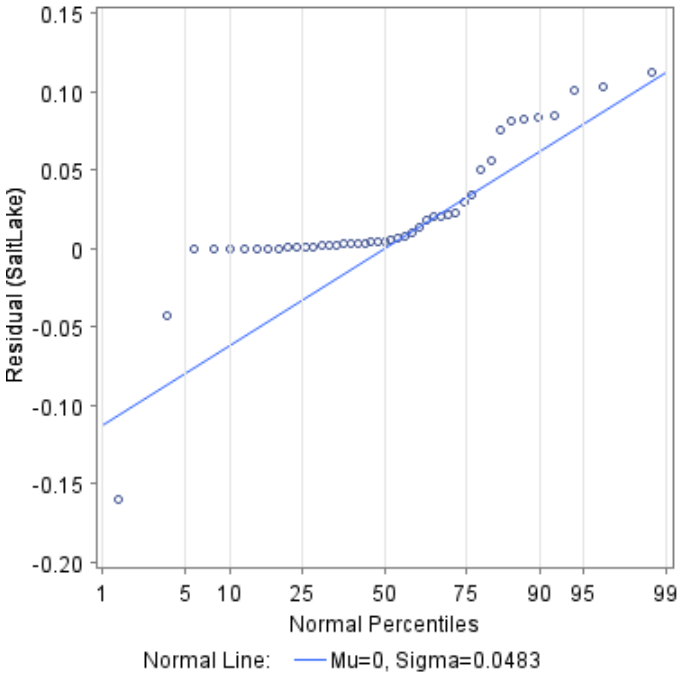

Figure D.77. Residual normality plot—90th-percentile TTI—Salt Lake City.

Table D.29. Residual Analysis—90th-Percentile TTI—Salt Lake City

Table D.29.a. Basic Summary

Location		Variability	
Mean	0.0195	Std deviation	0.0446
Median	0.0048	Variance	0.0020
Min	–0.1603	Range	0.2729
Max	0.1126	Interquartile range	0.0284

Table D.29.b. Estimated Confidence Limits Assuming Normality

Parameter	Estimate	95% Confidence Limits	
Mean	0.0195	0.0061	0.0329
Std deviation	0.0446	0.0369	0.0564
Variance	0.0020	0.0014	0.0038

Table D.29.c. Student's t-Test of Zero Residual Mean

Test	Statistic	*p*-Value
Student's *t*-test	2.9347	0.0053

Spokane

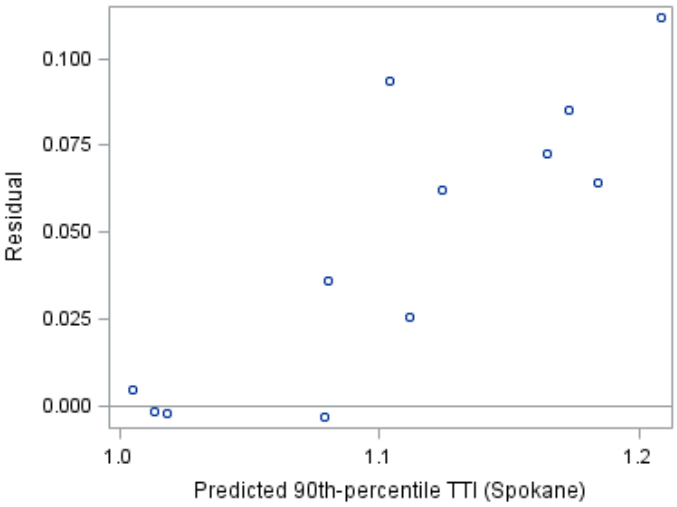

Figure D.78. Residual plot—90th-percentile TTI—Spokane.

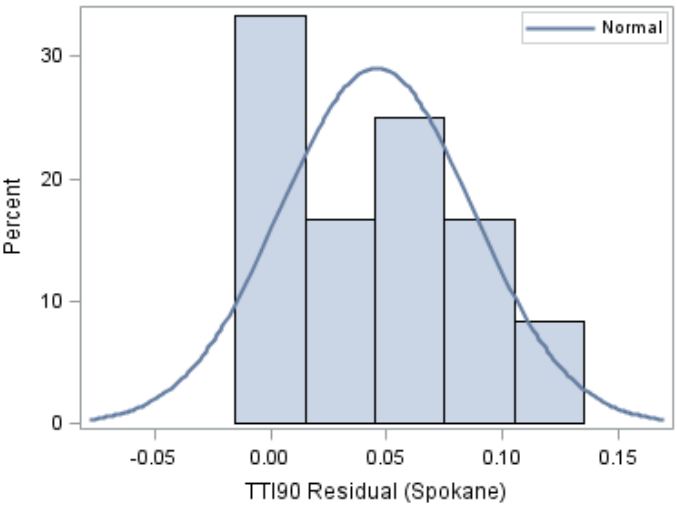

Figure D.79. Residual histogram—90th-percentile TTI—Spokane.

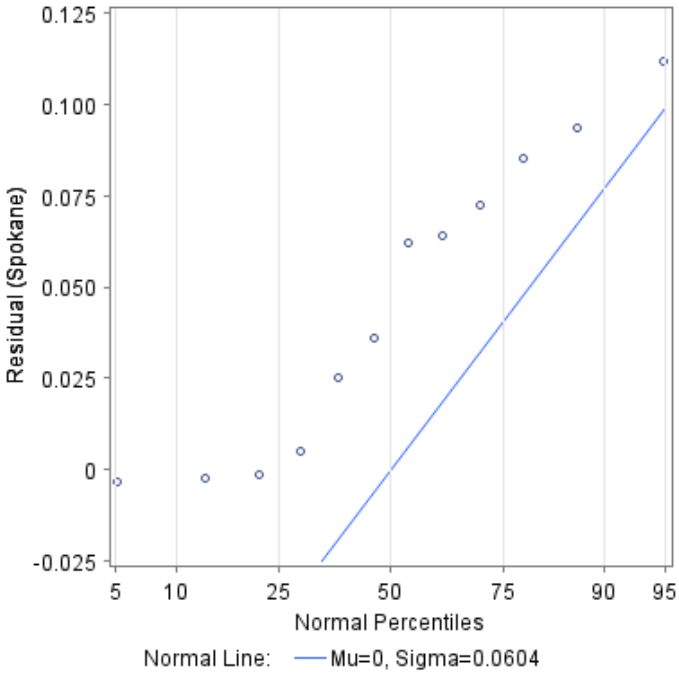

Figure D.80. Residual normality plot—90th-percentile TTI—Spokane.

Table D.30. Residual Analysis—90th-Percentile TTI—Spokane

Table D.30.a. Basic Summary

Location		Variability	
Mean	0.0457	Std deviation	0.0412
Median	0.0491	Variance	0.0017
Min	–0.0033	Range	0.1151
Max	0.1118	Interquartile range	0.0773

Table D.30.b. Estimated Confidence Limits Assuming Normality

Parameter	Estimate	95% Confidence Limits	
Mean	0.0457	0.0195	0.0719
Std deviation	0.0412	0.0292	0.0700
Variance	0.0017	0.0009	0.0049

Table D.30.c. Student's t-Test of Zero Residual Mean

Test	Statistic	*p*-Value
Student's *t*-test	3.8418	0.0027

80th-Percentile TTI Model

California

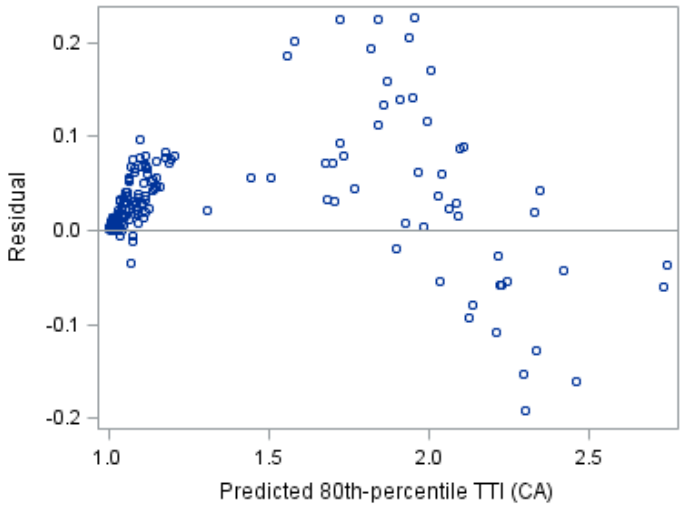

Figure D.81. Residual plot—80th-percentile TTI—California.

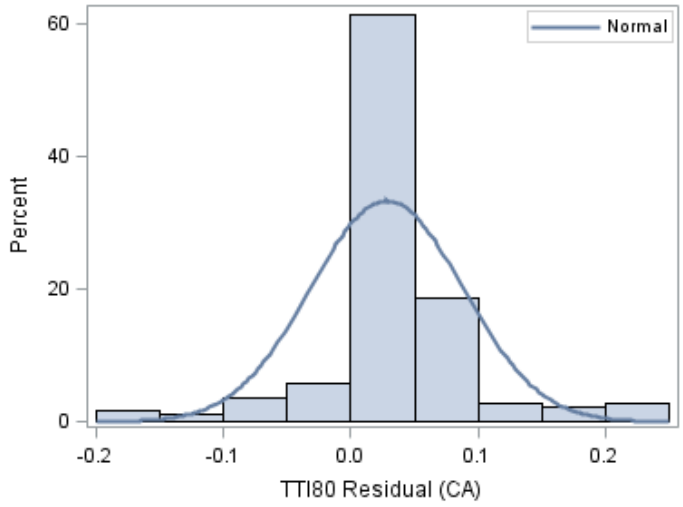

Figure D.82. Residual histogram—80th-percentile TTI—California.

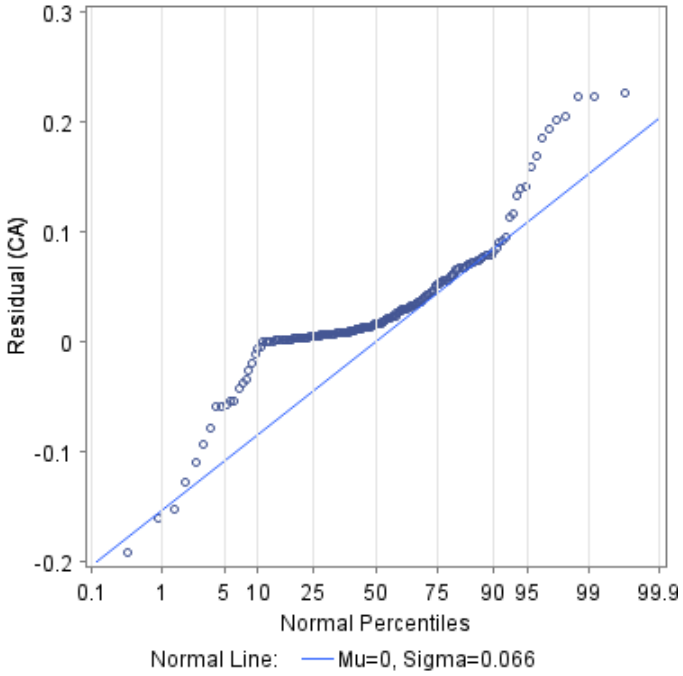

Figure D.83. Residual normality plot—80th-percentile TTI—California.

Table D.31. Residual Analysis—80th-Percentile TTI—California

Table D.31.a. Basic Summary

Location		Variability	
Mean	0.0282	Std deviation	0.0598
Median	0.0159	Variance	0.0036
Min	–0.1918	Range	0.4181
Max	0.2263	Interquartile range	0.0473

Table D.31.b. Estimated Confidence Limits Assuming Normality

Parameter	Estimate	95% Confidence Limits	
Mean	0.0282	0.0196	0.0369
Std deviation	0.0598	0.0543	0.0665
Variance	0.0036	0.0029	0.0044

Table D.31.c. Student's t-Test of Zero Residual Mean

Test	Statistic	*p*-Value
Student's *t*-test	6.4630	<0.0001

Minnesota

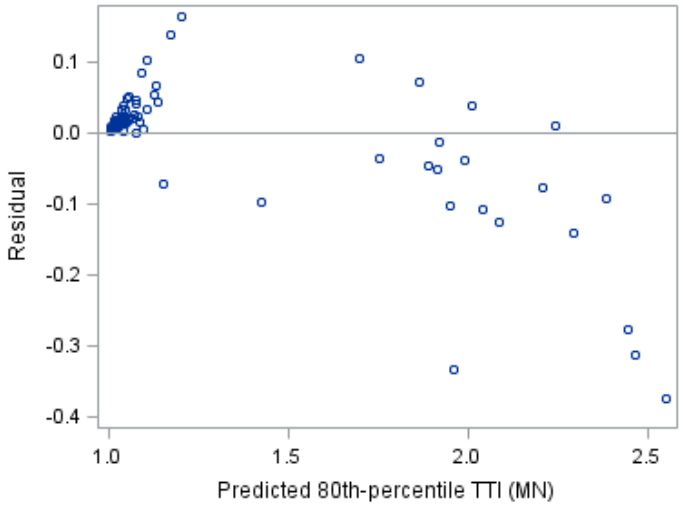

Figure D.84. Residual plot—80th-percentile TTI—Minnesota.

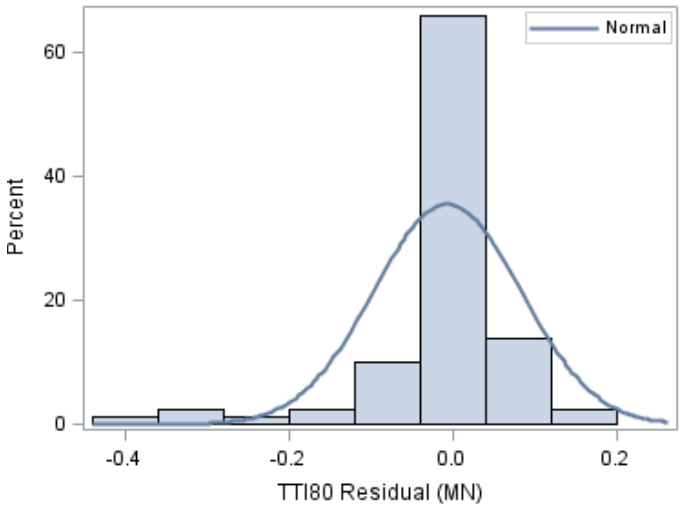

Figure D.85. Residual histogram—80th-percentile TTI—Minnesota.

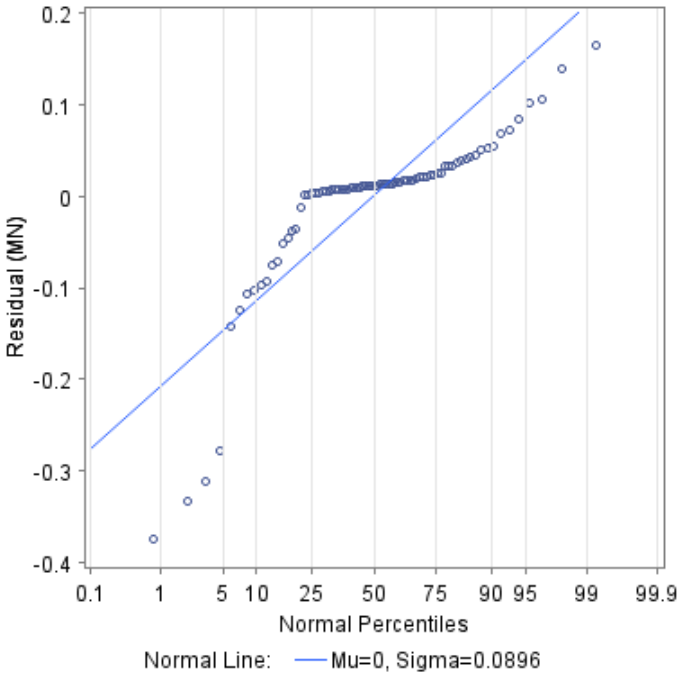

Figure D.86. Residual normality plot—80th-percentile TTI—Minnesota.

Table D.32. Residual analysis—80th-Percentile TTI—Minnesota

Table D.32.a. Basic Summary

Location		Variability	
Mean	–0.0068	Std deviation	0.0899
Median	0.0123	Variance	0.0081
Min	–0.3750	Range	0.5394
Max	0.1644	Interquartile range	0.0211

Table D.32.b. Estimated Confidence Limits Assuming Normality

Parameter	Estimate	95% Confidence Limits	
Mean	–0.0068	–0.0269	0.0134
Std deviation	0.0899	0.0777	0.1066
Variance	0.0081	0.0060	0.0114

Table D.32.c. Student's t-Test of Zero Residual Mean

Test	Statistic	*p*-Value
Student's *t*-test	–0.6700	0.5049

Salt Lake City

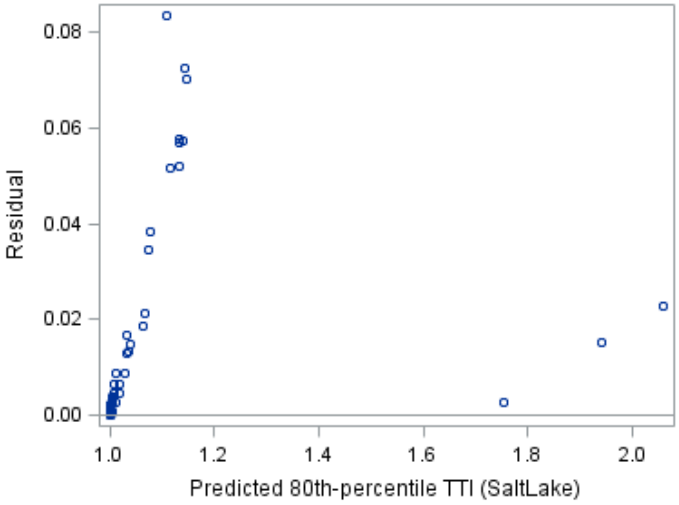

Figure D.87. Residual plot—80th-percentile TTI—Salt Lake City.

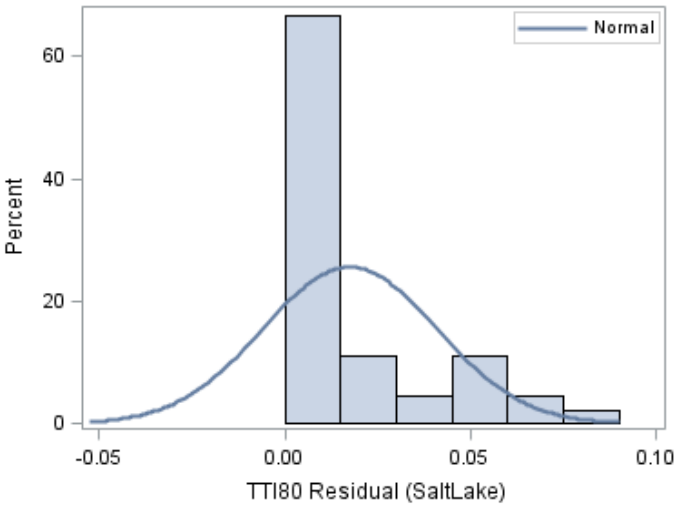

Figure D.88. Residual histogram—80th-percentile TTI—Salt Lake City.

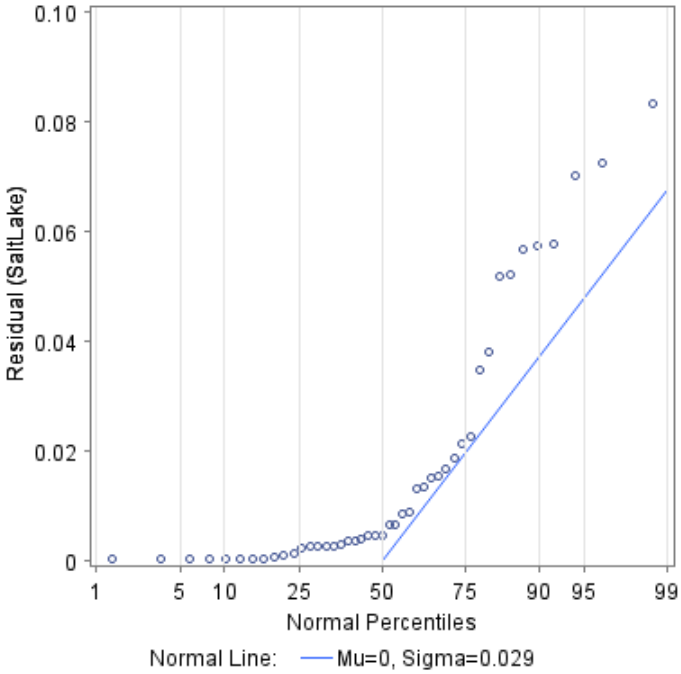

Figure D.89. Residual normality plot—80th-percentile TTI—Salt Lake City.

Table D.33. Residual Analysis—80th-Percentile TTI—Salt Lake City

Table D.33.a. Basic Summary

Location		Variability	
Mean	0.017496	Std deviation	0.02340
Median	0.004669	Variance	0.0005477
Min	0.000173969	Range	0.08334
Max	0.0835138	Interquartile range	0.01919

Table D.33.b. Estimated Confidence Limits Assuming Normality

Parameter	Estimate	95% Confidence Limits	
Mean	0.017496	0.010465	0.024527
Std deviation	0.023403	0.019374	0.029563
Variance	0.000548	0.000375	0.000874

Table D.33.c. Student's t*-Test of Zero Residual Mean*

Test	Statistic	*p*-Value
Student's *t*-test	5.015032	<0.0001

Spokane

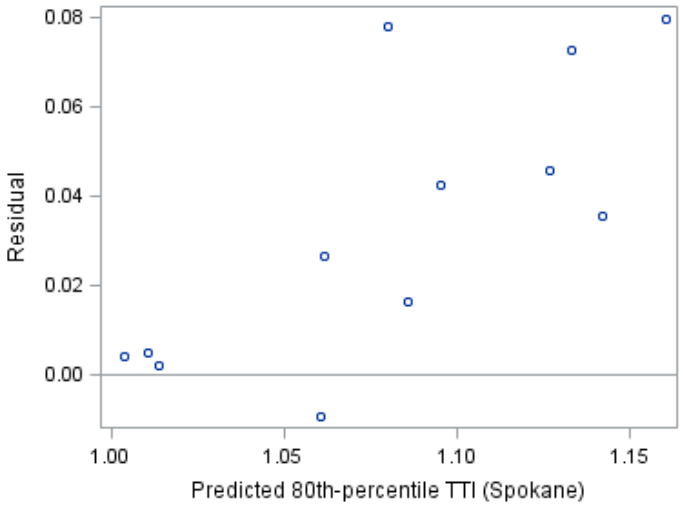

Figure D.90. Residual plot—80th-percentile TTI—Spokane.

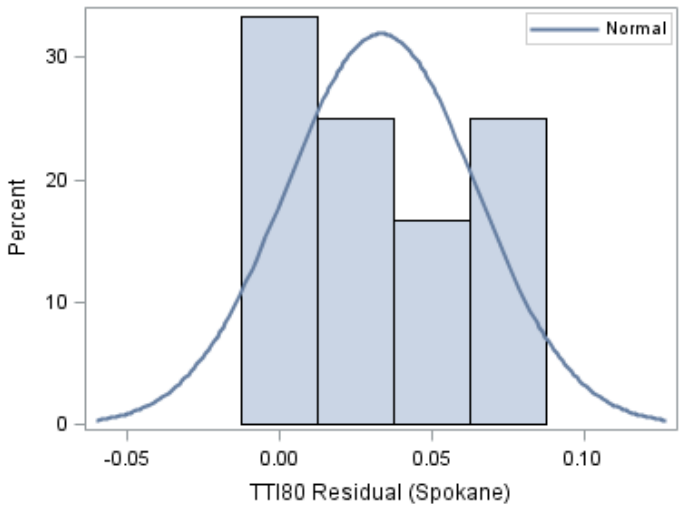

Figure D.91. Residual histogram—80th-percentile TTI—Spokane.

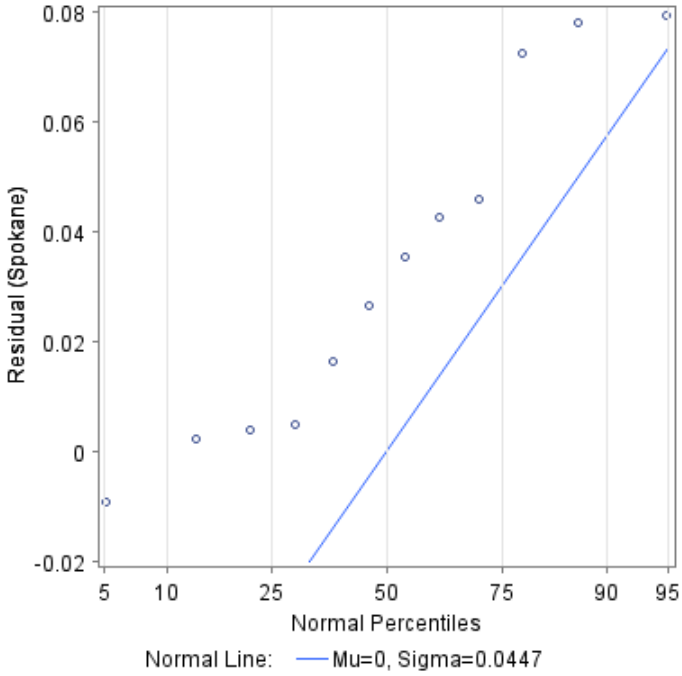

Figure D.92. Residual normality plot—80th-percentile TTI—Spokane.

Table D.34. Residual Analysis—80th-Percentile TTI—Spokane

Table D.34.a. Basic Summary

Location		Variability	
Mean	0.0332	Std deviation	0.0312
Median	0.0310	Variance	0.0010
Min	–0.0093	Range	0.0887
Max	0.0794	Interquartile range	0.0549

Table D.34.b. Estimated Confidence Limits Assuming Normality

Parameter	Estimate	95% Confidence Limits	
Mean	0.0332	0.0134	0.0531
Std deviation	0.0312	0.0221	0.0530
Variance	0.0010	0.0005	0.0028

Table D.34.c. Student's t-Test of Zero Residual Mean

Test	Statistic	*p*-Value
Student's *t*-test	3.6870	0.0036

Standard Deviation of TTI Model

California

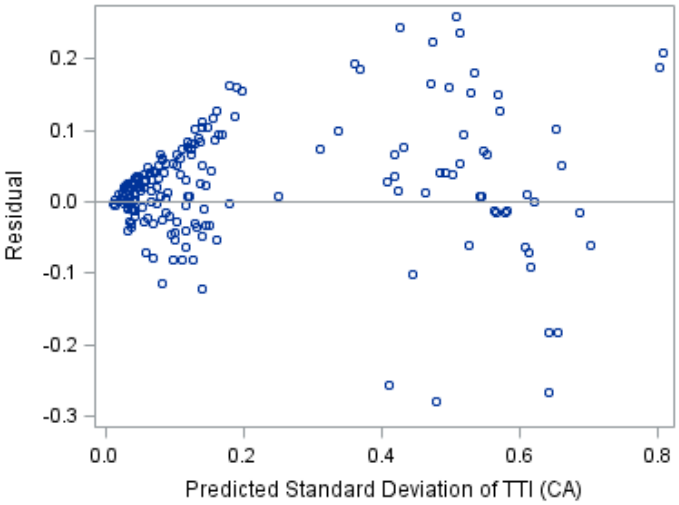

Figure D.93. Residual plot—standard deviation of TTI—California.

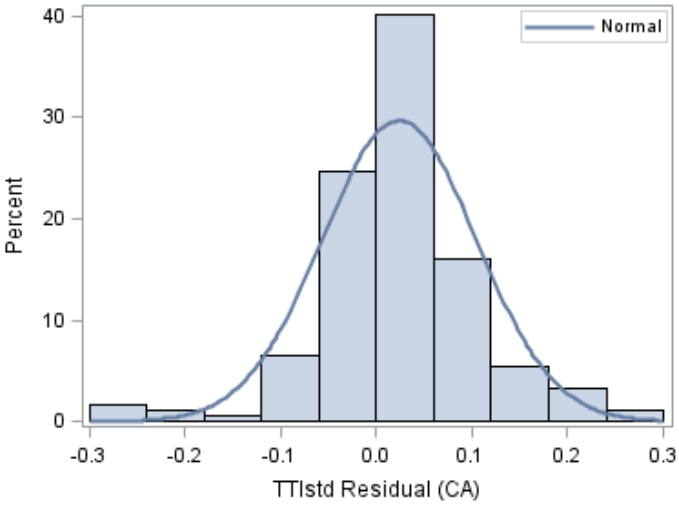

Figure D.94. Residual histogram—standard deviation of TTI—California.

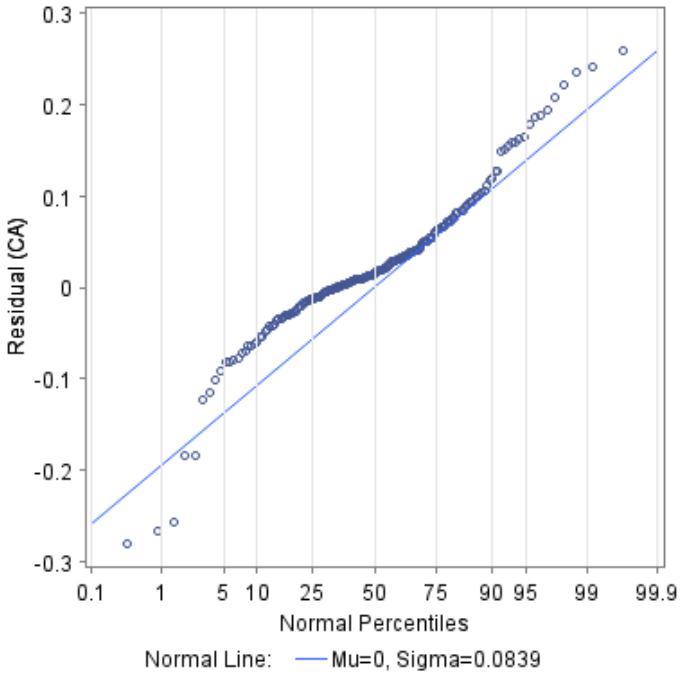

Figure D.95. Residual normality plot—standard deviation of TTI—California.

Table D.35. Residual Analysis—Standard Deviation of TTI—California

Table D.35.a. Basic Summary

Location		Variability	
Mean	0.0235	Std deviation	0.0808
Median	0.0160	Variance	0.0065
Min	–0.2805	Range	0.5395
Max	0.2590	Interquartile range	0.0739

Table D.35.b. Estimated Confidence Limits Assuming Normality

Parameter	Estimate	95% Confidence Limits	
Mean	0.0808	0.0118	0.0351
Std deviation	0.0065	0.0733	0.0899
Variance	0.5395	0.0054	0.0081

Table D.35.c. Student's t-Test of Zero Residual Mean

Test	Statistic	*p*-Value
Student's *t*-test	3.9710	0.0001

Minnesota

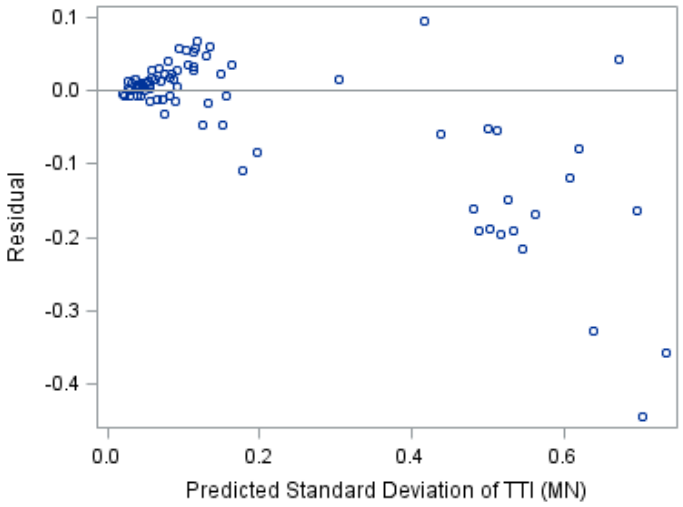

Figure D.96. Residual plot—standard deviation of TTI—Minnesota.

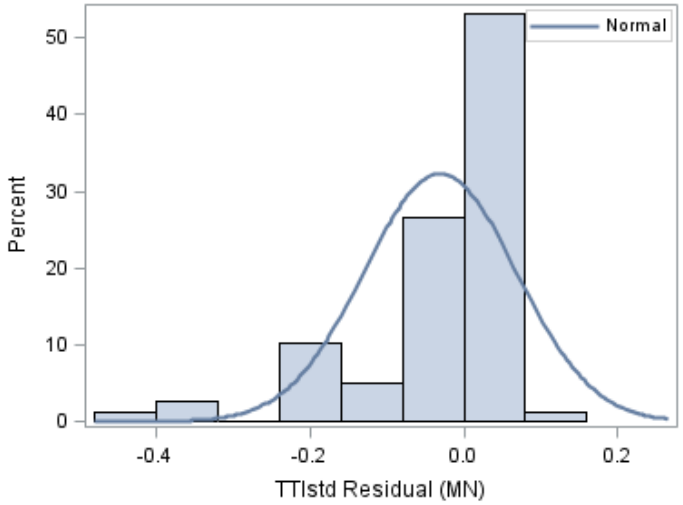

Figure D.97. Residual histogram—standard deviation of TTI—Minnesota.

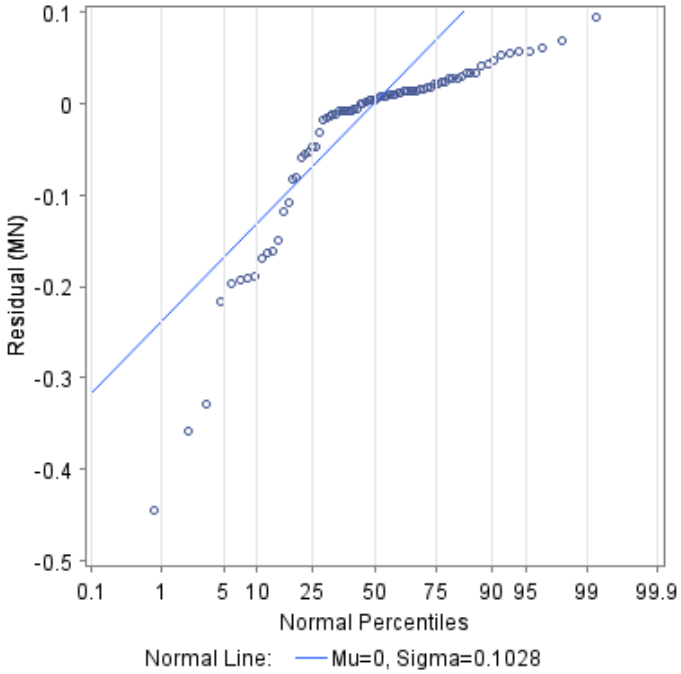

Figure D.98. Residual normality plot—standard deviation of TTI—Minnesota.

Table D.36. Residual Analysis—Standard Deviation of TTI—Minnesota

Table D.36.a. Basic Summary

Location		Variability	
Mean	–0.0309	Std deviation	0.0987
Median	0.0033	Variance	0.0097
Min	–0.4453	Range	0.5404
Max	0.0950	Interquartile range	0.0693

Table D.36.b. Estimated Confidence Limits Assuming Normality

Parameter	Estimate	95% Confidence Limits	
Mean	–0.0309	–0.0530	–0.0088
Std deviation	0.0987	0.0853	0.1170
Variance	0.0097	0.0073	0.0137

Table D.36.c. Student's t-Test of Zero Residual Mean

Test	Statistic	*p*-Value
Student's *t*-test	–2.7848	0.0067

Salt Lake City

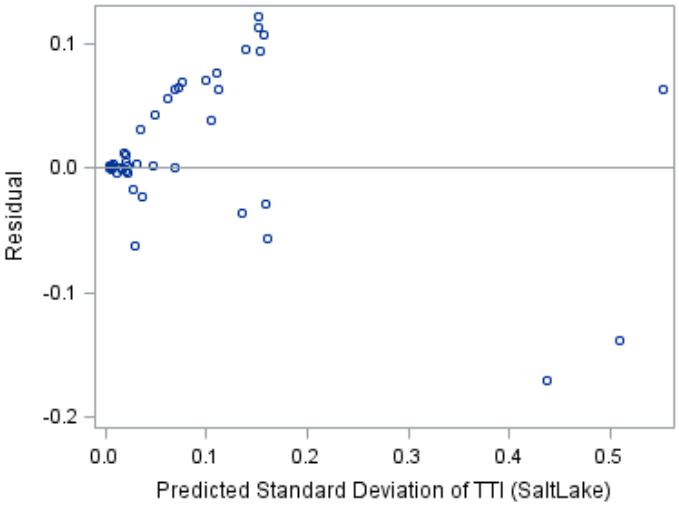

Figure D.99. Residual plot—standard deviation of TTI—Salt Lake City.

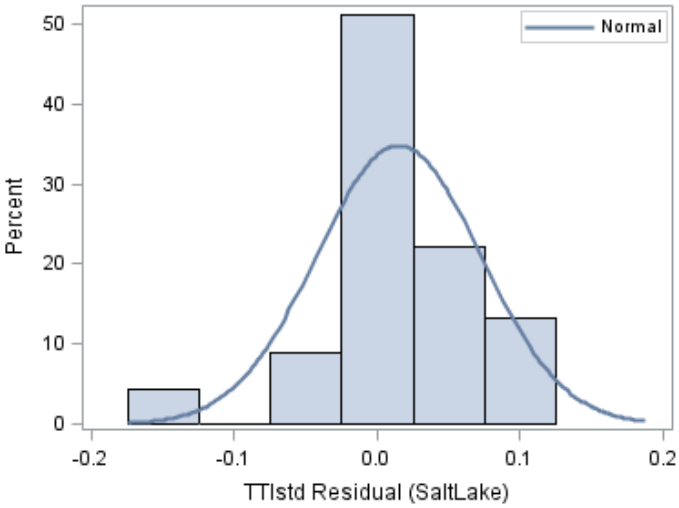

Figure D.100. Residual histogram—standard deviation of TTI—Salt Lake City.

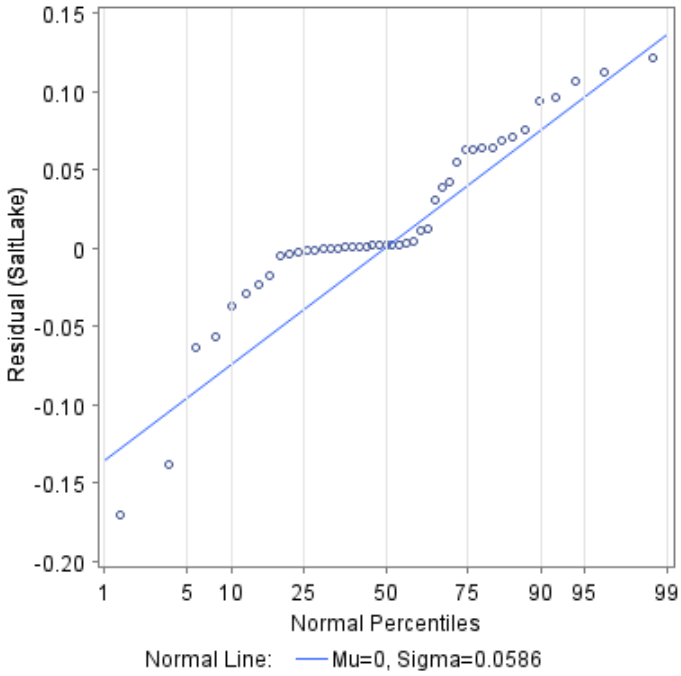

Figure D.101. Residual normality plot—standard deviation of TTI—Salt Lake City.

Table D.37. Residual Analysis—Standard Deviation of TTI—Salt Lake City

Table D.37.a. Basic Summary

Location		Variability	
Mean	0.0148	Std deviation	0.0574
Median	0.0021	Variance	0.0033
Min	–0.1706	Range	0.2922
Max	0.1216	Interquartile range	0.0645

Table D.37.b. Estimated Confidence Limits Assuming Normality

Parameter	Estimate	95% Confidence Limits	
Mean	0.0148	–0.0024	0.0320
Std deviation	0.0573	0.0475	0.0724
Variance	0.0033	0.0023	0.0052

Table D.37.c. Student's t-Test of Zero Residual Mean

Test	Statistic	*p*-Value
Student's *t*-test	1.7297	0.0907

Spokane

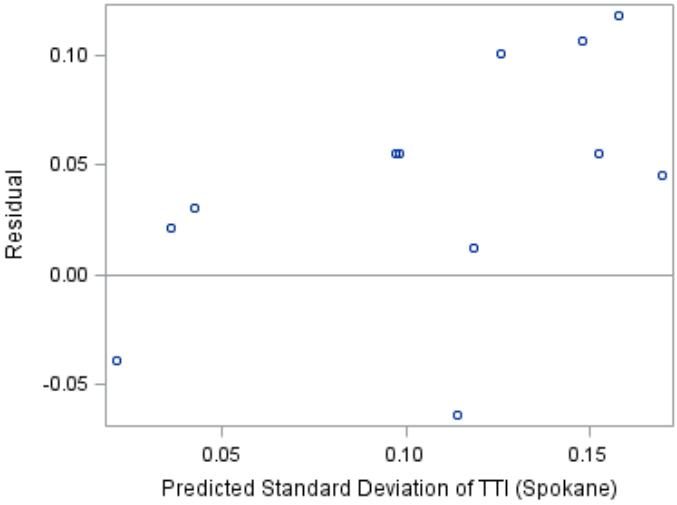

Figure D.102. Residual plot—standard deviation of TTI—Spokane.

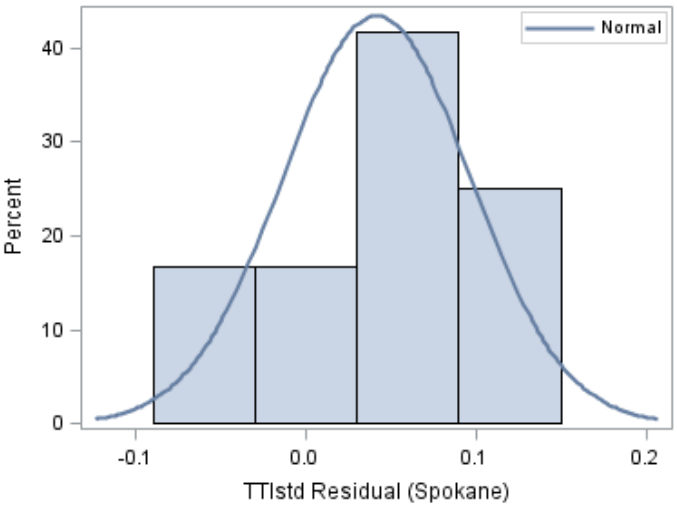

Figure D.103. Residual histogram—standard deviation of TTI—Spokane.

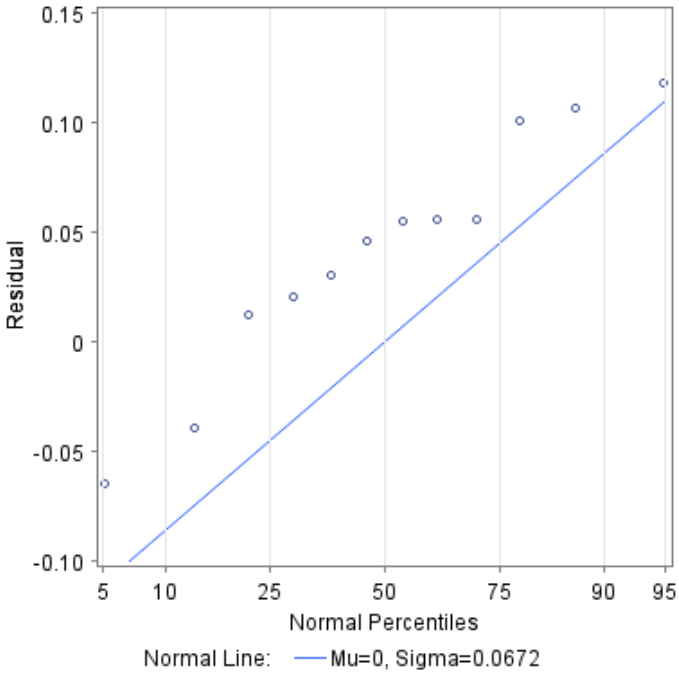

Figure D.104. Residual normality plot—standard deviation of TTI—Spokane.

Table D.38. Residual Analysis—Standard Deviation of TTI—Spokane

Table D.38.a. Basic Summary

Location		Variability	
Mean	0.0415	Std deviation	0.0551
Median	0.0504	Variance	0.0030
Min	–0.0645	Range	0.1829
Max	0.1184	Interquartile range	0.0616

Table D.38.b. Estimated Confidence Limits Assuming Normality

Parameter	Estimate	95% Confidence Limits	
Mean	0.0415	0.0065	0.0766
Std deviation	0.0551	0.0390	0.0936
Variance	0.0030	0.0015	0.0088

Table D.38.c. Student's t-Test of Zero Residual Mean

Test	Statistic	*p*-Value
Student's *t*-test	2.6108	0.0242

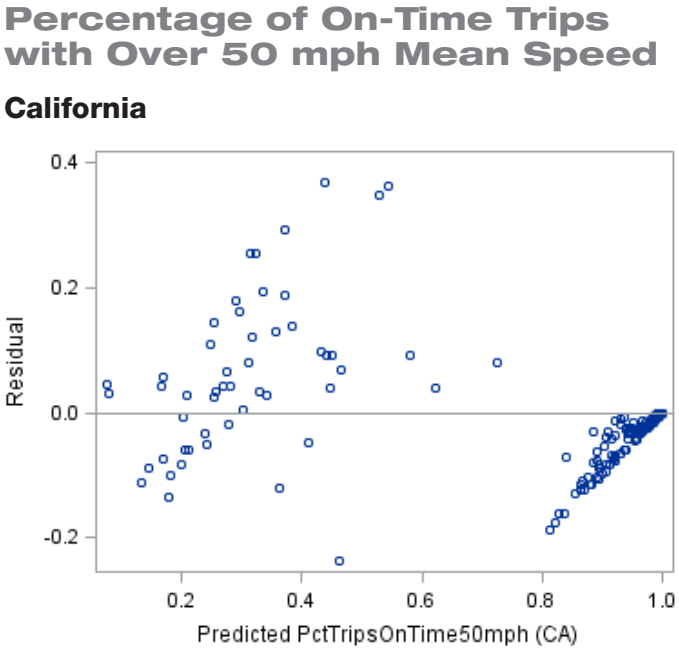

Figure D.105. Residual plot—percentage of on-time trips over 50 mph—California.

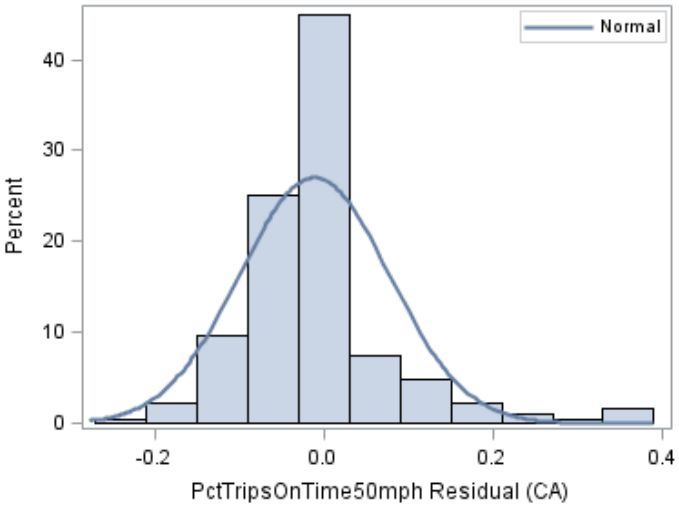

Figure D.106. Residual histogram—percentage of on-time trips over 50 mph—California.

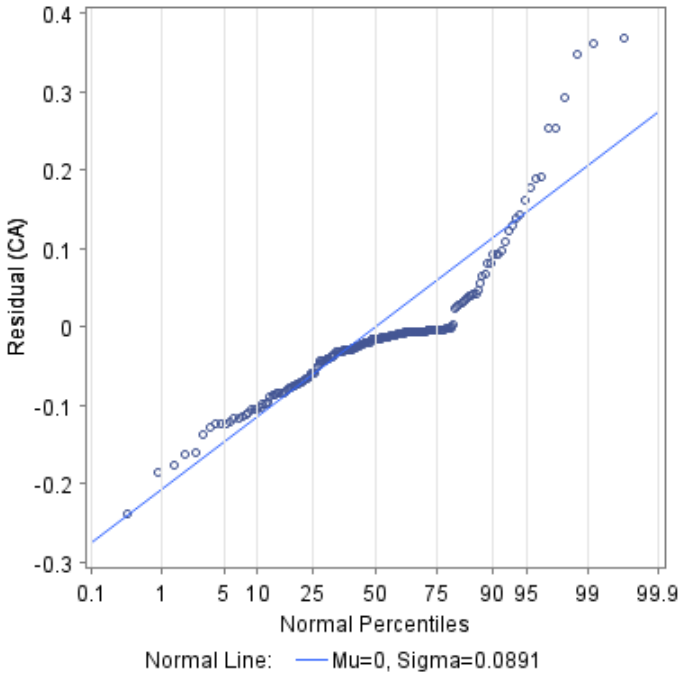

Figure D.107. Residual normality plot—percentage of on-time trips over 50 mph—California.

Table D.39. Residual Analysis—Percentage of On-Time Trips Over 50 mph—California

Table D.39.a. Basic Summary

Location		Variability	
Mean	–0.0117	Std deviation	0.0886
Median	–0.0153	Variance	0.0079
Min	–0.2374	Range	0.6062
Max	0.3687	Interquartile range	0.0559

Table D.39.b. Estimated Confidence Limits Assuming Normality

Parameter	Estimate	95% Confidence Limits	
Mean	–0.0117	–0.0245	0.0011
Std deviation	0.0886	0.0804	0.0986
Variance	0.0079	0.0065	0.0097

Table D.39.c. Student's t-Test of Zero Residual Mean

Test	Statistic	*p*-Value
Student's *t*-test	–1.8041	0.0728

Minnesota

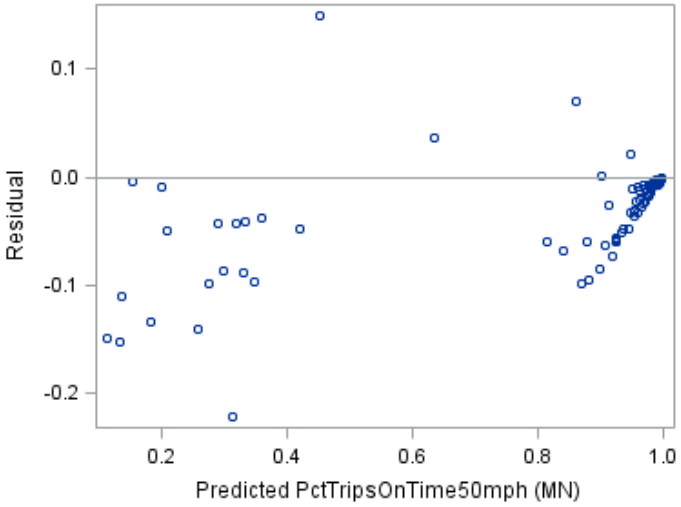

Figure D.108. Residual plot—percentage of on-time trips over 50 mph—Minnesota.

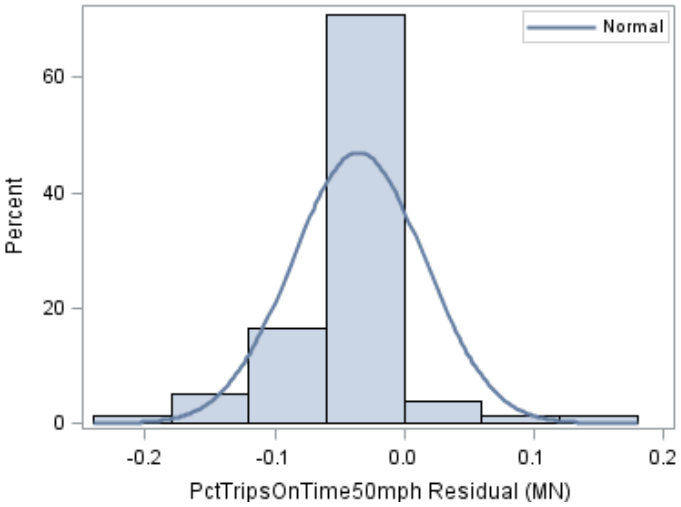

Figure D.109. Residual histogram—percentage of on-time trips over 50 mph—Minnesota.

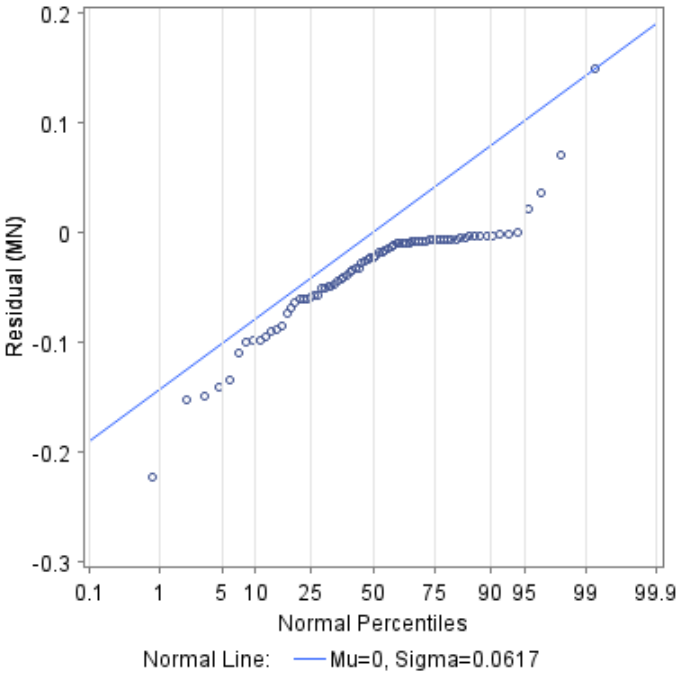

Figure D.110. Residual normality plot—percentage of on-time trips over 50 mph—Minnesota.

Table D.40. Residual Analysis—Percentage of On-Time Trips Over 50 mph—Minnesota

Table D.40.a. Basic Summary

Location		Variability	
Mean	–0.0353	Std deviation	0.0510
Median	–0.0221	Variance	0.0026
Min	–0.2230	Range	0.3729
Max	0.1499	Interquartile range	0.0526

Table D.40.b. Estimated Confidence Limits Assuming Normality

Parameter	Estimate	95% Confidence Limits	
Mean	–0.0353	–0.0467	–0.0239
Std deviation	0.0510	0.0441	0.0604
Variance	0.0026	0.0019	0.0037

Table D.40.c. Student's t-Test of Zero Residual Mean

Test	Statistic	*p*-Value
Student's *t*-test	–6.1620	<0.0001

Salt Lake City

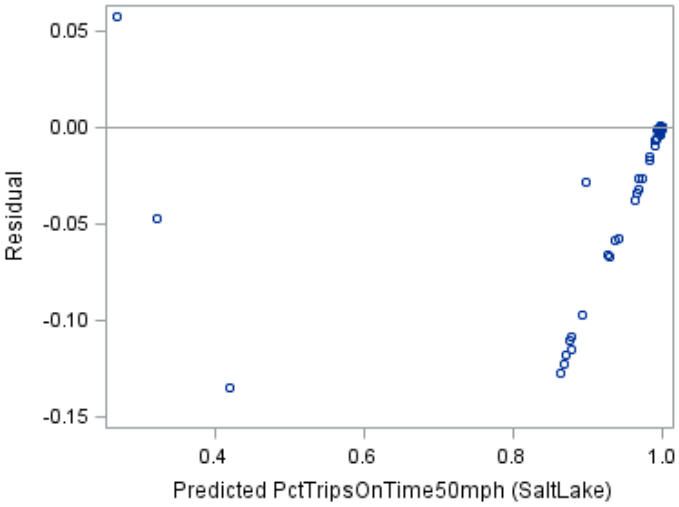

Figure D.111. Residual plot—percentage of on-time trips over 50 mph—Salt Lake City.

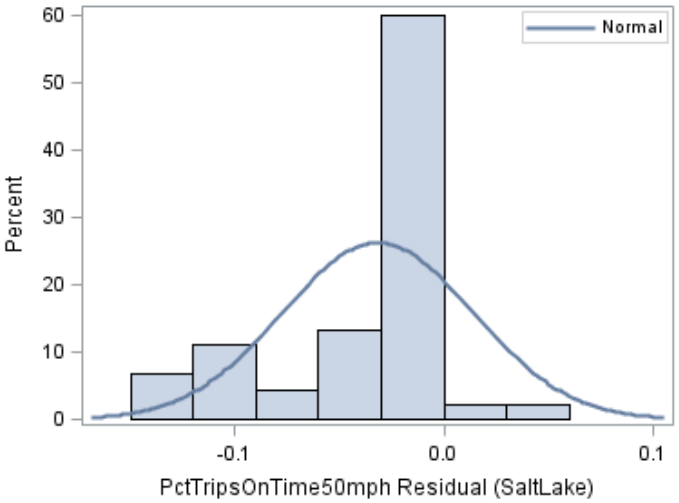

Figure D.112. Residual histogram—percentage of on-time trips over 50 mph—Salt Lake City.

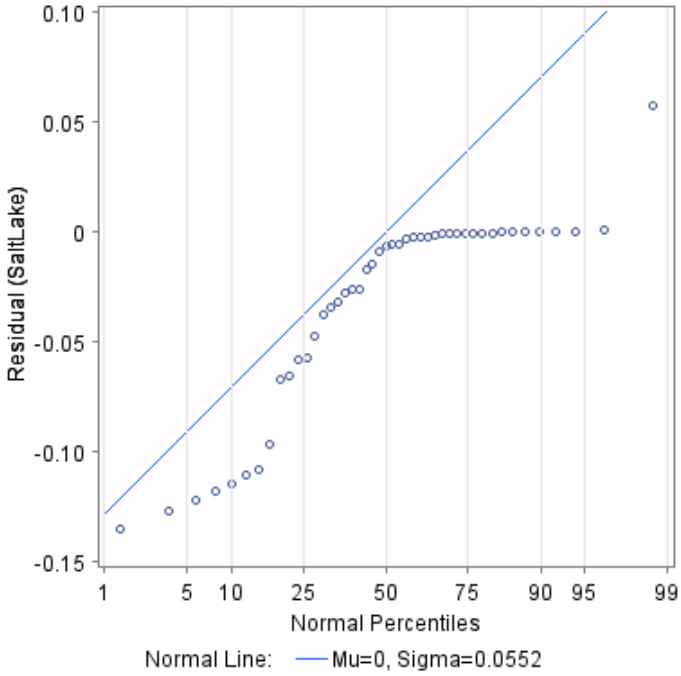

Figure D.113. Residual normality plot—percentage of on-time trips over 50 mph—Salt Lake City.

Table D.41. Residual Analysis—Percentage of On-Time Trips Over 50 mph—Salt Lake City

Table D.41.a. Basic Summary

Location		Variability	
Mean	–0.0318	Std deviation	0.0457
Median	–0.0066	Variance	0.0021
Min	–0.1350	Range	0.1927
Max	0.0577	Interquartile range	0.0568

Table D.41.b. Estimated Confidence Limits Assuming Normality

Parameter	Estimate	95% Confidence Limits	
Mean	–0.0318	–0.0455	–0.0181
Std deviation	0.0457	0.0378	0.0577
Variance	0.0021	0.0014	0.0033

Table D.41.c. Student's t-Test of Zero Residual Mean

Test	Statistic	*p*-Value
Student's *t*-test	–4.6715	<0.0001

Spokane

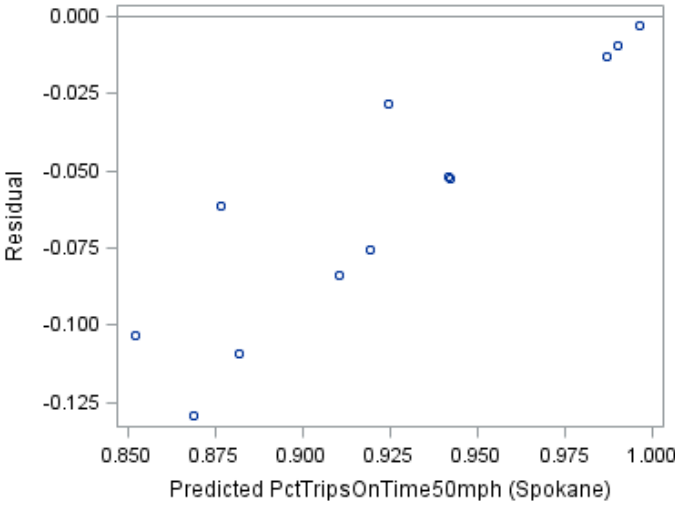

Figure D.114. Residual plot—percentage of on-time trips over 50 mph—Spokane.

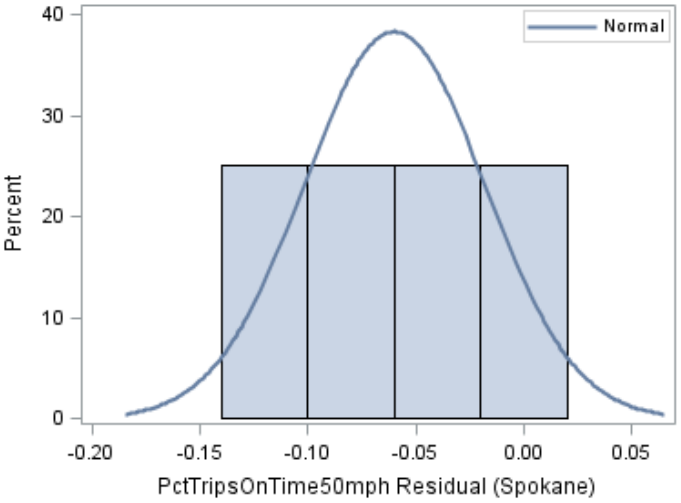

Figure D.115. Residual histogram—percentage of on-time trips over 50 mph—Spokane.

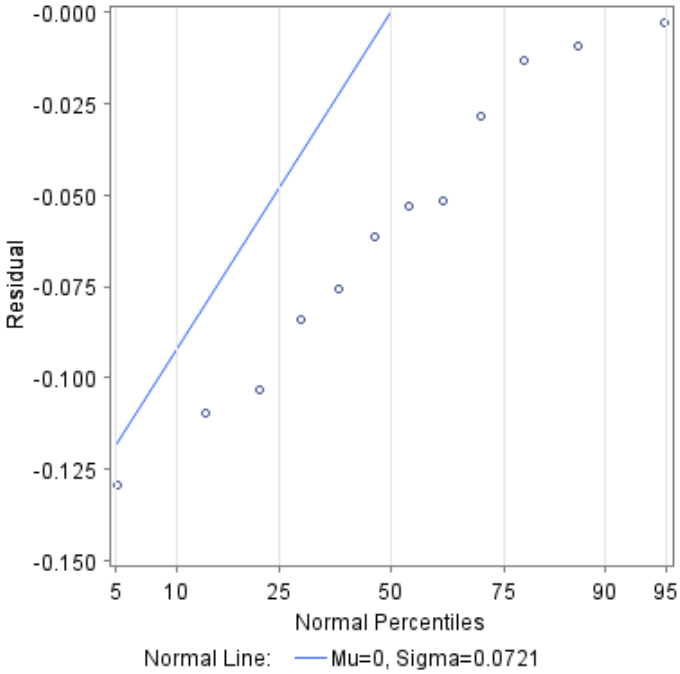

Figure D.116. Residual normality plot—percentage of on-time trips over 50 mph—Spokane.

Table D.42. Residual Analysis—Percentage of On-Time Trips Over 50 mph—Spokane

Table D.42.a. Basic Summary

Location		Variability	
Mean	–0.0601	Std deviation	0.0417
Median	–0.0570	Variance	0.0017
Min	–0.1295	Range	0.1266
Max	–0.0029	Interquartile range	0.0728

Table D.42.b. Estimated Confidence Limits Assuming Normality

Parameter	Estimate	95% Confidence Limits	
Mean	–0.0601	–0.0866	–0.0336
Std deviation	0.0417	0.0295	0.0708
Variance	0.0017	0.0009	0.0050

Table D.42.c. Student's t-Test of Zero Residual Mean

Test	Statistic	*p*-Value
Student's *t*-test	–4.9958	0.0004

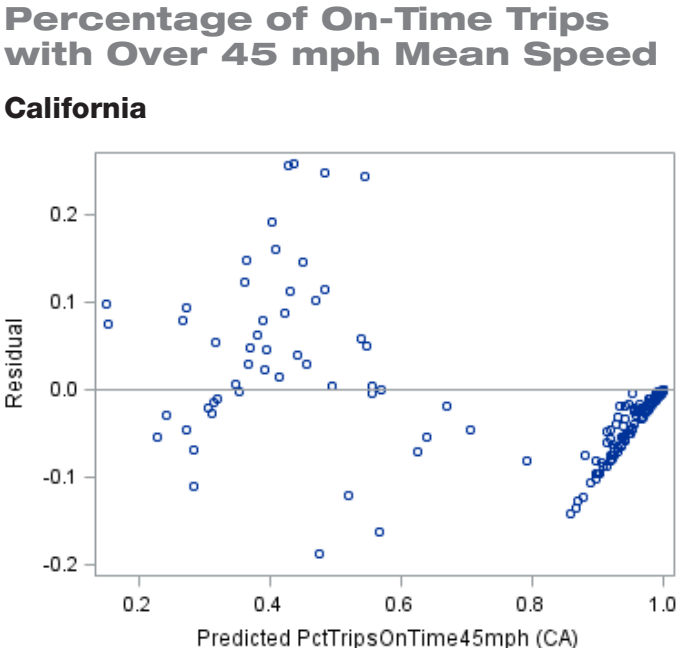

Figure D.117. Residual plot—percentage of on-time trips over 45 mph—California.

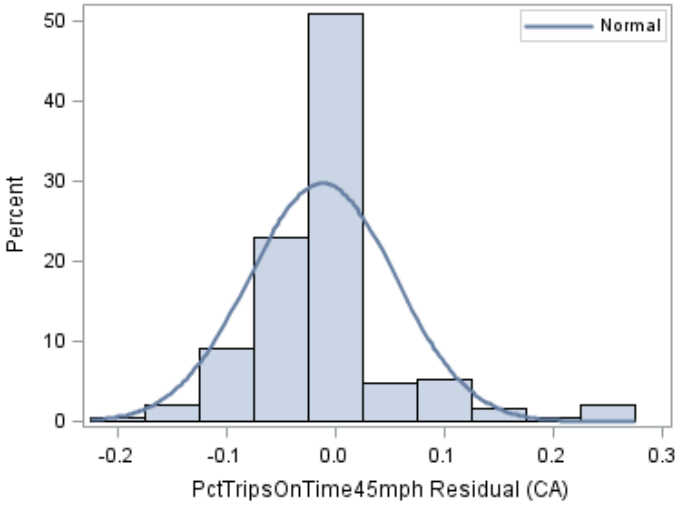

Figure D.118. Residual histogram—percentage of on-time trips over 45 mph—California.

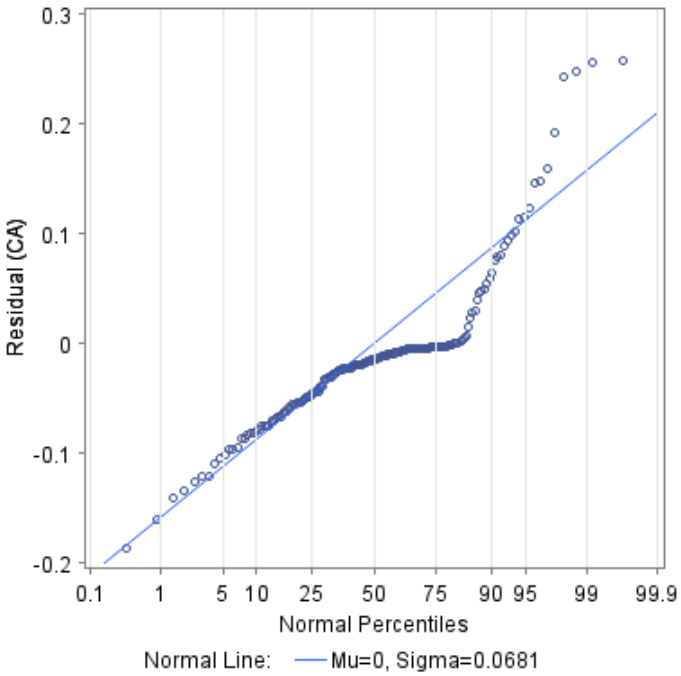

Figure D.119. Residual normality plot—percentage of on-time trips over 45 mph—California.

Table D.43. Residual Analysis—Percentage of On-Time Trips Over 45 mph—California

Table D.43.a. Basic Summary

Location		Variability	
Mean	–0.01220	Std deviation	0.06721
Median	–0.01415	Variance	0.00452
Min	–0.1876805	Range	0.44630
Max	0.2586168	Interquartile range	0.04294

Table D.43.b. Estimated Confidence Limits Assuming Normality

Parameter	Estimate	95% Confidence Limits	
Mean	–0.0122	–0.0219	–0.0025
Std deviation	0.0672	0.0610	0.0748
Variance	0.0045	0.0037	0.0056

Table D.43.c. Student's t-Test of Zero Residual Mean

Test	Statistic	*p*-Value
Student's *t*-test	–2.4815	0.0140

Minnesota

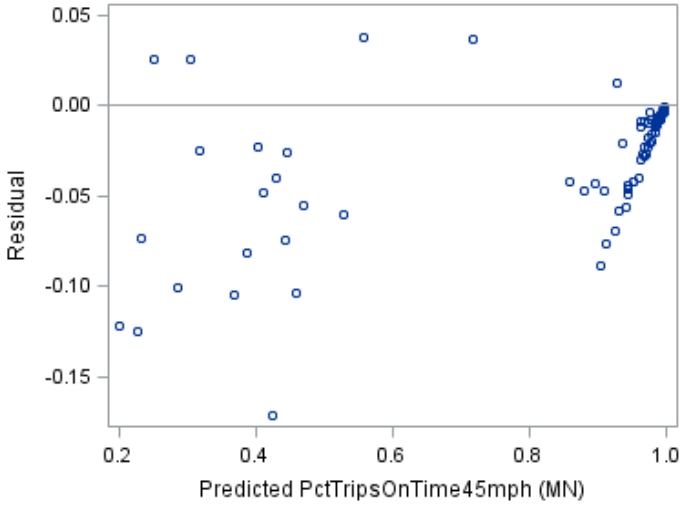

Figure D.120. Residual plot—percentage of on-time trips over 45 mph—Minnesota.

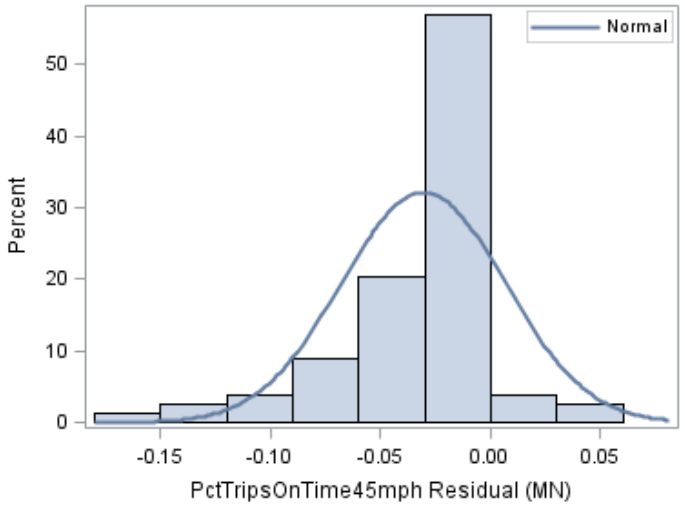

Figure D.121. Residual histogram—percentage of on-time trips over 45 mph—Minnesota.

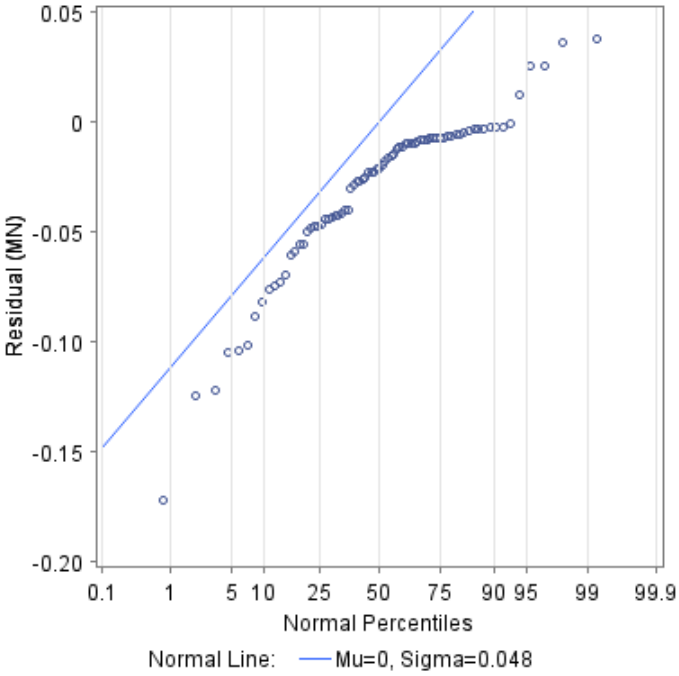

Figure D.122. Residual normality plot—percentage of on-time trips over 45 mph—Minnesota.

Table D.44. Residual Analysis – Percentage of On-Time Trips Over 45 mph—Minnesota

Table D.44.a. Basic Summary

Location		Variability	
Mean	–0.0306	Std deviation	0.0372
Median	–0.0208	Variance	0.0014
Min	–0.1719	Range	0.2103
Max	0.0383	Interquartile range	0.0400

Table D.44.b. Estimated Confidence Limits Assuming Normality

Parameter	Estimate	95% Confidence Limits	
Mean	–0.0306	–0.0389	–0.0222
Std deviation	0.0372	0.0322	0.0441
Variance	0.0014	0.0010	0.0019

Table D.44.c. Student's t-Test of Zero Residual Mean

Test	Statistic	*p*-Value
Student's *t*-test	–7.3038	<0.0001

Salt Lake City

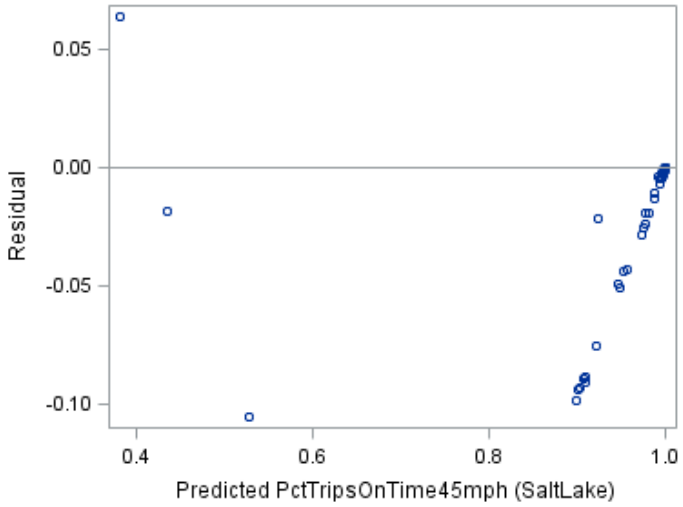

Figure D.123. Residual plot—percentage of on-time trips over 45 mph—Salt Lake City.

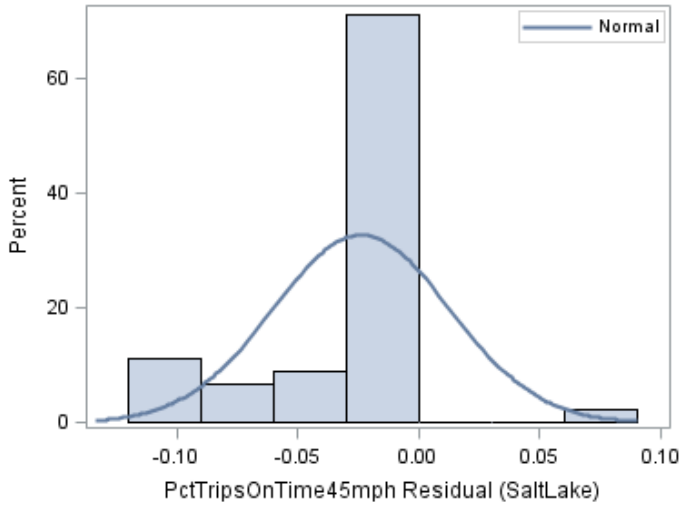

Figure D.124. Residual histogram—percentage of on-time trips over 45 mph—Salt Lake City.

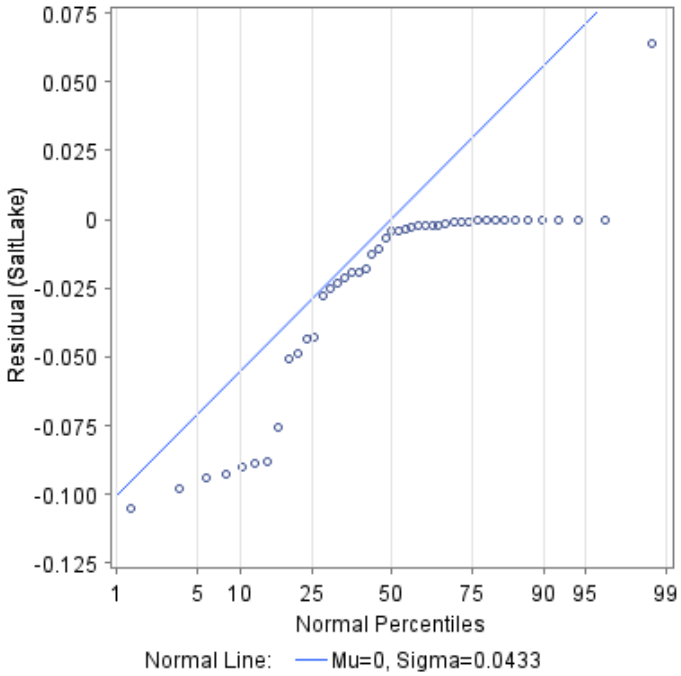

Figure D.125. Residual normality plot—percentage of on-time trips over 45 mph—Salt Lake City.

Table D.45. Residual Analysis—Percentage of On-Time Trips Over 45 mph—Salt Lake City

Table D.45.a. Basic Summary

Location		Variability	
Mean	–0.0238	Std deviation	0.0366
Median	–0.0043	Variance	0.0013
Min	–0.1053	Range	0.1695
Max	0.0642	Interquartile range	0.0425

Table D.45.b. Estimated Confidence Limits Assuming Normality

Parameter	Estimate	95% Confidence Limits	
Mean	–0.0238	–0.0348	–0.0128
Std deviation	0.0366	0.0303	0.0462
Variance	0.0013	0.0009	0.0021

Table D.45.c. Student's t-Test of Zero Residual Mean

Test	Statistic	*p*-Value
Student's *t*-test	–4.3584	<0.0001

Spokane

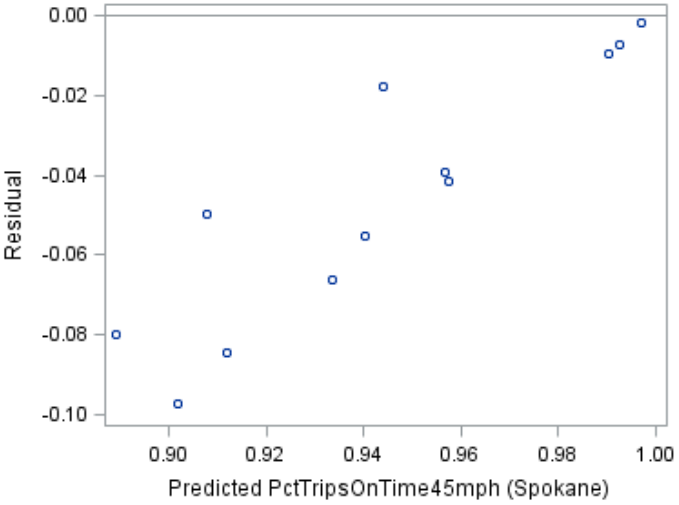

Figure D.126. Residual plot—percentage of on-time trips over 45 mph—Spokane.

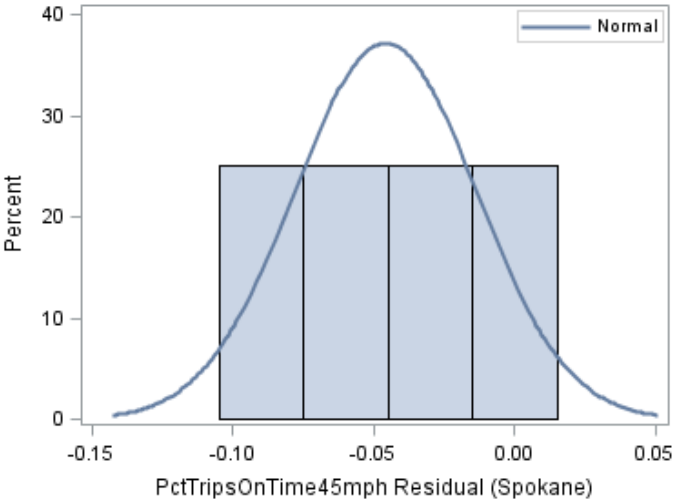

Figure D.127. Residual histogram—percentage of on-time trips over 45 mph—Spokane.

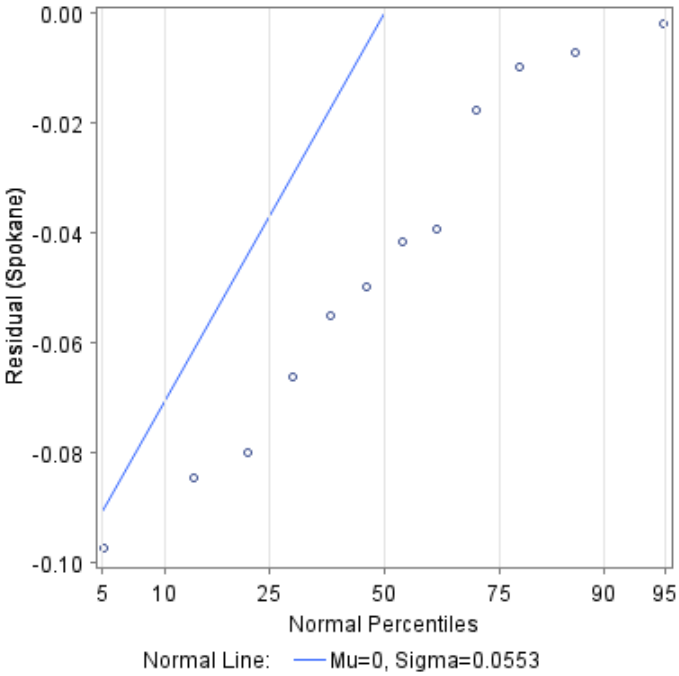

Figure D.128. Residual normality plot—percentage of on-time trips over 45 mph—Spokane.

Table D.46. Residual Analysis—Percentage of On-Time Trips Over 45 mph—Spokane

Table D.46.a. Basic Summary

Location		Variability	
Mean	–0.0459	Std deviation	0.0322
Median	–0.0458	Variance	0.0010
Min	–0.0973	Range	0.0953
Max	–0.0020	Interquartile range	0.0594

Table D.46.b. Estimated Confidence Limits Assuming Normality

Parameter	Estimate	95% Confidence Limits	
Mean	–0.04591	–0.0664	–0.0254
Std deviation	0.0322	0.0228	0.0547
Variance	0.0010	0.0005	0.0030

Table D.46.c. Student's t-Test of Zero Residual Mean

Test	Statistic	*p*-Value
Student's *t*-test	–4.9369	0.0004

Percentage of On-Time Trips with Over 30 mph Mean Speed

California

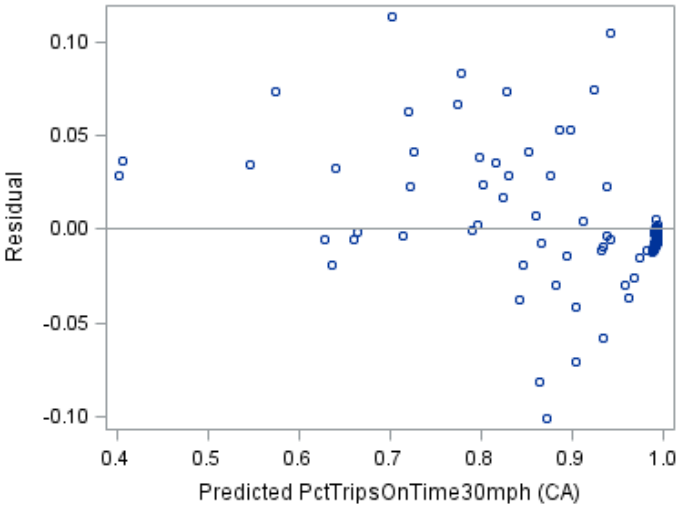

Figure D.129. Residual plot—percentage of on-time trips over 30 mph—California.

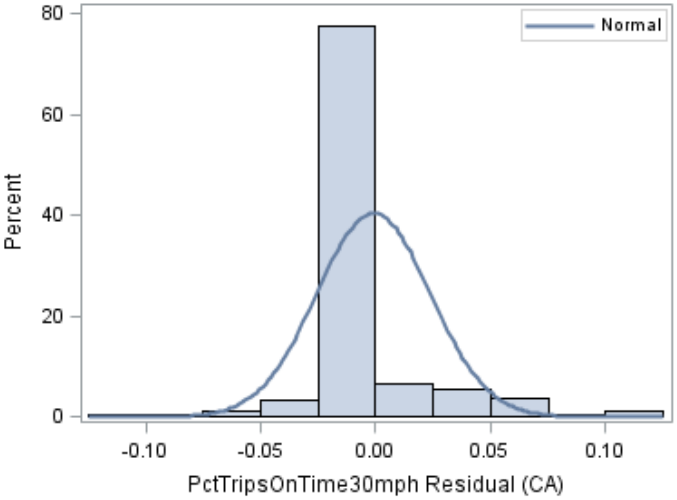

Figure D.130. Residual histogram—percentage of on-time trips over 30 mph—California.

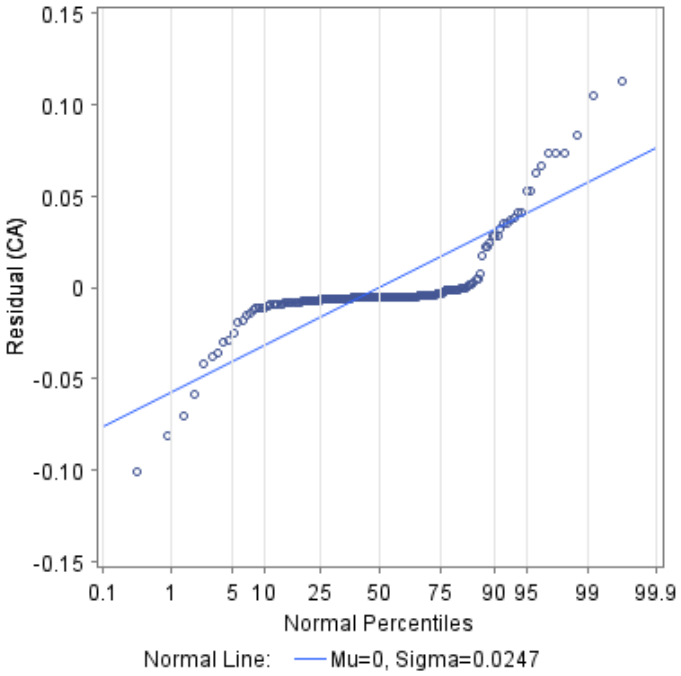

Figure D.131. Residual normality plot—percentage of on-time trips over 30 mph—California.

Table D.47. Residual Analysis—Percentage of On-Time Trips Over 30 mph—California

Table D.47.a. Basic Summary

Location		Variability	
Mean	–0.0009	Std deviation	0.0247
Median	–0.0055	Variance	0.0006
Min	–0.1009	Range	0.2143
Max	0.1134	Interquartile range	0.0037

Table D.47.b. Estimated Confidence Limits Assuming Normality

Parameter	Estimate	95% Confidence Limits	
Mean	–0.0009	–0.0045	0.0026
Std deviation	0.0247	0.0224	0.0275
Variance	0.0006	0.0005	0.0008

Table D.47.c. Student's t-Test of Zero Residual Mean

Test	Statistic	*p*-Value
Student's *t*-test	–0.5185	0.6048

Minnesota

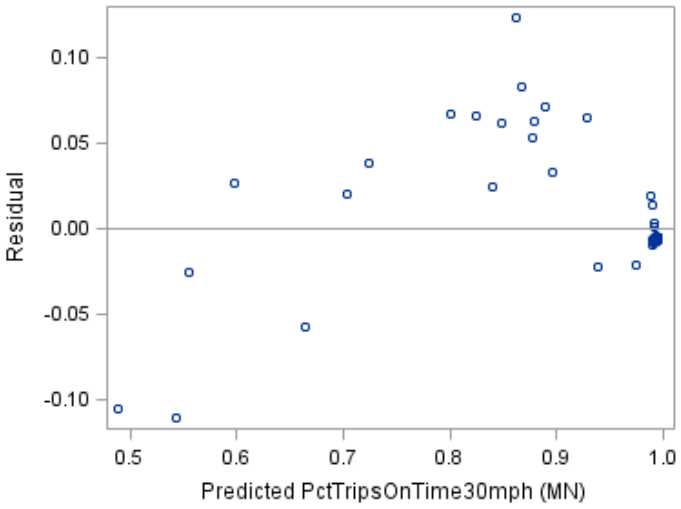

Figure D.132. Residual plot—percentage of on-time trips over 30 mph—Minnesota.

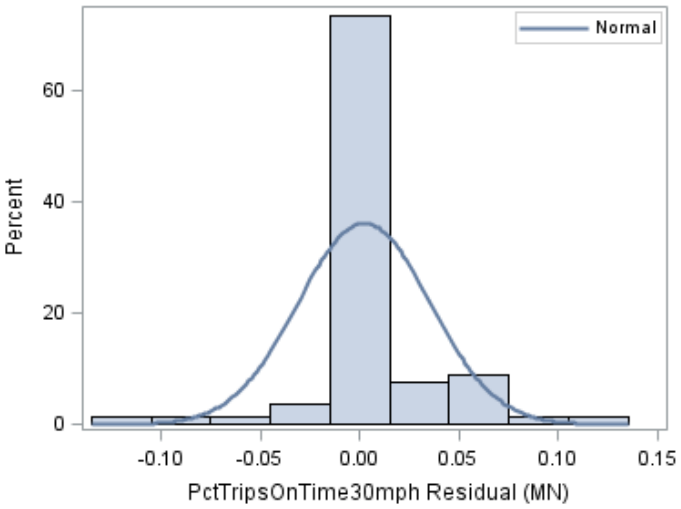

Figure D.133. Residual histogram—percentage of on-time trips over 30 mph—Minnesota.

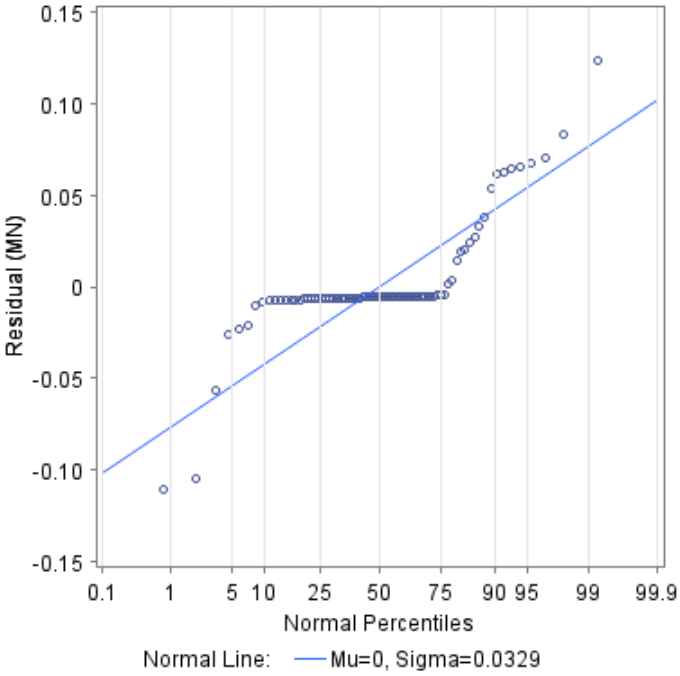

Figure D.134. Residual normality plot—percentage of on-time trips over 30 mph—Minnesota.

Table D.48. Residual Analysis—Percentage of On-Time Trips Over 30 mph—Minnesota

Table D.48.a. Basic Summary

Location		Variability	
Mean	0.0021	Std deviation	0.0331
Median	–0.0056	Variance	0.0011
Min	–0.1103	Range	0.2336
Max	0.1233	Interquartile range	0.0016

Table D.48.b. Estimated Confidence Limits Assuming Normality

Parameter	Estimate	95% Confidence Limits	
Mean	0.0021	–0.0053	0.0095
Std deviation	0.0331	0.0286	0.0392
Variance	0.0011	0.0008	0.0015

Table D.48.c. Student's t-Test of Zero Residual Mean

Test	Statistic	*p*-Value
Student's *t*-test	0.5652	0.5736

Salt Lake City

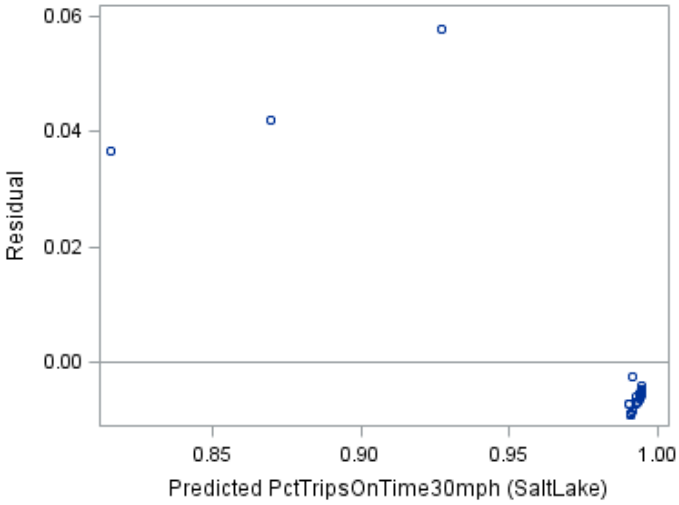

Figure D.135. Residual plot—percentage of on-time trips over 30 mph—Salt Lake City.

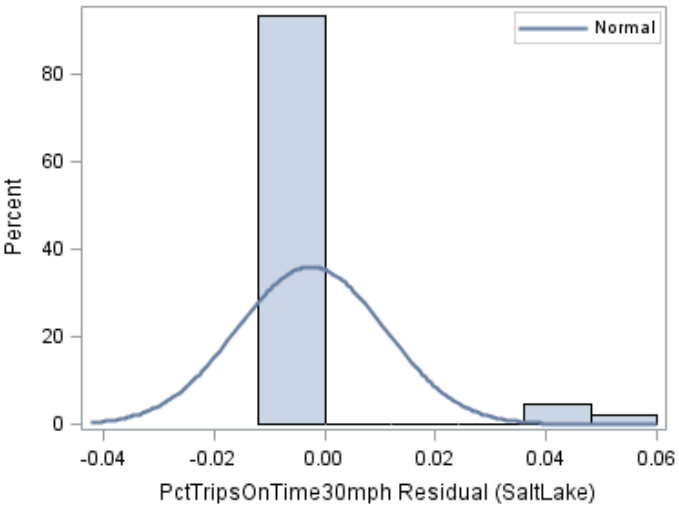

Figure D.136. Residual histogram—percentage of on-time trips over 30 mph—Salt Lake City.

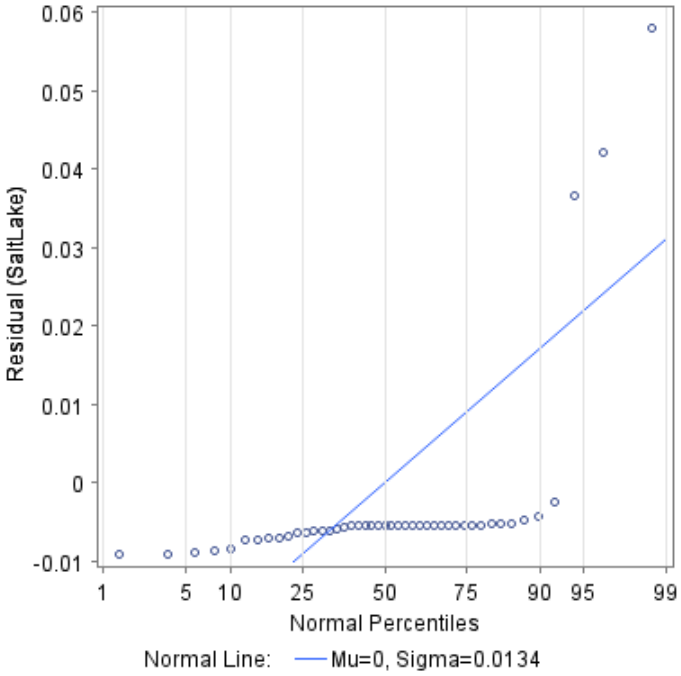

Figure D.137. Residual normality plot—percentage of on-time trips over 30 mph—Salt Lake City.

Table D.49. Residual Analysis—Percentage of On-Time Trips Over 30 mph—Salt Lake City

Table D.49.a. Basic Summary

Location		Variability	
Mean	–0.0026	Std deviation	0.0133
Median	–0.0054	Variance	0.0002
Min	–0.0092	Range	0.0671
Max	0.0579	Interquartile range	0.0009

Table D.49.b. Estimated Confidence Limits Assuming Normality

Parameter	Estimate	95% Confidence Limits	
Mean	–0.0026	–0.0065	0.0014
Std deviation	0.0133	0.0110	0.0168
Variance	0.0002	0.0001	0.0003

Table D.49.c. Student's t-Test of Zero Residual Mean

Test	Statistic	*p*-Value
Student's *t*-test	–1.2873	0.2047

Spokane

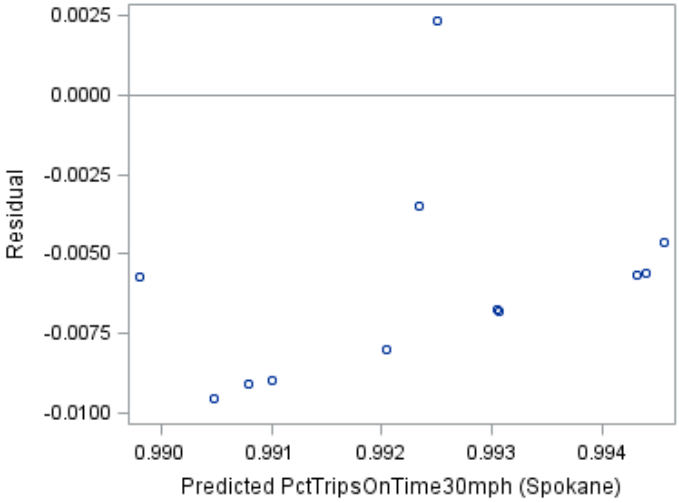

Figure D.138. Residual plot—percentage of on-time trips over 30 mph—Spokane.

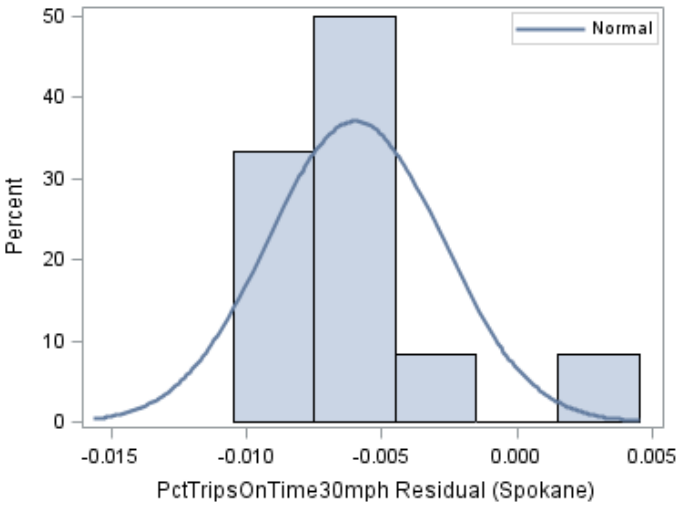

Figure D.139. Residual histogram—percentage of on-time trips over 30 mph—Spokane.

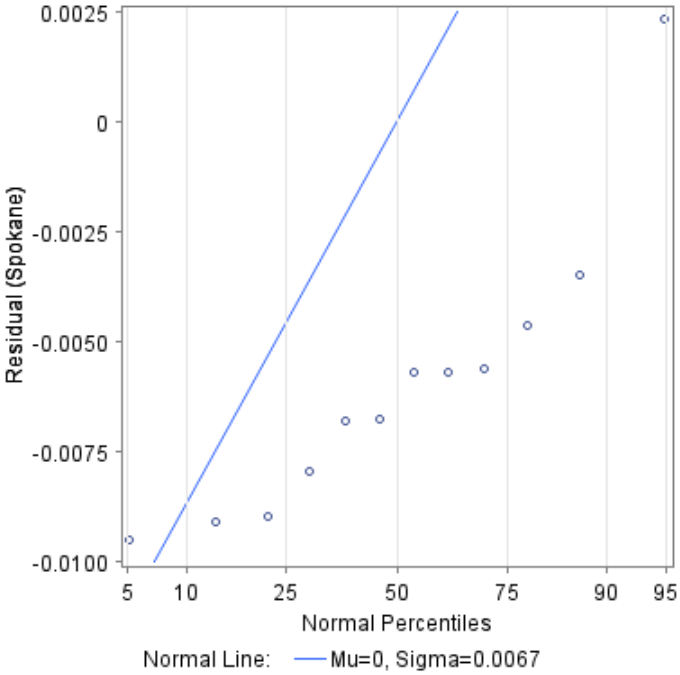

Figure D.140. Residual normality plot—percentage of on-time trips over 30 mph—Spokane.

Table D.50. Residual Analysis—Percentage of On-Time Trips Over 30 mph—Spokane

Table D.50.a. Basic Summary

Location		Variability	
Mean	–0.0060	Std deviation	0.0032
Median	–0.0062	Variance	0.0000
Min	–0.0095	Range	0.0119
Max	0.0024	Interquartile range	0.0034

Table D.50.b. Estimated Confidence Limits Assuming Normality

Parameter	Estimate	95% Confidence Limits	
Mean	–0.0060	–0.0080	–0.0039
Std deviation	0.0032	0.0023	0.0055
Variance	0.0000	0.0000	0.0000

Table D.50.c. Student's t-Test of Zero Residual Mean

Test	Statistic	*p*-Value
Student's *t*-test	–6.4287	<0.0001

APPENDIX E

Model Enhancements

Overview

This appendix presents the results of the recalibration of the L03 data-poor models and the development of new model forms for the 95th-, 90th-, and 80th-percentile predictive equations for the travel time index (TTI).

Recalibration

For each recalibration, model statistics along with diagnostic figures are presented. The model statistics show the overall model performance measures, such as the mean squared error (MSE) and the *F*-test. R^2 is also presented if applicable, but it may be redefined in different cases. The model statistics also include parameter-associated results, such as the parameter estimates and the *t*-test results. The figures include (if applicable)

1. Fit plot in the original scale. This scatter plot shows the measured data samples and the recalibrated model line.
2. Fit plot showing a similar scatter plot, but the *x*-axis is in logarithm scale. This is the linear recalibrated model form. The 95% prediction confidence limits are also indicated.
3. Observed-by-predicted plot. If the model fits well, the scattered points should fall on the two sides of the reference line.
4. Residual-by-predicted plot. This is an important method to analyze the residuals; same method is used in the model validation analysis to evaluate the model performance.
5. Outlier and leverage plot. This is to analyze the outliers and leverage points that may raise questions in model building.
6. Histogram. This is used to display the distribution of the residuals.
7. Normality plot. This is used to show how close the residual distribution is to a normal distribution.

Note that these statistics and plots are presented to evaluate the model from different perspectives; however, it is almost always impossible to build a real world model that perfectly satisfies all the criteria. Some of the measures are more important than others.

From the recalibration results we can see that the nonconstant variance is still a common problem for almost all cases; however, due to the characteristics of the data, it may not be fully resolvable.

95th-Percentile TTI

The recalibration of the 95th-percentile TTI model is conducted by building a linear model between the response variable, 95th-percentile TTI, and the independent variable, log-transformed mean TTI—ln(meanTTI)—with the restriction that the intercept is fixed at 1. Due to the restriction, the R^2 is redefined.

AllData

The recalibrated model for the 95th-percentile TTI with the AllData set is

$$\text{95th-percentile TTI}_{\text{AllData}} = 1 + 3.4201 * \ln(\text{meanTTI})$$

Overall, this model can predict the measured data with good accuracy (Table E.1). The *F*-test (Table E.2) shows strong evidence that the model can explain most of the variance of the response variable. The *t*-test (Table E.3) for individual predictors also shows strong evidence for significance of the independent variable.

We need to further analyze the goodness-of-fit of the model. The scatter plot (Figure E.1) shows how the regional data identified by different colors are scattered along the model line in the original scale (nontransformed). The observation that most blue dots (representing Minnesota data) are beyond the model line while most of the red dots (representing the California data) are below the model line indicates that regional calibration may be necessary.

Table E.1. Root MSE and R-Square, Recalibrated 95th-Percentile TTI Model, AllData

Root MSE	0.17230	*R*-Square	0.9884

Table E.2. Analysis of Variance, Recalibrated 95th-Percentile TTI Model, AllData

Source	DF	Sum of Squares	Mean Square	*F*-Value	Pr > *F*
Model	1	813.98823	813.98823	27418.0	<0.0001
Error	322	9.55957	0.02969		
Uncorrected total	323	823.54780			

Figures E.1 through E.7 evaluate the model performance from different perspectives. The scatter plot (Figure E.1) shows that the model can predict the data trend closely. From the fit plot (Figure E.2) we can see that some of the data samples fall outside the confidence limits, which may be outliers. The predicted versus measured plot (Figure E.3) shows in another way how the model fits the data. In the case of perfect fit, the data samples would fall on the equal value line; however, with noise in the measured data, they are supposed to scatter along the diagonal line. The pattern in the figure shows that the model can predict the data samples with a good satisfactory level. The residual plot (Figure E.4) shows that the residuals are generally randomly scattered, although the increasing residual variance problem still exists, and there is some nonrandom pattern around the origin. The outlier and leverage plot (Figure E.5) shows the identified outliers and leverage points. The histogram and the normality plot (Figures E.6 and E.7) show that even with recalibration, the residuals may still not satisfy the normal distribution assumption perfectly.

Table E.3. Parameter Estimates, Recalibrated 95th-Percentile TTI Model, AllData

Variable	DF	Parameter Estimate	Standard Error	*t*-Value	Pr > |*t*|	95% Confidence Limits	
Intercept	1	1.00000	0	Infty	<0.0001	1.00000	1.00000
ln(mean TTI) (AllData)	1	3.42007	0.04034	84.78	<0.0001	3.34071	3.49944
RESTRIC	–1	–2.54913	2.60948	–0.98	0.3294[a]	–7.66023	2.56198

[a] The model restricts the intercept to be 1 (unity).
Note: Infty = infinity.

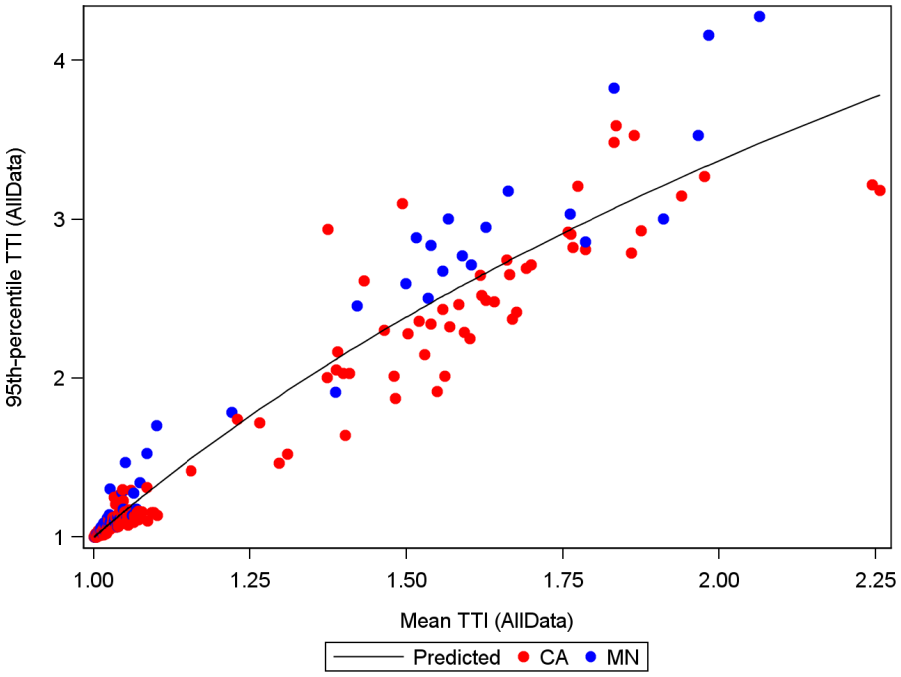

Figure E.1. Scatter plot in original scale, recalibrated 95th-percentile TTI model, AllData.

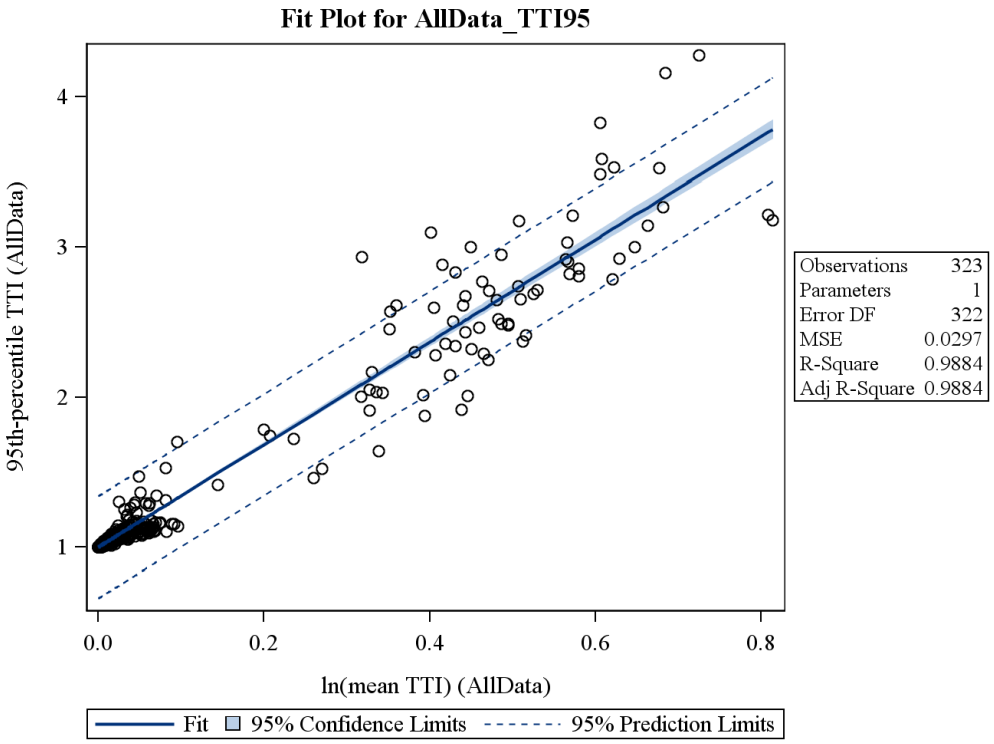

Figure E.2. Fit plot in x-axis log scale, recalibrated 95th-percentile TTI model, AllData.

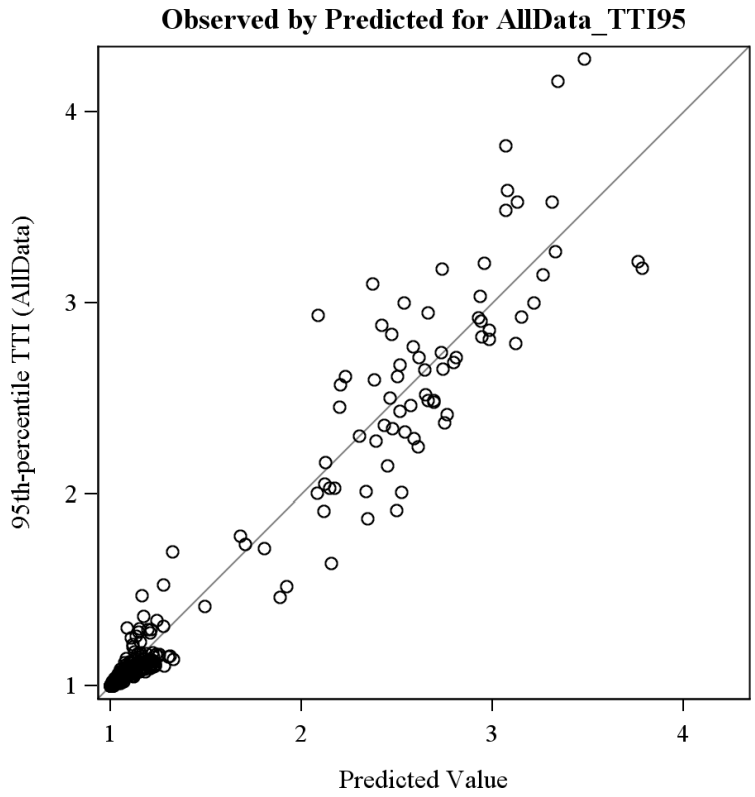

Figure E.3. Observed-by-predicted plot, recalibrated 95th-percentile TTI model, AllData.

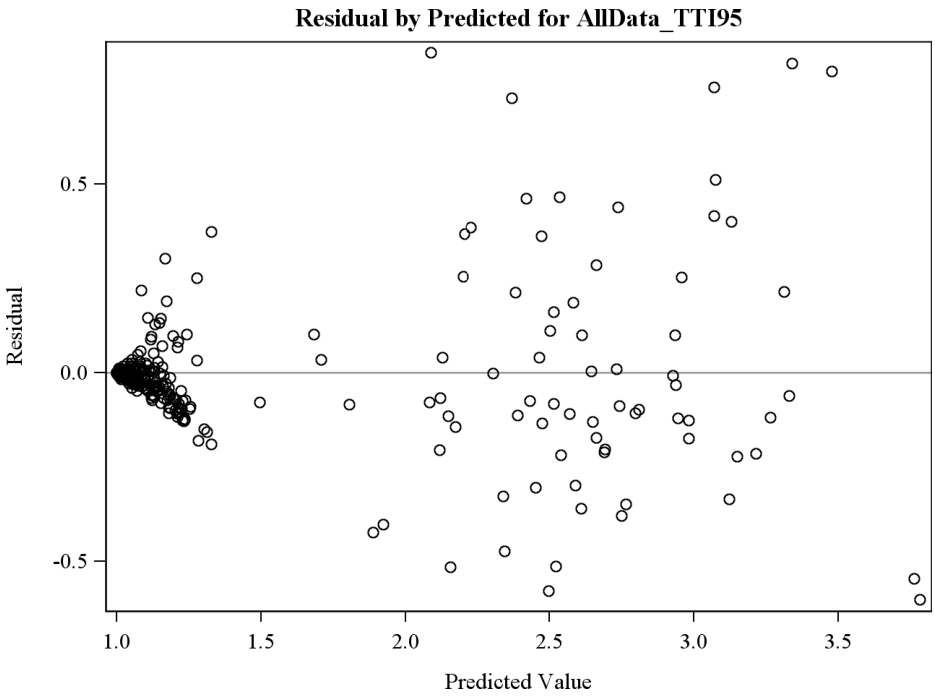

Figure E.4. Residual-by-predicted plot, recalibrated 95th-percentile TTI model, AllData.

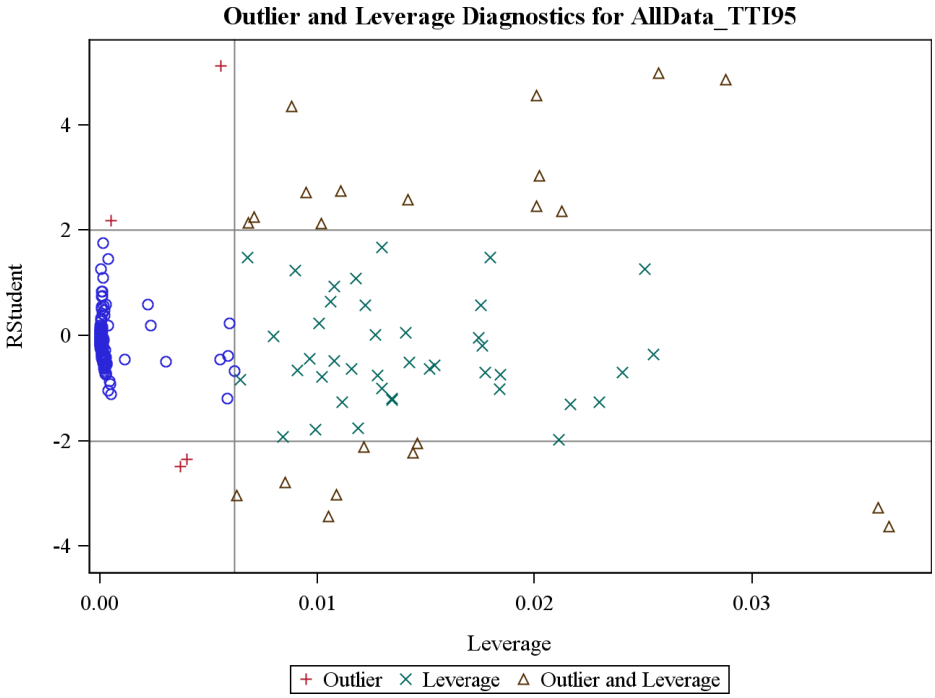

Figure E.5. Outlier and leverage plot, recalibrated 95th-percentile TTI model, AllData.

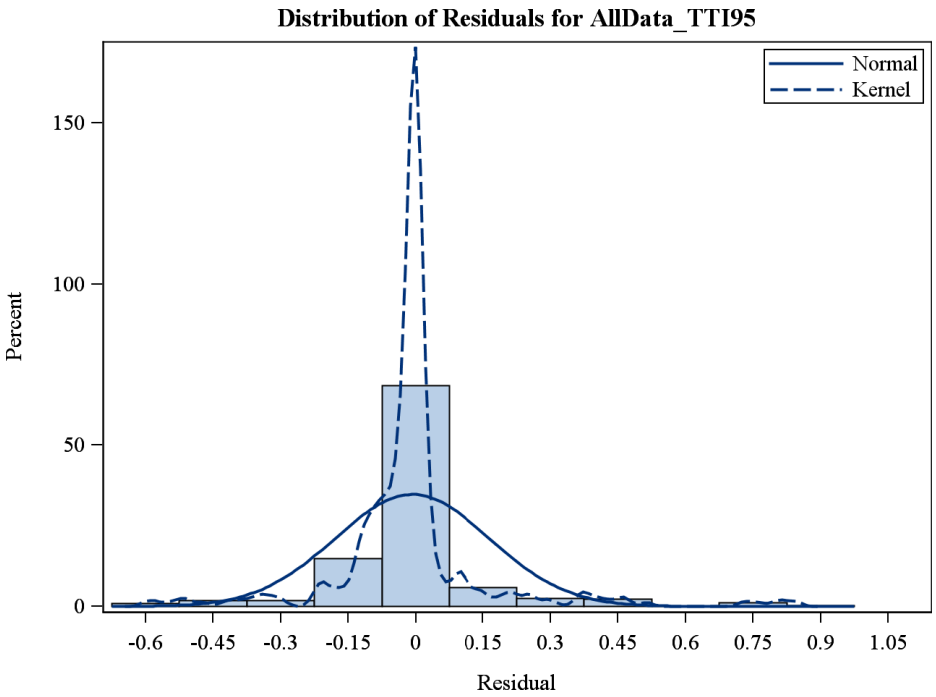

Figure E.6. Distribution of residuals, recalibrated 95th-percentile TTI model, AllData.

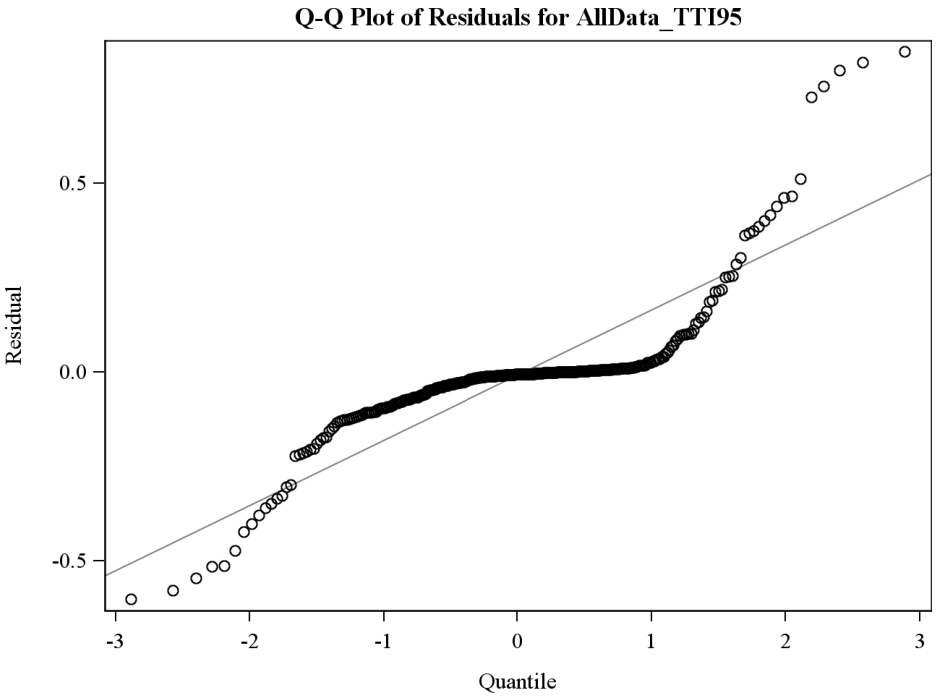

Figure E.7. Quantile-quantile (Q-Q) plot of residuals, recalibrated 95th-percentile TTI model, AllData.

Table E.4. Root MSE and R-Square, Recalibrated 95th-Percentile TTI Model, California

Root MSE	0.16425	*R*-Square	0.9898

Table E.5. Analysis of Variance, Recalibrated 95th-Percentile TTI Model, California

Source	DF	Sum of Squares	Mean Square	*F*-Value	Pr > *F*
Model	1	484.90978	484.90978	17974.2	<0.0001
Error	186	5.01793	0.02698		
Uncorrected total	187	489.92771			

California

The recalibrated model for the 95th-percentile TTI with the California (CA) set is

$$95\text{th-percentile TTI}_{CA} = 1 + 3.1818 * \ln(\text{meanTTI})$$

The root MSE and *R*-Square are given in Table E.4. The *F*-test (Table E.5) yields nearly zero *p*-values, indicating strong confidence in the model validity. Student's *t*-tests (Table E.6) also show the significance of the model parameters. The scatter plot, fit plot, and the observed-by-predicted plot all show that the model can predict the data trend well (refer to Figures E.8 through E.14 for interpretation of the observations). However, the residual-by-predicted plot indicates the possibility of inadequate model form as the residuals seem not to be randomly scattered along the reference line. The outlier and leverage plot show that outliers and leverage points may exist, while the histogram and the normality plot show that the residual distribution does not perfectly follow a normal distribution.

Table E.6. Parameter Estimates, Recalibrated 95th-Percentile TTI Model, California

Variable	DF	Parameter Estimate	Standard Error	*t*-Value	Pr > |*t*|	95% Confidence Limits	
Intercept	1	1.00000	0	Infty	<0.0001	1.00000	1.00000
ln(mean TTI) (CA)	1	3.18182	0.04671	68.12	<0.0001	3.08966	3.27397
RESTRICT	–1	–1.46715	1.83910	–0.80	0.4265[a]	–5.06758	2.13327

[a] The model restricts the intercept to be 1 (unity).

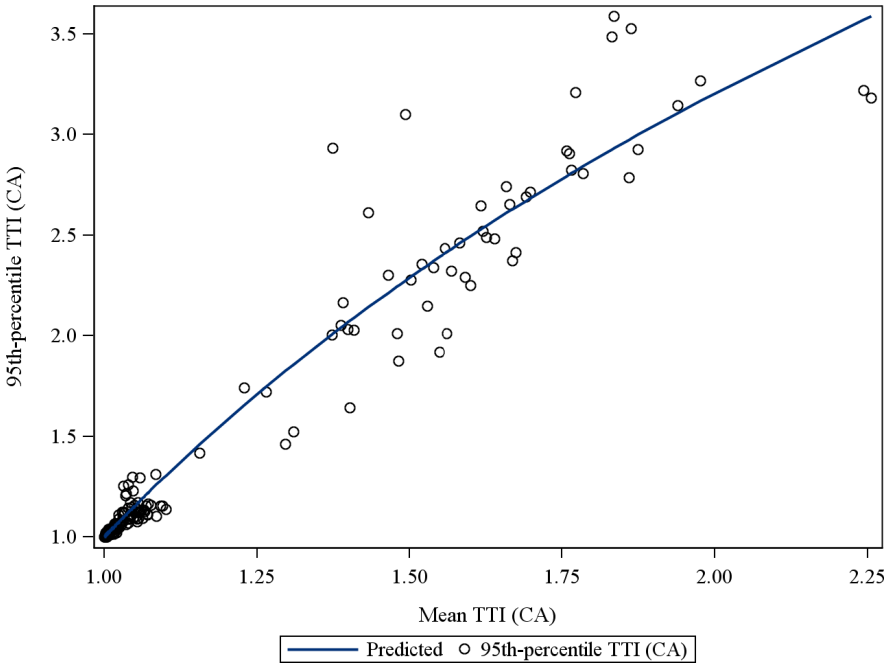

Figure E.8. Fit plot in original scale, recalibrated 95th-percentile TTI model, California.

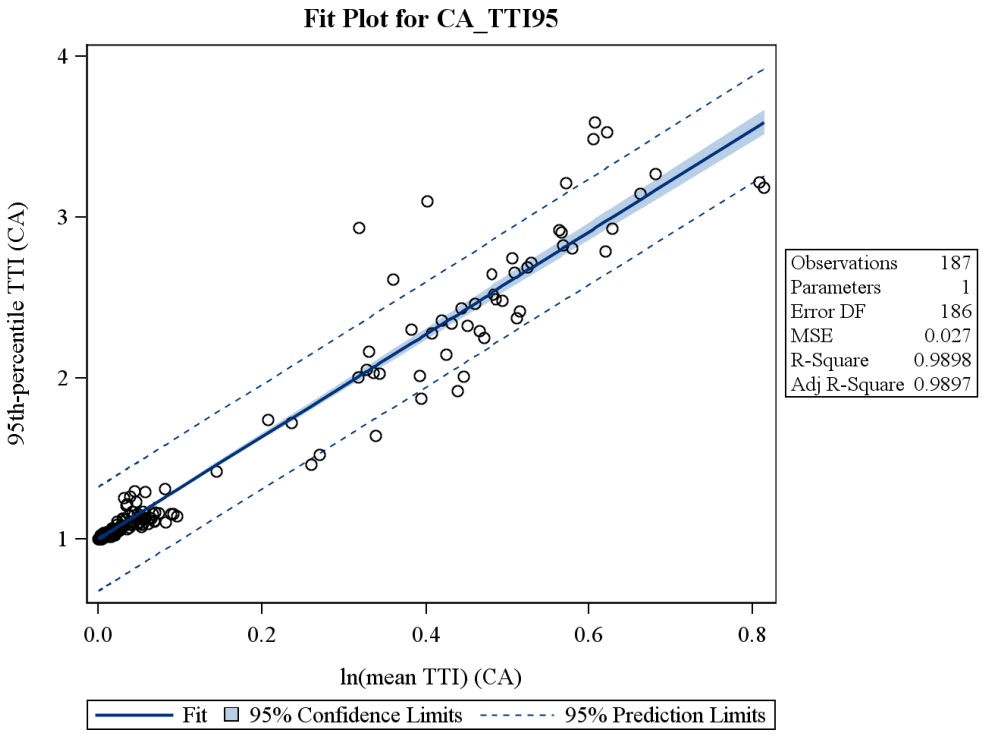

Figure E.9. Fit plot in x-axis log scale, recalibrated 95th-percentile TTI model, California.

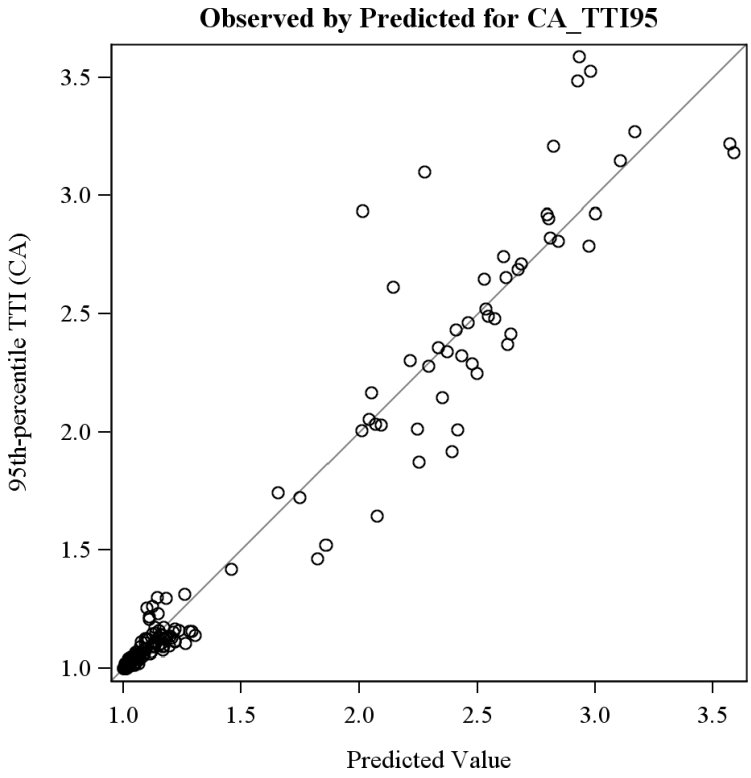

Figure E.10. Observed-by-predicted plot, recalibrated 95th-percentile TTI model, California.

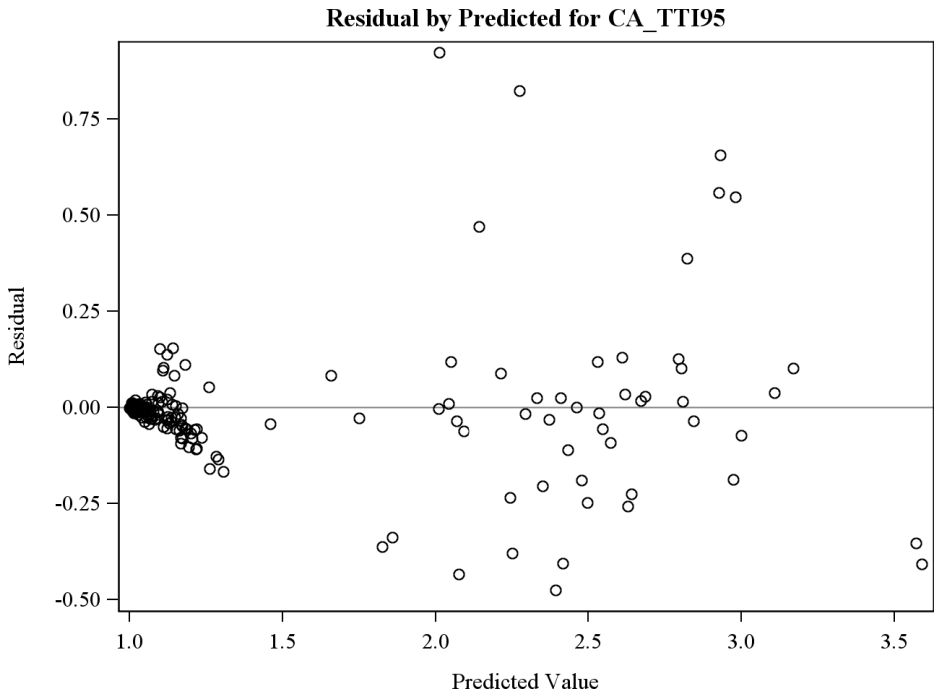

Figure E.11. Residual-by-predicted plot, recalibrated 95th-percentile TTI model, California.

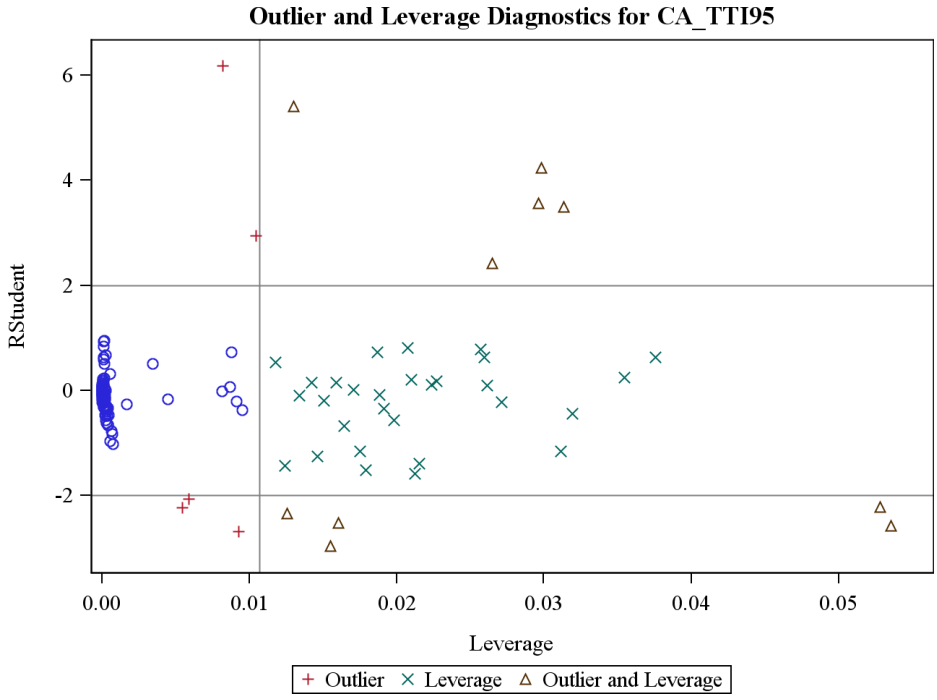

Figure E.12. Outlier and leverage plot, recalibrated 95th-percentile TTI model, California.

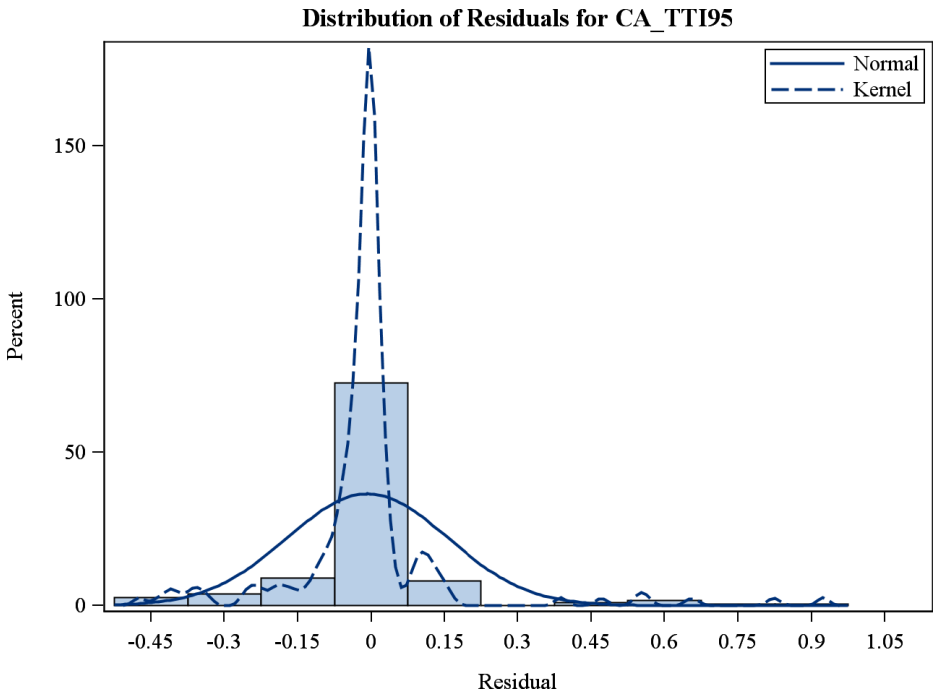

Figure E.13. Distribution of residuals, recalibrated 95th-percentile TTI model, California.

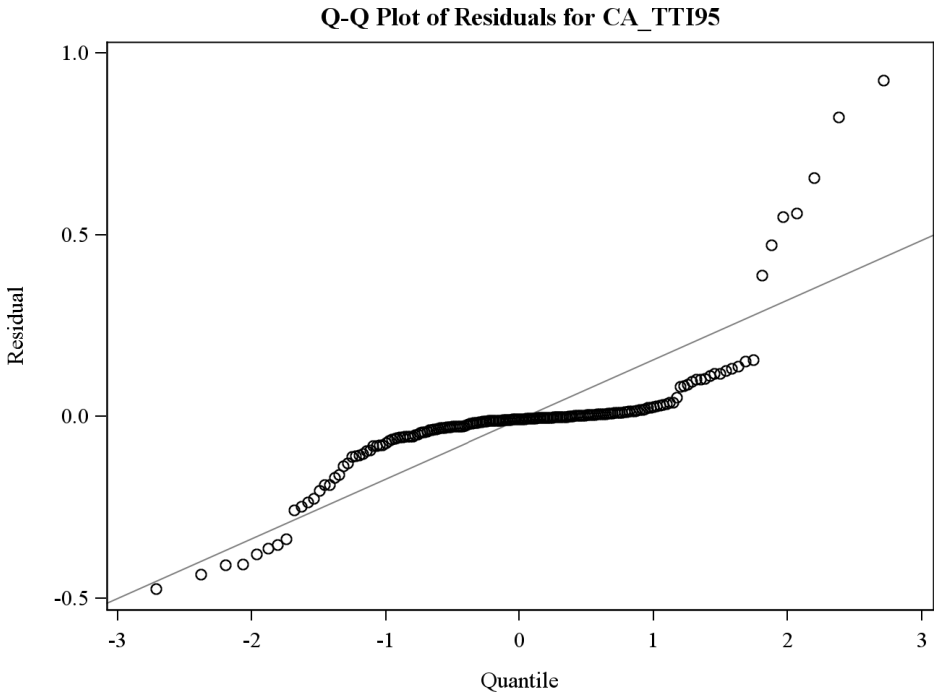

Figure E.14. Q-Q plot of residuals, recalibrated 95th-percentile TTI model, California.

Table E.7. Root MSE and R-Square, Recalibrated 95th-Percentile TTI Model, Minnesota

Root MSE	0.15298	*R*-Square	0.9928

Minnesota

The recalibrated model for the 95th-percentile TTI with the Minnesota (MN) set is

$$95\text{th-percentile TTI}_{MN} = 1 + 3.9787 * \ln(\text{meanTTI})$$

Table E.7 gives the root MSE and *R*-Square values. The *F*-test (Table E.8) yields a large *F*-value and a nearly zero *p*-value, showing strong confidence that the model can explain most of the variance of the response variable. The Student's *t*-test (Table E.9) also shows strong evidence that the model parameter is not zero. From the plots we can see that the model can predict the data trend well: the residual-by-predicted plot shows a generally random pattern although the nonconstant variance problem still exists; some of the samples may be outliers and leverage points; and the residual distribution does not perfectly follow a normal distribution (refer to Figures E.15 through E.21 for interpretation of the observations).

Table E.8. Analysis of Variance, Recalibrated 95th-Percentile TTI Model, Minnesota

Source	DF	Sum of Squares	Mean Square	*F*-Value	Pr > *F*
Model	1	252.12485	252.12485	10773.6	<0.0001
Error	78	1.82537	0.02340		
Uncorrected total	79	253.95022			

Table E.9. Parameter Estimates, Recalibrated 95th-Percentile TTI Model, Minnesota

Variable	Label	DF	Parameter Estimate	Standard Error	*t*-Value	Pr > |*t*|	95% Confidence Limits	
Intercept	Intercept	1	1.00000	0	Infty	<0.0001	1.00000	1.00000
MN_TTImean_ln	ln(mean TTI) (MN)	1	3.97871	0.06673	59.63	<0.0001	3.84587	4.11156
RESTRICT	*RESTRICT*	–1	0.27267	1.13445	0.24	0.8118[a]	–1.94456	2.48990

[a] The model restricts the intercept to be 1 (unity).

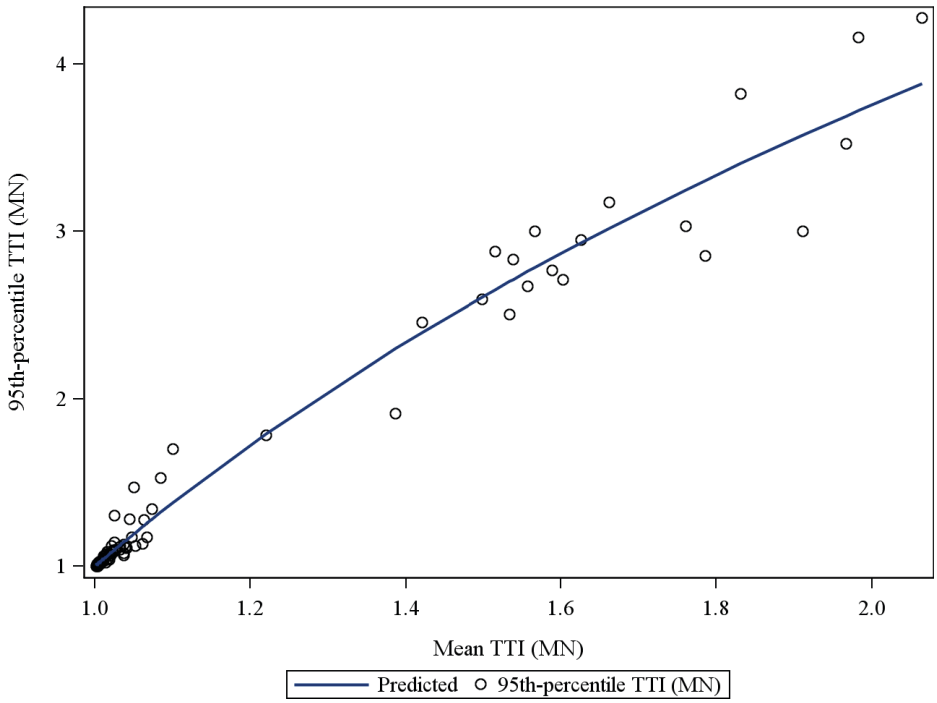

Figure E.15. Fit plot in original scale, recalibrated 95th-percentile TTI model, Minnesota.

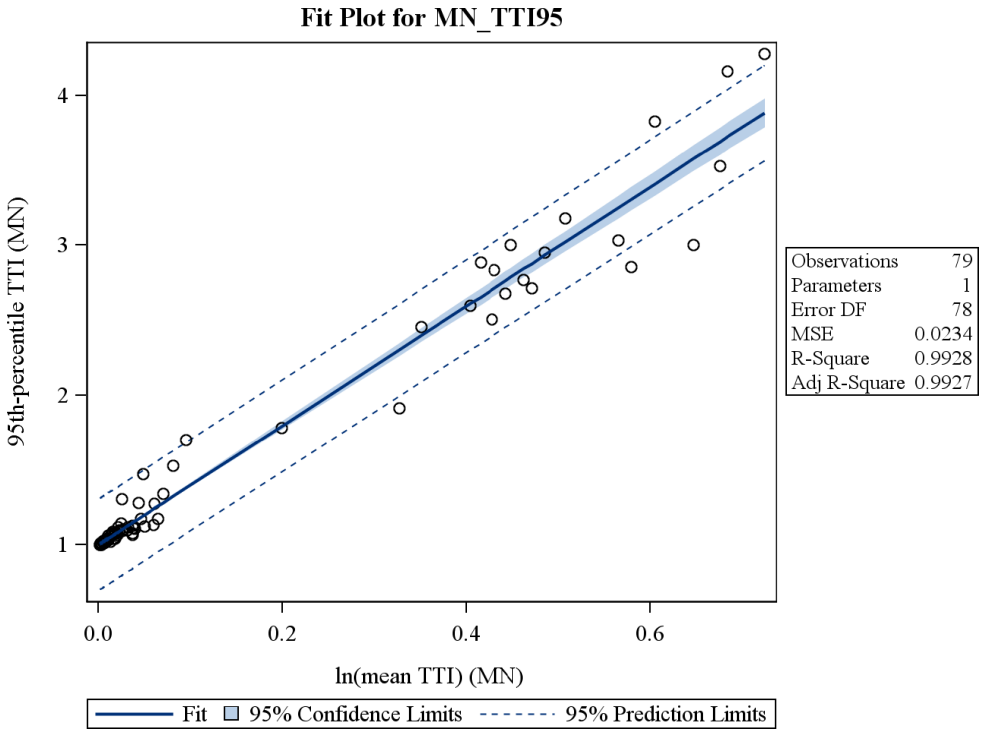

Figure E.16. Fit plot in x-axis log scale, recalibrated 95th-percentile TTI model, Minnesota.

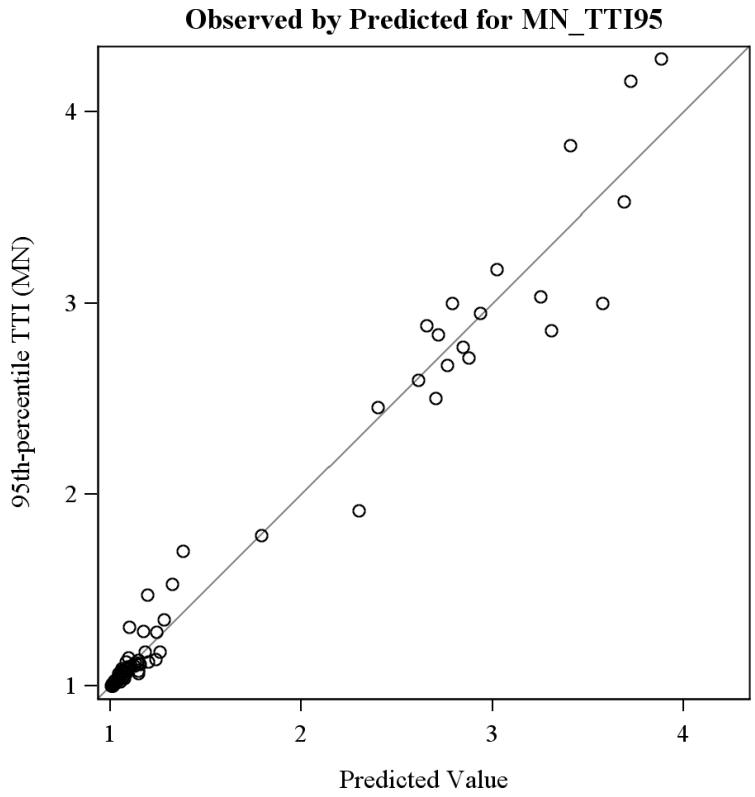

Figure E.17. Observed-by-predicted plot, recalibrated 95th-percentile TTI model, Minnesota.

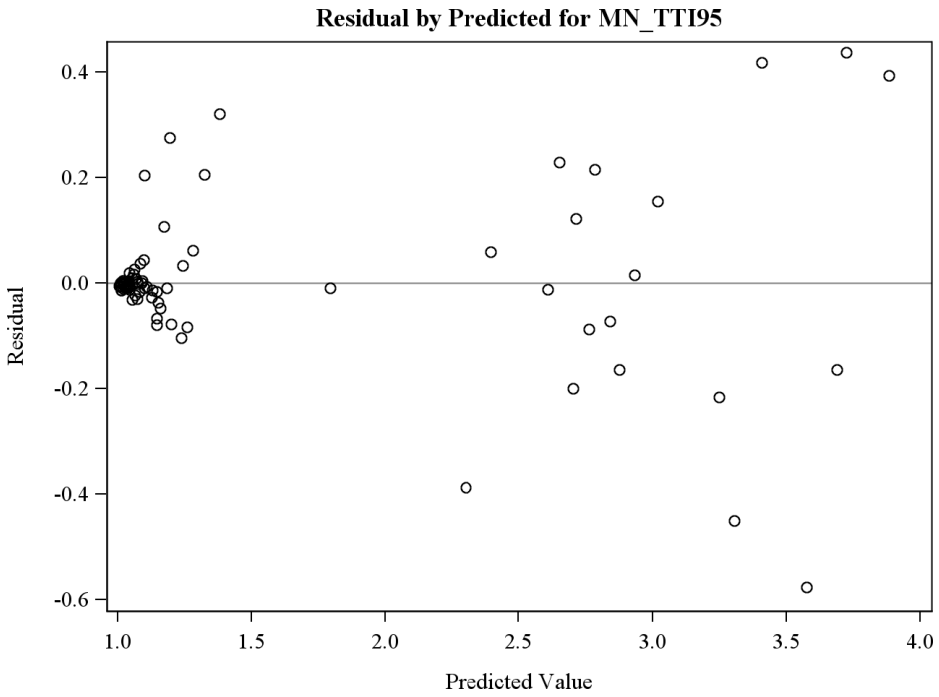

Figure E.18. Residual-by-predicted plot, recalibrated 95th-percentile TTI model, Minnesota.

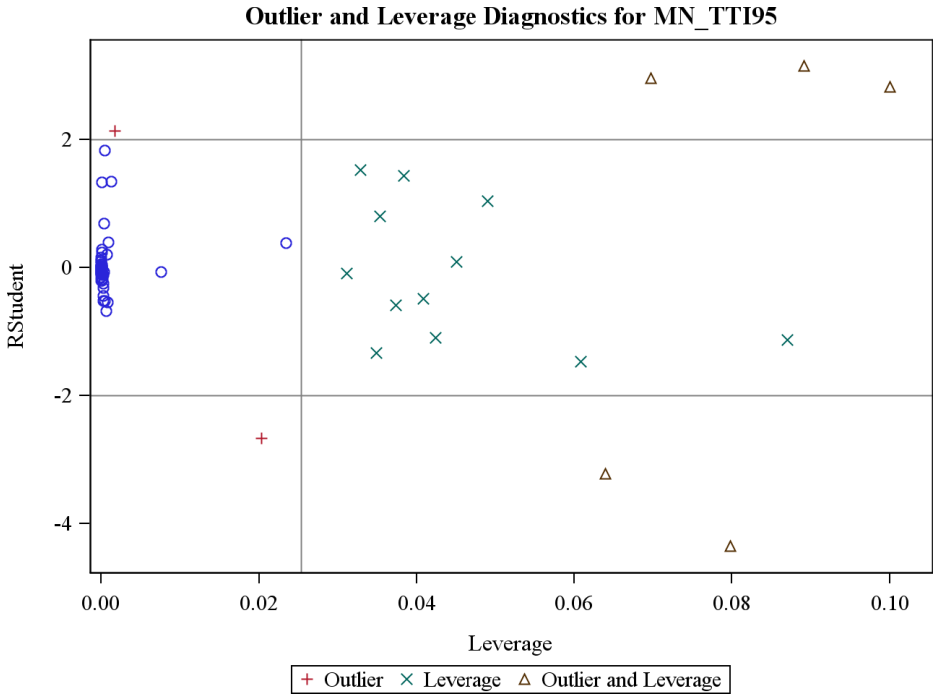

Figure E.19. Outlier and leverage plot, recalibrated 95th-percentile TTI model, Minnesota.

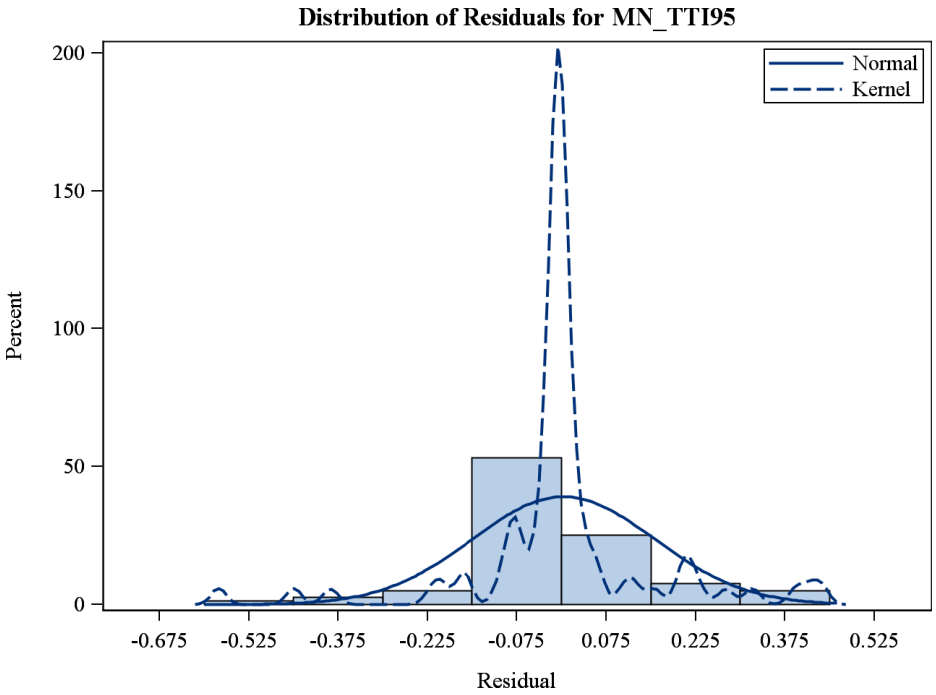

Figure E.20. Distribution of residuals, recalibrated 95th-percentile TTI model, Minnesota.

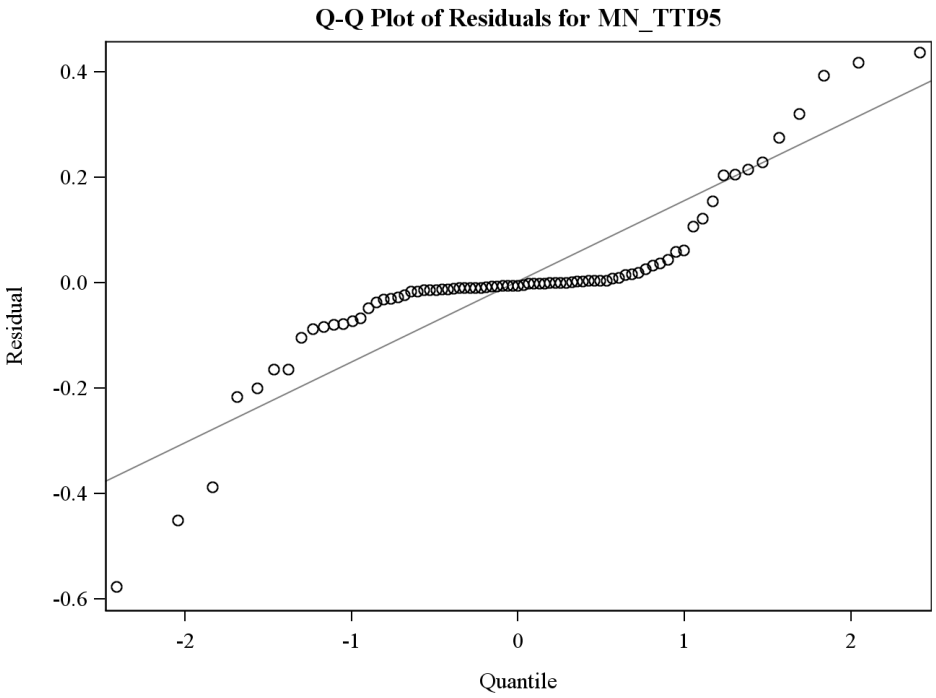

Figure E.21. Q-Q plot of residuals, recalibrated 95th-percentile TTI model, Minnesota.

Table E.10. Analysis of Variance, Recalibrated 90th-Percentile TTI Model, AllData

Source	DF	Sum of Squares	Mean Square	*F*-Value	Pr > *F*
Model	1	688.14766	688.14766	48802.7	<0.0001
Error	322	4.54040	0.01410		
Uncorrected total	323	692.68806			

Table E.11. Root MSE and R-Square, Recalibrated 90th-Percentile TTI Model, AllData

Root MSE	0.11875	*R*-Square	0.9934

90th-percentile TTI

The recalibration of the 90th-percentile TTI model is conducted by building a linear model between the response variable, 90th-percentile TTI, and the independent variable, log-transformed mean TTI—ln(mean TTI)—with the restriction that the intercept is fixed at 1. Due to the restriction, the R^2 is redefined.

AllData

The recalibrated model for the 90th-percentile TTI with the AllData set is

$$\text{90th-percentile TTI}_{\text{AllData}} = 1 + 2.8189 * \ln(\text{meanTTI})$$

The statistical test results (Tables E.10 through E.12) show that both the model and the parameters are significant. We need to further analyze the goodness-of-fit of the model. The scatter plot (Figure E.22) shows that the model can predict the trend of the data samples, but there may be two questionable patterns. First, the blue points representing the MN data samples are mostly beyond the model line, while the red points representing the CA data are mostly below the model line, indicating regional disparity. Another pattern (Figure E.23) is that there are more points beyond the upper 95% prediction confidence limit than below the lower 95% prediction confidence limit, which may indicate that the model form may not be adequate; perhaps the 90th-percentile TTI increases faster than the log-line. Figure E.24 shows the predicted versus observed plot. The residual-by-predicted plot (Figure E.25) shows a generally random pattern with the nonconstant variance problem. Other plots show the existence of outlier and leverage points (Figure E.26) and that the residual distribution does not perfectly follow a normal distribution because skewness exists (Figures E.27 and E.28).

California

The recalibrated model for the 90th-percentile TTI with the CA set is

$$\text{90th-percentile TTI}_{\text{CA}} = 1 + 2.6631 * \ln(\text{meanTTI})$$

The statistical tests results (Tables E.13 through E.15) show that both the model and the parameters are significant. The scatter plots (Figures E.29 through E.31) show that the model predicts the data samples well. The residual plots (Figures E.32 and E.35) show that the nonconstant variance problem still exists, and the residuals seem to present a nonrandom pattern. Figure E.33 shows the outlier and leverage plot. The histogram and the normality plot (Figures E.34 and E.35) show that the residual distribution does not perfectly follow a normal distribution.

Minnesota

The recalibrated model for the 90th-percentile TTI with the MN set is

$$\text{90th-percentile TTI}_{\text{MN}} = 1 + 3.2008 * \ln(\text{meanTTI})$$

The statistical test results (Tables E.16 through E.18) show that both the model and the parameters are significant. The scatter plots and the residual-by-predicted plot (Figures E.36 through E.40) show that the model can predict the data trend well, and the residuals present a random pattern along the zero reference line, although the nonconstant variance problem still exists. The histogram and the normality plot (Figures E.41 and E.42) show that the residual may not perfectly follow a normal distribution.

(text continues on page 242)

Table E.12. Parameter Estimates, Recalibrated 90th-Percentile TTI Model, AllData

Variable	DF	Parameter Estimate	Standard Error	*t*-Value	Pr > |*t*|	95% Confidence Limits	
Intercept	1	1.00000	0	Infty	<0.0001	1.00000	1.00000
ln(mean TTI) (AllData)	1	2.81886	0.02780	101.39	<0.0001	2.76416	2.87355
RESTRICT	–1	–6.40766	1.79838	–3.56	0.0003[a]	–9.93010	–2.88523

[a] The model restricts the intercept to be 1 (unity).

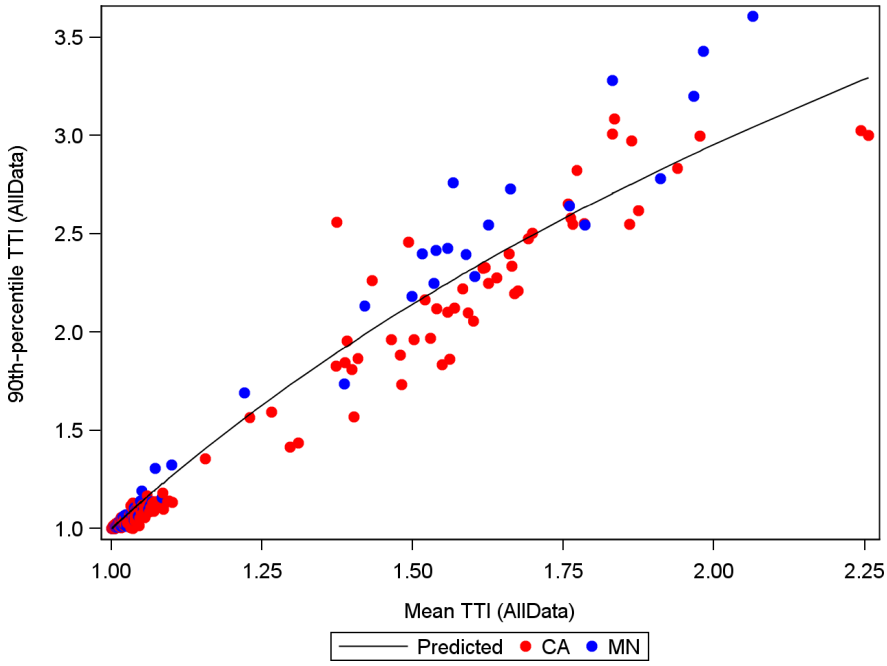

Figure E.22. Scatter plot in original scale, recalibrated 90th-percentile TTI model, AllData.

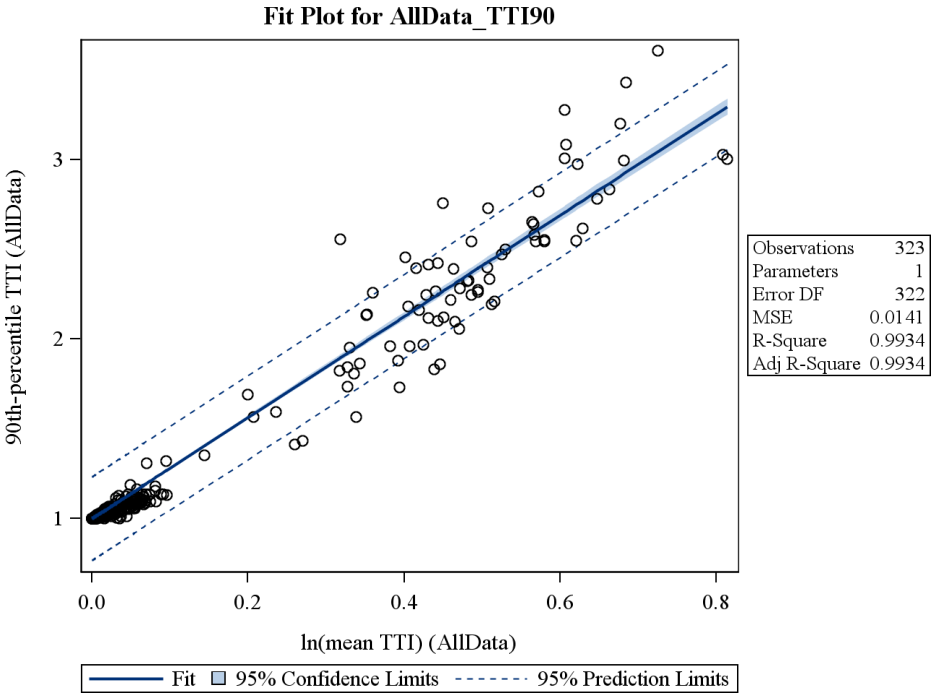

Figure E.23. Fit plot in x-axis log scale, recalibrated 90th-percentile TTI model, AllData.

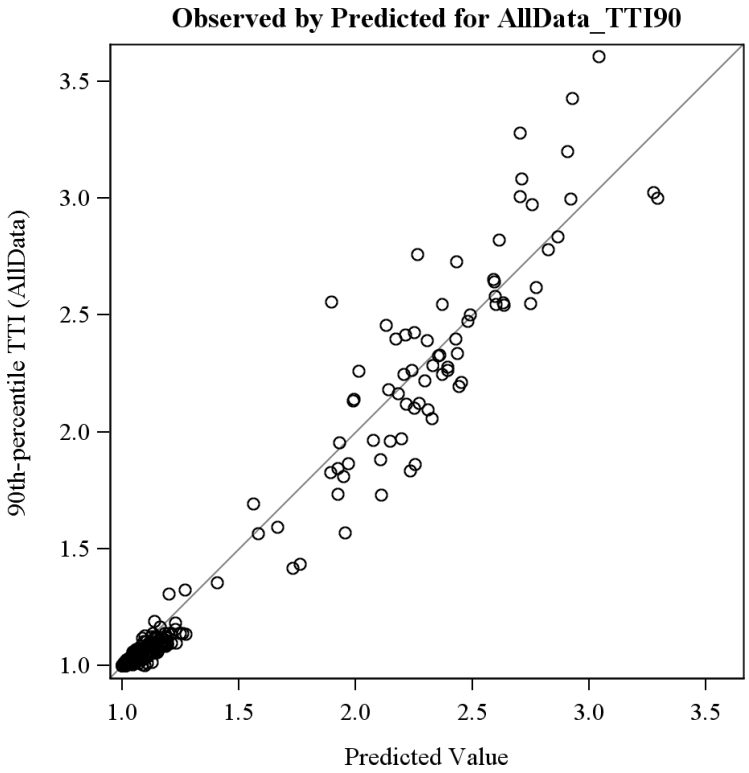

Figure E.24. Observed-by-predicted plot, recalibrated 90th-percentile TTI model, AllData.

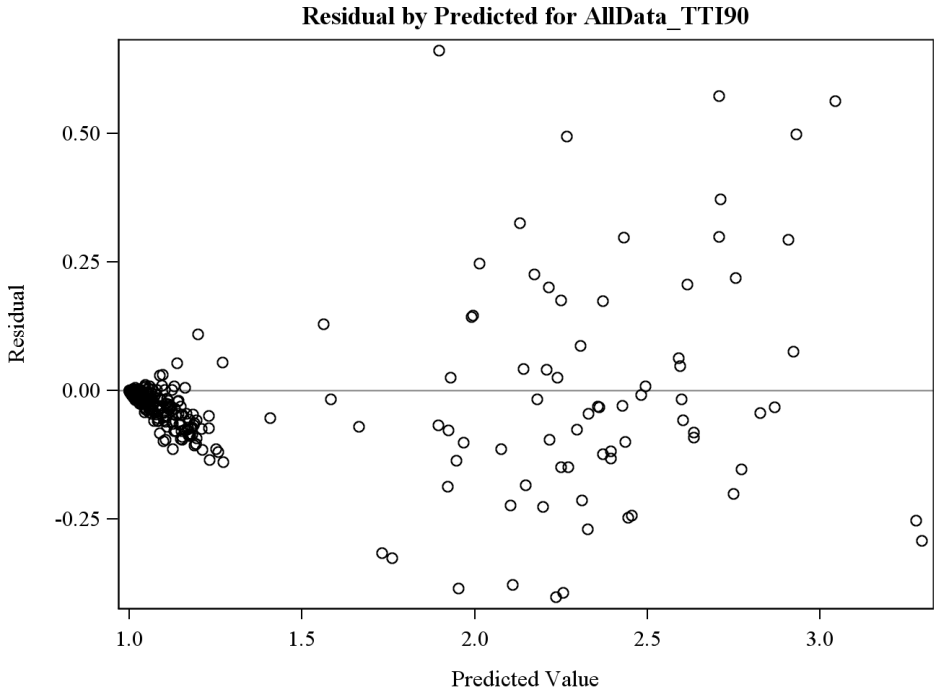

Figure E.25. Residual-by-predicted plot, recalibrated 90th-percentile TTI model, AllData.

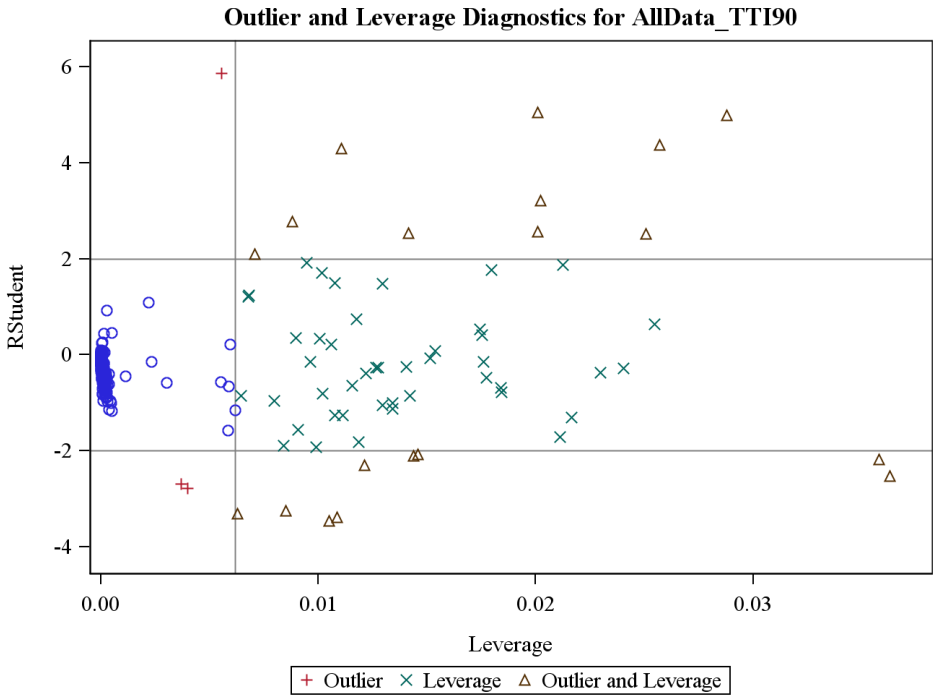

Figure E.26. Outlier and leverage plot, recalibrated 90th-percentile TTI model, AllData.

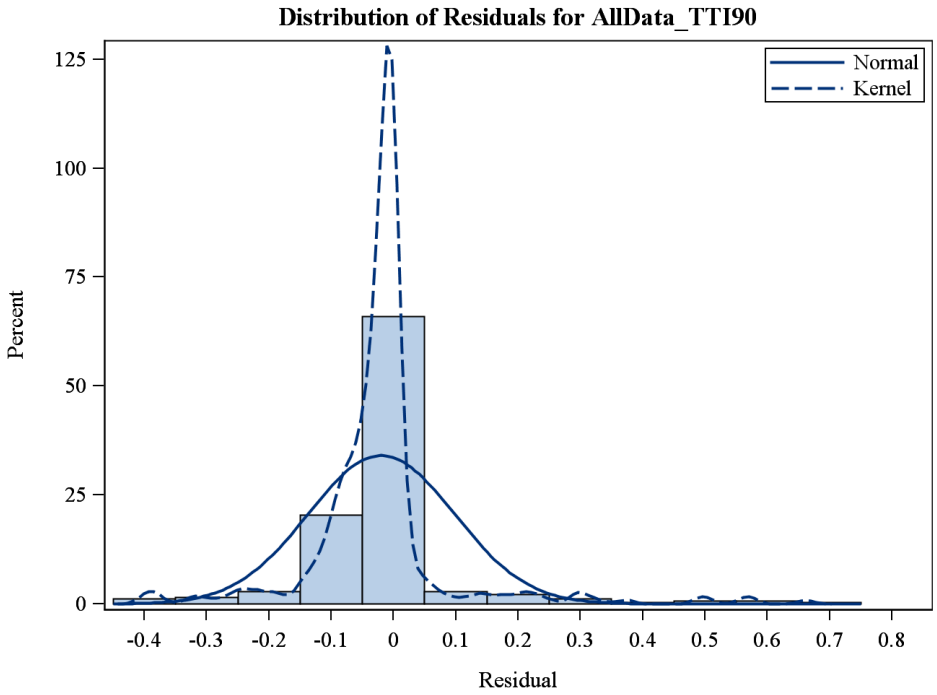

Figure E.27. Distribution of residuals, recalibrated 90th-percentile TTI model, AllData.

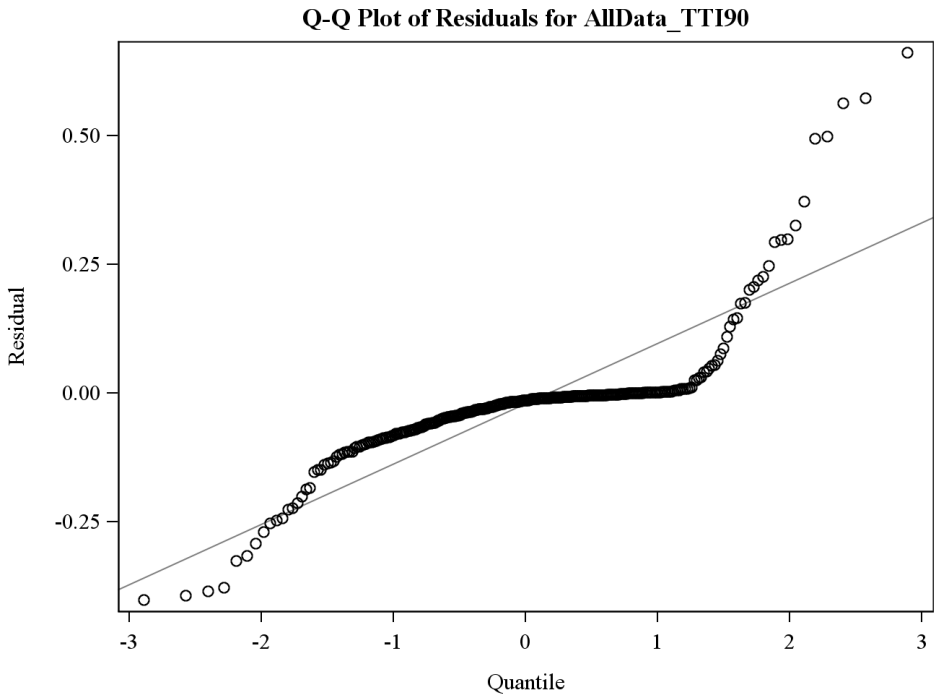

Figure E.28. Q-Q plot of residuals, recalibrated 90th-percentile TTI model, AllData.

Table E.13. Analysis of Variance, Recalibrated 90th-Percentile TTI Model, California

Source	DF	Sum of Squares	Mean Square	*F*-Value	Pr > *F*
Model	1	414.83485	414.83485	31320.3	<0.0001
Error	186	2.46355	0.01324		
Uncorrected total	187	417.29840			

Table E.14. Root MSE and R-Square, Recalibrated 90th-Percentile TTI Model, California

Root MSE	0.11509	*R*-Square	0.9941

Table E.15. Parameter Estimates, Recalibrated 90th-Percentile TTI Model, California

Variable	Label	DF	Parameter Estimate	Standard Error	*t*-Value	Pr > |*t*|	95% Confidence Limits	
Intercept	Intercept	1	1.00000	0	Infty	<0.0001	1.00000	1.00000
CA_TTImean_ln	ln(mean TTI) (CA)	1	2.66311	0.03273	81.37	<0.0001	2.59854	2.72767
RESTRICT		–1	–3.44219	1.28862	–2.67	0.0072[a]	–5.96493	–0.91945

[a] The model restricts the intercept to be 1 (unity).

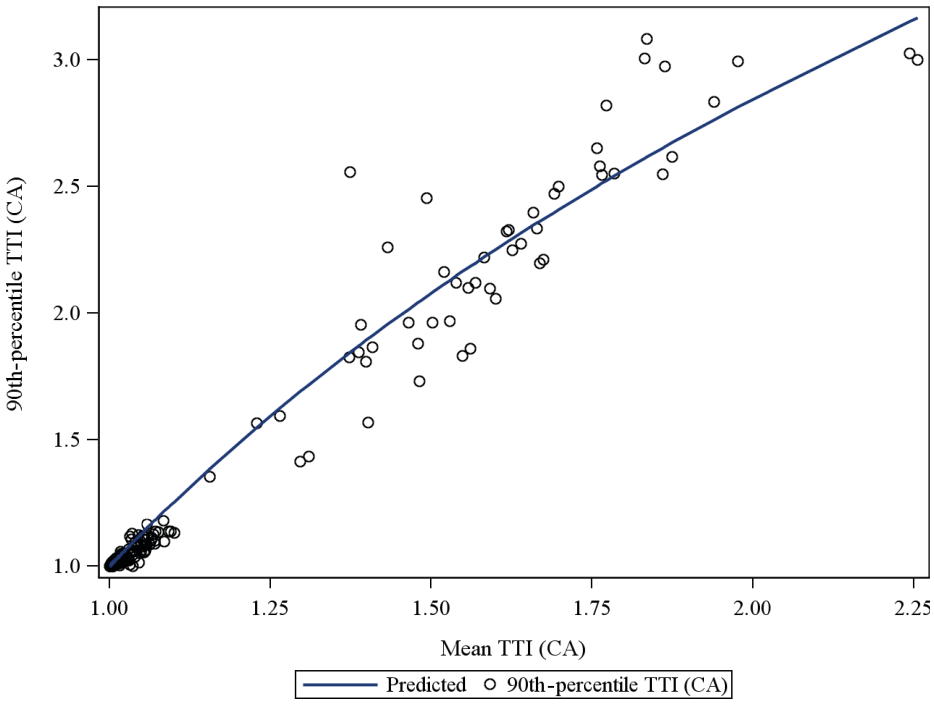

Figure E.29. Fit plot in original scale, recalibrated 90th-percentile TTI model, California.

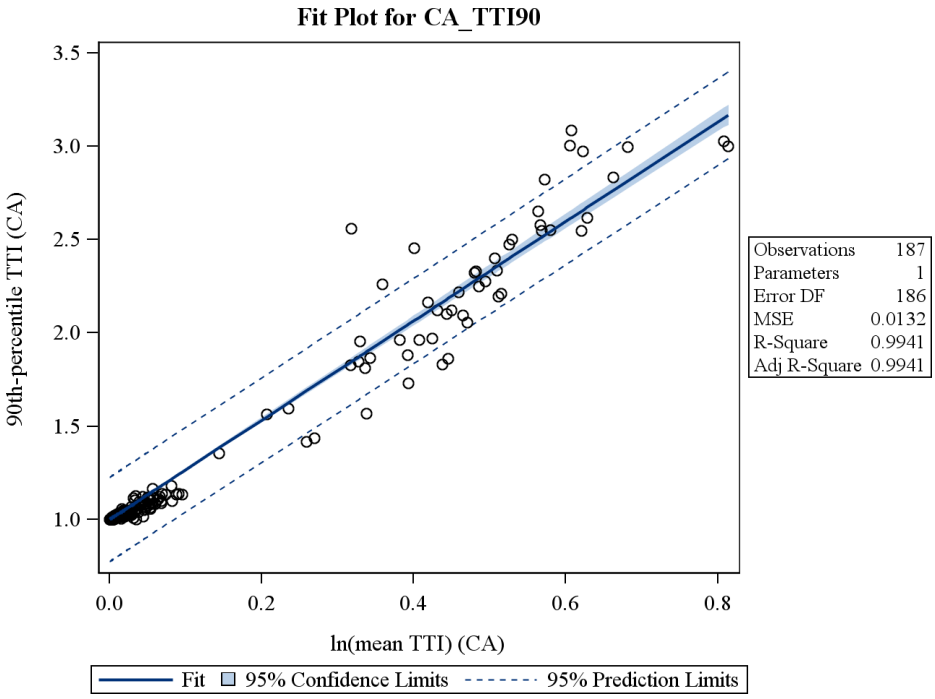

Figure E.30. Fit plot in x-axis log scale, recalibrated 90th-percentile TTI model, California.

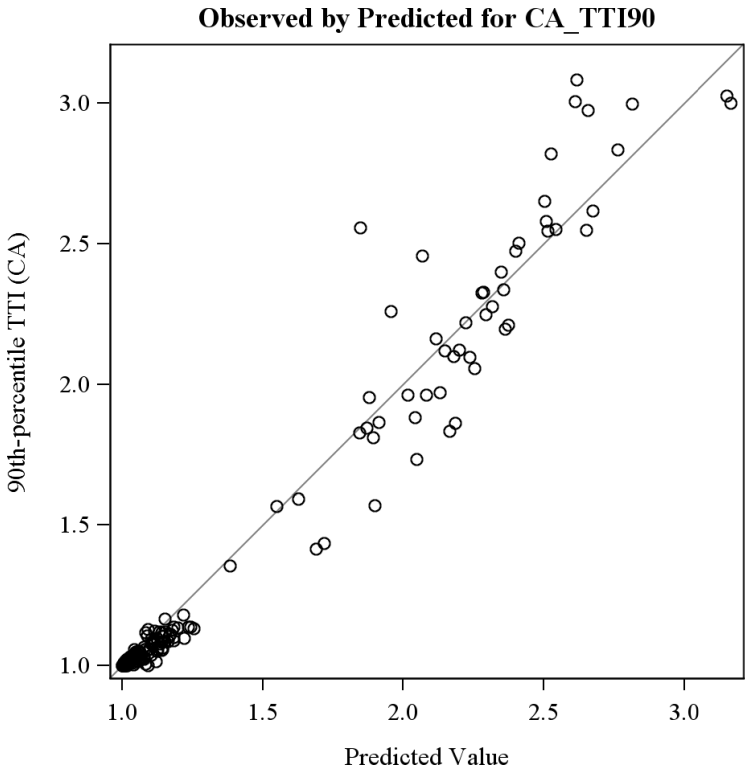

Figure E.31. Observed-by-predicted plot, recalibrated 90th-percentile TTI model, California.

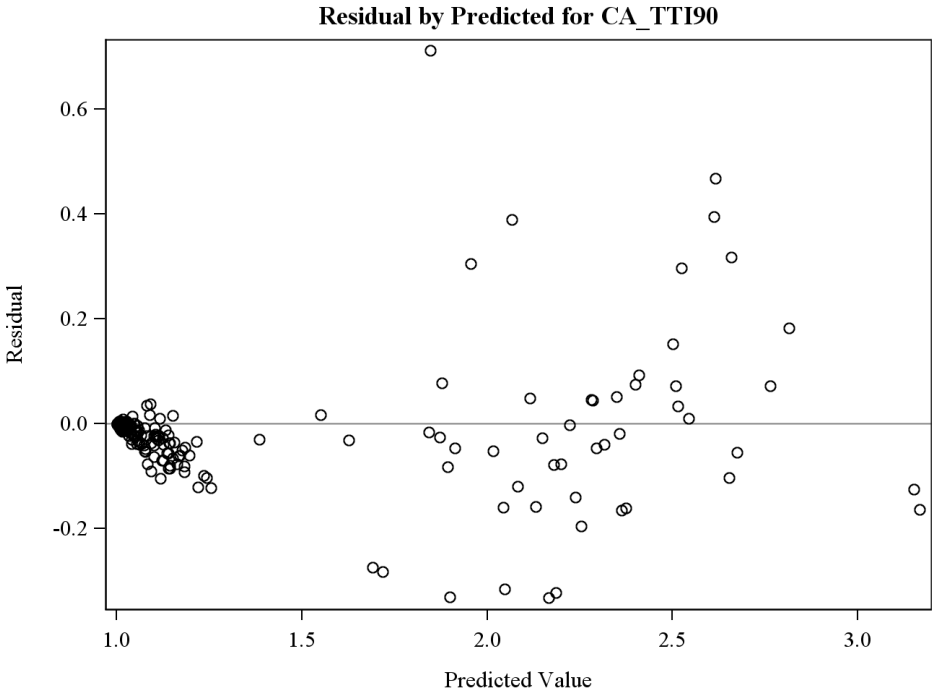

Figure E.32. Residual-by-predicted plot, recalibrated 90th-percentile TTI model, California.

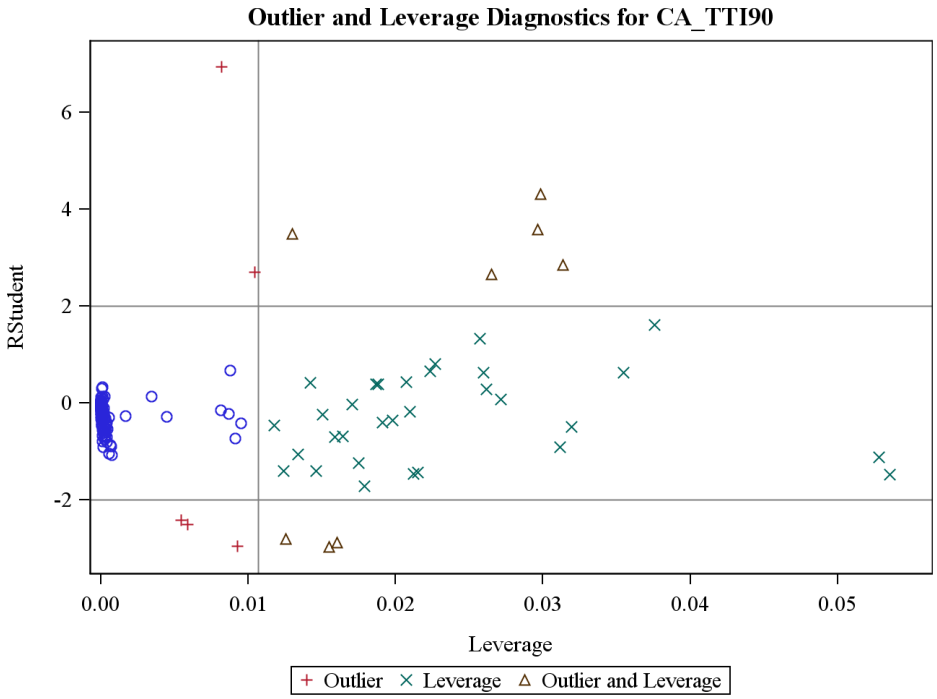

Figure E.33. Outlier and leverage plot, recalibrated 90th-percentile TTI model, California.

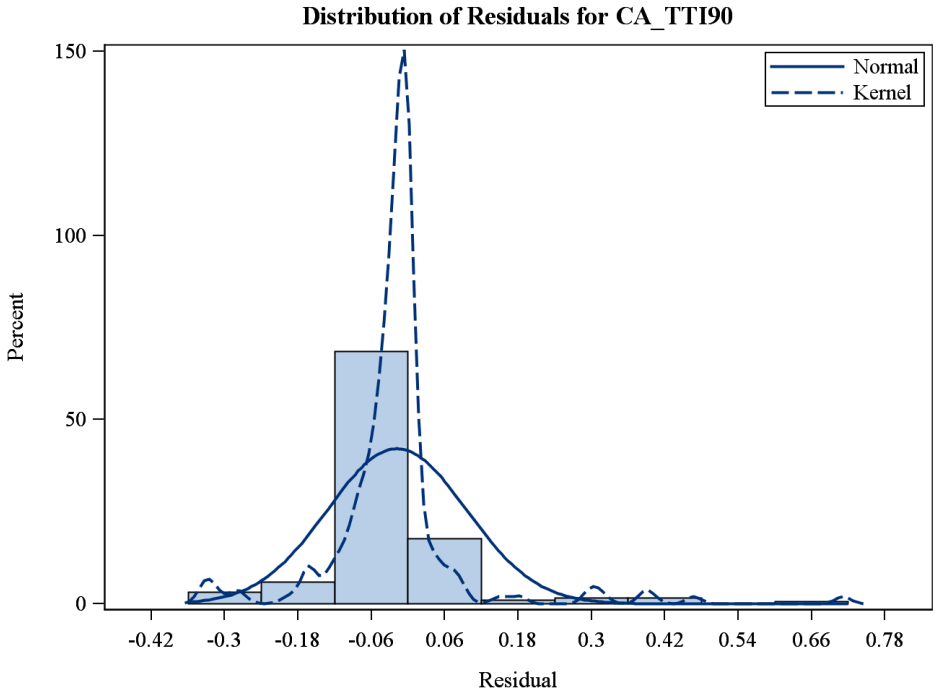

Figure E.34. Distribution of residuals, recalibrated 90th-percentile TTI model, California.

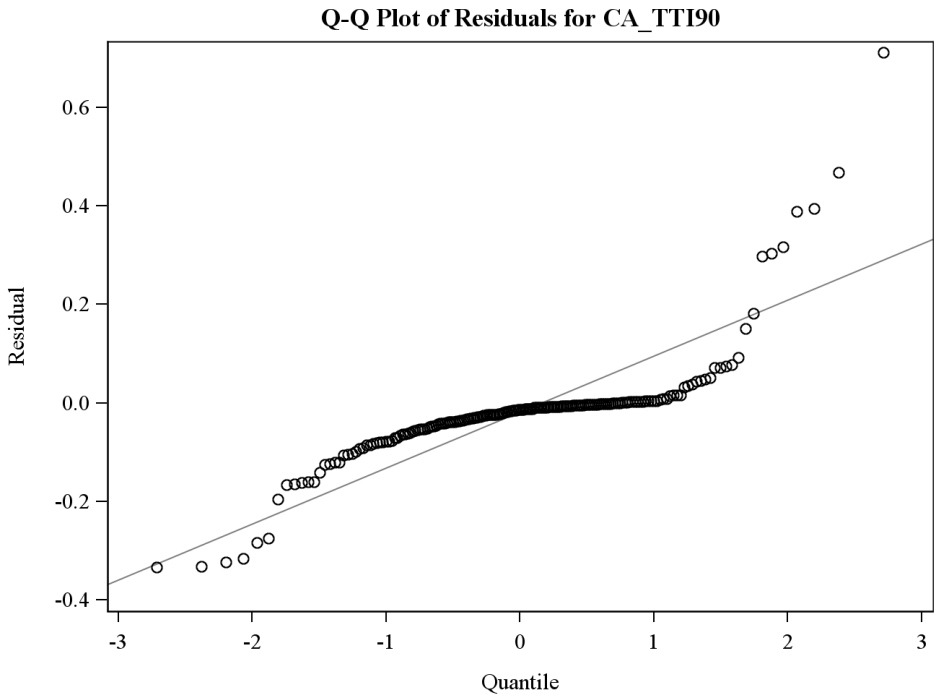

Figure E.35. Q-Q plot of residuals, recalibrated 90th-percentile TTI model, California.

Table E.16. Analysis of Variance, Recalibrated 90th-Percentile TTI Model, Minnesota

Source	DF	Sum of Squares	Mean Square	*F*-Value	Pr > *F*
Model	1	201.88201	201.88201	18388.9	<0.0001
Error	78	0.85632	0.01098		
Uncorrected total	79	202.73833			

Table E.17. Root MSE and R-Square, Recalibrated 90th-Percentile TTI Model, Minnesota

Root MSE	0.10478	*R*-Square	0.9958

Table E.18. Parameter Estimates, Recalibrated 90th-Percentile TTI Model, Minnesota

Variable	Label	DF	Parameter Estimate	Standard Error	*t*-Value	Pr > |*t*|	95% Confidence Limits	
Intercept	Intercept	1	1.00000	0	Infty	<0.0001	1.00000	1.00000
MN_TTImean_ln	ln(mean TTI) (MN)	1	3.20080	0.04570	70.03	<0.0001	3.10981	3.29179
RESTRICT		–1	–1.43443	0.77701	–1.85	0.0645[a]	–2.95306	0.08421

[a] The model restricts the intercept to be 1 (unity).

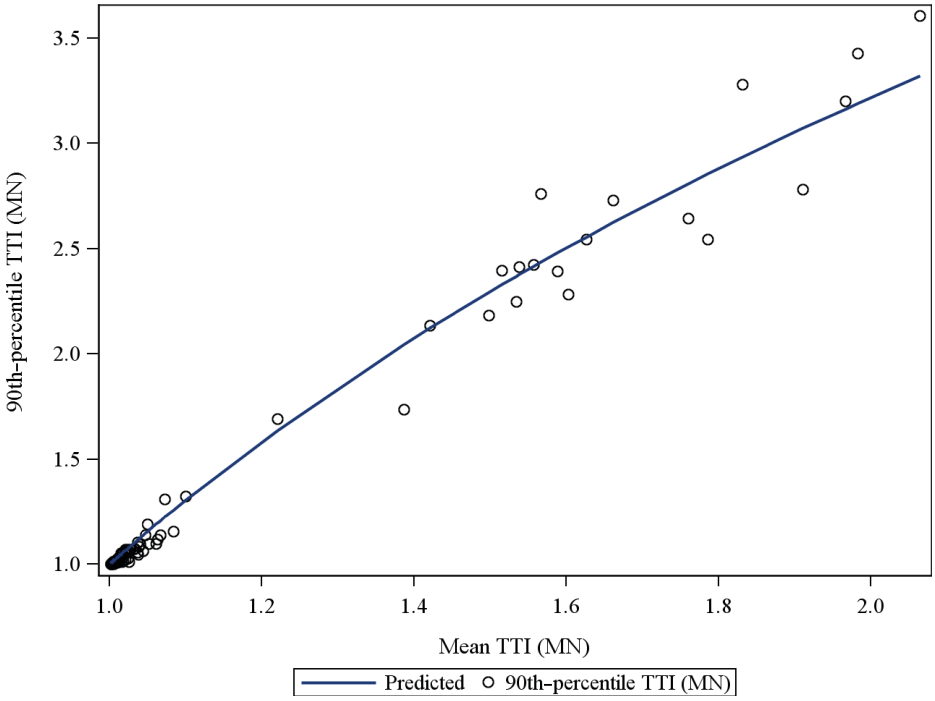

Figure E.36. Fit plot in original scale, recalibrated 90th-percentile TTI model, Minnesota.

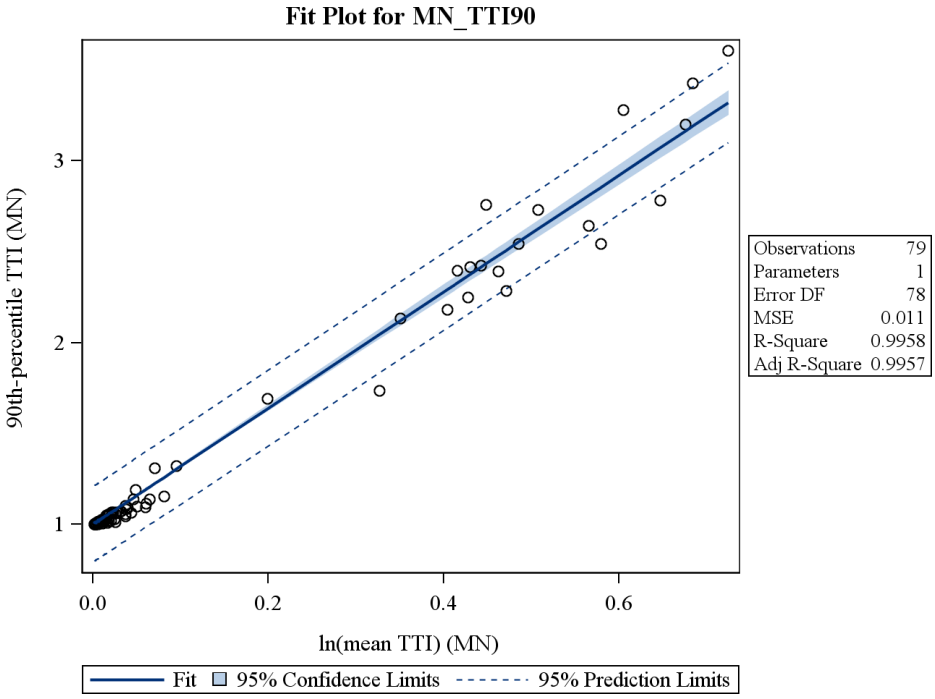

Figure E.37. Fit plot in x-axis log scale, recalibrated 90th-percentile TTI model, Minnesota.

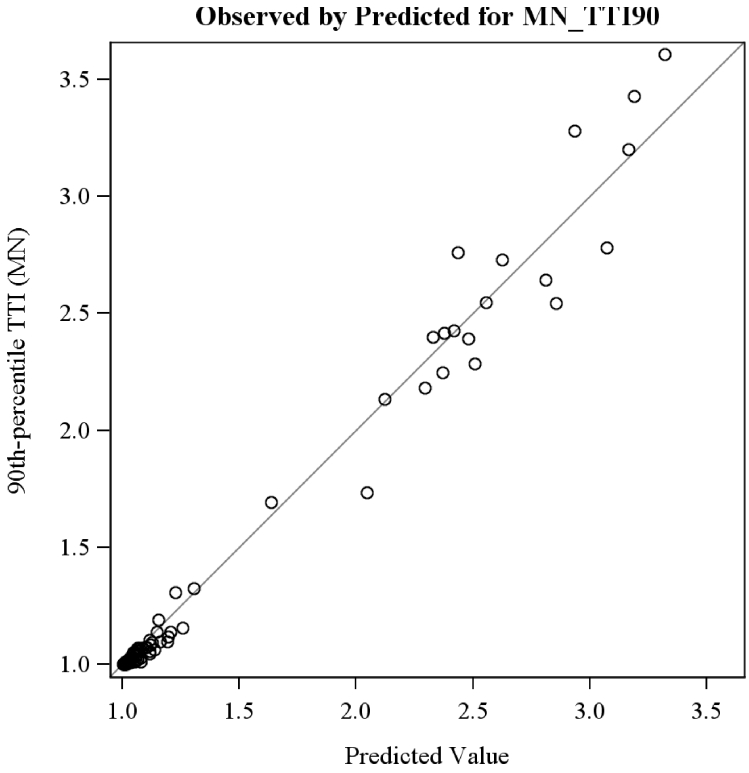

Figure E.38. Observed-by-predicted plot, recalibrated 90th-percentile TTI model, Minnesota.

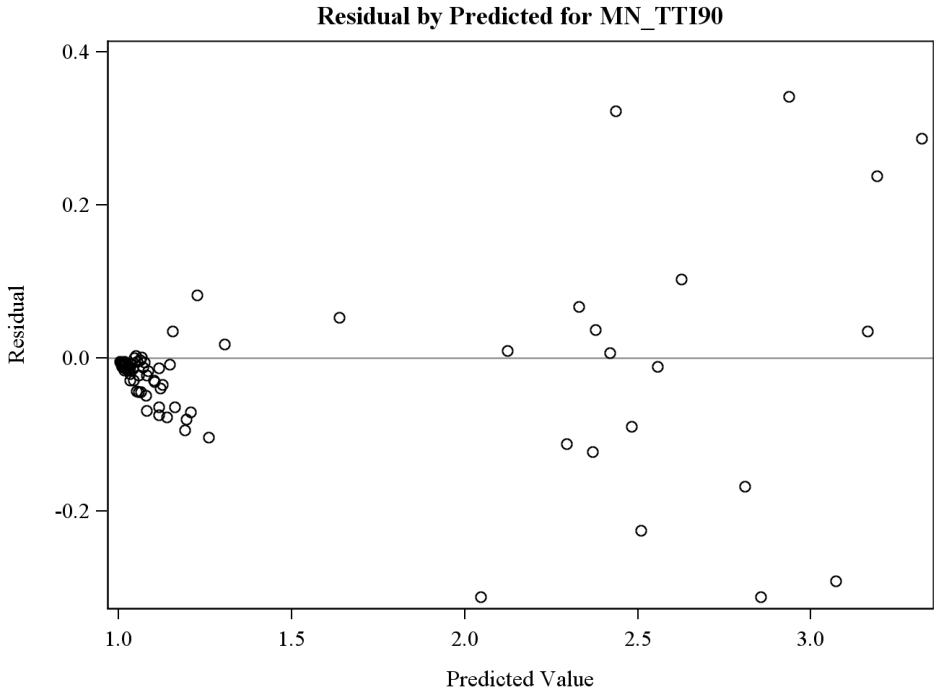

Figure E.39. Residual-by-predicted plot, recalibrated 90th-percentile TTI model, Minnesota.

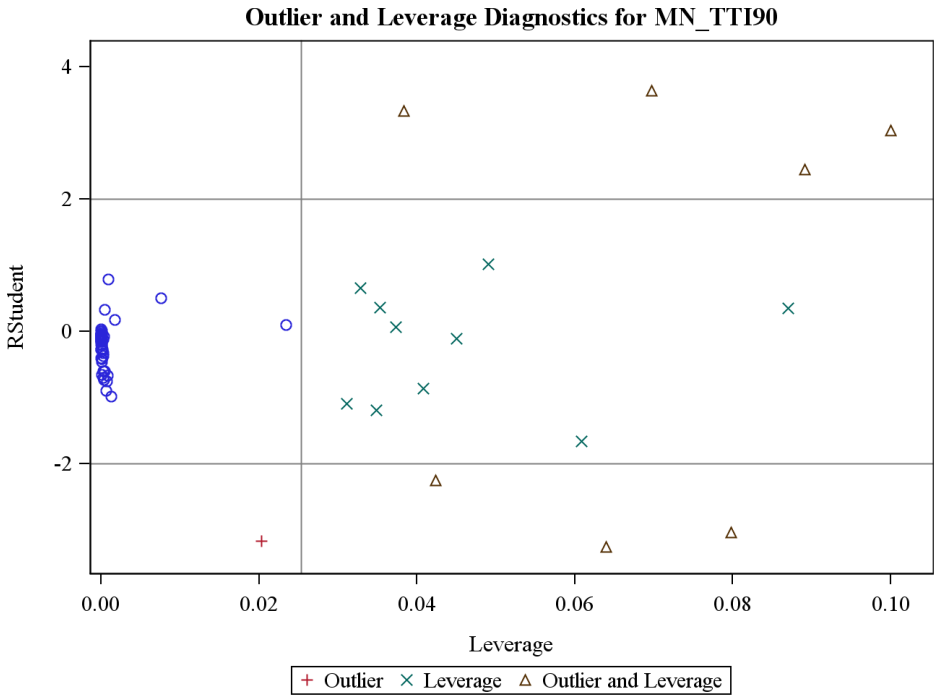

Figure E.40. Outlier and leverage plot, recalibrated 90th-percentile TTI model, Minnesota.

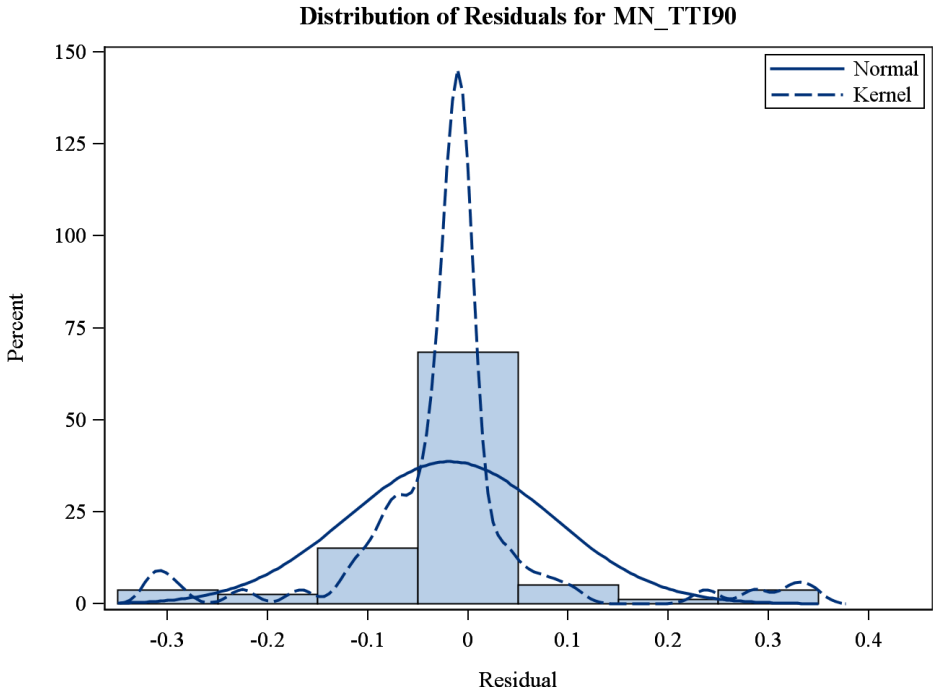

Figure E.41. Distribution of residuals, recalibrated 90th-percentile TTI model, Minnesota.

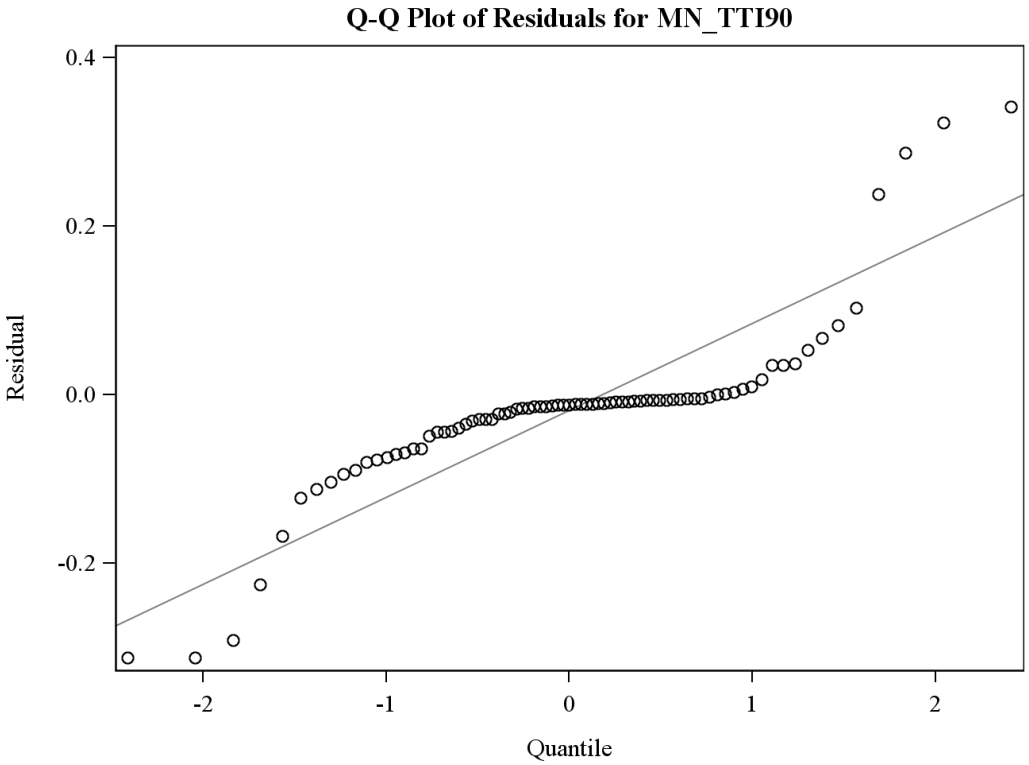

Figure E.42. Q-Q plot of residuals, recalibrated 90th-percentile TTI model, Minnesota.

80th-Percentile TTI

The recalibration of the 80th-percentile TTI model is conducted by building a linear model between the response variable, 80th-percentile TTI, and the independent variable, log-transformed mean TTI—ln(mean TTI)—with the restriction that the intercept is fixed at 1. Due to the restriction, the R^2 is redefined.

AllData

The recalibrated model for the 80th-percentile TTI with the AllData set is

$$\text{80th-percentile TTI}_{\text{AllData}} = 1 + 2.1598 * \ln(\text{meanTTI})$$

The statistical test results (Tables E.19 through E.21) show that both the model and the parameters are significant, which indicates that overall the model is valid. We need to further analyze the goodness-of-fit of the model. The scatter plot (Figure E.43), fit plot (Figure E.44), and observed-by-predicted plot (Figure E.45) show that although the model can generally predict the data trend, the model form may not be adequate. The residual-by-predicted plot (Figure E.46) also indicates the same problem because a nonrandom pattern exists. The outlier and leverage plot is shown in Figure E.47. The histogram and the normality plot (Figures E.48 and E.49) show that the residuals may not closely follow a normal distribution.

Table E.19. Analysis of Variance, Recalibrated 80th-Percentile TTI Model, AllData

Source	DF	Sum of Squares	Mean Square	*F*-Value	Pr > *F*
Model	1	573.17609	573.17609	122817	<0.0001
Error	322	1.50274	0.00467		
Uncorrected total	323	574.67883			

Table E.20. Root MSE and R-Square, Recalibrated 80th-Percentile TTI Model, AllData

Root MSE	0.06831	*R*-Square	0.9974

Table E.21. Parameter Estimates, Recalibrated 80th-Percentile TTI Model, AllData

Variable	Label	DF	Parameter Estimate	Standard Error	*t*-Value	Pr > |*t*|	95% Confidence Limits	
Intercept	Intercept	1	1.00000	0	Infty	<0.0001	1.00000	1.00000
AllData_TTImean_ln	ln(mean TTI) (AllData)	1	2.15981	0.01599	135.04	<0.0001	2.12835	2.19128
RESTRICT		–1	–6.72653	1.03461	–6.50	<0.0001[a]	–8.75299	–4.70007

[a] The model restricts the intercept to be 1 (unity).

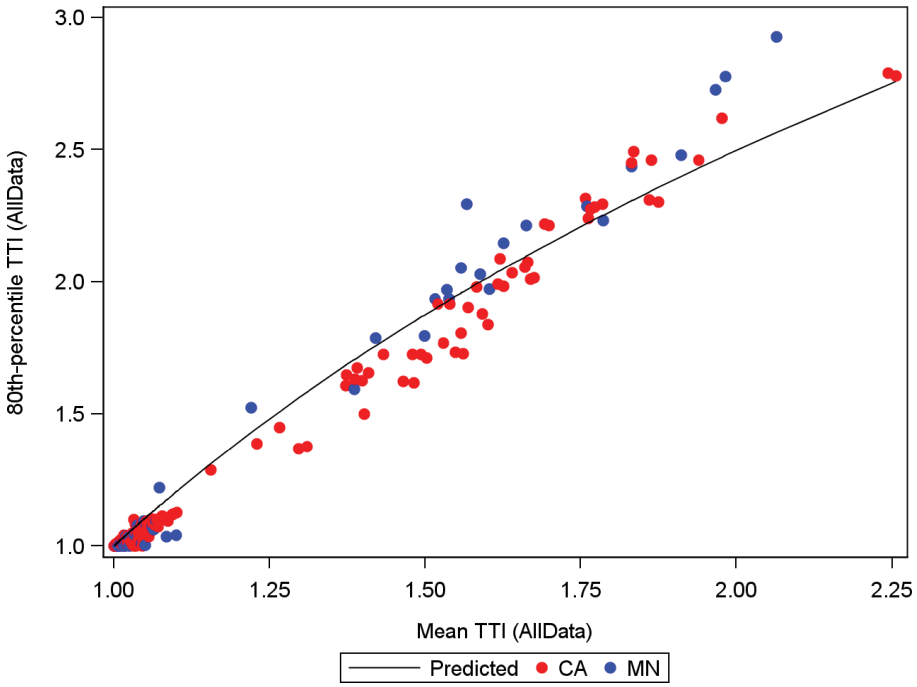

Figure E.43. Scatter plot in original scale, recalibrated 80th-percentile TTI model, AllData.

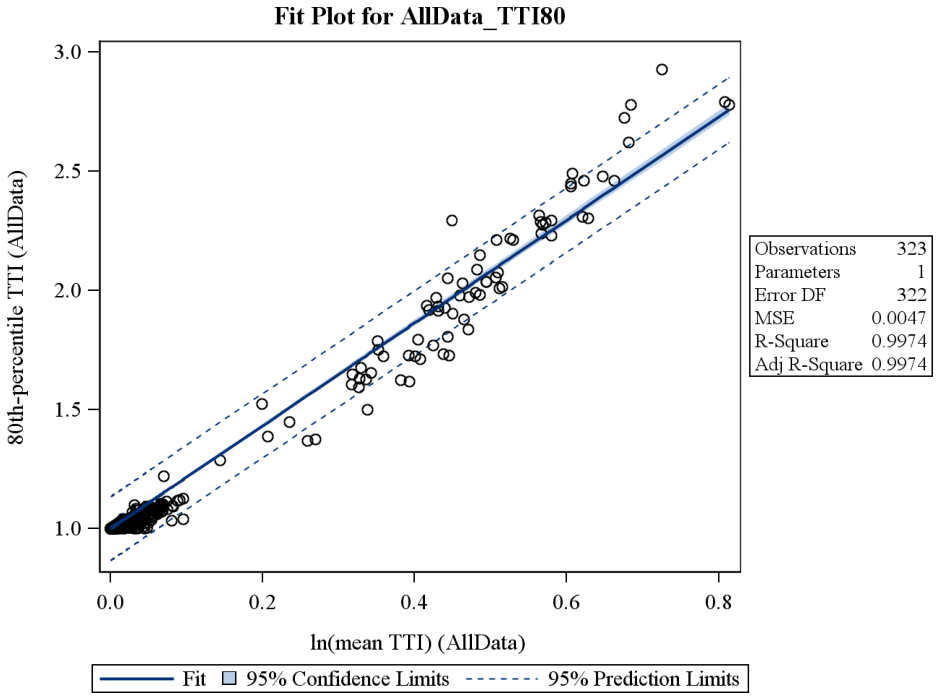

Figure E.44. Fit plot in x-axis log scale, recalibrated 80th-percentile TTI model, AllData.

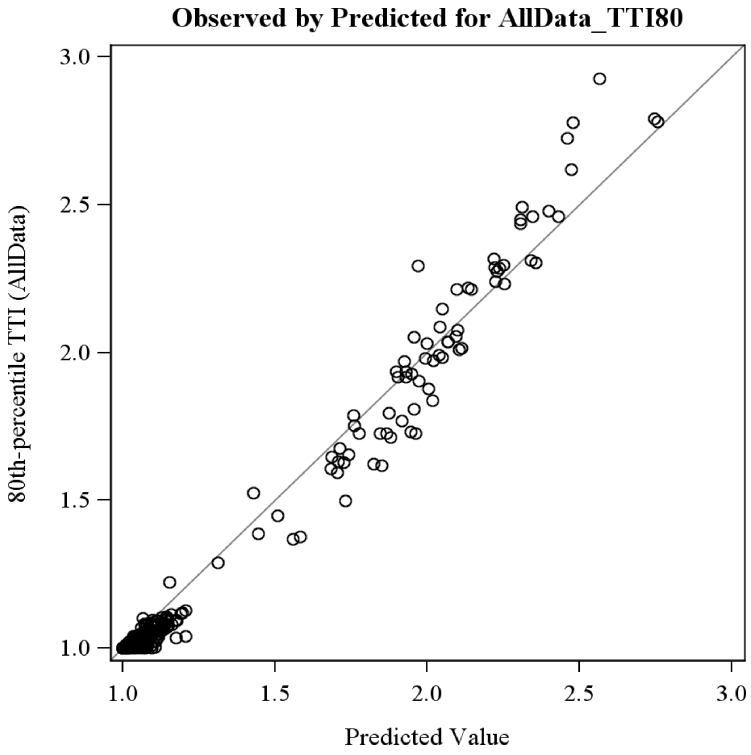

Figure E.45. Observed-by-predicted plot, recalibrated 80th-percentile TTI model, AllData.

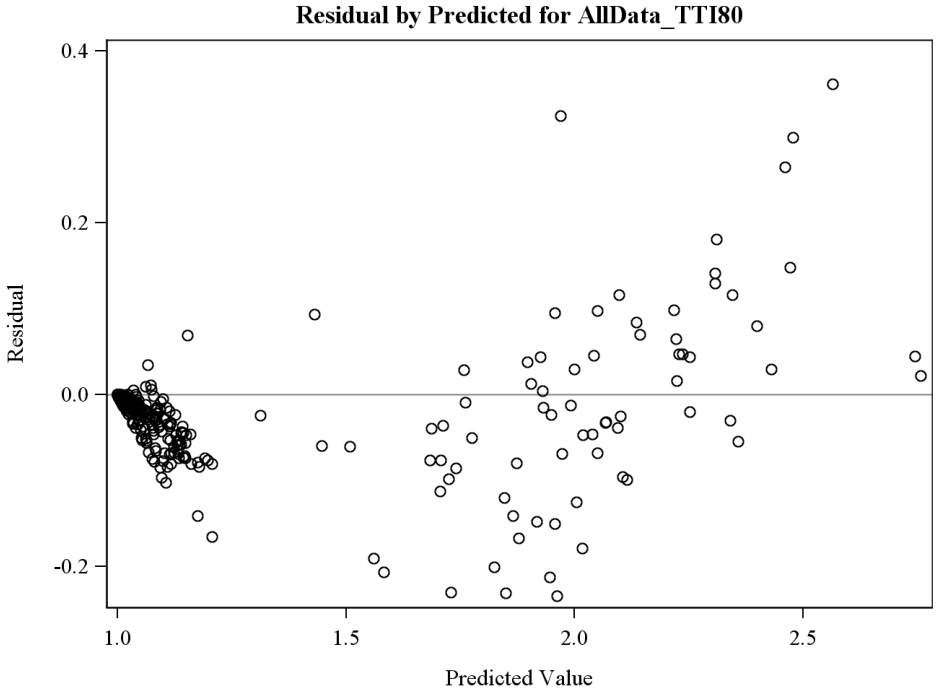

Figure E.46. Residual-by-predicted plot, recalibrated 80th-percentile TTI model, AllData.

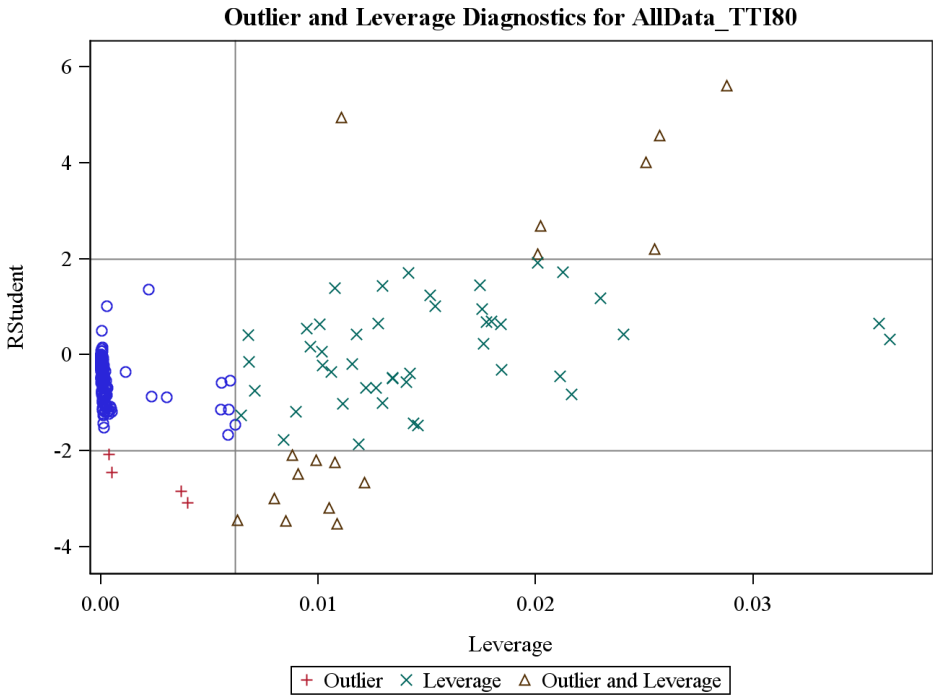

Figure E.47. Outlier and leverage plot, recalibrated 80th-percentile TTI model, AllData.

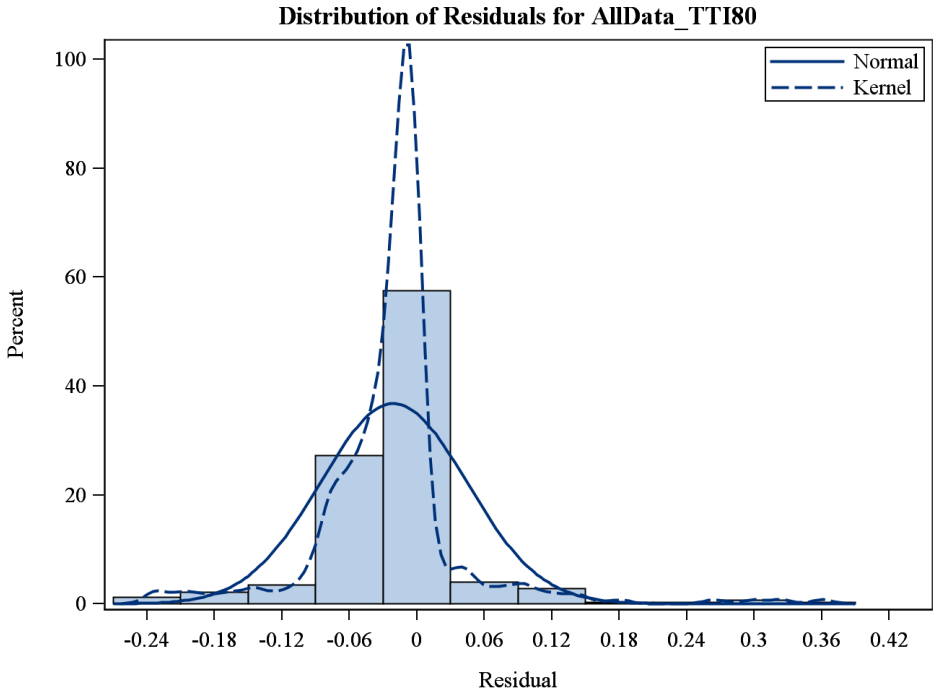

Figure E.48. Distribution of residuals, recalibrated 80th-percentile TTI model, AllData.

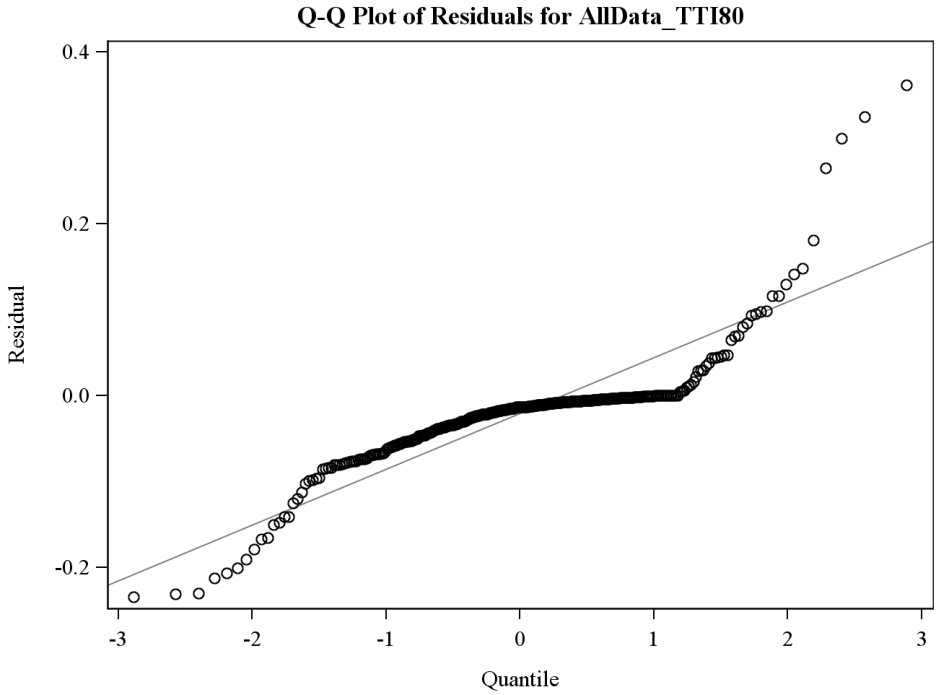

Figure E.49. Q-Q plot of residuals, recalibrated 80th-percentile TTI model, AllData.

California

The recalibrated model for the 80th-percentile TTI with the CA set is

$$80\text{th-percentile TTI}_{CA} = 1 + 2.0844 * \ln(\text{meanTTI})$$

The statistical test results (Tables E.22 through E.24) show that both the model and the parameters are significant. From the scatter plots (Figures E.50 through E.52) and the residual plot (Figure E.53) we can see that the model form may not be adequate because the 80th-percentile TTI seems to increase faster than the model line when the mean TTI is large. Figure E.54 shows the outlier and leverage plot. The histogram and the normality plot (Figures E.55 and E.56) show that the residual distribution does not closely follow a normal distribution.

Table E.22. Analysis of Variance, Recalibrated 80th-Percentile TTI Model, California

Source	DF	Sum of Squares	Mean Square	*F*-Value	Pr > *F*
Model	1	348.33950	348.33950	83662.1	<0.0001
Error	186	0.77444	0.00416		
Uncorrected total	187	349.11394			

Table E.23. Root MSE and R-Square, Recalibrated 80th-Percentile TTI Model, California

Root MSE	0.06453	*R*-Square	0.9978

Table E.24. Parameter Estimates, Recalibrated 80th-Percentile TTI Model, California

Variable	Label	DF	Parameter Estimate	Standard Error	*t*-Value	Pr > |*t*|	95% Confidence Limits	
Intercept	Intercept	1	1.00000	0	Infty	<0.0001	1.00000	1.00000
CA_TTImean_ln	ln(mean TTI) (CA)	1	2.08443	0.01835	113.59	<0.0001	2.04823	2.12063
RESTRICT		–1	–3.73107	0.72250	–5.16	<0.0001[a]	–5.14551	–2.31663

[a] The model restricts the intercept to be 1 (unity).

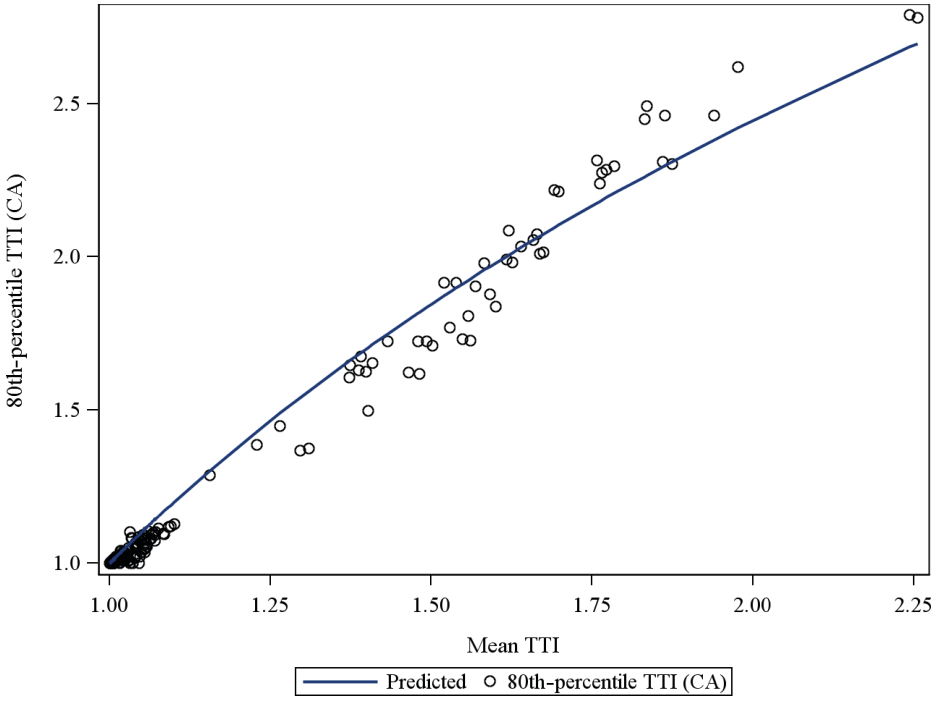

Figure E.50. Fit plot in original scale, recalibrated 80th-percentile TTI model, California.

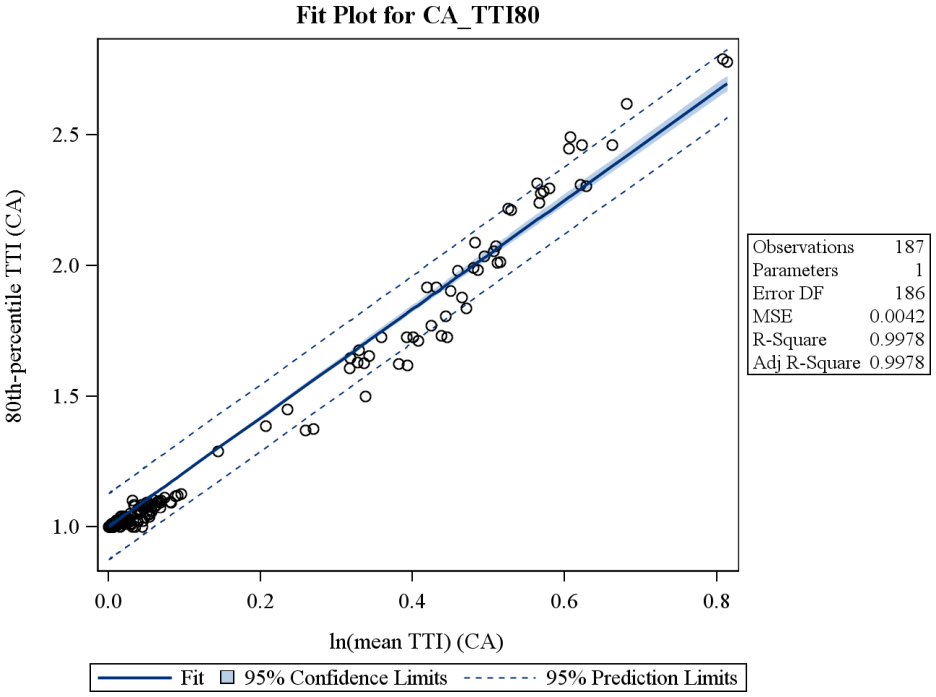

Figure E.51. Fit plot in x-axis log scale, recalibrated 80th-percentile TTI model, California.

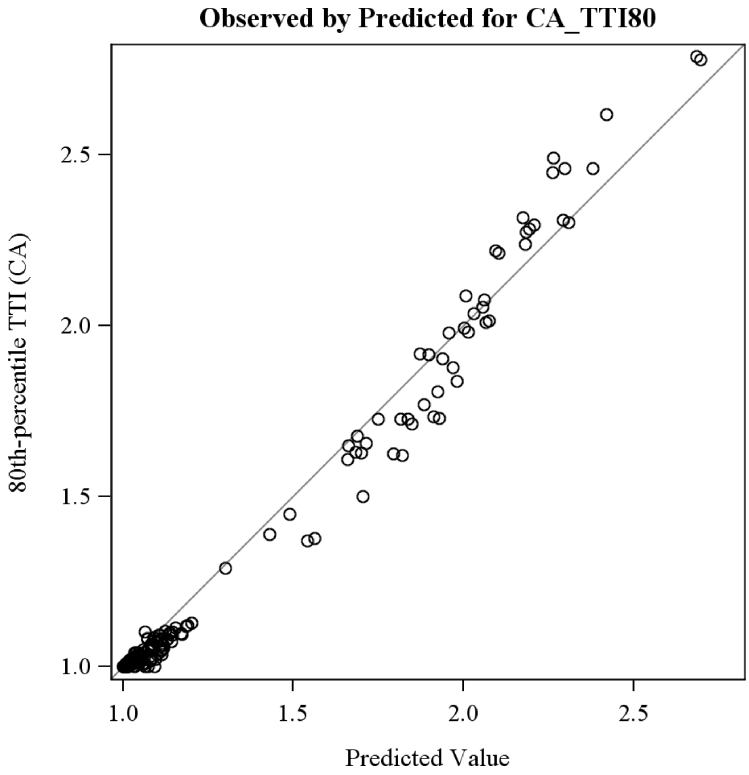

Figure E.52. Observed-by-predicted plot, recalibrated 80th-percentile TTI model, California.

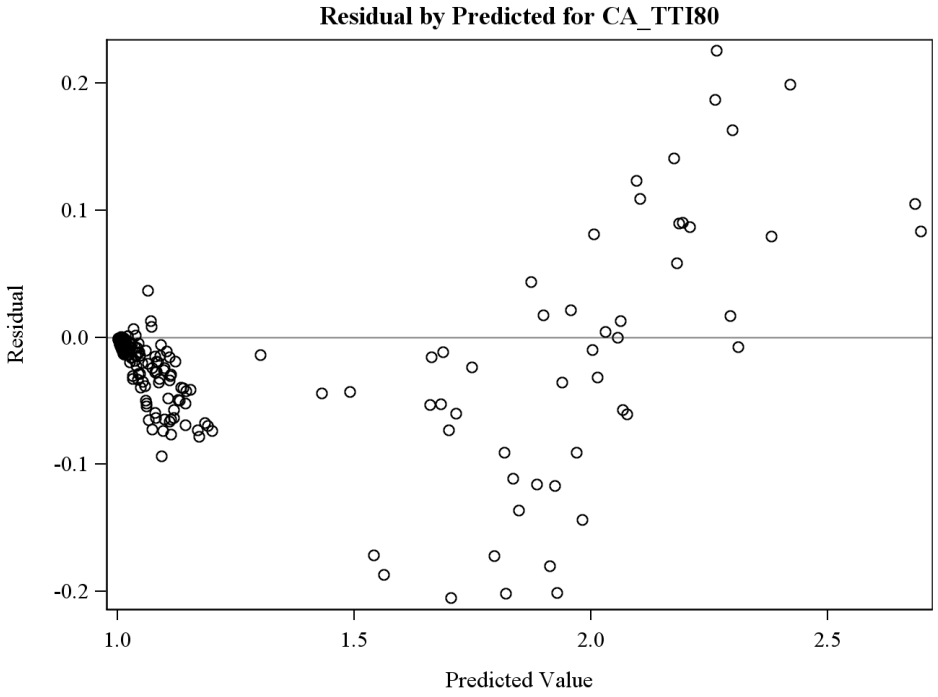

Figure E.53. Residual-by-predicted plot, recalibrated 80th-percentile TTI model, California.

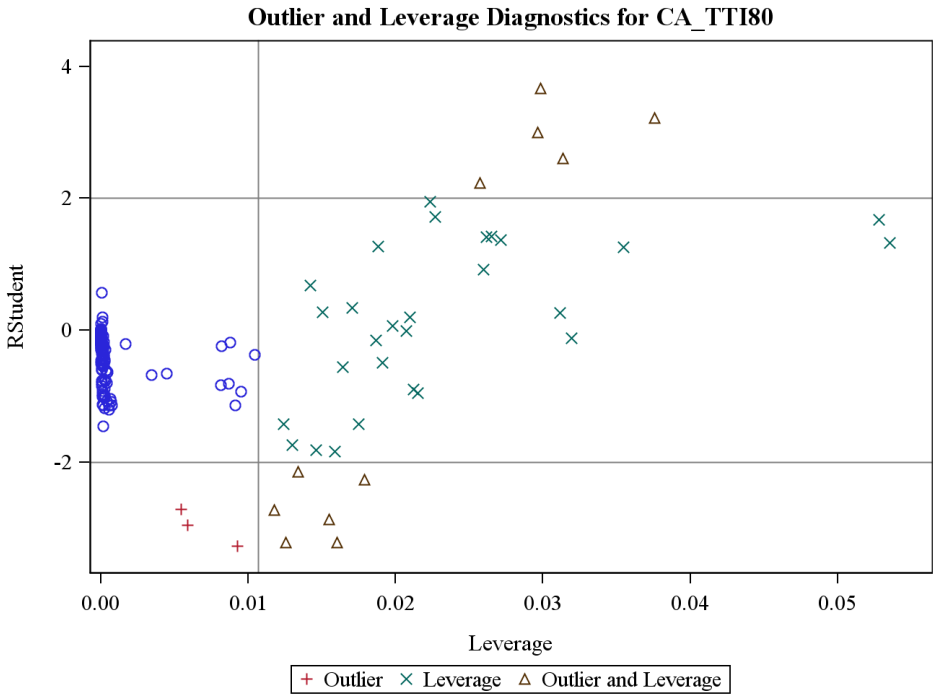

Figure E.54. Outlier and leverage plot, recalibrated 80th-percentile TTI model, California.

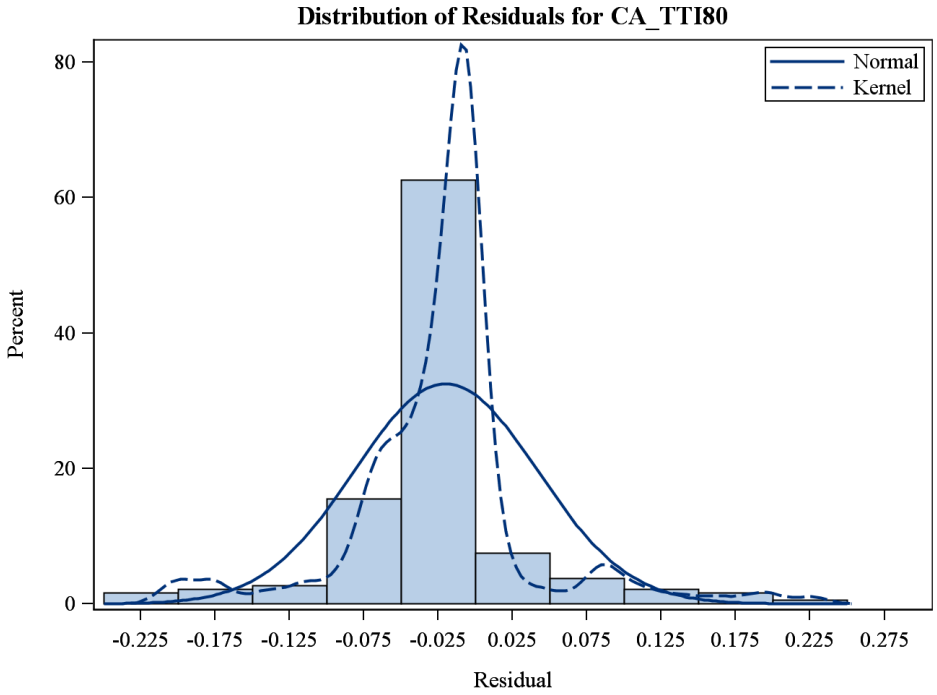

Figure E.55. Distribution of residuals, recalibrated 80th-percentile TTI model, California.

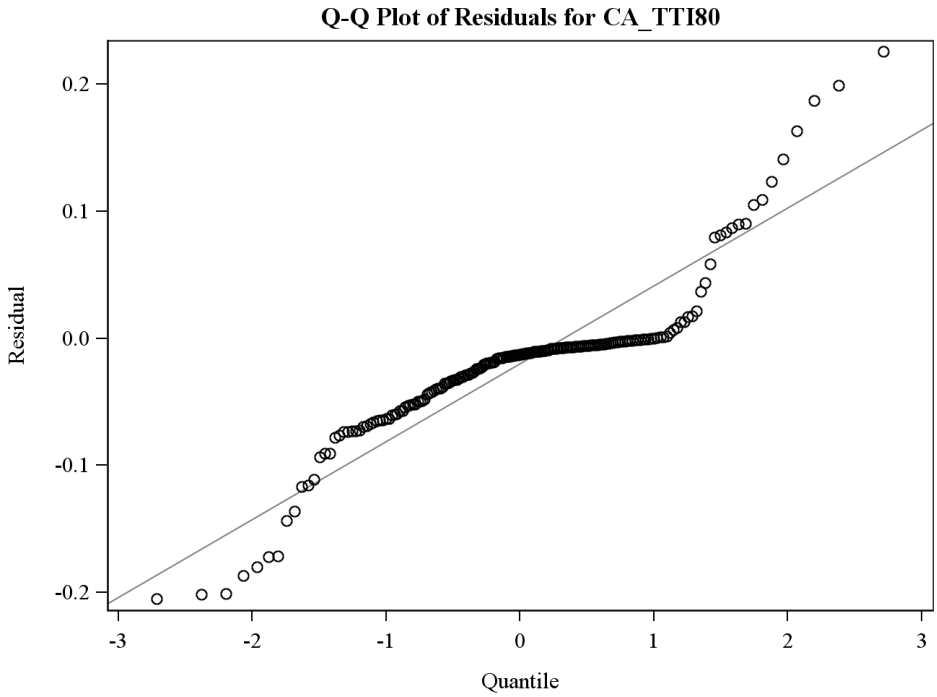

Figure E.56. Q-Q plot of residuals, recalibrated 80th-percentile TTI model, California.

Minnesota

The recalibrated model for the 80th-percentile TTI with the MN set is

$$80\text{th-percentile TTI}_{MN} = 1 + 2.3539 * \ln(\text{meanTTI})$$

The statistical test results (Tables E.25 through E.27) show that both the model and the parameters are significant. The scatter plots (Figures E.57 through E.59) show that the model can predict the trend in data samples. However, the residual plot (Figure E.60) shows that the data samples are not evenly distributed along the zero reference line. Figure E.61 shows the outlier and leverage diagnostics. The histogram and the normality plot (Figures E.62 and E.63) show that the residual distribution does not closely follow a normal distribution.

Table E.25. Analysis of Variance, Recalibrated 80th-Percentile TTI Model, Minnesota

Source	DF	Sum of Squares	Mean Square	*F*-Value	Pr > *F*
Model	1	157.28090	157.28090	31059.9	<0.0001
Error	78	0.39498	0.00506		
Uncorrected total	79	157.67587			

Table E.26. Root MSE and R-Square, Recalibrated 80th-Percentile TTI Model, Minnesota

Root MSE	0.07116	*R*-Square	0.9975

Table E.27. Parameter Estimates, Recalibrated 80th-Percentile TTI Model, Minnesota

Variable	Label	DF	Parameter Estimate	Standard Error	*t*-Value	Pr > |*t*|	95% Confidence Limits	
Intercept	Intercept	1	1.00000	0	Infty	<0.0001	1.00000	1.00000
MN_TTImean_ln	ln(mean TTI) (MN)	1	2.35394	0.03104	75.84	<0.0001	2.29214	2.41573
RESTRICT		–1	–1.86088	0.52771	–3.53	0.0003[a]	–2.89227	–0.82950

[a] The model restricts the intercept to be 1 (unity).

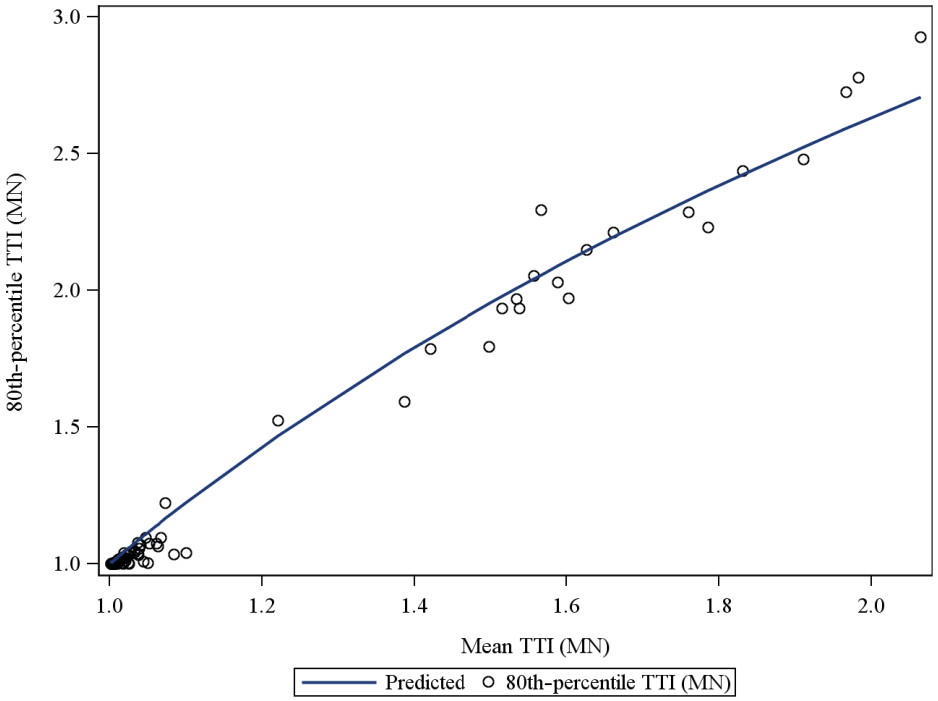

Figure E.57. Fit plot in original scale, recalibrated 80th-percentile TTI model, Minnesota.

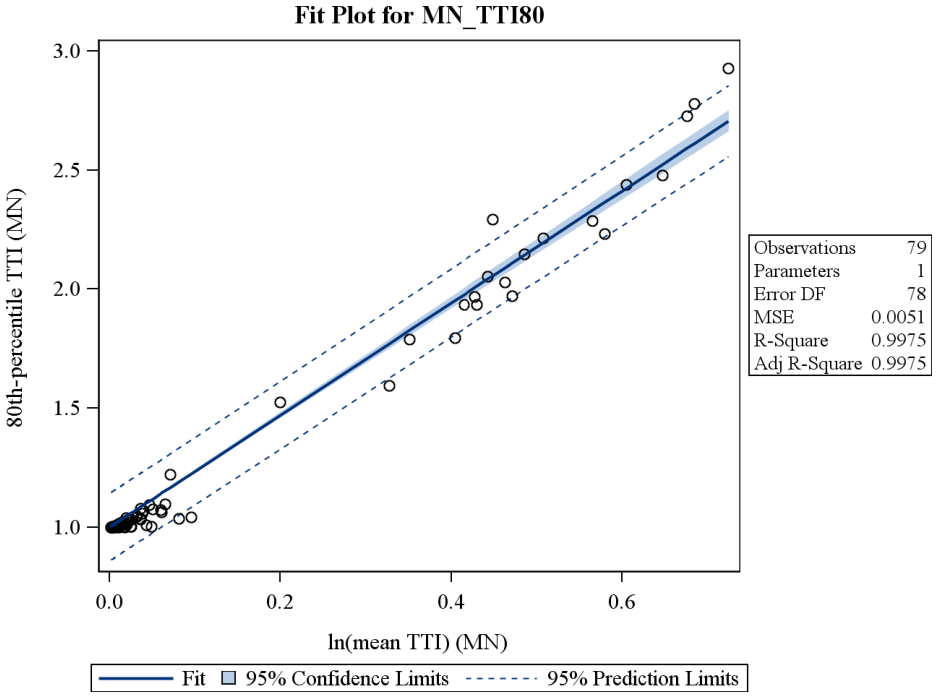

Figure E.58. Fit plot in x-axis log scale, recalibrated 80th-percentile TTI model, Minnesota.

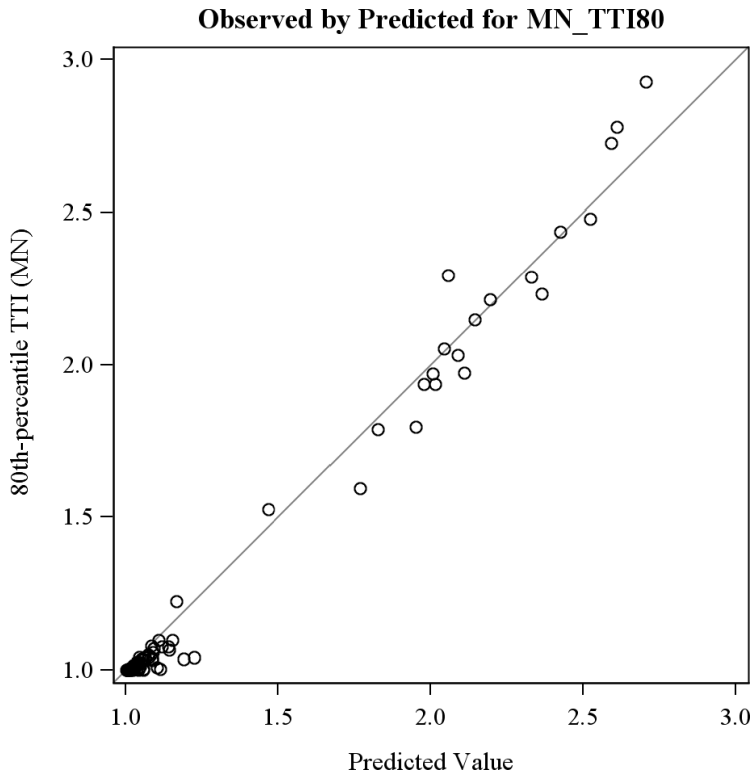

Figure E.59. Observed-by-predicted plot, recalibrated 80th-percentile TTI model, Minnesota.

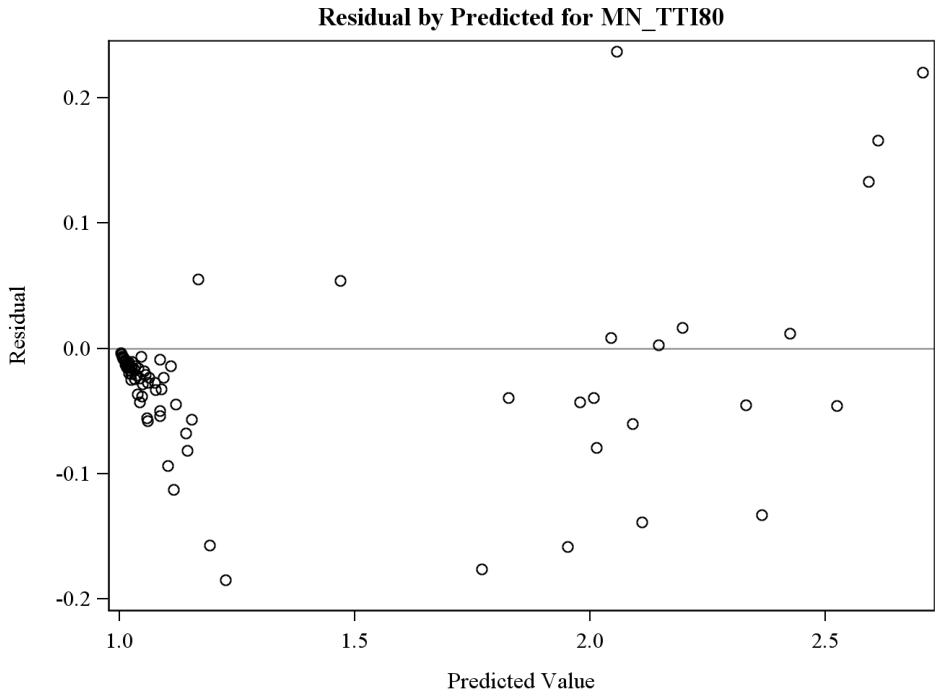

Figure E.60. Residual-by-predicted plot, recalibrated 80th-percentile TTI model, Minnesota.

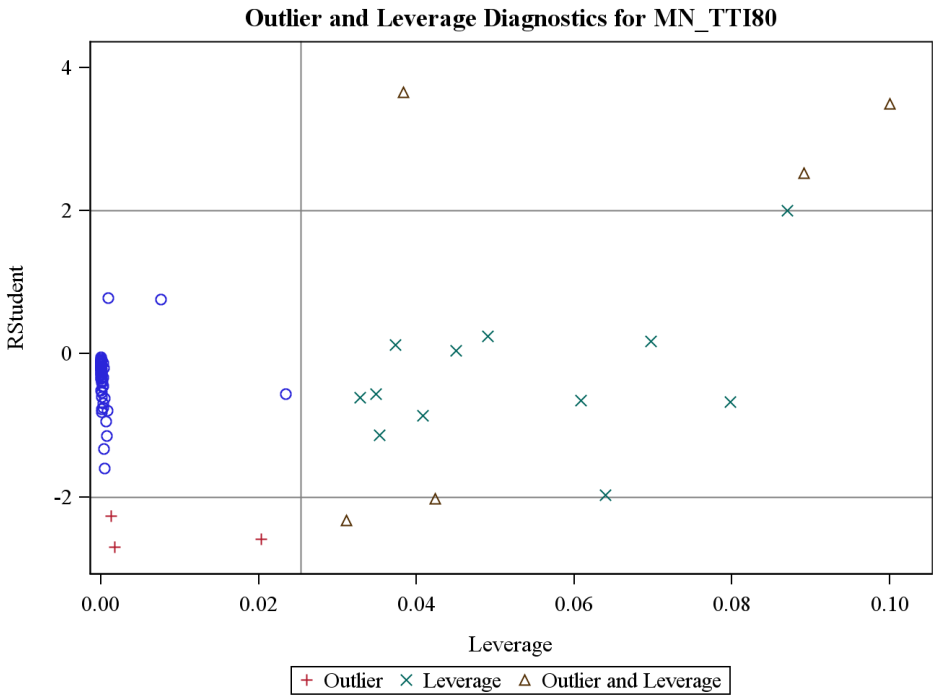

Figure E.61. Outlier and leverage plot, recalibrated 80th-percentile TTI model, Minnesota.

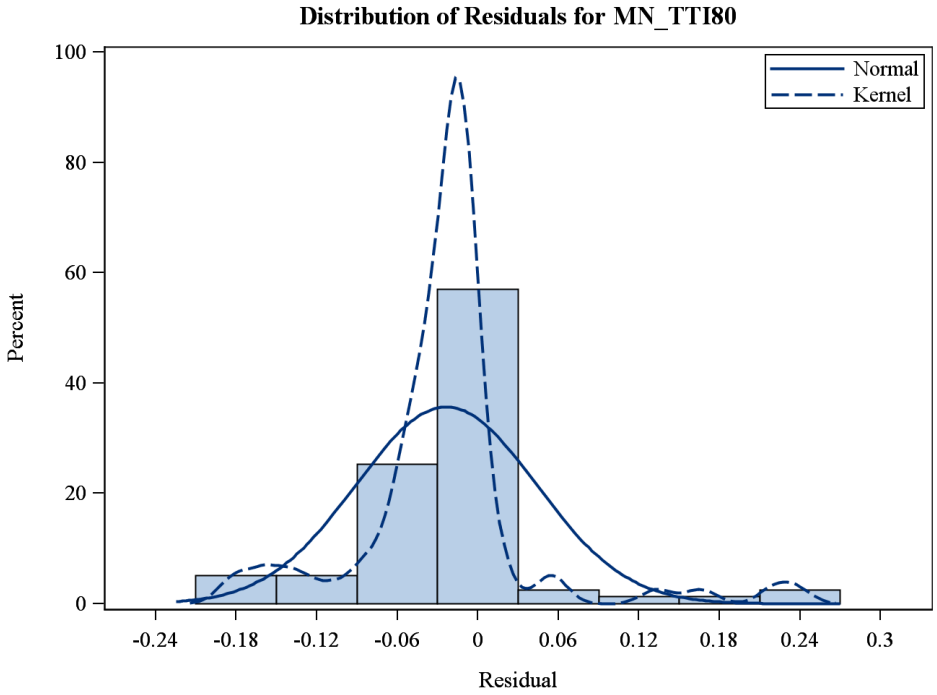

Figure E.62. Distribution of residuals, recalibrated 80th-percentile TTI model, Minnesota.

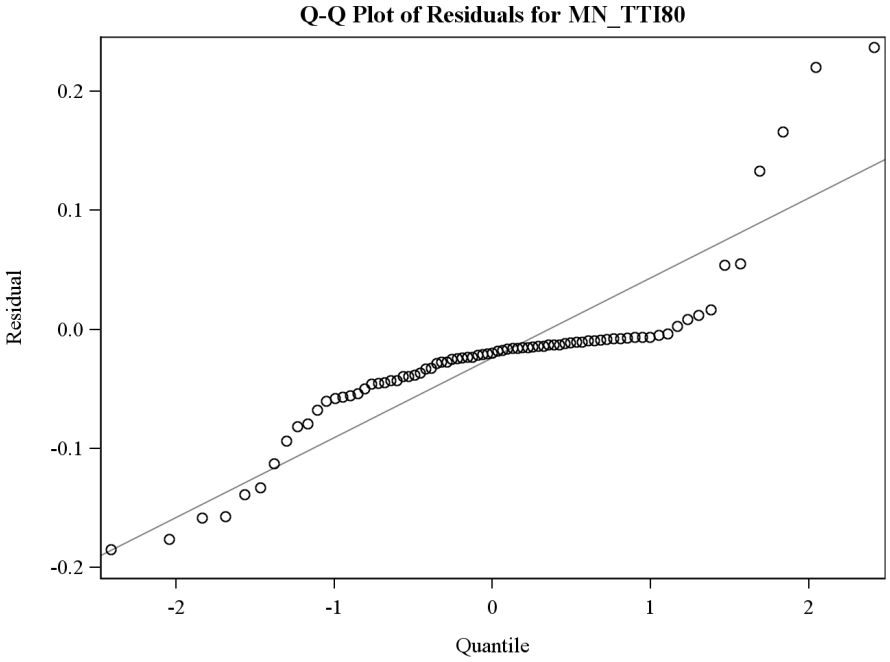

Figure E.63. Q-Q plot of residuals, recalibrated 80th-percentile TTI model, Minnesota.

Standard Deviation of TTI

The recalibration of the standard deviation of the TTI model is conducted by building a nonlinear model between the response variable, the standard deviation of TTI, and the independent variable, mean TTI. The model form is the same as the L03 data-poor model form, described as

$$\text{StdDevTTI} = a * (\text{meanTTI} - 1)^b$$

where a and b are the model parameters to be calibrated. Note that a similar model can be built by adopting a linear model form using log-transformed dependent and independent variables; however, it is found that the nonlinear model and the transformed linear model are quite different, and the nonlinear model line is closer to the measured data trend.

AllData

The recalibrated model for the standard deviation of TTI with the AllData set is

$$\text{StdDevTTI}_{\text{AllData}} = 0.7775 * (\text{meanTTI} - 1)^{0.6810}$$

The *F*-test results (Table E.28) show that the model is significant. The parameter estimation results are shown in Table E.29. The scatter plot (Figure E.64), the fit plot (Figure E.65), and the observed-by-predicted plot (Figure E.66) all show that the model can generally predict the trend of the measured data. From the scatter plot we can also see that most of the blue points representing the MN data samples are beyond the model line, while a greater portion of the red points representing the CA samples are below the model line, indicating regional difference. The residual-by-predicted plot (Figure E.67) indicates the problem of nonconstant variance; however, this problem may not be totally fixed due to the characteristics of the data. The histogram and the normality plot (Figures E.68 and E.69) show that the residual distribution is generally close to a normal distribution but with long tails.

Table E.28. Analysis of Variance, Recalibrated Standard Deviation TTI Model, AllData

Source	DF	Sum of Squares	Mean Square	*F*-Value	Approx. Pr > *F*
Model	2	25.3386	12.6693	1896.51	<0.0001
Error	321	2.1444	0.00668		
Uncorrected total	323	27.4829			

Table E.29. Parameter Estimates, Recalibrated Standard Deviation TTI Model, AllData

Parameter	Estimate	Approx. Std Error	Approx. 95% Confidence Limits	
a	0.7775	0.0158	0.7464	0.8086
b	0.6810	0.0242	0.6334	0.7287

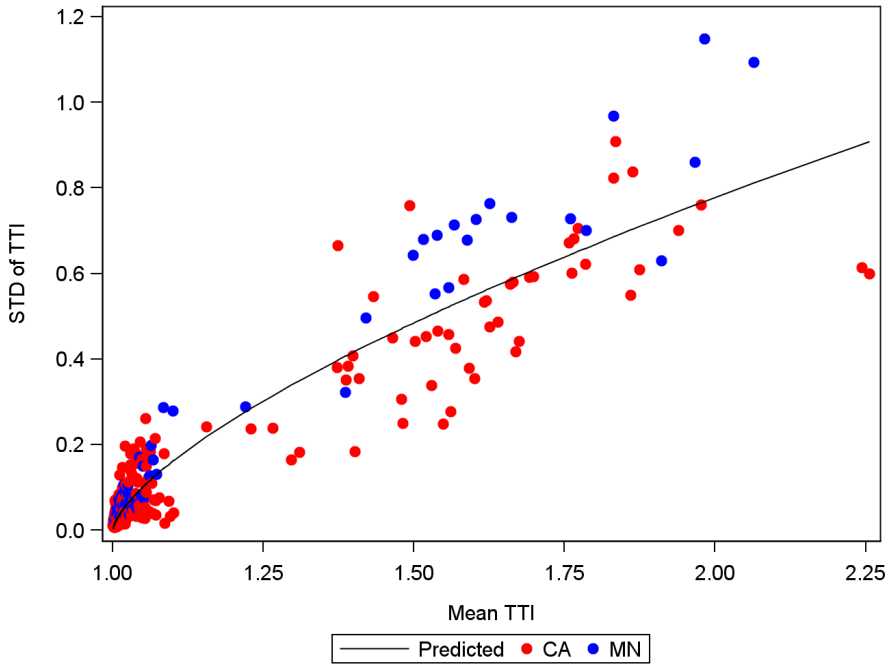

Figure E.64. Scatter plot in original scale, recalibrated standard deviation TTI model, AllData.

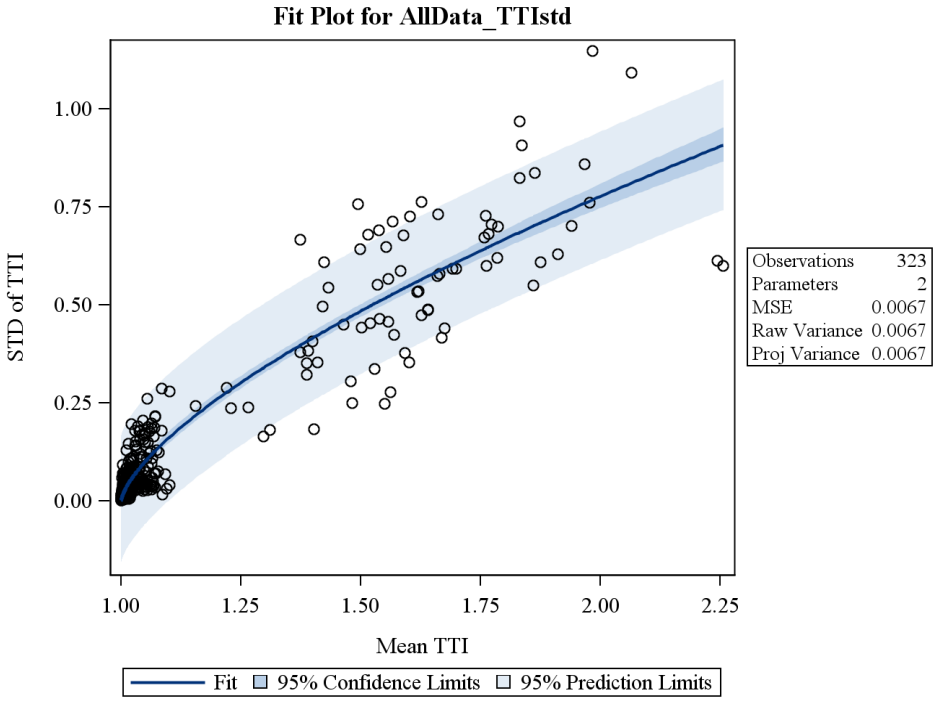

Figure E.65. Fit plot in original scale, recalibrated standard deviation TTI model, AllData.

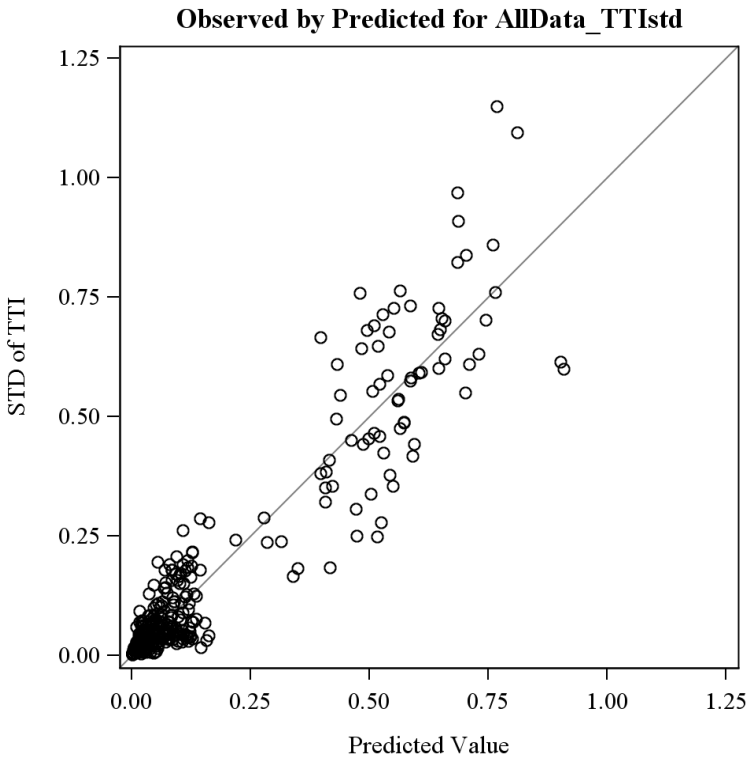

Figure E.66. Observed-by-predicted plot, recalibrated standard deviation TTI model, AllData.

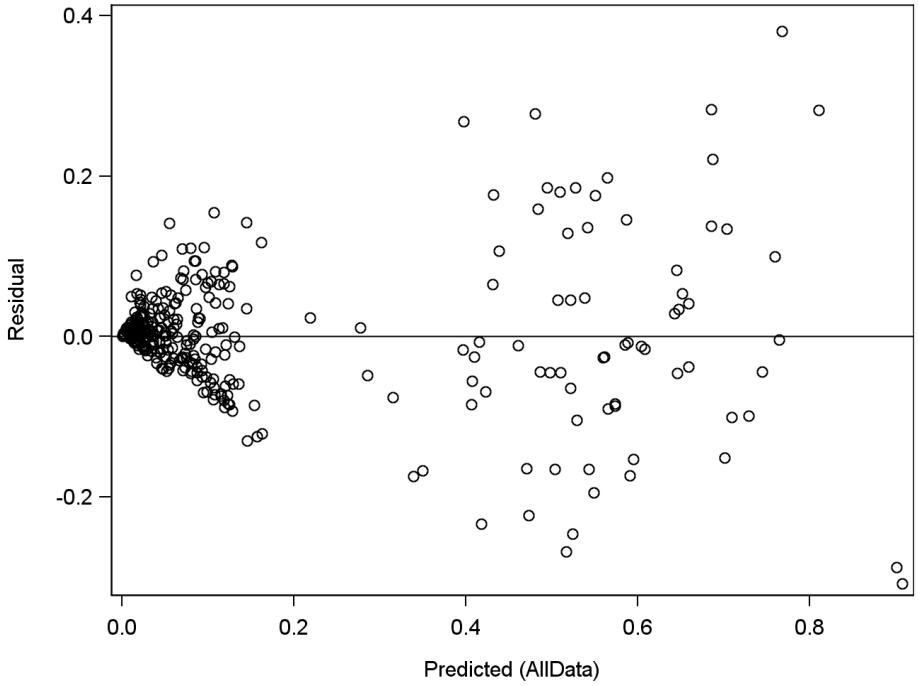

Figure E.67. Residual-by-predicted plot, recalibrated standard deviation TTI model, AllData.

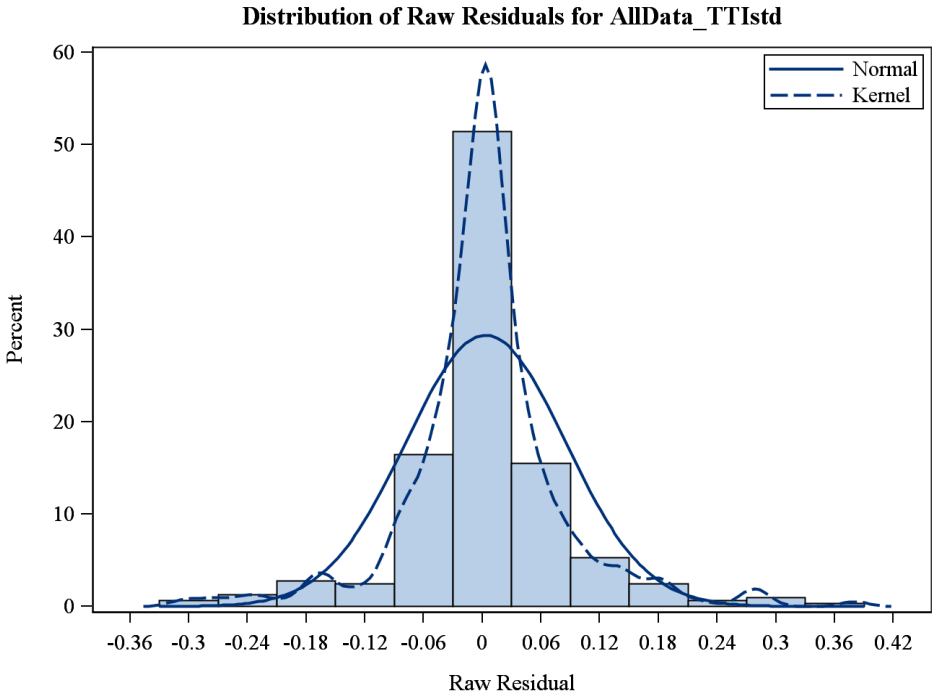

Figure E.68. Distribution of raw residuals, recalibrated standard deviation TTI model, AllData.

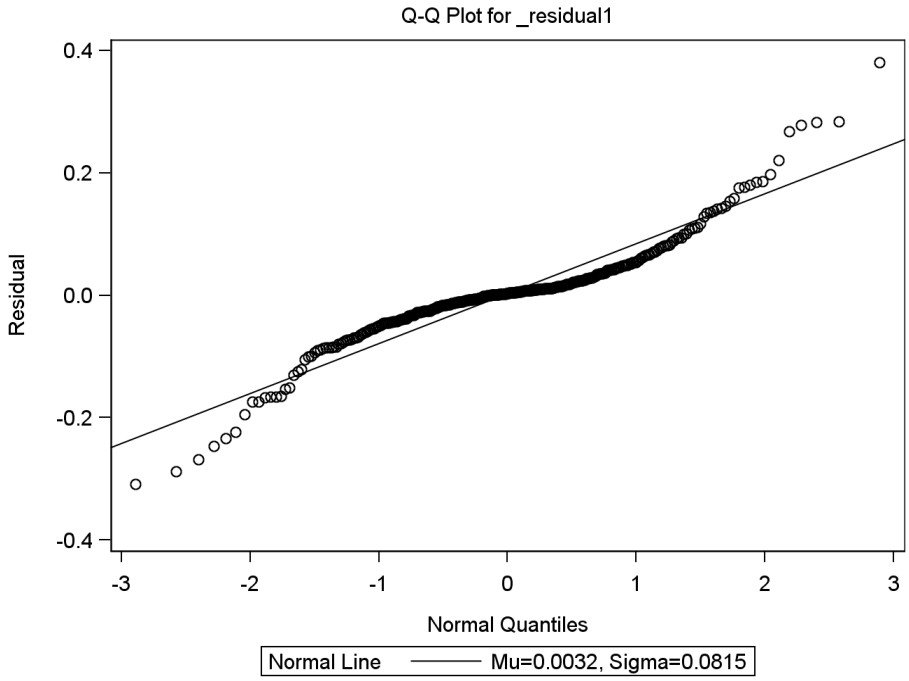

Figure E.69. Q-Q plot of residuals, recalibrated standard deviation TTI model, AllData.

California

The recalibrated model for the standard deviation of TTI with the CA set is

$$\text{StdDevTTI}_{CA} = 0.6886 * (\text{meanTTI} - 1)^{0.6444}$$

The *F*-test (Table E.30) results show that the model is significant. Table E.31 shows the parameter estimates. The fit plot (Figure E.70) and the observed-by-predicted plot (Figure E.71) show that the model generally fits the data. The residual-by-predicted plot (Figure E.72) shows that the nonconstant variance problem still exists. The histogram and the normality plot (Figures E.73 and E.74) show that the residual distribution closely follows a normal distribution but with a long right tail.

Table E.30. Analysis of Variance, Recalibrated Standard Deviation TTI Model, California

Source	DF	Sum of Squares	Mean Square	*F*-Value	Approx. Pr > *F*
Model	2	13.9468	6.9734	1107.15	<0.0001
Error	185	1.1652	0.00630		
Uncorrected total	187	15.1121			

Table E.31. Parameter Estimates, Recalibrated Standard Deviation TTI Model, California

Parameter	Estimate	Approx. Std Error	Approx. 95% Confidence Limits	
a	0.6886	0.0184	0.6523	0.7250
b	0.6444	0.0310	0.5833	0.7055

Minnesota

The recalibrated model for the standard deviation of TTI with the MN set is

$$\text{StdDevTTI}_{MN} = 0.9611 * (\text{meanTTI} - 1)^{0.6961}$$

The *F*-test results (Table E.32) show that the model is significant. Table E.33 shows the parameter estimation. The fit plot (Figure E.75) and the observed-by-predicted plot (Figure E.76) show that the model generally fits the data. The residual-by-predicted plot (Figure E.77) presents a random pattern, but the nonconstant variance problem still exists. The histogram and the normality plot (Figures E.78 and E.79) show that the residual distribution closely follows a normal distribution but with a long left tail.

(text continues on page 264)

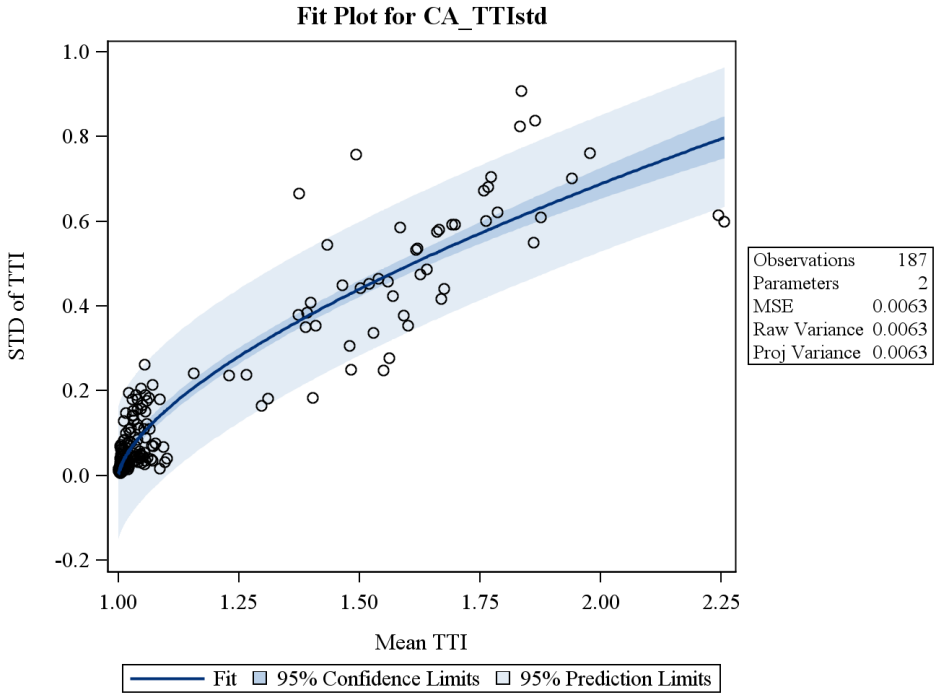

Figure E.70. Fit plot in original scale, recalibrated standard deviation TTI model, California.

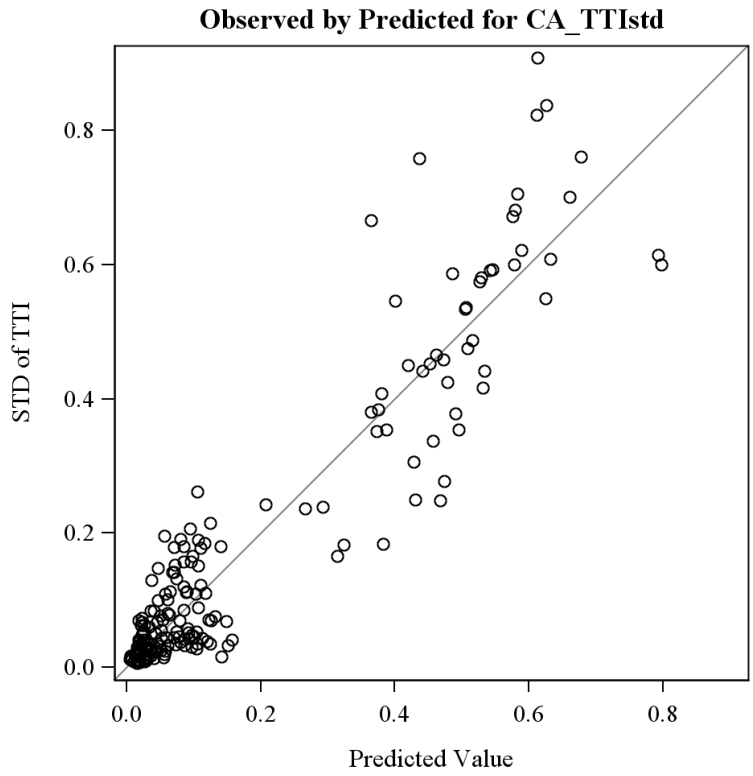

Figure E.71. Observed-by-predicted plot, recalibrated standard deviation TTI model, California.

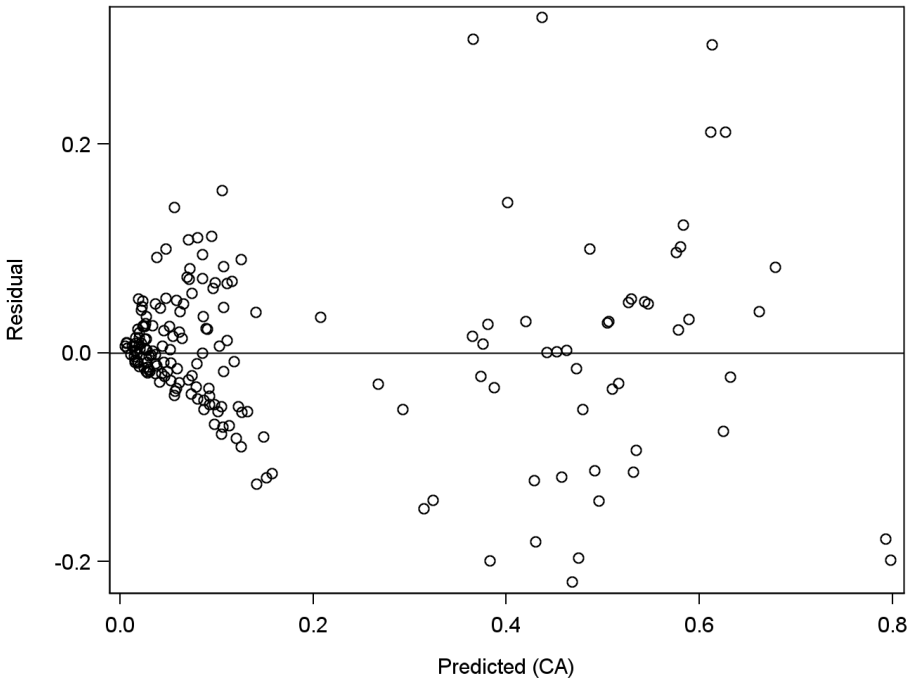

Figure E.72. Residual-by-predicted plot, recalibrated standard deviation TTI model, California.

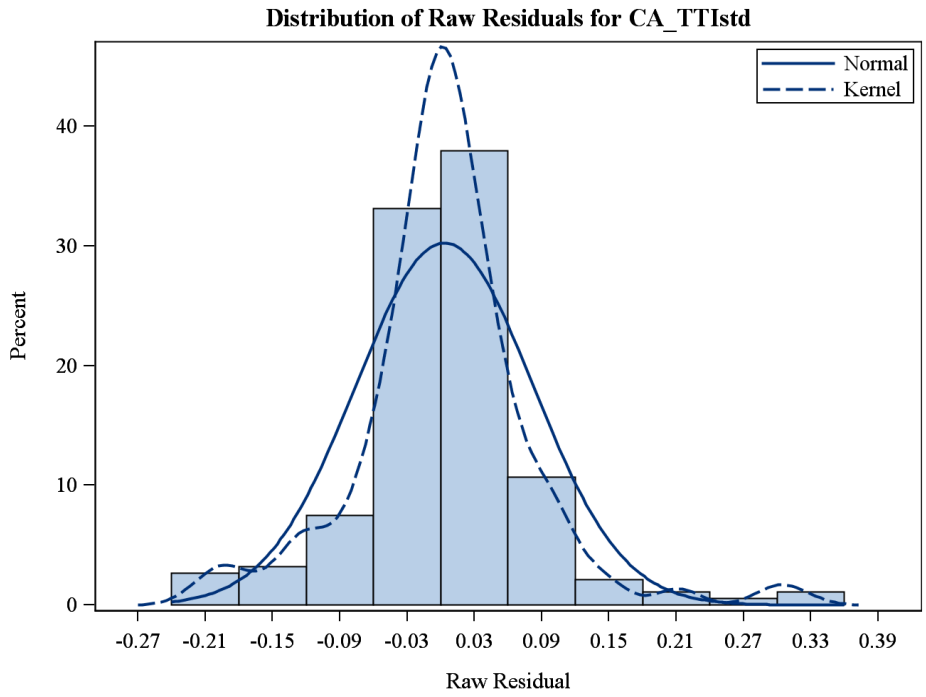

Figure E.73. Distribution of raw residuals, recalibrated standard deviation TTI model, California.

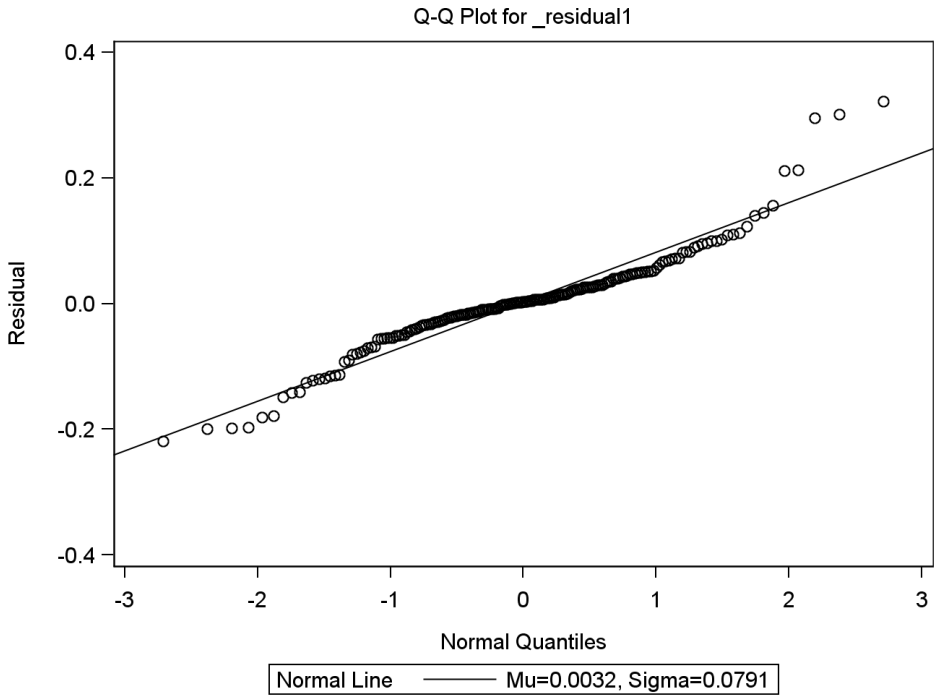

Figure E.74. Q-Q plot of residuals, recalibrated standard deviation TTI model, California.

Table E.32. Analysis of Variance, Recalibrated Standard Deviation TTI Model, Minnesota

Source	DF	Sum of Squares	Mean Square	*F*-Value	Approx. Pr > *F*
Model	2	10.8257	5.4129	1485.34	<0.0001
Error	77	0.2806	0.00364		
Uncorrected total	79	11.1063			

Table E.33. Parameter Estimates, Recalibrated Standard Deviation TTI Model, Minnesota

Parameter	Estimate	Approx. Std Error	Approx. 95% Confidence Limits	
a	0.9611	0.0217	0.9179	1.0043
b	0.6961	0.0306	0.6353	0.7570

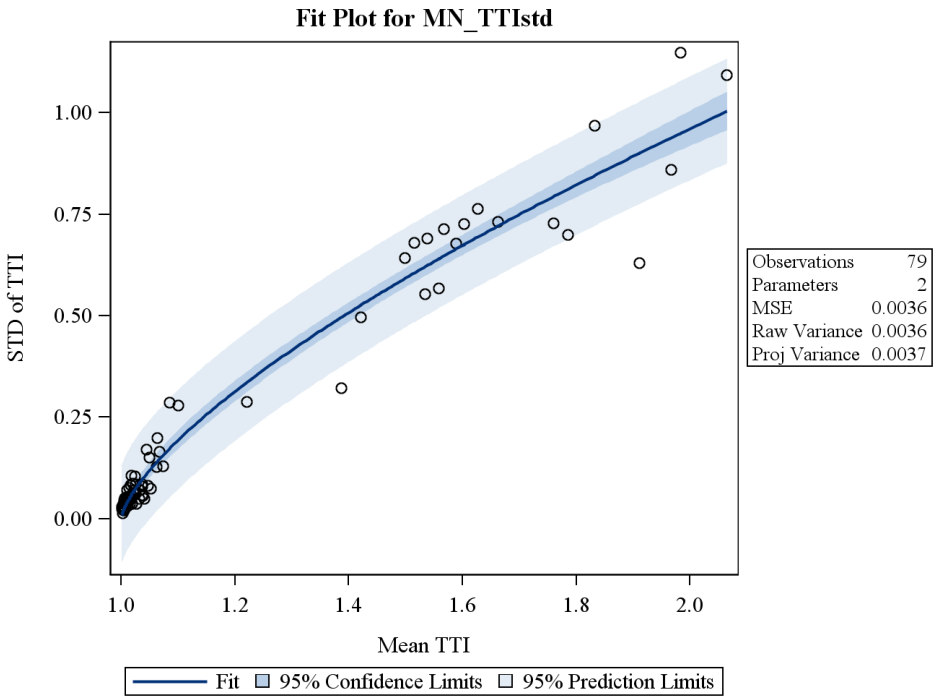

Figure E.75. Fit plot in original scale, recalibrated standard deviation TTI model, Minnesota.

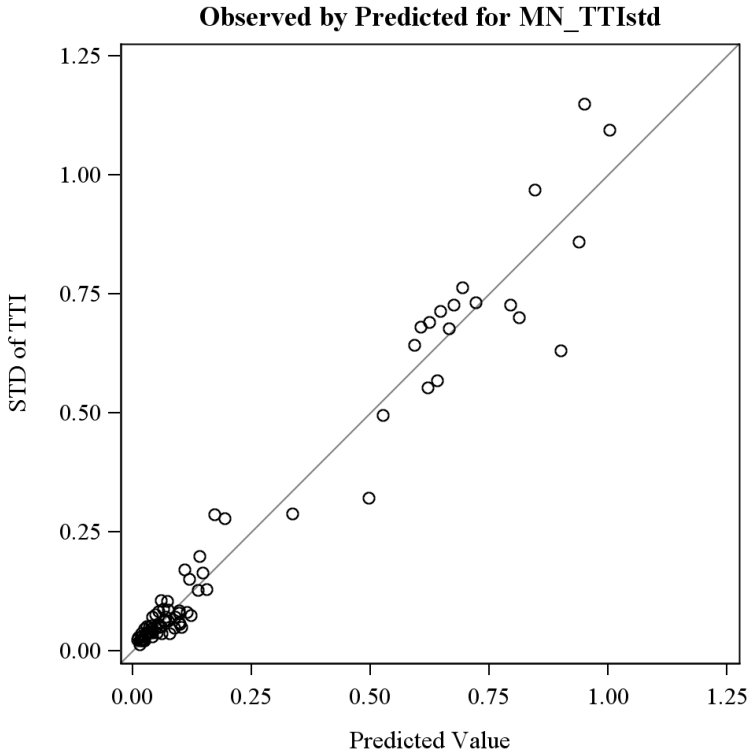

Figure E.76. Observed-by-predicted plot, recalibrated standard deviation TTI model, Minnesota.

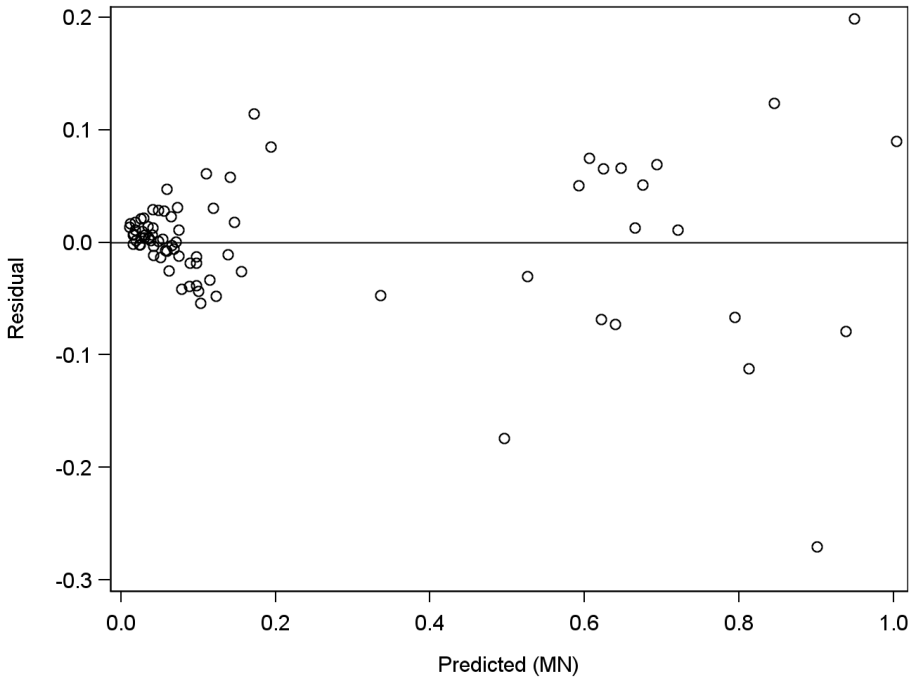

Figure E.77. Residual-by-predicted plot, recalibrated standard deviation TTI model, Minnesota.

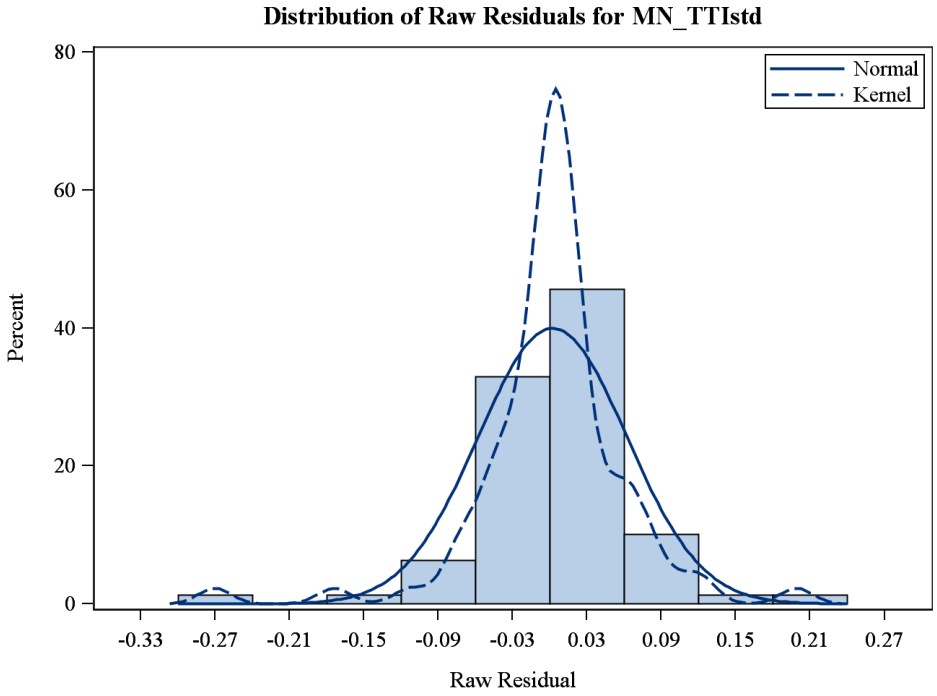

Figure E.78. Distribution of raw residuals, recalibrated standard deviation TTI model, Minnesota.

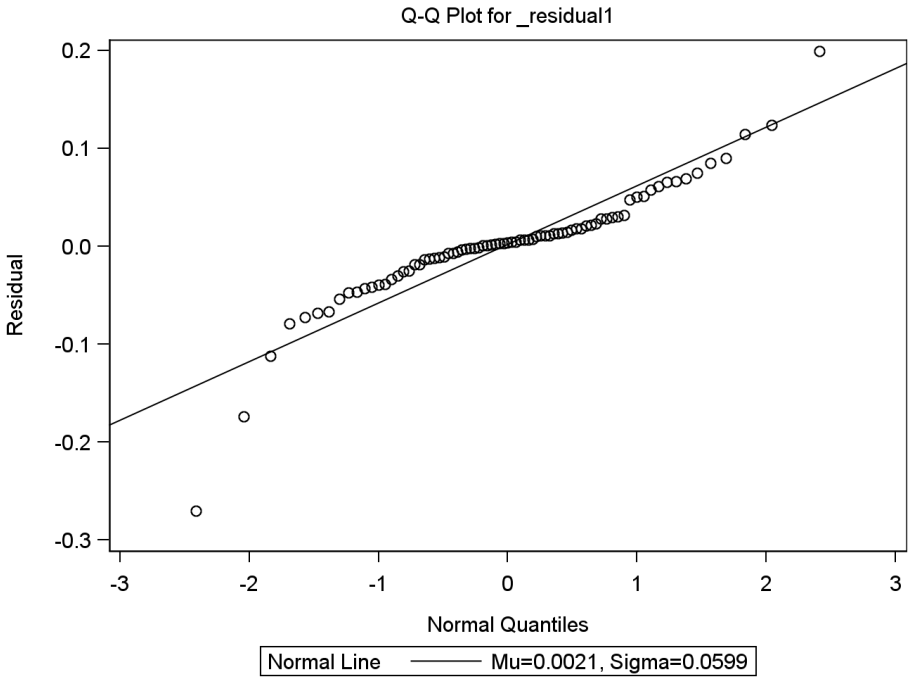

Figure E.79. Q-Q plot of residuals, recalibrated standard deviation TTI model, Minnesota.

PctTripsOnTime50mph

The recalibration of the PctTripsOnTime50mph model is conducted by building a nonlinear model between the response variable, PctTripsOnTime50mph, and the independent variable, mean TTI. The model form is the same as the L03 data-poor model form, described as

$$\text{PctTripsOnTime50mph} = e^{a*[\text{meanTTI}-1]}$$

where a is the model parameter to be calibrated.

AllData

The recalibrated model for the PctTripsOnTime50mph with the AllData set is

$$\text{PctOnTimeTrip50mph}_{\text{AllData}} = e^{-2.0293*[\text{meanTTI}-1]}$$

The *F*-test results (Table E.34) show that the model is significant. The parameter estimates are shown in Table E.35. The scatter plot (Figure E.80) shows that the regional pattern may still exist; that is, when the mean TTI is larger than 1.25, the blue points representing MN data tend to scatter beyond the model line while the red points representing CA data tend to scatter below the blue line. Note that around the origin the measured samples are scattered out forming a cone shape, but almost all of them are beyond the model line. This results in the nonrandom pattern on the right side of the residual-by-predicted value plot (Figure E.83). The nonconstant variance problem still exists in the residual-by-predicted plot. These unsatisfactory patterns may mainly be due to the characteristics of the data. The fit plot (Figure E.81) and observed-by-predicted plot (Figure E.82) are also given. The histogram and the normality plot (Figures E.84 and E.85) show that the residual distribution is close to a normal distribution when the residual is positive but has an unusual long tail on the negative side.

Table E.34. Analysis of Variance, Recalibrated PctTripsOnTime50mph Model, AllData

Source	DF	Sum of Squares	Mean Square	*F*-Value	Approx. Pr > *F*
Model	1	247.3	247.3	40121.7	<0.0001
Error	322	1.9848	0.00616		
Uncorrected total	323	249.3			

Table E.35. Parameter Estimates, Recalibrated PctTripsOnTime50mph Model, AllData

Parameter	Estimate	Approx. Std Error	Approx. 95% Confidence Limits	
a	–2.0293	0.0514	–2.1305	–1.9281

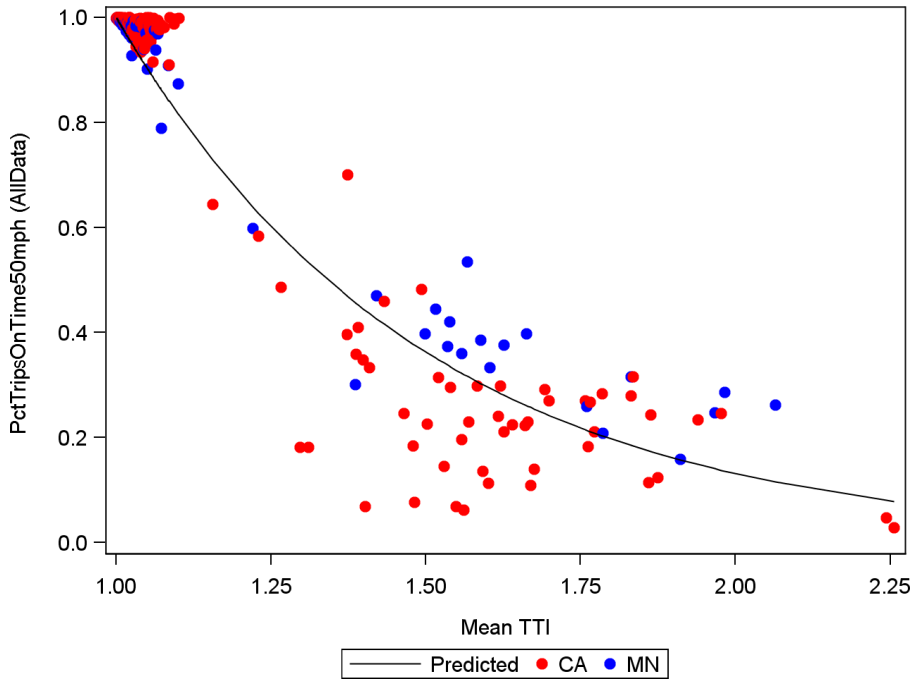

Figure E.80. Scatter plot in original scale, recalibrated PctTripsOnTime50mph model, AllData.

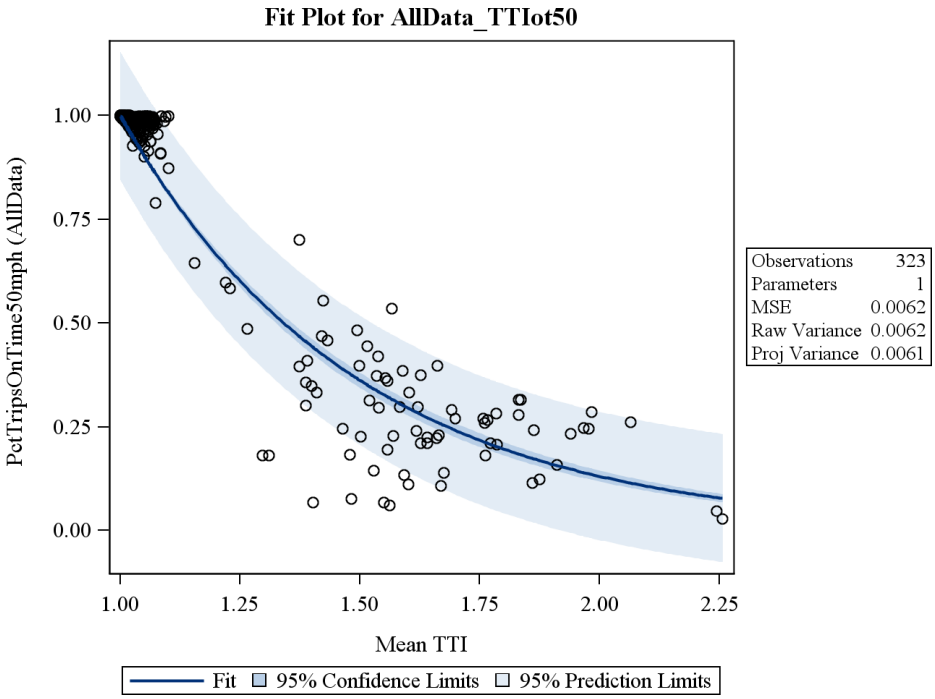

Figure E.81. Fit plot in original scale, recalibrated PctTripsOnTime50mph model, AllData.

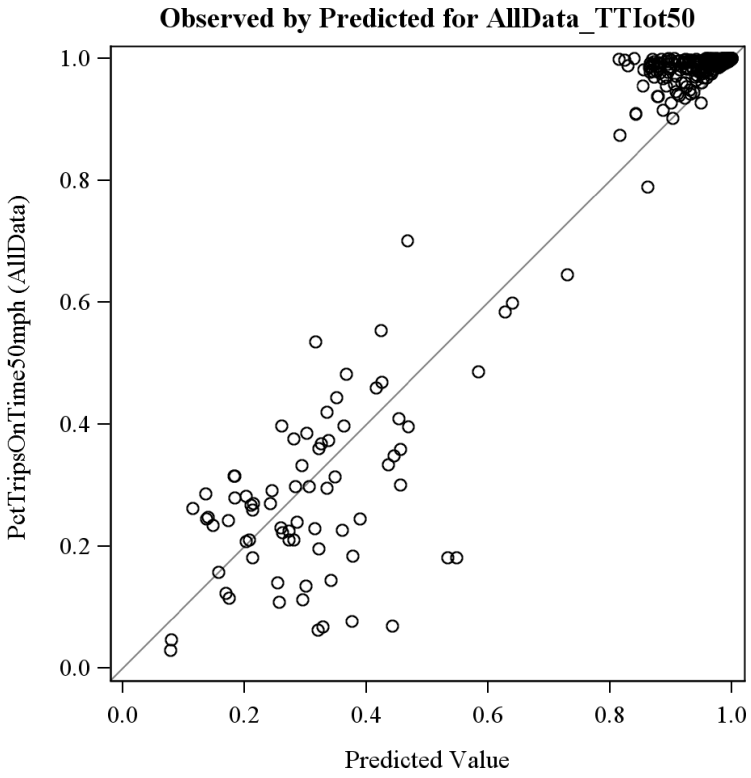

Figure E.82. Observed-by-predicted plot, recalibrated PctTripsOnTime50mph model, AllData.

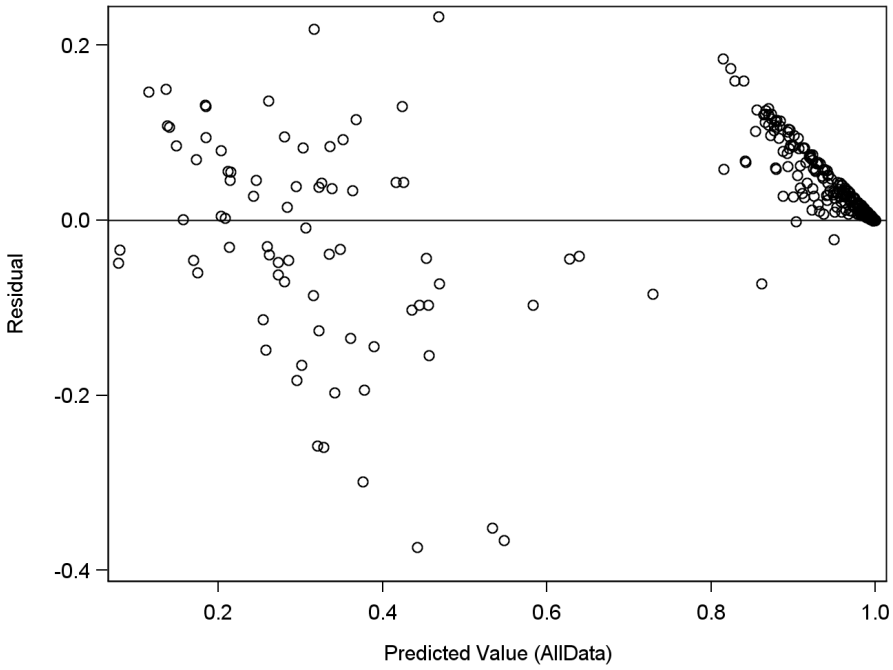

Figure E.83. Residual-by-predicted plot, recalibrated PctTripsOnTime50mph model, AllData.

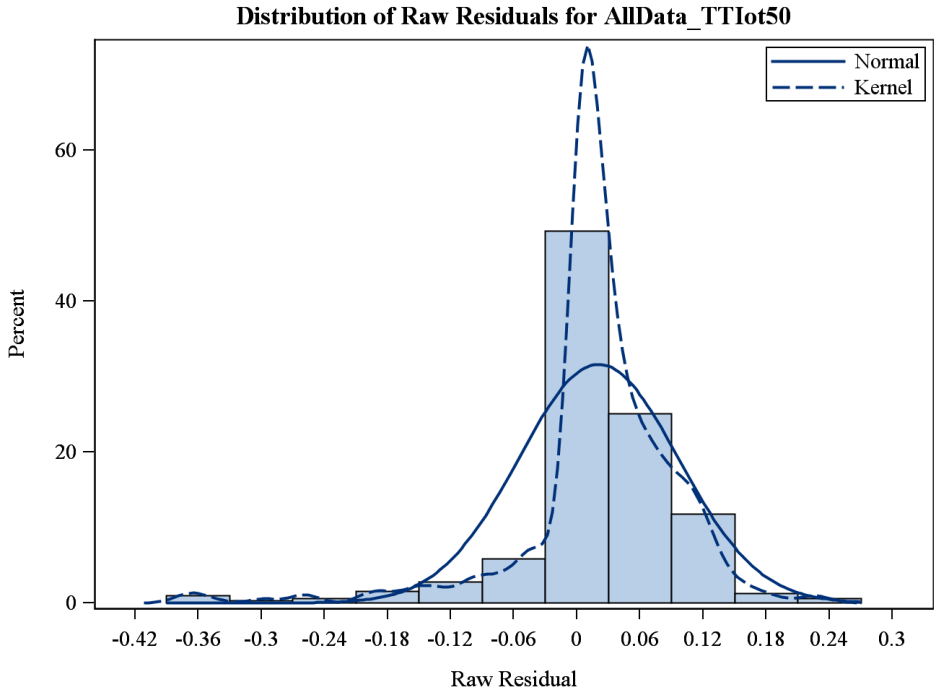

Figure E.84. Distribution of raw residuals, recalibrated PctTripsOnTime50mph model, AllData.

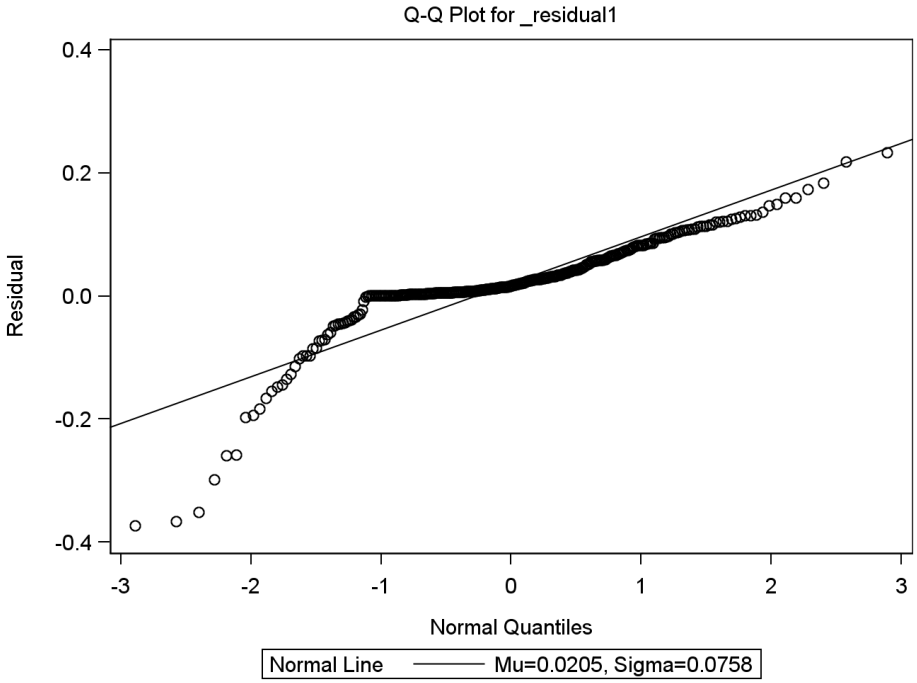

Figure E.85. Q-Q plot of residuals, recalibrated PctTripsOnTime50mph model, AllData.

California

The recalibrated model for the PctTripsOnTime50mph with the CA set is

$$\text{PctTripsOnTime50mph}_{CA} = e^{-2.2663*[\text{meanTTI}-1]}$$

The *F*-test results (Table E.36) show that the model is significant. Parameter estimates are shown in Table E.37. The fitted-curve-to-data plot (fit plot) (Figure E.86) shows a very similar pattern to that of the AllData set. The most obvious unusual pattern is that when the mean TTI is close to 1, the measured response values are almost all larger than the model predicted values (Figure E.87). The nonconstant variance problem also exists. The residual-by-predicted plot is shown in Figure E.88. The histogram and the normality plot (Figures E.89 and E.90) show that the residual distribution is close to a normal distribution when it is positive but has a long negative tail.

Table E.36. Analysis of Variance, Recalibrated PctTripsOnTime50mph Model, California

Source	DF	Sum of Squares	Mean Square	*F*-Value	Approx. Pr > *F*
Model	1	135.0	135.0	17643.1	<0.0001
Error	186	1.4229	0.00765		
Uncorrected total	187	136.4			

Minnesota

The recalibrated model for the PctTripsOnTime50mph with the MN set is

$$\text{PctTripsOnTime50mph}_{MN} = e^{-1.6422*[\text{meanTTI}-1]}$$

The *F*-test results (Table E.38) show that the model is significant. Parameter estimation is shown in Table E.39. The fit plot (Figure E.91) shows that the data samples are in general randomly scattered out along the model line, indicating that the regionally recalibrated model performs better for the MN model than the model built on the AllData set. The observed-by-predicted plot is shown in Figure E.92. The residual plot (Figure E.93) shows that when the mean TTI is close to 1, it is still unbalanced. The histogram and the normality plot (Figures E.94 and E.95) show that the residual distribution is not perfectly following a normal distribution.

(text continues on page 273)

Table E.37. Parameter Estimates, Recalibrated PctTripsOnTime50mph Model, California

Parameter	Estimate	Approx. Std Error	Approx. 95% Confidence Limits	
a	–2.2663	0.0787	–2.4215	–2.1111

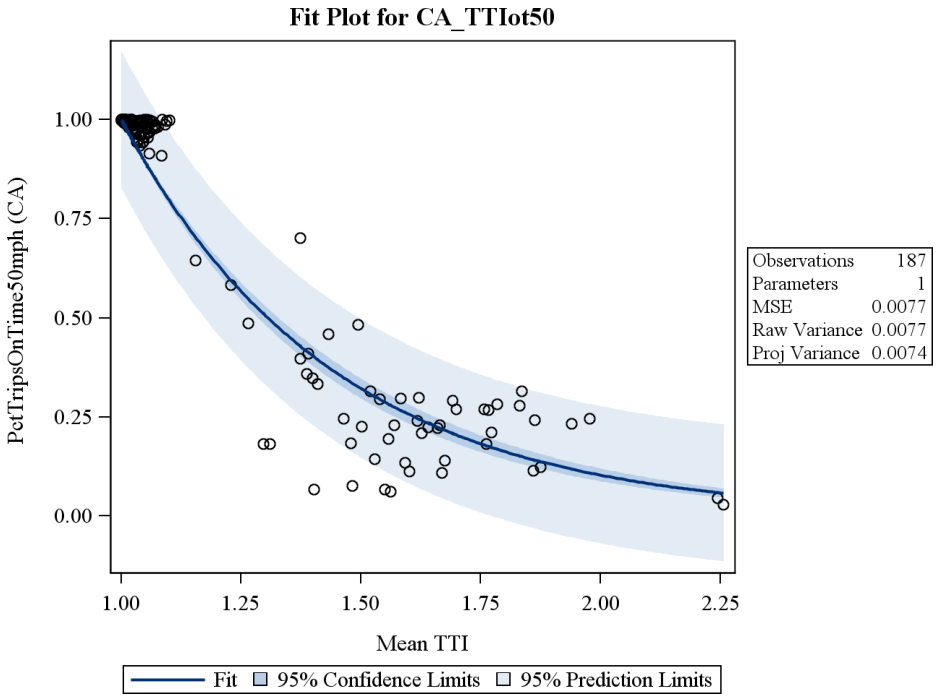

Figure E.86. Fit plot in original scale, recalibrated PctTripsOnTime50mph model, California.

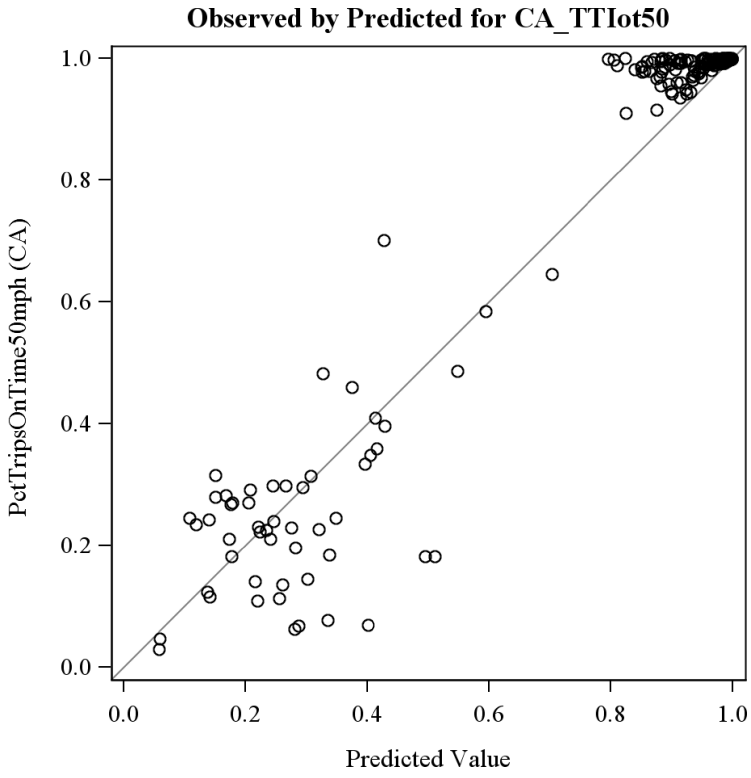

Figure E.87. Observed-by-predicted plot, recalibrated PctTripsOnTime50mph model, California.

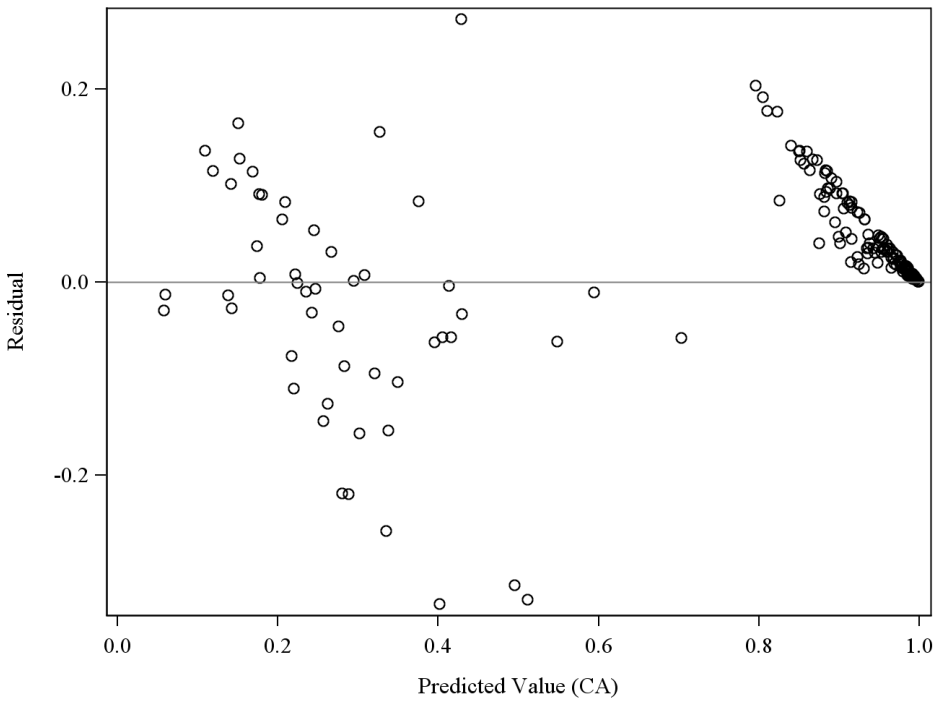

Figure E.88. Residual-by-predicted plot, recalibrated PctTripsOnTime50mph model, California.

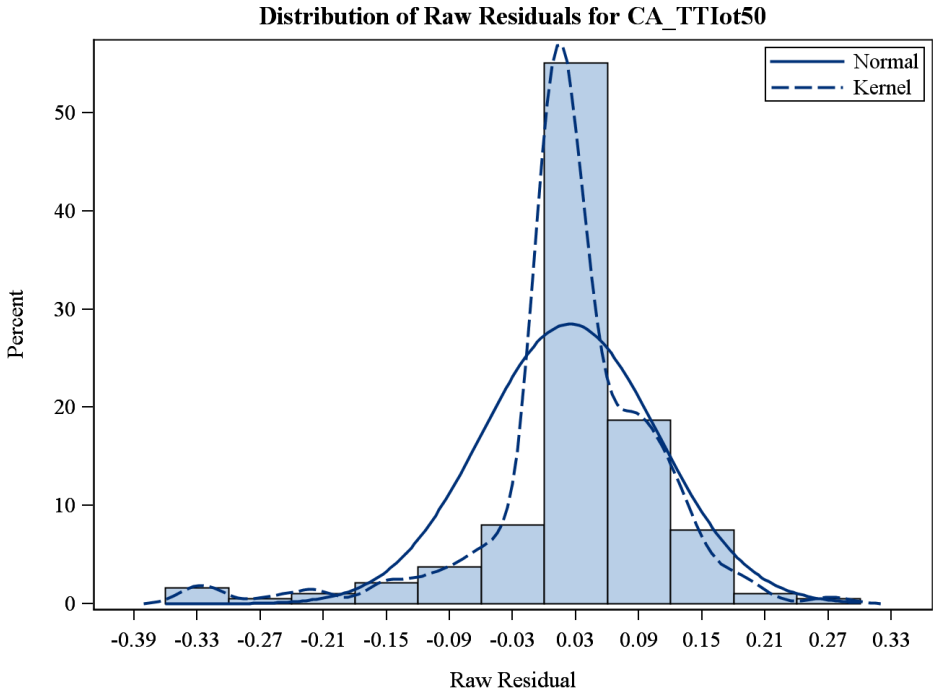

Figure E.89. Distribution of raw residuals, recalibrated PctTripsOnTime50mph model, California.

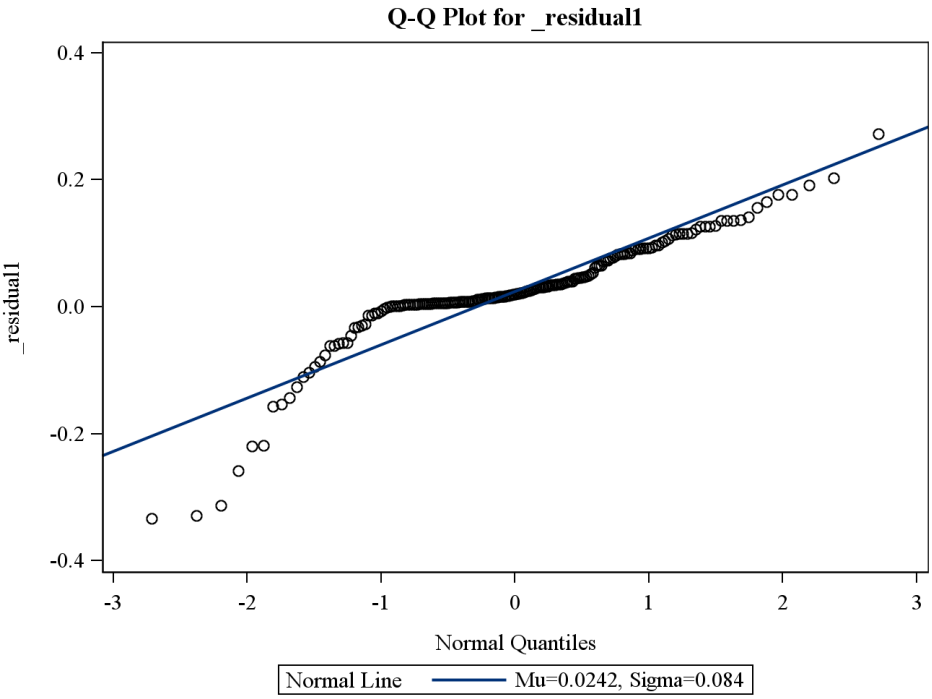

Figure E.90. Q-Q plot of residuals, recalibrated PctTripsOnTime50mph model, California.

Table E.38. Analysis of Variance, Recalibrated PctTripsOnTime50mph Model, Minnesota

Source	DF	Sum of Squares	Mean Square	*F*-Value	Approx. Pr > *F*
Model	1	59.0003	59.0003	26281.6	<0.0001
Error	78	0.1751	0.00224		
Uncorrected total	79	59.1754			

Table E.39. Parameter Estimates, Recalibrated PctTripsOnTime50mph Model, Minnesota

Parameter	Estimate	Approx. Std Error	Approx. 95% Confidence Limits	
a	–1.6422	0.0486	–1.7390	–1.5454

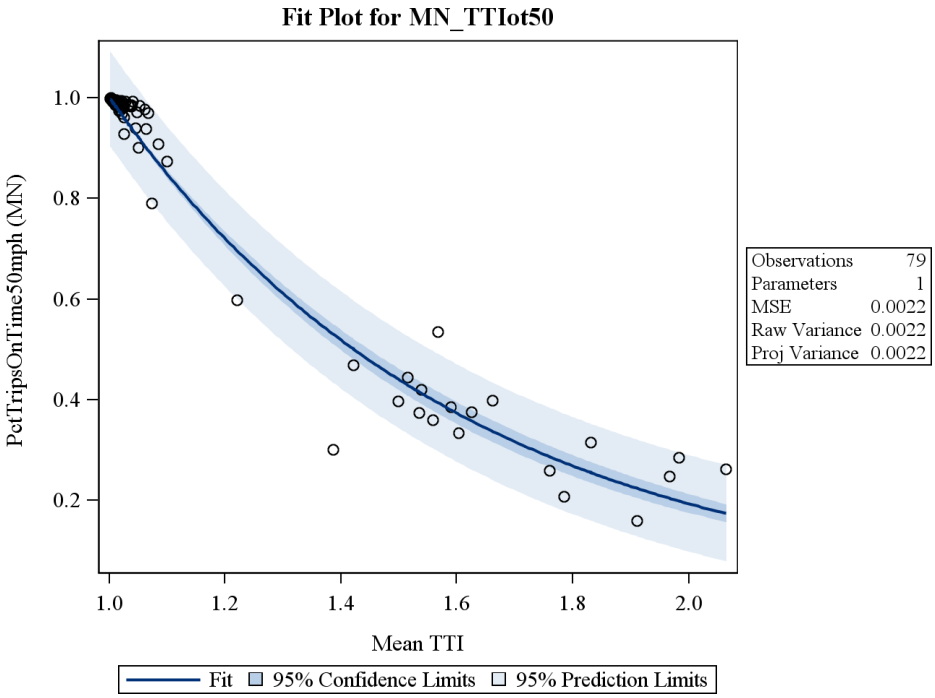

Figure E.91. Fit plot in original scale, recalibrated PctTripsOnTime50mph model, Minnesota.

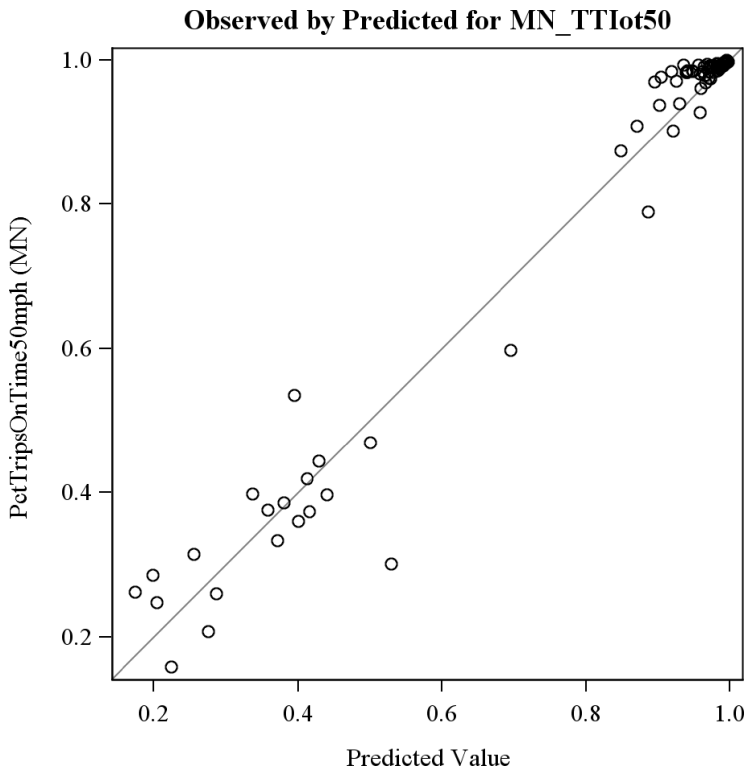

Figure E.92. Observed-by-predicted plot, recalibrated PctTripsOnTime50mph model, Minnesota.

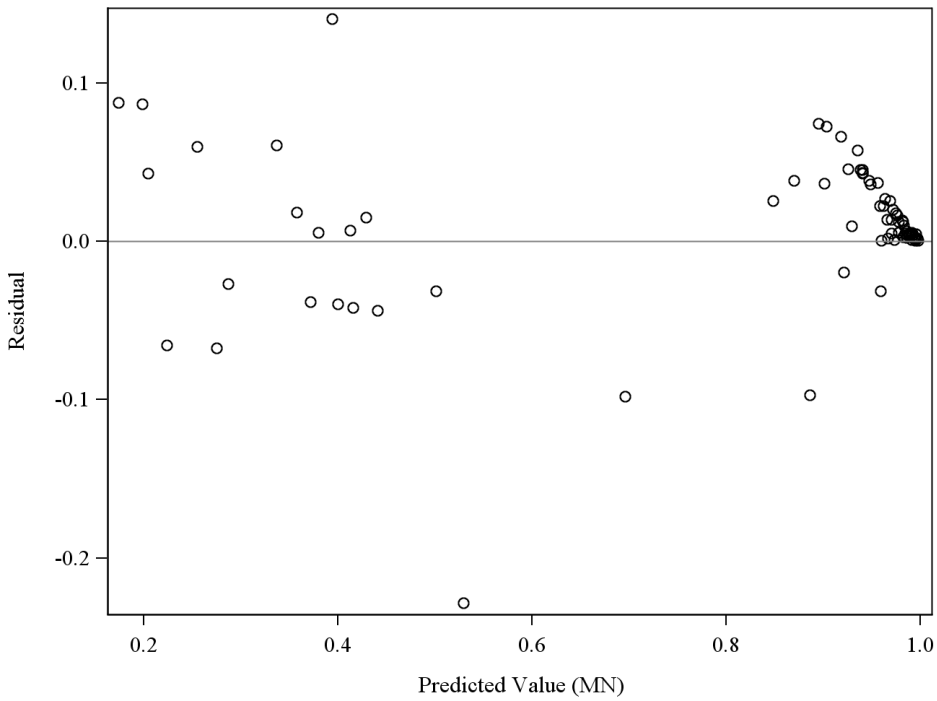

Figure E.93. Residual-by-predicted plot, recalibrated PctTripsOnTime50mph model, Minnesota.

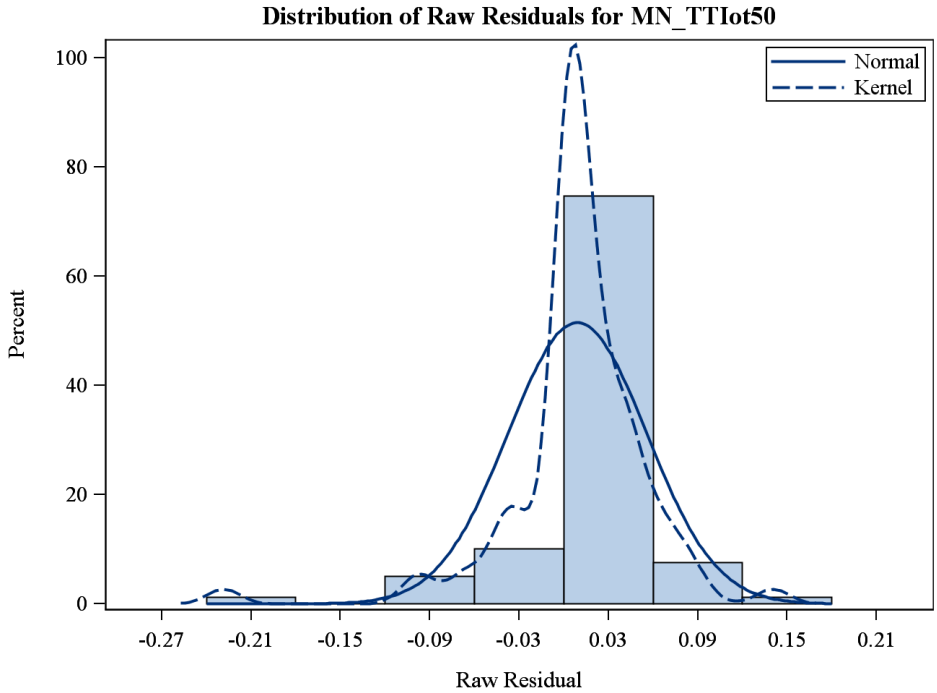

Figure E.94. Distribution of raw residuals, recalibrated PctTripsOnTime50mph model, Minnesota.

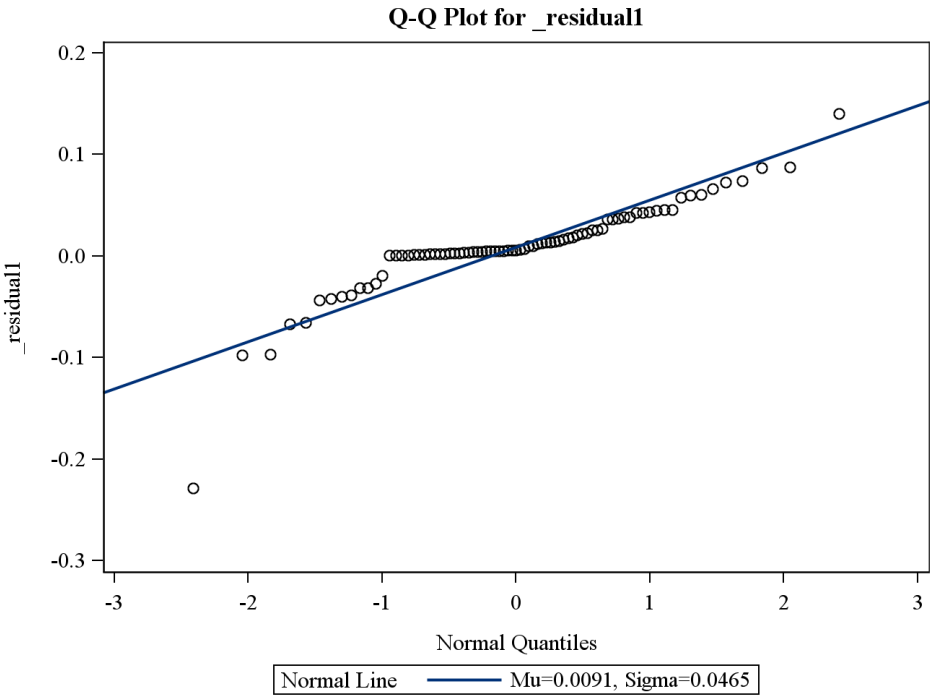

Figure E.95. Q-Q plot of residuals, recalibrated PctTripsOnTime50mph model, Minnesota.

PctTripsOnTime45mph

The recalibration of the PctTripsOnTime45mph model is conducted by building a nonlinear model between the response variable, PctTripsOnTime45mph, and the independent variable, mean TTI. The model form is the same as the L03 data-poor model form, described as

$$\text{PctTripsOnTime45mph} = e^{a*[\text{meanTTI}-1]}$$

where a is the model parameter to be calibrated.

AllData

The recalibrated model for the PctTripsOnTime45mph with the AllData set is

$$\text{PctTripsOnTime45mph}_{\text{AllData}} = e^{-1.4874*[\text{meanTTI}-1]}$$

The model form for the PctTripsOnTime45mph is the same as that for the PctTripsOnTime50mph, and the patterns shown in the recalibrated models are also very similar. As for this recalibrated PctTripsOnTime45mph model, the *F*-test results (Table E.40) show that overall the model is significant. The parameter estimation is shown in Table E.41. The scatter plot (Figure E.96), fit plot (Figure E.97), and the measured-by-predicted plot (Figure E.98) show that the recalibrated model line can generally predict the trend in the measured data. The regional difference can also be noticed from the scatter plot where the blue points representing MN data tend to scatter beyond the model line while the red points representing CA data tend to scatter below the blue line when the mean TTI is larger than 1.25. The nonconstant variance problem can be identified in the residual-by-predicted plot (Figure E.99). The histogram and the normality plot (Figures E.100 and E.101) show that the residual distribution has a longer negative tail compared to a normal distribution.

Table E.40. Analysis of Variance, Recalibrated PctTripsOnTime45mph Model, AllData

Source	DF	Sum of Squares	Mean Square	*F*-Value	Approx. Pr > *F*
Model	1	257.4	257.4	70942.6	<0.0001
Error	322	1.1685	0.00363		
Uncorrected total	323	258.6			

Table E.41. Parameter Estimates, Recalibrated PctTripsOnTime45mph Model, AllData

Parameter	Estimate	Approx. Std Error	Approx. 95% Confidence Limits	
a	–1.4874	0.0290	–1.5446	–1.4303

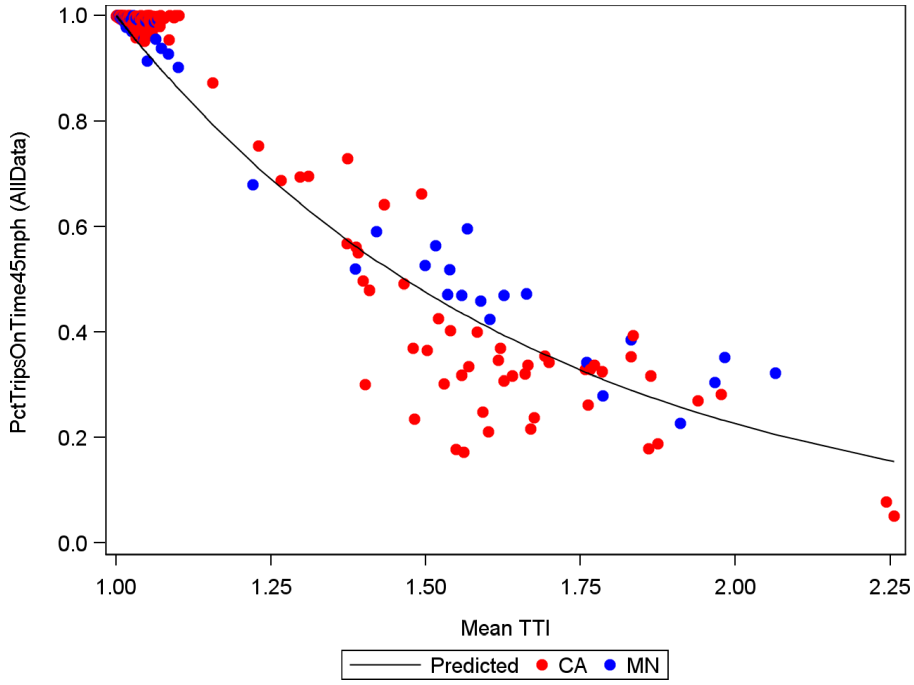

Figure E.96. Scatter plot in original scale, recalibrated PctTripsOnTime45mph model, AllData.

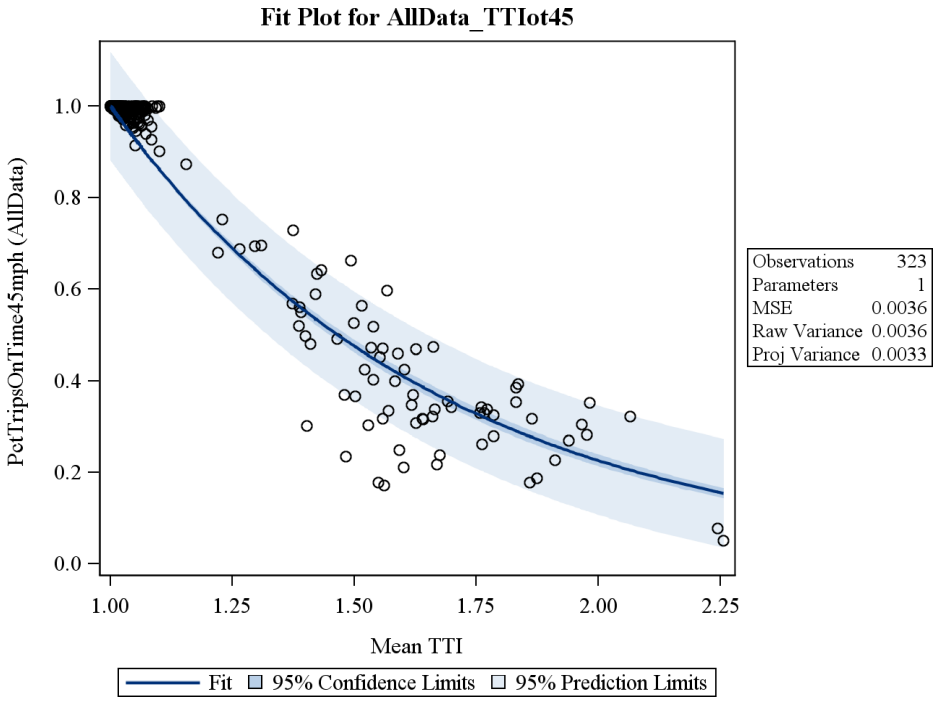

Figure E.97. Fit plot in original scale, recalibrated PctTripsOnTime45mph model, AllData.

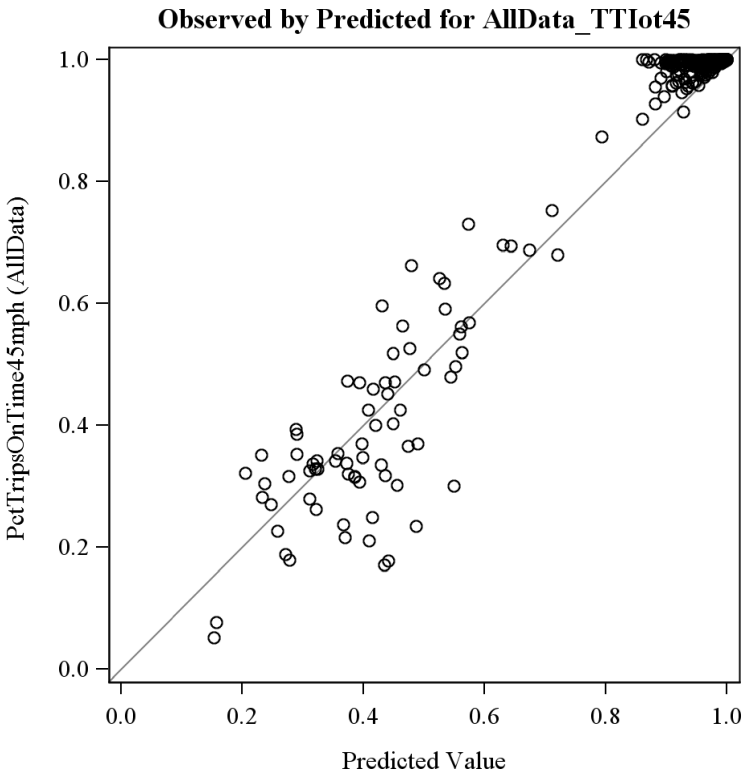

Figure E.98. Observed-by-predicted plot, recalibrated PctTripsOnTime45mph model, AllData.

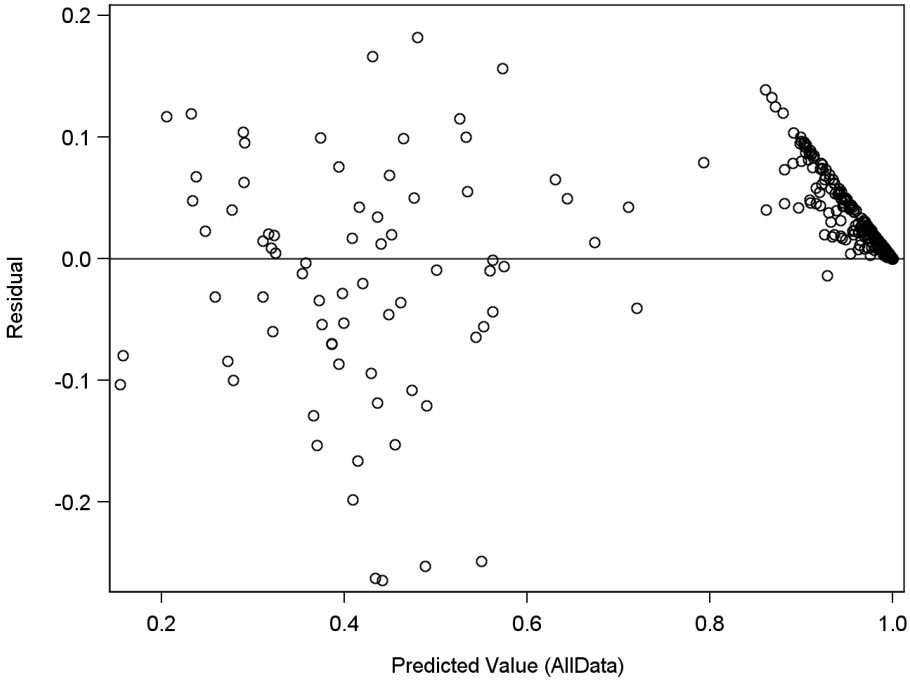

Figure E.99. Residual-by-predicted plot, recalibrated PctTripsOnTime45mph model, AllData.

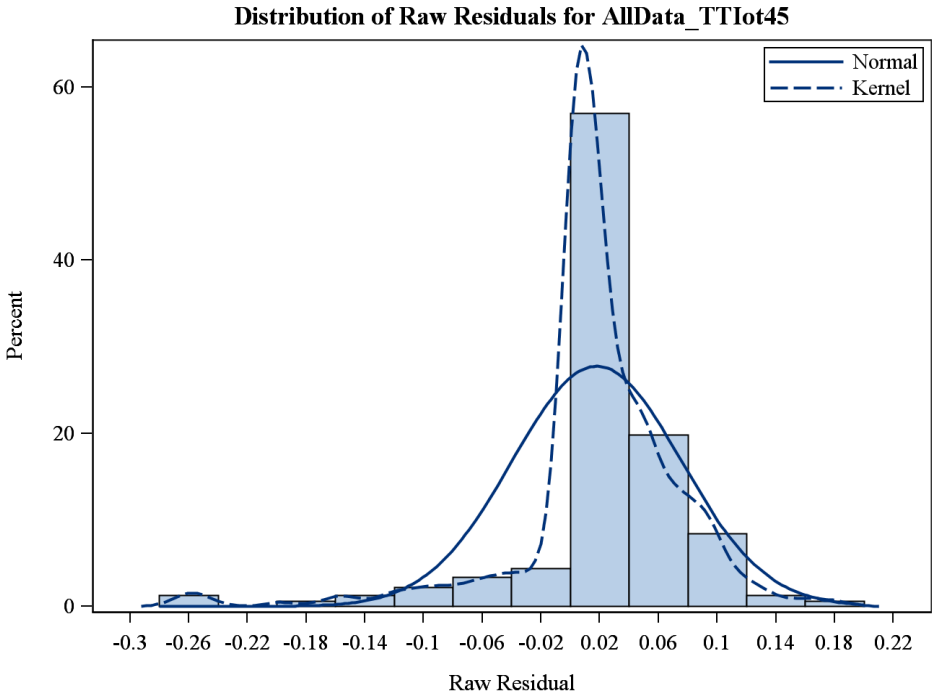

Figure E.100. Distribution of raw residuals, recalibrated PctTripsOnTime45mph model, AllData.

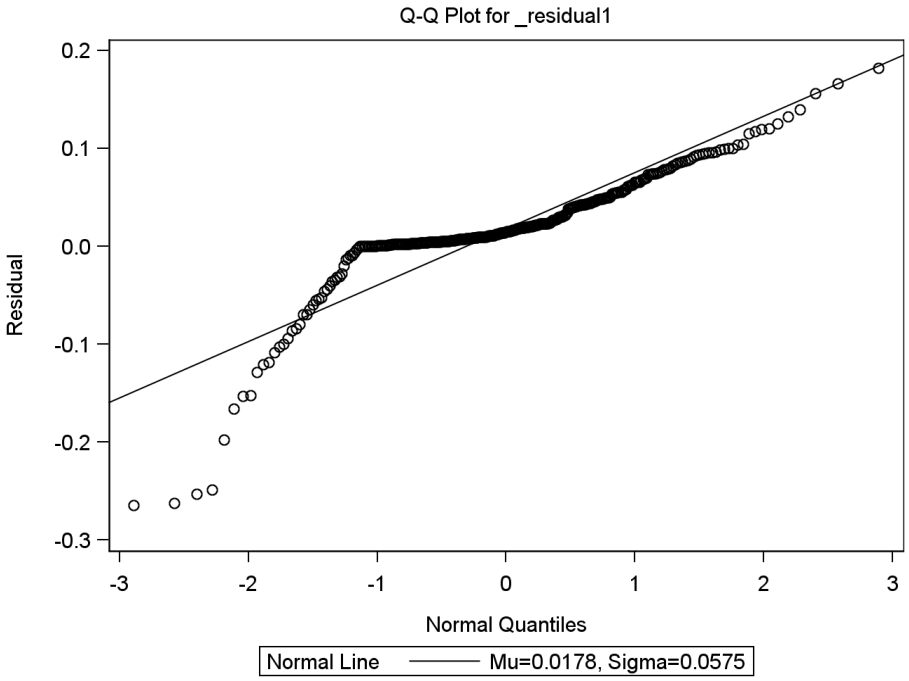

Figure E.101. Q-Q plot of residuals, recalibrated PctTripsOnTime45mph model, AllData.

California

The recalibrated model for the PctTripsOnTime45mph with the CA set is

$$\text{PctTripsOnTime45mph}_{CA} = e^{-1.6125*[\text{meanTTI}-1]}$$

The recalibrated model for the CA data set presents similar results to that for the AllData set. The *F*-test results (Table E.42) show that the model is significant. The parameter estimation is shown in Table E.43. From the fit plot (Figure E.102) we can see that when the mean TTI is close to 1, the measured response values are almost all larger than the model predicted values (Figure E.103). The nonconstant variance problem also exists. The residual-by-predicted plot is shown in Figure E.104. The histogram and the normality plot (Figures E.105 and E.106) show that the residual distribution is close to a normal distribution when it is positive but has a long negative tail.

Minnesota

The recalibrated model for the PctTripsOnTime45mph with the MN set is

$$\text{PctTripsOnTime45mph}_{MN} = e^{-1.2568*[\text{meanTTI}-1]}$$

Similar to the PctTripsOnTime50mph case, the regionally recalibrated model works better for the MN data set than the model built on the AllData set because the measured samples

Table E.42. Analysis of Variance, Recalibrated PctTripsOnTime45mph Model, California

Source	DF	Sum of Squares	Mean Square	*F*-Value	Approx. Pr > *F*
Model	1	141.7	141.7	31390.1	<0.0001
Error	186	0.8396	0.00451		
Uncorrected total	187	142.5			

Table E.43. Parameter Estimates, Recalibrated PctTripsOnTime45mph Model, California

Parameter	Estimate	Approx. Std Error	Approx. 95% Confidence Limits	
a	–1.6125	0.0423	–1.6959	–1.5291

are in general randomly scattered out on both sides of the model line, although when the mean TTI is close to 1, the model tends to underestimate the response variable. The *F*-test results (Table E.44) show that the model is significant. The parameter estimation is shown in Table E.45. The fit plot is shown in Figure E.107. The observed-by-predicted plot is shown in Figure E.108. The residual-by-predicted plot is shown in Figure E.109. The histogram and the normality plot (Figure E.110 and Figure E.111) show that the residual distribution is not perfectly following a normal distribution.

(text continues on page 283)

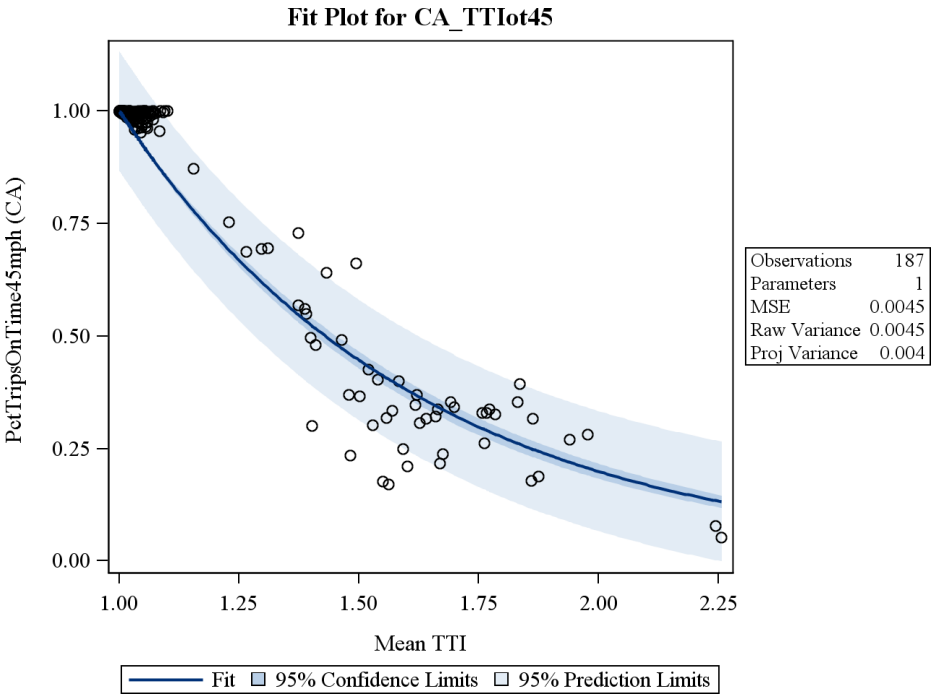

Figure E.102. Fit plot in original scale, recalibrated PctTripsOnTime45mph model, California.

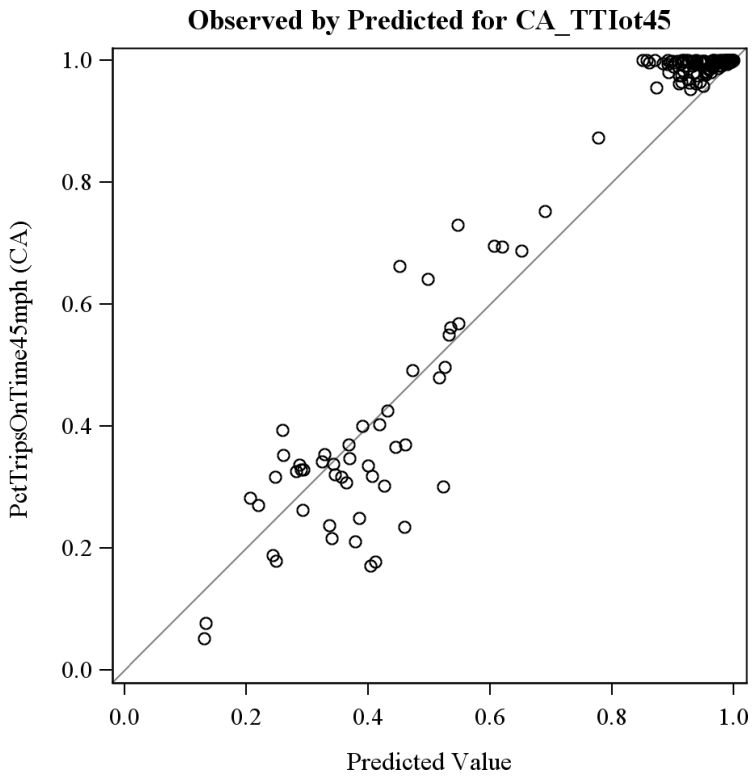

Figure E.103. Observed-by-predicted plot, recalibrated PctTripsOnTime45mph model, California.

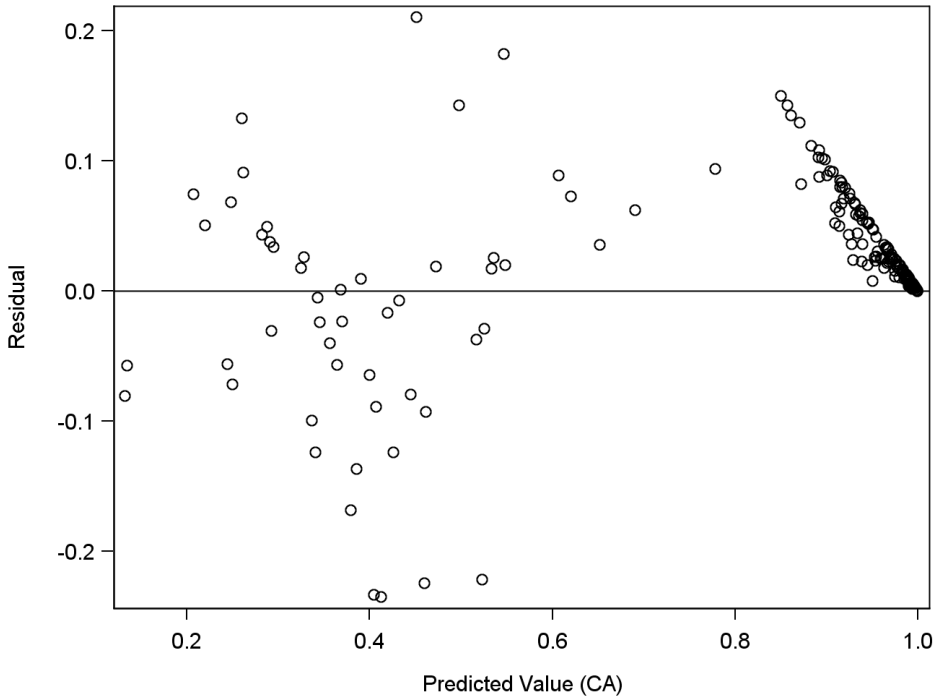

Figure E.104. Residual-by-predicted plot, recalibrated PctTripsOnTime45mph model, California.

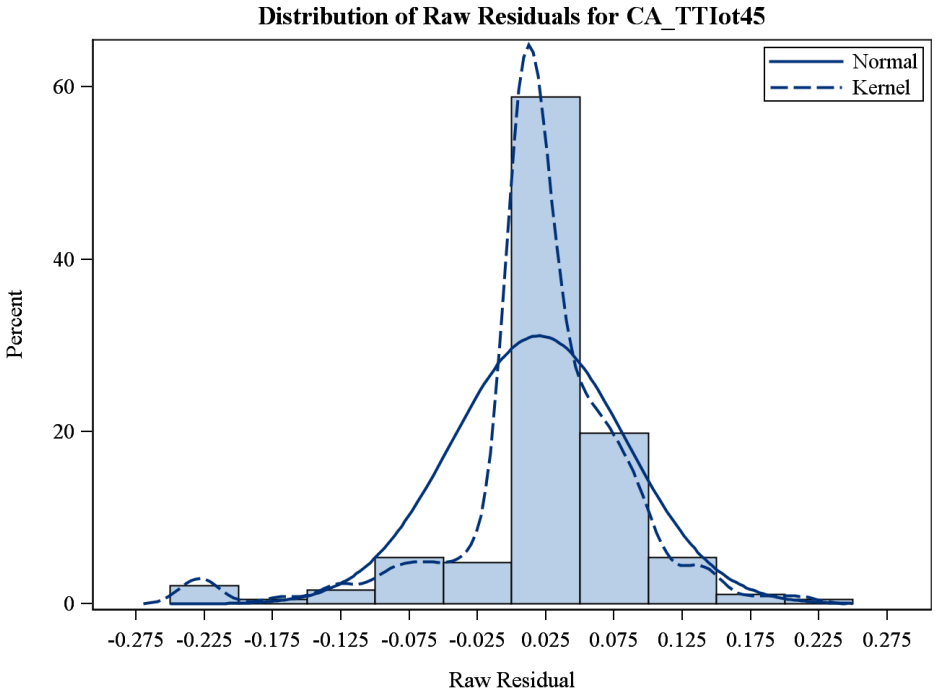

Figure E.105. Distribution of raw residuals, recalibrated PctTripsOnTime45mph model, California.

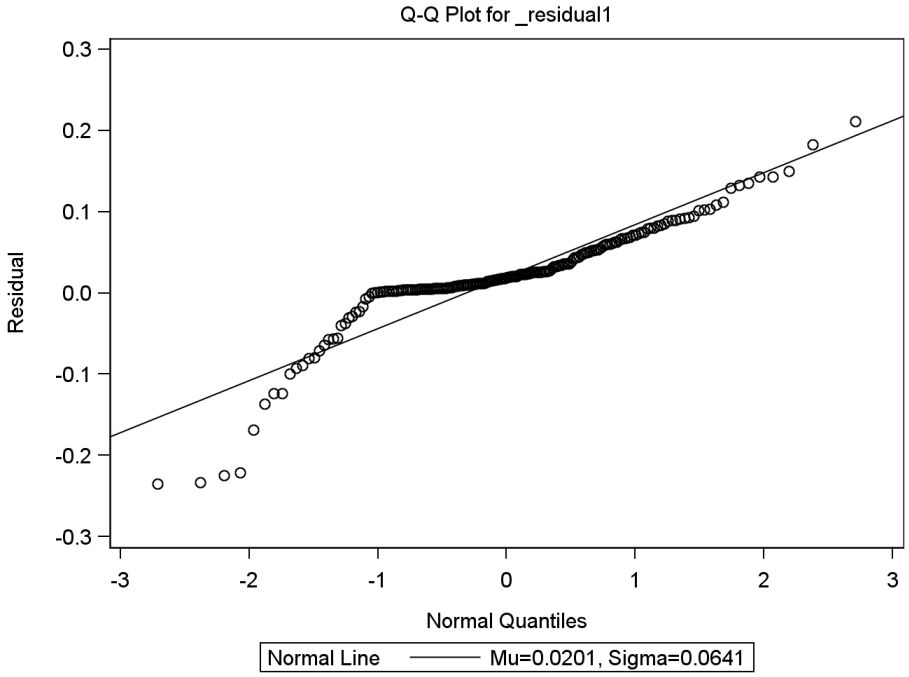

Figure E.106. Q-Q plot of residuals, recalibrated PctTripsOnTime45mph model, California.

Table E.44. Analysis of Variance, Recalibrated PctTripsOnTime45mph Model, Minnesota

Source	DF	Sum of Squares	Mean Square	*F*-Value	Approx. Pr > *F*
Model	1	61.7399	61.7399	50278.5	<0.0001
Error	78	0.0958	0.00123		
Uncorrected total	79	61.8357			

Table E.45. Parameter Estimates, Recalibrated PctTripsOnTime45mph Model, Minnesota

Parameter	Estimate	Approx. Std Error	Approx. 95% Confidence Limits	
a	–1.2568	0.0281	–1.3128	–1.2008

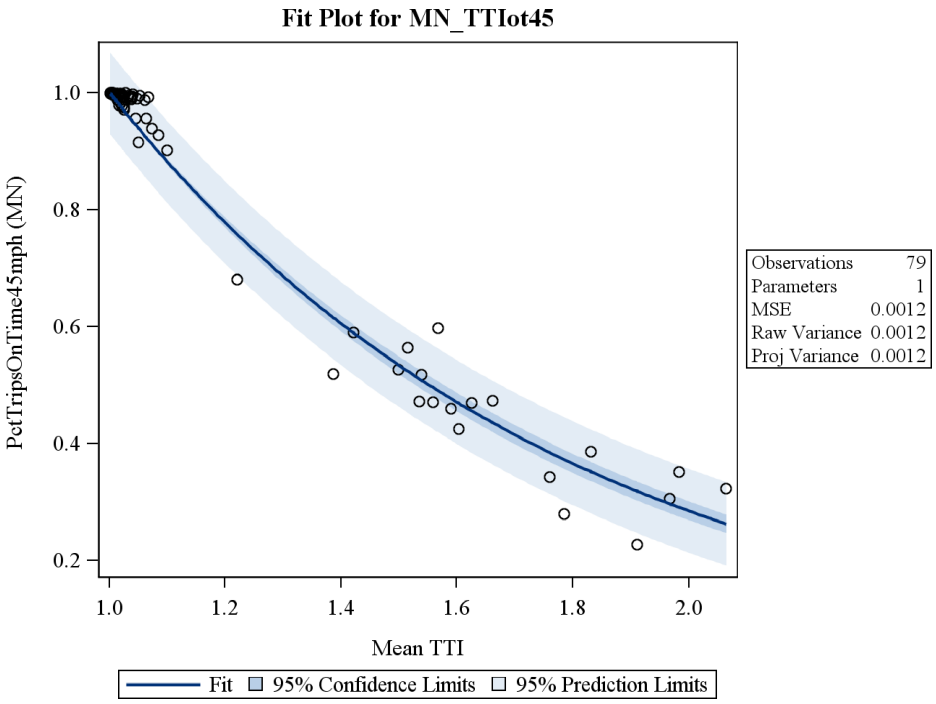

Figure E.107. Fit plot in original scale, recalibrated PctTripsOnTime45mph model, Minnesota.

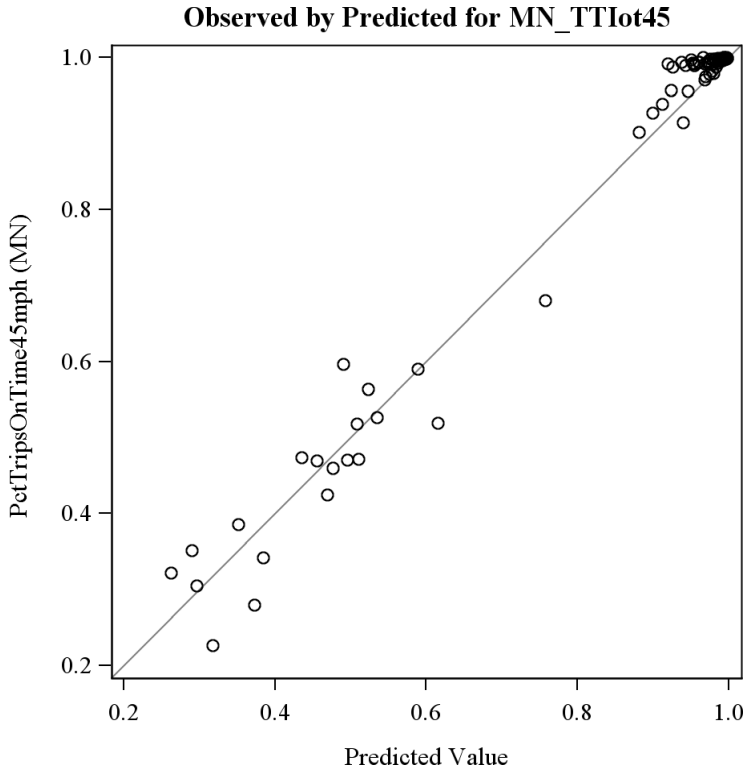

Figure E.108. Observed-by-predicted plot, recalibrated PctTripsOnTime45mph model, Minnesota.

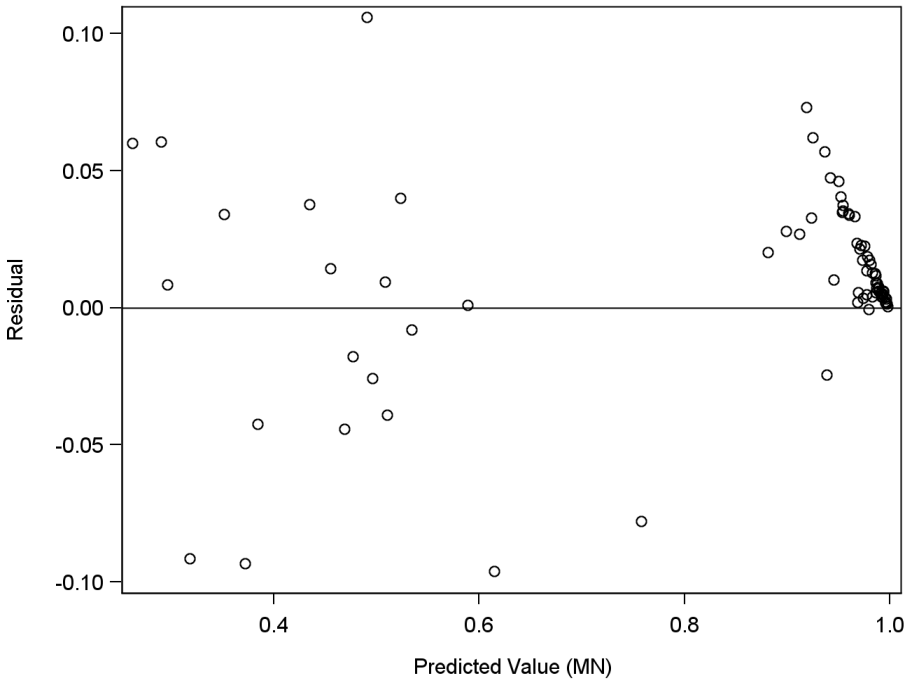

Figure E.109. Residual-by-predicted plot, recalibrated PctTripsOnTime45mph model, Minnesota.

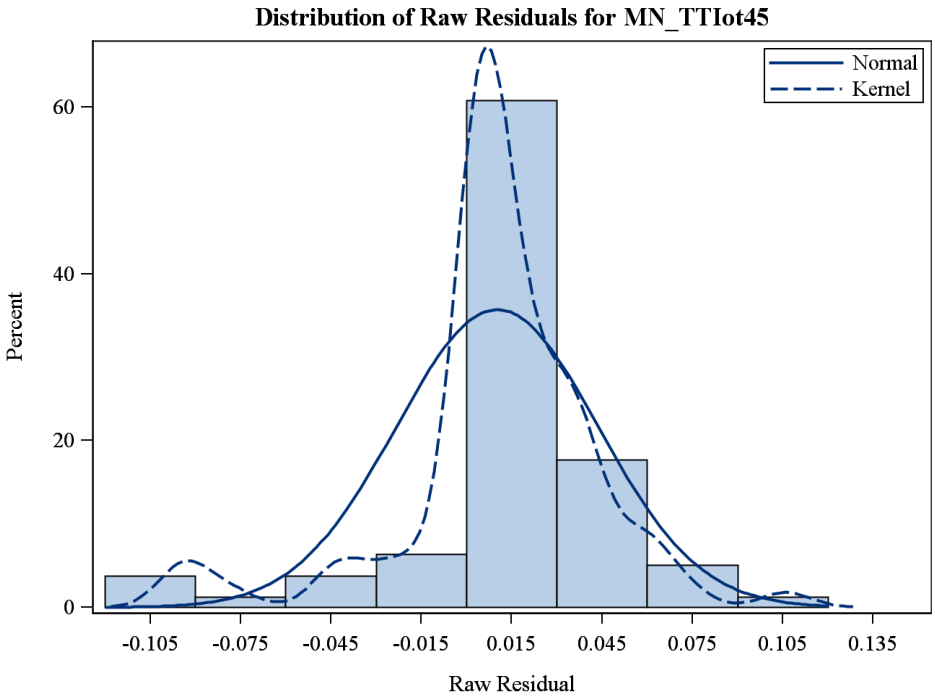

Figure E.110. Distribution of raw residuals, recalibrated PctTripsOnTime45mph model, Minnesota.

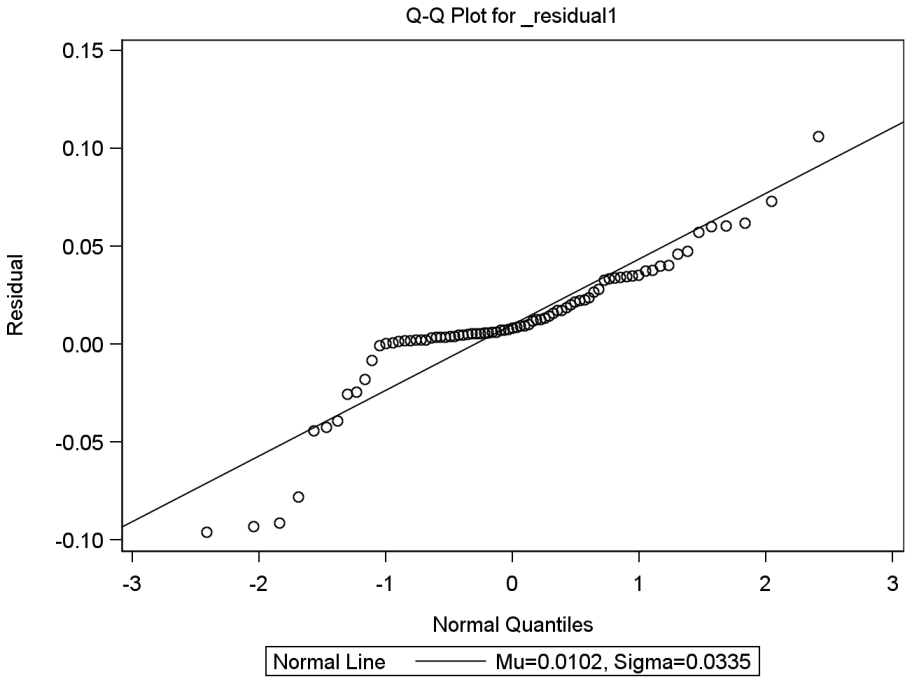

Figure E.111. Q-Q plot of residuals, recalibrated PctTripsOnTime45mph model, Minnesota.

PctTripsOnTime30mph

The recalibration of the PctTripsOnTime30mph model is conducted by building a nonlinear model between the response variable, PctTripsOnTime30mph, and the independent variable, mean TTI. The model form is the same as the L03 data-poor model form, described as

$$\text{PctTripsOnTime30mph} = a + \frac{b-a}{1+\exp(c*[\text{meanTTI}-d])}$$

where a, b, c, d are the four model parameters to be calibrated.

AllData

The recalibrated model for the PctTripsOnTime30mph with the AllData set is

$$\text{PctTripsOnTime30mph}_{\text{AllData}} = 0.3401 + \frac{0.6803}{1+\exp(4.5026*[\text{meanTTI}-1.7890])}$$

The *F*-test results (Table E.46) show that overall the model is significant. The parameter estimation is shown in Table E.47. The scatter plots (Figures E.112 through E.114) show that the model line can generally predict the trend in the data, indicating that the model is satisfactory in general. The residual plot (Figure E.115) presents a general random scatter, except for the slight nonconstant variance pattern on the right side of the figure. The histogram and the normality plot (Figures E.116 and E.117) show that the residual distribution does not closely follow a normal distribution, which may largely be due to the disproportional number of residuals close to zero.

Table E.46. Analysis of Variance, Recalibrated PctTripsOnTime30mph Model, AllData

Source	DF	Sum of Squares	Mean Square	*F*-Value	Approx. Pr > *F*
Model	3	3.8334	1.2778	2396.81	<0.0001
Error	319	0.1701	0.000533		
Corrected total	322	4.0035			

Table E.47. Parameter Estimates, Recalibrated PctTripsOnTime30mph Model, AllData

Parameter	Estimate	Approx. Std Error	Approx. 95% Confidence Limits	
a	0.3401	0.0312	0.2787	0.4016
b	0.6803	0.0343	0.6129	0.7478
c	4.5026	0.2817	3.9485	5.0568
d	1.7890	0.0221	1.8324	1.7455

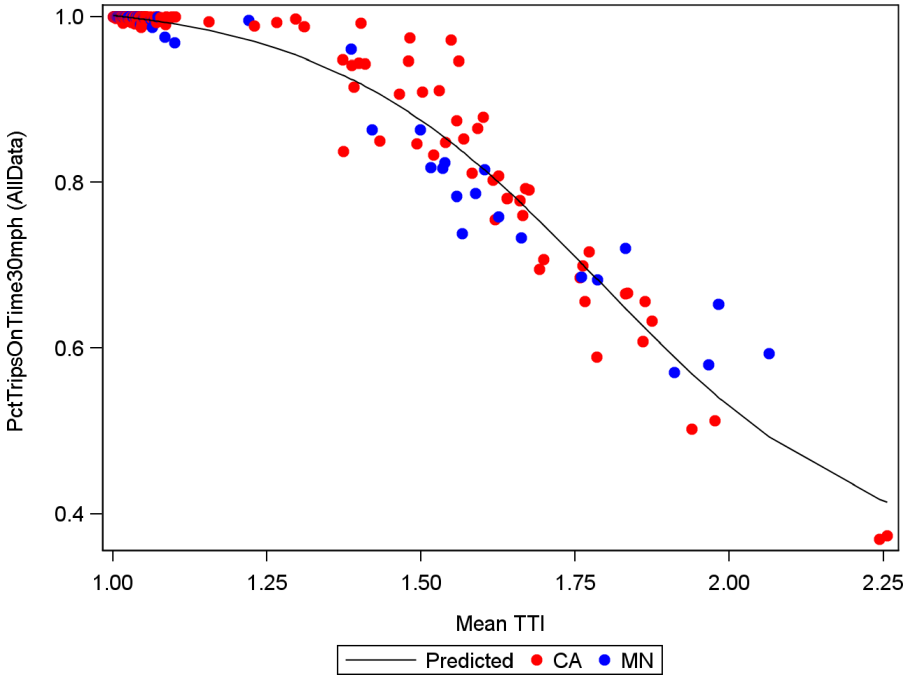

Figure E.112. Scatter plot in original scale, recalibrated PctTripsOnTime30mph model, AllData.

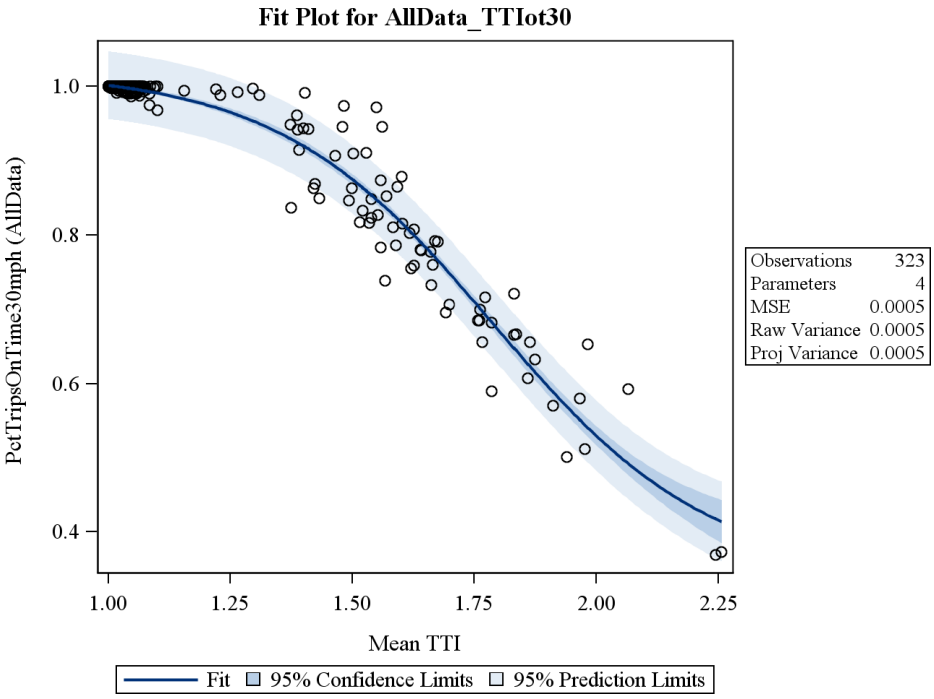

Figure E.113. Fit plot in original scale, recalibrated PctTripsOnTime30mph model, AllData.

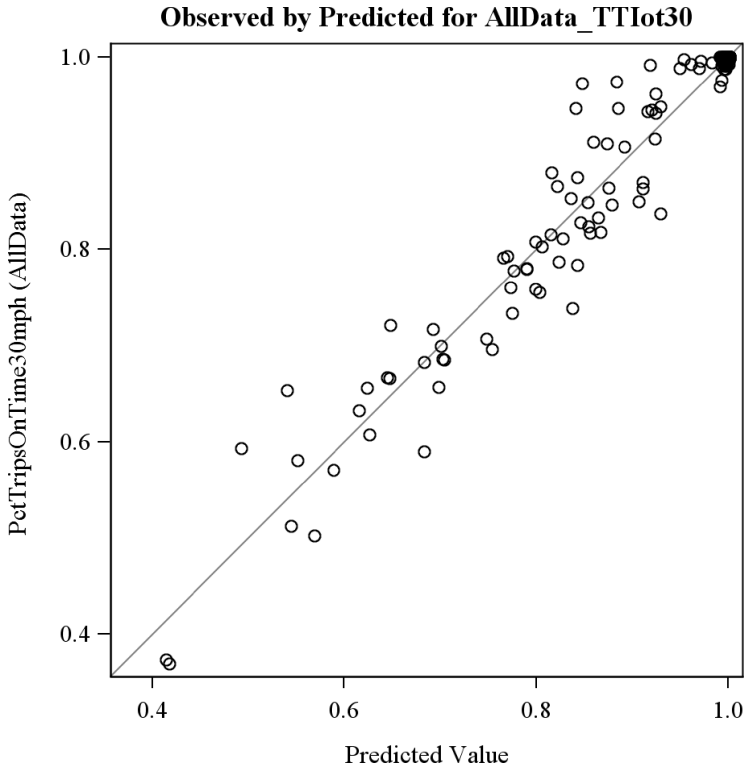

Figure E.114. Observed-by-predicted plot, recalibrated PctTripsOnTime30mph model, AllData.

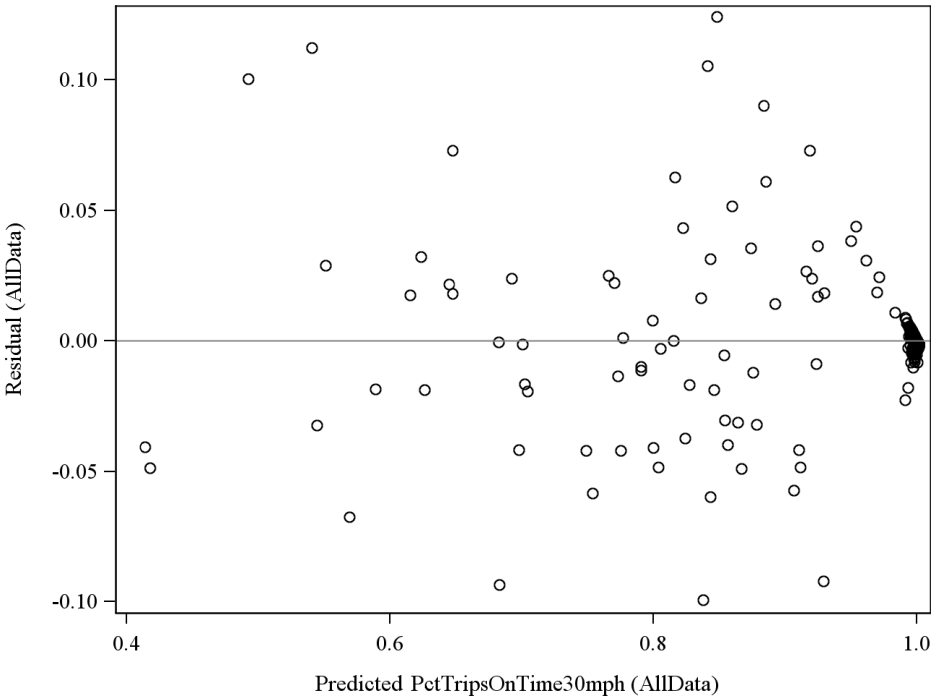

Figure E.115. Residual-by-predicted plot, recalibrated PctTripsOnTime30mph model, AllData.

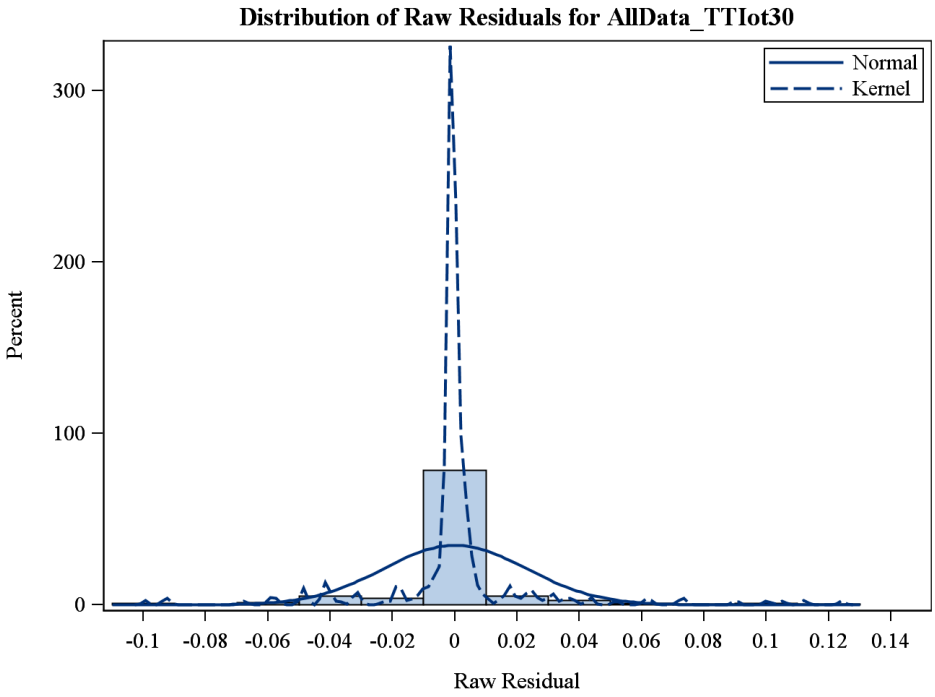

Figure E.116. Distribution of raw residuals, recalibrated PctTripsOnTime30mph model, AllData.

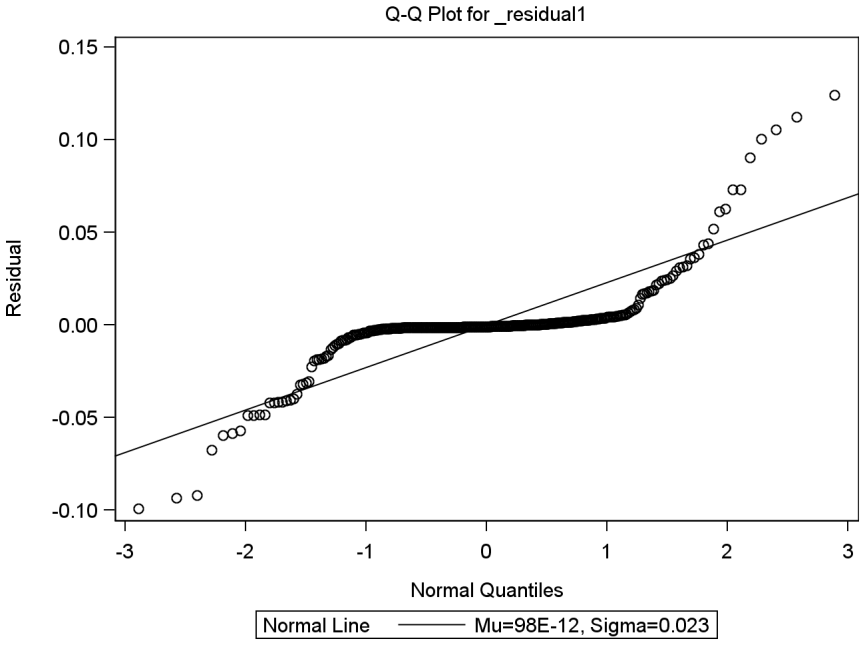

Figure E.117. Q-Q plot of residuals, recalibrated PctTripsOnTime30mph model, AllData.

California

The recalibrated model for the PctTripsOnTime30mph with the CA set is

$$\text{PctTripsOnTime30mph}_{CA} = 0.3263 + \frac{0.6827}{1+\exp(5.4915 * [\text{meanTTI} - 1.7916])}$$

The *F*-test (Table E.48) has a small *p*-value, indicating that overall the model is valid. The parameter estimates are shown in Table E.49. The fit plot (Figure E.118) and the measured-by-predicted plot (Figure E.119) confirm that the model can predict the trend in the data samples. The residual-by-predicted plot (Figure E.120) presents a random pattern in general. The histogram and the normality plot (Figures E.121 and E.122) show that the residual distribution does not closely follow a normal distribution.

Minnesota

The recalibrated model for the PctTripsOnTime30mph with the MN set is

$$\text{PctTripsOnTime30mph}_{MN} = 0.5795 + \frac{0.4341}{1+\exp(6.1112 * [\text{meanTTI} - 1.5715])}$$

The *F*-test (Table E.50) has a small *p*-value, indicating that overall the model is valid. The parameter estimates are shown in Table E.51. The fit plot (Figure E.123) and the measured-by-predicted plot (Figure E.124) confirm that the model can predict the trend in the data samples, resulting in the random pattern in the residual-by-predicted plot (Figure E.125) although the nonconstant variance problem may still slightly exist (Figures E.126 and E.127).

(text continues on page 292)

Table E.48. Analysis of Variance, Recalibrated PctTripsOnTime30mph Model, California

Source	DF	Sum of Squares	Mean Square	*F*-Value	Approx. Pr > *F*
Model	3	2.6242	0.8747	1744.94	<0.0001
Error	183	0.0917	0.000501		
Corrected total	186	2.7159			

Table E.49. Parameter Estimates, Recalibrated PctTripsOnTime30mph Model, California

Parameter	Estimate	Approx. Std Error	Approx. 95% Confidence Limits	
a	0.3263	0.0248	0.2774	0.3752
b	0.6827	0.0263	0.6307	0.7346
c	5.4915	0.2995	4.9005	6.0824
d	1.7916	0.0157	1.8226	1.7605

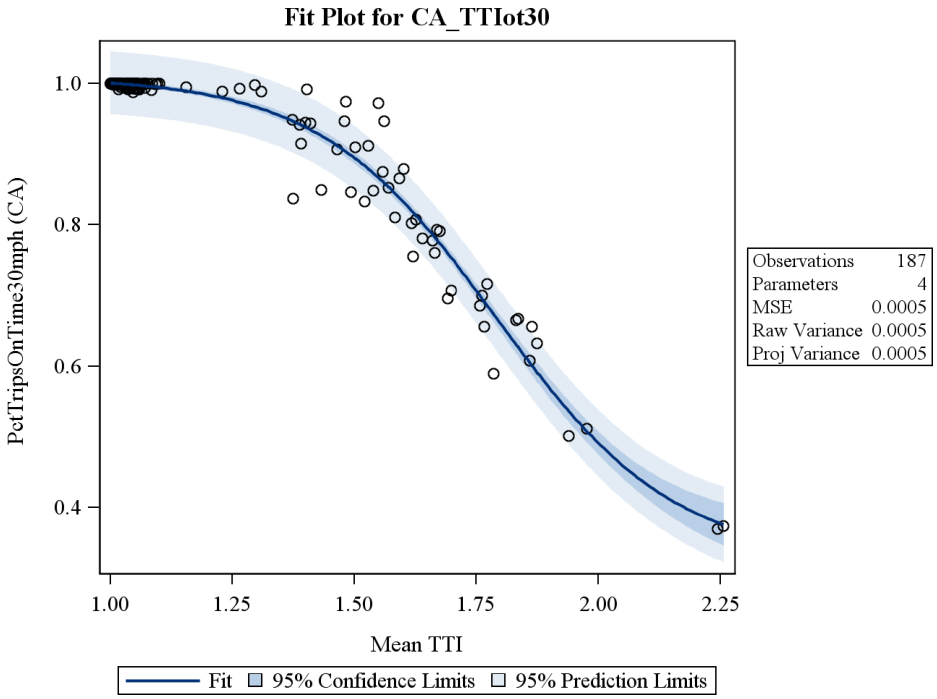

Figure E.118. Fit plot in original scale, recalibrated PctTripsOnTime30mph model, California.

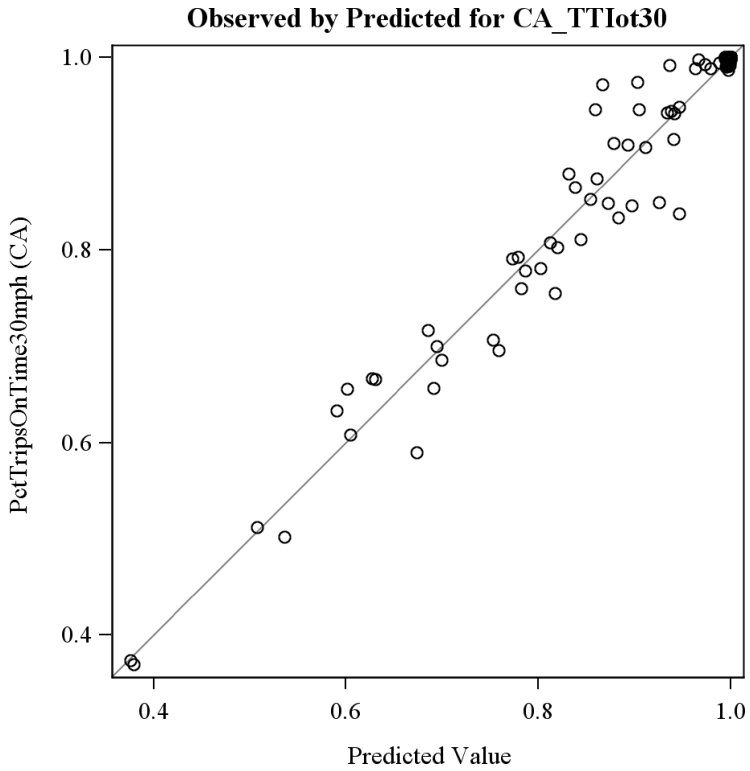

Figure E.119. Observed-by-predicted plot, recalibrated PctTripsOnTime30mph model, California.

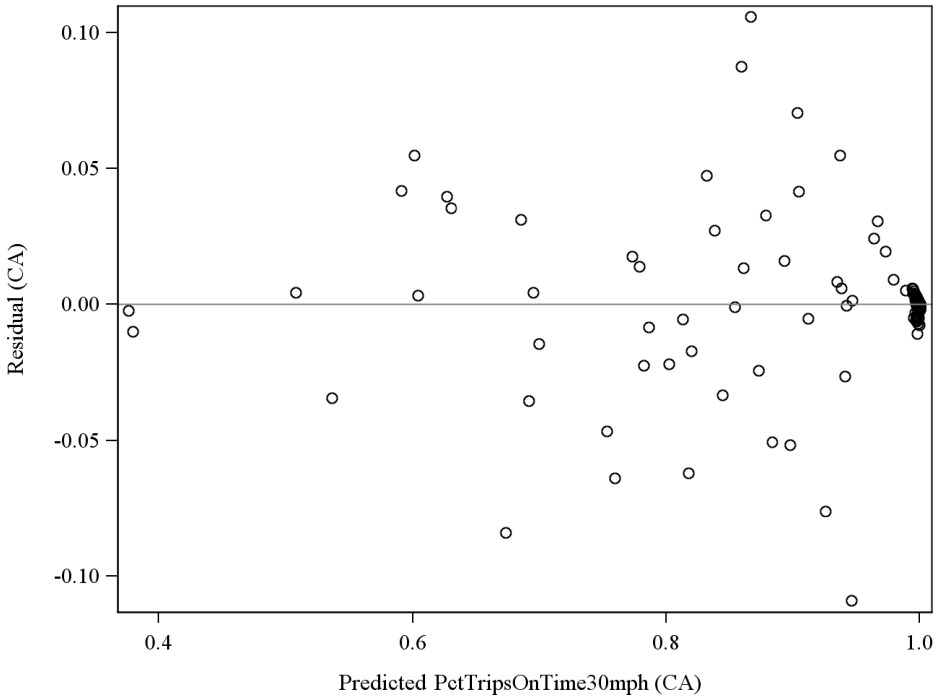

Figure E.120. Residual-by-predicted plot, recalibrated PctTripsOnTime30mph model, California.

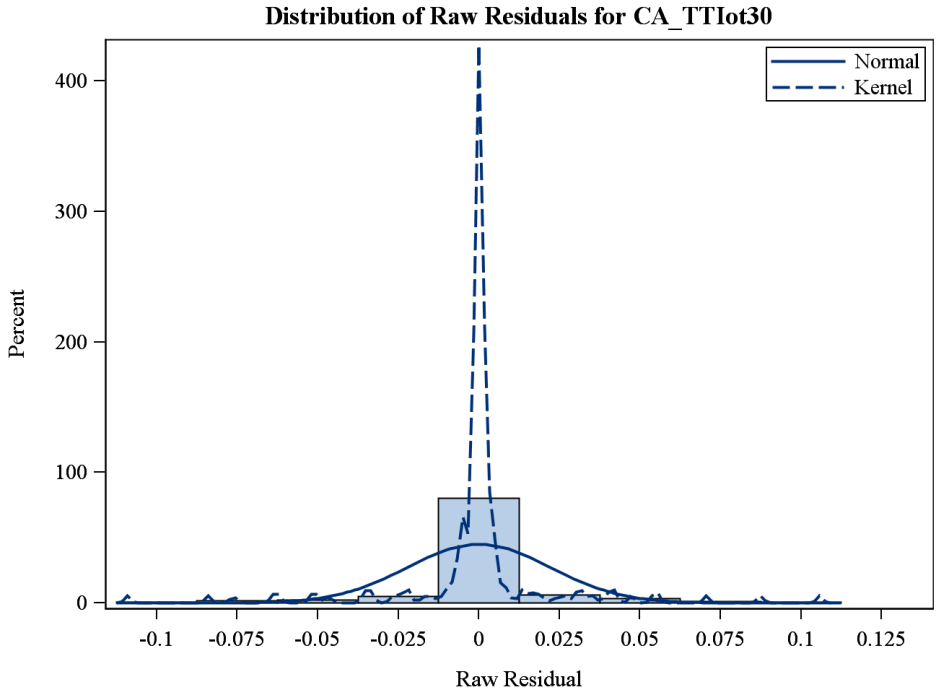

Figure E.121. Distribution of raw residuals, recalibrated PctTripsOnTime30mph model, California.

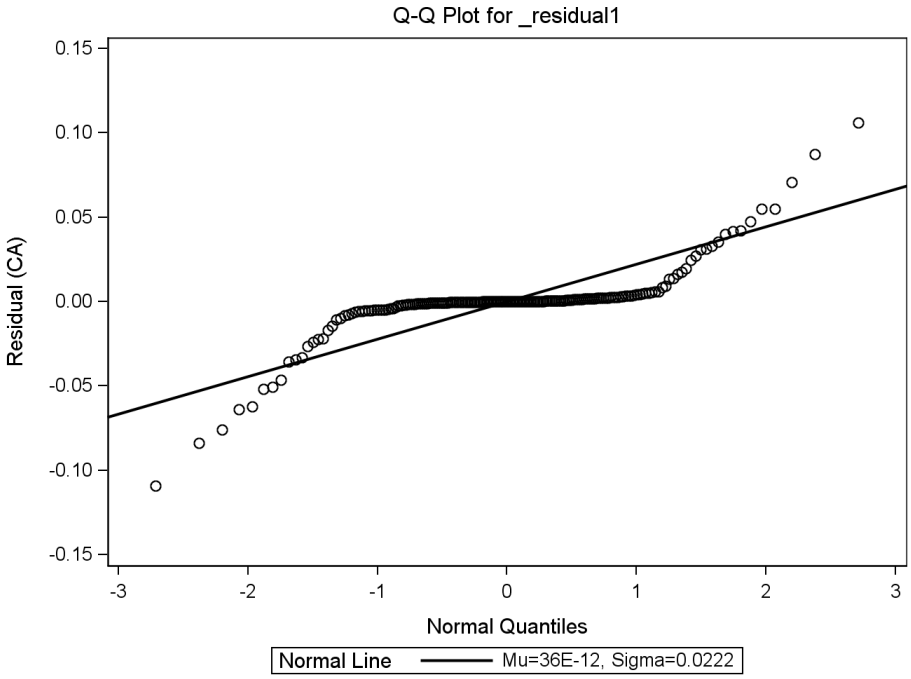

Figure E.122. Q-Q plot of residuals, recalibrated PctTripsOnTime30mph model, California.

Table E.50. Analysis of Variance, Recalibrated PctTripsOnTime30mph Model, Minnesota

Source	DF	Sum of Squares	Mean Square	*F*-Value	Approx. Pr > *F*
Model	3	1.0652	0.3551	1168.55	<0.0001
Error	75	0.0228	0.000304		
Corrected total	78	1.0880			

Table E.51. Parameter Estimates, Recalibrated PctTripsOnTime30mph Model, Minnesota

Parameter	Estimate	Approx. Std Error	Approx. 95% Confidence Limits	
a	0.5795	0.0191	0.5414	0.6175
b	0.4341	0.0247	0.3850	0.4833
c	6.1112	0.7944	4.5287	7.6937
d	1.5715	0.0157	1.6028	1.5402

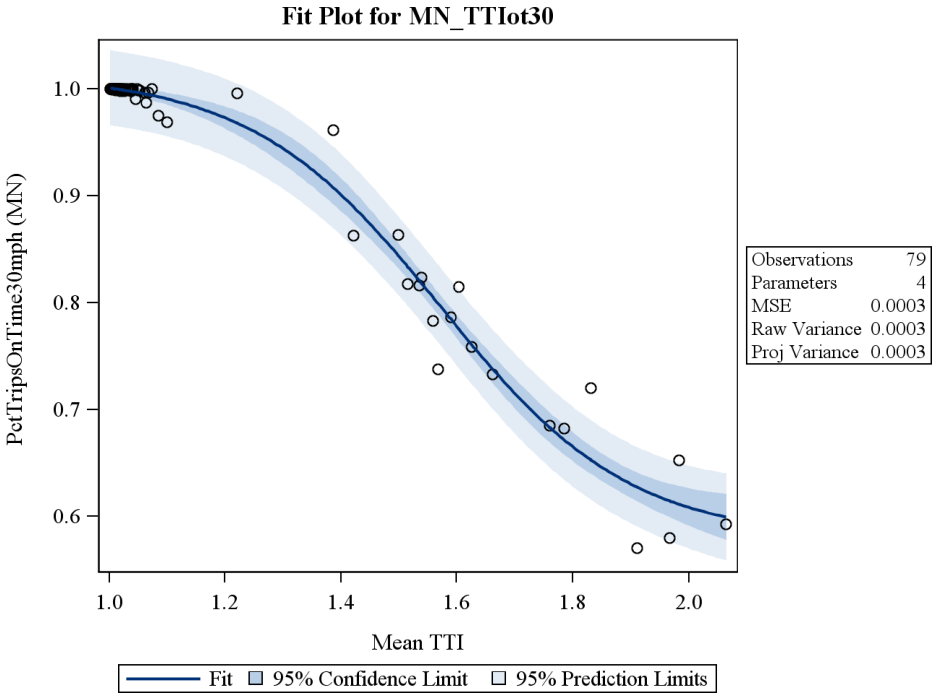

Figure E.123. Fit plot in original scale, recalibrated PctTripsOnTime30mph model, Minnesota.

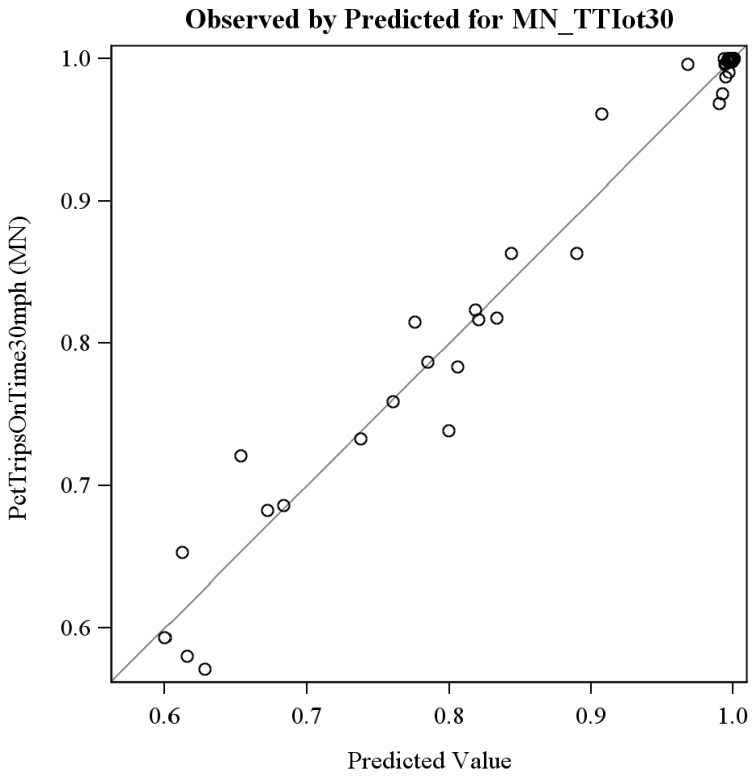

Figure E.124. Observed-by-predicted plot, recalibrated PctTripsOnTime30mph model, Minnesota.

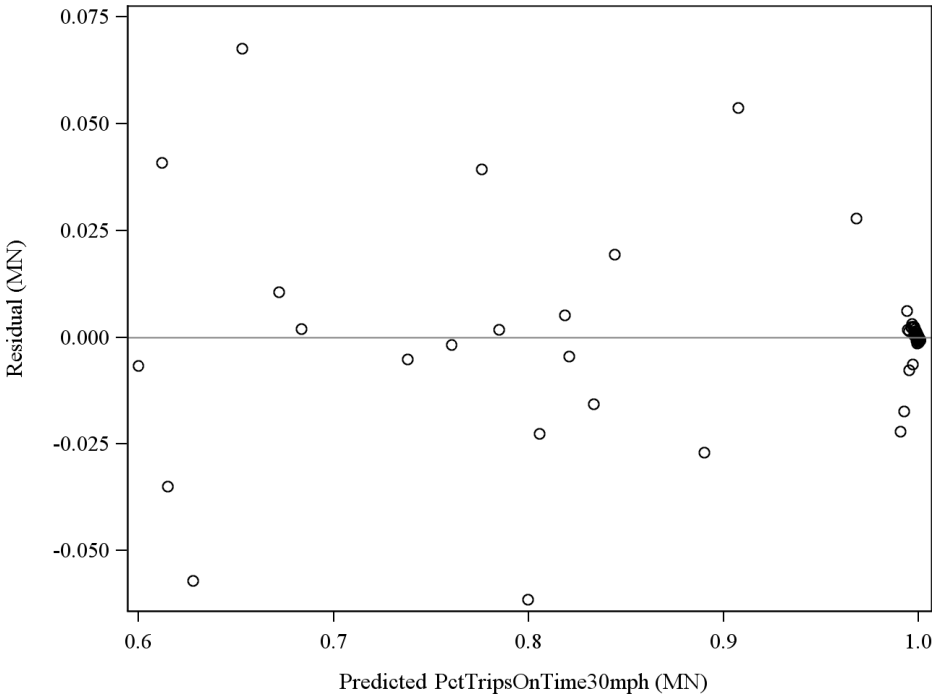

Figure E.125. Residual-by-predicted plot, recalibrated PctTripsOnTime30mph model, Minnesota.

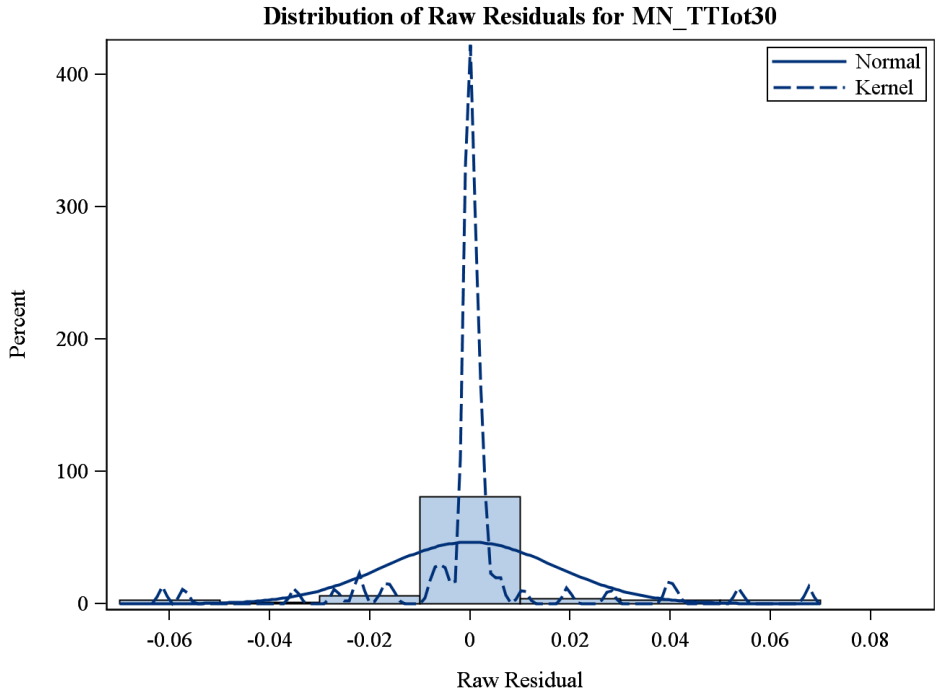

Figure E.126. Distribution of raw residuals, recalibrated PctTripsOnTime30mph model, Minnesota.

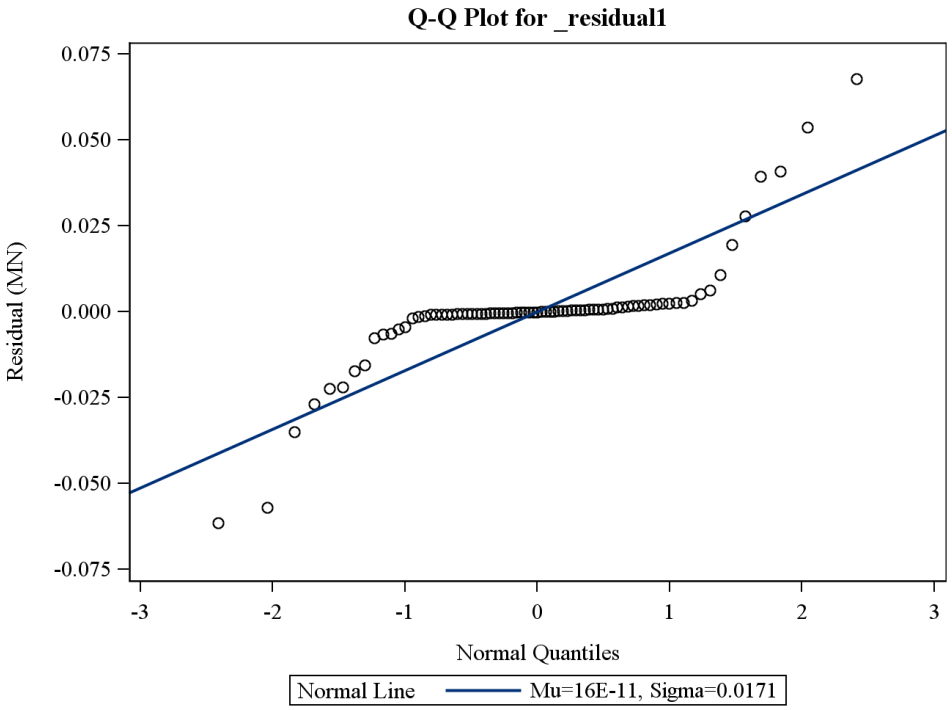

Figure E.127. Q-Q plot of residuals, recalibrated PctTripsOnTime30mph model, Minnesota.

New Models

This chapter presents the results of the new model development for the 95th-, 90th-, and 80th-percentile TTI SHRP 2 L03 models. The new model development was performed on three of the L33 data sets: California, Minnesota, and AllData (representing roadway sections in both CA and MN). Three enhanced models were developed: (1) a single-parameter power form model; (2) a two-parameter power form model; and (3) a two-parameter polynomial model. For each of the measures, this appendix contains a summary table of the mean square error (MSE) for the recalibrated model and the three new models. Note that all modeling results in this chapter are built on a reduced data set that excludes two outlier samples. As such, the MSE values for the recalibration models shown in this chapter may be different from those presented in the previous chapter. The new models show the most significant improvements for the 80th-percentile TTI model and the least improvement for the 95th-percentile TTI model. Based on the results of the data-poor recalibration and enhancement, the L33 project team recommends that the SHRP 2 program recommend the new models for adoption. This recommendation is based on the following reasons:

1. The residual-by-predicted value plot shows improvement in the shape and in the balance of scatter around the origin, indicating that the new models better satisfy the assumptions of regression. Note that there is still a problem with the nonconstant variance that, due to data characteristics, may not be possible to fully solve.
2. The new models allow for a consistent model form between different percentile TTI measures.
3. Since the variance of travel times tends to increase with the mean travel time, reliability model curves should show an increasing pattern at an increasing rate. The new models satisfy this characteristic in a way that the original L03 data-poor models (which show a decreasing rate of increase) do not.

95th-Percentile TTI

Summary

The MSE summary table (Table E.52) shows that the recalibrated 95th-percentile TTI model has a smaller MSE value than the new models. However, due to the reasons stated above and the fact that the MSE values are similar between the recalibrated and new models, we still propose that the SHRP 2 program adopt the new models.

When evaluating the MSE tables, it is important to keep in mind that there is no benchmark to decide how much smaller

Table E.52. MSE Summary Table (Comparable)

Model Name	Formula	AllData	CA	MN
Recalibration	$y = 1 + a * \ln(x)$	0.0277	0.0255	0.0234
1-parameter power	$y = x^b$	0.0300	0.0273	0.0408
2-parameter power	$y = a * x^b$	0.0286	0.0264	0.0345
2-parameter polynomial	$y = a * x + b * x^2$	0.0289	0.0268	0.0352

of an MSE makes the model better. In this case, due to the fact that the validation data sets have a relatively small range in the mean TTI, each of the four types of models has predictive power. However, the research team believes the new models are more consistent with professional knowledge and real world experience.

The following three sections present the new models built for the 95th-percentile TTI with the AllData (Tables E.54, E.56, and E.58), CA (Tables E.60, E.62, and E.64), and MN (Tables E.66, E.68, and E.70) data sets. The three models present very similar results in terms of fit plot (Figures E.128, E.129, E.134, E.135, E.140, E.141, E.146, E.151, E.156, E.161, E.166, and E.171) and residual-by-predicted plot (Figures E.131, E.137, E.143, E.148, E.153, E.158, E.163, E.168, and E.173). Regional differences can be identified in the plots. All the models passed the *F*-test (Tables E.53, E.55, E.57, E.59, E.61, E.63, E.65, E.67, and E.69), indicating overall validity. The fit plots and the observed-by-predicted plots (Figures E.130, E.136, E.142, E.147, E.152, E.157, E.162, E.167, and E.172) show that the model can predict the trend in the data set. The residual-by-predicted plots show an improvement in the nonrandom pattern around the origin, although the nonconstant variance problem still exists. The histograms (Figures E.132, E.138, E.144, E.149, E.154, E.159, E.164, E.169, and E.174) and the normality plots (Figures E.133, E.139, E.145, E.150, E.155, E.160, E.165, E.170 and E.175) indicate that the normality assumption may still be violated. Due to the validation data characteristics, the nonconstant variance problem and the violation of normality problem may be hard to get rid of.

The MN modeling results raise a questionable pattern because the residual-by-predicted plots for all three new model forms show an unbalanced distribution of residual points and a concave shape. In fact, the original data-poor model for the 95th-percentile TTI model fits better. However, such results may be due to insufficient data points. Although the MN data set has 79 samples, most of them are around the origin area (low mean TTI and high reliability). To make the model form consistent, the team still proposes adopting the three new model forms.

AllData

Power Form Model with a Single Parameter

Model:

$$95\text{th-percentile TTI}_{\text{AllData}} = \text{meanTTI}^{1.9566}$$

Power Form Model with Two Parameters

Model:

$$95\text{th-percentile TTI}_{\text{AllData}} = 1.0406 * \text{meanTTI}^{1.8821}$$

Polynomial Form Model with Two Parameters

Model:

$$95\text{th-percentile TTI}_{\text{AllData}} = 1.1494 * \text{meanTTI} + 0.8902 * \text{meanTTI}^2$$

(text continues on page 304)

Table E.53. Analysis of Variance, New Model: Power Form with a Single Parameter, 95th-Percentile TTI, AllData

Source	DF	Sum of Squares	Mean Square	*F*-Value	Approx. Pr > *F*
Model	1	793.5	793.5	26492.1	<0.0001
Error	320	9.5845	0.0300		
Uncorrected total	321	803.1			

Table E.54. Parameter Estimates, New Model: Power Form with a Single Parameter, 95th-Percentile TTI, AllData

Parameter	Estimate	Approx. Std Error	Approx. 95% Confidence Limits	
b	1.9566	0.0146	1.9279	1.9853

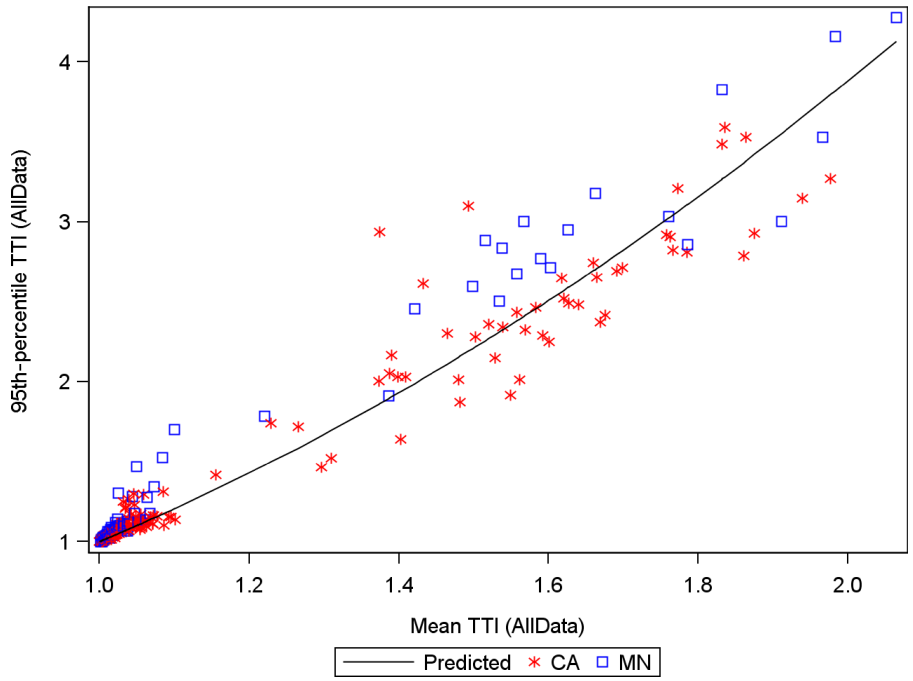

Figure E.128. Fit plot by region, new model: power form with a single parameter, 95th-percentile TTI, AllData.

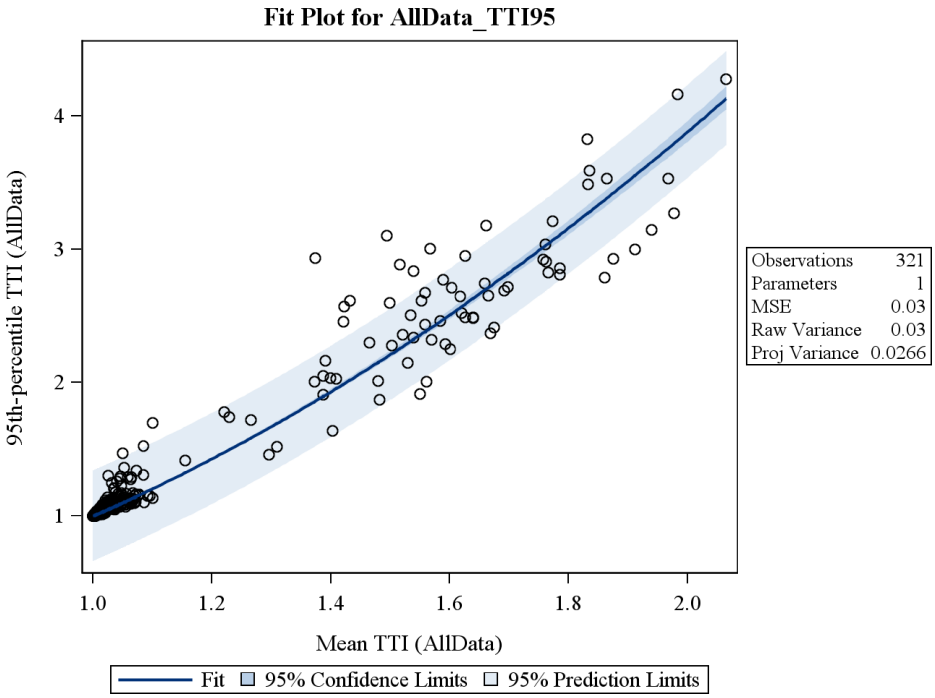

Figure E.129. Fit plot, new model: power form with a single parameter, 95th-percentile TTI, AllData.

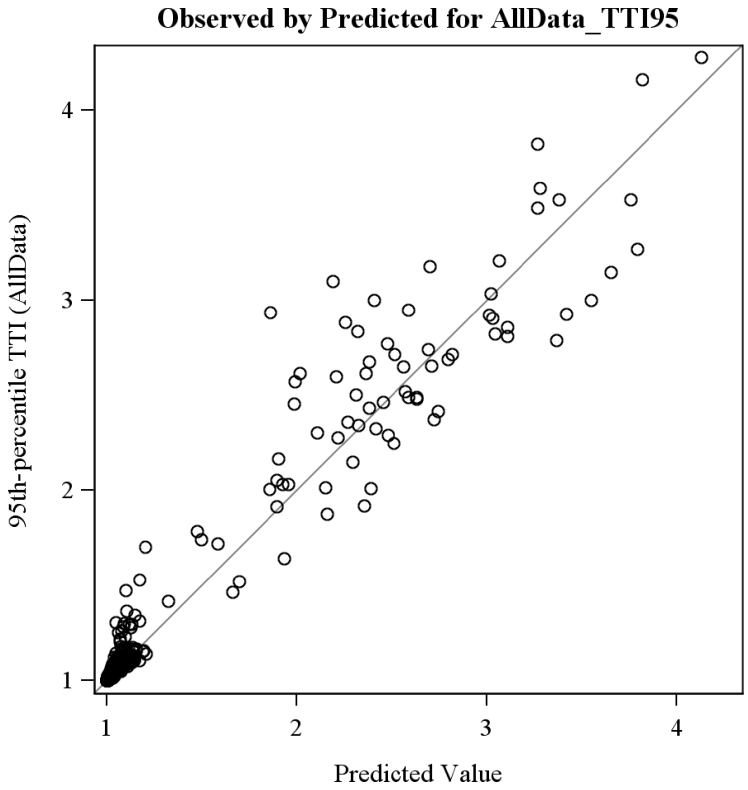

Figure E.130. Observed-by-predicted plot, new model: power form with a single parameter, 95th-percentile TTI, AllData.

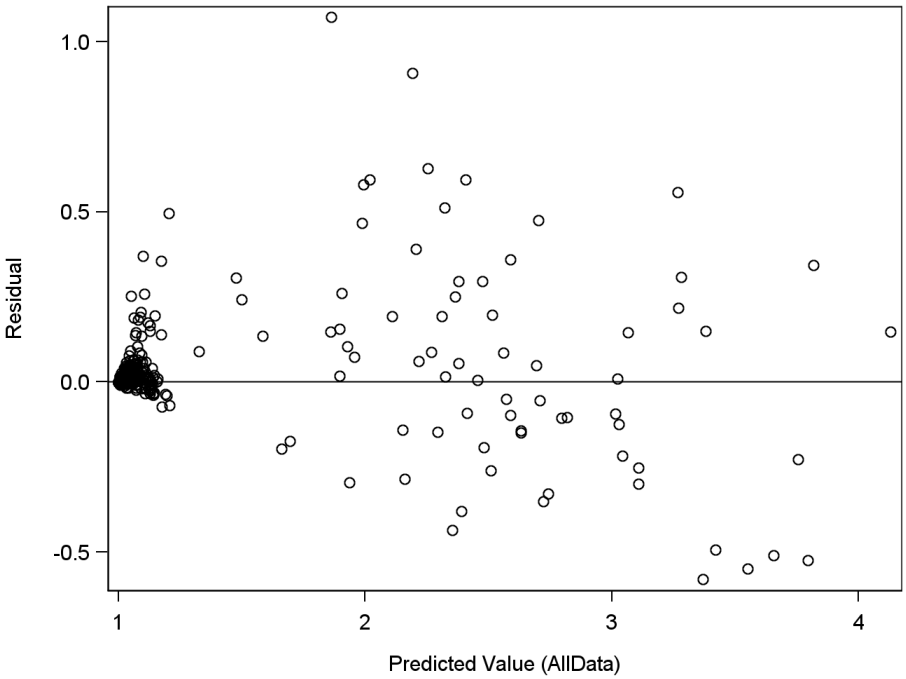

Figure E.131. Residual-by-predicted plot, new model: power form with a single parameter, 95th-percentile TTI, AllData.

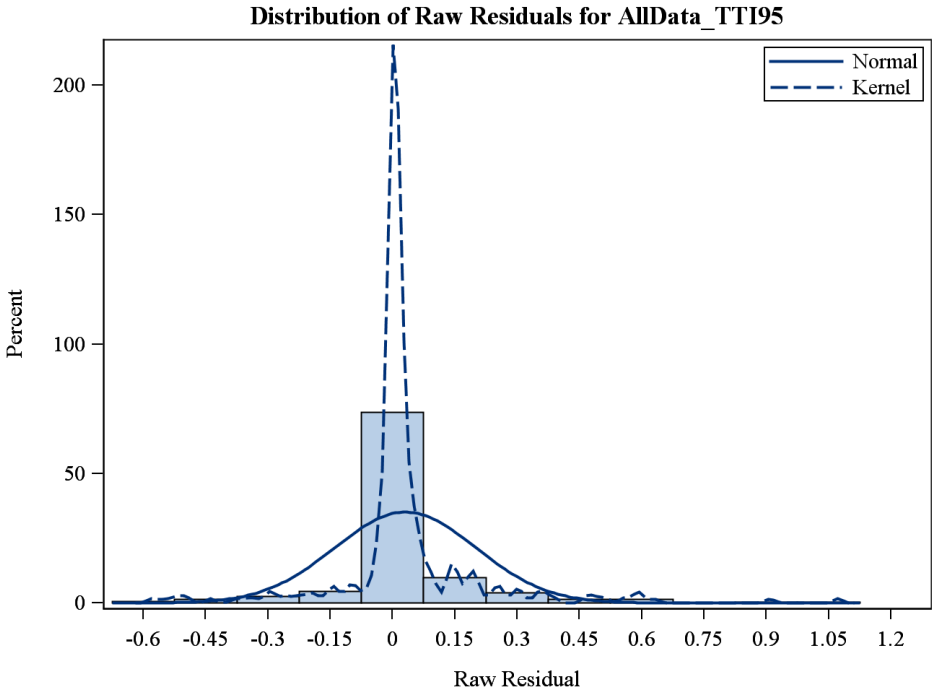

Figure E.132. Distribution of residuals, new model: power form with a single parameter, 95th-percentile TTI, AllData.

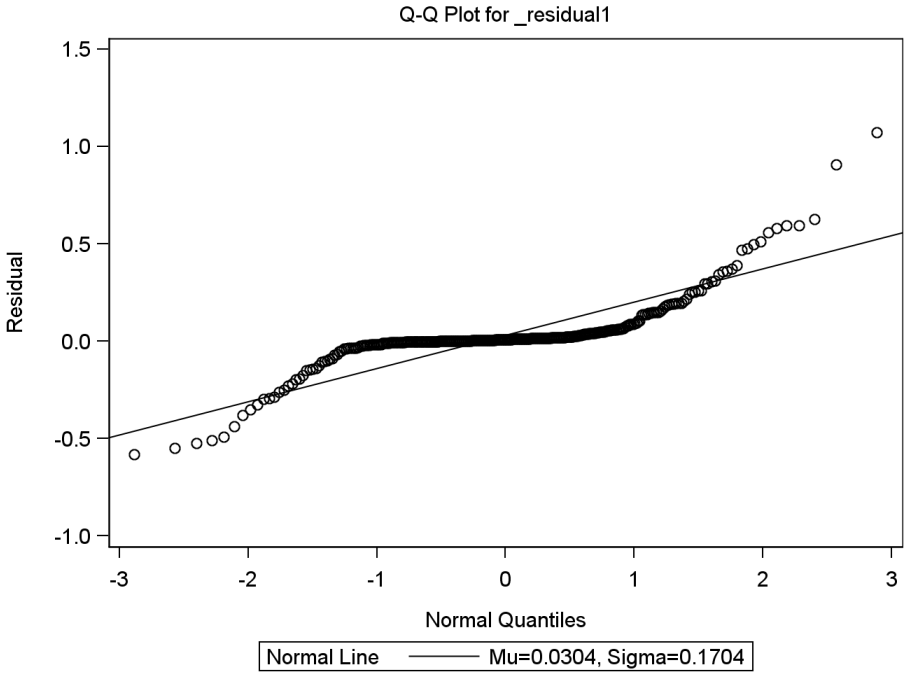

Figure E.133. Q-Q plot of residuals, new model: power form with a single parameter, 95th-percentile TTI, AllData.

Table E.55. Analysis of Variance, New Model: Power Form with Two Parameters, 95th-Percentile TTI, AllData

Source	DF	Sum of Squares	Mean Square	*F*-Value	Approx. Pr > *F*
Model	2	793.9	397.0	13865.6	<0.0001
Error	319	9.1328	0.0286		
Uncorrected total	321	803.1			

Table E.56. Parameter Estimates, New Model: Power Form with Two Parameters, 95th-Percentile TTI, AllData

Parameter	Estimate	Approx. Std Error	Approx. 95% Confidence Limits	
a	1.0406	0.0103	1.0203	1.0609
b	1.8821	0.0236	1.8358	1.9285

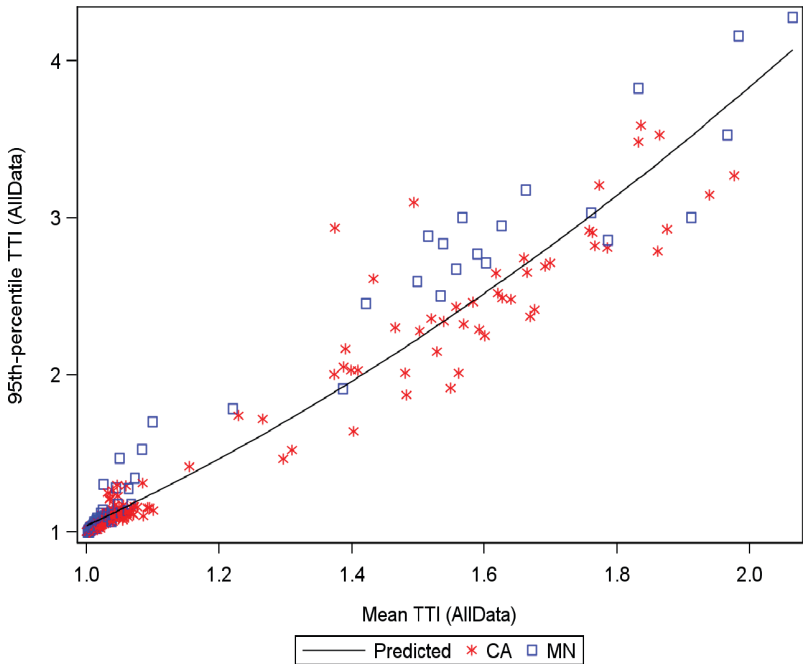

Figure E.134. Fit plot by region, new model: power form with two parameters, 95th-percentile TTI, AllData.

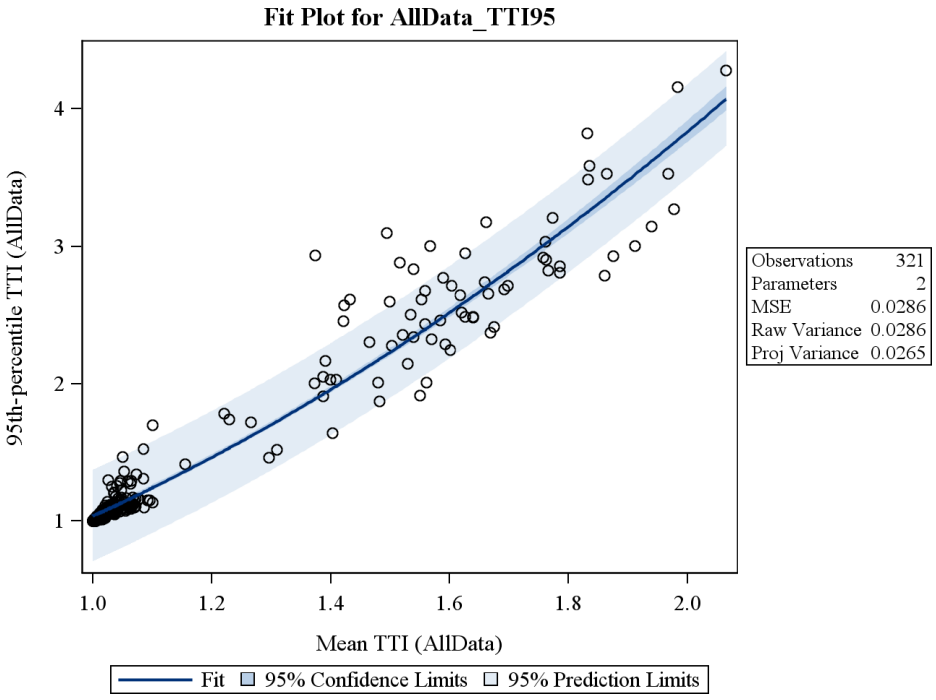

Figure E.135. Fit plot, new model: power form with two parameters, 95th-percentile TTI, AllData.

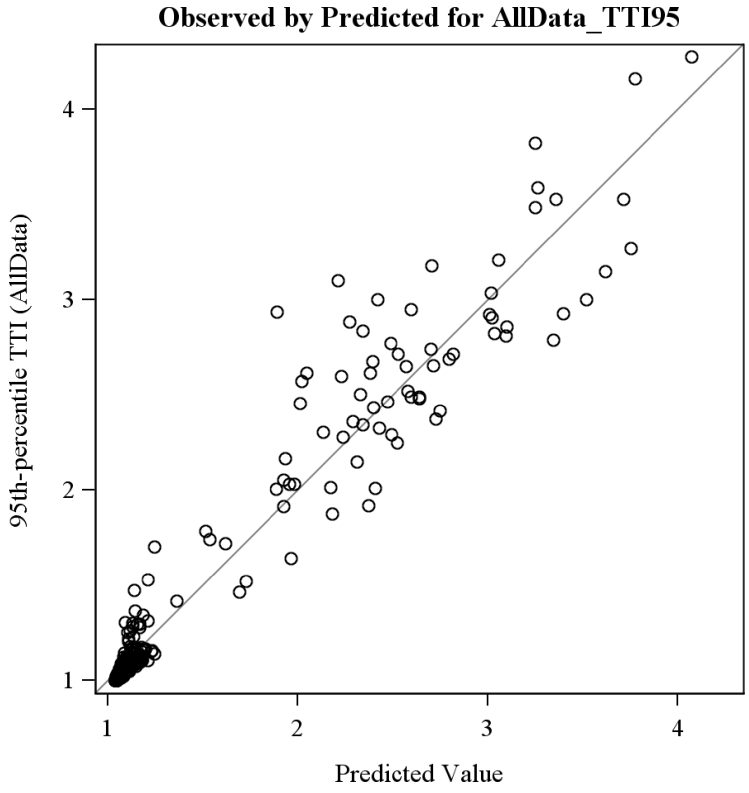

Figure E.136. Observed-by-predicted plot, new model: power form with two parameters, 95th-percentile TTI, AllData.

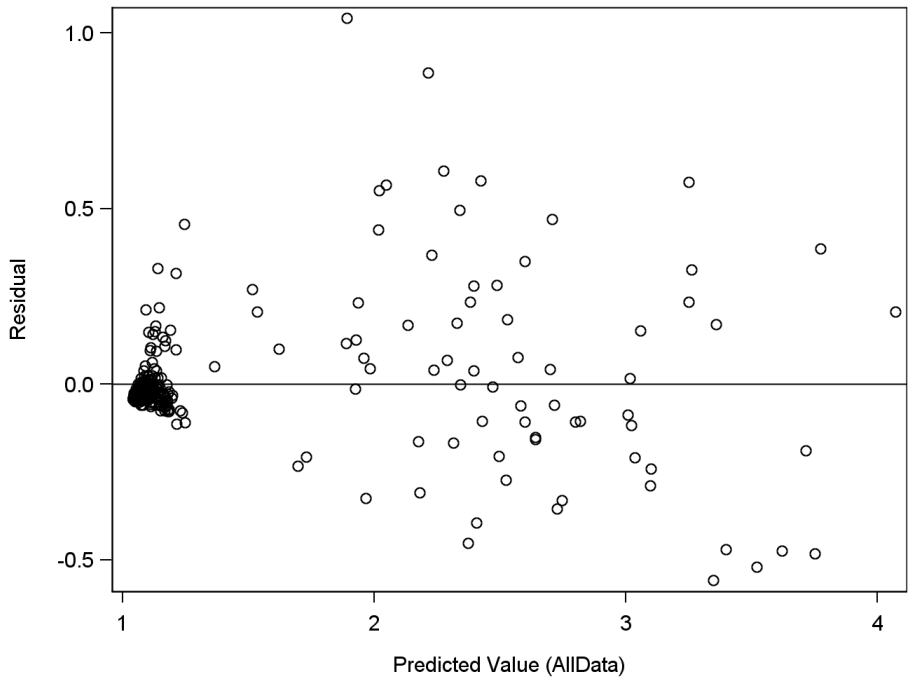

Figure E.137. Residual-by-predicted plot, new model: power form with two parameters, 95th-percentile TTI, AllData.

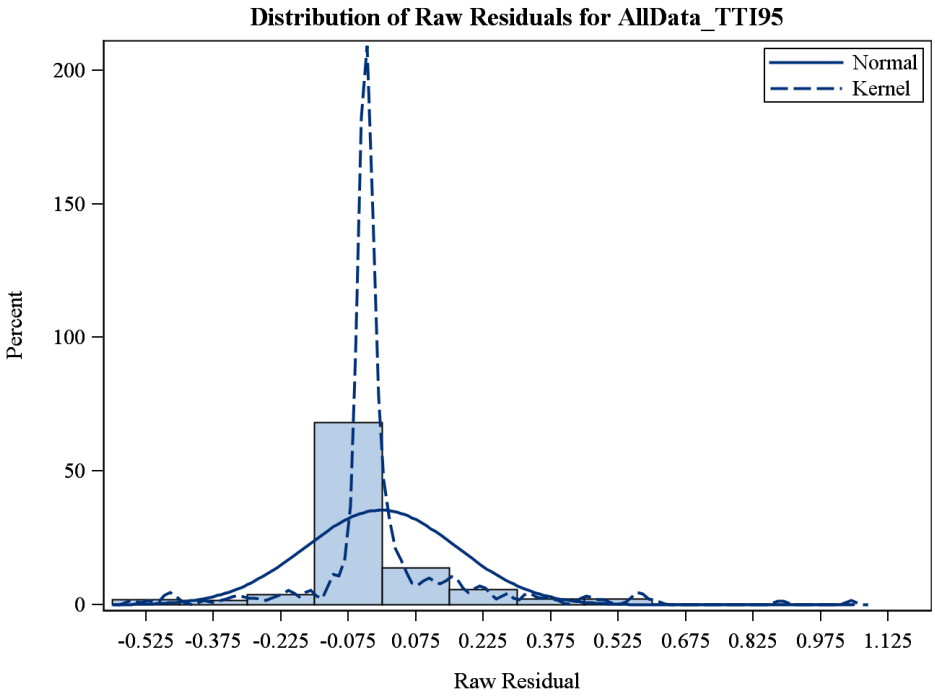

Figure E.138. Distribution of residuals, new model: power form with two parameters, 95th-percentile TTI, AllData.

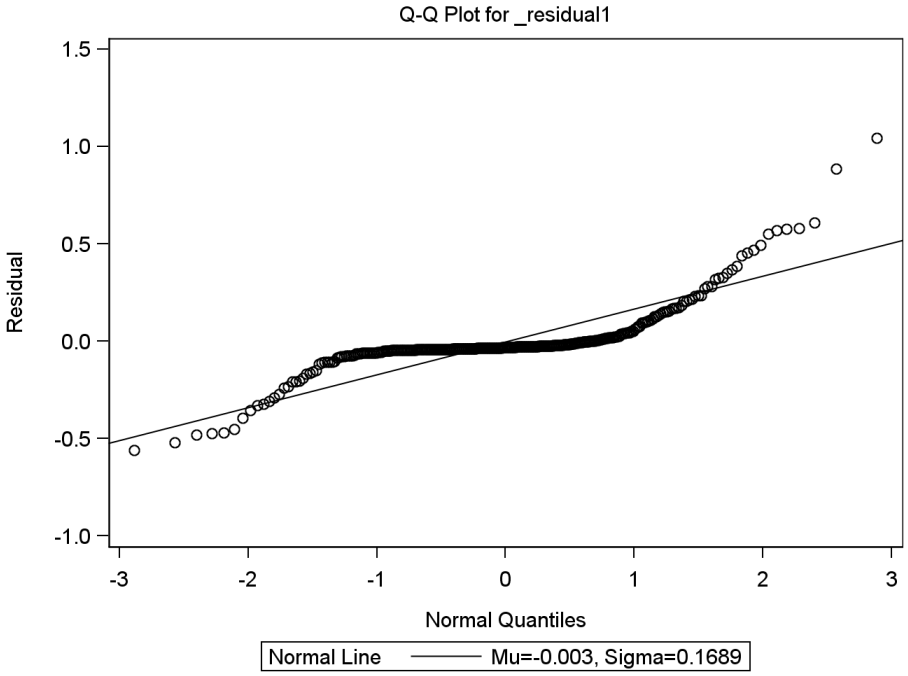

Figure E.139. Q-Q plot of residuals, new model: power form with two parameters, 95th-percentile TTI, AllData.

Table E.57. Analysis of Variance, New Model: Polynomial Form with Two Parameters, 95th-Percentile TTI, AllData

Source	DF	Sum of Squares	Mean Square	*F*-Value	Approx. Pr > *F*
Model	2	793.8	396.9	13716.8	<0.0001
Error	319	9.2308	0.0289		
Uncorrected total	321	803.1			

Table E.58. Parameter Estimates, New Model: Polynomial Form with Two Parameters, 95th-Percentile TTI, AllData

Parameter	Estimate	Approx. Std Error	Approx. 95% Confidence Limits	
a	0.1494	0.0321	0.0862	0.2125
b	0.8902	0.0241	0.8427	0.9378

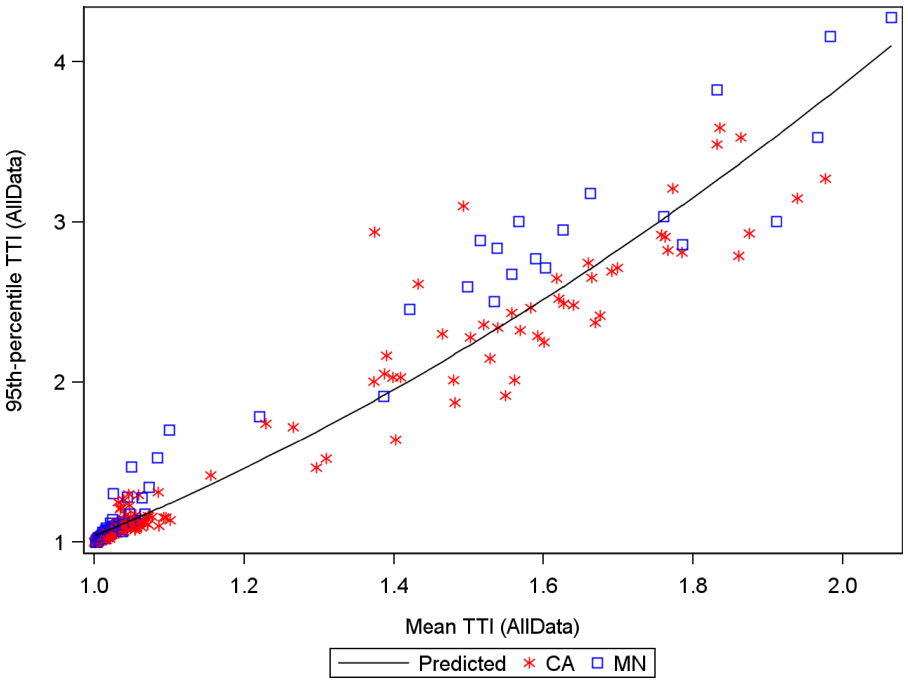

Figure E.140. Fit plot by region, new model: polynomial form with two parameters, 95th-percentile TTI, AllData.

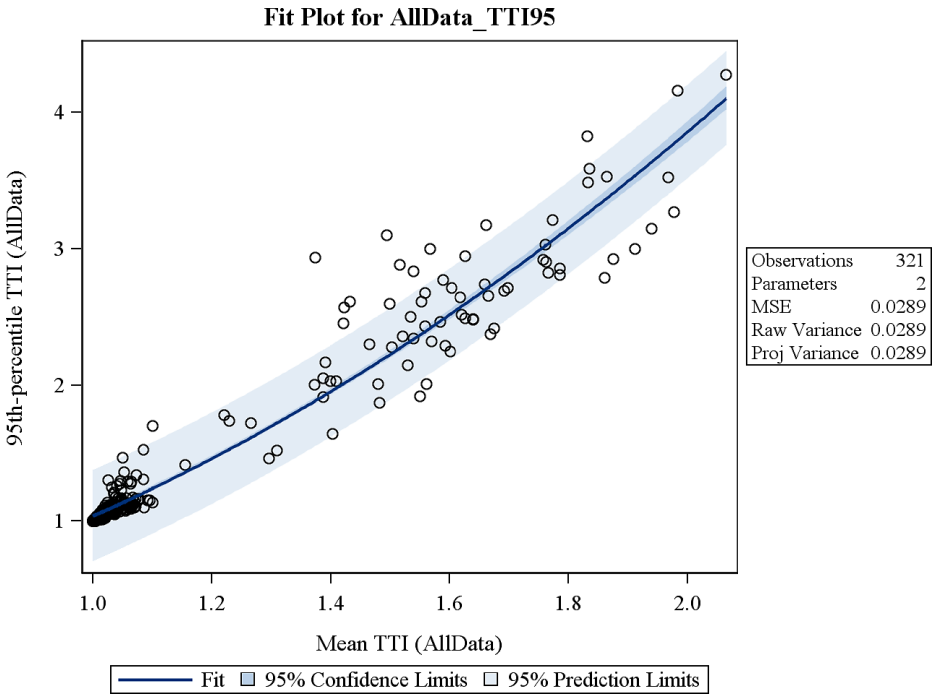

Figure E.141. Fit plot, new model: polynomial form with two parameters, 95th-percentile TTI, AllData.

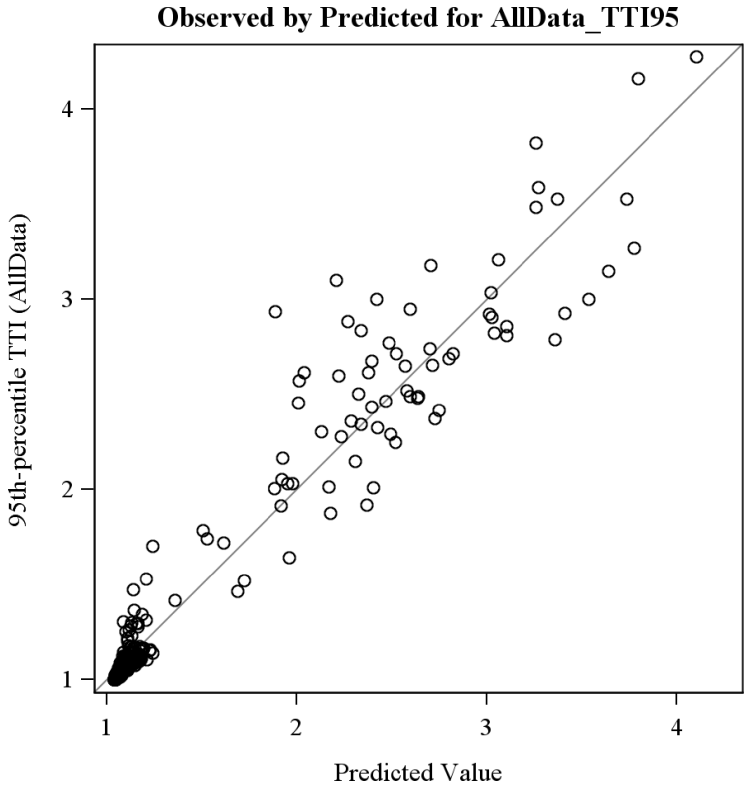

Figure E.142. Observed-by-predicted plot, new model: polynomial form with two parameters, 95th-percentile TTI, AllData.

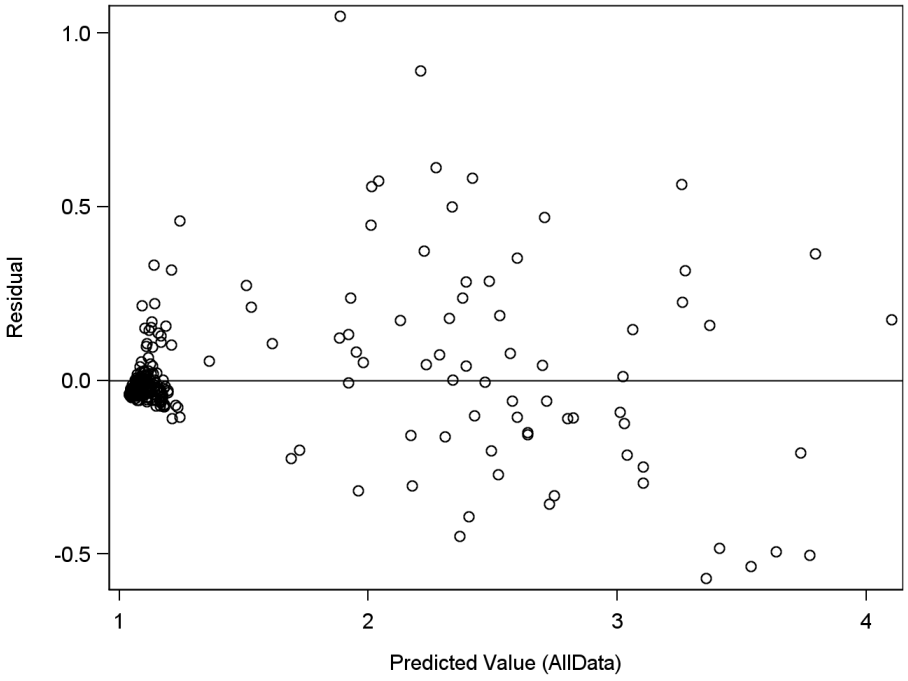

Figure E.143. Residual-by-predicted plot, new model: polynomial form with two parameters, 95th-percentile TTI, AllData.

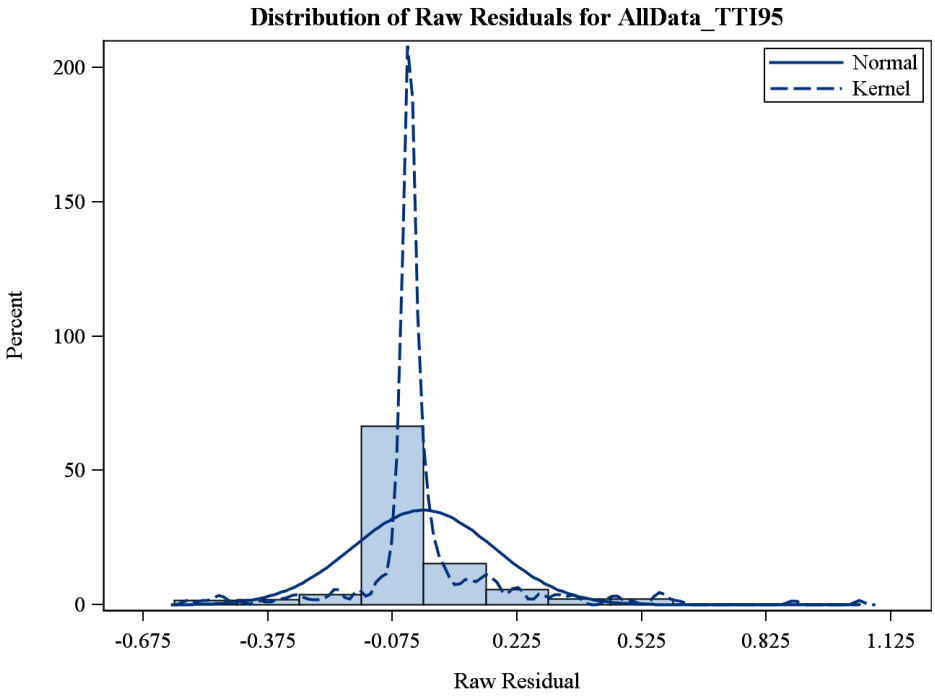

Figure E.144. Distribution of residuals, new model: polynomial form with two parameters, 95th-percentile TTI, AllData.

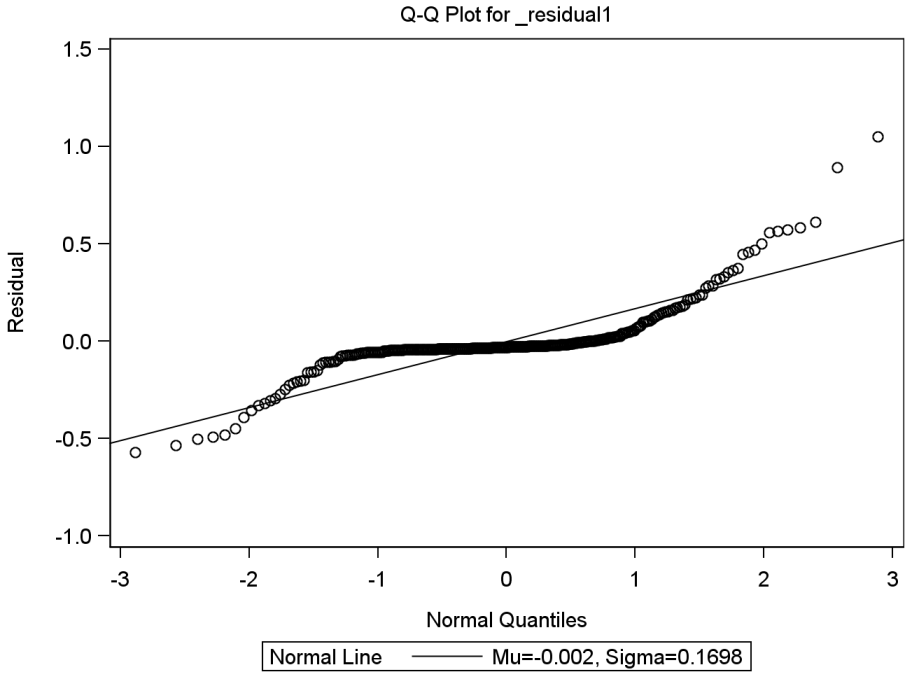

Figure E.145. Q-Q plot of residuals, new model: polynomial form with two parameters, 95th-percentile TTI, AllData.

California

Power Form Model with a Single Parameter

Model:

$$95\text{th-percentile TTI}_{CA} = \text{meanTTI}^{1.8922}$$

Power Form Model with Two Parameters

Model:

$$95\text{th-percentile TTI}_{CA} = 1.0363 * \text{meanTTI}^{1.8232}$$

Polynomial Form Model with Two Parameters

Model:

$$95\text{th-percentile TTI}_{CA} = 0.2245 * \text{meanTTI} + 0.8119 * \text{meanTTI}^2$$

Minnesota

Power Form Model with a Single Parameter

Model:

$$95\text{th-percentile TTI}_{MN} = \text{meanTTI}^{2.0516}$$

Power Form Model with Two Parameters

Model:

$$95\text{th-percentile TTI}_{MN} = 1.0871 * \text{meanTTI}^{1.9081}$$

Table E.59. Analysis of Variance, New Model: Power Form with a Single Parameter, 95th-Percentile TTI, California

Source	DF	Sum of Squares	Mean Square	*F*-Value	Approx. Pr > *F*
Model	1	464.4	464.4	16991.0	<0.0001
Error	184	5.0293	0.0273		
Uncorrected total	185	469.4			

Table E.60. Parameter Estimates, New Model: Power Form with a Single Parameter, 95th-Percentile TTI, California

Parameter	Estimate	Approx. Std Error	Approx. 95% Confidence Limits	
b	1.8922	0.0184	1.8559	1.9285

Polynomial Form Model with Two Parameters

Model:

$$95\text{th-percentile TTI}_{MN} = 0.1122 * \text{meanTTI} + 0.9701 * \text{meanTTI}^2$$

(text continues on page 322)

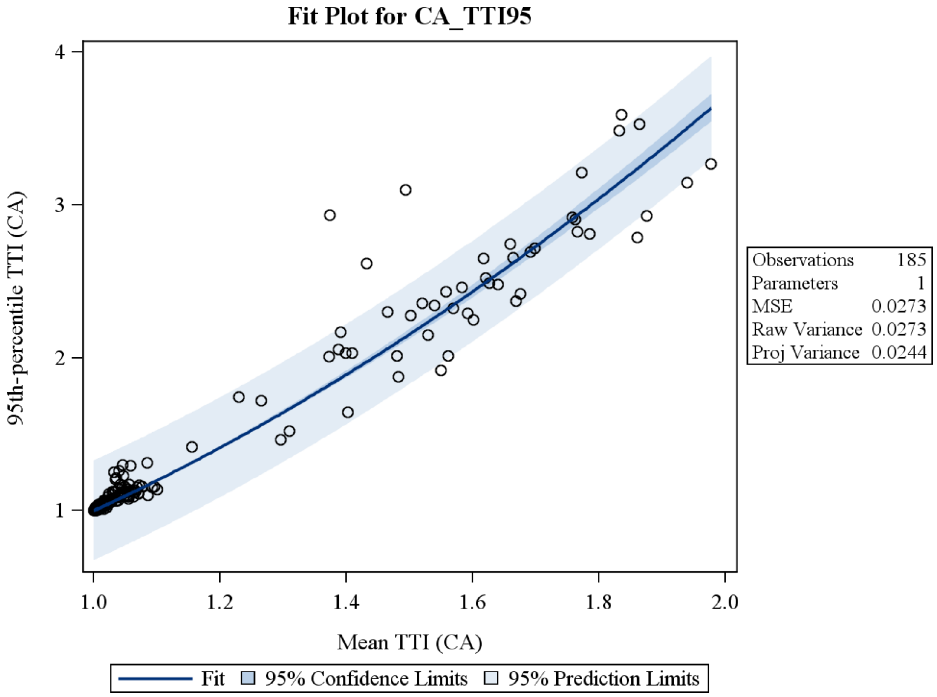

Figure E.146. Fit plot, new model: power form with a single parameter, 95th-percentile TTI, California.

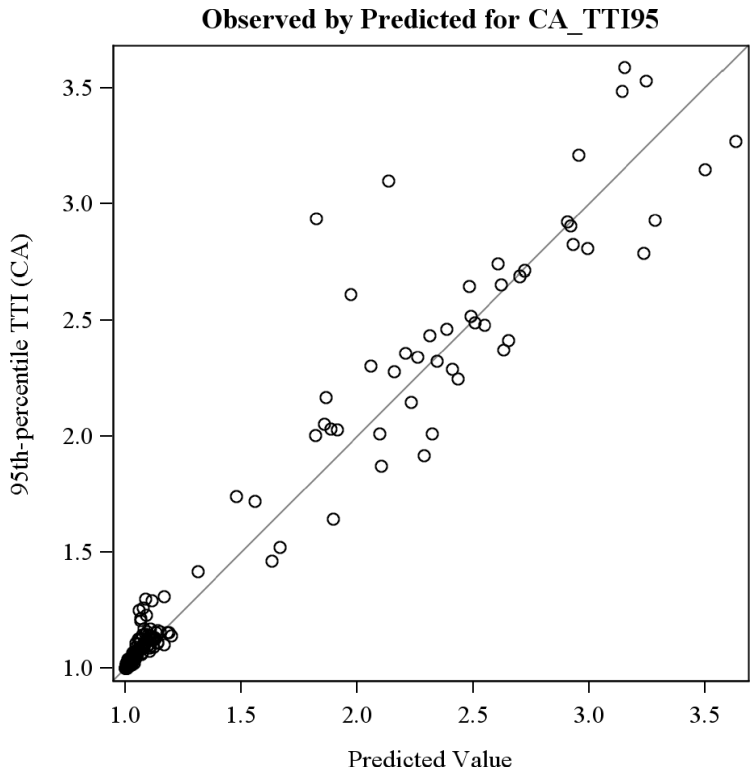

Figure E.147. Observed-by-predicted plot, new model: power form with a single parameter, 95th-percentile TTI, California.

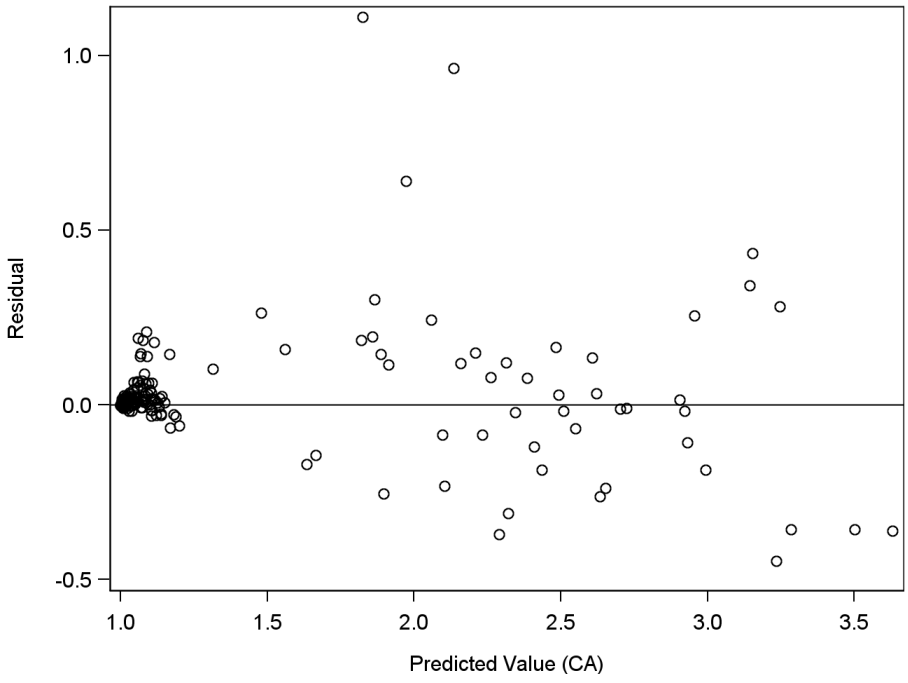

Figure E.148. Residual-by-predicted plot, new model: power form with a single parameter, 95th-percentile TTI, California.

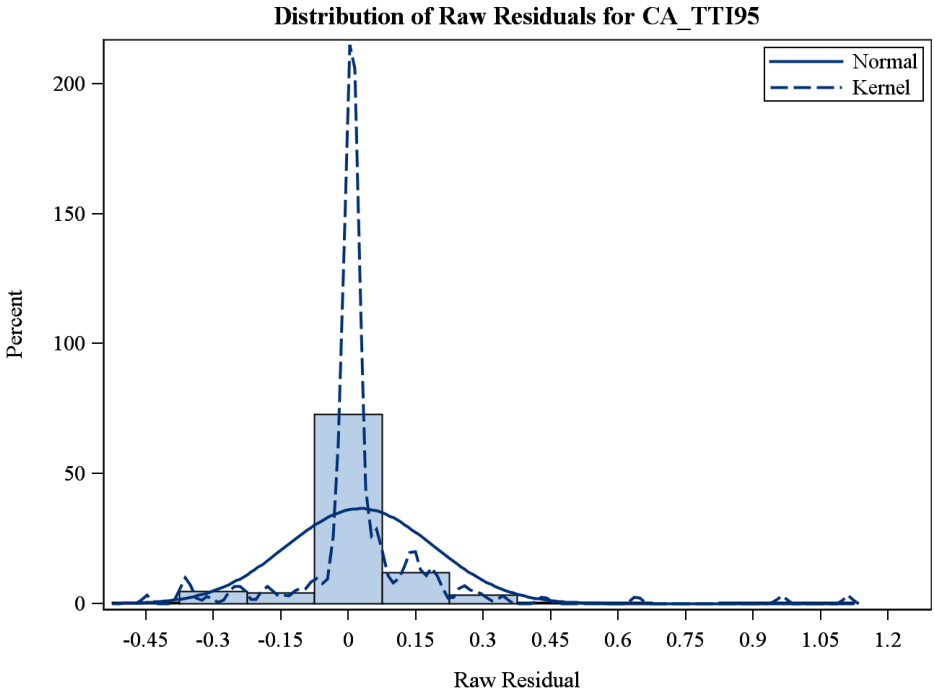

Figure E.149. Distribution of residuals, new model: power form with a single parameter, 95th-percentile TTI, California.

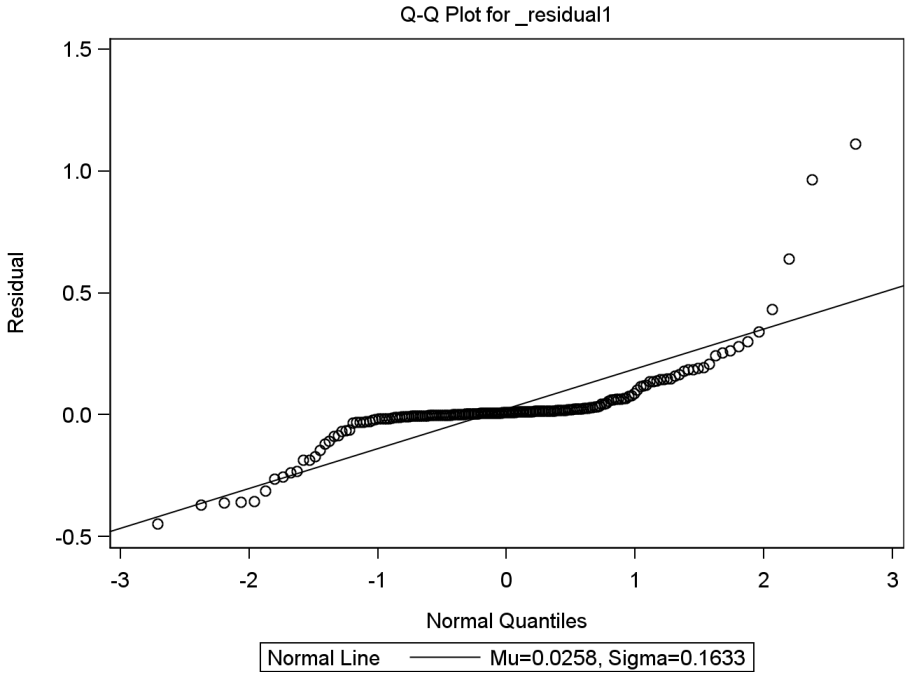

Figure E.150. Q-Q plot of residuals, new model: power form with a single parameter, 95th-percentile TTI, California.

Table E.61. Analysis of Variance, New Model: Power Form with Two Parameters, 95th-Percentile TTI, California

Source	DF	Sum of Squares	Mean Square	*F*-Value	Approx. Pr > *F*
Model	2	464.6	232.3	8797.71	<0.0001
Error	183	4.8322	0.0264		
Uncorrected total	185	469.4			

Table E.62. Parameter Estimates, New Model: Power Form with Two Parameters, 95th-Percentile TTI, California

Parameter	Estimate	Approx. Std Error	Approx. 95% Confidence Limits	
a	1.0363	0.0134	1.0099	1.0627
b	1.8232	0.0311	1.7619	1.8845

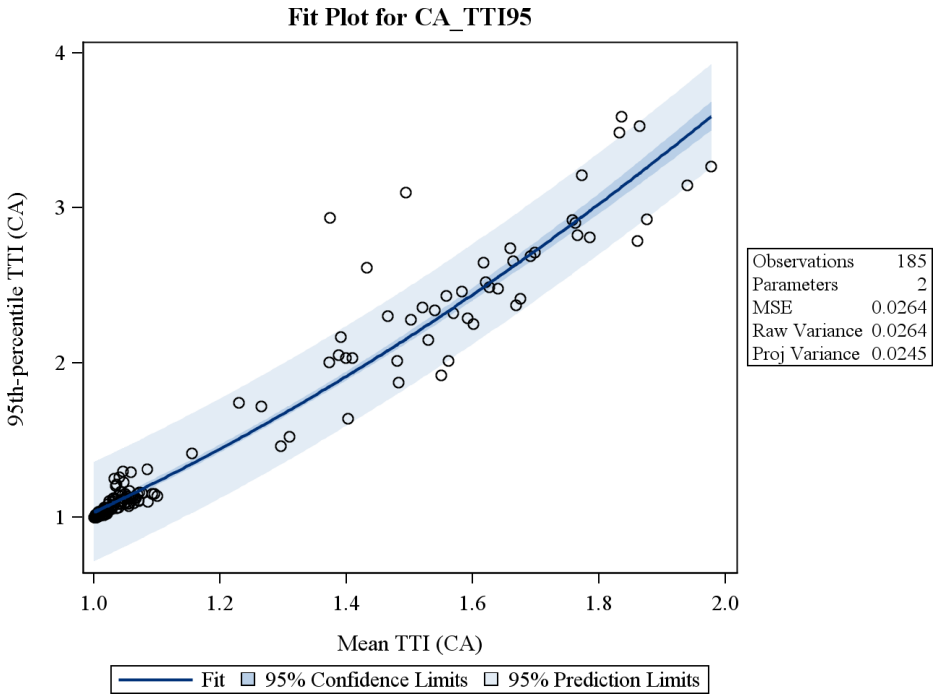

Figure E.151. Fit plot, new model: power form with two parameters, 95th-percentile TTI, California.

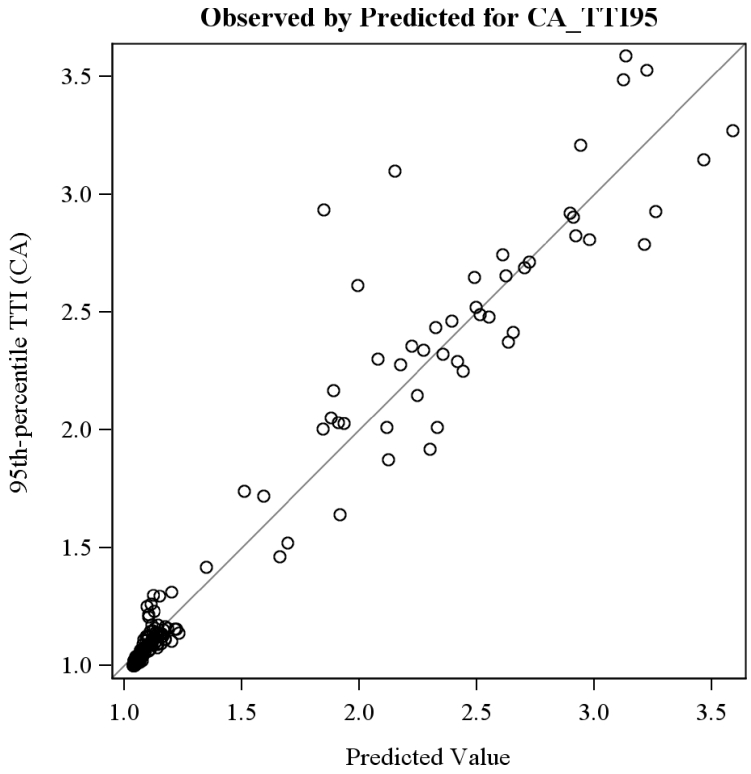

Figure E.152. Observed-by-predicted plot, new model: power form with two parameters, 95th-percentile TTI, California.

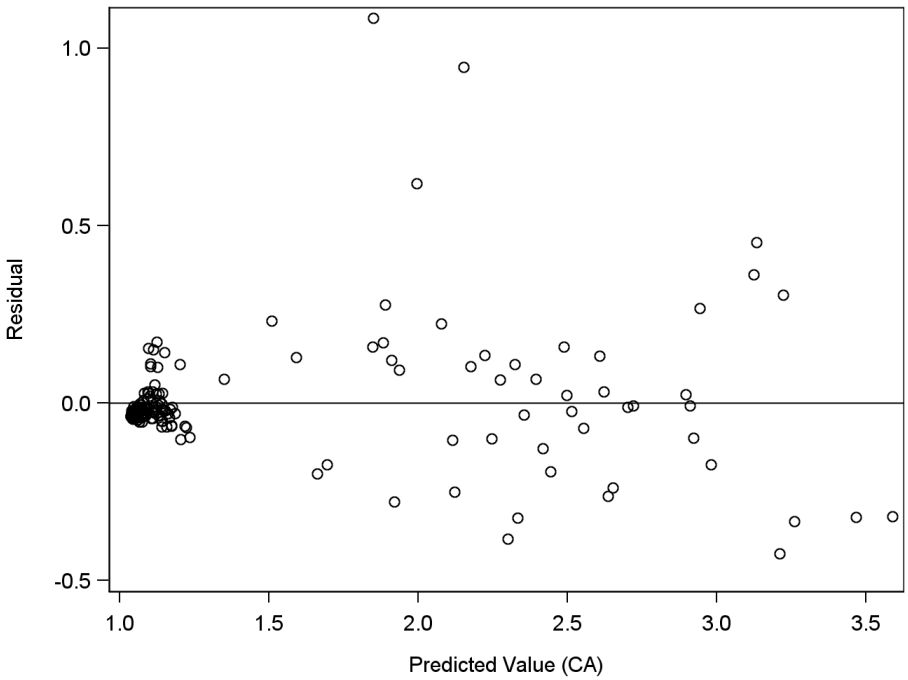

Figure E.153. Residual-by-predicted plot, new model: power form with two parameters, 95th-percentile TTI, California.

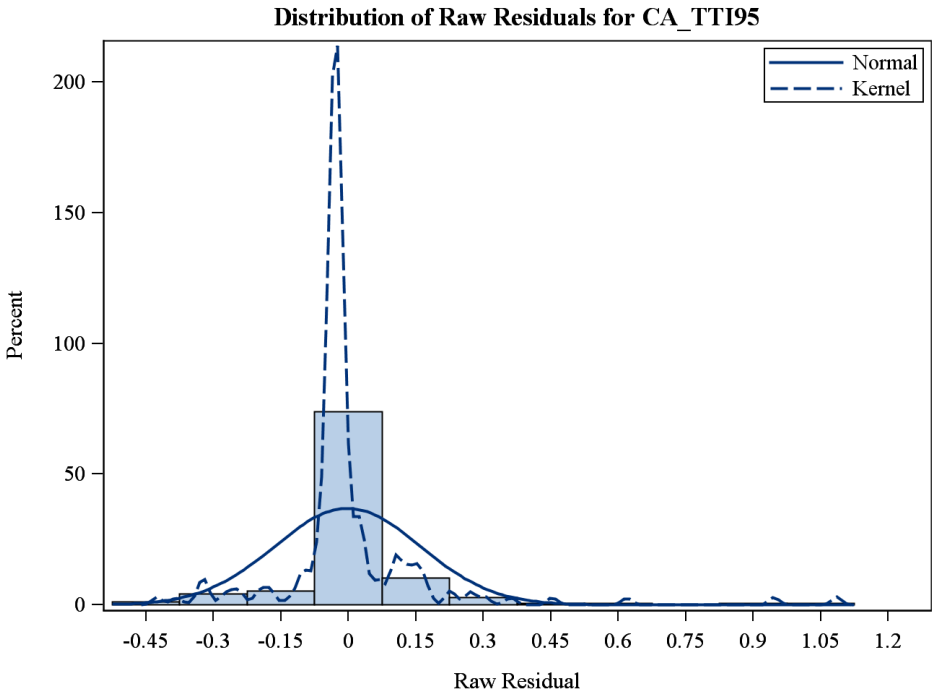

Figure E.154. Distribution of residuals, new model: power form with two parameters, 95th-percentile TTI, California.

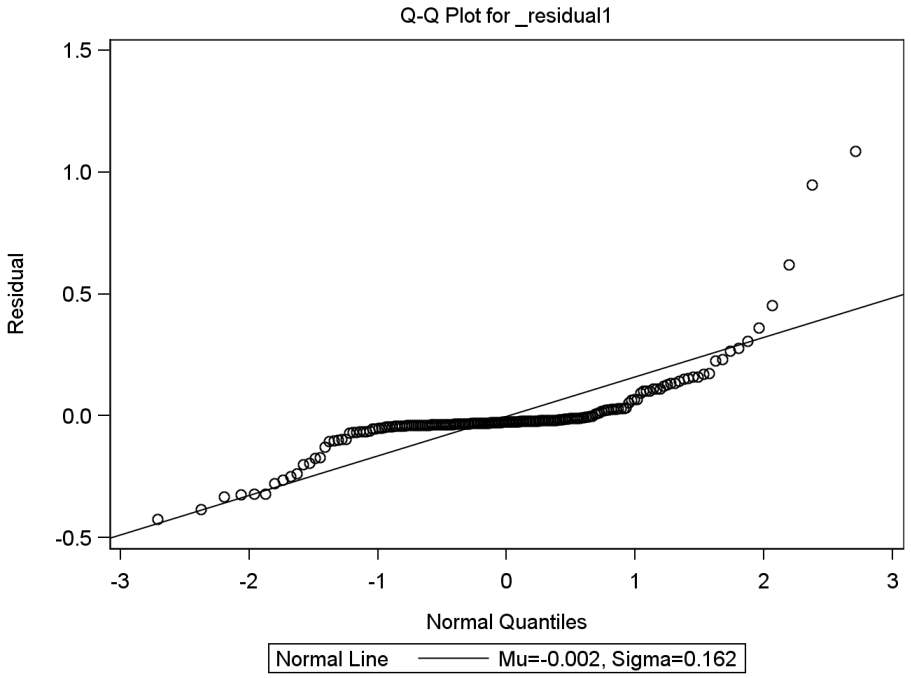

Figure E.155. Q-Q plot of residuals, new model: power form with two parameters, 95th-percentile TTI, California.

Table E.63. Analysis of Variance, New Model: Polynomial Form with Two Parameters, 95th-Percentile TTI, California

Source	DF	Sum of Squares	Mean Square	*F*-Value	Approx. Pr > *F*
Model	2	464.5	232.3	8670.53	<0.0001
Error	183	4.9023	0.0268		
Uncorrected total	185	469.4			

Table E.64. Parameter Estimates, New Model: Polynomial Form with Two Parameters, 95th-Percentile TTI, California

Parameter	Estimate	Approx. Std Error	Approx. 95% Confidence Limits	
a	0.2245	0.0414	0.1428	0.3062
b	0.8119	0.0307	0.7514	0.8725

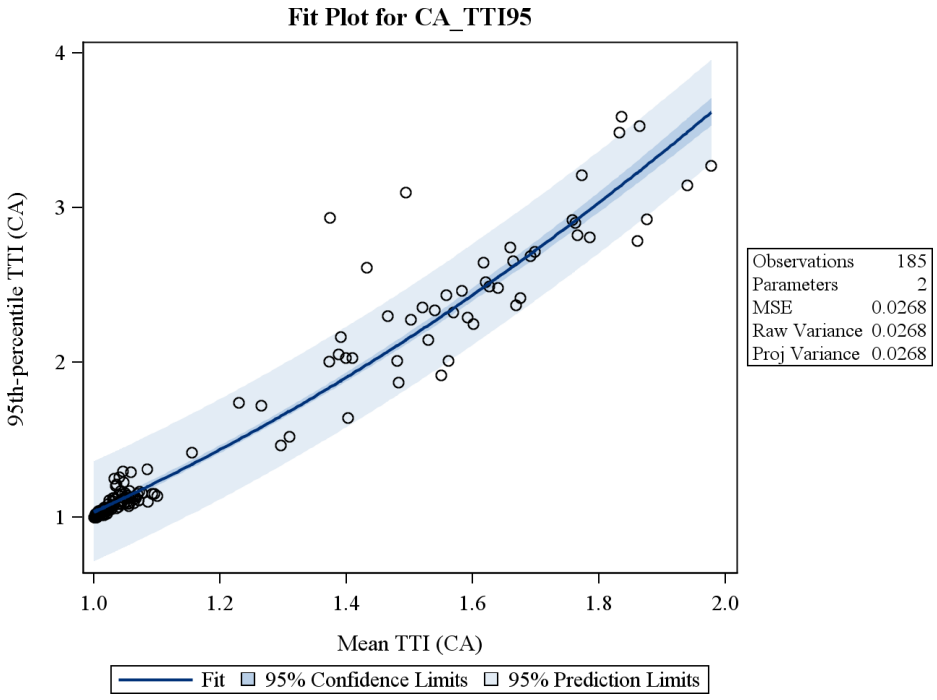

Figure E.156. Fit plot, new model: polynomial form with two parameters, 95th-percentile TTI, California.

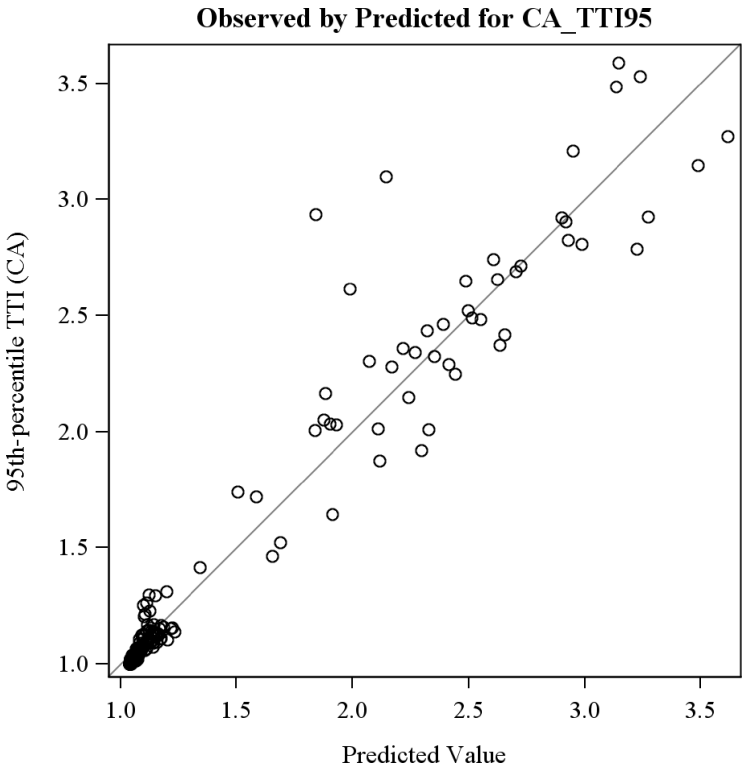

Figure E.157. Observed-by-predicted plot, new model: polynomial form with two parameters, 95th-percentile TTI, California.

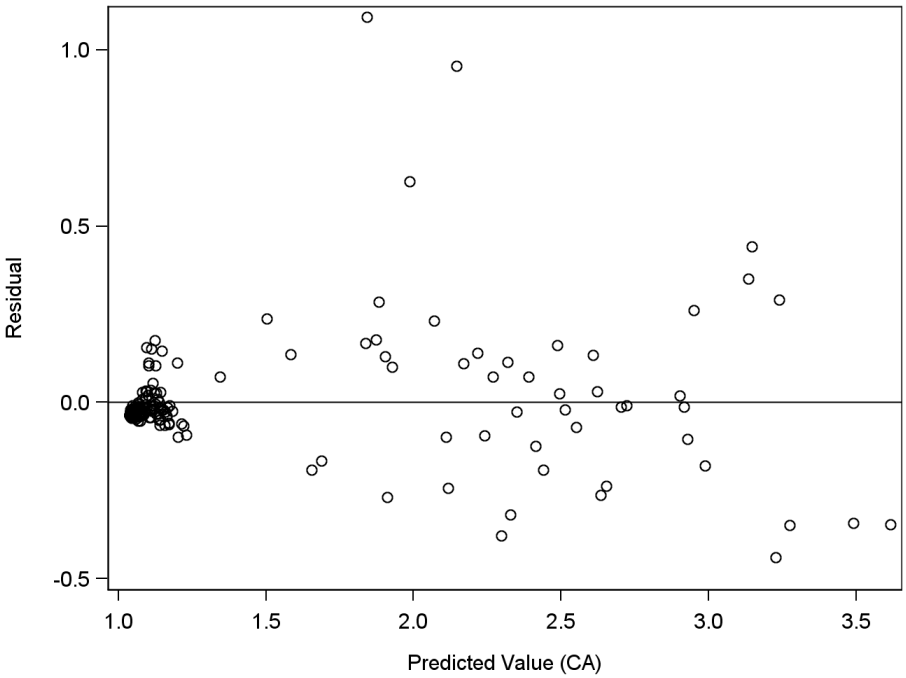

Figure E.158. Residual-by-predicted plot, new model: polynomial form with two parameters, 95th-percentile TTI, California.

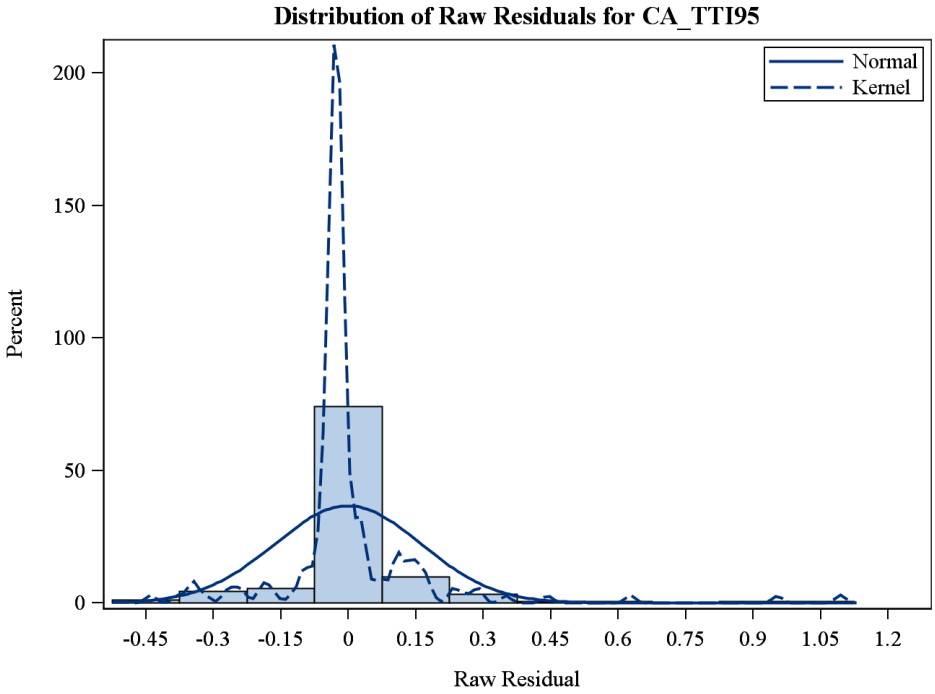

Figure E.159. Distribution of residuals, new model: polynomial form with two parameters, 95th-percentile TTI, California.

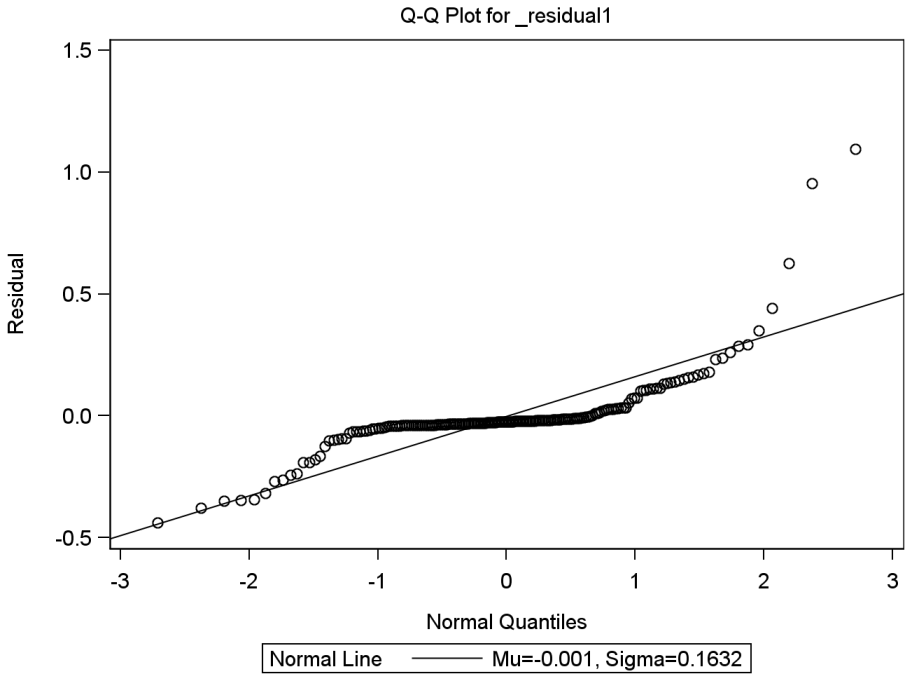

Figure E.160. Q-Q plot of residuals, new model: polynomial form with two parameters, 95th-percentile TTI, California.

Table E.65. Analysis of Variance, New Model: Power Form with a Single Parameter, 95th-Percentile TTI, Minnesota

Source	DF	Sum of Squares	Mean Square	*F*-Value	Approx. Pr > *F*
Model	1	250.8	250.8	6151.90	<0.0001
Error	78	3.1795	0.0408		
Uncorrected total	79	254.0			

Table E.66. Parameter Estimates, New Model: Power Form with a Single Parameter, 95th-Percentile TTI, Minnesota

Parameter	Estimate	Approx. Std Error	Approx. 95% Confidence Limits	
b	2.0516	0.0268	1.9983	2.1048

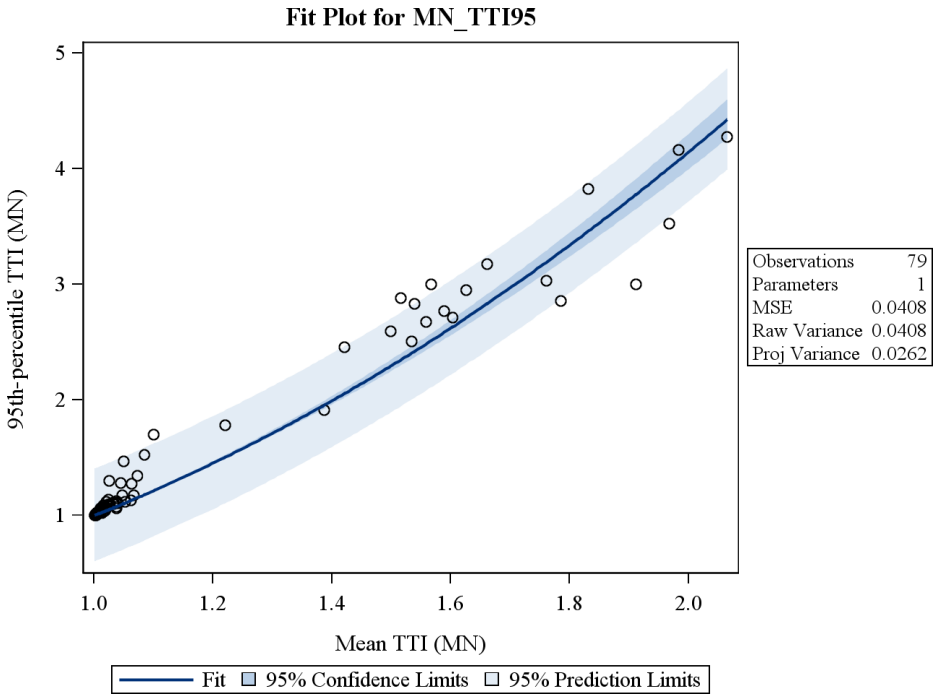

Figure E.161. Fit plot, new model: power form with a single parameter, 95th-percentile TTI, Minnesota.

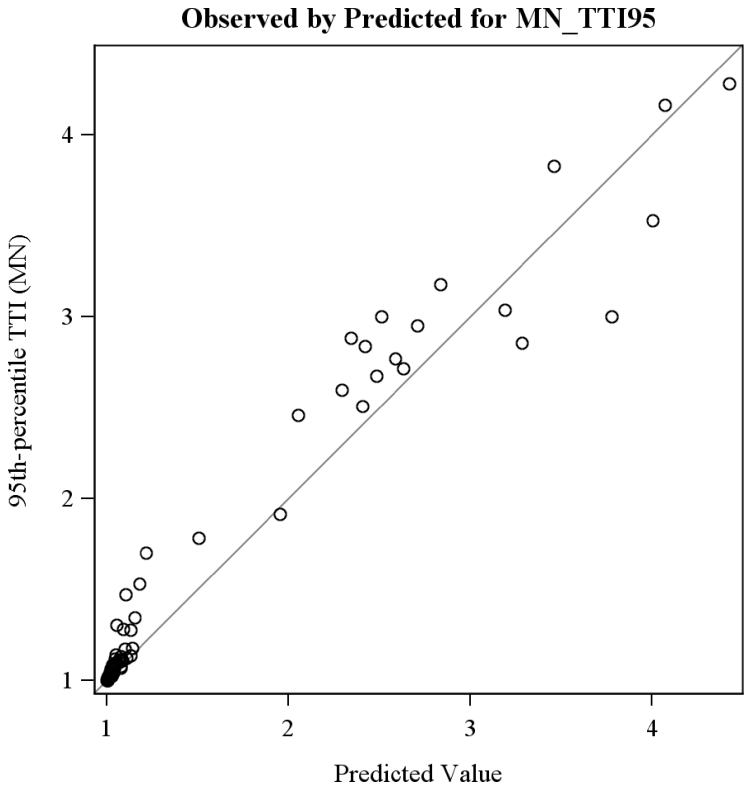

Figure E.162. Observed-by-predicted plot, new model: power form with a single parameter, 95th-percentile TTI, Minnesota.

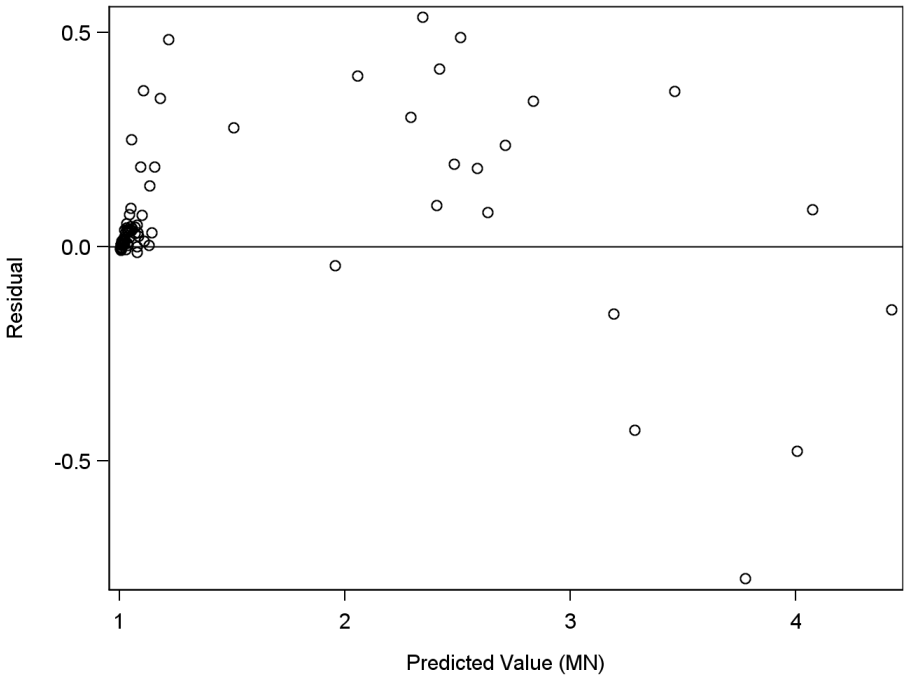

Figure E.163. Residual-by-predicted plot, new model: power form with a single parameter, 95th-percentile TTI, Minnesota.

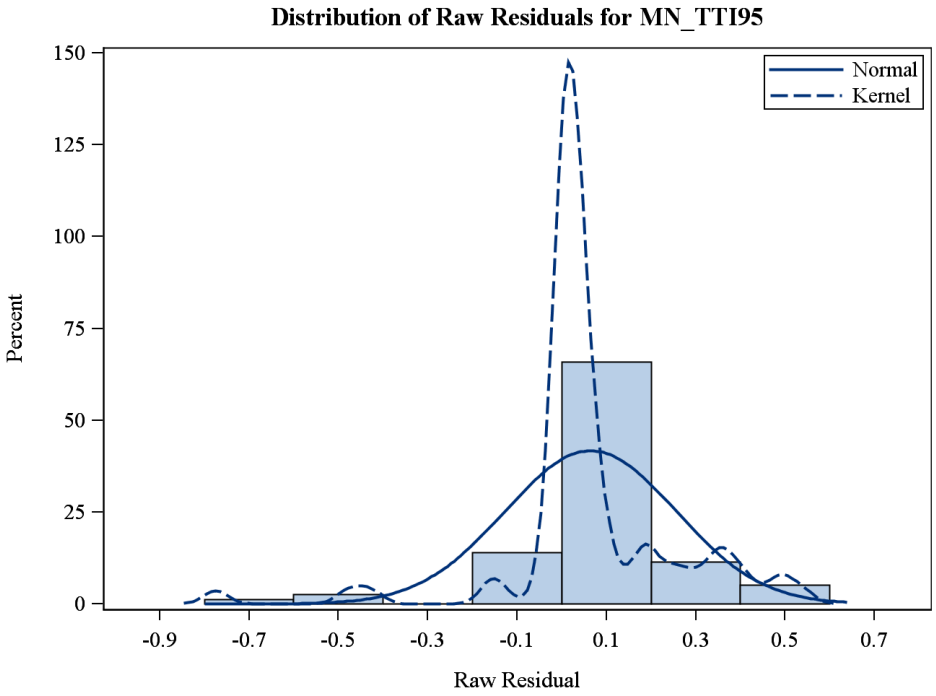

Figure E.164. Distribution of residuals, new model: power form with a single parameter, 95th-percentile TTI, Minnesota.

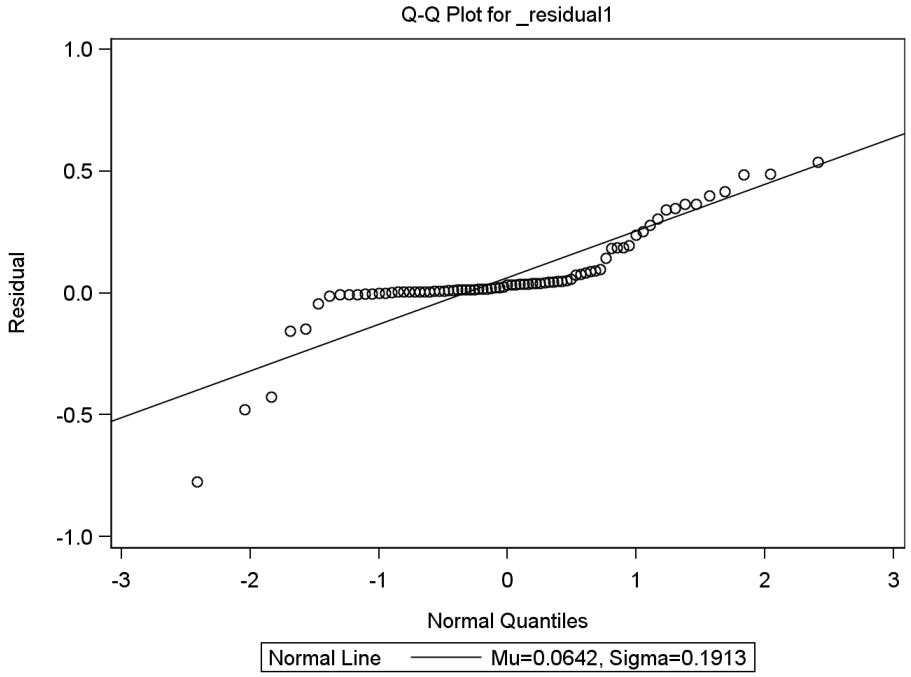

Figure E.165. Q-Q plot of residuals, new model: power form with a single parameter, 95th-percentile TTI, Minnesota.

Table E.67. Analysis of Variance, New Model: Power Form with Two Parameters, 95th-Percentile TTI, Minnesota

Source	DF	Sum of Squares	Mean Square	*F*-Value	Approx. Pr > *F*
Model	2	251.3	125.6	3638.20	<0.0001
Error	77	2.6592	0.0345		
Uncorrected total	79	254.0			

Table E.68. Parameter Estimates, New Model: Power Form with Two Parameters, 95th-Percentile TTI, Minnesota

Parameter	Estimate	Approx. Std Error	Approx. 95% Confidence Limits	
a	1.0871	0.0228	1.0416	1.1325
b	1.9081	0.0443	1.8200	1.9963

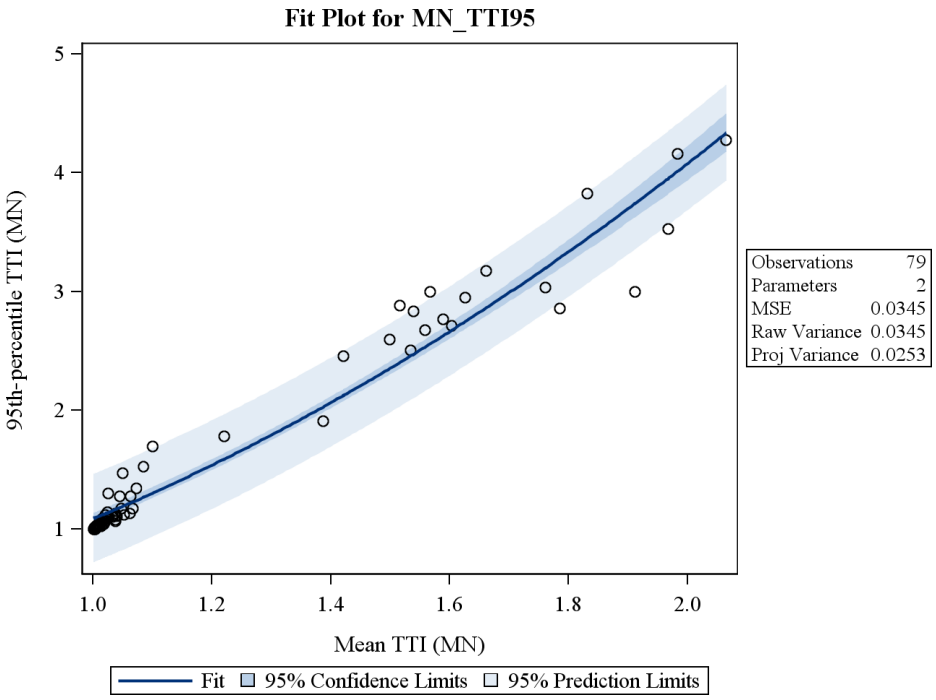

Figure E.166. Fit plot, new model: power form with two parameters, 95th-percentile TTI, Minnesota.

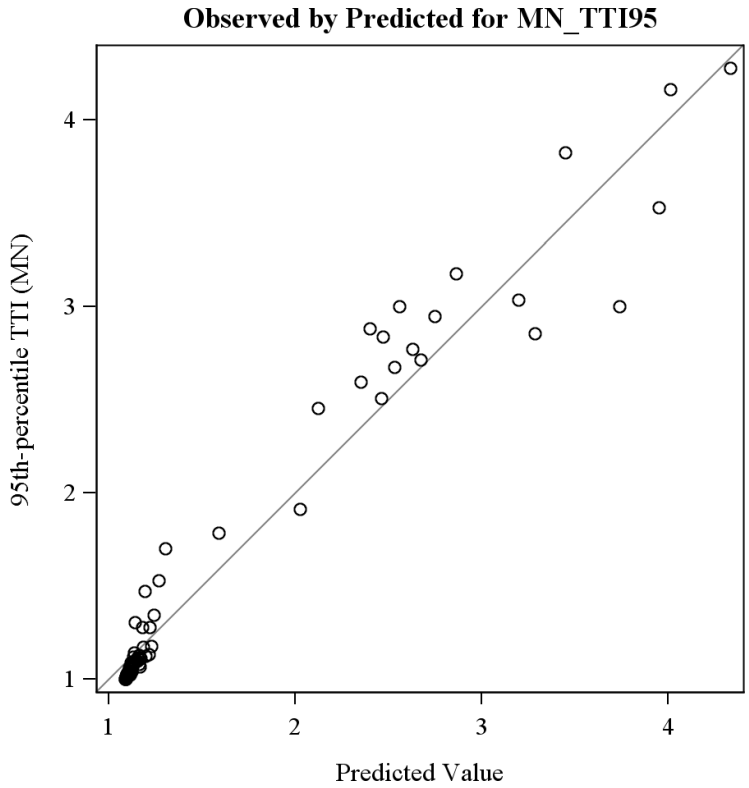

Figure E.167. Observed-by-predicted plot, new model: power form with two parameters, 95th-percentile TTI, Minnesota.

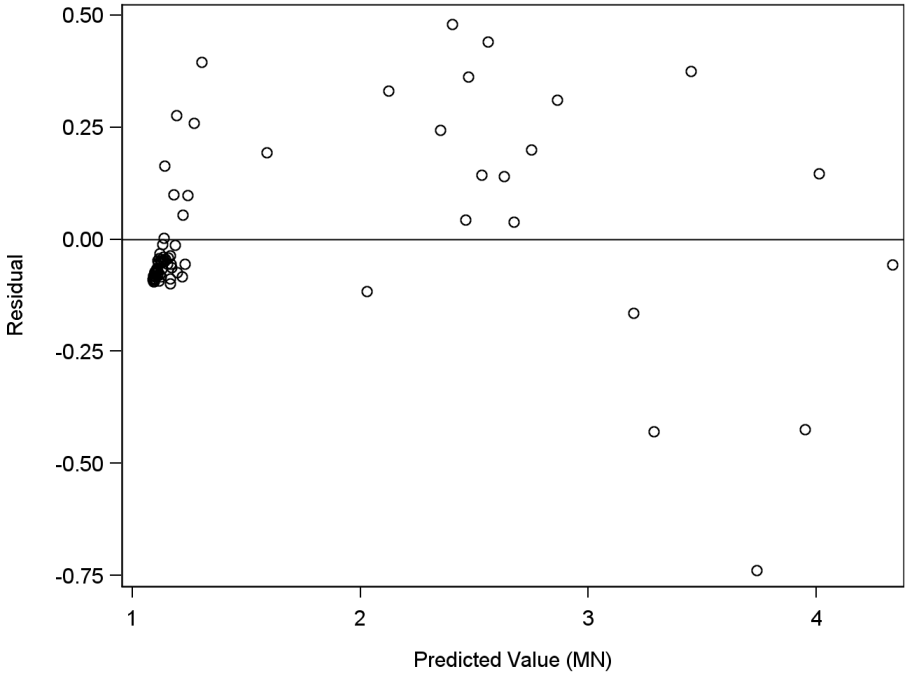

Figure E.168. Residual-by-predicted plot, new model: power form with two parameters, 95th-percentile TTI, Minnesota.

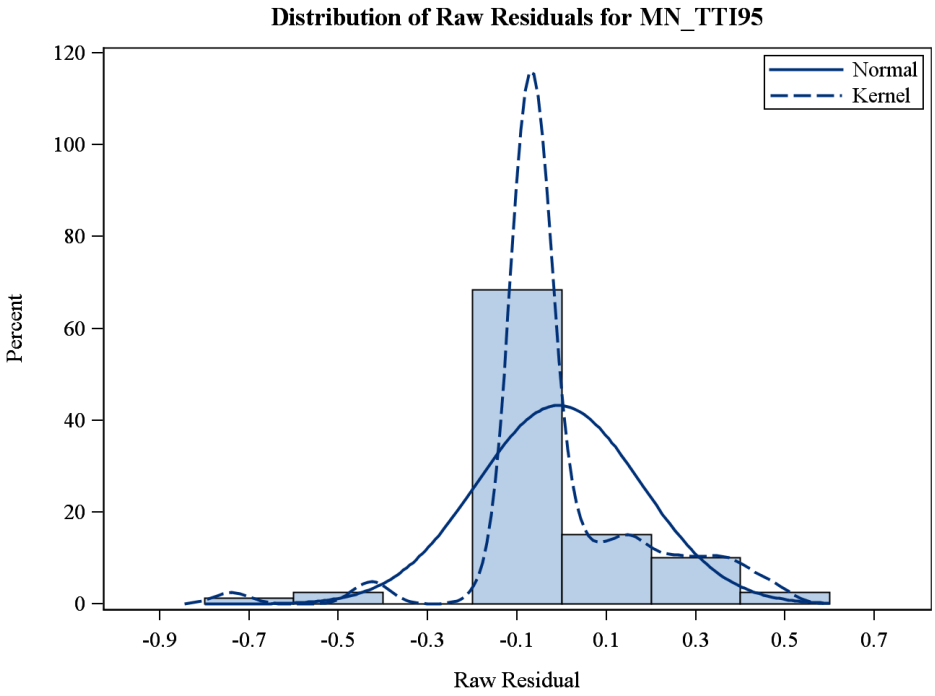

Figure E.169. Distribution of residuals, new model: power form with two parameters, 95th-percentile TTI, Minnesota.

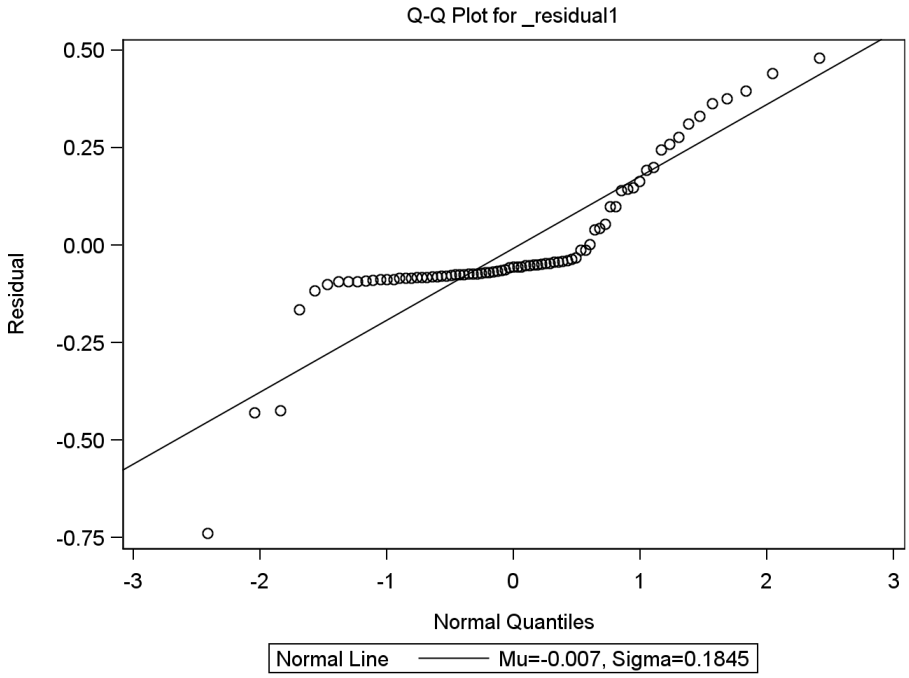

Figure E.170. Q-Q plot of residuals, new model: power form with two parameters, 95th-percentile TTI, Minnesota.

Table E.69. Analysis of Variance, New Model: Polynomial Form with Two Parameters, 95th-Percentile TTI, Minnesota

Source	DF	Sum of Squares	Mean Square	*F*-Value	Approx. Pr > *F*
Model	2	251.2	125.6	3572.65	<0.0001
Error	77	2.7075	0.0352		
Uncorrected total	79	254.0			

Table E.70. Parameter Estimates, New Model: Polynomial Form with Two Parameters, 95th-Percentile TTI, Minnesota

Parameter	Estimate	Approx. Std Error	Approx. 95% Confidence Limits	
a	0.1122	0.0652	–0.0176	0.2419
b	0.9701	0.0466	0.8772	1.0630

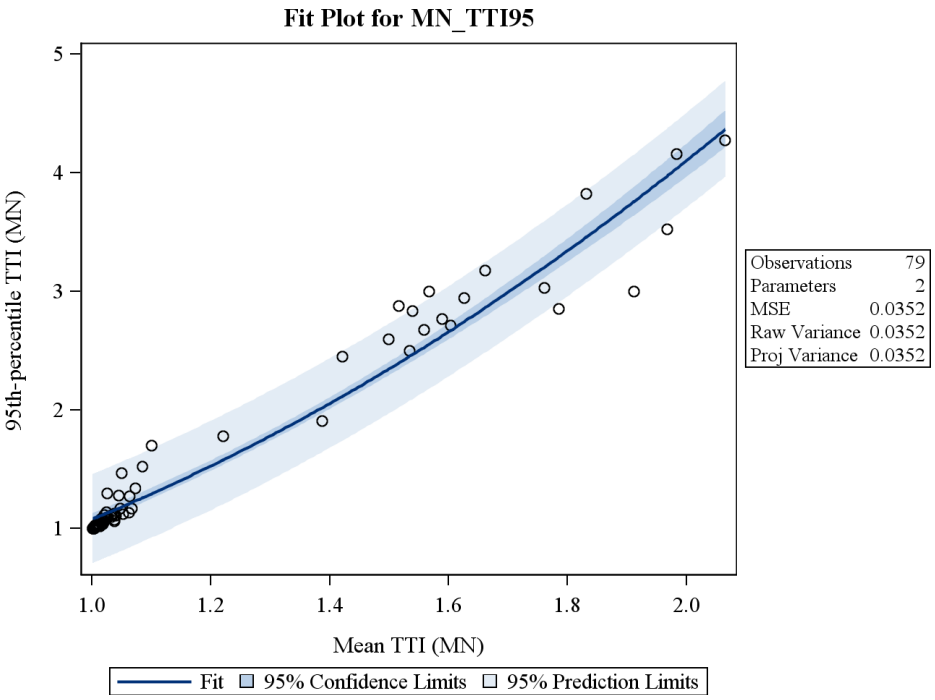

Figure E.171. Fit plot, new model: polynomial form with two parameters, 95th-percentile TTI, Minnesota.

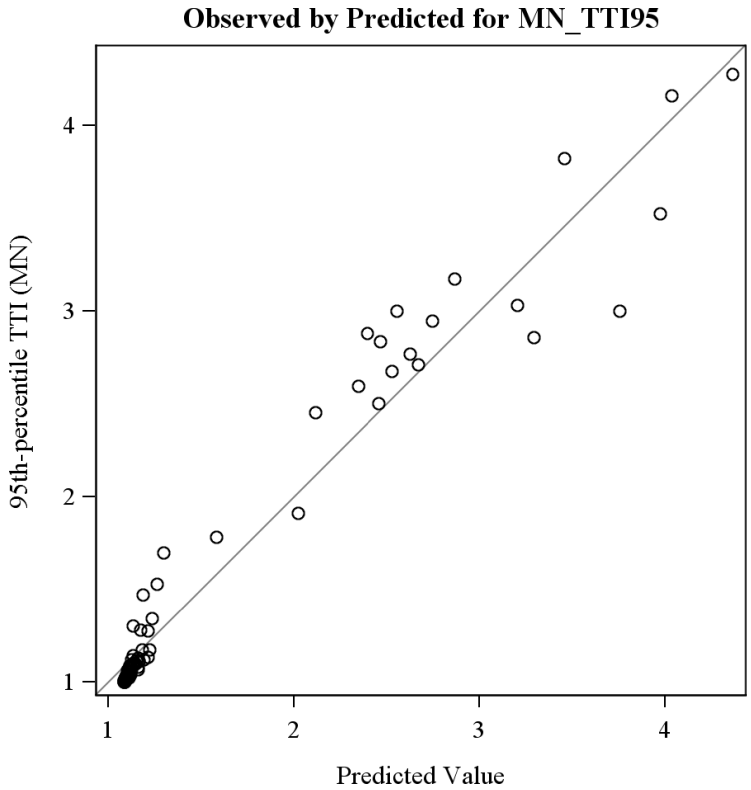

Figure E.172. Observed-by-predicted plot, new model: polynomial form with two parameters, 95th-percentile TTI, Minnesota.

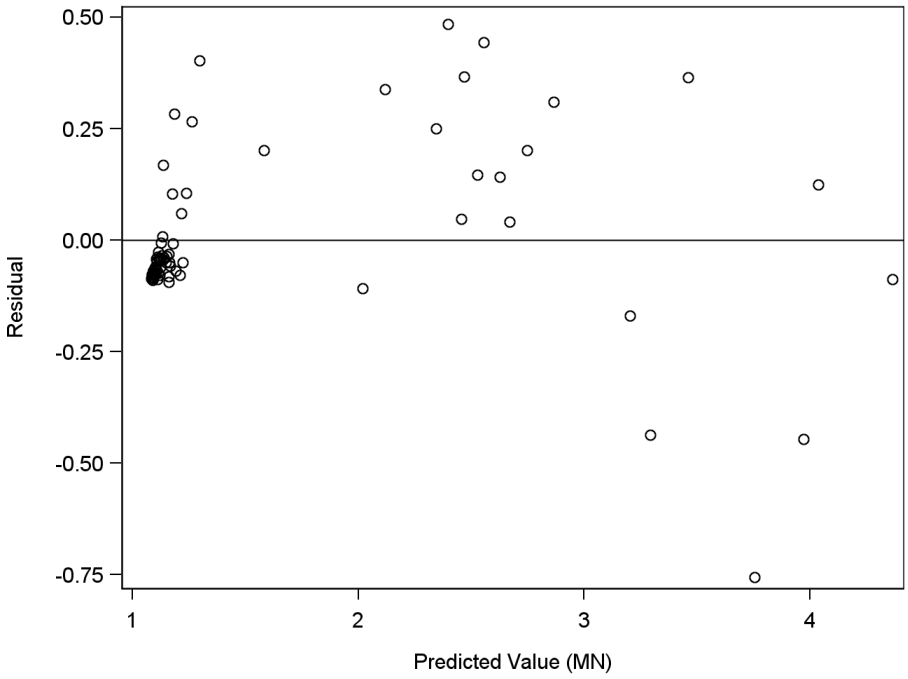

Figure E.173. Residual-by-predicted plot, new model: polynomial form with two parameters, 95th-percentile TTI, Minnesota.

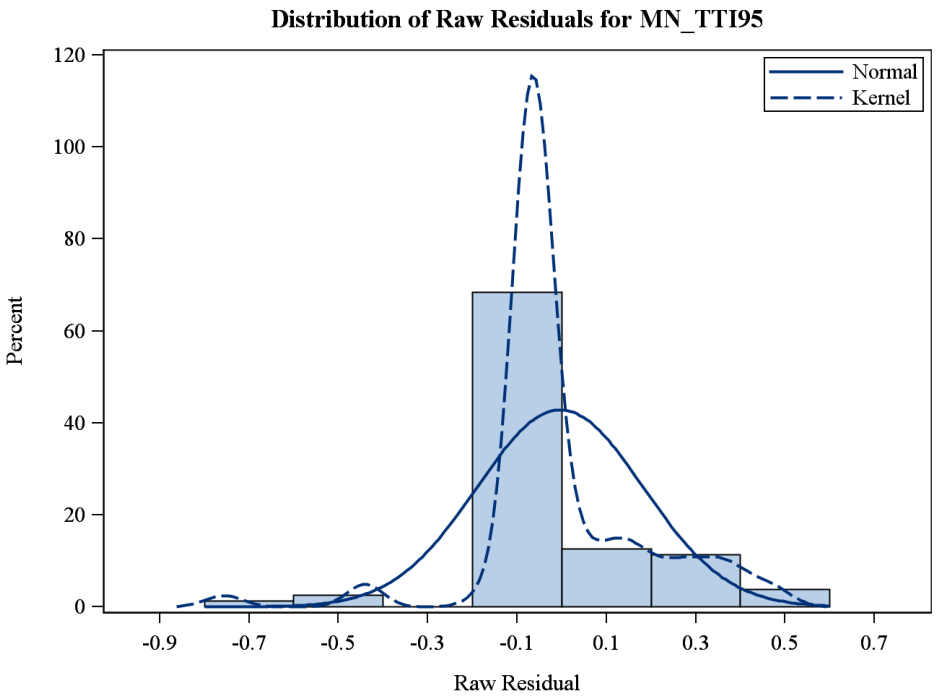

Figure E.174. Distribution of residuals, new model: polynomial form with two parameters, 95th-percentile TTI, Minnesota.

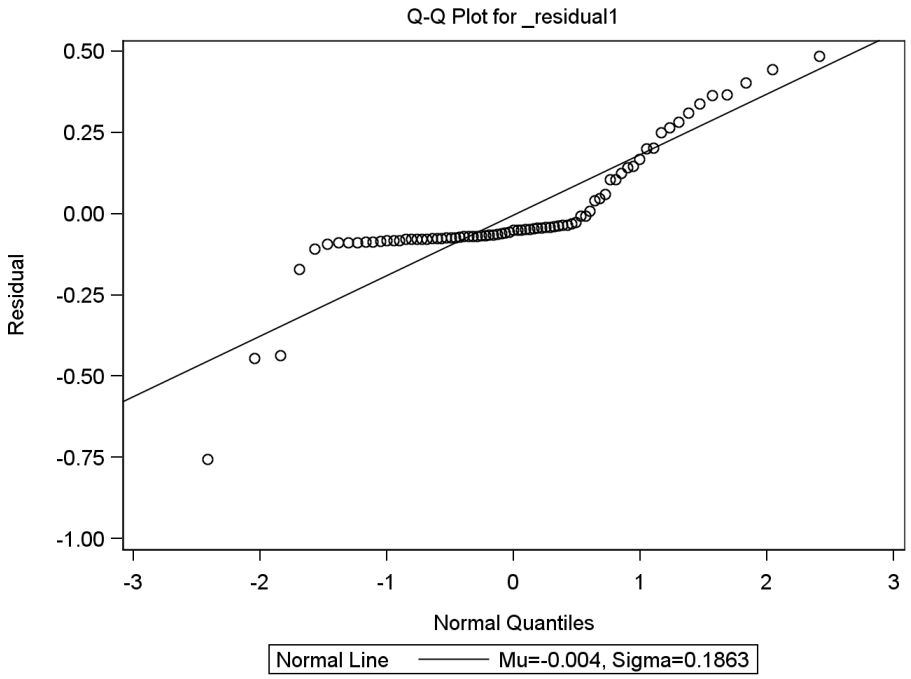

Figure E.175. Q-Q plot of residuals, new model: polynomial form with two parameters, 95th-percentile TTI, Minnesota.

90th-Percentile TTI

Summary

For the 90th-percentile TTI models, the MSE table (Table E.71) shows that the MSE values for the AllData and the CA data sets are smaller with the new models. For the MN data set, the recalibration model has the smallest MSE.

The new models (Tables E.73, E.75, E.77, E.79, E.81, E.83, E.85, E.87, and E.89) all passed the *F*-test (Tables E.72, E.74, E.76, E.78, E.80, E.82, E.84, E.86, and E.88), indicating overall validity. The fit plots (Figures E.176, E.177, E.182, E.183, E.188, E.189, E.194, E.199, E.204, E.209, E.214, and E.219) show that the new models can predict the data trend well and also show the regional differences. The residual-by-predicted plots (Figures E.179, E.185, E.191, E.196, E.201, E.206, E.211, E.216, and E.221) show improved residual pattern compared with the recalibrated models in that the residual samples are more randomly balanced on the two sides of the zero reference line and around the origin. The nonconstant variance problem still exists. The histograms (Figures E.180, E.186, E.192, E.197, E.202, E.207, E.212, E.217, and E.222) and the normality plots (Figures E.181, E.187, E.193, E.198, E.203, E.208, E.213, E.218, and E.223) show that the residuals may not perfectly follow a normal distribution. The observed-by-predicted plots are shown in Figures E.178, E.184, E.190, E.195, E.200, E.205, E.210, E.215, and E.220.

AllData

Power Form Model with a Single Parameter

Model:

$$90\text{th-percentile TTI}_{\text{AllData}} = \text{meanTTI}^{1.7324}$$

Power Form Model with Two Parameters

Model:

$$90\text{th-percentile TTI}_{\text{AllData}} = 1.0099 * \text{meanTTI}^{1.7137}$$

Table E.71. MSE Summary Table (Comparable)

Model Name	Formula	AllData	CA	MN
Recalibration	$y = 1 + a * \ln(x)$	0.0137	0.0131	0.0110
1-parameter power	$y = x^b$	0.0122	0.0118	0.0151
2-parameter power	$y = a * x^b$	0.0121	0.0118	0.0144
2-parameter polynomial	$y = a * x + b * x^2$	0.0125	0.0121	0.0153

Table E.72. Analysis of Variance, New Model: Power Form with a Single Parameter, 90th-Percentile TTI, AllData

Source	DF	Sum of Squares	Mean Square	*F*-Value	Approx. Pr > *F*
Model	1	670.6	670.6	55066.8	<0.0001
Error	320	3.8971	0.0122		
Uncorrected total	321	674.5			

Table E.73. Parameter Estimates, New Model: Power Form with a Single Parameter, 90th-Percentile TTI, AllData

Parameter	Estimate	Approx. Std Error	Approx. 95% Confidence Limits	
b	1.7324	0.0106	1.7116	1.7532

Polynomial Form Model with Two Parameters

Model:

$$90\text{th-percentile TTI}_{\text{AllData}} = 0.3528 * \text{meanTTI} + 0.6591 * \text{meanTTI}^2$$

California

Power Form Model with a Single Parameter

Model:

$$90\text{th-percentile TTI}_{\text{CA}} = \text{meanTTI}^{1.6826}$$

Power Form Model with Two Parameters

Model:

$$90\text{th-percentile TTI}_{\text{CA}} = 1.0090 * \text{meanTTI}^{1.6651}$$

Polynomial Form Model with Two Parameters

Model:

$$90\text{th-percentile TTI}_{\text{CA}} = 0.4060 * \text{meanTTI} + 0.6055 * \text{meanTTI}^2$$

(text continues on page 342)

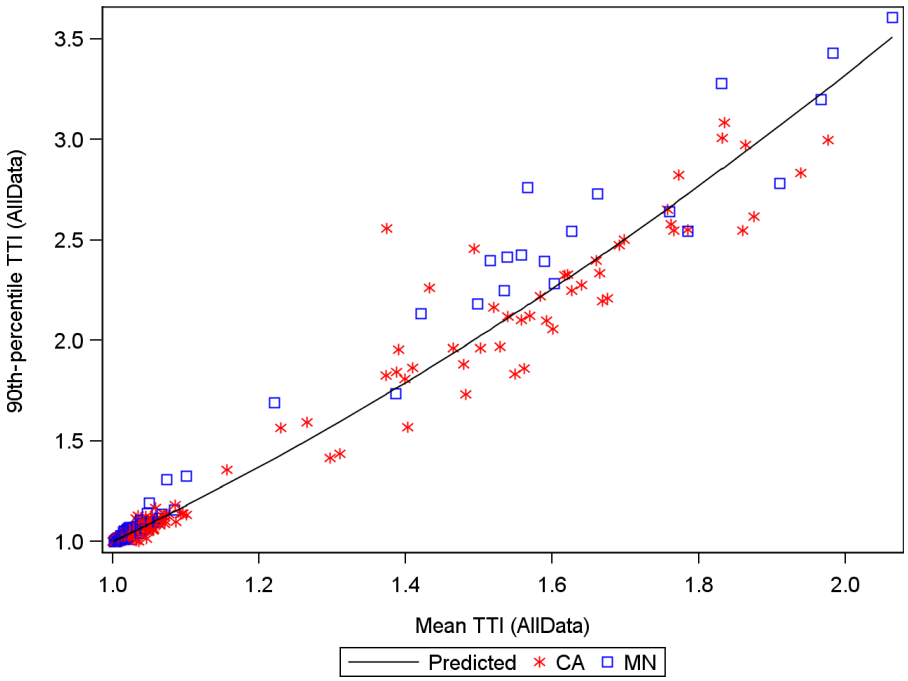

Figure E.176. Fit plot by region, new model: power form with a single parameter, 90th-percentile TTI, AllData.

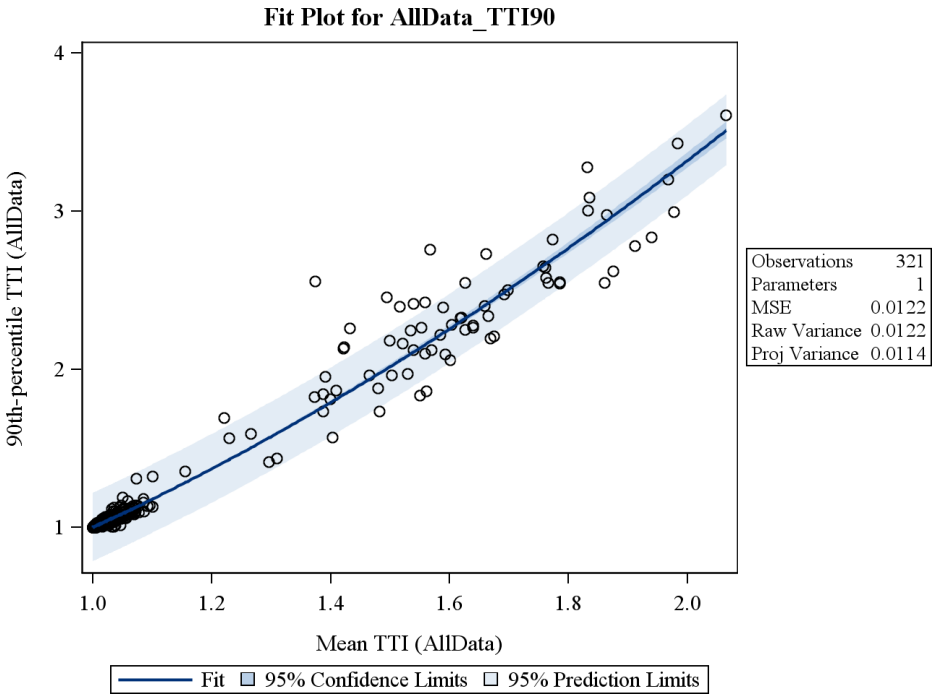

Figure E.177. Fit plot, new model: power form with a single parameter, 90th-percentile TTI, AllData.

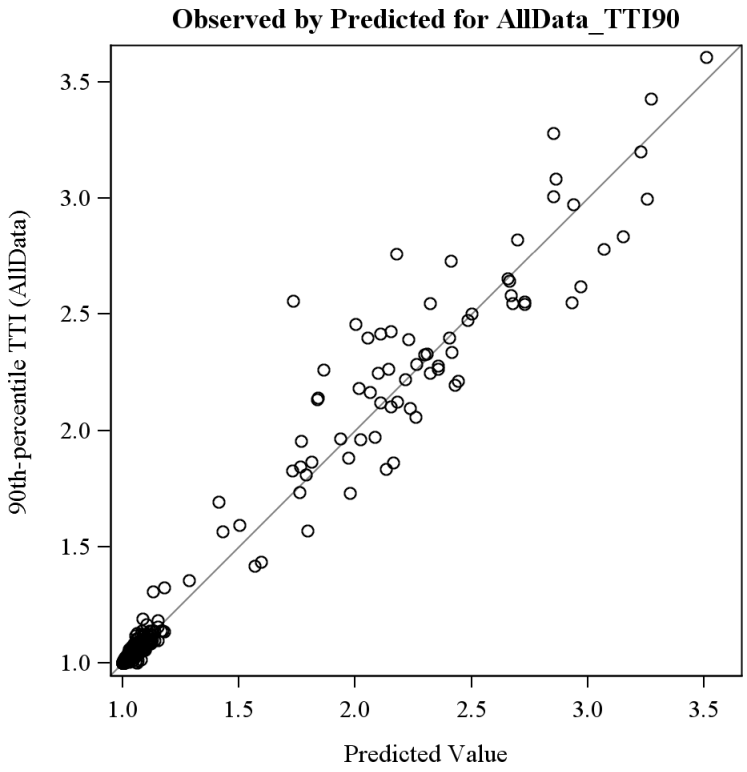

Figure E.178. Observed-by-predicted plot, new model: power form with a single parameter, 90th-percentile TTI, AllData.

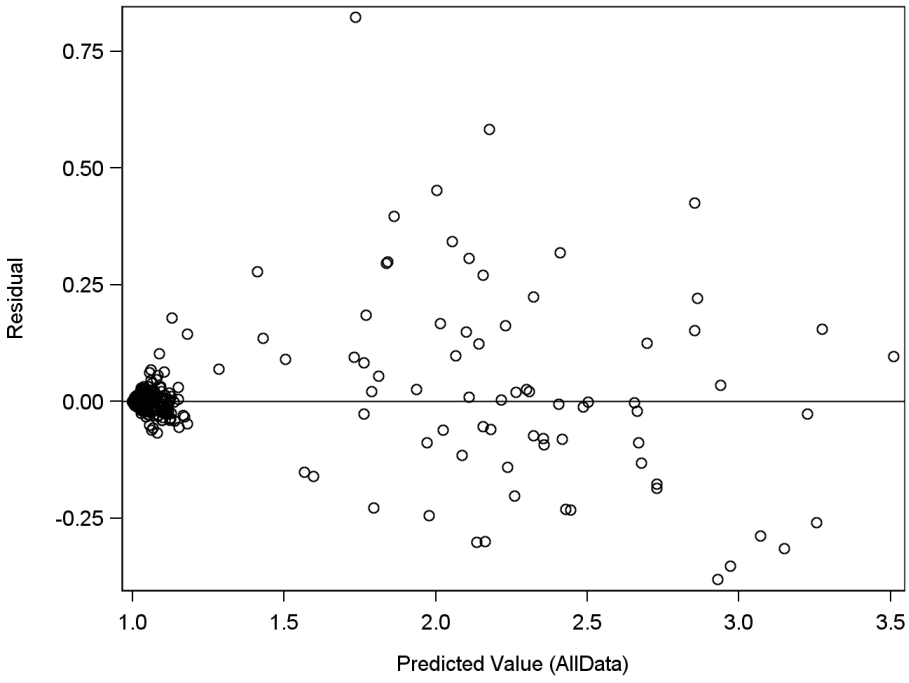

Figure E.179. Residual-by-predicted plot, new model: power form with a single parameter, 90th-percentile TTI, AllData.

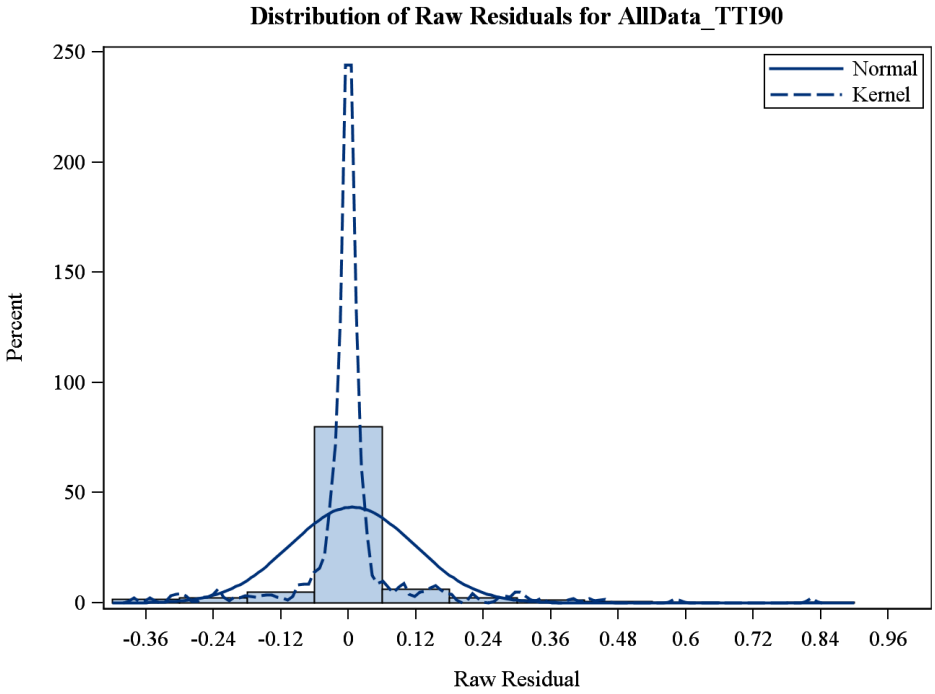

Figure E.180. Distribution of residuals, new model: power form with a single parameter, 90th-percentile TTI, AllData.

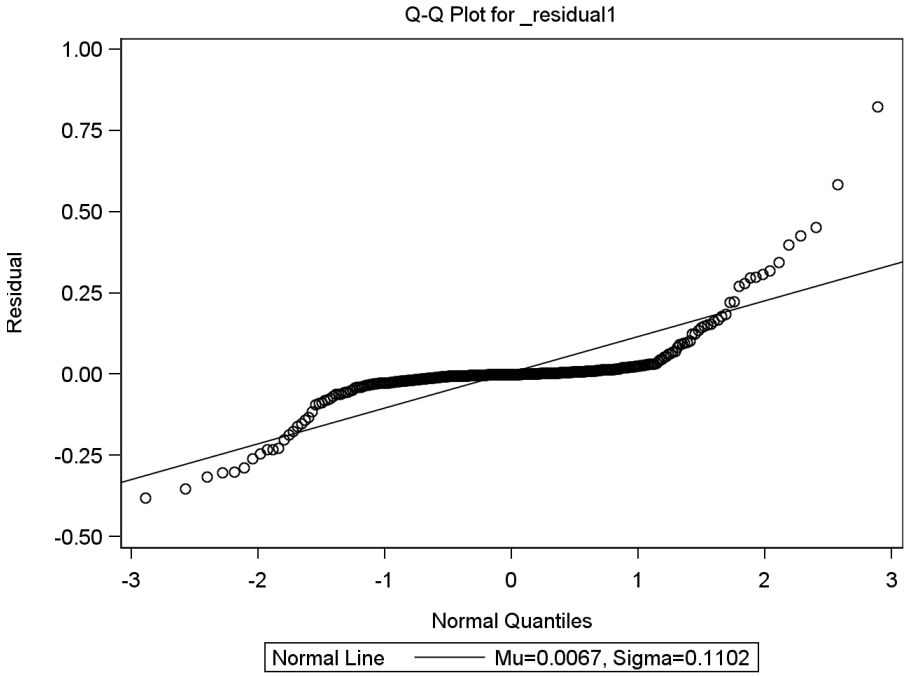

Figure E.181. Q-Q plot of residuals, new model: power form with a single parameter, 90th-percentile TTI, AllData.

Table E.74. Analysis of Variance, New Model: Power Form with Two Parameters, 90th-Percentile TTI, AllData

Source	DF	Sum of Squares	Mean Square	*F*-Value	Approx. Pr > *F*
Model	2	670.6	335.3	27631.9	<0.0001
Error	319	3.8712	0.0121		
Uncorrected total	321	674.5			

Table E.75. Parameter Estimates, New Model: Power Form with Two Parameters, 90th-Percentile TTI, AllData

Parameter	Estimate	Approx. Std Error	Approx. 95% Confidence Limits	
a	1.0099	0.00677	0.9965	1.0232
b	1.7137	0.0166	1.6810	1.7464

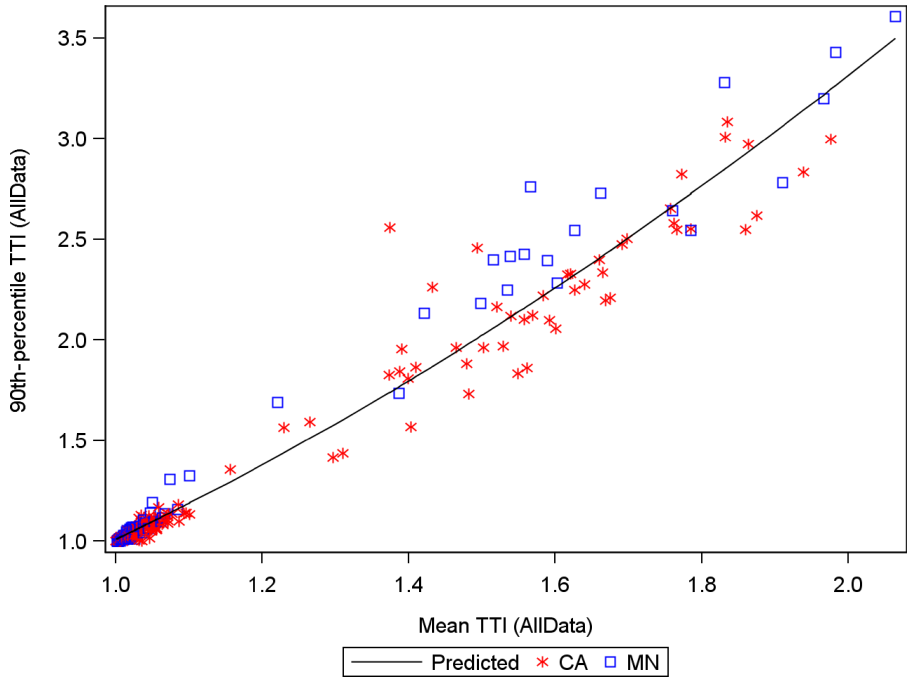

Figure E.182. Fit plot by region, new model: power form with two parameters, 90th-percentile TTI, AllData.

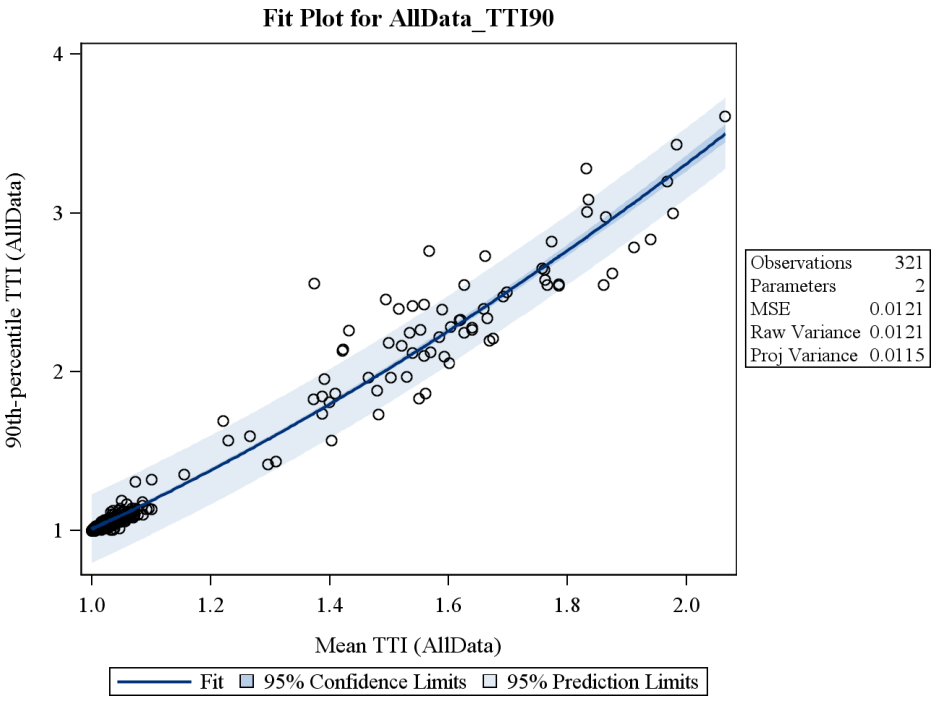

Figure E.183. Fit plot, new model: power form with two parameters, 90th-percentile TTI, AllData.

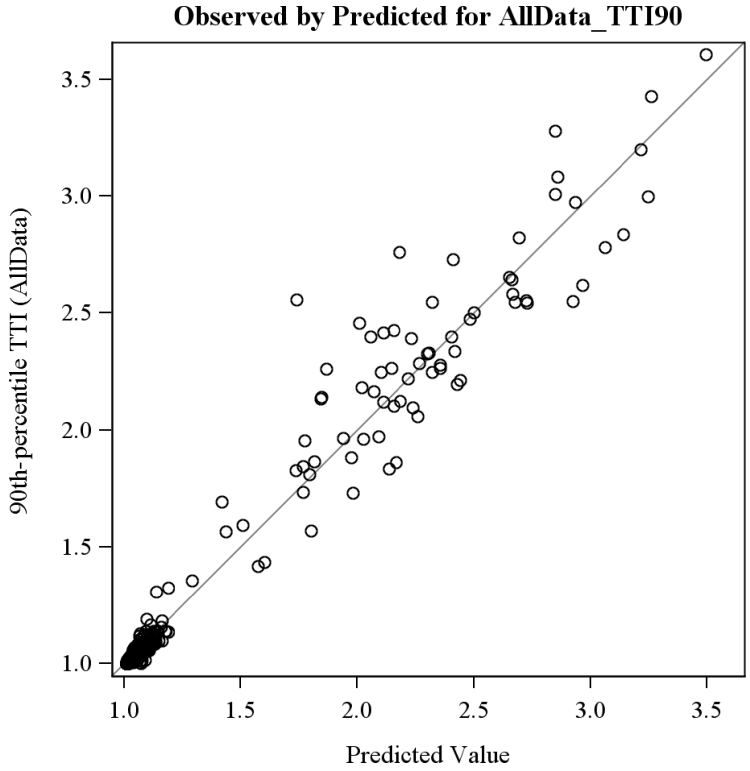

Figure E.184. Observed-by-predicted plot, new model: power form with two parameters, 90th-percentile TTI, AllData.

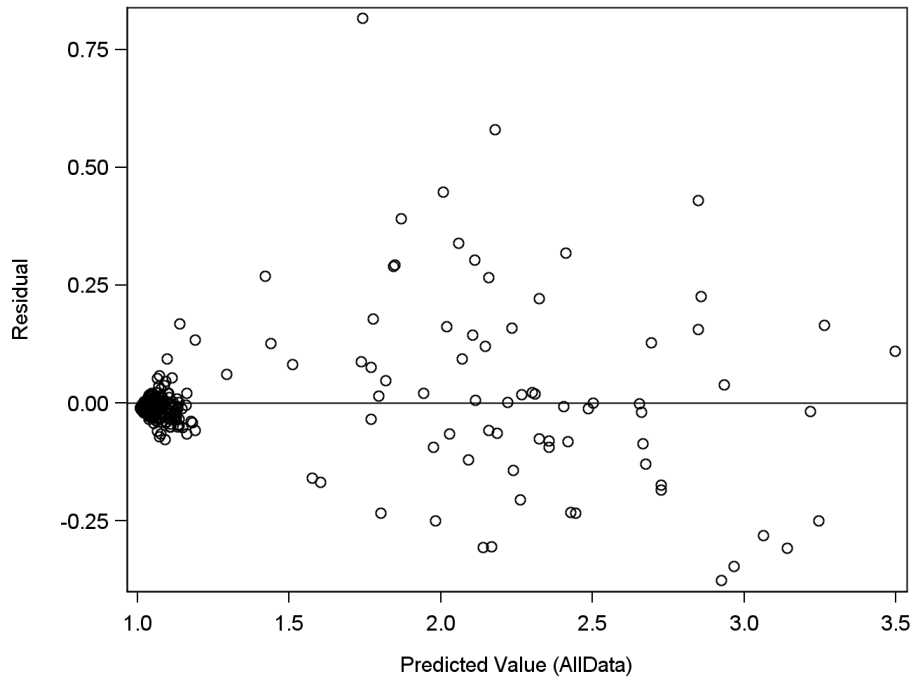

Figure E.185. Residual-by-predicted plot, new model: power form with two parameters, 90th-percentile TTI, AllData.

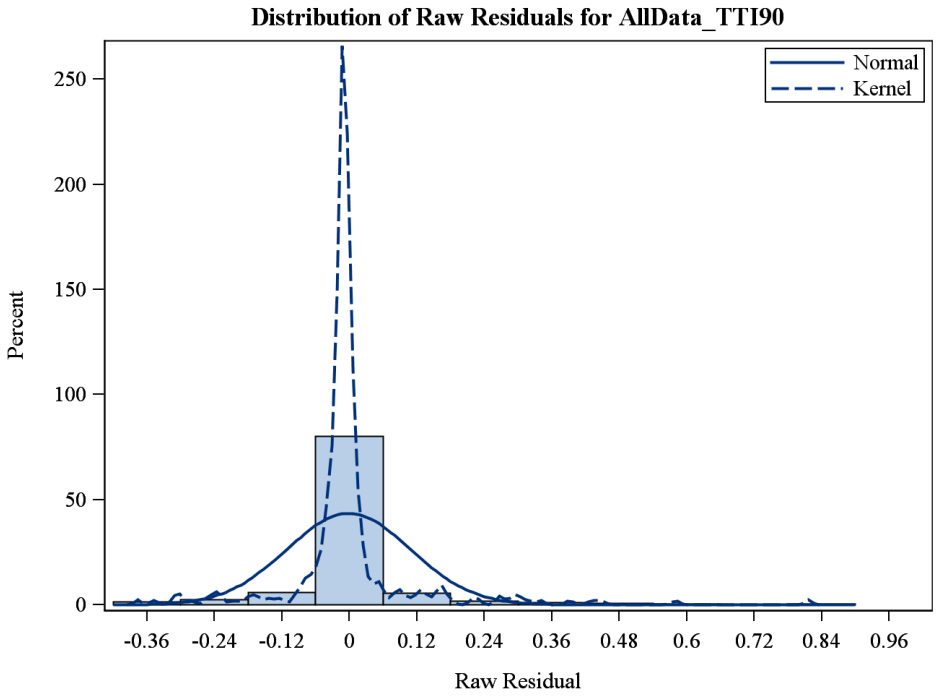

Figure E.186. Distribution of residuals, new model: power form with two parameters, 90th-percentile TTI, AllData.

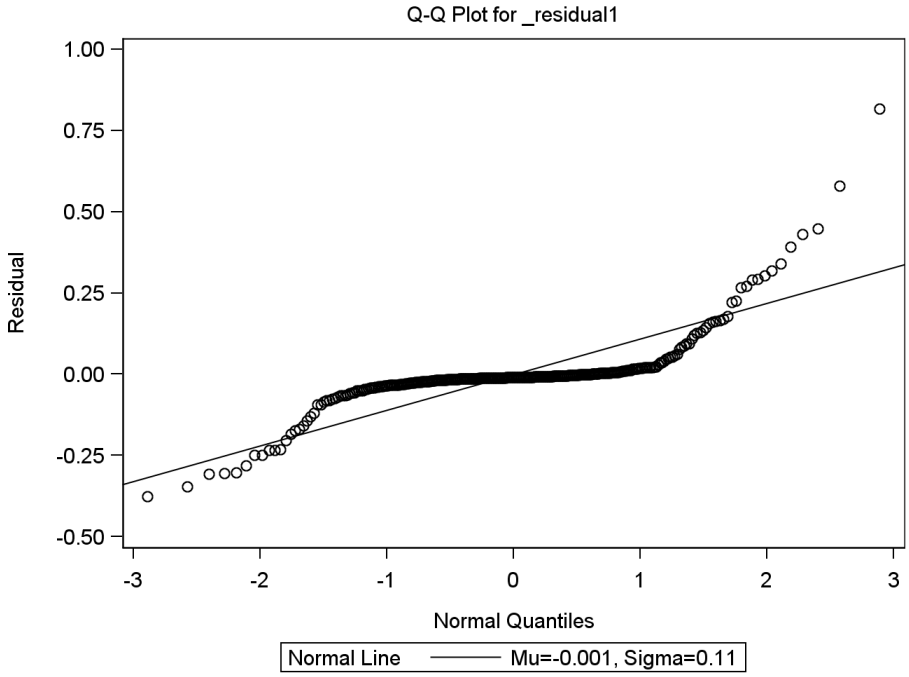

Figure E.187. Q-Q plot of residuals, new model: power form with two parameters, 90th-percentile TTI, AllData.

Table E.76. Analysis of Variance, New Model: Polynomial Form with Two Parameters, 90th-Percentile TTI, AllData

Source	DF	Sum of Squares	Mean Square	*F*-Value	Approx. Pr > *F*
Model	2	670.5	335.3	26887.0	<0.0001
Error	319	3.9778	0.0125		
Uncorrected total	321	674.5			

Table E.77. Parameter Estimates, New Model: Polynomial Form with Two Parameters, 90th-Percentile TTI, AllData

Parameter	Estimate	Approx. Std Error	Approx. 95% Confidence Limits	
a	0.3528	0.0211	0.3114	0.3943
b	0.6591	0.0159	0.6279	0.6903

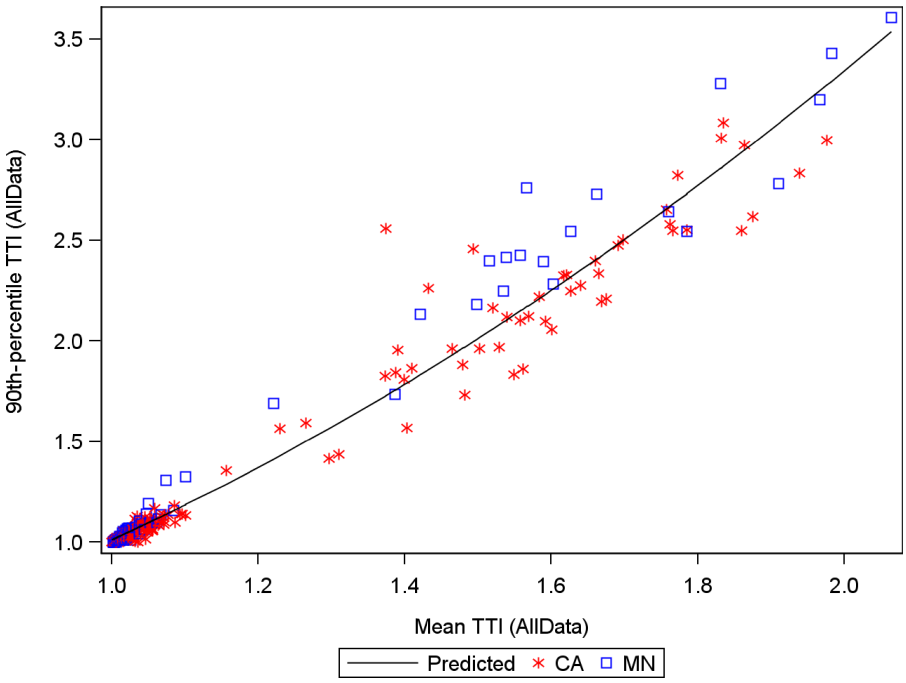

Figure E.188. Fit plot by region, new model: polynomial form with two parameters, 90th-percentile TTI, AllData.

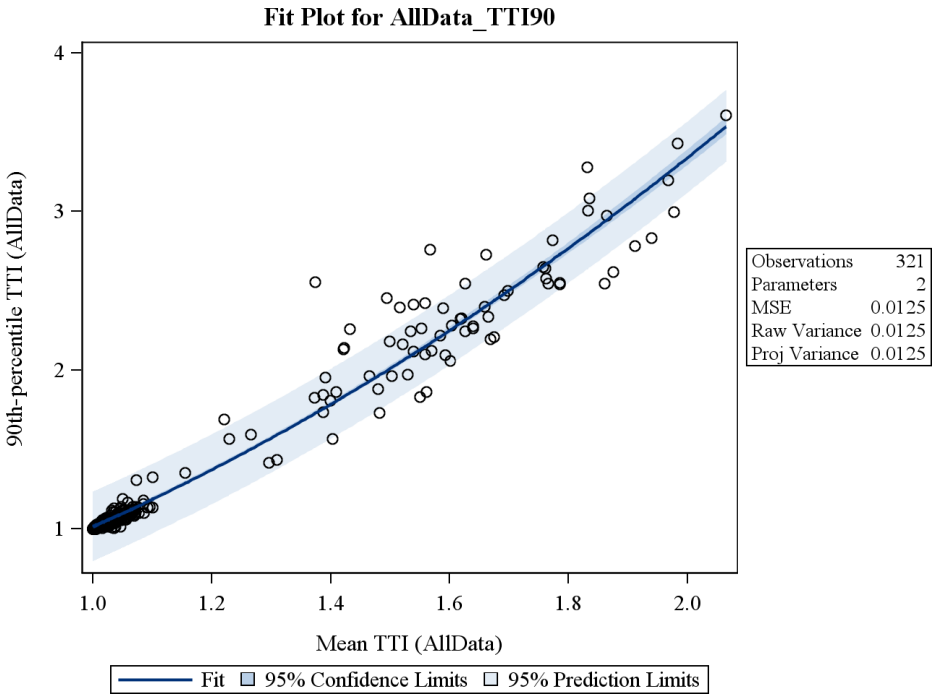

Figure E.189. Fit plot, new model: polynomial form with two parameters, 90th-percentile TTI, AllData.

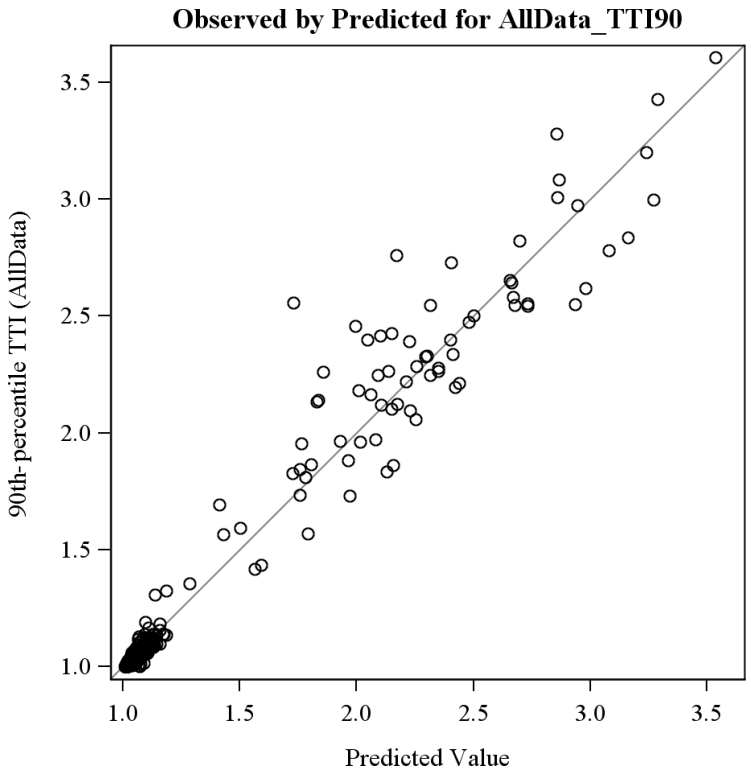

Figure E.190. Observed-by-predicted plot, new model: polynomial form with two parameters, 90th-percentile TTI, AllData.

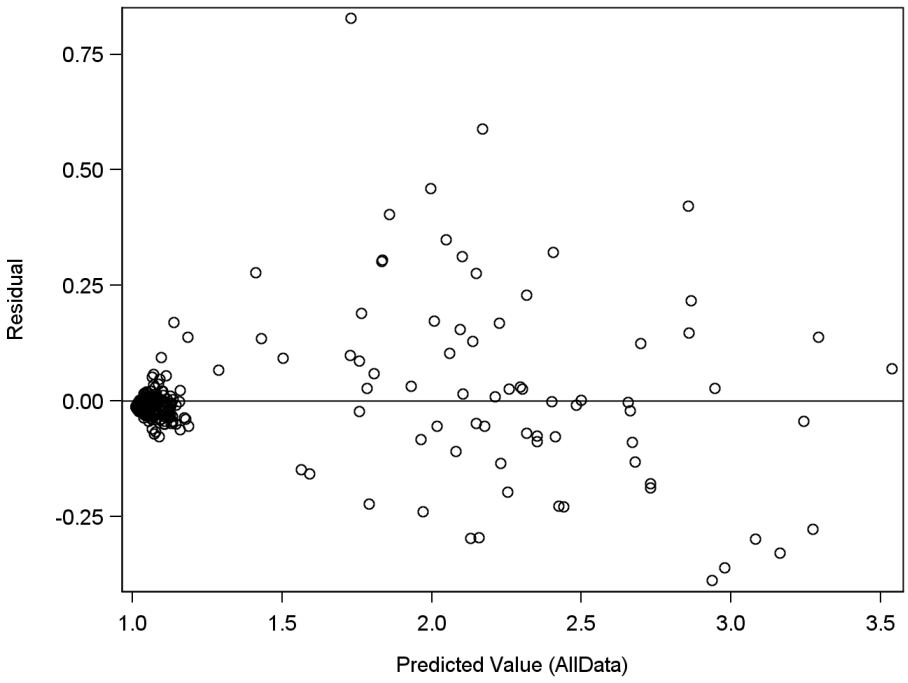

Figure E.191. Residual-by-predicted plot, new model: polynomial form with two parameters, 90th-percentile TTI, AllData.

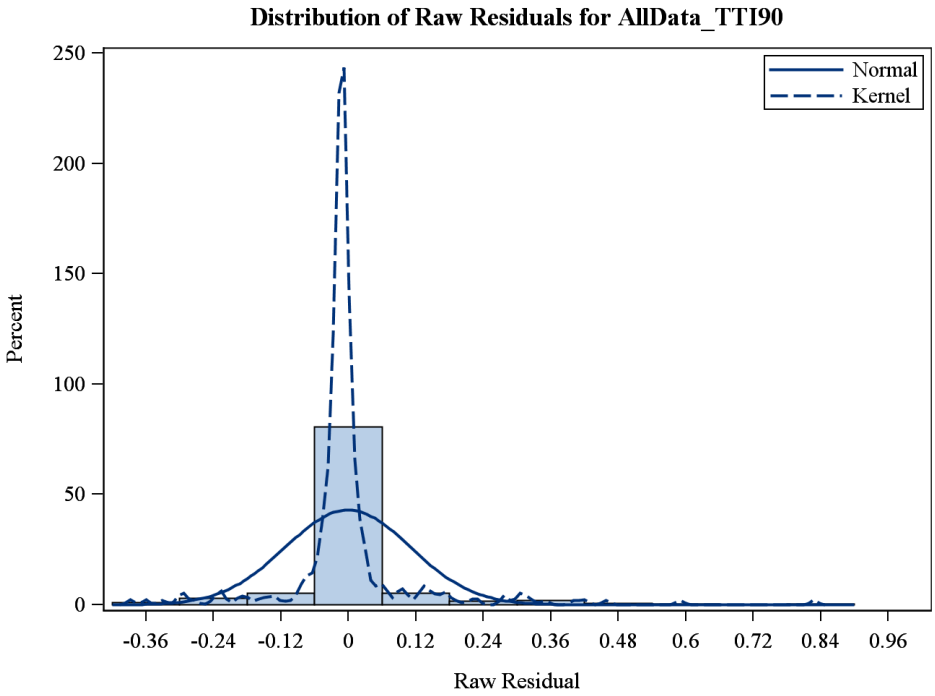

Figure E.192. Distribution of residuals, new model: polynomial form with two parameters, 90th-percentile TTI, AllData.

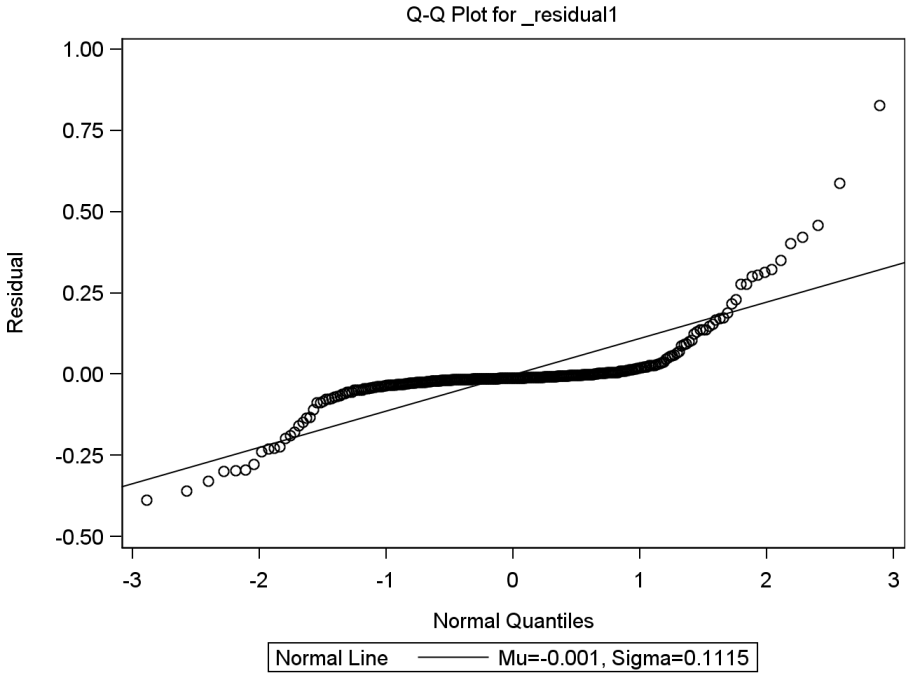

Figure E.193. Q-Q plot of residuals, new model: polynomial form with two parameters, 90th-percentile TTI, AllData.

Table E.78. Analysis of Variance, New Model: Power Form with a Single Parameter, 90th-Percentile TTI, California

Source	DF	Sum of Squares	Mean Square	*F*-Value	Approx. Pr > *F*
Model	1	397.0	397.0	33589.4	<0.0001
Error	184	2.1745	0.0118		
Uncorrected total	185	399.1			

Table E.79. Parameter Estimates, New Model: Power Form with a Single Parameter, 90th-Percentile TTI, California

Parameter	Estimate	Approx. Std Error	Approx. 95% Confidence Limits	
b	1.6826	0.0136	1.6559	1.7094

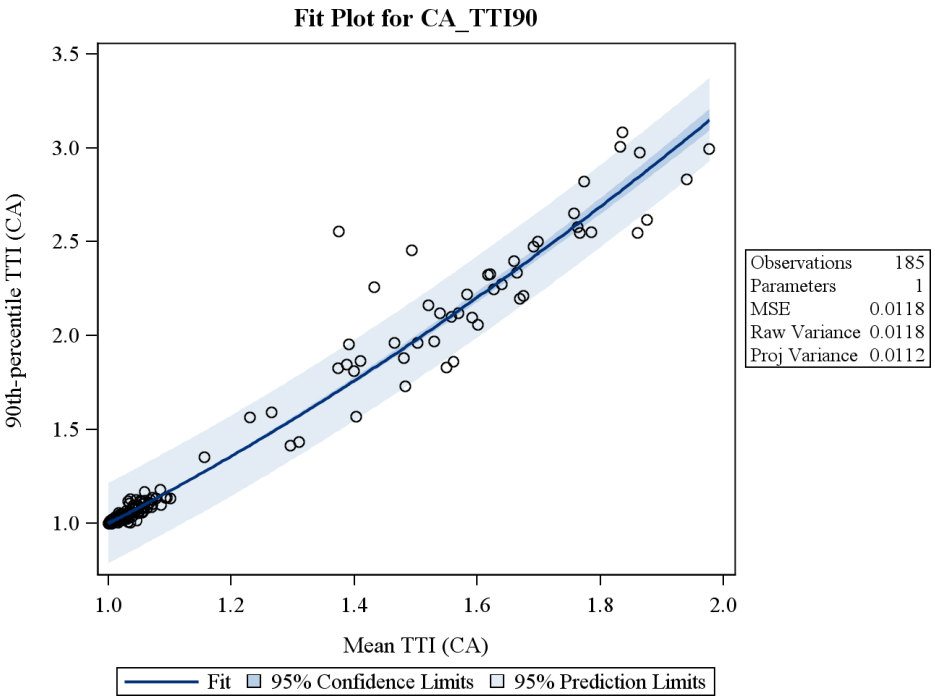

Figure E.194. Fit plot by region, new model: power form with a single parameter, 90th-percentile TTI, California.

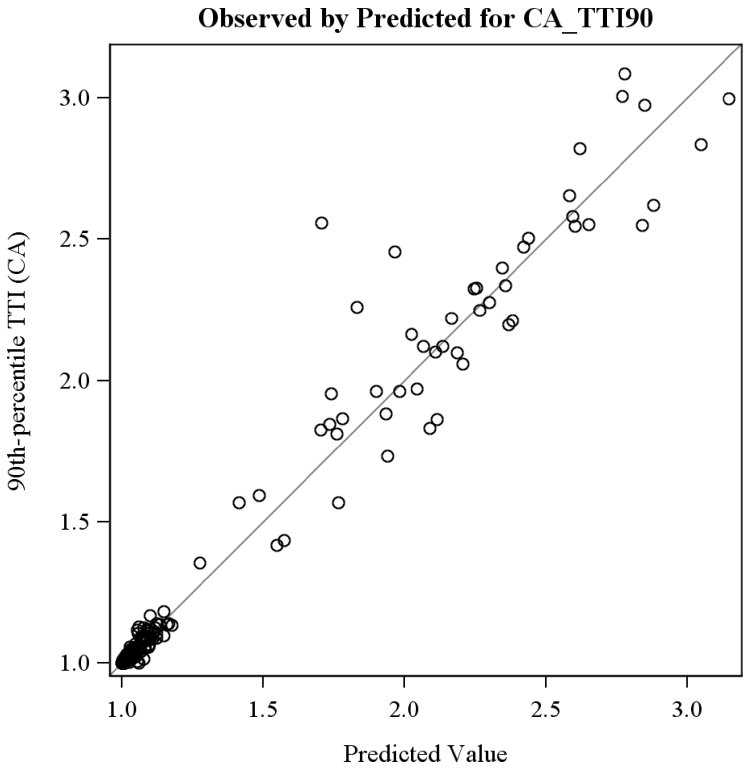

Figure E.195. Observed-by-predicted plot, new model: power form with a single parameter, 90th-percentile TTI, California.

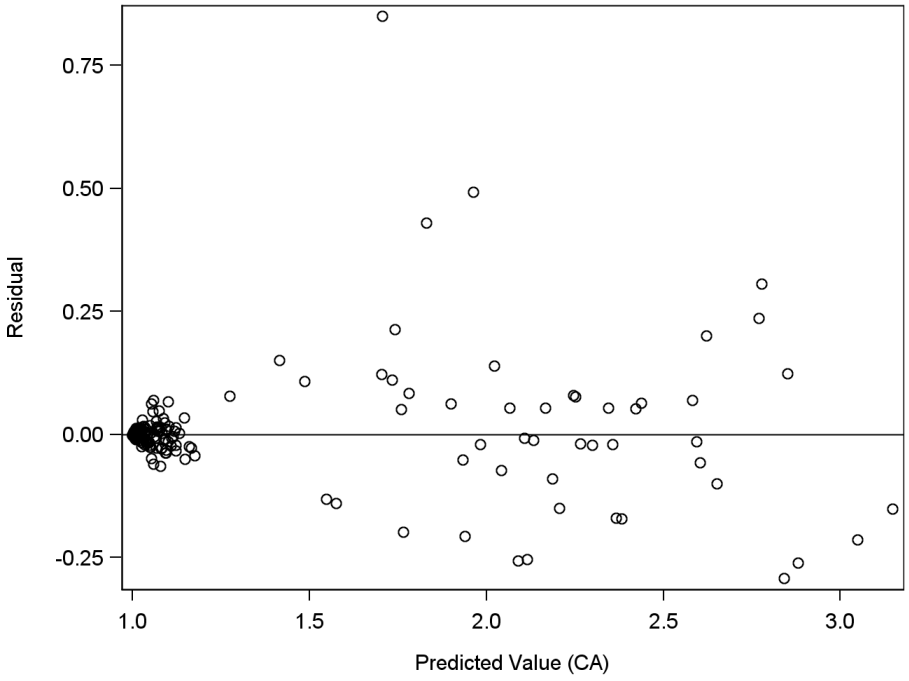

Figure E.196. Residual-by-predicted plot, new model: power form with a single parameter, 90th-percentile TTI, California.

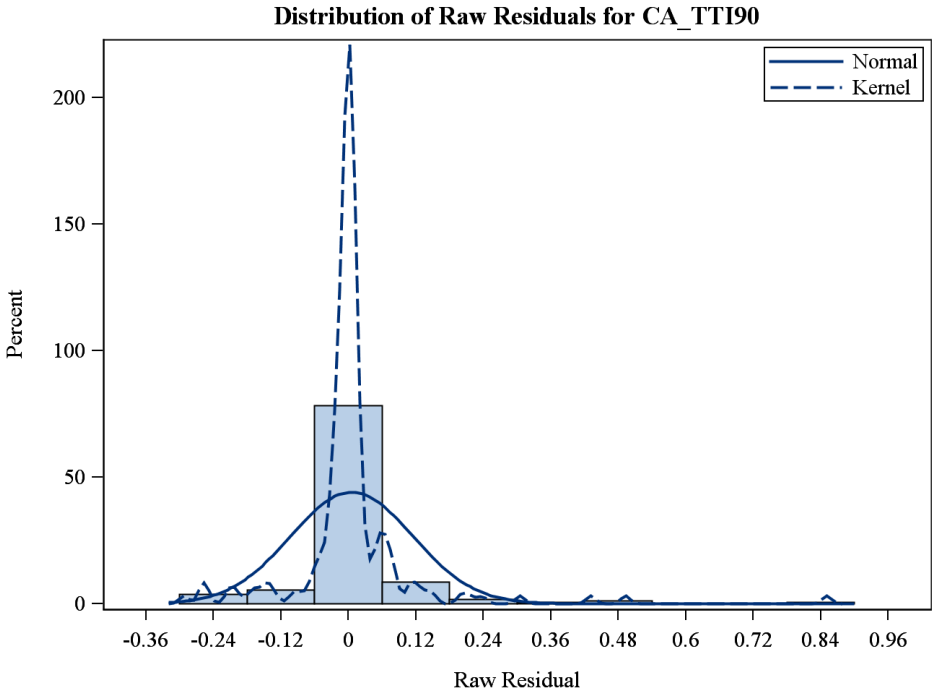

Figure E.197. Distribution of residuals, new model: power form with a single parameter, 90th-percentile TTI, California.

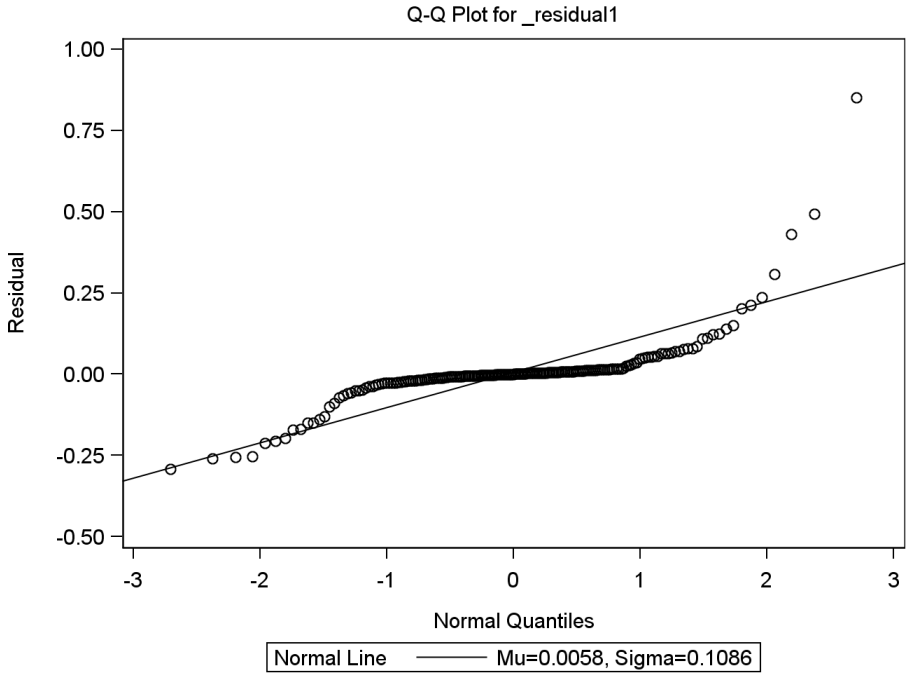

Figure E.198. Q-Q plot of residuals, new model: power form with a single parameter, 90th-percentile TTI, California.

Table E.80. Analysis of Variance, New Model: Power Form with Two Parameters, 90th-Percentile TTI, California

Source	DF	Sum of Squares	Mean Square	*F*-Value	Approx. Pr > *F*
Model	2	397.0	198.5	16793.9	<0.0001
Error	183	2.1628	0.0118		
Uncorrected total	185	399.1			

Table E.81. Parameter Estimates, New Model: Power Form with Two Parameters, 90th-Percentile TTI, California

Parameter	Estimate	Approx. Std Error	Approx. 95% Confidence Limits	
a	1.0090	0.00905	0.9911	1.0268
b	1.6651	0.0223	1.6212	1.7091

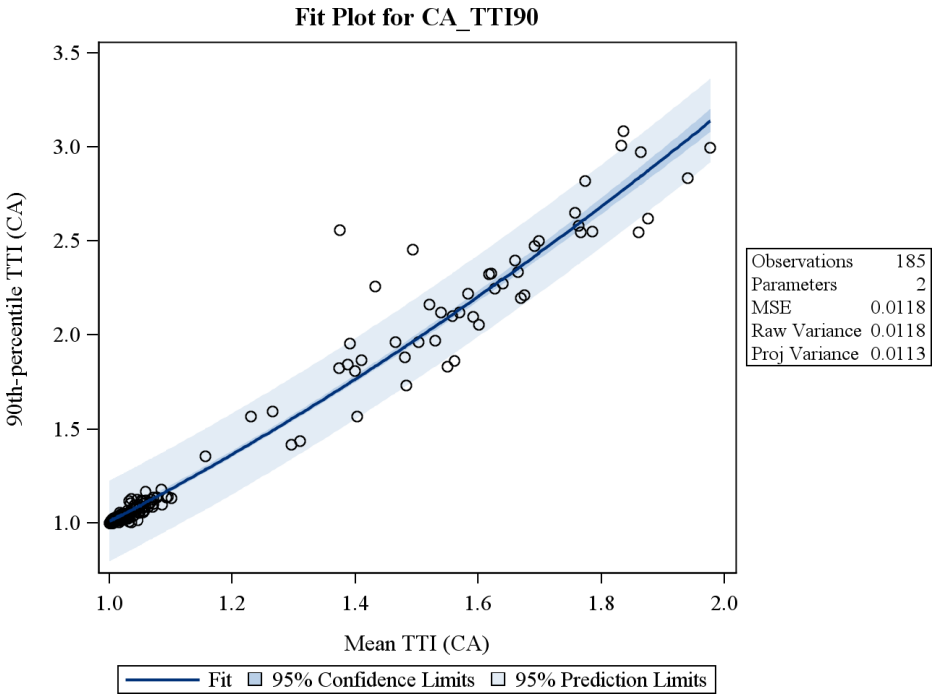

Figure E.199. Fit plot, new model: power form with two parameters, 90th-percentile TTI, California.

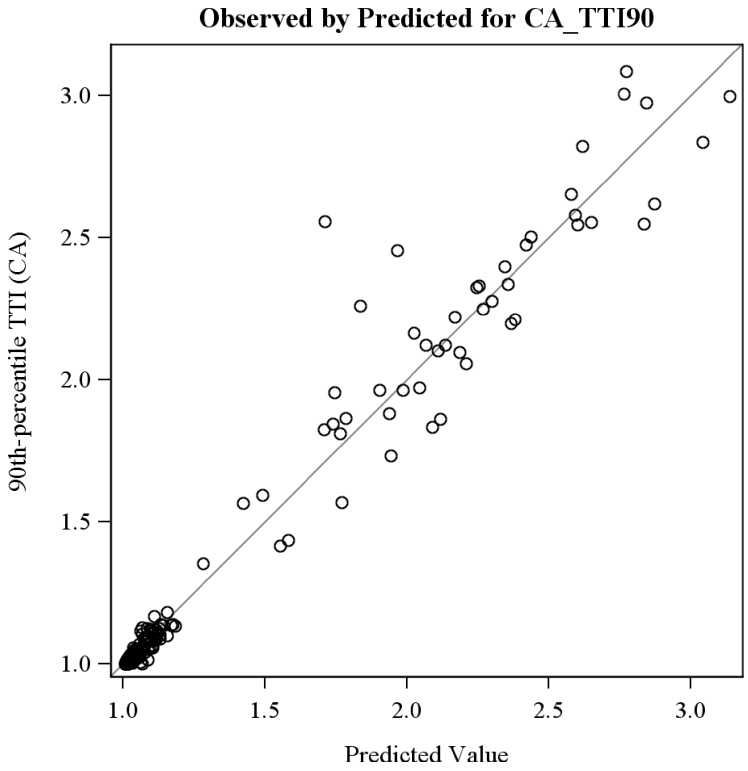

Figure E.200. Observed-by-predicted plot, new model: power form with two parameters, 90th-percentile TTI, California.

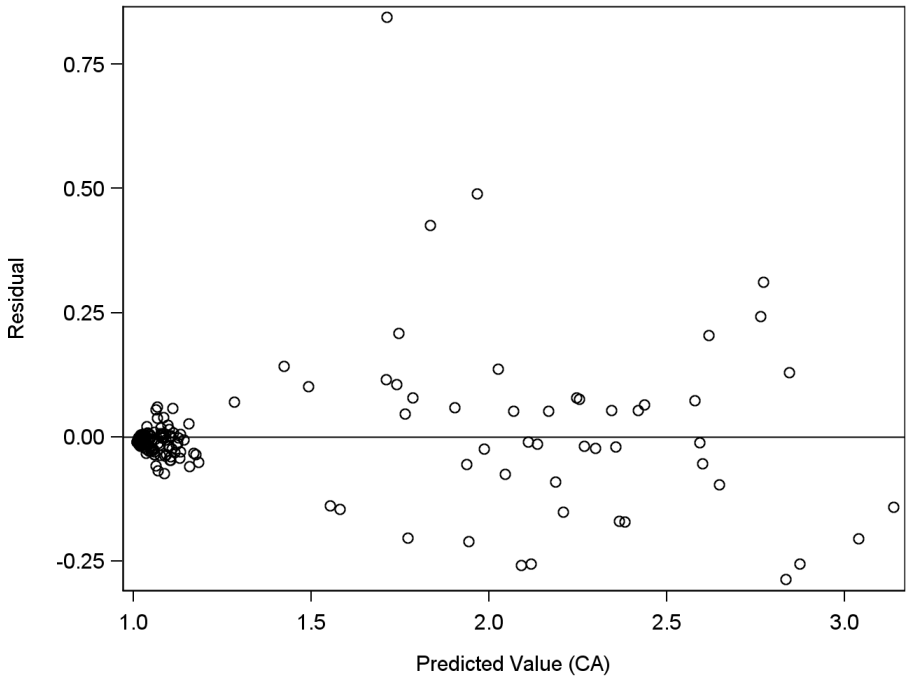

Figure E.201. Residual-by-predicted plot, new model: power form with two parameters, 90th-percentile TTI, California.

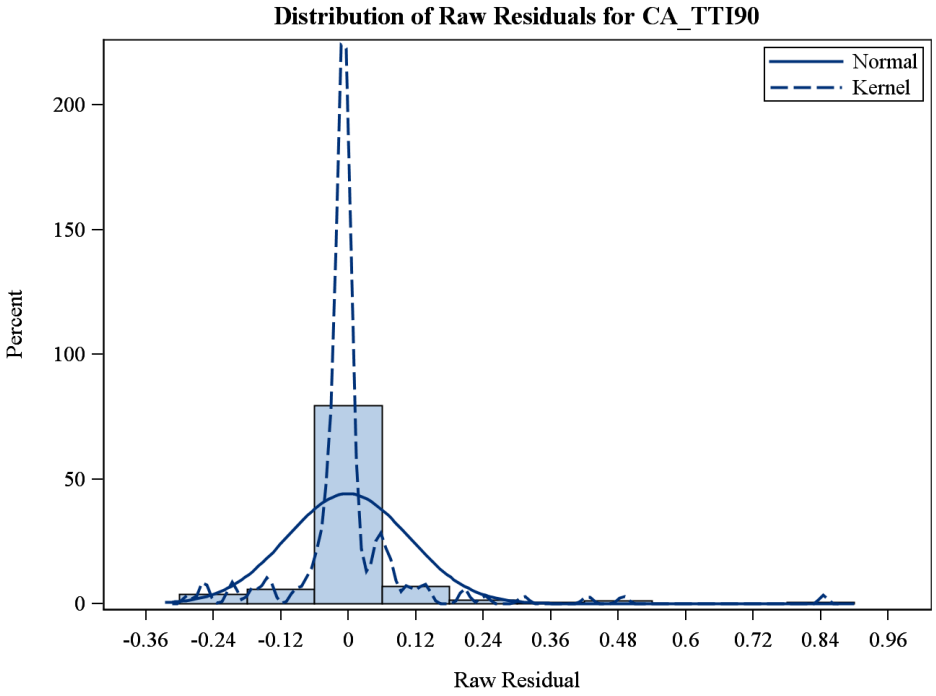

Figure E.202. Distribution of residuals, new model: power form with two parameters, 90th-percentile TTI, California.

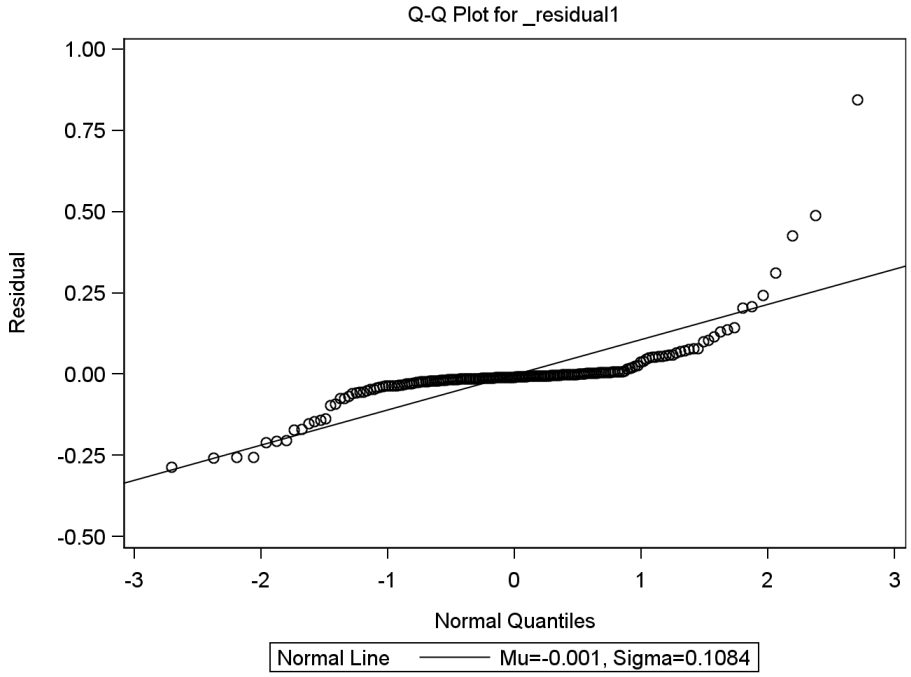

Figure E.203. Q-Q plot of residuals, new model: power form with two parameters, 90th-percentile TTI, California.

Table E.82. Analysis of Variance, New Model: Polynomial Form with Two Parameters, 90th-Percentile TTI, California

Source	DF	Sum of Squares	Mean Square	*F*-Value	Approx. Pr > *F*
Model	2	396.9	198.5	16354.7	<0.0001
Error	183	2.2206	0.0121		
Uncorrected total	185	399.1			

Table E.83. Parameter Estimates, New Model: Polynomial Form with Two Parameters, 90th-Percentile TTI, California

Parameter	Estimate	Approx. Std Error	Approx. 95% Confidence Limits	
a	0.4060	0.0279	0.3510	0.4610
b	0.6055	0.0207	0.5648	0.6463

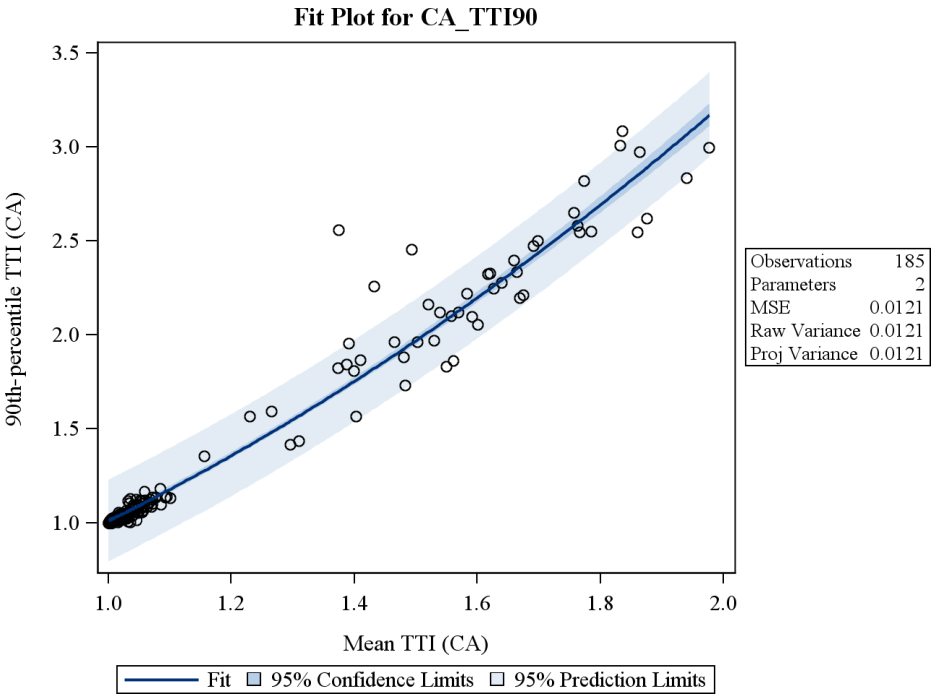

Figure E.204. Fit plot, new model: polynomial form with two parameters, 90th-percentile TTI, California.

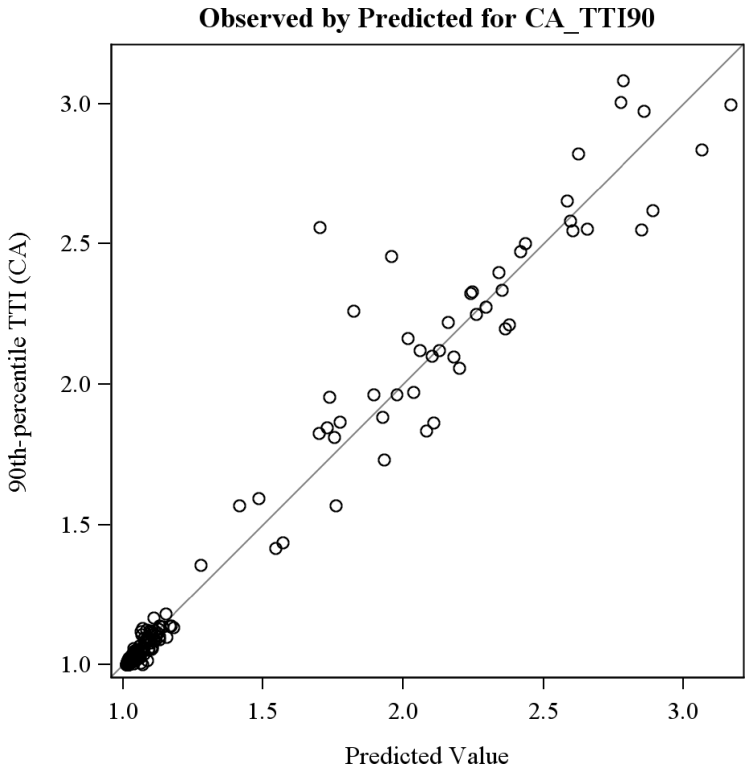

Figure E.205. Observed-by-predicted plot, new model: polynomial form with two parameters, 90th-percentile TTI, California.

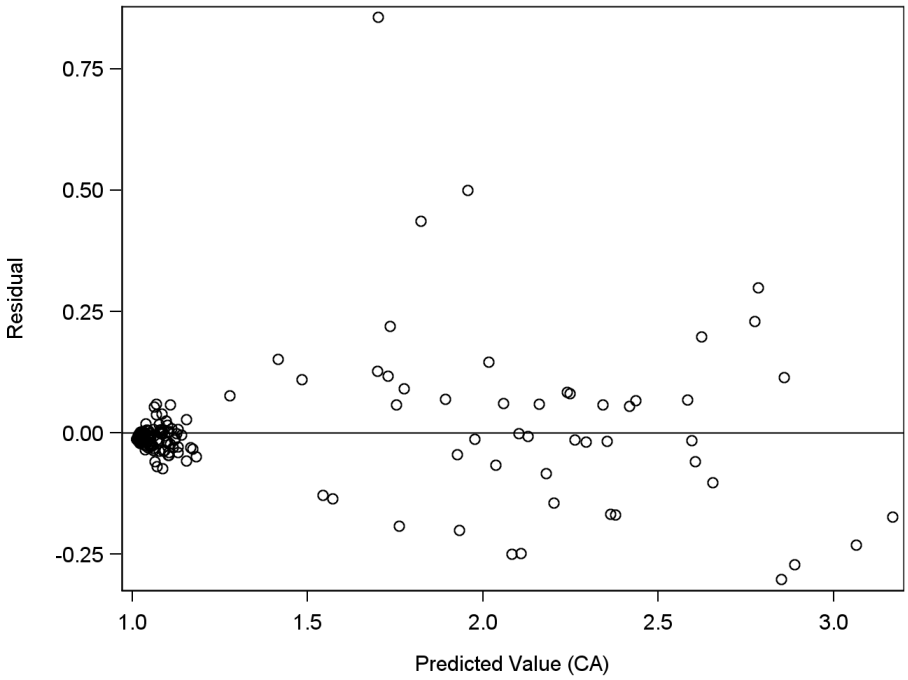

Figure E.206. Residual-by-predicted plot, new model: polynomial form with two parameters, 90th-percentile TTI, California.

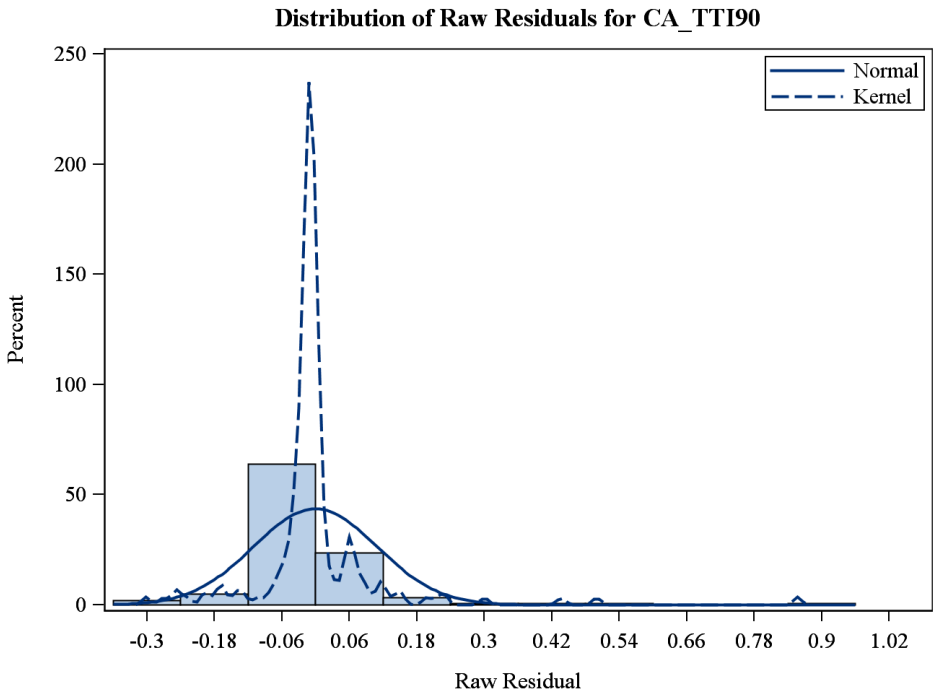

Figure E.207. Distribution of residuals, new model: polynomial form with two parameters, 90th-percentile TTI, California.

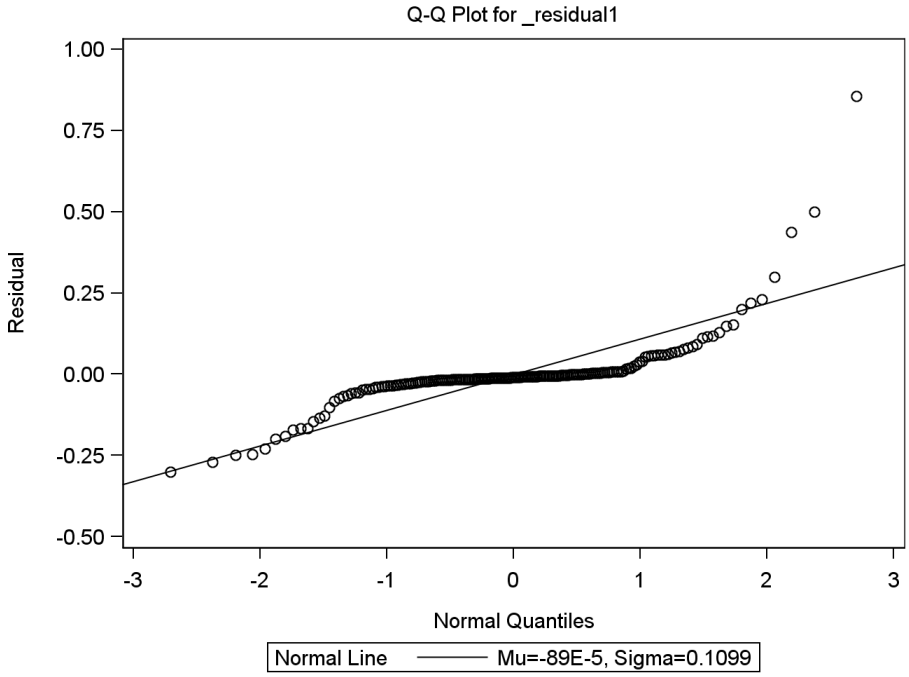

Figure E.208. Q-Q plot of residuals, new model: polynomial form with two parameters, 90th-percentile TTI, California.

Minnesota

Power Form Model with a Single Parameter

Model:

$$90\text{th-percentile TTI}_{MN} = \text{meanTTI}^{1.8113}$$

Power Form Model with Two Parameters

Model:

$$90\text{th-percentile TTI}_{MN} = 1.0320 * \text{meanTTI}^{1.7562}$$

Polynomial Form Model with Two Parameters

Model:

$$90\text{th-percentile TTI}_{MN} = 0.3102 * \text{meanTTI} + 0.7225 * \text{meanTTI}^2$$

(text continues on page 351)

Table E.84. Analysis of Variance, New Model: Power Form with a Single Parameter, 90th-Percentile TTI, Minnesota

Source	DF	Sum of Squares	Mean Square	*F*-Value	Approx. Pr > *F*
Model	1	201.6	201.6	13391.4	<0.0001
Error	78	1.1740	0.0151		
Uncorrected total	79	202.7			

Table E.85. Parameter Estimates, New Model: Power Form with a Single Parameter, 90th-Percentile TTI, Minnesota

Parameter	Estimate	Approx. Std Error	Approx. 95% Confidence Limits	
b	1.8113	0.0188	1.7739	1.8488

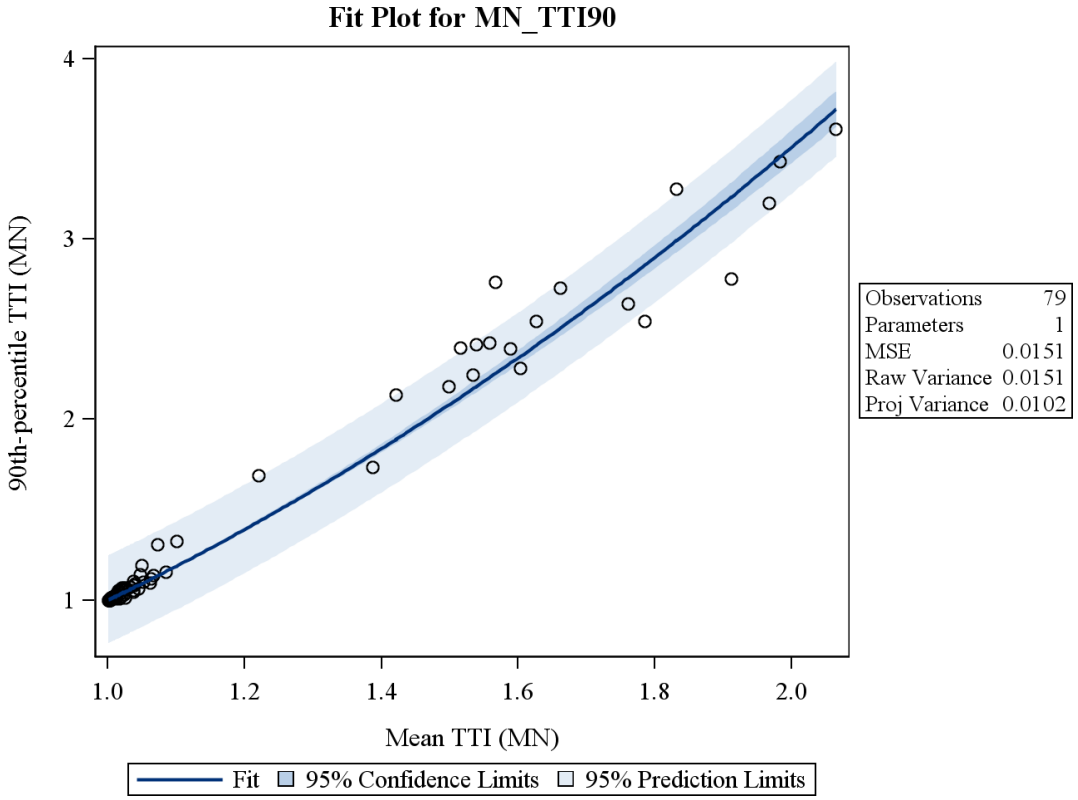

Figure E.209. Fit plot, new model: power form with a single parameter, 90th-percentile TTI, Minnesota.

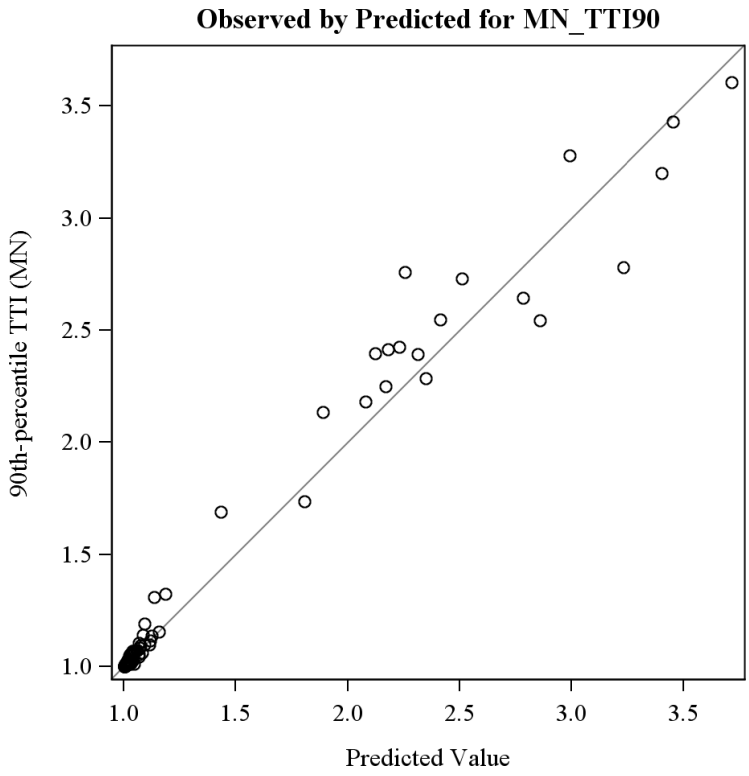

Figure E.210. Observed-by-predicted plot, new model: power form with a single parameter, 90th-percentile TTI, Minnesota.

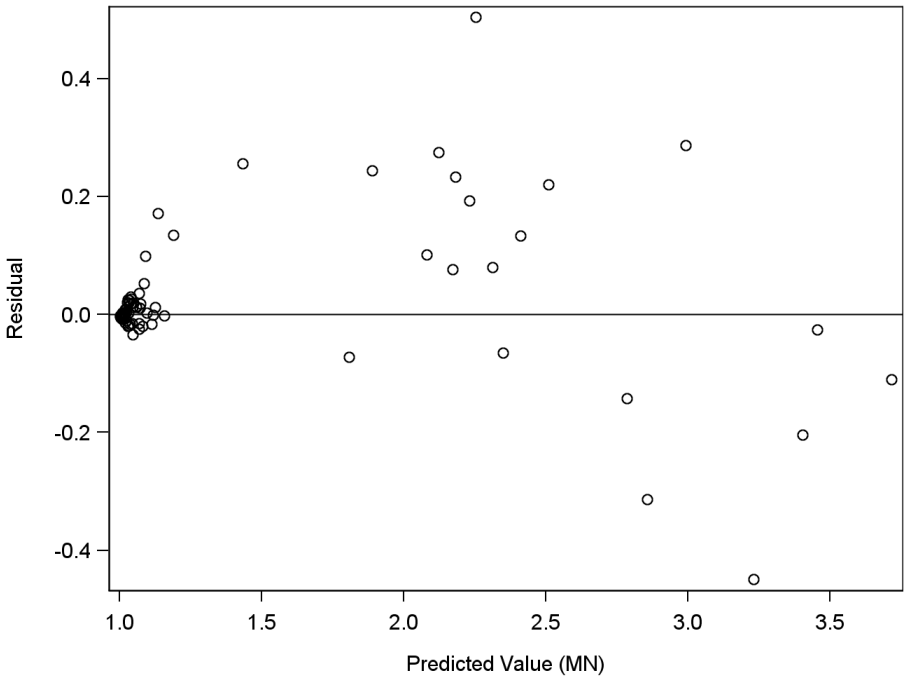

Figure E.211. Residual-by-predicted plot, new model: power form with a single parameter, 90th-percentile TTI, Minnesota.

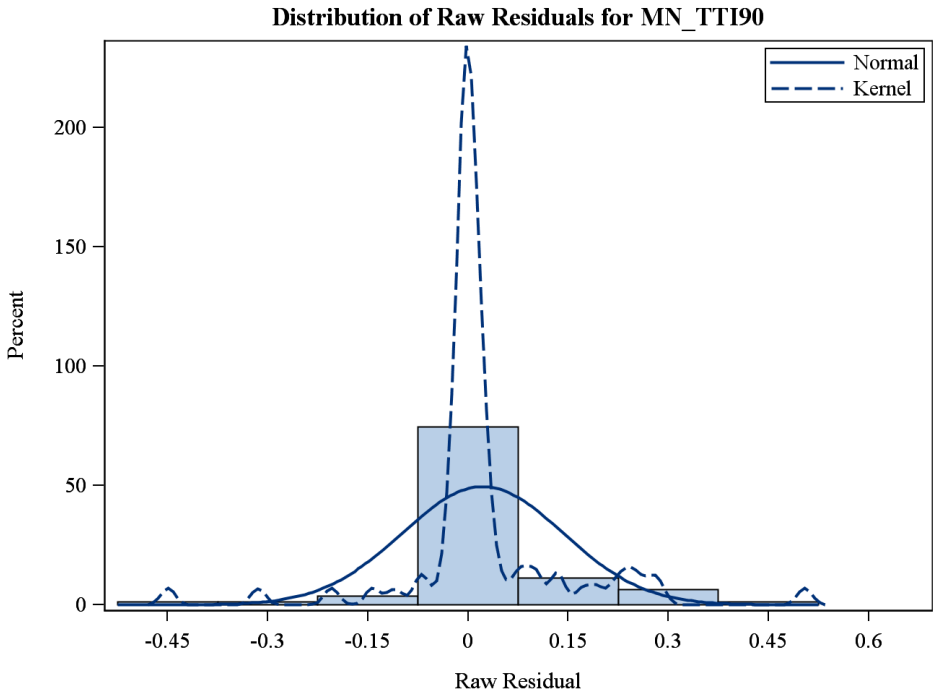

Figure E.212. Distribution of residuals, new model: power form with a single parameter, 90th-percentile TTI, Minnesota.

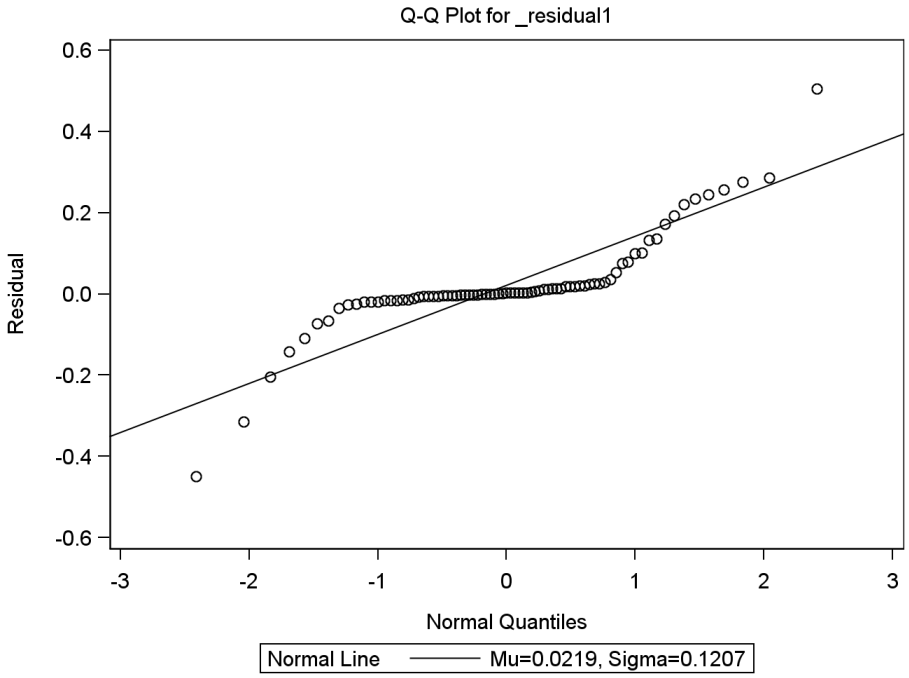

Figure E.213. Q-Q plot of residuals, new model: power form with a single parameter, 90th-percentile TTI, Minnesota.

Table E.86. Analysis of Variance, New Model: Power Form with Two Parameters, 90th-Percentile TTI, Minnesota

Source	DF	Sum of Squares	Mean Square	*F*-Value	Approx. Pr > *F*
Model	2	201.6	100.8	7018.73	<0.0001
Error	77	1.1060	0.0144		
Uncorrected total	79	202.7			

Table E.87. Parameter Estimates, New Model: Power Form with Two Parameters, 90th-Percentile TTI, Minnesota

Parameter	Estimate	Approx. Std Error	Approx. 95% Confidence Limits	
a	1.0320	0.0149	1.0024	1.0617
b	1.7562	0.0314	1.6937	1.8188

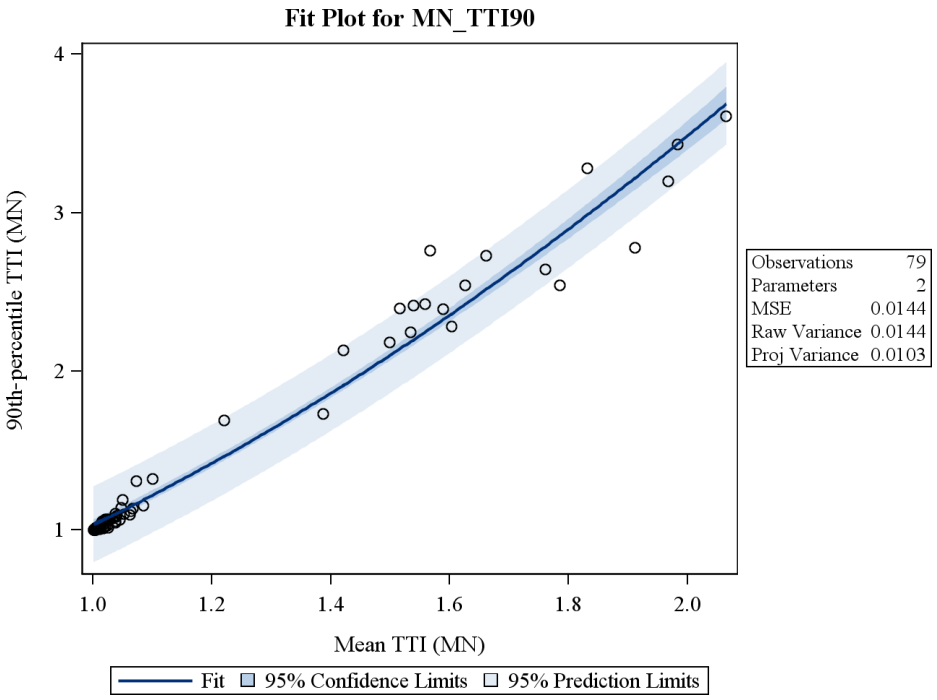

Figure E.214. Fit plot, new model: power form with two parameters, 90th-percentile TTI, Minnesota.

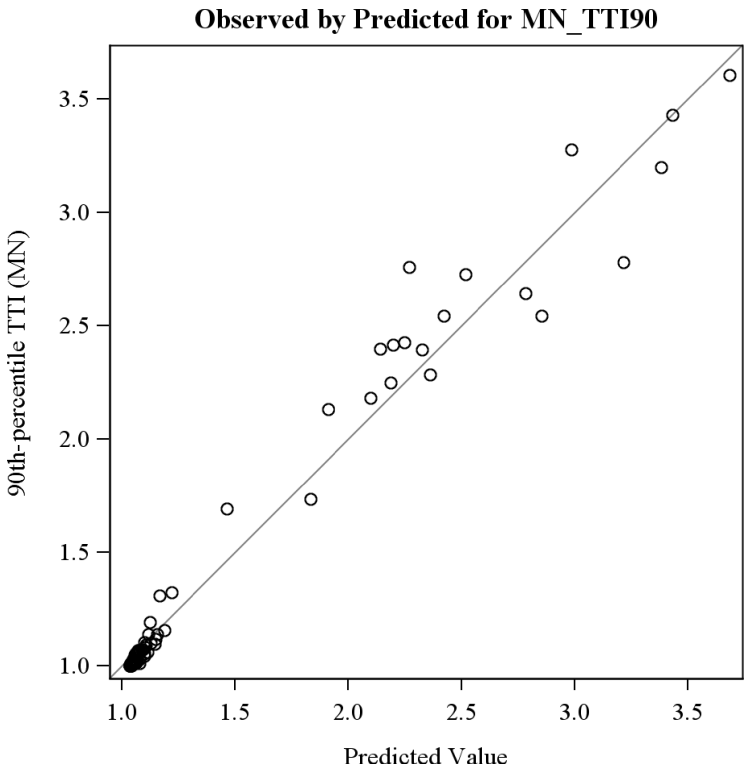

Figure E.215. Observed-by-predicted plot, new model: power form with two parameters, 90th-percentile TTI, Minnesota.

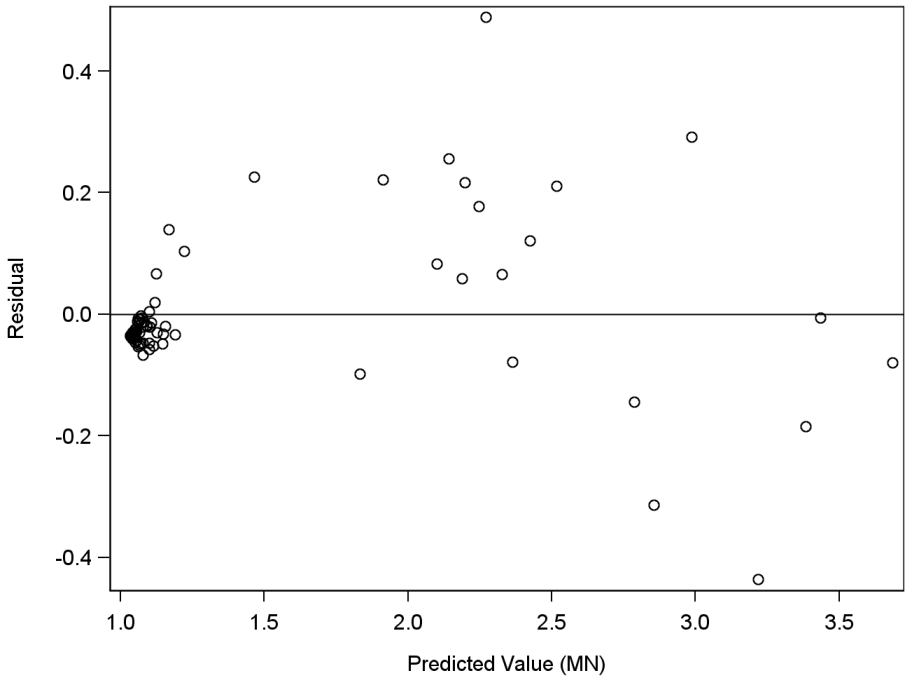

Figure E.216. Residual-by-predicted plot, new model: power form with two parameters, 90th-percentile TTI, Minnesota.

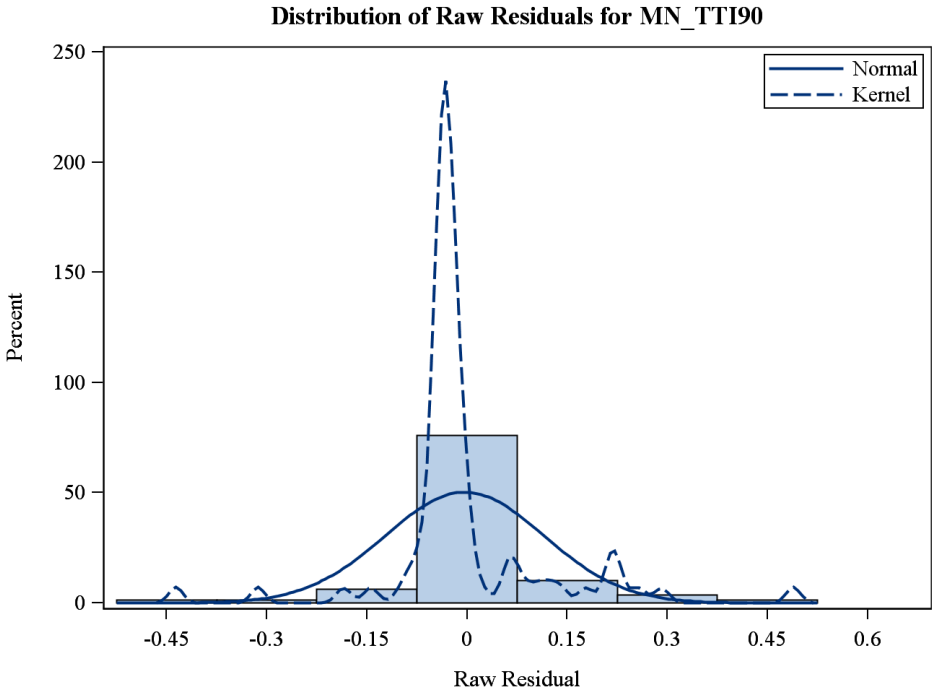

Figure E.217. Distribution of residuals, new model: power form with two parameters, 90th-percentile TTI, Minnesota.

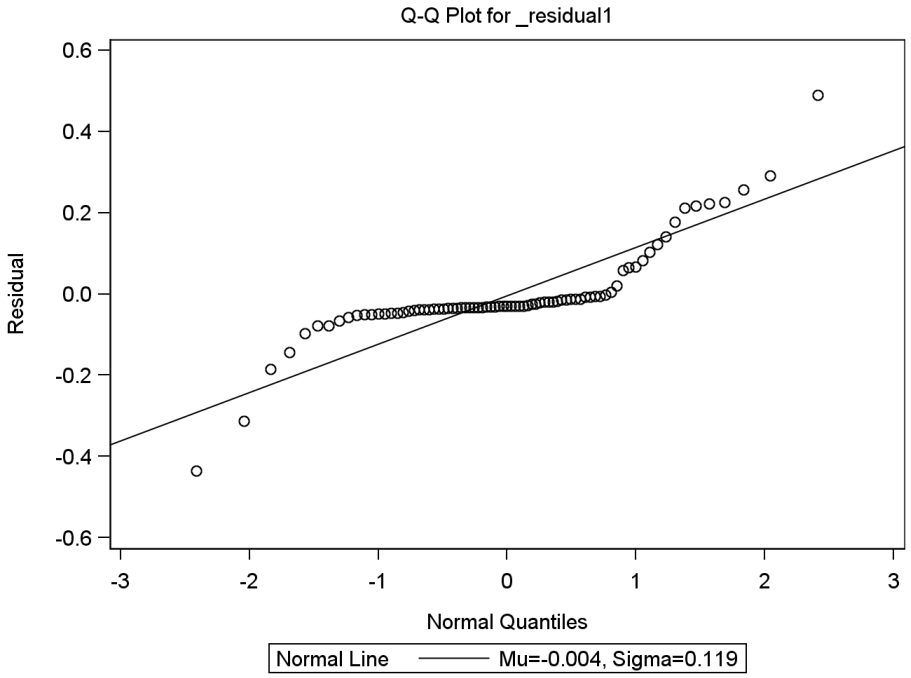

Figure E.218. Q-Q plot of residuals, new model: power form with two parameters, 90th-percentile TTI, Minnesota.

Table E.88. Analysis of Variance, New Model: Polynomial Form with Two Parameters, 90th-Percentile TTI, Minnesota

Source	DF	Sum of Squares	Mean Square	*F*-Value	Approx. Pr > *F*
Model	2	201.6	100.8	6606.74	<0.0001
Error	77	1.1746	0.0153		
Uncorrected total	79	202.7			

Table E.89. Parameter Estimates, New Model: Polynomial Form with Two Parameters, 90th-Percentile TTI, Minnesota

Parameter	Estimate	Approx. Std Error	Approx. 95% Confidence Limits	
a	0.3102	0.0429	0.2247	0.3956
b	0.7225	0.0307	0.6614	0.7837

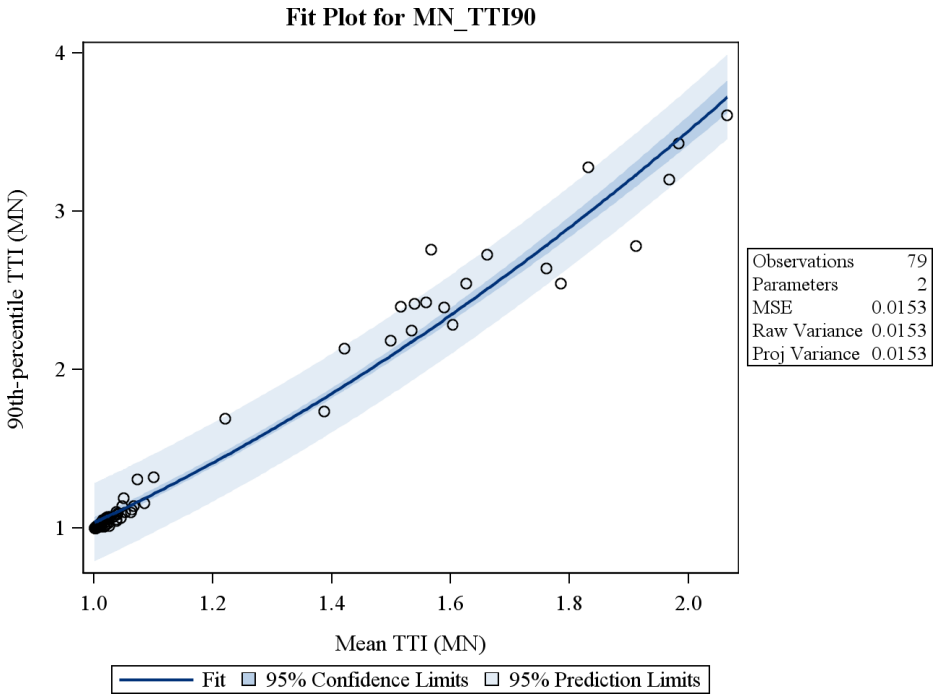

Figure E.219. Fit plot, new model: polynomial form with two parameters, 90th-percentile TTI, Minnesota.

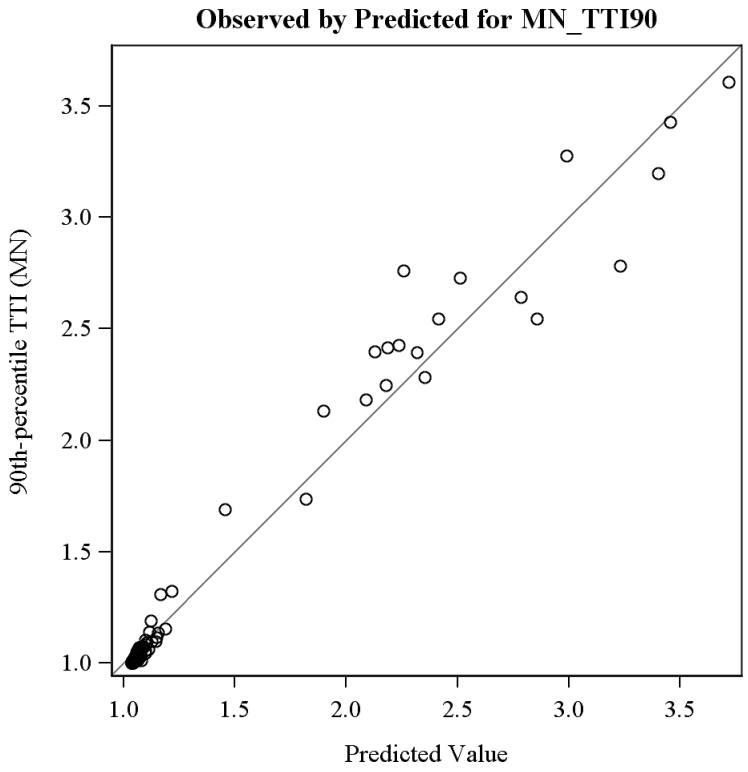

Figure E.220. Observed-by-predicted plot, new model: polynomial form with two parameters, 90th-percentile TTI, Minnesota.

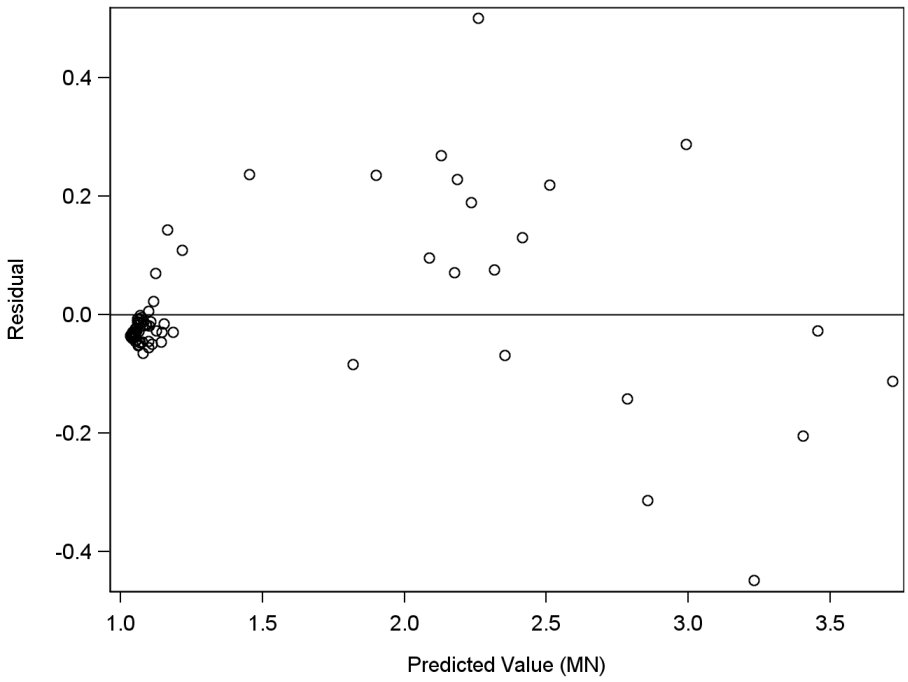

Figure E.221. Residual-by-predicted plot, new model: polynomial form with two parameters, 90th-percentile TTI, Minnesota.

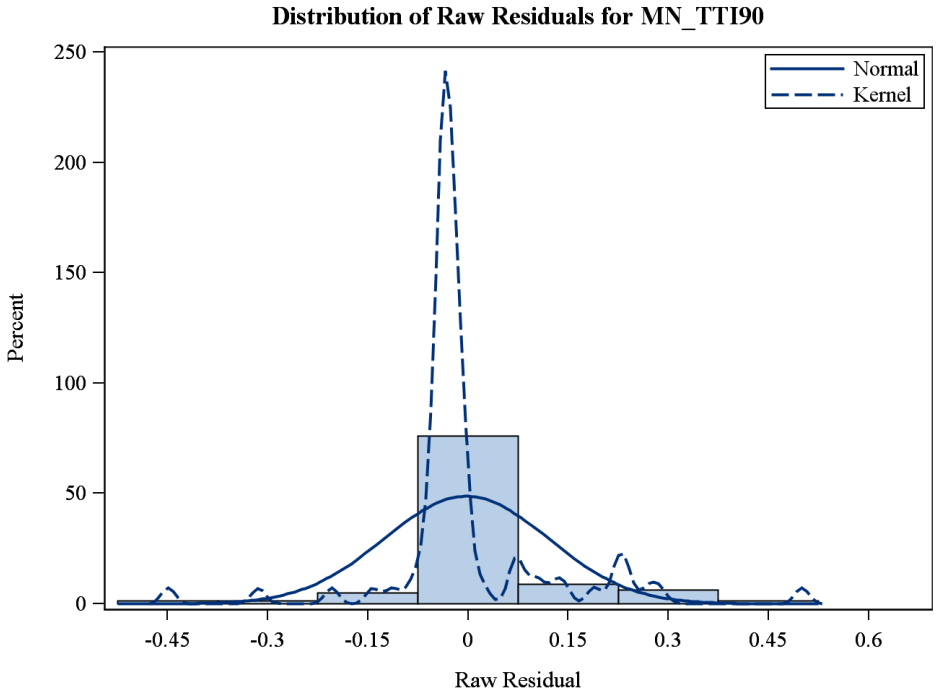

Figure E.222. Distribution of residuals, new model: polynomial form with two parameters, 90th-percentile TTI, Minnesota.

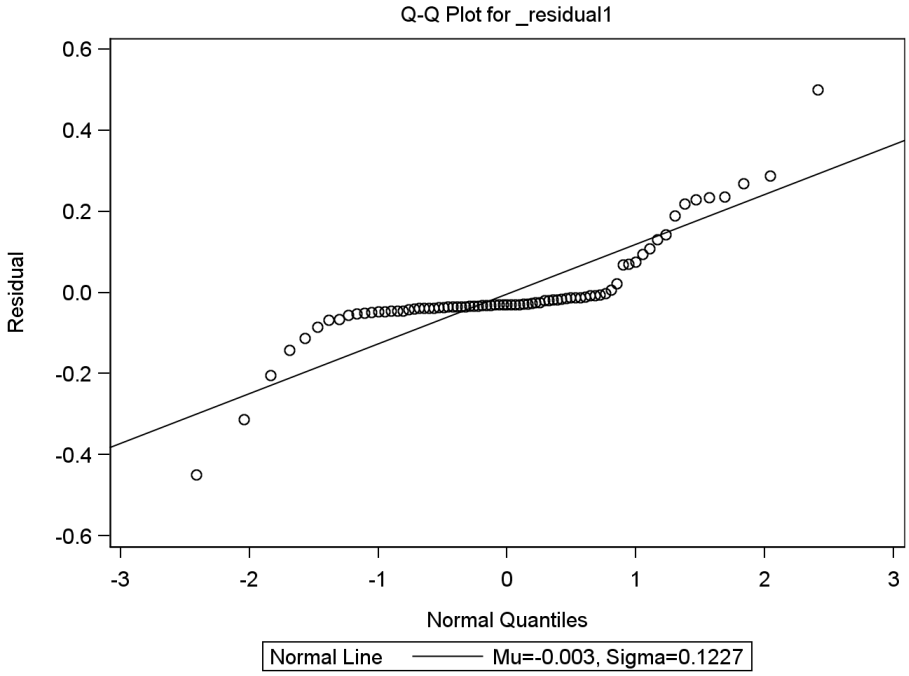

Figure E.223. Q-Q plot of residuals, new model: polynomial form with two parameters, 90th-percentile TTI, Minnesota.

80th-Percentile TTI

Summary

For the 80th-percentile TTI, the new models all have smaller MSE values than the recalibrated model. The MSE for the AllData set is reduced by almost 50% with the new models (Table E.90).

The new models (Tables E.92, E.94, E.96, E.98, E.100, E.102, E.104, E.106, and E.108) perform much better than the L03 data-poor models for the 80th-percentile TTI (*F*-tests shown in Tables E.91, E.93, E.95, E.97, E.99, E.101, E.103, E.105, and E.107). The significant improvement is shown in both the fit plots (Figures E.224, E.229, E.234, E.239, E.244, E.249, E.254, E.259, and E.264) and the observed-by-predicted plots (Figures E.225, E.230, E.235, E.240, E.245, E.250, E.255, E.260, and E.265). The residual-by-predicted plots (Figures E.226, E.231, E.236, E.241, E.246, E.251, E.256, E.261, and E.266) all show generally random patterns, although the nonconstant problem still exists. The histograms (Figures E.227, E.232, E.237, E.242, E.247, E.252, E.257, E.262, and E.267) and the normality plots (Figures E.228, E.233, E.238, E.243, E.248, E.253, E.258, E.263, and E.268) show that the residual distributions may not perfectly follow a normal distribution. Overall, the new models work much better than the L03 data-poor model for the 80th-percentile TTI.

AllData

Power Form Model with a Single Parameter

Model:

$$80\text{th-percentile TTI}_{\text{AllData}} = \text{meanTTI}^{1.4448}$$

Power Form Model with Two Parameters

Model:

$$80\text{th-percentile TTI}_{\text{AllData}} = 0.9943 * \text{meanTTI}^{1.4559}$$

Table E.90. MSE Summary Table (Comparable)

Model Name	Formula	AllData	CA	MN
Recalibration	$y = 1 + a * \ln(x)$	0.00469	0.00410	0.00506
1-parameter power	$y = x^b$	0.00239	0.00178	0.00384
2-parameter power	$y = a * x^b$	0.00237	0.00176	0.00389
2-parameter polynomial	$y = a * x + b * x^2$	0.00245	0.00179	0.00436

Table E.91. Analysis of Variance, New Model: Power Form with a Single Parameter, 80th-Percentile TTI, AllData

Source	DF	Sum of Squares	Mean Square	*F*-Value	Approx. Pr > *F*
Model	1	558.4	558.4	233468	<0.0001
Error	320	0.7654	0.00239		
Uncorrected total	321	559.2			

Table E.92. Parameter Estimates, New Model: Power Form with a Single Parameter, 80th-Percentile TTI, AllData

Parameter	Estimate	Approx. Std Error	Approx. 95% Confidence Limits	
b	1.4448	0.00549	1.4340	1.4556

Polynomial Form Model with Two Parameters

Model:

$$80\text{th-percentile TTI}_{\text{AllData}} = 0.6166 * \text{meanTTI} + 0.3809 * \text{meanTTI}^2$$

California

Power Form Model with a Single Parameter

Model:

$$80\text{th-percentile TTI}_{\text{CA}} = \text{meanTTI}^{1.4148}$$

Power Form Model with Two Parameters

Model:

$$80\text{th-percentile TTI}_{\text{CA}} = 0.9943 * \text{meanTTI}^{1.4264}$$

Polynomial Form Model with Two Parameters

Model:

$$80\text{th-percentile TTI}_{\text{CA}} = 0.6428 * \text{meanTTI} + 0.3547 * \text{meanTTI}^2$$

(text continues on page 369)

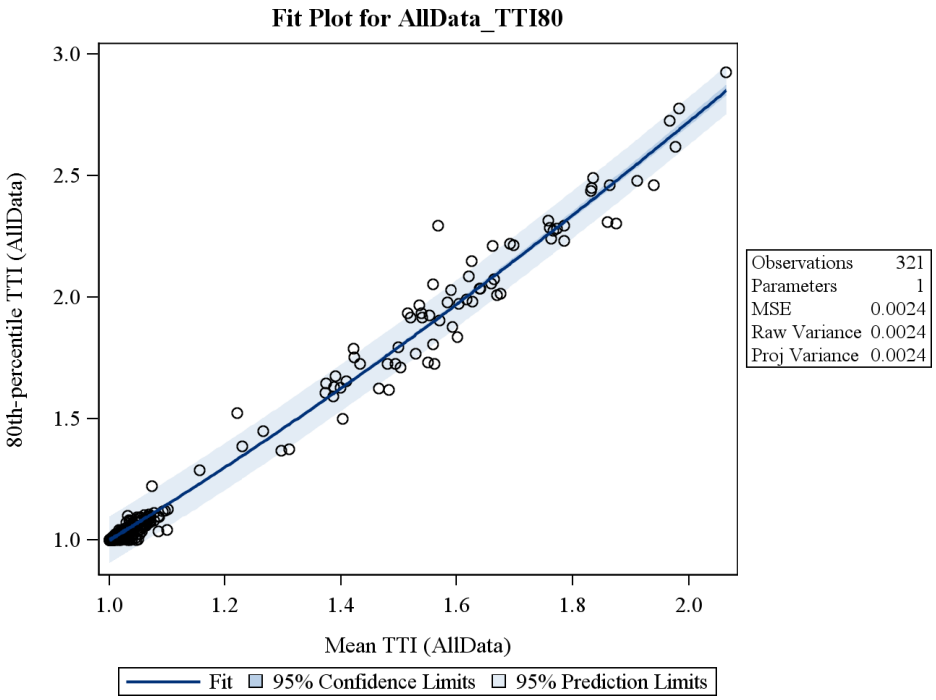

Figure E.224. Fit plot, new model: power form with a single parameter, 80th-percentile TTI, AllData.

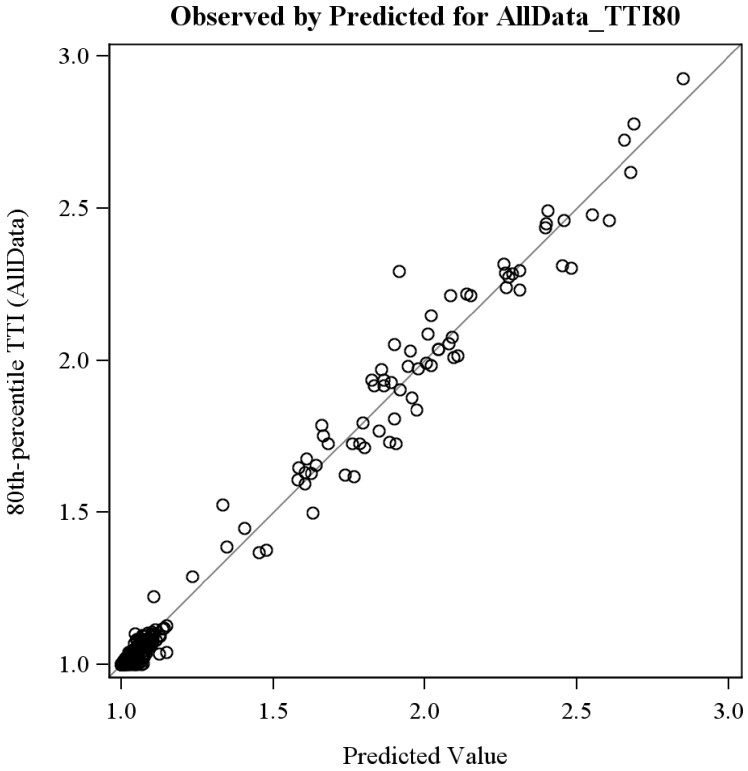

Figure E.225. Observed-by-predicted plot, new model: power form with a single parameter, 80th-percentile TTI, AllData.

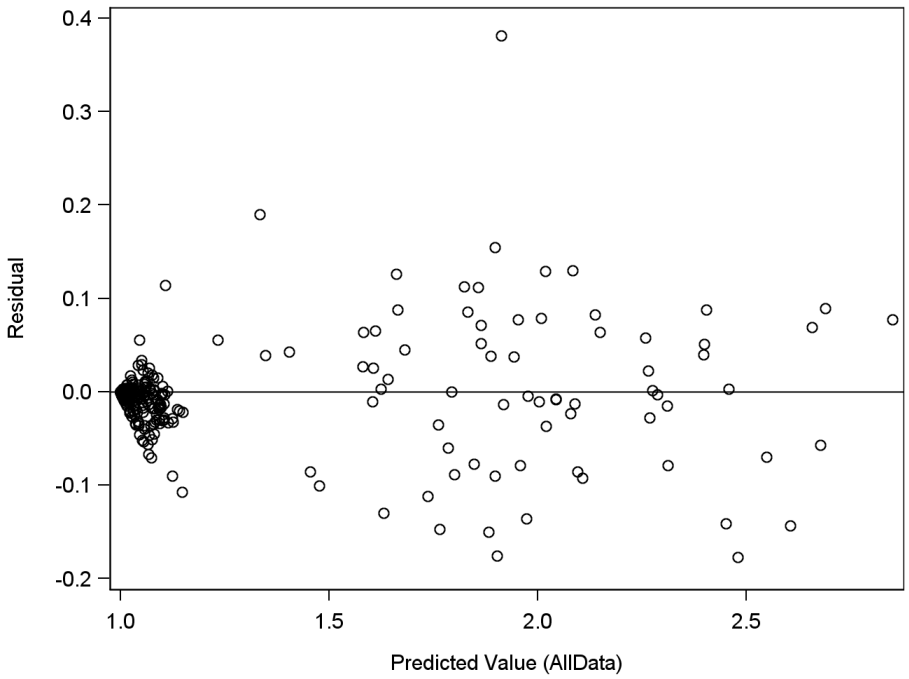

Figure E.226. Residual-by-predicted plot, new model: power form with a single parameter, 80th-percentile TTI, AllData.

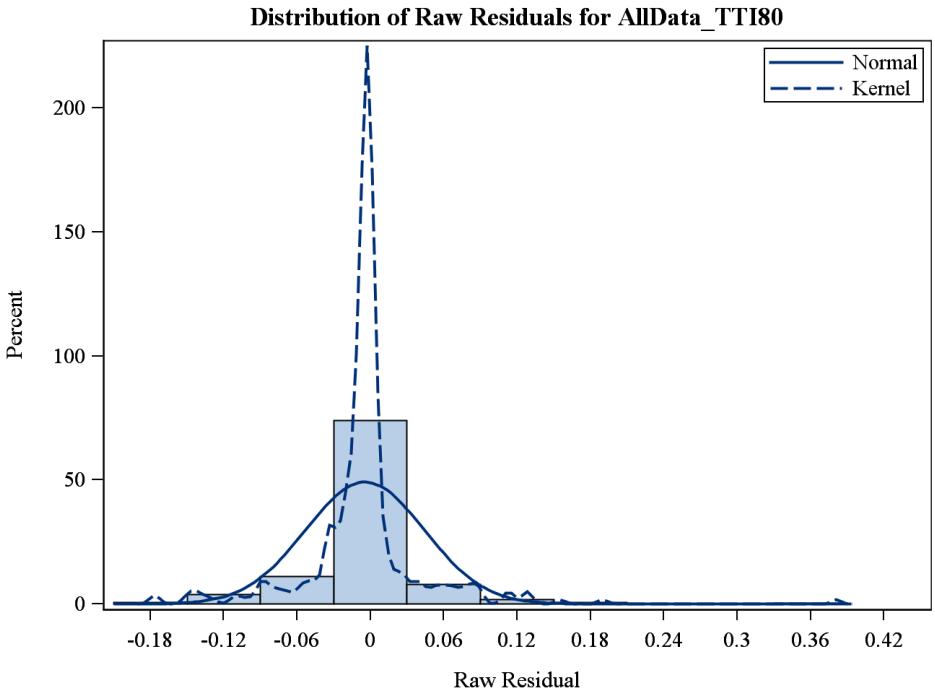

Figure E.227. Distribution of residuals, new model: power form with a single parameter, 80th-percentile TTI, AllData.

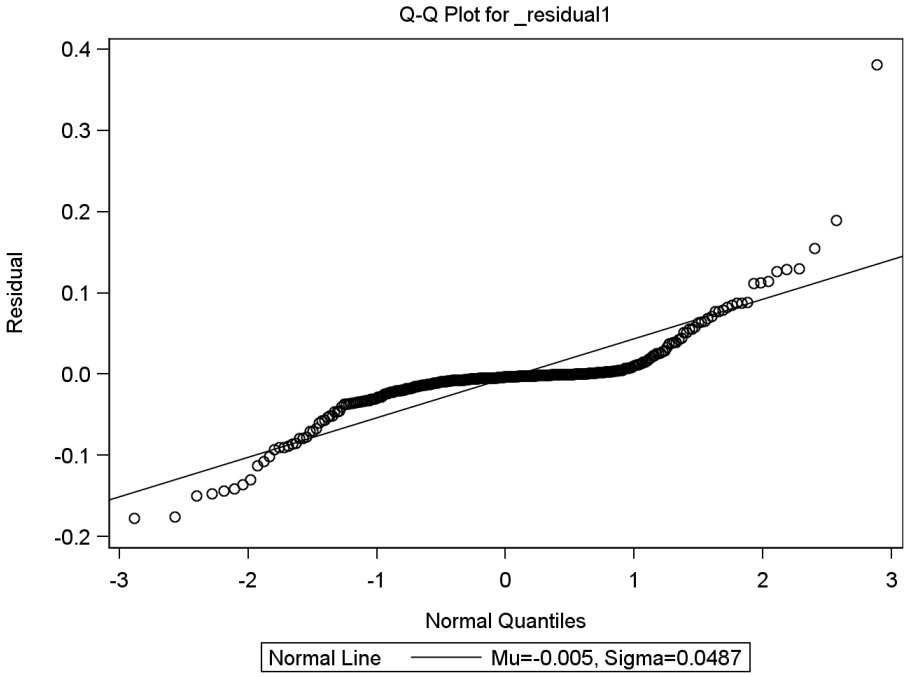

Figure E.228. Q-Q plot of residuals, new model: power form with a single parameter, 80th-percentile TTI, AllData.

Table E.93. Analysis of Variance, New Model: Power Form with Two Parameters, 80th-Percentile TTI, AllData

Source	DF	Sum of Squares	Mean Square	*F*-Value	Approx. Pr > *F*
Model	2	558.4	279.2	117639	<0.0001
Error	319	0.7571	0.00237		
Uncorrected total	321	559.2			

Table E.94. Parameter Estimates, New Model: Power Form with Two Parameters, 80th-Percentile TTI, AllData

Parameter	Estimate	Approx. Std Error	Approx. 95% Confidence Limits	
a	0.9943	0.00304	0.9884	1.0003
b	1.4559	0.00810	1.4399	1.4718

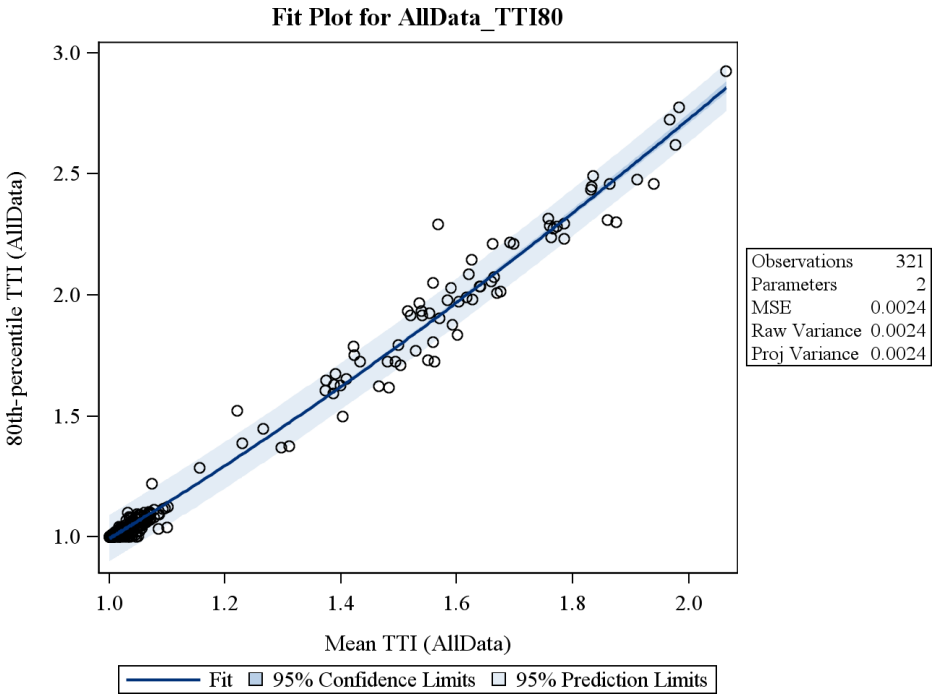

Figure E.229. Fit plot, new model: power form with two parameters, 80th-percentile TTI, AllData.

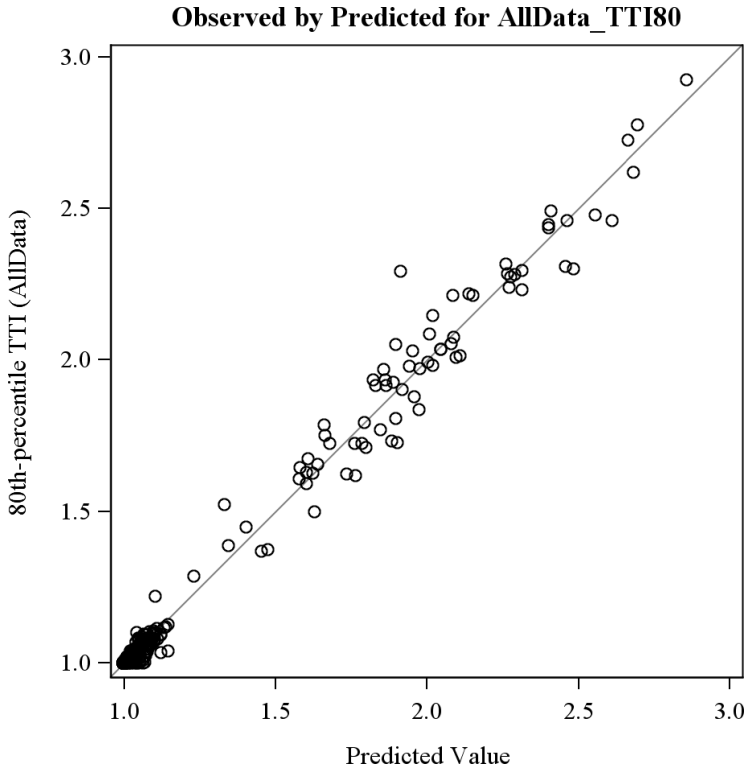

Figure E.230. Observed-by-predicted plot, new model: power form with two parameters, 80th-percentile TTI, AllData.

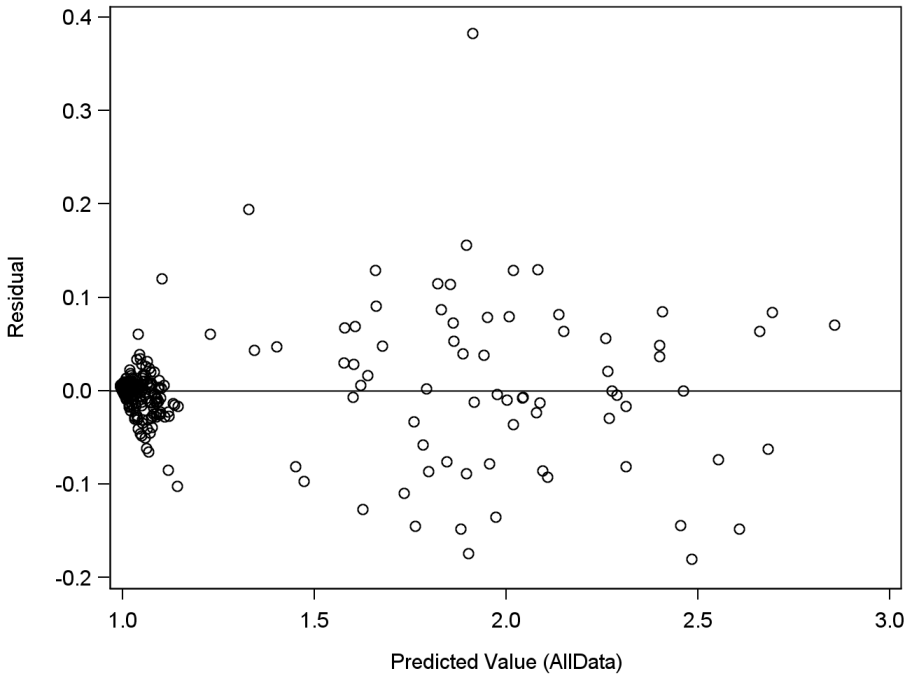

Figure E.231. Residual-by-predicted plot, new model: power form with two parameters, 80th-percentile TTI, AllData.

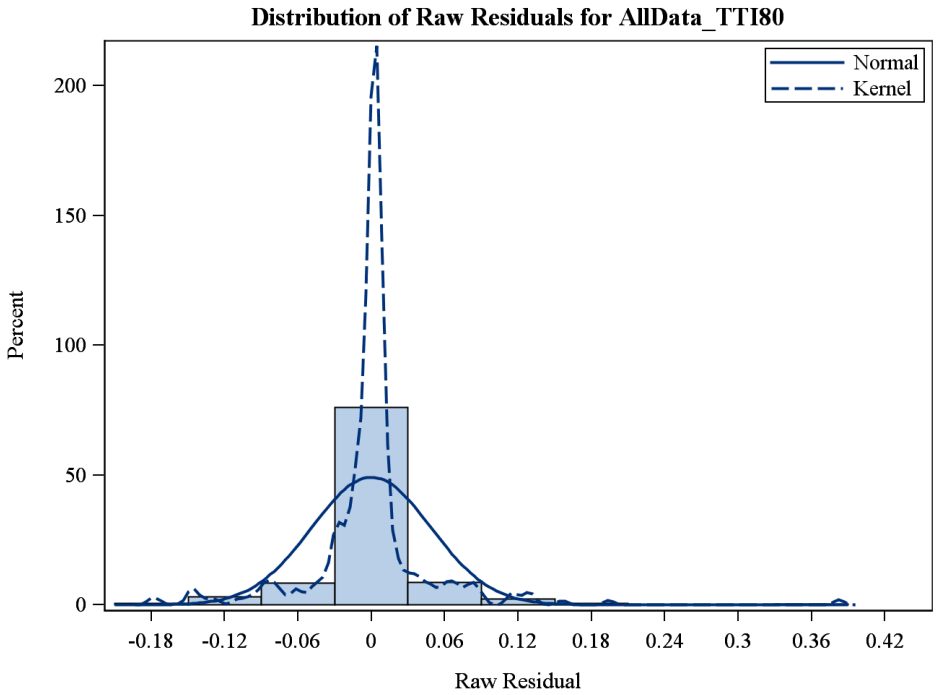

Figure E.232. Distribution of residuals, new model: power form with two parameters, 80th-percentile TTI, AllData.

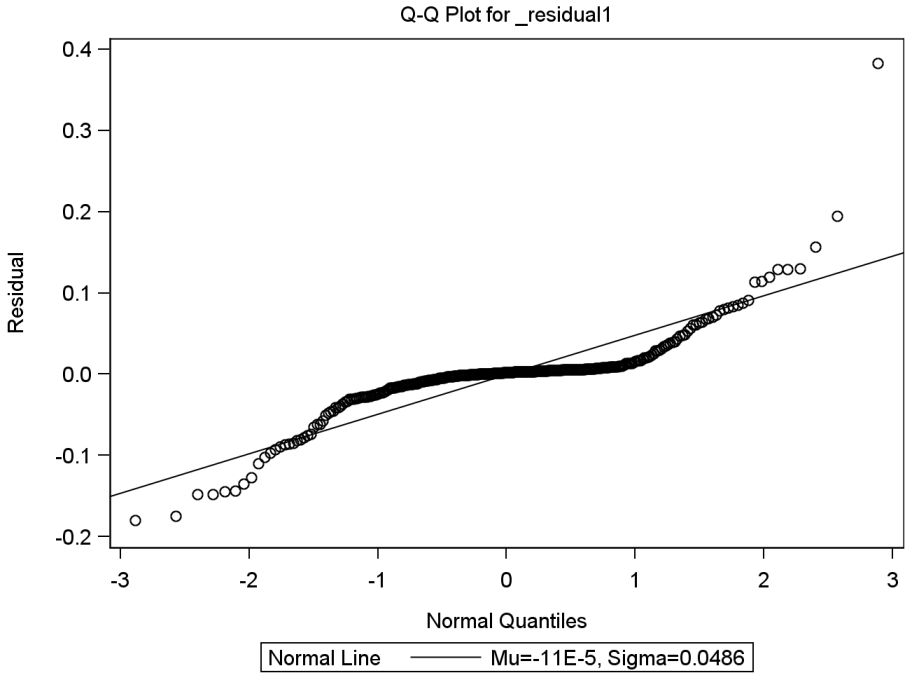

Figure E.233. Q-Q plot of residuals, new model: power form with two parameters, 80th-percentile TTI, AllData.

Table E.95. Analysis of Variance, New Model: Polynomial Form with Two Parameters, 80th-Percentile TTI, AllData

Source	DF	Sum of Squares	Mean Square	*F*-Value	Approx. Pr > *F*
Model	2	558.4	279.2	113766	<0.0001
Error	319	0.7829	0.00245		
Uncorrected total	321	559.2			

Table E.96. Parameter Estimates, New Model: Polynomial Form with Two Parameters, 80th-Percentile TTI, AllData

Parameter	Estimate	Approx. Std Error	Approx. 95% Confidence Limits	
a	0.6166	0.00935	0.5983	0.6350
b	0.3809	0.00703	0.3671	0.3948

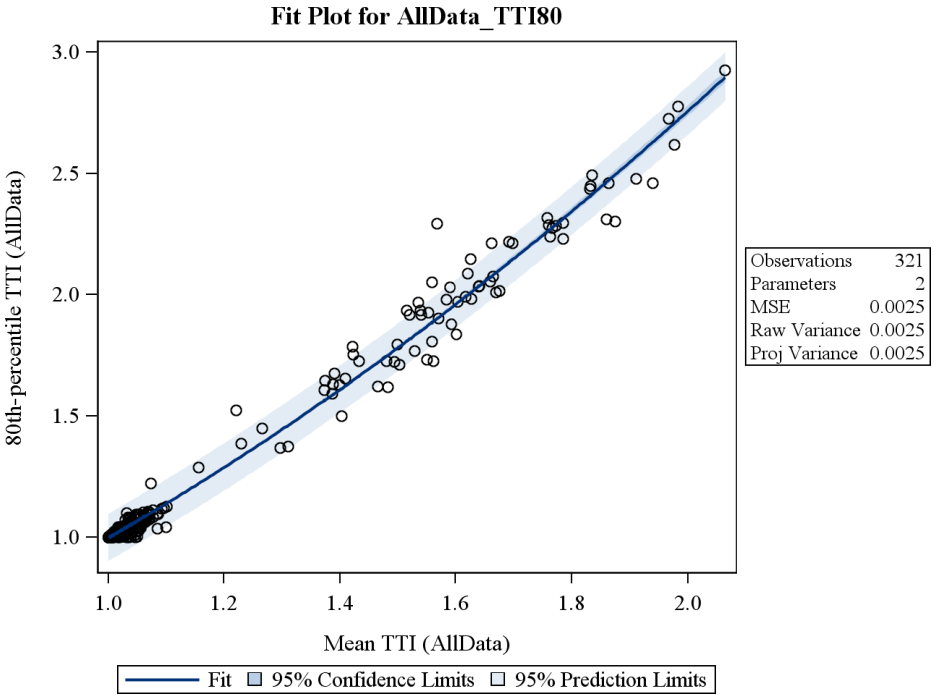

Figure E.234. Fit plot, new model: polynomial form with two parameters, 80th-percentile TTI, AllData.

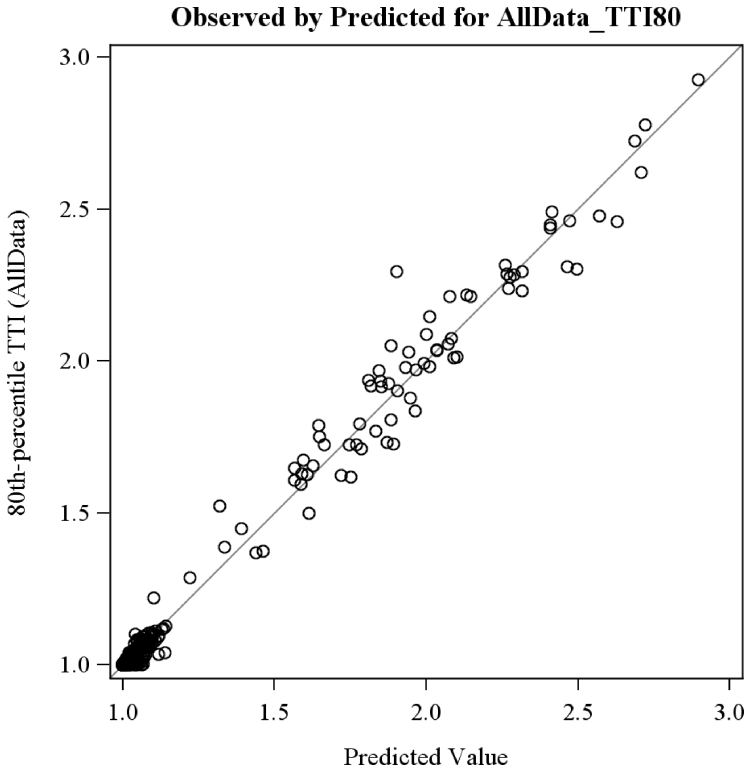

Figure E.235. Observed-by-predicted plot, new model: polynomial form with two parameters, 80th-percentile TTI, AllData.

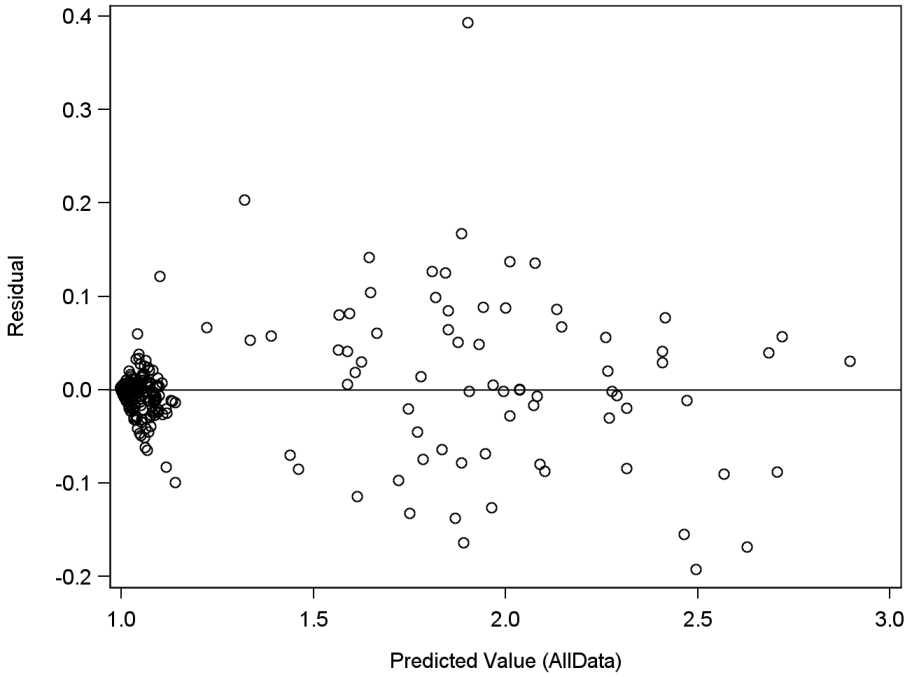

Figure E.236. Residual-by-predicted plot, new model: polynomial form with two parameters, 80th-percentile TTI, AllData.

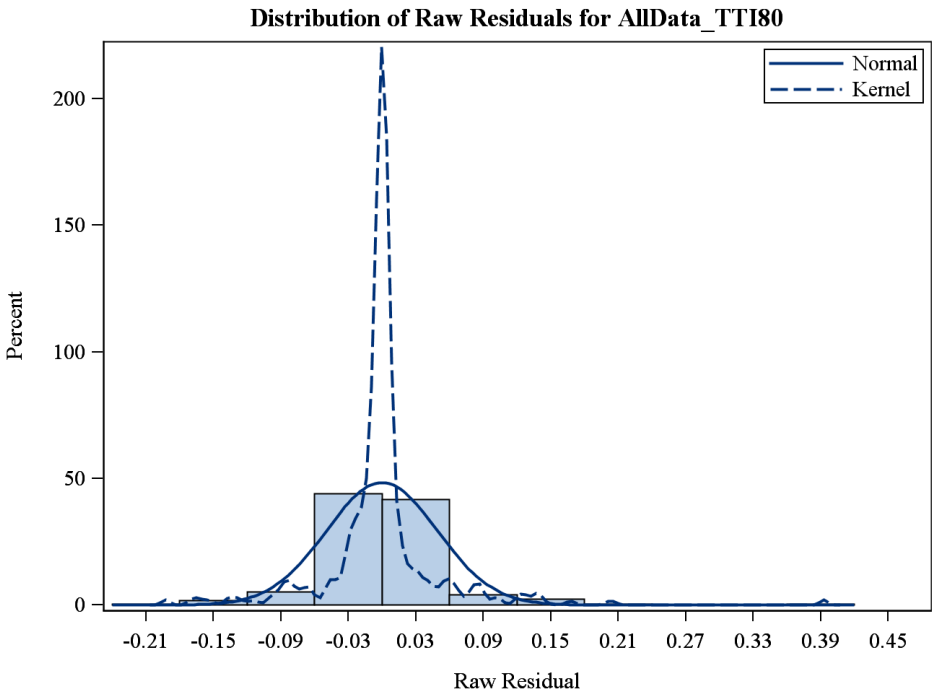

Figure E.237. Distribution of residuals, new model: polynomial form with two parameters, 80th-percentile TTI, AllData.

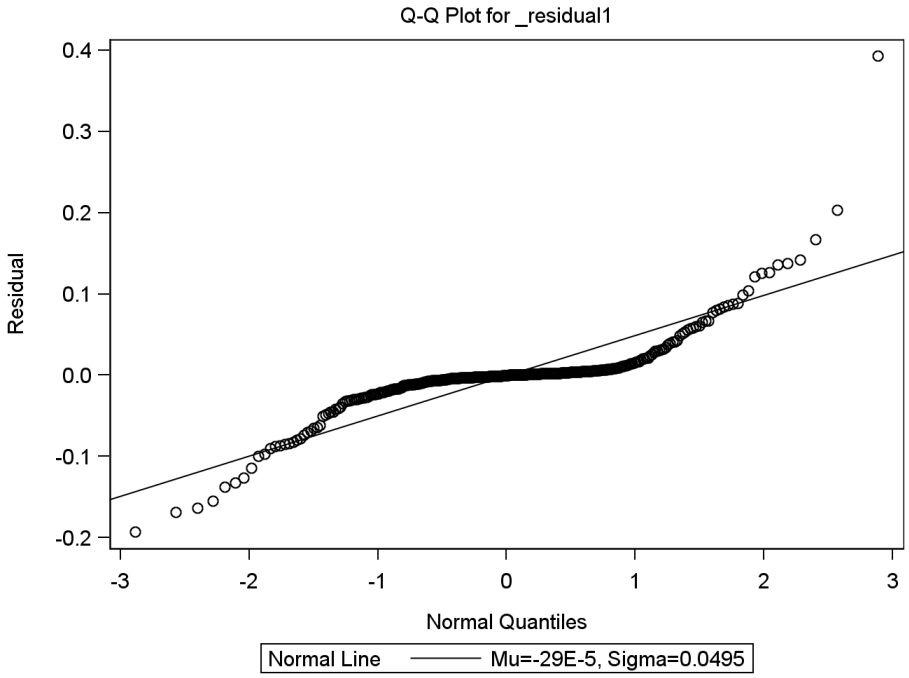

Figure E.238. Q-Q plot of residuals, new model: polynomial form with two parameters, 80th-percentile TTI, AllData.

Table E.97. Analysis of Variance, New Model: Power Form with a Single Parameter, 80th-Percentile TTI, California

Source	DF	Sum of Squares	Mean Square	*F*-Value	Approx. Pr > *F*
Model	1	333.3	333.3	187478	<0.0001
Error	184	0.3271	0.00178		
Uncorrected total	185	333.6			

Table E.98. Parameter Estimates, New Model: Power Form with a Single Parameter, 80th-Percentile TTI, California

Parameter	Estimate	Approx. Std Error	Approx. 95% Confidence Limits	
b	1.4148	0.00607	1.4029	1.4268

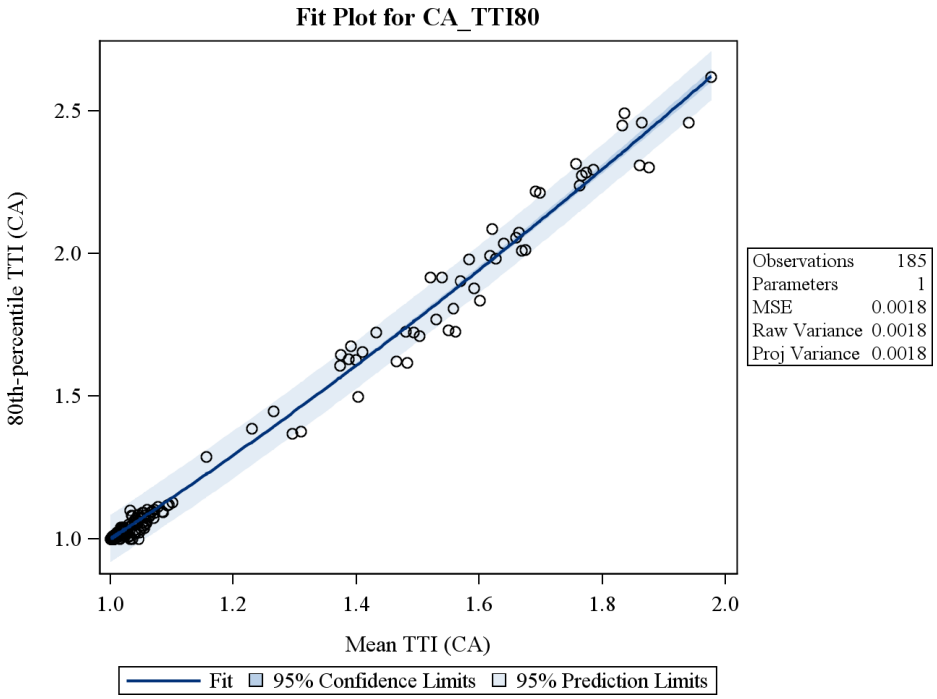

Figure E.239. Fit plot, new model: power form with a single parameter, 80th-percentile TTI, California.

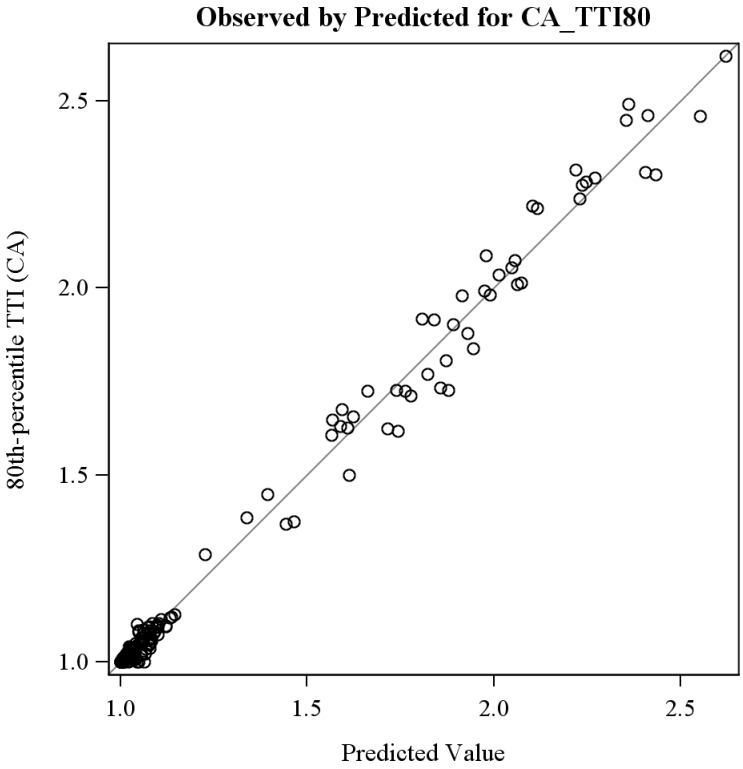

Figure E.240. Observed-by-predicted plot, new model: power form with a single parameter, 80th-percentile TTI, California.

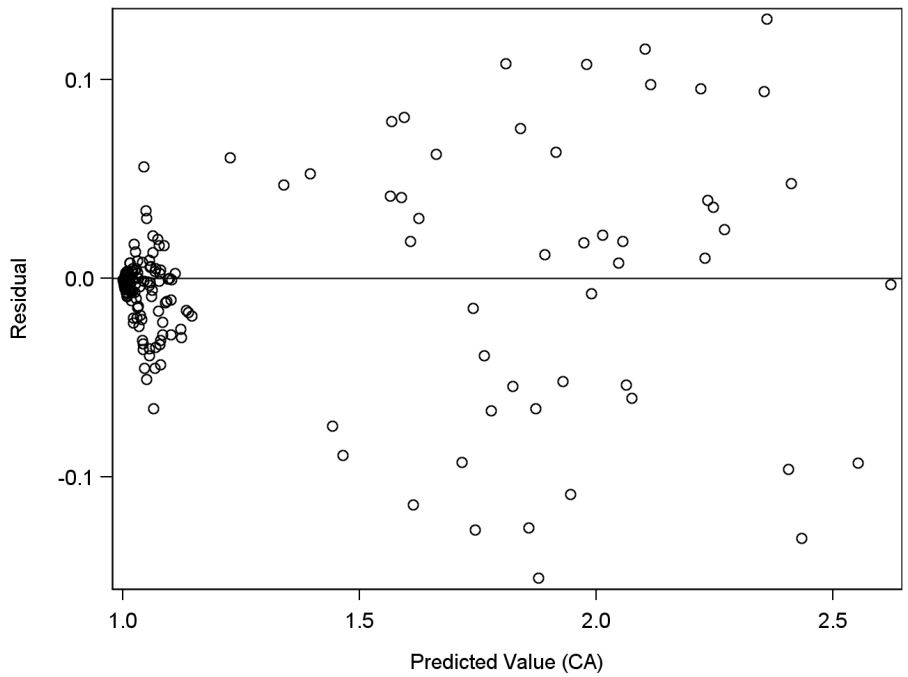

Figure E.241. Residual-by-predicted plot, new model: power form with a single parameter, 80th-percentile TTI, California.

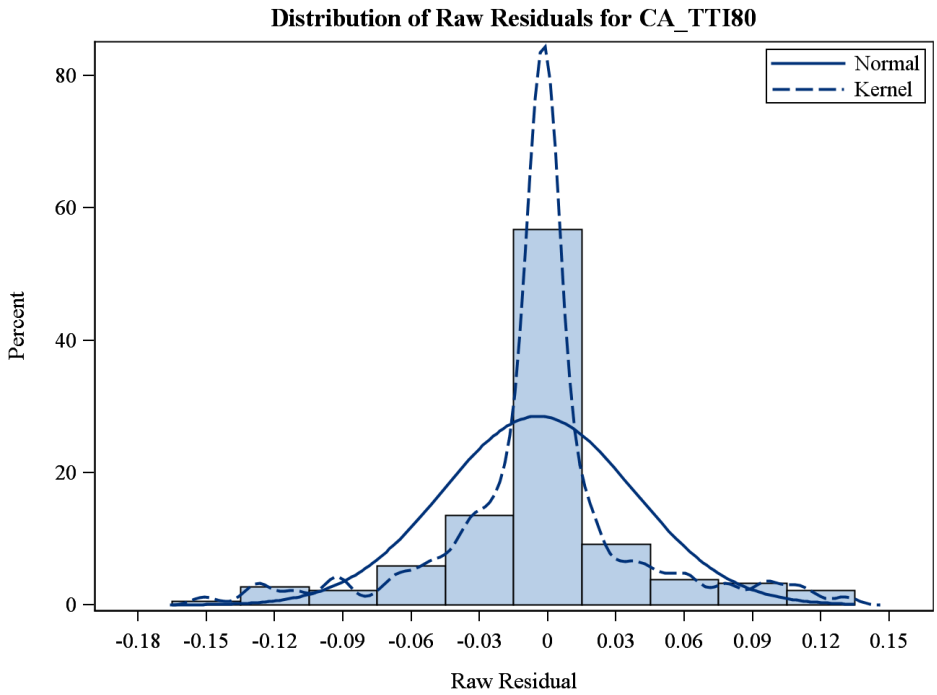

Figure E.242. Distribution of residuals, new model: power form with a single parameter, 80th-percentile TTI, California.

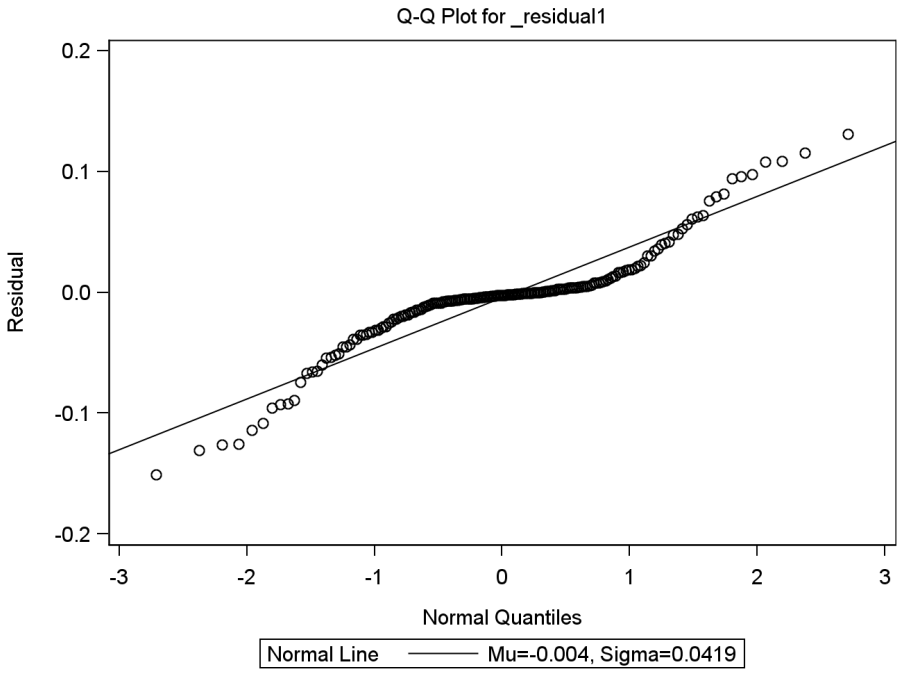

Figure E.243. Q-Q plot of residuals, new model: power form with a single parameter, 80th-percentile TTI, California.

Table E.99. Analysis of Variance, New Model: Power Form with Two Parameters, 80th-Percentile TTI, California

Source	DF	Sum of Squares	Mean Square	*F*-Value	Approx. Pr > *F*
Model	2	333.3	166.6	94557.3	<0.0001
Error	183	0.3225	0.00176		
Uncorrected total	185	333.6			

Table E.100. Parameter Estimates, New Model: Power Form with Two Parameters, 80th-Percentile TTI, California

Parameter	Estimate	Approx. Std Error	Approx. 95% Confidence Limits	
a	0.9943	0.00354	0.9873	1.0013
b	1.4264	0.00936	1.4079	1.4448

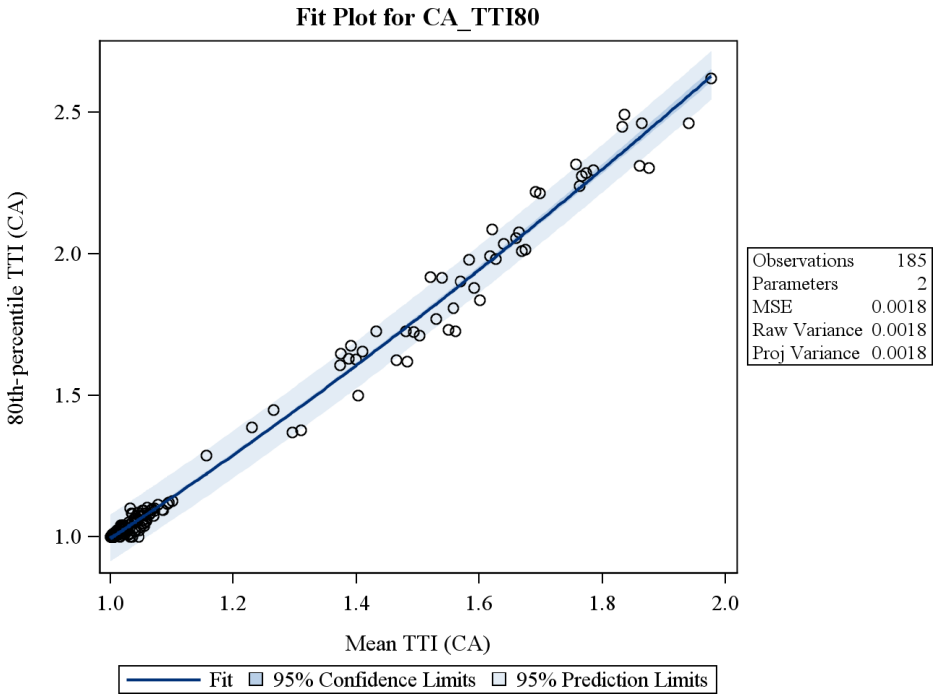

Figure E.244. Fit plot, new model: power form with two parameters, 80th-percentile TTI, California.

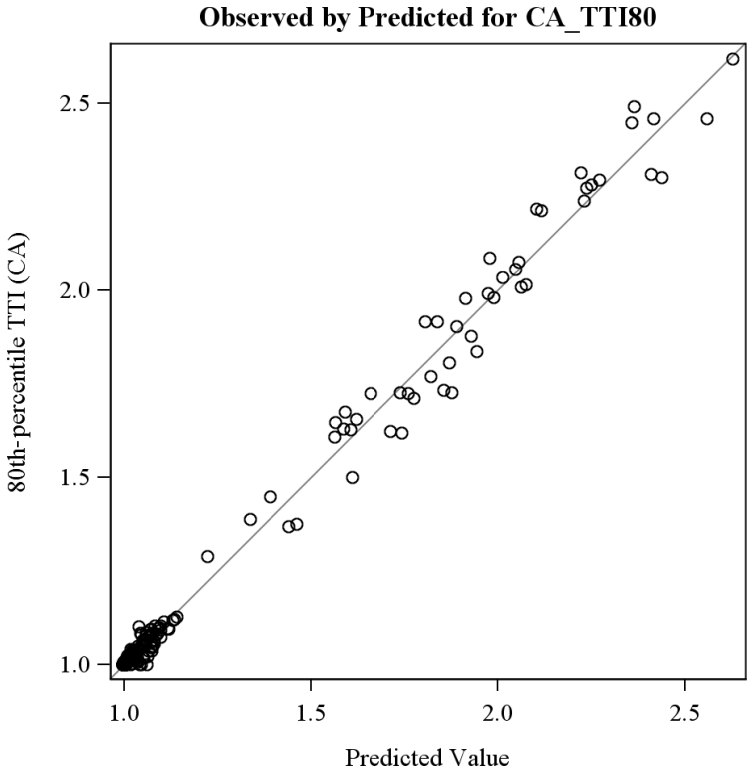

Figure E.245. Observed-by-predicted plot, new model: power form with two parameters, 80th-percentile TTI, California.

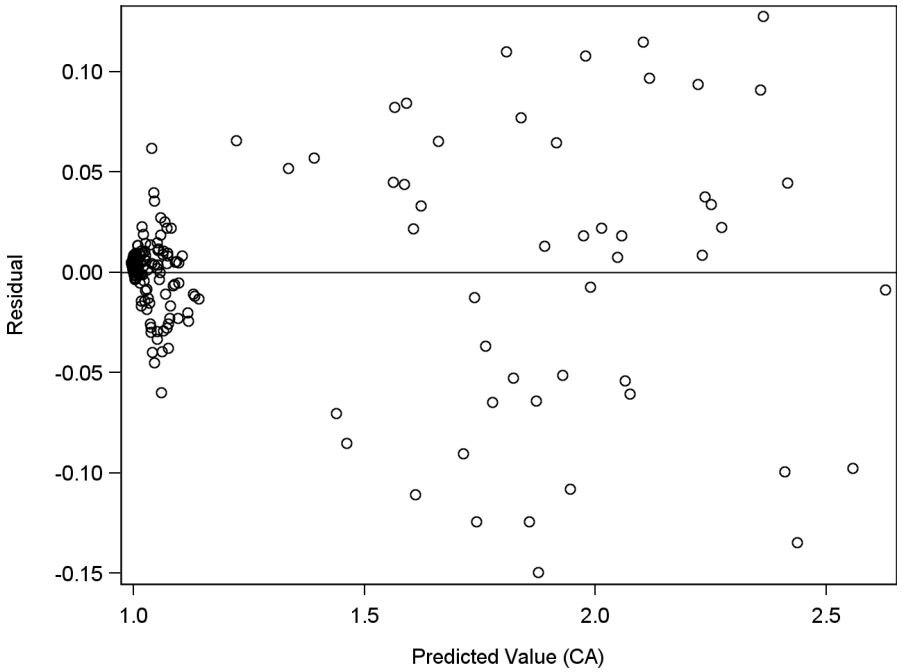

Figure E.246. Residual-by-predicted plot, new model: power form with two parameters, 80th-percentile TTI, California.

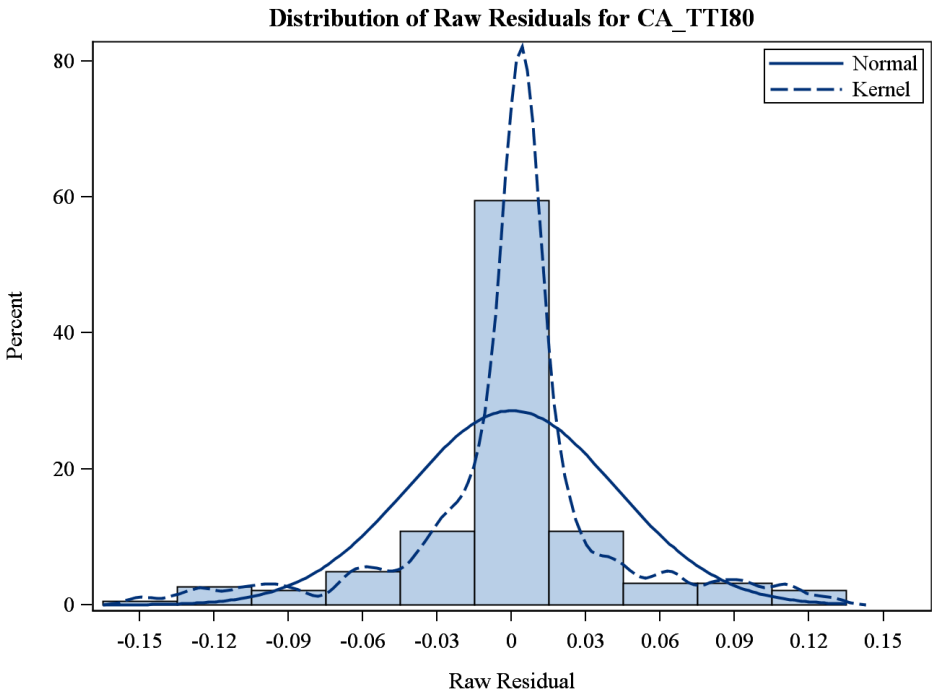

Figure E.247. Distribution of residuals, new model: power form with two parameters, 80th-percentile TTI, California.

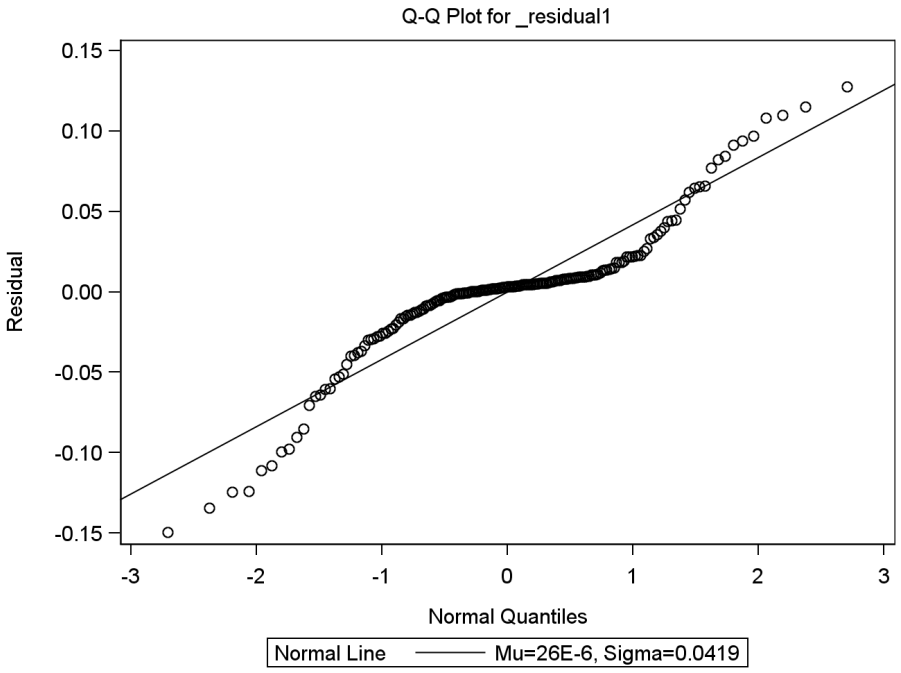

Figure E.248. Q-Q plot of residuals, new model: power form with two parameters, 80th-percentile TTI, California.

Table E.101. Analysis of Variance, New Model: Polynomial Form with Two Parameters, 80th-Percentile TTI, California

Source	DF	Sum of Squares	Mean Square	*F*-Value	Approx. Pr > *F*
Model	2	333.3	166.6	93176.0	<0.0001
Error	183	0.3273	0.00179		
Uncorrected total	185	333.6			

Table E.102. Parameter Estimates, New Model: Polynomial Form with Two Parameters, 80th-Percentile TTI, California

Parameter	Estimate	Approx. Std Error	Approx. 95% Confidence Limits	
a	0.6428	0.0107	0.6217	0.6639
b	0.3547	0.00793	0.3391	0.3704

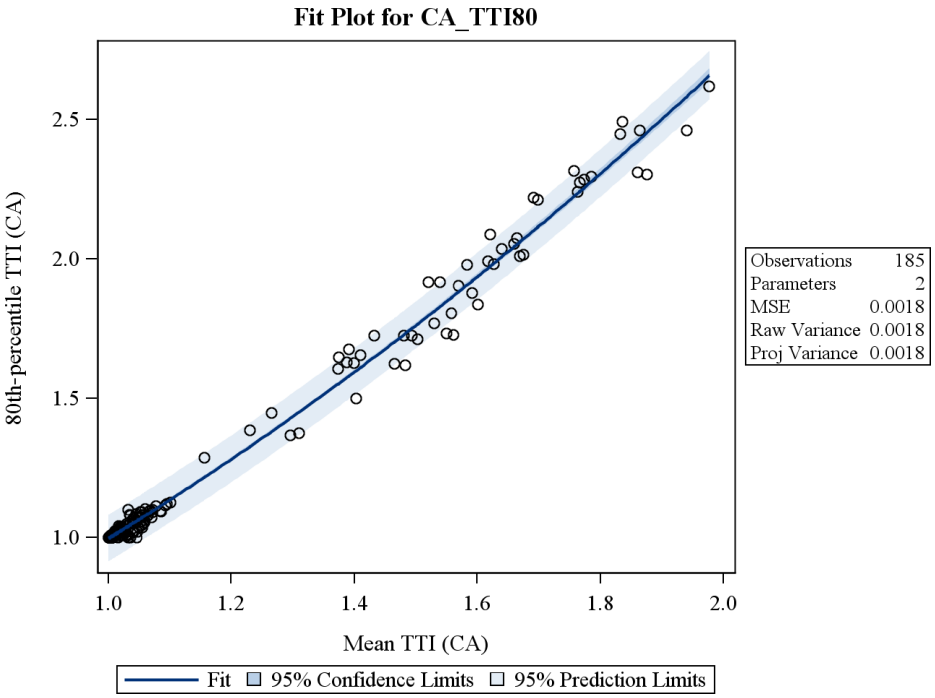

Figure E.249. Fit plot, new model: polynomial form with two parameters, 80th-percentile TTI, California.

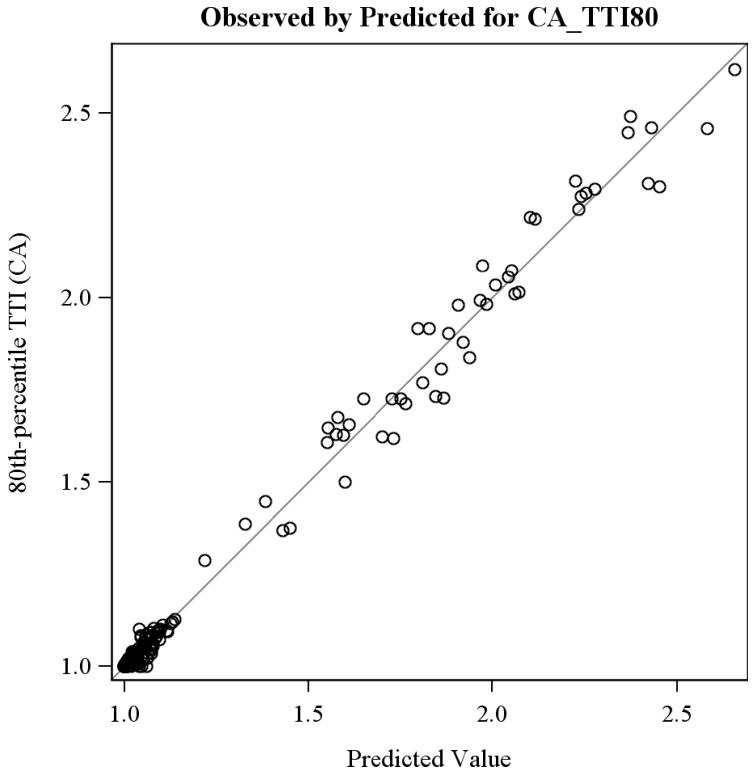

Figure E.250. Observed-by-predicted plot, new model: polynomial form with two parameters, 80th-percentile TTI, California.

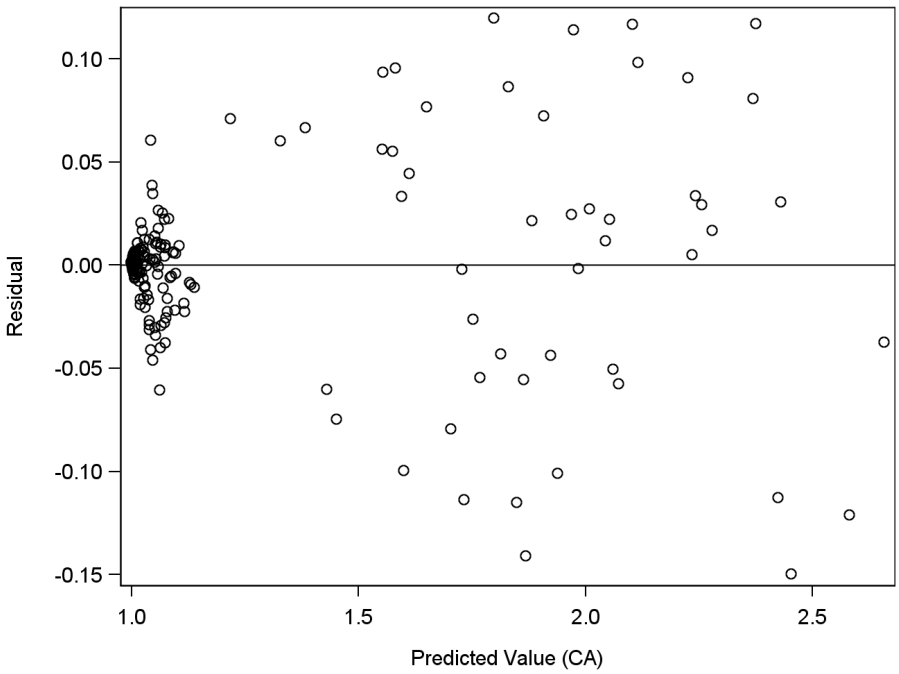

Figure E.251. Residual-by-predicted plot, new model: polynomial form with two parameters, 80th-percentile TTI, California.

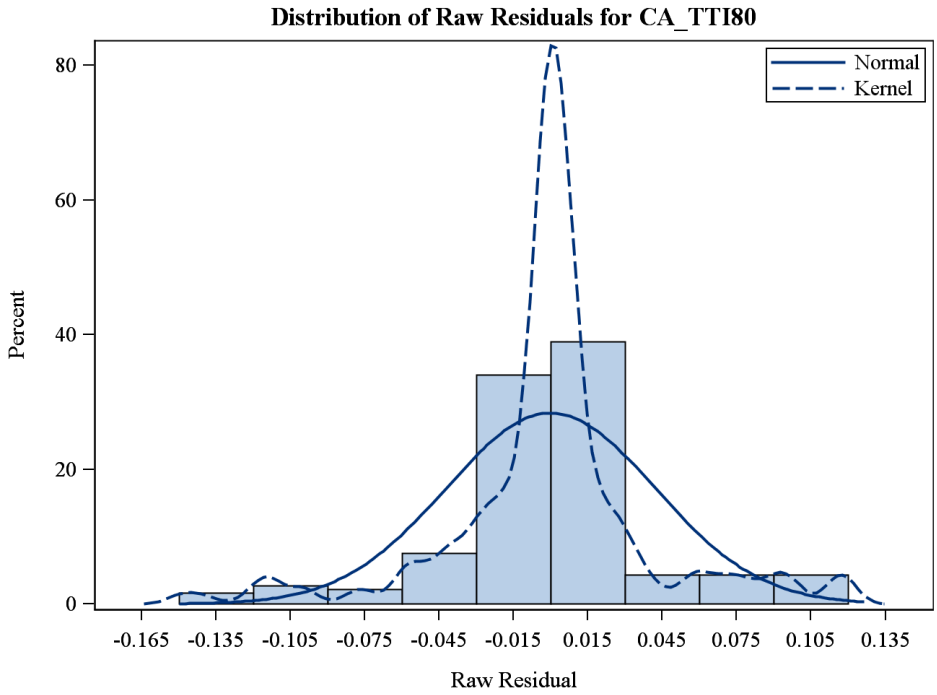

Figure E.252. Distribution of residuals, new model: polynomial form with two parameters, 80th-percentile TTI, California.

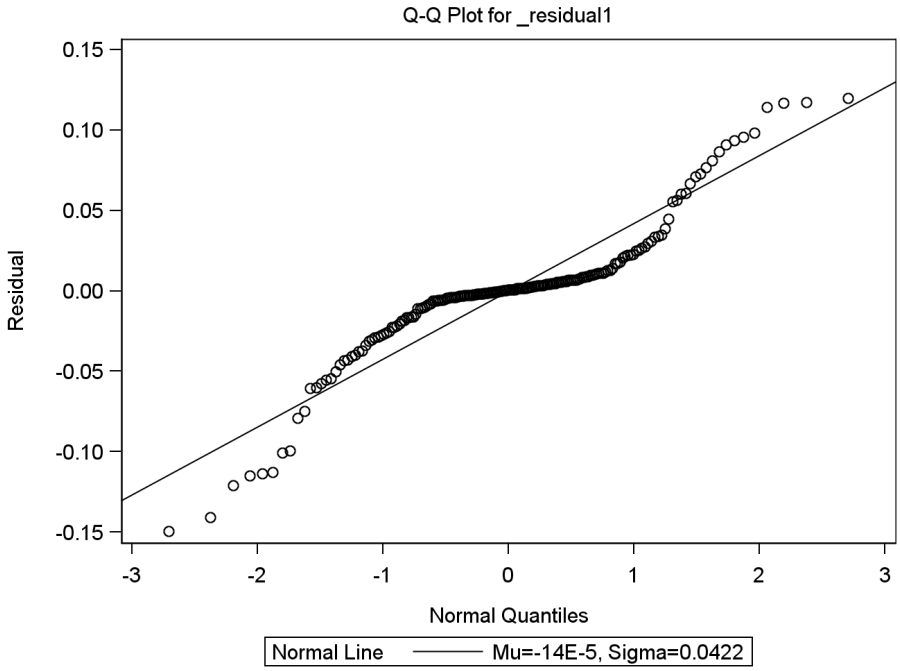

Figure E.253. Q-Q plot of residuals, new model: polynomial form with two parameters, 80th-percentile TTI, California.

Minnesota

Power Form Model with a Single Parameter

Model:

$$80\text{th-percentile TTI}_{MN} = \text{meanTTI}^{1.4955}$$

Power Form Model with Two Parameters

Model:

$$80\text{th-percentile TTI}_{MN} = 0.9992 * \text{meanTTI}^{1.4969}$$

Polynomial Form Model with Two Parameters

Model:

$$80\text{th-percentile TTI}_{MN} = 0.5858 * \text{meanTTI} + 0.4173 * \text{meanTTI}^2$$

Table E.103. Analysis of Variance, New Model: Power Form with a Single Parameter, 80th-Percentile TTI, Minnesota

Source	DF	Sum of Squares	Mean Square	*F*-Value	Approx. Pr > *F*
Model	1	157.4	157.4	41002.4	<0.0001
Error	78	0.2994	0.00384		
Uncorrected total	79	157.7			

Table E.104. Parameter Estimates, New Model: Power Form with a Single Parameter, 80th-Percentile TTI, Minnesota

Parameter	Estimate	Approx. Std Error	Approx. 95% Confidence Limits	
b	1.4955	0.0115	1.4727	1.5183

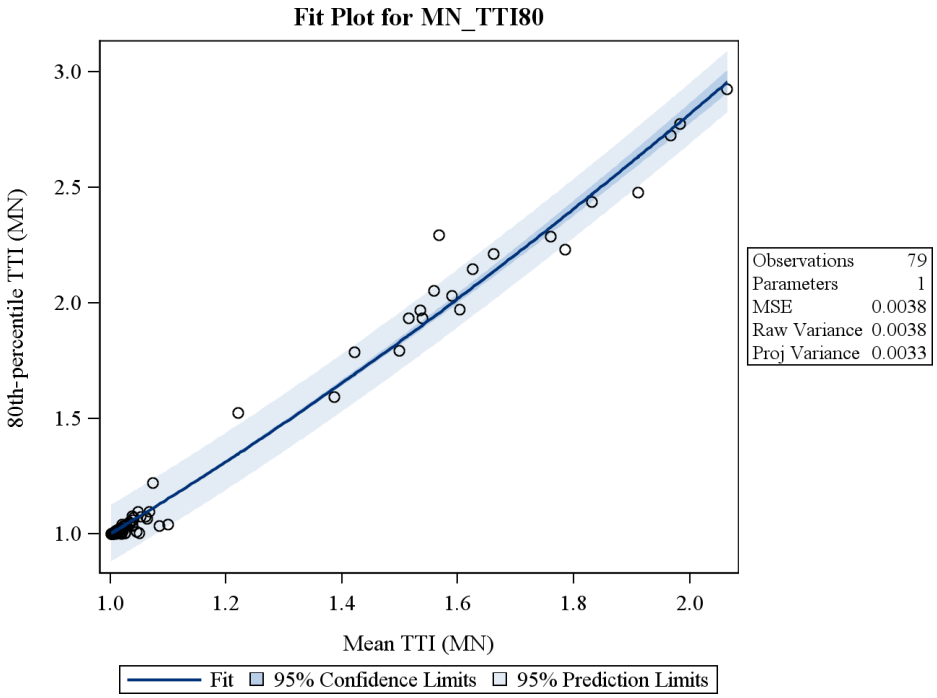

Figure E.254. Fit plot, new model: power form with a single parameter, 80th-percentile TTI, Minnesota.

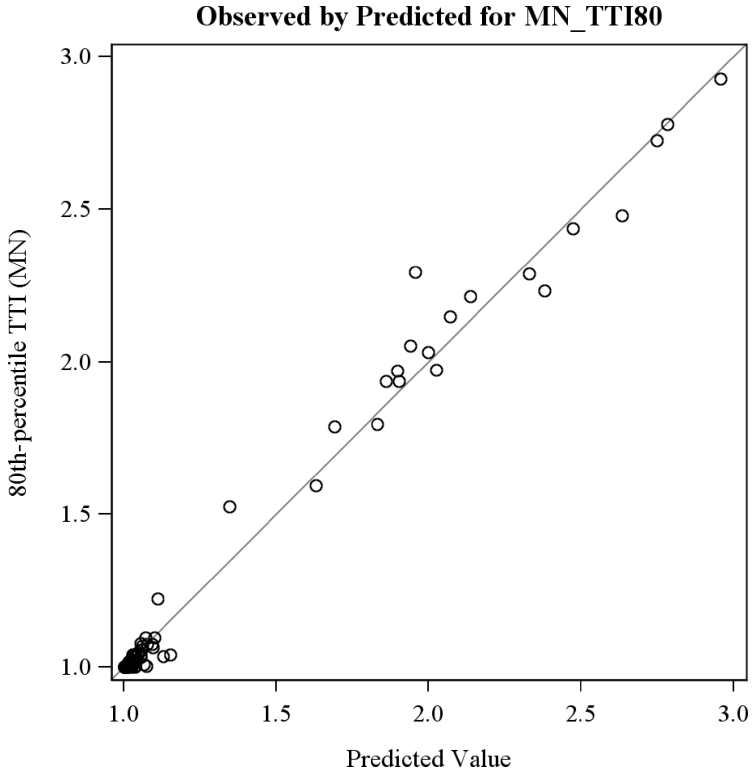

Figure E.255. Observed-by-predicted plot, new model: power form with a single parameter, 80th-percentile TTI, Minnesota.

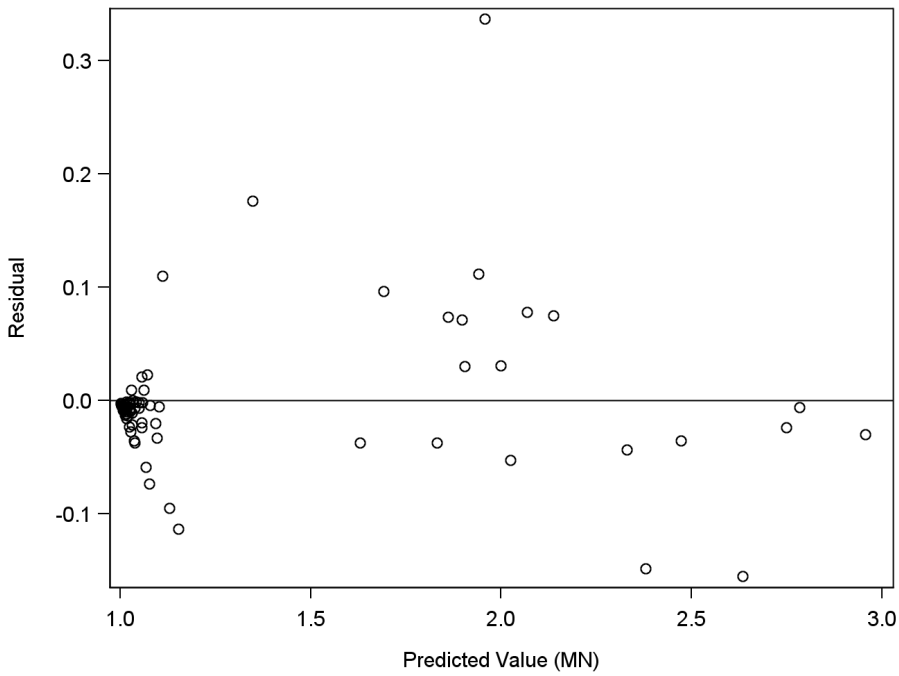

Figure E.256. Residual-by-predicted plot, new model: power form with a single parameter, 80th-percentile TTI, Minnesota.

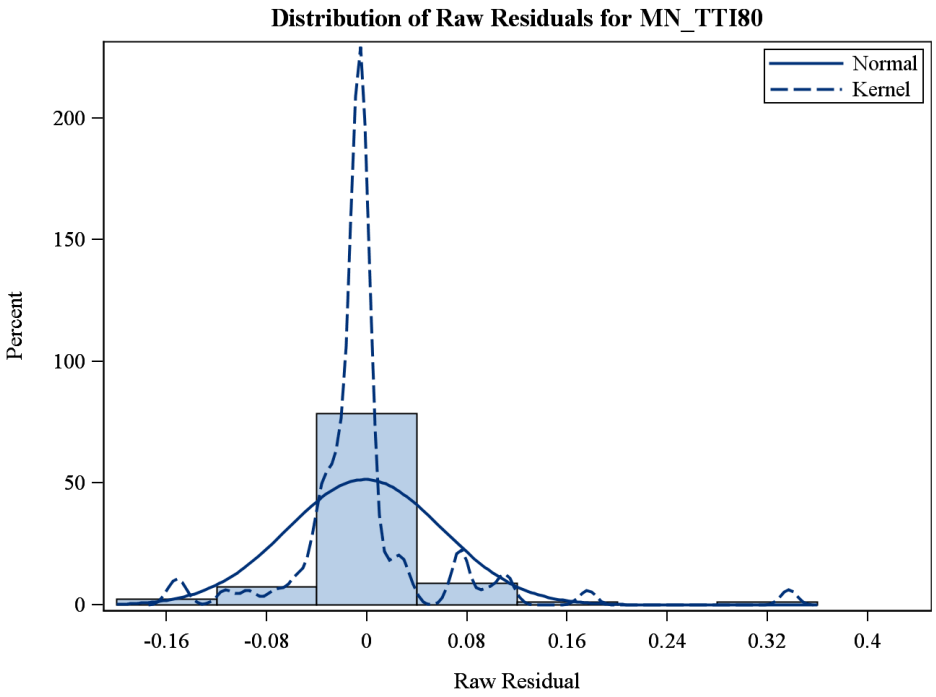

Figure E.257. Distribution of residuals, new model: power form with a single parameter, 80th-percentile TTI, Minnesota.

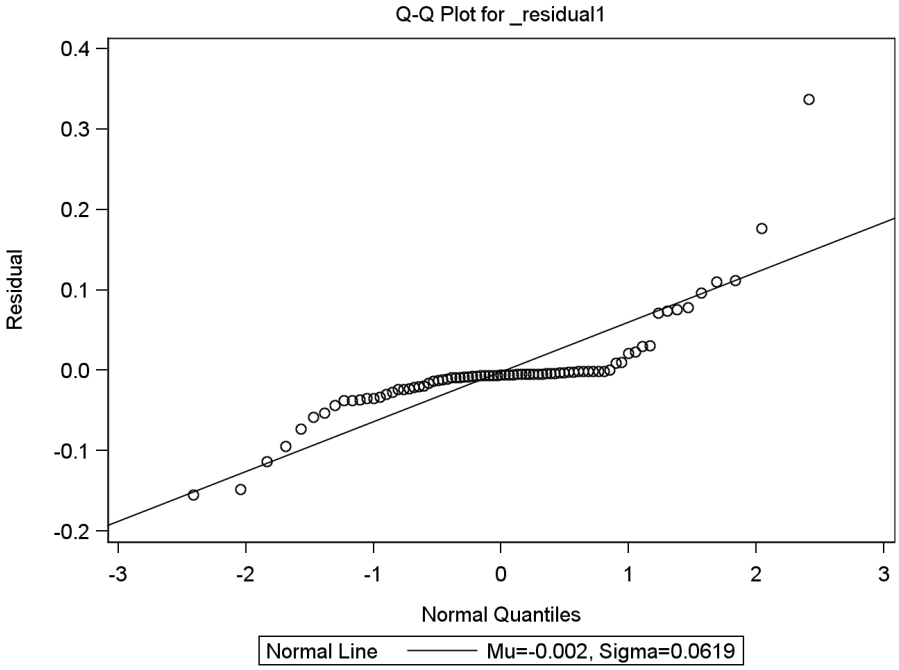

Figure E.258. Q-Q plot of residuals, new model: power form with a single parameter, 80th-percentile TTI, Minnesota.

Table E.105. Analysis of Variance, New Model: Power Form with Two Parameters, 80th-Percentile TTI, Minnesota

Source	DF	Sum of Squares	Mean Square	*F*-Value	Approx. Pr > *F*
Model	2	157.4	78.6883	20241.1	<0.0001
Error	77	0.2993	0.00389		
Uncorrected total	79	157.7			

Table E.106. Parameter Estimates, New Model: Power Form with Two Parameters, 80th-Percentile TTI, Minnesota

Parameter	Estimate	Approx. Std Error	Approx. 95% Confidence Limits	
a	0.9992	0.00786	0.9835	1.0149
b	1.4969	0.0183	1.4605	1.5333

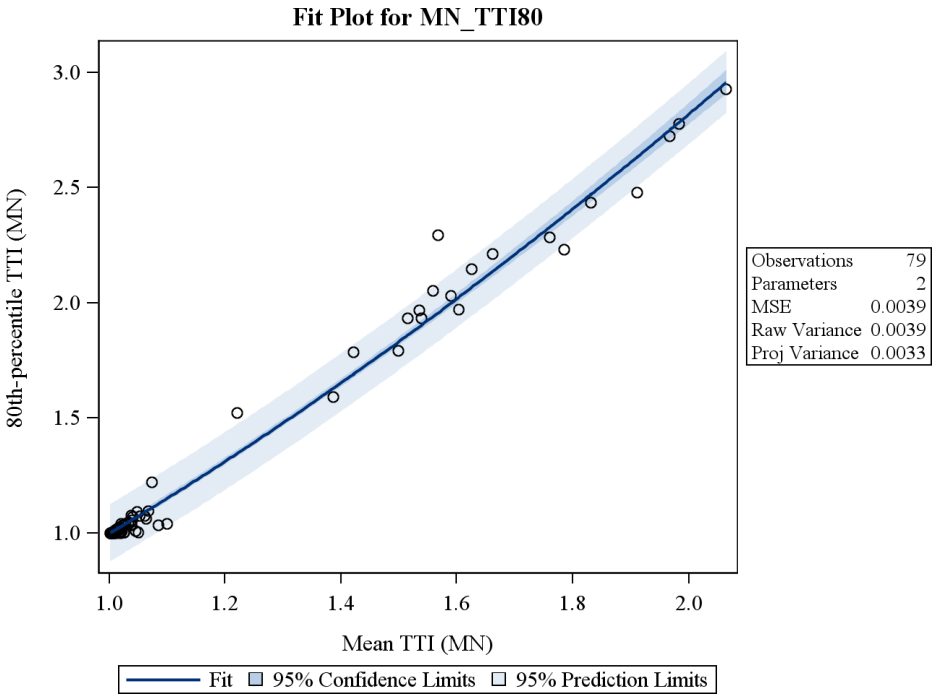

Figure E.259. Fit plot, new model: power form with two parameters, 80th-percentile TTI, Minnesota.

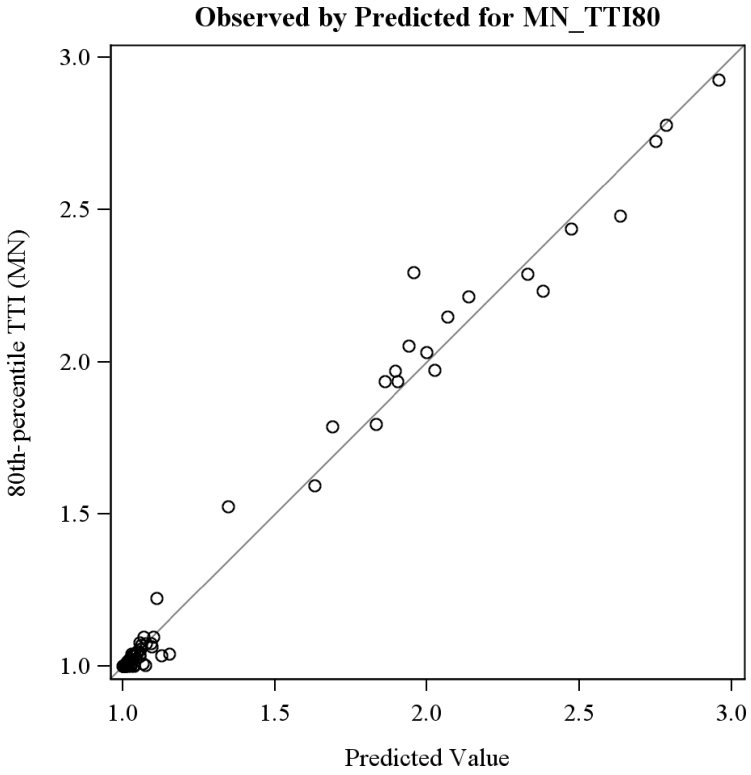

Figure E.260. Observed-by-predicted plot, new model: power form with two parameters, 80th-percentile TTI, Minnesota.

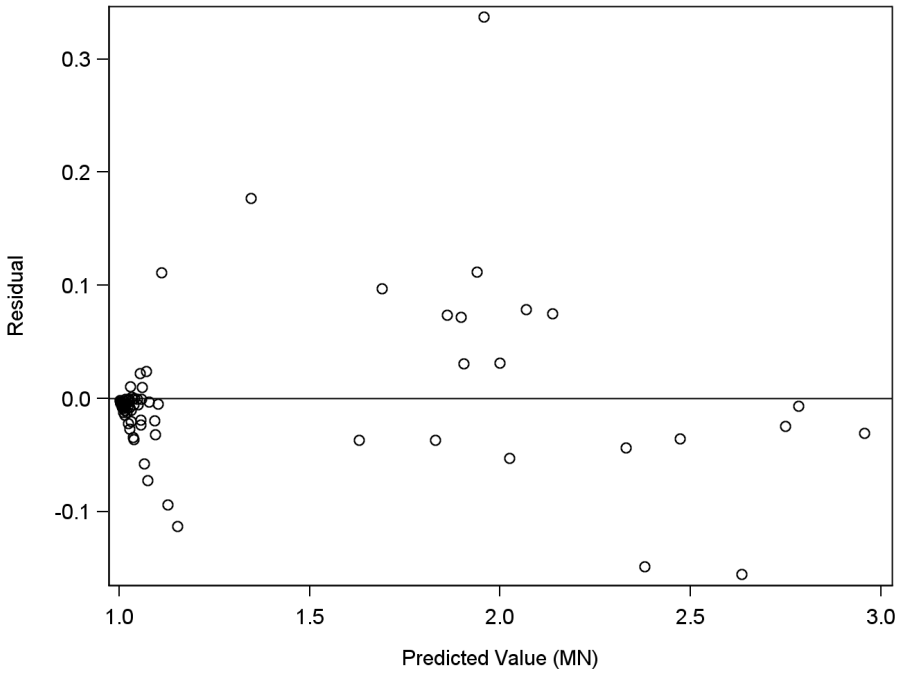

Figure E.261. Residual-by-predicted plot, new model: power form with two parameters, 80th-percentile TTI, Minnesota.

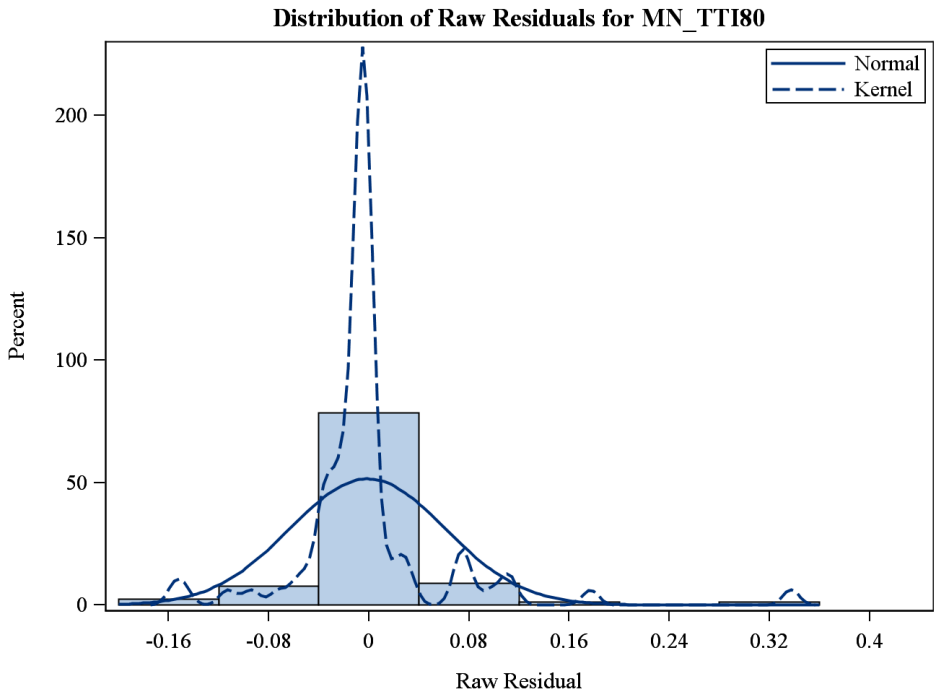

Figure E.262. Distribution of residuals, new model: power form with two parameters, 80th-percentile TTI, Minnesota.

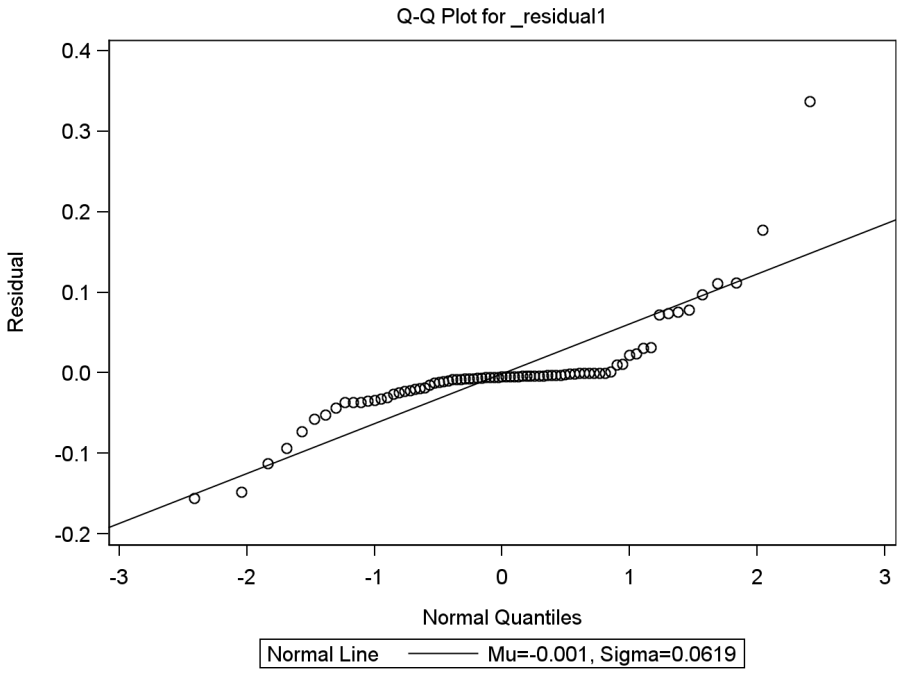

Figure E.263. Q-Q plot of residuals, new model: power form with two parameters, 80th-percentile TTI, Minnesota.

Table E.107. Analysis of Variance, New Model: Polynomial Form with Two Parameters, 80th-Percentile TTI, Minnesota

Source	DF	Sum of Squares	Mean Square	*F*-Value	Approx. Pr > *F*
Model	2	157.3	78.6702	18059.0	<0.0001
Error	77	0.3354	0.00436		
Uncorrected total	79	157.7			

Table E.108. Parameter Estimates, New Model: Polynomial Form with Two Parameters, 80th-Percentile TTI, Minnesota

Parameter	Estimate	Approx. Std Error	Approx. 95% Confidence Limits	
a	0.5858	0.0229	0.5401	0.6315
b	0.4173	0.0164	0.3846	0.4500

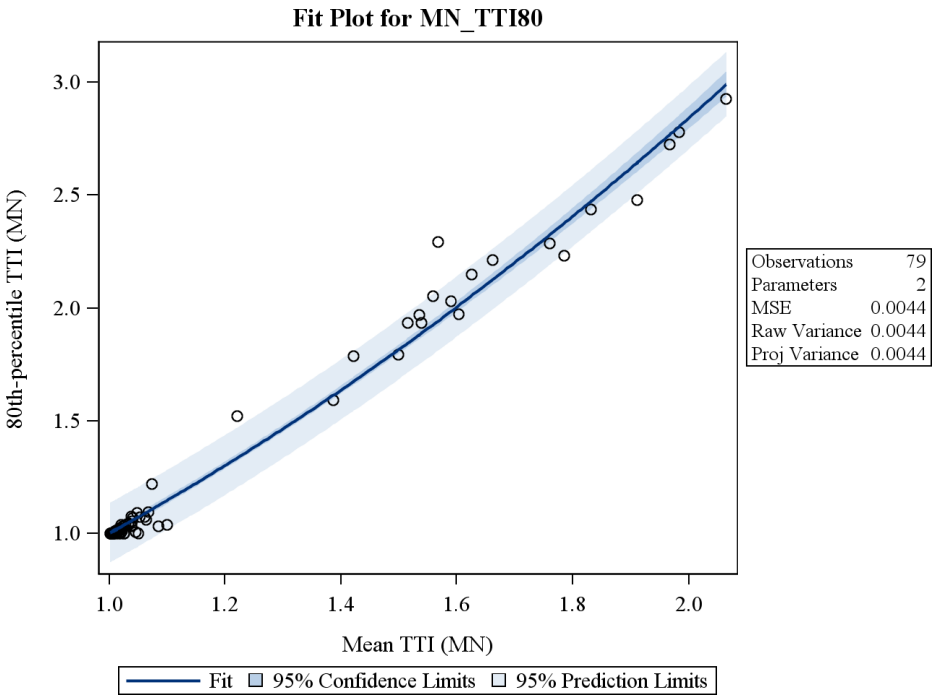

Figure E.264. Fit plot, new model: polynomial form with two parameters, 80th-percentile TTI, Minnesota.

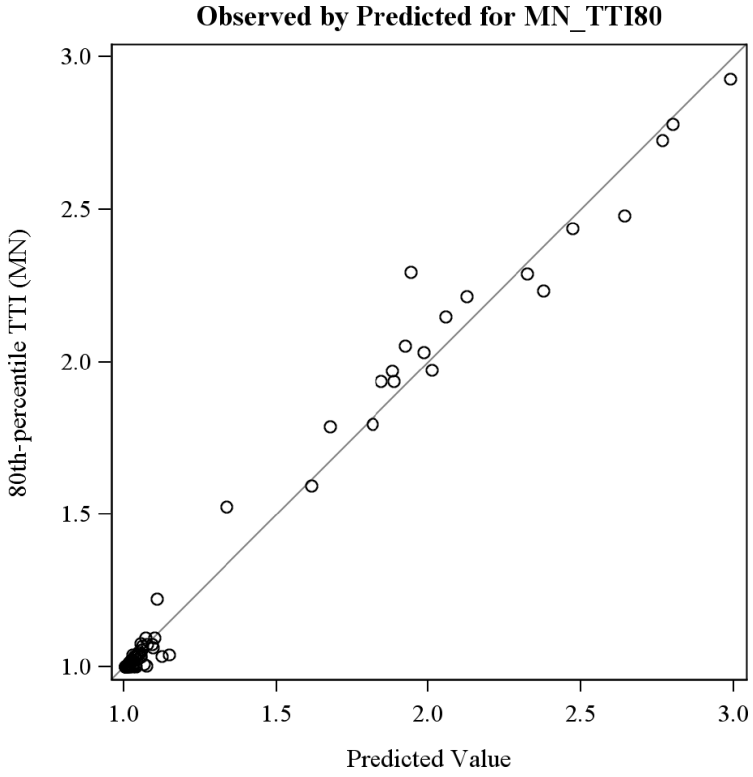

Figure E.265. Observed-by-predicted plot, new model: polynomial form with two parameters, 80th-percentile TTI, Minnesota.

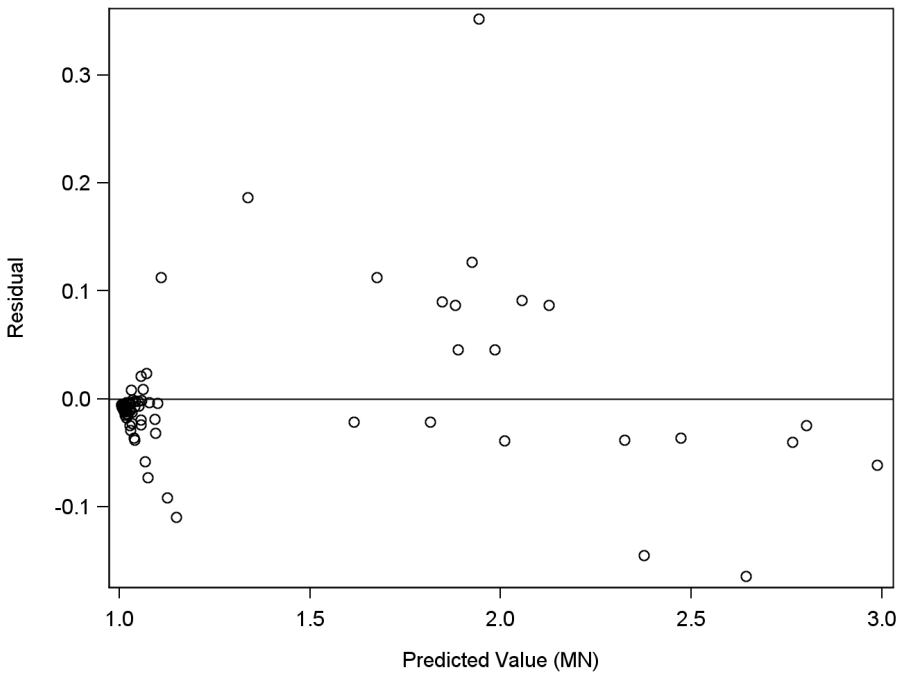

Figure E.266. Residual-by-predicted plot, new model: polynomial form with two parameters, 80th-percentile TTI, Minnesota.

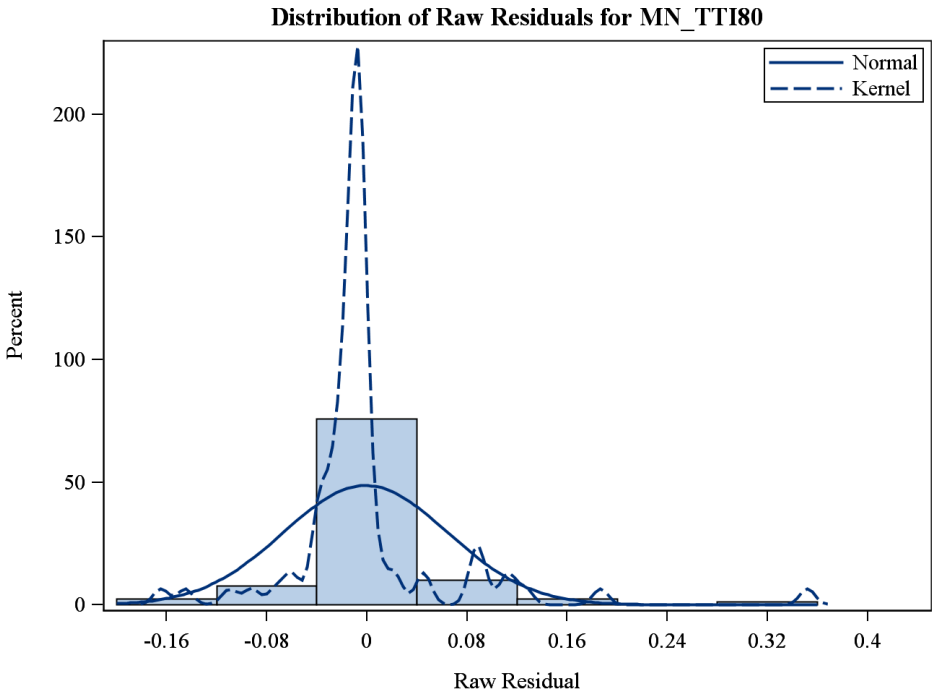

Figure E.267. Distribution of residuals, new model: polynomial form with two parameters, 80th-percentile TTI, Minnesota.

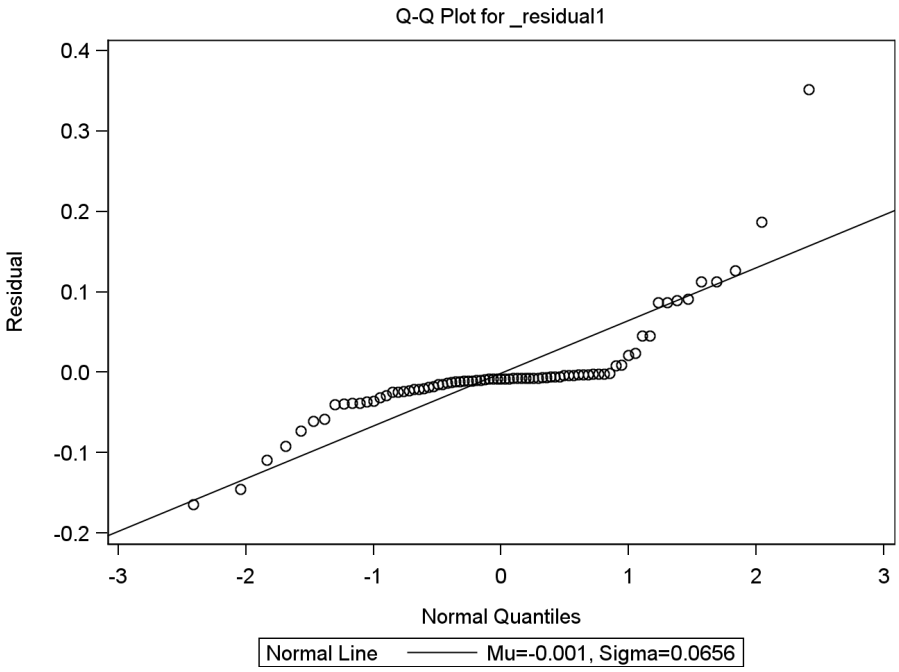

Figure E.268. Q-Q plot of residuals, new model: polynomial form with two parameters, 80th-percentile TTI, Minnesota.

TRB OVERSIGHT COMMITTEE FOR THE STRATEGIC HIGHWAY RESEARCH PROGRAM 2*

CHAIR: **Kirk T. Steudle,** *Director, Michigan Department of Transportation*

MEMBERS

H. Norman Abramson, *Executive Vice President (retired), Southwest Research Institute*
Alan C. Clark, *MPO Director, Houston–Galveston Area Council*
Frank L. Danchetz, *Vice President, ARCADIS-US, Inc. (deceased January 2015)*
Malcolm Dougherty, *Director, California Department of Transportation*
Stanley Gee, *Executive Deputy Commissioner, New York State Department of Transportation*
Mary L. Klein, *President and CEO, NatureServe*
Michael P. Lewis, *Director, Rhode Island Department of Transportation*
John R. Njord, *Executive Director (retired), Utah Department of Transportation*
Charles F. Potts, *Chief Executive Officer, Heritage Construction and Materials*
Ananth K. Prasad, *Secretary, Florida Department of Transportation*
Gerald M. Ross, *Chief Engineer (retired), Georgia Department of Transportation*
George E. Schoener, *Executive Director, I-95 Corridor Coalition*
Kumares C. Sinha, *Olson Distinguished Professor of Civil Engineering, Purdue University*
Paul Trombino III, *Director, Iowa Department of Transportation*

EX OFFICIO MEMBERS

Victor M. Mendez, *Administrator, Federal Highway Administration*
David L. Strickland, *Administrator, National Highway Transportation Safety Administration*
Frederick "Bud" Wright, *Executive Director, American Association of State Highway and Transportation Officials*

LIAISONS

Ken Jacoby, *Communications and Outreach Team Director, Office of Corporate Research, Technology, and Innovation Management, Federal Highway Administration*
Tony Kane, *Director, Engineering and Technical Services, American Association of State Highway and Transportation Officials*
Jeffrey F. Paniati, *Executive Director, Federal Highway Administration*
John Pearson, *Program Director, Council of Deputy Ministers Responsible for Transportation and Highway Safety, Canada*
Michael F. Trentacoste, *Associate Administrator, Research, Development, and Technology, Federal Highway Administration*

* Membership as of January 2015.

RELIABILITY TECHNICAL COORDINATING COMMITTEE*

CHAIR: **Carlos Braceras,** *Deputy Director and Chief Engineer, Utah Department of Transportation*
VICE CHAIR: **John Corbin,** *Director, Bureau of Traffic Operations, Wisconsin Department of Transportation*
VICE CHAIR: **Mark F. Muriello,** *Assistant Director, Tunnels, Bridges, and Terminals, The Port Authority of New York and New Jersey*

MEMBERS

Malcolm E. Baird, *Consultant*
Mike Bousliman, *Chief Information Officer, Information Services Division, Montana Department of Transportation*
Kevin W. Burch, *President, Jet Express, Inc.*
Leslie S. Fowler, *ITS Program Manager, Intelligent Transportation Systems, Bureau of Transportation Safety and Technology, Kansas Department of Transportation*
Steven Gayle, *Consultant, Gayle Consult, LLC*
Bruce R. Hellinga, *Professor, Department of Civil and Environmental Engineering, University of Waterloo, Ontario, Canada*
Sarath C. Joshua, *ITS and Safety Program Manager, Maricopa Association of Governments*
Sandra Q. Larson, *Systems Operations Bureau Director, Iowa Department of Transportation*
Dennis Motiani, *Executive Director, Transportation Systems Management, New Jersey Department of Transportation*
Richard J. Nelson, *Nevada Department of Transportation*
Richard Phillips, *Director (retired), Administrative Services, Washington State Department of Transportation*
Mark Plass, *District Traffic Operations Engineer, Florida Department of Transportation*
Constance S. Sorrell, *Chief of Systems Operations, Virginia Department of Transportation*
William Steffens, *Vice President and Regional Manager, McMahon Associates*
Jan van der Waard, *Program Manager, Mobility and Accessibility, Netherlands Institute for Transport Policy Analysis*
John P. Wolf, *Assistant Division Chief, Traffic Operations, California Department of Transportation (Caltrans)*

FHWA LIAISONS

Robert Arnold, *Director, Transportation Management, Office of Operations, Federal Highway Administration*
Joe Conway, *SHRP 2 Implementation Director, National Highway Institute*
Jeffrey A. Lindley, *Associate Administrator for Operations, Federal Highway Administration*

U.S. DEPARTMENT OF TRANSPORTATION LIAISON

Patricia S. Hu, *Director, Bureau of Transportation Statistics, U.S. Department of Transportation*

AASHTO LIAISON

Gummada Murthy, *Associate Program Director, Operations*

CANADA LIAISON

Andrew Beal, *Manager, Traffic Office, Highway Standards Branch, Ontario Ministry of Transportation*

* Membership as of July 2014.

Related SHRP 2 Research

Analytical Procedures for Determining the Impacts of Reliability Mitigation Strategies (L03)

Evaluation of Cost-Effectiveness of Highway Design Features (L07)